



AMERICAN ACADEMY
OF OPHTHALMOLOGY®
Protecting Sight. Empowering Lives.

12 | Retina and Vitreous

2022–2023 **BCSC**® Basic and Clinical Science Course™

Editorial Committee

Stephen J. Kim, MD, *Chair*

Amani Fawzi, MD

Jaclyn L. Kovach, MD

Shriji Patel, MD, MBA

Franco M. Recchia, MD

Lucia Sobrin, MD, MPH

Jennifer K. Sun, MD, MPH

Charles C. Wykoff, MD, PhD



AMERICAN ACADEMY
OF OPHTHALMOLOGY®
Protecting Sight. Empowering Lives.

12 | Retina and Vitreous

2022–2023
BCSC
**Basic and Clinical
Science Course™**

*Funded in part by the Educational Trust
Fund/Retina Research Foundation*



Published after collaborative
review with the European Board
of Ophthalmology subcommittee

The American Academy of Ophthalmology is accredited by the Accreditation Council for Continuing Medical Education (ACCME) to provide continuing medical education for physicians.

The American Academy of Ophthalmology designates this enduring material for a maximum of 15 *AMA PRA Category 1 Credits*[™]. Physicians should claim only the credit commensurate with the extent of their participation in the activity.

CME expiration date: June 1, 2025. *AMA PRA Category 1 Credits*[™] may be claimed only once between June 1, 2022, and the expiration date.

BCSC[®] volumes are designed to increase the physician's ophthalmic knowledge through study and review. Users of this activity are encouraged to read the text and then answer the study questions provided at the back of the book.

To claim *AMA PRA Category 1 Credits*[™] upon completion of this activity, learners must demonstrate appropriate knowledge and participation in the activity by taking the posttest for Section 12 and achieving a score of 80% or higher. For further details, please see the instructions for requesting CME credit at the back of the book.

The Academy provides this material for educational purposes only. It is not intended to represent the only or best method or procedure in every case, nor to replace a physician's own judgment or give specific advice for case management. Including all indications, contraindications, side effects, and alternative agents for each drug or treatment is beyond the scope of this material. All information and recommendations should be verified, prior to use, with current information included in the manufacturers' package inserts or other independent sources, and considered in light of the patient's condition and history. Reference to certain drugs, instruments, and other products in this course is made for illustrative purposes only and is not intended to constitute an endorsement of such. Some material may include information on applications that are not considered community standard, that reflect indications not included in approved FDA labeling, or that are approved for use only in restricted research settings. **The FDA has stated that it is the responsibility of the physician to determine the FDA status of each drug or device he or she wishes to use, and to use them with appropriate, informed patient consent in compliance with applicable law.** The Academy specifically disclaims any and all liability for injury or other damages of any kind, from negligence or otherwise, for any and all claims that may arise from the use of any recommendations or other information contained herein.

All trademarks, trade names, logos, brand names, and service marks of the American Academy of Ophthalmology (AAO), whether registered or unregistered, are the property of AAO and are protected by US and international trademark laws. These trademarks include, but are not limited to, AAO; AAOE; AMERICAN ACADEMY OF OPHTHALMOLOGY; BASIC AND CLINICAL SCIENCE COURSE; BCSC; EYENET; EYEWIKI; FOCAL POINTS; FOCUS DESIGN (logo on cover); IRIS; IRIS REGISTRY; ISRS; OKAP; ONE NETWORK; OPHTHALMOLOGY; OPHTHALMOLOGY GLAUCOMA; OPHTHALMOLOGY RETINA; OPHTHALMOLOGY SCIENCE; OPHTHALMOLOGY WORLD NEWS; PREFERRED PRACTICE PATTERN; PROTECTING SIGHT. EMPOWERING LIVES.; THE OPHTHALMIC NEWS AND EDUCATION NETWORK.

Cover image: Confocal scanning laser ophthalmoscopy multicolor fundus image (30° field of view) of a healthy eye. (Courtesy of Lucia Sobrin, MD.)



Copyright © 2022 American Academy of Ophthalmology. All rights reserved. No part of this publication may be reproduced without written permission.

Printed in China.

Basic and Clinical Science Course



Christopher J. Rapuano, MD, Philadelphia, Pennsylvania
Senior Secretary for Clinical Education



J. Timothy Stout, MD, PhD, MBA, Houston, Texas
Secretary for Lifelong Learning and Assessment



Colin A. McCannel, MD, Los Angeles, California
BCSC Course Chair

Section 12

Faculty for the Major Revision



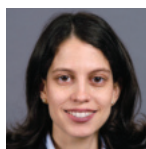
Stephen J. Kim, MD
Chair
Nashville, Tennessee



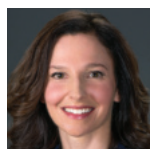
Franco M. Recchia, MD
Nashville, Tennessee



Amani Fawzi, MD
Chicago, Illinois



Lucia Sobrin, MD, MPH
Boston, Massachusetts



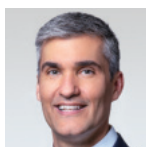
Jaclyn L. Kovach, MD
Naples, Florida



Jennifer K. Sun, MD, MPH
Boston, Massachusetts



Shriji Patel, MD, MBA
Nashville, Tennessee



Charles C. Wykoff, MD, PhD
Houston, Texas

The Academy acknowledges the *American Society of Retina Specialists (ASRS)*, the *Macula Society*, and the *Retina Society* for recommending faculty members to the BCSC Section 12 committee.

The Academy also acknowledges the following committees for review of this edition:

Committee on Aging: Christopher R. Henry, MD, Houston, Texas

Vision Rehabilitation Committee: Linda A. Lam, MD, MBA, Los Angeles, California

BCSC Resident/Fellow Reviewers: Sharon L. Jick, MD, *Chair*, St Louis, Missouri; Sunil Belur, MD; Gordon S. Crabtree, MD; Maria Paula Fernandez, MD; Michael J. Heiferman, MD; Hong-Uyen Hua, MD; Hong-Gam T. Le, MD; Danny Mammo, MD; Archana Nair, MD; Daniel J. Oh, MD; Ivy Zhu, MD

Practicing Ophthalmologists Advisory Committee for Education: Gaurav K. Shah, MD, *Primary Reviewer*, Town and Country, Missouri; Cynthia S. Chiu, MD, Oakland, California; George S. Ellis Jr, MD, New Orleans, Louisiana; Bradley D. Fouraker, MD, Tampa, Florida; Philip R. Rizzuto, MD, Providence, Rhode Island; Rosa A. Tang, MD, MPH, MBA, Houston, Texas; Troy M. Tanji, MD, Waipahu, Hawaii; Michelle S. Ying, MD, Ladson, South Carolina

In addition, the Academy acknowledges the following committee for assistance in developing Study Questions and Answers for this BCSC Section:

Resident Self-Assessment Committee: Evan L. Waxman, MD, PhD, *Chair*, Pittsburgh, Pennsylvania; Robert A. Beaulieu, MD, Southfield, Michigan; Benjamin W. Botsford, MD, New York, New York; Olga M. Ceron, MD, Grafton, Massachusetts; Kevin Halenda, MD, Cleveland, Ohio; Amanda D. Henderson, MD, Baltimore, Maryland; Andrew M. Hendrick, MD, Atlanta, Georgia; Joshua Hendrix, MD, Dalton, Georgia; Matthew B. Kaufman, MD, Portland, Oregon; Zachary A. Koretz, MD, MPH, Pittsburgh, Pennsylvania; Kevin E. Lai, MD, Indianapolis, Indiana; Kenneth C. Lao, MD, Temple, Texas; Yasha S. Modi, MD, New York, New York; Mark E. Robinson, MD, MPH, Columbia, South Carolina; Jamie B. Rosenberg, MD, New York, New York; Tahira M. Scholle, MD, Houston, Texas; Ann Shue, MD, Sunnyvale, California; Jeong-Hyeon Sohn, MD, Shavano Park, Texas; Misha F. Syed, MD, League City, Texas; Parisa Taravati, MD, Seattle, Washington; Sarah Van Tassel, MD, New York, New York; Matthew S. Wieder, MD, Scarsdale, New York; Jules A. Winokur, MD, Great Neck, New York



European Board of Ophthalmology: Lotte Welinder, MD, *Liaison*, Aalborg, Denmark; Katja Christina Schielke, MBBS, Aalborg, Denmark

Financial Disclosures

Academy staff members who contributed to the development of this product state that within the 24 months prior to their contributions to this CME activity and for the duration of development, they have had no financial interest in or other relationship with any entity that produces, markets, resells, or distributes health care goods or services consumed by or used in patients, or with any competing commercial product or service.

The authors and reviewers state that within the 24 months prior to their contributions to this CME activity and for the duration of development, they have had the following financial relationships:*

Dr Fouraker: Addition Technology (C, L), AJL Ophthalmic, SA (C, L), Alcon (C, L), OASIS Medical (C, L)

Dr Fawzi: Bayer (L), Boehringer Ingelheim (C), Novartis (C), Regeneron Pharmaceuticals (C), Roche (C)

Dr Henry: Aldeyra Therapeutics (C), Alimera Sciences (C), Castle Biosciences (C), Clear-side Biomedical (C), Lexitas (C)

Dr Kovach: Novartis (L), Regeneron Pharmaceuticals (L)

Dr Lai: Twenty/Twenty Therapeutics (C)

Dr Lam: Ocutrux (C)

Dr Modi: Alimera Sciences (C), Allergan (C), Carl Zeiss (C), Genentech (C), Novartis (C), Théa Laboratories (C)

Dr Patel: Alcon (S)

Dr Recchia: Adverum Biotechnologies (S), Astellas Pharma (S), Chengdu Kanghong (S), Genentech (S), Kodiak Sciences (S), Mylan (S), Novartis (S), Regeneron Pharmaceuticals (S), REGENXBIO (S)

Dr Robinson: Horizon Therapeutics (O)

Dr Shah: Allergan (C, L, S), Bausch + Lomb (L), DORC Dutch Ophthalmic Research Center (International) BV (S), Regeneron Pharmaceuticals (C, L, S)

Dr Sobrin: Novartis (C), Santen (C)

Dr Sun: Adaptive Sensory Technology (S), Boehringer Ingelheim (S), Boston Micro-machines (S), Genentech (S), *JAMA Ophthalmology* (C), KalVista Pharmaceuticals (S), Merck (C), Novartis (C, S), Novo Nordisk (C, S), Optovue (S), Regeneron Pharmaceuticals (S), Roche (C, S)

Dr Tang: EMD Serono (L), Horizon Therapeutics (C, S), Immunovant (S), Novartis (S), Quark Pharmaceuticals (C, S), Regenera Pharma (S), Sanofi (L), ZEISS (L)

Dr Van Tassel: AbbVie (C), Aerie Pharmaceuticals (C), Allergan (C), Bausch + Lomb (C), Carl Zeiss Meditec (C), Equinox (C), New World Medical (C, L)

Dr Wykoff: AbbVie (C), Acucela (C), Adverum Biotechnologies (C, S), Aerie Pharmaceuticals (C, S), Aerpio Pharmaceuticals (C, S), Alcon (C, S), Aldeyra (S), Alimera Sciences (C, S), Alkahest (S), Allegro Ophthalmics (C, S), Allergan (C, L, S), Apellis (C, S), AsclepiX Therapeutics (S), Astellas Pharma (S), Bausch + Lomb (C), Bayer (C, S), Boehringer Ingelheim (S),

* C = consultant fee, paid advisory boards, or fees for attending a meeting; E = employed by or received a W2 from a commercial company; L = lecture fees or honoraria, travel fees or reimbursements when speaking at the invitation of a commercial company; O = equity ownership/stock options in publicly or privately traded firms, excluding mutual funds; P = patents and/or royalties for intellectual property; S = grant support or other financial support to the investigator from all sources, including research support from government agencies, foundations, device manufacturers, and/or pharmaceutical companies

Chengdu Kanghong (C, S), Clearside Biomedical (C, S), EyePoint Pharmaceuticals (C), Gemini Therapeutics (S), Genentech (C, S), Graybug Vision (S), Gyroscope (C, S), Ionis Pharmaceuticals (S), Iveric Bio (C, S), Kato Pharmaceuticals (C), Kodiak Sciences (C, S), Merck (C), Nanoscope (S), Neurotech (S), NGM Biopharmaceuticals (C, S), Notal Vision (C), Novartis (C, S), OccuRx (C), Ocular Therapeutix (C), OHR Pharmaceuticals (S), ONL Therapeutics (C), Ophthotech Corporation (S), Opthea (C, S), Outlook Therapeutics (S), Oxurion (C, S), Palatin (C), PolyPhotonix (C), RecensMedical (C, O, S), Regeneron Pharmaceuticals (C, L, S), RegenxBio (C, S), Roche (C, S), SamChunDang Pharm (S), Samsung (S), Santen (C, S), SciFluor Life Sciences (S), Senju Pharmaceutical Co, Ltd (S), Takeda (C), Théa Open Innovation (C), ThromboGenics (S), Tyrogenex (S), Valo Health (C), Visgenx (O), Vitranu (C), Xbrane Biopharma (S)

The other authors and reviewers state that within the 24 months prior to their contributions to this CME activity and for the duration of development, they have had no financial interest in or other relationship with any entity that produces, markets, resells, or distributes health care goods or services consumed by or used in patients, or with any competing commercial product or service.

Recent Past Faculty

Audina M. Berrocal, MD
Graham E. Holder, PhD
Brian C. Leonard, MD
Colin A. McCannel, MD
Richard B. Rosen, MD
Richard F. Spaide, MD

In addition, the Academy gratefully acknowledges the contributions of numerous past faculty and advisory committee members who have played an important role in the development of previous editions of the Basic and Clinical Science Course.

American Academy of Ophthalmology Staff

Dale E. Fajardo, EdD, MBA, *Vice President, Education*
Beth Wilson, *Director, Continuing Professional Development*
Denise Evenson, *Director, Brand & Creative*
Susan Malloy, *Acquisitions and Development Manager*
Stephanie Tanaka, *Publications Manager*
Rayna Ungersma, *Manager, Curriculum Development*
Jasmine Chen, *Manager, E-Learning*
Sarah Page, *Online Education & Licensing Manager*
Lana Ip, *Senior Designer*
Beth Collins, *Medical Editor*
Amanda Fernandez, *Publications Editor*
Eric Gerdes, *Interactive Designer*
Lynda Hanwella, *Publications Specialist*
Debra Marchi, *Administrative Assistant*

American Academy of Ophthalmology
655 Beach Street
Box 7424
San Francisco, CA 94120-7424

Contents

Introduction to the BCSC	xvii
Introduction to Section 12	xix

Objectives	1
-----------------------------	----------

PART I Fundamentals and Diagnostic Approaches 3

1 Basic Anatomy.	5
Highlights	5
Vitreous	5
Neurosensory Retina	7
Retinal Topography	7
Retinal Layers and Neurosensory Elements	9
Retinal Vasculature and Oxygen Supply	13
Retinal Pigment Epithelium	15
Bruch Membrane	17
Choroid	17
Sclera	19

2 Diagnostic Approach to Retinal and Choroidal Disease	21
Highlights	21
Introduction	21
Ophthalmoscopy	22
Examination With the Binocular Indirect Ophthalmoscope	22
Indirect Ophthalmoscopy With the Slit Lamp	22
Imaging Technologies	23
Fundus Camera Imaging	23
Scanning Laser Ophthalmoscopy	24
Optical Coherence Tomography.	26
Optical Coherence Tomography Angiography.	28
Fundus Autofluorescence.	29
Adaptive Optics Imaging.	32
Retinal Angiographic Techniques	32
Ultrasonography	39

3 Retinal Physiology and Psychophysics	43
Highlights	43
Electrophysiologic Testing	43

Electroretinography	44
Full-Field (Ganzfeld) Electroretinography	45
Multifocal Electroretinography	49
Pattern Electroretinography	51
Clinical Considerations	52
Electro-oculography	53
Visual Evoked Potentials	55
Microperimetry	56
Psychophysical Testing	56
Color Vision	57
Contrast Sensitivity	59
Dark Adaptometry	61

PART II Diseases of the Retina and Vitreous 63

4 Age-Related Macular Degeneration and Other Causes of Choroidal Neovascularization 65

Highlights	65
Age-Related Macular Degeneration	66
Genetics and AMD	68
Nonneovascular AMD	69
Neovascular AMD	77
Other Causes of Choroidal Neovascularization	93
Ocular Histoplasmosis Syndrome	93
Angioid Streaks	95
Pathologic Myopia	96
Idiopathic CNV and Miscellaneous Causes of CNV	97

5 Diabetic Retinopathy 99

Highlights	99
Introduction	99
Terminology and Classification	100
Diabetes Terminology	100
Diabetic Retinopathy Terminology	100
Epidemiology of Diabetic Retinopathy	101
Pathogenesis of Diabetic Retinopathy	102
Recommended Diabetes Mellitus–Related	
Ophthalmic Examinations	103
Systemic Medical Management of Diabetic Retinopathy	104
Nonproliferative Diabetic Retinopathy	108
Treatment of Nonproliferative Diabetic Retinopathy	111
Proliferative Diabetic Retinopathy	111
Management of Proliferative Diabetic Retinopathy	
and Its Complications	115
Additional Vision-Threatening Complications	
of Diabetic Retinopathy	119

Diabetic Macular Edema	121
Classification of Diabetic Macular Edema	122
Management of Diabetic Macular Edema.	123
Cataract Surgery in Patients With Diabetes Mellitus	128

6 Retinal Vascular Diseases Associated With Cardiovascular Disease. 131

Highlights	131
Systemic Arterial Hypertension and Associated Ocular Diseases	131
Hypertensive Retinopathy	132
Hypertensive Choroidopathy	133
Hypertensive Optic Neuropathy.	134
Retinal Venous Occlusion	134
Overview of Retinal Venous Occlusion.	134
Branch Retinal Vein Occlusion	145
Central Retinal Vein Occlusion	148
Ocular Ischemic Syndrome and Retinopathy of Carotid Occlusive Disease.	152
Symptoms and Signs of OIS.	152
Etiology and Course of OIS.	153
Treatment of OIS	154
Arterial Occlusive Disease	154
Cotton-Wool Spots	154
Branch Retinal Artery Occlusion	155
Central Retinal Artery Occlusion	158
Cilioretinal Artery Occlusion	162
Ophthalmic Artery Occlusion.	162
Paracentral Acute Middle Maculopathy	164
Arterial Macroaneurysms	165

7 Other Retinal Vascular Diseases. 167

Highlights	167
Sickle Cell Disease and Retinopathy	167
Sickle Cell Disease.	167
Stages of Sickle Cell Retinopathy	168
Nonproliferative Sickle Cell Retinopathy	168
Proliferative Sickle Cell Retinopathy	168
Other Ocular Abnormalities in Sickle Cell Hemoglobinopathies	171
Management of Sickle Cell Retinopathy and Its Complications	174
Vasculitis	175
Cystoid Macular Edema	176
Etiologies of CME.	176
Treatment of CME	178
Coats Disease	178
Coats-like Reaction in Other Retinal Conditions	179

Macular Telangiectasia	180
Macular Telangiectasia Type 1	180
Macular Telangiectasia Type 2	180
Macular Telangiectasia Type 3	181
Phakomatoses	181
Von Hippel–Lindau Syndrome	181
Wyburn-Mason Syndrome	186
Retinal Cavernous Hemangioma	186
Radiation Retinopathy.	187
Valsalva Retinopathy	189
Purtscher Retinopathy and Purtscher-like Retinopathy.	190
Terson Syndrome	192

8 Retinopathy of Prematurity 193

Highlights	193
Introduction	193
Epidemiology.	193
Classification, Terminology, and Clinical Features.	194
Pathophysiology of ROP	199
Natural Course	201
Screening Recommendations.	201
Screening Criteria.	201
Screening Intervals	202
Fundus Photographic Screening of ROP	203
Prevention and Risk Factors	203
Treatment of Acute ROP.	204
Laser and Cryoablation Surgery	207
Anti-VEGF Drugs.	207
Vitrectomy and Scleral Buckling Surgery	209
Associated Conditions and Late Sequelae of ROP	209
Medicolegal Aspects of ROP	211

9 Choroidal Disease. 215

Highlights	215
Scope of Chapter	215
Central Serous Chorioretinopathy.	215
Demographics and Features	215
Systemic Associations	217
Imaging	217
Differential Diagnosis	218
Treatment	221
Choroidal Perfusion Abnormalities	222
Arteritic Disease	222
Nonarteritic Disease.	222
Choriocapillaris Blood Flow Abnormalities	225
Increased Venous Pressure	226
Age-Related Choroidal Atrophy.	227

Choroidal Folds	230
Choroidal Hemangiomas	231
Uveal Effusion Syndrome	231
Bilateral Diffuse Uveal Melanocytic Proliferation	233
10 Myopia and Pathologic Myopia	235
Highlights	235
Definition, Prevalence, and Epidemiology	235
Prevention of Pathologic Myopia	235
The Retina and Choroid	236
The Retina	236
Bruch Membrane	239
Choroidal Neovascularization	239
The Choroid	240
The Sclera	243
The Optic Nerve	246
11 Focal and Diffuse Retinal and Choroidal Inflammation	249
Highlights	249
Overview	249
Noninfectious Retinal and Choroidal Inflammation	250
White Dot Syndromes	250
Chorioretinal Autoimmune Conditions	261
Sympathetic Ophthalmia	263
Uveitis Masquerade: Intraocular Lymphoma	264
Infectious Retinal and Choroidal Inflammation	267
Cytomegalovirus Retinitis	267
Non-CMV Necrotizing Herpetic Retinitis	268
Endogenous Bacterial Endophthalmitis	270
Fungal Endophthalmitis	271
Ocular Tuberculosis	272
Syphilitic Retinochoroiditis	274
Ocular Bartonellosis	274
Toxoplasmic Chorioretinitis	274
Toxocariasis	277
Ocular Lyme Borreliosis	278
Diffuse Unilateral Subacute Neuroretinitis	279
West Nile Virus Chorioretinitis	279
Zika Virus Chorioretinitis	279
Ebola Virus Panuveitis	281
Chikungunya Virus Retinitis	281
12 Hereditary Retinal and Choroidal Disease	283
Highlights	283
Color Vision Abnormalities	283
Congenital Color Deficiency	283

Night Vision Abnormalities	285
Congenital Night-Blinding Disorders With Normal Fundi	285
Congenital Night-Blinding Disorders With Fundus Abnormality	286
Retinal and Choroidal Dystrophies	288
Classification and Terminology	288
General Diagnostic Considerations	289
General Genetic Considerations.	290
General Management Considerations	290
Diffuse Dystrophies: Photoreceptor Dystrophies.	291
Diffuse Dystrophies: Choroidal Dystrophies	297
Macular Dystrophies	300
Inner Retinal Dystrophies	310

13 Retinal Degenerations Associated

With Systemic Disease	315
Highlights	315
Introduction	315
Retinal Degeneration With Systemic Involvement	315
Infantile-Onset to Early Childhood-Onset Syndromes	318
Bardet-Biedl Syndrome	318
Hearing Loss and Pigmentary Retinopathy: Usher Syndrome	319
Neuromuscular Disorders	319
Diseases Affecting Other Organ Systems	320
Paraneoplastic and Autoimmune Retinopathies	322
Metabolic Diseases	324
Albinism.	324
Metabolic Diseases With Central Nervous System Abnormalities	325
Amino Acid Disorders	329
Mitochondrial Disorders	330

14 Systemic Drug-Induced Retinal Toxicity. 333

Highlights	333
Overview	333
Drugs Causing Abnormalities of the Retinal Pigment Epithelium/Photoreceptor Complex	333
Chloroquine Derivatives	333
Phenothiazines	337
Miscellaneous Medications	337
Drugs Causing Occlusive Retinopathy or Microvasculopathy	342
Drugs Causing Ganglion Cell Damage and Optic Neuropathy.	343
Drugs Causing Macular Edema.	343
Drugs Causing Crystalline Retinopathy	344
Drugs Causing Color Vision or ERG Abnormalities	347
Drugs Causing Other Ocular Toxicities	347

15 Diseases of the Vitreous and Vitreoretinal

Interface	349
Highlights	349
Posterior Vitreous Detachment	349
Epiretinal Membranes	351
Vitreomacular Traction Diseases	354
Idiopathic Macular Holes	355
Developmental Abnormalities	358
Tunica Vasculosa Lentis	358
Prepapillary Vascular Loops	358
Persistent Fetal Vasculature	360
Hereditary Hyaloideoretinopathies With Optically Empty Vitreous:	
Wagner and Stickler Syndromes	360
Familial Exudative Vitreoretinopathy	362
Vitreous Opacities	364
Opacities Associated With Vitreous Degeneration and Detachment	364
Asteroid Hyalosis	364
Vitreous Hemorrhage	365
Pigment Granules	365
Cholesterolosis	366
Amyloidosis	366

16 Retinal Detachment and Predisposing Lesions 369

Highlights	369
Examination and Management of Posterior Vitreous Detachment	369
Lesions That Predispose Eyes to Retinal Detachment	371
Lattice Degeneration	371
Vitreoretinal Tufts	371
Meridional Folds, Enclosed Ora Bays, and Peripheral Retinal Excavations	374
Lesions That Do Not Predispose Eyes to Retinal Detachment	374
Paving-Stone Degeneration	374
Retinal Pigment Epithelial Hyperplasia	375
Retinal Pigment Epithelial Hypertrophy	375
Peripheral Cystoid Degeneration	375
Retinal Breaks	376
Traumatic Breaks	376
Trauma in Young Eyes	377
Prophylactic Treatment of Retinal Breaks	379
Symptomatic Retinal Breaks	380
Asymptomatic Retinal Breaks	380
Lattice Degeneration	380
Aphakia and Pseudophakia	381
Fellow Eye in Patients With Retinal Detachment	381
Subclinical Retinal Detachment	381

Retinal Detachment	381
Rhegmatogenous Retinal Detachment	382
Traction Retinal Detachment	387
Exudative Retinal Detachment	388
Differential Diagnosis of Retinal Detachment.	389
Retinoschisis	389
Differentiation of Retinoschisis From Rhegmatogenous Retinal Detachment.	391
Macular Lesions Associated With Retinal Detachment.	392
Optic Pit Maculopathy.	392
Macular Holes in High Myopia	394
17 Posterior Segment Manifestations of Trauma	395
Highlights	395
Classification of Ocular Globe Trauma.	395
Evaluation of the Patient After Ocular Trauma	396
Blunt Trauma Without a Break in the Eye Wall	397
Comotio Retinae	398
Choroidal Rupture	398
Posttraumatic Macular Hole	399
Vitreous Hemorrhage	400
Traumatic Chorioretinal Disruption	401
Open-Globe Injuries	401
Scleral Rupture	401
Lacerating and Penetrating Injuries	402
Perforating Injuries	402
Surgical Management	402
Intraocular Foreign Bodies	404
Posttraumatic Endophthalmitis.	407
Prognostication of Globe Injuries	409
Sympathetic Ophthalmia	410
Avulsion of the Optic Nerve Head	410
Abusive Head Trauma.	411
Photoc Damage.	412
Solar Retinopathy	412
Phototoxicity From Ophthalmic Instrumentation	413
Occupational Light Toxicity	414
Laser-Pointer Injury	414
PART III Selected Therapeutic Topics	417
18 Laser Therapy and Cryotherapy for Posterior Segment Diseases	419
Highlights	419
Basic Principles of Photocoagulation	419
Choice of Laser Wavelength	420

Practical Aspects of Laser Photocoagulation	421
Complications of Photocoagulation	424
Transpupillary Thermotherapy	425
Photodynamic Therapy	426
Complications of Photodynamic Therapy.	426
Cryotherapy	426
Cryopexy Technique.	427
19 Vitreoretinal Surgery and Intravitreal Injections	429
Highlights	429
Pars Plana Vitrectomy	429
Vitrectomy for Selected Macular Diseases	431
Macular Epiretinal Membranes	431
Vitreomacular Traction Diseases	432
Submacular Hemorrhage.	434
Vitrectomy for Vitreous Opacities.	435
Vitrectomy for Complications of Diabetic Retinopathy.	435
Vitreous Hemorrhage	436
Diabetic Traction Retinal Detachment	436
Diabetic Macular Edema	437
Vitrectomy for Posterior Segment Complications of Anterior	
Segment Surgery	437
Postoperative Endophthalmitis	437
Retained Lens Fragments After Phacoemulsification	441
Posteriorly Dislocated Intraocular Lenses.	442
Cystoid Macular Edema	443
Suprachoroidal Hemorrhage	443
Needle Injury of the Globe	445
Rhegmatogenous Retinal Detachment Surgery	445
Techniques for Surgical Repair of Retinal Detachments.	447
Outcomes Following Retinal Reattachment Surgery	450
Complications of Pars Plana Vitrectomy	451
Intravitreal Injections	452
20 Gene Therapy	455
Highlights	455
Introduction	455
Gene Augmentation Therapy.	456
Optogenetics.	458
Genome Editing	458
Current Limitations.	458
Additional Materials and Resources	459
Requesting Continuing Medical Education Credit.	461
Study Questions	463
Answers.	473
Index	481

Introduction to the BCSC

The Basic and Clinical Science Course (BCSC) is designed to meet the needs of residents and practitioners for a comprehensive yet concise curriculum of the field of ophthalmology. The BCSC has developed from its original brief outline format, which relied heavily on outside readings, to a more convenient and educationally useful self-contained text. The Academy updates and revises the course annually, with the goals of integrating the basic science and clinical practice of ophthalmology and of keeping ophthalmologists current with new developments in the various subspecialties.

The BCSC incorporates the effort and expertise of more than 100 ophthalmologists, organized into 13 Section faculties, working with Academy editorial staff. In addition, the course continues to benefit from many lasting contributions made by the faculties of previous editions. Members of the Academy Practicing Ophthalmologists Advisory Committee for Education, Committee on Aging, and Vision Rehabilitation Committee review every volume before major revisions, as does a group of select residents and fellows. Members of the European Board of Ophthalmology, organized into Section faculties, also review volumes before major revisions, focusing primarily on differences between American and European ophthalmology practice.

Organization of the Course

The Basic and Clinical Science Course comprises 13 volumes, incorporating fundamental ophthalmic knowledge, subspecialty areas, and special topics:

- 1 Update on General Medicine
- 2 Fundamentals and Principles of Ophthalmology
- 3 Clinical Optics and Vision Rehabilitation
- 4 Ophthalmic Pathology and Intraocular Tumors
- 5 Neuro-Ophthalmology
- 6 Pediatric Ophthalmology and Strabismus
- 7 Oculofacial Plastic and Orbital Surgery
- 8 External Disease and Cornea
- 9 Uveitis and Ocular Inflammation
- 10 Glaucoma
- 11 Lens and Cataract
- 12 Retina and Vitreous
- 13 Refractive Surgery

References

Readers who wish to explore specific topics in greater detail may consult the references cited within each chapter and listed in the Additional Materials and Resources section at the back of the book. These references are intended to be selective rather than exhaustive,

chosen by the BCSC faculty as being important, current, and readily available to residents and practitioners.

Multimedia

This edition of Section 12, *Retina and Vitreous*, includes videos related to topics covered in the book and interactive content, or “activities,” developed by members of the BCSC faculty. The videos and activities are available to readers of the print and electronic versions of Section 12 (www.aao.org/bcscvideo_section12 and www.aao.org/bcscactivity_section12). Mobile-device users can scan the QR codes below (a QR-code reader may need to be installed on the device) to access the videos and activities.



Videos



Activities

Self-Assessment and CME Credit

Each volume of the BCSC is designed as an independent study activity for ophthalmology residents and practitioners. The learning objectives for this volume are given on page 1. The text, illustrations, and references provide the information necessary to achieve the objectives; the study questions allow readers to test their understanding of the material and their mastery of the objectives. Physicians who wish to claim CME credit for this educational activity may do so by following the instructions given at the end of the book.*

Conclusion

The Basic and Clinical Science Course has expanded greatly over the years, with the addition of much new text, numerous illustrations, and video content. Recent editions have sought to place greater emphasis on clinical applicability while maintaining a solid foundation in basic science. As with any educational program, it reflects the experience of its authors. As its faculties change and medicine progresses, new viewpoints emerge on controversial subjects and techniques. Not all alternate approaches can be included in this series; as with any educational endeavor, the learner should seek additional sources, including Academy Preferred Practice Pattern Guidelines.

The BCSC faculty and staff continually strive to improve the educational usefulness of the course; you, the reader, can contribute to this ongoing process. If you have any suggestions or questions about the series, please do not hesitate to contact the faculty or the editors.

The authors, editors, and reviewers hope that your study of the BCSC will be of lasting value and that each Section will serve as a practical resource for quality patient care.

*This activity meets the Self-Assessment CME requirements defined by the American Board of Ophthalmology (ABO). Please be advised that the ABO is not an accrediting body for purposes of any CME program. ABO does not sponsor this or any outside activity, and ABO does not endorse any particular CME activity. Complete information regarding the ABO Self-Assessment CME Maintenance of Certification requirements is available at <https://abop.org/maintain-certification/cme-self-assessment/>.

Introduction to Section 12

BCSC Section 12, *Retina and Vitreous*, is arranged into 3 parts. Part I, Fundamentals and Diagnostic Approaches, covers retinal anatomy, imaging, and functional evaluation in 3 chapters. Chapter 1 provides an overview of the anatomy of the posterior segment. Chapter 2 discusses examination techniques, including dilated slit-lamp biomicroscopy in combination with precorneal non-contact or contact lenses, as well as indirect ophthalmoscopy, which is often aided by scleral indentation to facilitate viewing the anterior retina.

Documenting clinical findings, either by description or by illustration, remains an essential element of a complete posterior segment examination. Ancillary testing, such as fundus photography, autofluorescence, fluorescein angiography, indocyanine green angiography, optical coherence tomography (OCT), scanning laser ophthalmoscopy, microperimetry, and electrophysiology, may provide additional diagnostic information or help detect changes over time. The various incarnations of OCT (time-domain, spectral-domain, and swept-source) deserve special mention. OCT has become perhaps the most commonly ordered ancillary ophthalmic test and is revolutionizing our understanding of many vitreoretinal conditions. Ultrasonography (also called *echography*) employing both A- and B-scan techniques, is useful for examining patients with opaque media, can aid in the diagnosis of retinal or choroidal lesions, and can be used to monitor a lesion's size. Chapter 3 reviews electrophysiologic tests and their significance in diagnosis and follow-up of retinal disease.

Part II, Diseases of the Retina and Vitreous, which includes Chapters 4 through 17, covers specific diseases of and trauma to the posterior segment. Appropriate diagnostic techniques are indicated throughout these discussions. By necessity, the illustrative findings associated with the described vitreoretinal diseases are presented as highlights—using schematics as well as the different imaging technologies—rather than as a comprehensive collection. Narratives describing the management of, and therapy for, the retinal diseases covered in Part II are complemented by descriptions of the important clinical trials that have helped establish appropriate evidence-based practices. As part of the major revision of the book, content in Part II has been reorganized. Congenital and stationary retinal disease, discussed in a separate chapter in the last edition, is now part of Chapter 12, “Hereditary Retinal and Choroidal Disease.” Also, the chapter titled “Diseases of the Vitreous and Vitreoretinal Interface,” which previously appeared after “Retinal Detachment and Predisposing Lesions,” now precedes it, providing a more logical flow.

In Part III, Selected Therapeutic Topics, Chapters 18 and 19 offer more detailed information on the 3 most important posterior segment treatment approaches: vitreoretinal surgery, laser surgery, and intravitreal injection of effective pharmacologic agents, especially anti-vascular endothelial growth factor. The emergence of each of these treatment approaches has been associated with dramatic improvements in the outcomes that retina specialists can accomplish in terms of preserving or restoring patients' vision. The field of gene therapy has advanced tremendously over the last decade and offers great promise in

the treatment of retinal disease. This edition features a new chapter dedicated to this topic (Chapter 20, “Gene Therapy”).

Increasingly, when treating patients with vitreoretinal diseases, clinicians base treatment decisions on evidence from clinical trials. Readers should familiarize themselves with those topics that are important for interpreting the scientific literature, such as study design, levels of evidence, results interpretation, and clinical practice applications of trial results (see BCSC Section 1, *Update on General Medicine*).

This book is not meant as a thorough review of the field; rather, it serves as what a group of experts considers the most important and up-to-date highlights of the subspecialty. Readers interested in more comprehensive information can obtain additional detail from the selected references that appear throughout the chapters as well as from the references provided in the Additional Materials and Resources section at the end of the book.

Objectives

Upon completion of BCSC Section 12, *Retina and Vitreous*, the reader should be able to

- describe the basic structure and function of the retina and its relationship to the pigment epithelium, choroid, and vitreous
 - select appropriate methods of examination, based on an understanding of the relative benefits and disadvantages of different examination techniques
 - identify vitreoretinal diseases by their clinical appearance and features of supportive diagnostic testing
 - select appropriate ancillary studies to help establish the diagnosis of different vitreoretinal diseases and follow them over time
 - explain how to incorporate data from major prospective clinical trials in the management of vitreoretinal disorders
 - describe the effect of ocular conditions on the retina, such as in severe myopia
 - list the retinal manifestations of inherited diseases, as well as the likely course of these diseases over time
 - identify retinal toxicities of medications
 - describe the appropriateness and timing of prophylactic interventions
 - explain the urgency of intervention for different vitreoretinal conditions
 - describe the effect of trauma on the eye and vision, to better counsel patients about visual outcomes
 - explain the appropriateness and timing of surgical intervention for vitreoretinal diseases to patients
-

PART I

**Fundamentals
and
Diagnostic
Approaches**

Basic Anatomy

Highlights

- Spectral-domain optical coherence tomography is a noninvasive, high-resolution imaging technique that allows discernment of individual retinal layers which directly correlate with the layers seen in cross-sectional histologic preparations.
- The retinal pigment epithelium has many functions that are critical to retinal function, including absorbing light, forming the outer blood–ocular barrier, maintaining a fluid-free subretinal space, phagocytosing rod and cone outer segments, and recycling visual pigment.
- The choroid has the highest rate of blood flow per unit weight of any tissue in the body, supplying most of the metabolic needs of the retina.

Vitreous

The vitreous is a transparent gel composed principally of water, collagen, and hyaluronic acid. It occupies 80% of the volume of the eye. The vitreous body is divided into 2 main topographic areas: the central, or core, vitreous and the peripheral, or cortical, vitreous. Ultrastructurally, the vitreous gel is made up of collagen fibrils separated by hydrated hyaluronic acid molecules, which act as fillers between adjacent collagen fibrils.

The anterior surface of the vitreous body, called the *anterior cortical gel*, is made up of a condensation of collagenous fibers that attach to the posterior lens capsule, forming the Wieger ligament (Fig 1-1). The retrolental indentation of the anterior vitreous is called the *patellar fossa*. The potential space between the peripheral posterior lens and the anterior cortical gel bordered by the Wieger ligament is called the *Berger space*. In the vitreous base, the collagen fibers are particularly dense; they are firmly attached to the anterior retina and posterior pars plana, creating a ringlike area that extends approximately 2 mm anterior and 3–4 mm posterior to the ora serrata. The vitreous is not only attached at its base; it is also firmly attached to the posterior lens capsule, retinal vessels, optic nerve, and fovea. The densely packed collagen fibrils in the cortical vitreous form the cortical gel. Posteriorly, fibers course in a direction roughly parallel to the inner surface of the retina, forming the preretinal tract. The vitreous attaches to the retinal surface, specifically the internal limiting membrane, via the adhesion molecules fibronectin and laminin. There is no basement membrane between the vitreous base and lens, an area called the *annular gap*, which is a ringlike zone important for diffusion between the aqueous and vitreous

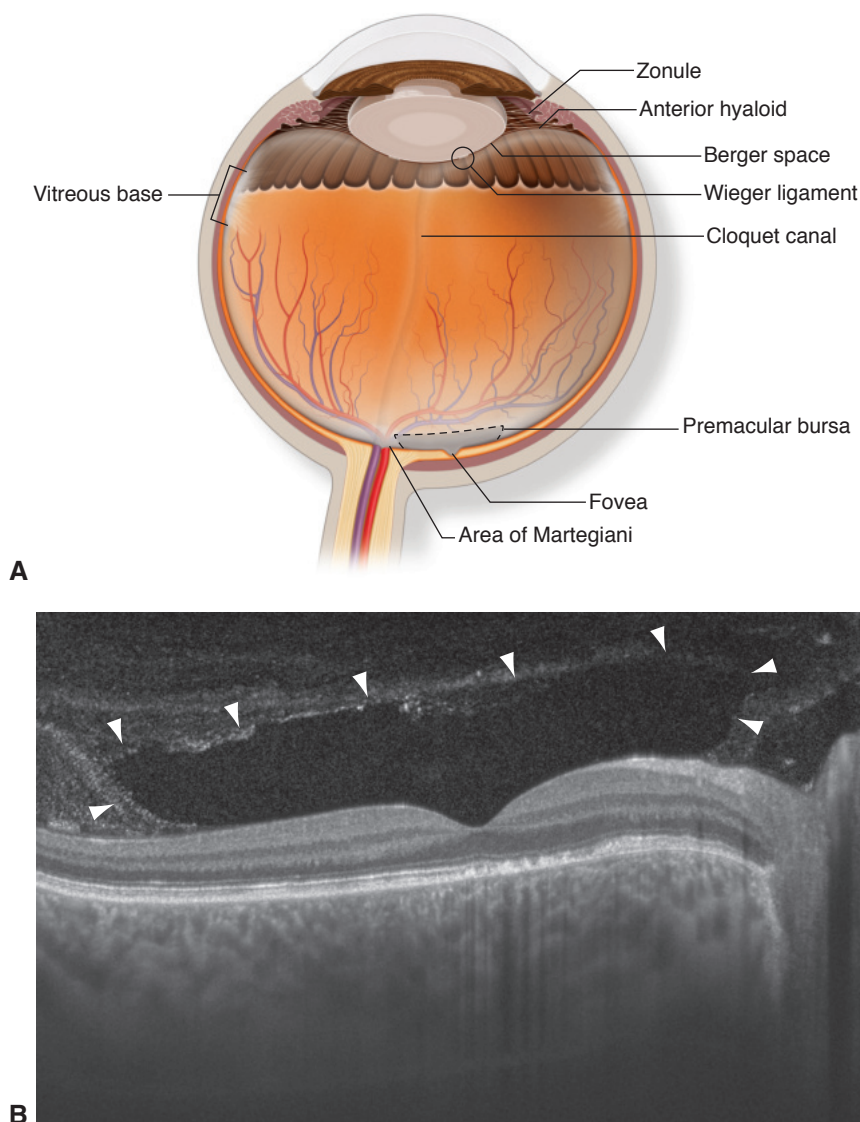


Figure 1-1 Cross section of vitreous anatomy. **A**, Diagram of the eye with emphasis on the anatomical features of the vitreous. The vitreous is most firmly attached to the retina at the vitreous base, and it also has adhesions at the optic nerve, along vessels, at the fovea, and to the posterior lens capsule. A prominent area of liquefaction of the premacular vitreous gel is called the *premacular bursa*, or *precortical vitreous pocket*. **B**, Swept-source optical coherence tomography image of the posterior vitreous and macular region demonstrates the signal void in the vitreous cavity in front of the macula that represents the premacular bursa (*arrowheads*). Note also the very thick macular choroid and photoreceptor disruption in the central macula, extending nasally. (Part A illustration by Mark M. Miller; part B courtesy of Srinivas Sadda, MD.)

compartments. The space known as the *premacular bursa*, or *precortical vitreous pocket* (see Fig 1-1), which is anterior to the posterior attachment of the vitreous to the macula, is believed to decrease the tractional forces generated during ocular motion. The vitreous inserts on the edges of the optic nerve head, creating a funnel-shaped void of vitreous. This void is the opening of the Cloquet canal and is referred to as the *area of Martegiani*. The anatomy of the vitreous is difficult to delineate *in vivo*; however, the vitreous appears to contain interconnected cisterns and canals, most notably the ciliobursal canal that connects the ciliary body and macula.

The vitreous also contains hyalocytes, which arise from bone marrow–derived stem cells. Oxygen is derived through diffusion from the choroidal and retinal circulation. Hyalocytes consume most of this, limiting the amount of oxygen that reaches the lens and anterior segment. However, the vitreous has high ascorbate levels, which protect against oxidative damage (eg, to the lens).

Worst JGF, Los LI. *Cisternal Anatomy of the Vitreous*. Kugler; 1995.

Neurosensory Retina

Retinal Topography

The central area of the retina, or macula (sometimes called the *area centralis*), measures approximately 5.5 mm in diameter and is centered between the optic nerve head and the temporal vascular arcades (Fig 1-2, Table 1-1). On histologic examination, this area features 2 or more layers of ganglion cells, accounting for half of all ganglion cells in the retina. Oxygenated carotenoids, in particular lutein and zeaxanthin, accumulate within the central macula and contribute to its yellow color.

The central 1.5 mm of the macula, which is called the *fovea* (or *fovea centralis*), is specialized for high spatial acuity and color vision. The fovea has a margin; a downward slope; and a floor known as the *foveola*, a 0.35-mm-diameter region where the cones are

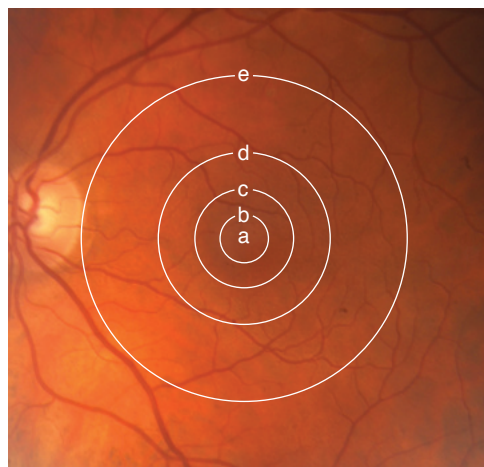


Figure 1-2 Anatomical macula, also known as the *area centralis* or *posterior pole*. The anatomical fovea and foveola are contained within the center of the anatomical macula. The borders of anatomical areas are indicated by letters: a = umbo; b = foveola; c = fovea; zone between c and d = parafoveal macula; zone between d and e = perifoveal macula; e = macula. (Courtesy of Hermann D. Schubert, MD.)

Table 1-1 Anatomical Terminology of the Macula (Area Centralis)

Term	Synonym	Histologic Definition	Clinical Observation and Size
Macula	Posterior pole Area centralis	Contains 2 or more ganglion cell layers	Area 5.5 mm in diameter centered between vascular arcades and optic nerve head; approx. 4.0 mm temporal and 0.8 mm inferior to center of optic nerve head
Perifovea		From the outer limit of the macula to the outermost limit of the parafovea	Ring 1.5 mm wide surrounding the parafovea
Parafovea		Margin, where the ganglion cell layer, inner nuclear layer, and outer plexiform (Henle fiber) layer are thickest (ie, the retina is thickest)	Ring 0.5 mm wide surrounding the fovea
Fovea	Fovea centralis	A depression in the inner retina; has a margin, slope, and floor, the photoreceptor layer of which consists entirely of cones	A concave central retinal depression seen on slit-lamp examination; 1.5 mm in diameter (approx. 1 disc diameter, or 5°)
Foveola		The floor of the fovea features cones only, arranged in the shape of a circle, where the inner nuclear layer and ganglion cell layer are laterally displaced	0.35 mm in diameter, usually smaller than the foveal avascular zone
Umbo	Fixation light reflex	Small (150–200 μ m) depression at center of floor of foveola; features elongated cones	Observed point corresponding to the normal light reflex but not solely responsible for this light reflex

slender, elongated, and densely packed. At the very center of the foveola is a small depression, 150–200 μ m in diameter, known as the *umbo*. Within the fovea is a region devoid of retinal vessels, the *foveal avascular zone (FAZ)*. The diameter of the FAZ ranges from 250 to 600 μ m or greater. The geometric center of the FAZ is often taken to be the center of the macula and thus the point of fixation; it is an important landmark in fluorescein angiography. Surrounding the fovea is the *parafovea*, a 0.5-mm-wide ring where the ganglion cell layer, inner nuclear layer, and outer plexiform layer (also known as *Henle fiber layer*) are thickest. Surrounding this zone is the *perifovea*, a ring approximately 1.5 mm wide. Thus, the umbo forms the center of the macula, and the periphery of the perifovea forms its margin.

The retina outside the macula, sometimes referred to as the *extra-areal periphery*, is commonly divided into a few concentric regions, starting with the *near periphery*, a 1.5-mm ring peripheral to the temporal major vascular arcades. The *equatorial retina* is the retina around the equator, and the region anterior to the equatorial retina is called the *peripheral retina*. In the far periphery, the border between the retina and the pars plana is called the *ora serrata* (Fig 1-3). The posterior border of the vitreous base is typically located between the ora serrata and the equator of the eye. This region is where most retinal tears occur.

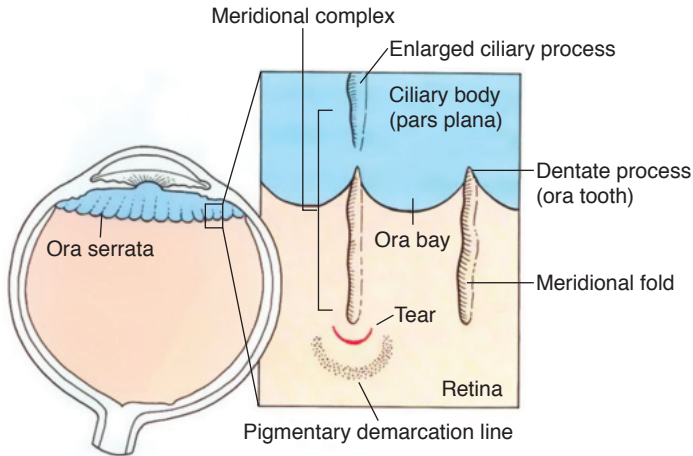


Figure 1-3 Schematic of the ora serrata, detail of which shows an ora bay, dentate process, and meridional folds (pleats of redundant retina). Tears may occur at the posterior end of such folds. Pigmentary demarcation lines may be a marker of chronicity. (Used with permission from Federman JL, Gouras P, Schubert H, et al. *Retina and Vitreous*. Mosby; 1998. Podos SM, Yanoff M, eds. *Textbook of Ophthalmology*; vol 9.)

Jetties of retinal tissue, called *dentate processes*, extend anteriorly into the pars plana. These processes are more prominent nasally. *Ora bays* are posterior extensions of the pars plana toward the retina. On occasion, dentate processes may wrap around a portion of an ora bay to form an enclosed ora bay. A *meridional fold* is a radially oriented, prominent thickening of retinal tissue that extends into the pars plana. When aligned with a ciliary process, such folds are known as a *meridional complex*.

Polyak SL. *The Retina*. University of Chicago Press; 1941.

Retinal Layers and Neurosensory Elements

The layers of the retina can be seen in cross-sectional histologic preparations, and most layers can be identified with spectral-domain optical coherence tomography (SD-OCT) (see Chapter 2, Activity 2-1), a noninvasive high-resolution imaging technique. The layers of the retina as seen in histologic sections and in corresponding OCT cross-sectional images are shown in Figure 1-4.

To reach the photoreceptors—retinal rods and cones—light must travel through the full thickness of the retina. The density and distribution of photoreceptors vary with their topographic location. In the fovea, the cones, which are predominantly red- and green-sensitive, are densely packed; their density exceeds 140,000 cones/mm². The foveola has no rods; the fovea contains only photoreceptors and processes of Müller cells. The number of cone photoreceptors decreases rapidly in areas farther from the center, even though 90% of cones overall reside outside the foveal region. The rods have their greatest density in a zone lying approximately 4 mm from the foveal center, or 12° from fixation, where they reach a peak density of about 160,000 rods/mm². The density of rods also decreases toward the periphery. A small area of high rod concentration (176,000 rods/mm²) has

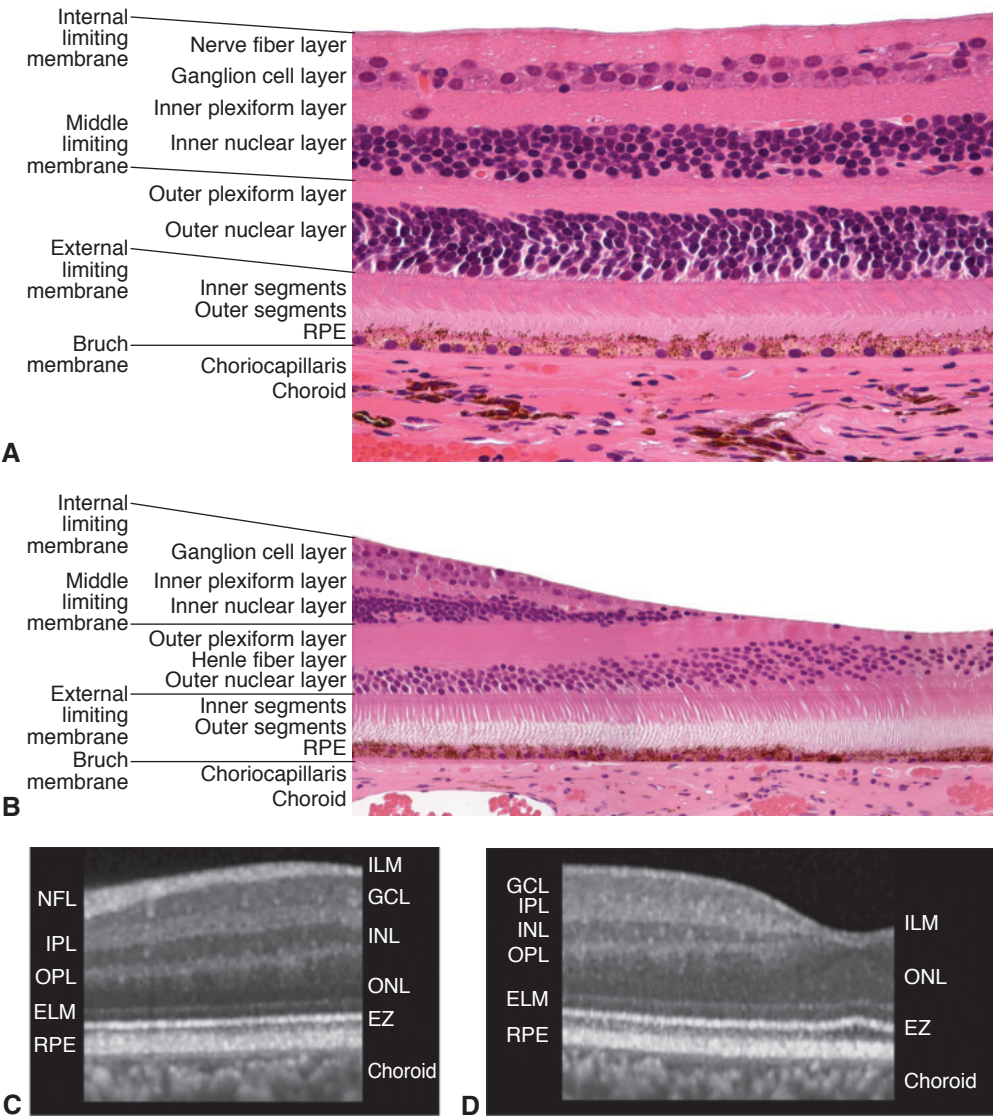


Figure 1-4 Cross-sectional images of peripheral macular (**A, C**) and foveal (**B, D**) retina. **A, B**, Photomicrographs (hematoxylin-eosin stain) of retina and choroid (*labeled*). In the fovea (**B**), the inner cellular layers are laterally displaced, and there is an increased density of pigment in the retinal pigment epithelium (RPE). Note that on the right edge of the image, the inner cellular layers are laterally displaced. This allows incident light to fall directly onto the photoreceptors, avoiding the inner retinal layers, thereby reducing the potential for scattering of light. **C, D**, Corresponding spectral-domain optical coherence tomography cross-sectional images of macular and foveal retina. Layers labeled from inner to outer retina, following the path of incident light: internal limiting membrane (ILM), nerve fiber layer (NFL), ganglion cell layer (GCL), inner plexiform layer (IPL), inner nuclear layer (INL), outer plexiform layer (OPL), outer nuclear layer (ONL), external limiting membrane (ELM), ellipsoid zone (EZ), RPE, and choroid. (*Parts A and B courtesy of Ralph Eagle, MD; parts C and D courtesy of Hannah J. Yu, BS, and Charles C. Wykoff, MD, PhD.*)

been found in the superior macula. The arrangement of rods and cones can be visualized with noninvasive adaptive optics imaging (Fig 1-5).

Each photoreceptor cell consists of an outer segment and an inner segment. The light-sensitive molecules in rods and cones are derived from vitamin A and are contained in the disc membranes of the photoreceptor outer segments (Fig 1-6). The discs are attached to a cilium, which is rooted through neurotubules in the ellipsoid and myoid of the inner segment. The ellipsoid, which is adjacent to the cilium, contains mitochondria and is

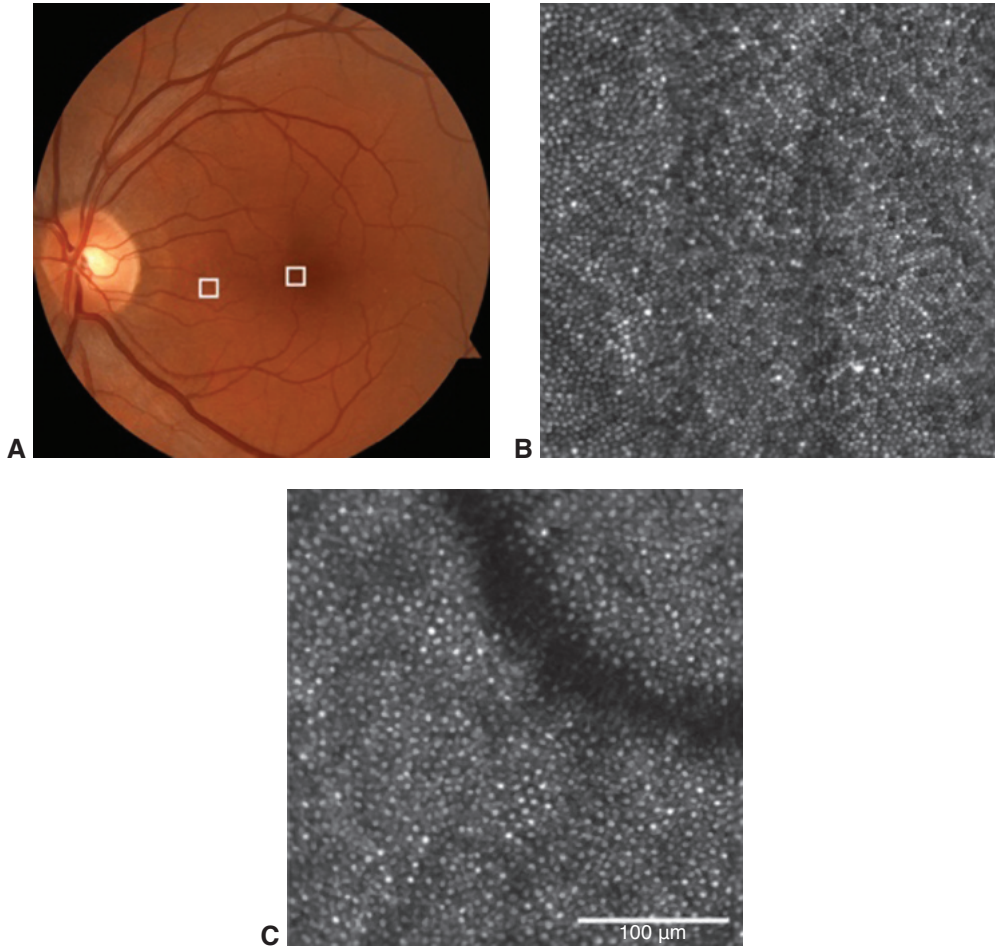


Figure 1-5 Comparison of a conventional fundus photograph and confocal adaptive optics scanning laser ophthalmoscope (AOSLO) images of a healthy left-eye macula. **A**, In the fundus photograph, the white box that is closer to the fovea is 0.5° from fixation and represents a $300 \times 300\text{-}\mu\text{m}$ area of macula. **B**, The corresponding AOSLO image of the retina within that white box shows cones that are smaller and very tightly packed; no rods are visible. **C**, AOSLO image corresponding to the white box in **A** that is closer to the optic nerve and 7° from fixation and also represents a $300 \times 300\text{-}\mu\text{m}$ area of macula. The image shows cones that are larger and less densely packed; intervening rods are starting to become visible. (Courtesy of Mina M. Chung, MD, and Hongxin Song, MD, PhD.)

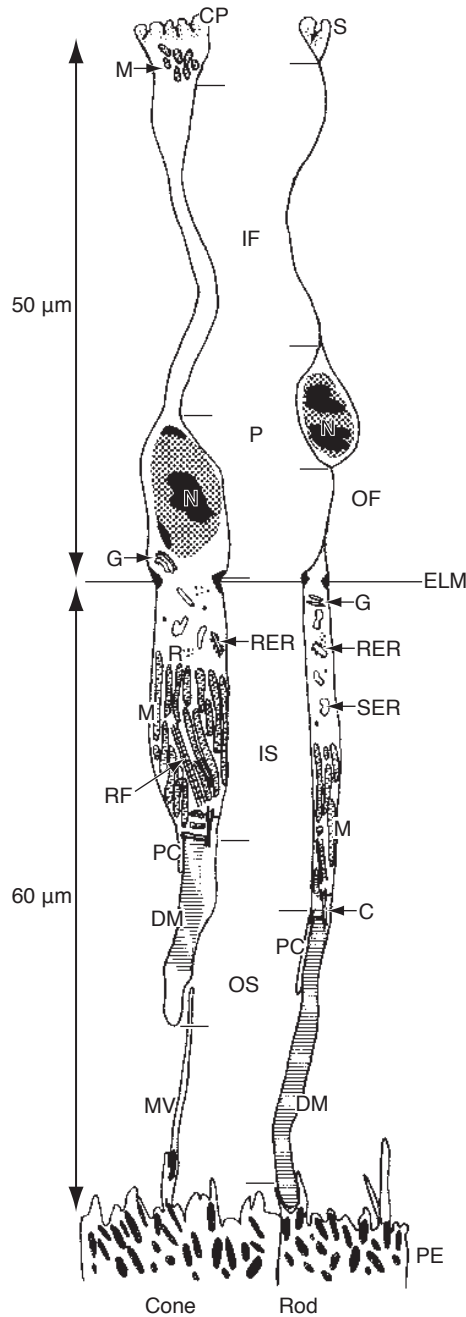


Figure 1-6 Schematic of a cone cell (*left*) and a rod cell (*right*) in the peripheral retina. In the diagram, light enters from the top; the pigmented epithelium is on the distal side. C=cilium; CP=cone cell pedicle; DM=membranous discs; ELM=external limiting membrane; G=Golgi apparatus; IF=inner fiber; IS=inner segment; M=mitochondria; MV=microvilli of pigment epithelial cells; N=nucleus; OF=outer fiber; OS=outer segment; P=perikaryon; PC=processus calycoides; PE=pigment epithelium; R=free ribosomes; RER=rough endoplasmic reticulum; RF=rootlet fiber; S=rod cell spherule; SER=smooth endoplasmic reticulum. (Adapted with permission from Springer Nature. Krebs W, Krebs I. Primate Retina and Choroid. Atlas of Fine Structure in Man and Monkey. 1991.)

responsible for the cone shape. The myoid, which is closer to the photoreceptor nucleus, contains endoplasmic reticulum. The mitochondria, cilia, and inner discs together form the *inner-outer segment junction*, which provides evidence of the origin of the photoreceptor as a modified sensory cilium prone to the full range of ciliopathies. Rod outer segments may contain up to 1000 discs stacked like coins. These discs are renewed in and shed from the outer retina and are phagocytosed by the retinal pigment epithelium (RPE) for processing and recycling of components.

Cone photoreceptors have a 1-to-1 synapse with a type of bipolar cell known as a *midget bipolar cell*. Other types of bipolar cells also synapse with each cone. Conversely, more than 1 rod—and sometimes more than 100 rods—converge on each bipolar cell. Bipolar cells, the first neurons of the visual pathway, synapse with ganglion cells, the second neurons of the visual pathway, in the inner plexiform layer (IPL). The ganglion cells summate responses from bipolar and amacrine cells and develop action potentials that are conducted to the dorsolateral geniculate nucleus and the third neuron in the brain. Amacrine cells in the inner portion of the inner nuclear layer (INL) help process signals by responding to specific alterations in retinal stimuli, such as sudden changes in light intensity or the presence of certain sizes of stimuli. The INL is composed of horizontal cells, bipolar cells, and amacrine cells. In the nerve fiber layer (NFL), axons of the ganglion cell layer (GCL) course along the inner portion of the retina to form the optic nerve, a brain tract. The internal limiting membrane (ILM), which is not a true membrane but is formed by the footplates of Müller cells, is attached to the posterior cortical gel of the vitreous (Fig 1-7).

Two additional intraretinal “membranes” identified by histologists, the external limiting membrane (ELM) and the middle limiting membrane (MLM), are actually junctional systems, not true membranes. At the outer extent of the Müller cells, zonular attachments between photoreceptors and Müller cells form the ELM, a structure visible with both light microscopy and OCT. Thus, the Müller cells, whose nuclei reside in the INL, course through almost the entire thickness of the retina. The inner third of the outer plexiform layer (OPL) has a linear density in which synaptic and desmosomal connections occur between the photoreceptor inner fibers and the processes of the bipolar cells. This linear density, which is also apparent with OCT, is the junctional system that has been called the MLM.

Retinal Vasculature and Oxygen Supply

The vascular supply of the retina comes from the retinal circulation for the inner retina and indirectly from the choroidal circulation for the avascular outer retina. The central retinal artery (a branch of the ophthalmic artery) enters the eye and divides into 4 branches, each supplying blood to a quadrant of the retina. These branches are located in the inner retina. A cilioretinal artery, derived from the ciliary circulation, supplies a portion of the inner retina in approximately one-third of human eyes (Fig 1-8). On a tissue level, the retina is supplied by up to 4 layers of vessels:

- *radial peripapillary capillary network*, located in the NFL and around the optic nerve head
- *superficial vascular plexus*, which includes the *superficial capillary plexus*, in the retinal GCL
- *deep capillary complex* with 2 capillary beds, one on either side of the INL

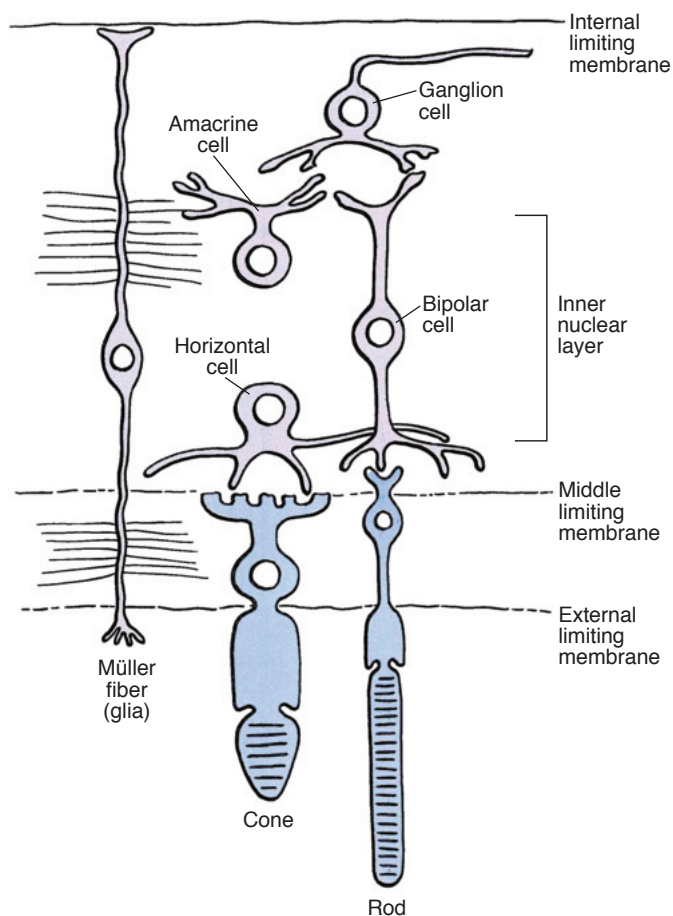


Figure 1-7 Schematic of the neuronal connections in the retina and participating cells. In the diagram, light enters from the top, at the ganglion cell layer. (Redrawn from Federman JL, Gouras P, Schubert H, et al. *Retina and Vitreous*. Mosby; 1988. Podos SM, Yanoff M, eds. *Textbook of Ophthalmology*; vol 9. Illustration by Mark Miller.)

Although the superficial layer of the deep capillary plexus is sometimes referred to as the *intermediate capillary plexus*, typically both layers are collectively referred to as the *deep capillary complex*. OCT angiography can visualize these distinct capillary layers. The retinal vasculature, including its capillaries, retains the blood–brain barrier with tight junctions between capillary endothelial cells. Blood from the capillaries is collected by the retinal venous system; it eventually leaves the eye through the central retinal vein by way of branch retinal veins.

The outer retinal layers, beginning with the OPL, derive their oxygen supply from the choroidal circulation. The exact boundary between the retinal vascular supply and the diffusion from the choriocapillaris varies according to the topographic location, retinal thickness, and amount of light present. For additional discussion, see the choroid section later in this chapter, as well as Part I, Anatomy, of BCSC Section 2, *Fundamentals and Principles of Ophthalmology*.

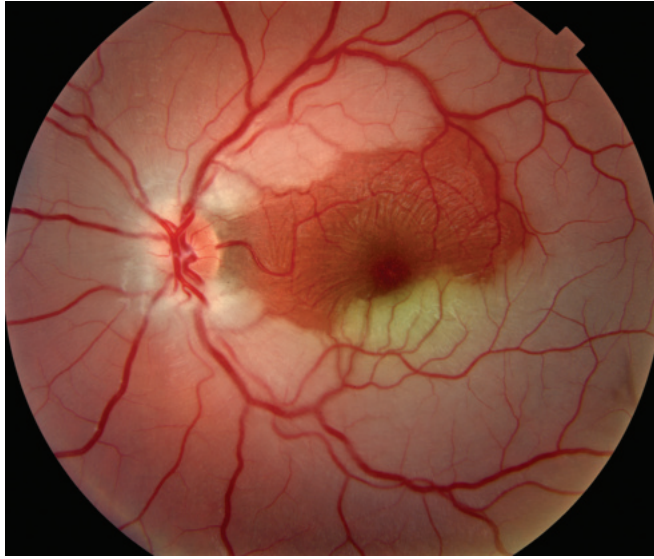


Figure 1-8 A central retinal artery occlusion in a young patient with a previously unknown patent foramen ovale. Presumably, an embolus from the systemic circulation passed through the patent foramen ovale and lodged in the central retinal artery, occluding its blood flow. Fortunately, a cilioretinal artery supplied part of the eye's retina. Note the retinal ischemic whitening in the distribution of the central retinal artery but preservation of the normal retinal transparency in the zone supplied by the cilioretinal artery. (Used with permission from Ho IV, Spaide RF. Central retinal artery occlusion associated with a patent foramen ovale. *Retina*. 2007;27(2):259–260. doi:10.1097/IAE.0b013e318030cc2)

Retinal Pigment Epithelium

The RPE is a monolayer of pigmented, hexagonal cells derived from the outer layer of the optic cup. This layer is continuous with the pigment epithelium of the ciliary body and iris. In the macula, RPE cells are taller and denser than in the periphery. The lateral surfaces of adjacent cells are closely apposed and joined by tight junctional complexes (zonulae occludentes) near the apices, forming apical girdles and the outer blood–ocular barrier. Each RPE cell has an apex and base; the apical portion envelops the outer segments of the photoreceptor cells with villous processes (Fig 1-9). The basal surface of the cells shows a rich infolding of the plasma membrane. The basement membrane does not follow these infoldings. The cytoplasm of the typical RPE cell contains several melanosomes, each designed to absorb light. Melanosomes are spheroidal; their melanin is distributed on protein fibers.

The RPE contributes to retinal function in several ways; it

- absorbs light
- phagocytoses rod and cone outer segments
- participates in retinal and polyunsaturated fatty acid metabolism
- forms the outer blood–ocular barrier
- maintains a fluid-free subretinal space
- heals and forms scar tissue
- regenerates and recycles visual pigment

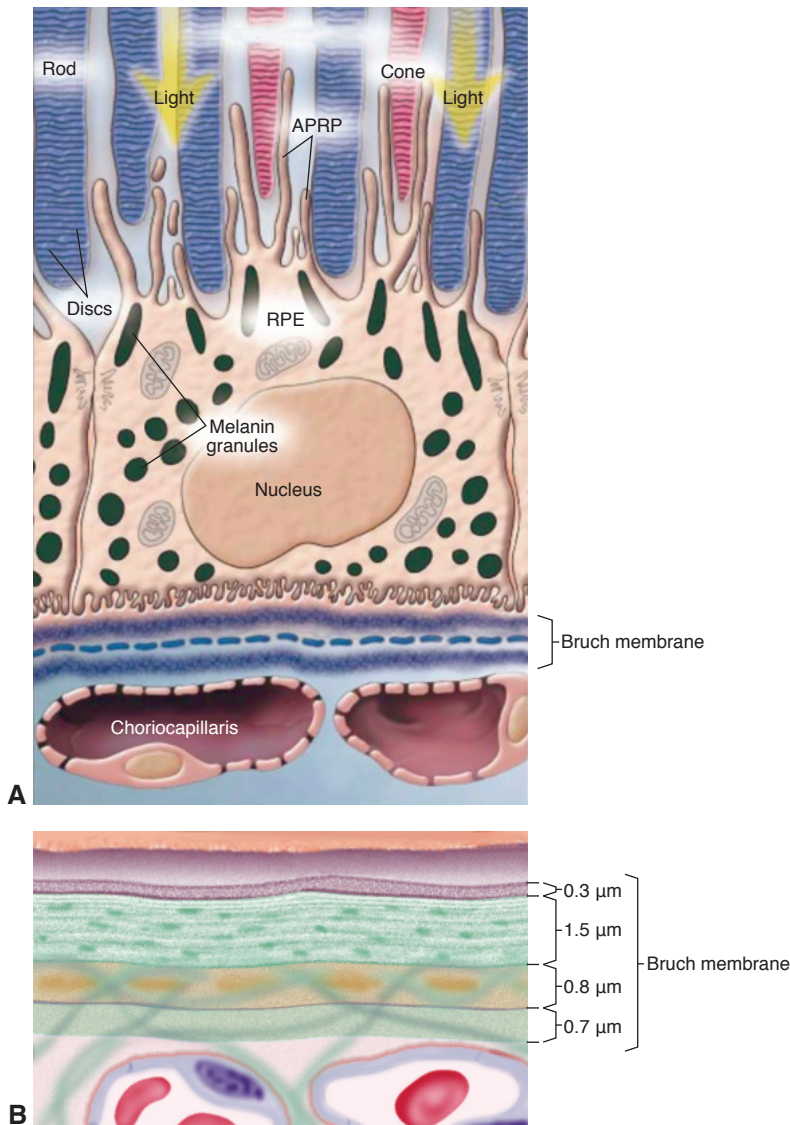


Figure 1-9 Illustrations of Bruch membrane. **A**, The RPE and its relationship to the photoreceptors and Bruch membrane. Note the interdigitations; villi from the RPE make contact with the outer segments of both rods and cones. **B**, The folded plasmalemma of the RPE rests on its smooth basement membrane (0.3 μm thick) bordering the inner collagenous zone (1.5 μm thick). The outer collagenous zone (0.7 μm thick) borders the elastic layer (0.8 μm thick) and is continuous with intercapillary bridges and the subcapillary fibrous tissue. APRP = apical process of the RPE. (Part A courtesy of the University of Rochester; part B illustration by Daniel Casper, MD, PhD.)

RPE cells serve a phagocytic function, continually ingesting the disc membranes shed by the outer segments of photoreceptor cells. Over the course of a lifetime, each RPE cell is thought to phagocytose billions of outer segments. This process of shedding, phagocytosis, and photoreceptor renewal follows a daily (circadian) rhythm. Rods shed discs at dawn,

and cones shed them at dusk. The ingested outer segments are digested gradually, broken down by enzymes from lysosomes.

Visual pigments contain 11-*cis*-retinaldehyde that is converted to 11-*trans*-retinaldehyde in the photoreceptor outer segments. Most of the regeneration of 11-*cis* to the 11-*trans* configuration occurs in the RPE and requires a highly efficient transfer of metabolites from the outer segments to the RPE cells and back. The interdigitation of the RPE and outer segments facilitates the regeneration by increasing the surface area of contact and allowing proximity. The visual pigments' biochemical cycle is discussed in more detail in BCSC Section 2, *Fundamentals and Principles of Ophthalmology*.

A variety of pathologic changes—caused by such factors as genetic defects, drugs, dietary insufficiency (of vitamin A), or senescence—can impair the process of phagocytosis and renewal. Physical separation of the retina from the RPE, which occurs when subretinal fluid (ie, retinal detachment) or blood is present, also disrupts the important exchange of metabolites.

The RPE functions as a barrier to prevent diffusion of metabolites between the choroid and the subretinal space. Because of this, the environment of the photoreceptors is largely regulated by the selective transport properties of the RPE. The RPE has a high capacity for water transport, so in a healthy eye, fluid does not accumulate in the subretinal space. This RPE-mediated dehydration of the subretinal space also modulates the bonding properties of the interphotoreceptor matrix, which acts as a bridge between the RPE and photoreceptors and helps bond the neurosensory retina to the RPE. With deterioration or loss of the RPE, there is corresponding atrophy of the overlying photoreceptors and underlying choriocapillaris.

Bruch Membrane

The basal portion of the RPE is attached to Bruch membrane, which has 5 layers. Starting with the innermost, the layers are as follows (see Fig 1-9):

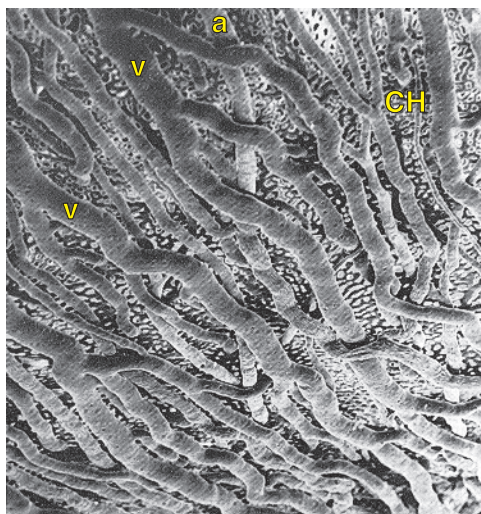
- basement membrane of the RPE
- inner collagenous zone
- middle layer of elastic fibers
- outer collagenous zone
- basement membrane of the endothelium of the choriocapillaris

Degeneration of Bruch membrane over time is associated with buildup of lipids and oxidatively damaged materials as well as calcification. In some disease states, extensive Bruch membrane calcification can lead to fractures, known as *angioid streaks*. In age-related macular degeneration, areas of calcification with microscopic breaks have also been found.

Choroid

The choroid nourishes the outer portion of the retina. Blood enters the choroid, which consists of 3 layers of vessels, through the posterior ciliary arteries (Fig 1-10). The outer layer

Figure 1-10 Scanning electron micrograph (70 \times) of the choroid. Vascular cast of the choroid from the posterior pole of a 62-year-old man, showing arteries (a), veins (v), and the choriocapillaris (CH). (Courtesy of A. Fryczkowski, MD.)



of large-caliber vessels, known as the *Haller layer*, is relatively thick. The vessels in this layer divide into smaller-diameter vessels and precapillary arterioles, which make up the middle layer, known as the *Sattler layer*. These smaller vessels distribute the blood throughout the choroid, reducing arterial pressure to the relatively low pressure found in the innermost layer, the *choriocapillaris*.

The choroid has a maximal thickness posteriorly. On histologic examination, it is 0.22 mm thick in the central macular region, becoming progressively thinner anteriorly; at the ora serrata, it is 0.1 mm thick. Subfoveal choroidal thickness, measured by SD-OCT in vivo in healthy volunteers with a mean age of 50 years, is approximately 287 μm . However, thickness changes with age and disease states of the eye. The presence of thin choroid (leptochoroid) and thick choroid (pachychoroid) may be associated with ocular diseases.

In the posterior pole, the choriocapillaris forms a plexus of capillaries, even though the capillaries themselves are not arranged strictly into lobules. The capillary arrangement becomes more irregular toward the periphery, where the capillaries are arranged more radially. Interspersed between the vessels of the choroid are loose connective tissue, fibroblasts, and melanocytes.

After passing through the choriocapillaris, the blood is collected in venules, which coalesce into collecting channels, or ampullae, of the vortex veins. Most eyes have 4 or 5 vortex veins, which exit the eye at or posterior to the equator. The vortex veins drain into the superior and inferior ophthalmic veins.

The choroid supplies the metabolic needs of the retina, which has one of the highest metabolic rates per gram of tissue in the body. In some estimates, the choroidal circulation supplies 90% of the oxygen consumed by the retina, primarily by the photoreceptors. The choroid also has the highest rate of blood flow per unit weight of any tissue in the body, and the venous blood exiting the choroid still has a very high oxygen tension. The RPE cells, which are anatomically closely associated with the choriocapillaris, are exposed to the highest oxygen tensions of any perfused tissue, increasing the risk of oxidative damage.

The rapid flow in the choroid also acts as a heat sink, removing thermal energy obtained by light absorption.

Mrejen S, Spaide RF. Optical coherence tomography: imaging of the choroid and beyond. *Surv Ophthalmol*. 2013;58(5):387–429.

Sclera

The sclera is composed of collagen and a few elastic fibers embedded in a matrix of proteoglycans. It terminates at the histologists' limbus. The sclera does not have uniform thickness. It is thinnest immediately behind the insertion of the rectus muscles, whereas it is thicker at the posterior pole, around the optic nerve head.

The sclera is normally permeable to the passage of molecules in both directions. Up to 40% of the aqueous leaves the eye via uveoscleral outflow, making the sclera an important path of fluid movement. Scleral permeability allows drugs to be delivered to the eye by means of injection into the sub-Tenon space. The sclera is a hydrophilic tissue and is therefore only variably permeable to hydrophobic or amphiphilic substances or medications. This characteristic is an important consideration for periocular injection of pharmacologic agents.

Hogan MJ, Alvarado JA, Weddell JE. *Histology of the Human Eye*. Saunders; 1971:chaps 5, 8, 9, 11.

CHAPTER 2

Diagnostic Approach to Retinal and Choroidal Disease



This chapter includes related videos. Go to www.aao.org/bcscvideo_section12 or scan the QR codes in the text to access this content.



This chapter also includes a related activity. Go to www.aao.org/bcscactivity_section12 or scan the QR code in the text to access this content.

Highlights

- A thorough history and full eye examination, including careful examination of the central and peripheral retina, are necessary for evaluation of retinal diseases.
- Many retinal imaging modalities are now available, each of which provides different, complementary information about retinal and choroidal disease processes.
- Obtaining and integrating information from multimodal imaging is necessary for efficient and precise diagnosis of retinal and choroidal diseases.

Introduction

Evaluating a patient for retinal disease begins with obtaining a thorough patient history, including family history, and a careful review of systems. The patient should undergo a detailed ophthalmic examination, beginning with visual acuity measurement and including careful examination of the central and peripheral retina and testing for a relative afferent pupillary defect. Testing for retinal disease is directed by findings from the clinical examination. In addition, in-office Amsler grid testing can be performed, as it can provide evidence of macular disease, when present.

This chapter explores some of the many imaging modalities used to evaluate retinal disease. No particular modality supplies all the information needed to appropriately evaluate every disease. Rather, each modality provides different, complementary information. Thus, integrating information from multimodal imaging is necessary for efficient and precise diagnosis of retinal and choroidal diseases.

Ophthalmoscopy

The direct ophthalmoscope provides an upright, monocular, high-magnification (15 \times) image of the retina. Because of its lack of stereopsis, small field of view (5°–8°), and poor view of the retinal periphery, the direct ophthalmoscope has limited use, and this technique has largely been supplanted by indirect ophthalmoscopy. In indirect ophthalmoscopy, light from the illumination source is directed into the eye through a condensing lens, which helps form a flat, inverted, and reversed aerial image of the patient's retina between the lens and the examiner. Indirect ophthalmoscopy can be performed with the binocular indirect ophthalmoscope or at the slit lamp. A variety of condensing lenses are available for use with the slit lamp or the binocular indirect ophthalmoscope, allowing the clinician to choose the best lens for the particular situation. The magnification is calculated by dividing the dioptric power of the examination lens into -60 . For example, a 20-diopter (D) lens would result in a magnification of -3 (the negative sign indicates an inverted image).

Examination With the Binocular Indirect Ophthalmoscope

The binocular indirect ophthalmoscope has a unitary magnification. Through the use of prisms, it reduces the distance between the pupils in the instrument, and using a mirror, it reduces the distance from the light source to the optical axis. The examiner's retina, the aerial image, and the patient's retina all become conjugate (see BCSC Section 3, *Clinical Optics and Vision Rehabilitation*, Chapter 9). Binocular indirect ophthalmoscopes allow stereopsis, have a field of view that depends on the dioptric power of the condensing lens (higher powers deliver wider angles of view but at a lower magnification), and with ocular steering, can visualize the entire fundus—unlike direct ophthalmoscopes. If the patient's pupil can be fully dilated, the ora serrata may be seen without the use of any additional instruments. If the pupil cannot be widely dilated or the clinician needs to see peripheral retinal details in profile, scleral depression can be performed. Disadvantages of binocular indirect ophthalmoscopy include the resulting low magnification from the condensing lens and the inverted and reversed image.

Indirect Ophthalmoscopy With the Slit Lamp

Indirect ophthalmoscopy can also be performed with a slit lamp by using a noncontact lens, for example, a 60-D or 78-D lens. With a 60-D lens, the magnification afforded by the lens is 1 \times ; however, the slit lamp typically has a magnification of 10 \times or 16 \times . The field of view provided by these lenses is good, a little less than 70° with the 60-D lens and more than 80° with the 78-D lens. Ocular steering can be used to evaluate a large area of the fundus. Lenses of higher dioptric powers can aid visualization of wide areas of the retina even if the pupil does not dilate. These lenses may have a field of view of 100° or more.

With *noncontact indirect biomicroscopy*, the power and capabilities of a slit lamp with a wide field of view may be employed without any contact with the eye; subsequent ocular imaging can proceed without a problem because no contact is made with the cornea. The main disadvantage is that the image created is inverted and reversed.

A contact lens provides one of the highest-resolution methods to view the fundus. Although these lenses provide no significant magnification, they nullify the refractive power, and potentially any astigmatism, of the cornea. The 3-mirror lens is one commonly used contact lens. The central portion is used to visualize the posterior pole directly and has a field of view of a little more than 20°. The 3 mirrors can be used to evaluate the midperiphery and far periphery of the retina as well as the iridocorneal angle. The 3-mirror lens produces a noninverted image; however, the field of view through any one component is limited, and rotation of the lens on the patient's eye is required to visualize 360° of the peripheral fundus. *Wide-field contact lenses* allow visualization of peripheral pathology with fields of view up to 160° without rotation of the lens, but they produce an inverted image. All contact lenses require use of a viscous coupling fluid, which may hinder subsequent ocular imaging.

Lenses are chosen at the discretion of the examining clinician, according to what is needed for the specific examination. For example, an opacified posterior capsule with a small posterior capsulotomy may inhibit good visualization of the retinal periphery with a 3-mirror lens but pose no significant problem for a wide-field contact lens. For more information about lens choice and indirect ophthalmoscopy, see the following reference.

Roybal CN. Indirect ophthalmoscopy 101. American Academy of Ophthalmology. May 15, 2017. Accessed January 17, 2022. <https://www.aao.org/young-ophthalmologists/yo-info/article/indirect-ophthalmoscopy-101>

Imaging Technologies

Fundus Camera Imaging

Fundus camera imaging employs the optical principles of indirect ophthalmoscopy. The objective lens is used to deliver a cone of light through the entrance pupil. Light reflected from the eye subsequently forms a flat, inverted aerial image within the body of the camera. This image is transferred to and projected onto an image sensor through a system of relay lenses. Fundus cameras use flash illumination to obtain high-quality images of the eye (a capacitor must be charged to power the flash unit; consequently, fundus cameras typically record images at a speed of only about once per second).

Color fundus photography provides photographic records of the state of a patient's fundus for their medical records; these images may also be used in research and for teaching. Because a large amount of information can be extracted from a simple color fundus photograph (Fig 2-1A, B), this mode of imaging has been the cornerstone of many large epidemiologic and treatment studies. The color rendition is the best of any imaging system in terms of color accuracy, noise, and resolution.

With the addition of different filters, the fundus camera can be used to perform fluorescein angiography, indocyanine green angiography, and fundus autofluorescence imaging (Fig 2-1C); these techniques are discussed later in the chapter.

Imaging from fundus cameras may be affected by cloudy media, with light scattering obscuring fundus details and reducing image contrast.

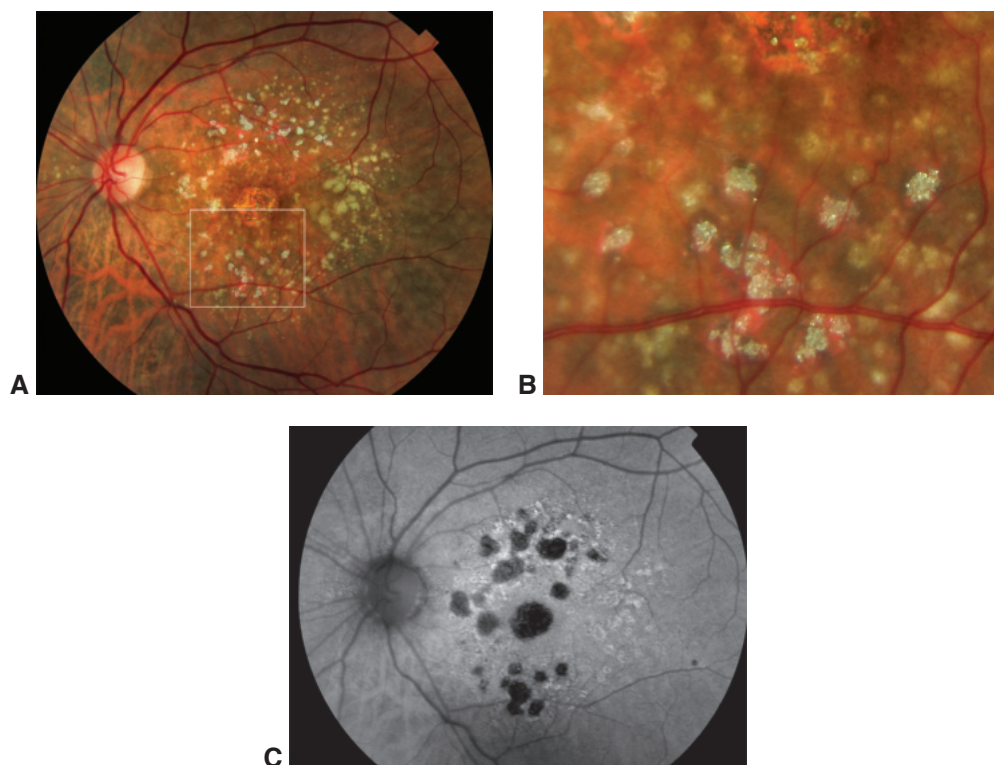


Figure 2-1 Multimodal imaging of refractile drusen and associated atrophy. **A**, Color fundus photograph of geographic atrophy with refractile drusen. **B**, Enlarging the section within the white square from **A** reveals a remarkable amount of information, even showing the diamondlike particles that seem to correspond to the hydroxyapatite spherules seen in histologic sections of drusen. **C**, Fundus autofluorescence (FAF) image shows attenuated autofluorescence in areas of geographic atrophy that are also depicted in the color photograph; in addition, FAF reveals an absence of autofluorescence colocalized to the locations of the refractile drusen. (Courtesy of Richard F. Spaide, MD.)

Scanning Laser Ophthalmoscopy

The confocal scanning laser ophthalmoscope (SLO) functions as both an ophthalmoscope and a fundus camera and allows additional applications, such as fluorescein angiography and autofluorescence imaging. The SLO generates retinal images by scanning an illuminated spot on the retina in a raster pattern and uses a Maxwellian view system to build the retinal image. Because the system is confocal, the scattered light can be rejected by the crystalline lens, as can the fluorescence, allowing for the use of shorter wavelengths in autofluorescence imaging. A photodiode is used to detect the light received from the eye.

A variety of wavelengths can be used as dictated by need. A fundus photograph can be reconstructed with 3 simultaneously acquired color laser images in the blue, green, and infrared spectra; however, the color in these multicolor images is unnatural compared with that in a traditional fundus photograph (Fig 2-2A, B). Infrared imaging alone can be used to evaluate the fundus; in some circumstances, it provides more comprehensive

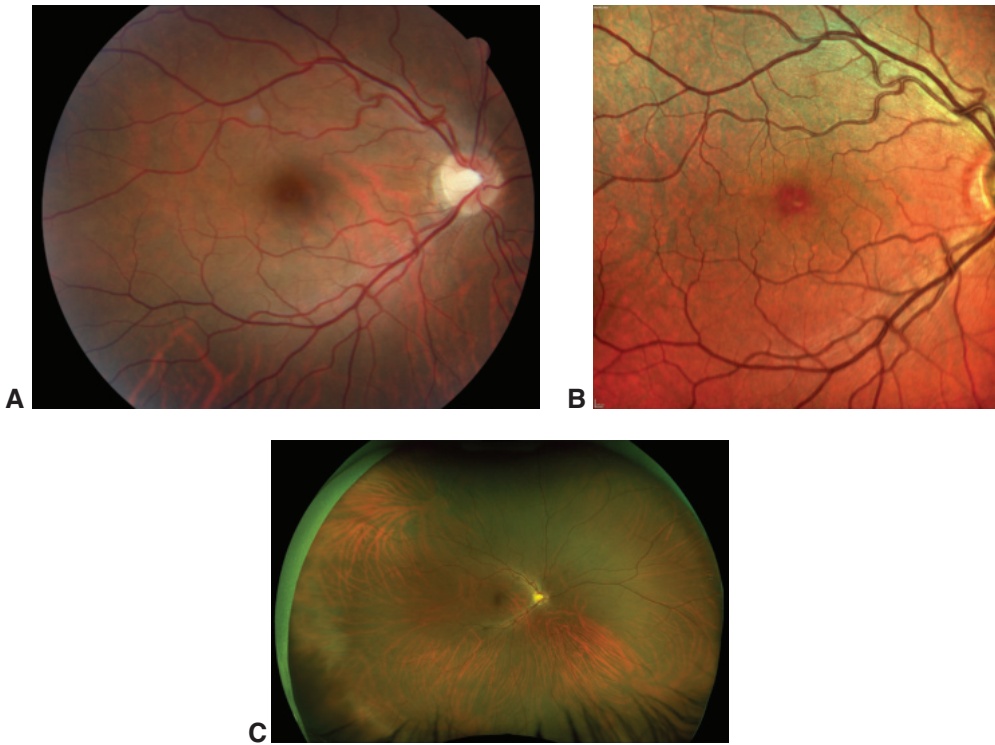


Figure 2-2 Images of a single healthy eye obtained with 3 different modalities. **A**, Traditional fundus photograph (50° field of view). **B**, Confocal scanning laser ophthalmoscopy (SLO) multi-color fundus image (30° field of view). **C**, Ultra-wide-field SLO fundus image produced by using an ellipsoidal mirror (200° field of view). (Courtesy of Lucia Sobrin, MD.)

information than that revealed by color photography. For example, some types of pseudo-drusen (ie, subretinal drusenoid deposits) are not very prominent in color fundus photographs but are easy to view in infrared images. Similarly, choroidal nevi reflect infrared light, consequently appearing bright in infrared imaging. The infrared image can be used to perform eye movement tracking.

In SLO angiography, fluorescein is injected intravenously to act as a contrast agent and then imaging begins. To obtain an autofluorescent image of the fundus, the excitation laser and barrier filter are put into place, but fluorescein dye is not used and the gain is turned up. This method uses a blue-green wavelength that is absorbed by macular pigment.

A second approach to SLO uses an ellipsoidal mirror. Commercial systems using this method can obtain images that are approximately 200° wide, or ultra wide field (Fig 2-2C). With ocular steering, nearly all of the retina can be imaged. In this method, 2 lasers, a red one and a green one, are employed to obtain a pseudo-color-scaled image. As with the SLO multicolor images mentioned earlier, the color in these images is unnatural; therefore, when evaluating lesion color, clinicians should rely on the ophthalmoscopic examination rather than these images. Angiography can be performed with the use of the appropriate

excitation lasers. The number of points imaged is large, and these systems do not record at video rates. Systems employing an ellipsoidal mirror have limited confocality. To obtain autofluorescent images, a green laser needs to be used.

Optical Coherence Tomography

Optical coherence tomography (OCT) is a noninvasive, noncontact imaging modality that produces micrometer-resolution images of tissue. Low-coherence light is simultaneously directed into tissue and into a reference arm. An interferometer combines the light returning from the tissue with the light from the reference arm, producing an interferogram. The benefit of using low-coherence light is that its spectral makeup changes rapidly with time; thus, light produced at a particular instant will not interfere substantially with light produced at other times. This means the exact position from which the interfering light came can be determined by the resolution dictated by the coherence length of the light source, which is typically 5–7 μm . In any given A-scan, the earlier technology of time-domain (TD) OCT is used to interrogate each point in the tissue sequentially. In more modern techniques, for example either spectral-domain (SD) or swept-source (SS) OCT, a more efficient approach is taken. In SD-OCT, a broad-spectrum light source is used, and the interferogram produced varies with the reflectivity of the tissue. SS-OCT uses a more complicated light source that sequentially scans through successive wavelengths of light across a spectral range. SS-OCT and SD-OCT produce higher-resolution images than TD-OCT and have largely replaced TD-OCT in the clinic.

Compared with SD-OCT, SS-OCT has the following advantages:

- generally faster image acquisition
- wider scanning ranges
- better simultaneous imaging of vitreous to choroid
- better penetration through opacities

On the other hand, SD-OCT imaging devices are less expensive than SS-OCT devices, and they have better axial resolution. Although simultaneous imaging of the vitreous to the choroid is better with SS-OCT, SD-OCT can image the choroid well by using enhanced depth imaging (EDI). EDI is useful for determining choroidal thickness.

Both SD-OCT and SS-OCT create an A-scan through tissue. B-scans consist of a collection of many A-scans conducted through a plane of tissue. A volume scan consists of an assembly of numerous B-scans; this volume scan is stored in computer memory as a block of data in which each memory location stores a value that corresponds to a specific small volume of tissue. The voxels (a portmanteau of *volume* and *pixels*) in the volume of data may be represented in many ways; one simple way is to make planar slices, producing an image called a *C-scan*. C-scans are difficult to interpret because in a curved structure, many planes of tissue can be crossed. Another, more advanced method is to segment the data according to tissue planes; a thickness of voxels presented this way is called an *en face scan*. This technique can be used to measure the thickness of various tissues, for example, the retinal nerve fiber layer. Maps of the thickness of the retina or a specific retinal layer can also be produced. Actual correlation between OCT scans and histology of the retina continues to be an area of active research (Activity 2-1).



ACTIVITY 2-1 Optical coherence tomography (OCT) terminology, based on the International Nomenclature for OCT Panel for Normal OCT Terminology.

Reproduced from Staurengi G, Sadda S, Chakravarthy U, Spaide RF; International Nomenclature for Optical Coherence Tomography (IN-OCT) Panel. Proposed lexicon for anatomic landmarks in normal posterior segment spectral-domain optical coherence tomography: the IN-OCT consensus. Ophthalmology. 2014;121(8):1572–1578. Copyright 2014, with permission from Elsevier.



In addition to B-scans and en face imaging, volume rendering of OCT data is possible and shows the 3-dimensional character of tissue (Fig 2-3). Compared with ordinary

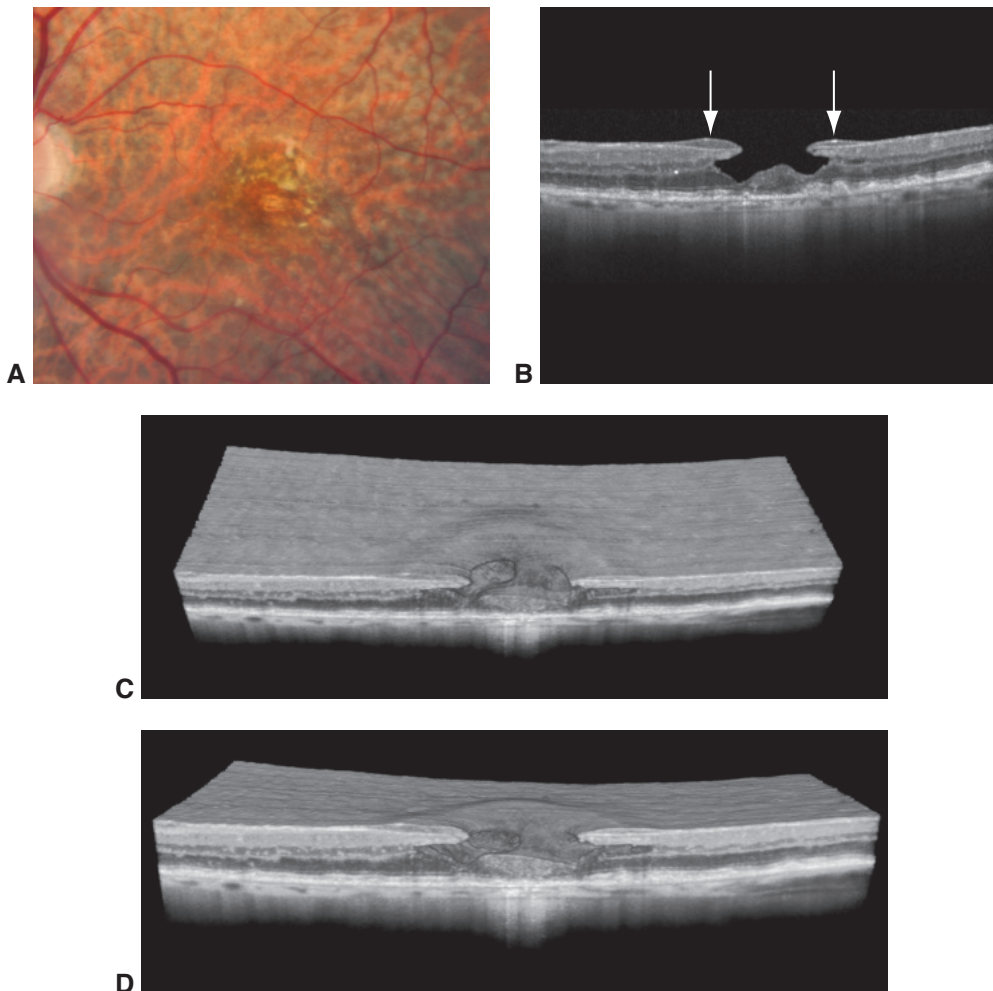


Figure 2-3 Imaging of an eye with drusen and a lamellar macular hole. **A**, Fundus photograph from a patient with prominent drusen and distorted vision. **B**, B-scan section of optical coherence tomography (OCT) imaging shows a lamellar hole with lamellar hole–associated epiretinal proliferation (LHEP). **C**, **D**, Two different views from volume-rendered imaging of the lamellar macular hole taken in sections, showing the thick epiretinal membrane, as well as the absence of induced distortion of the retina. Note the cavities within the undermined retina and the attachment of the LHEP to the central foveal tissue. (Courtesy of Richard F. Spaide, MD.)

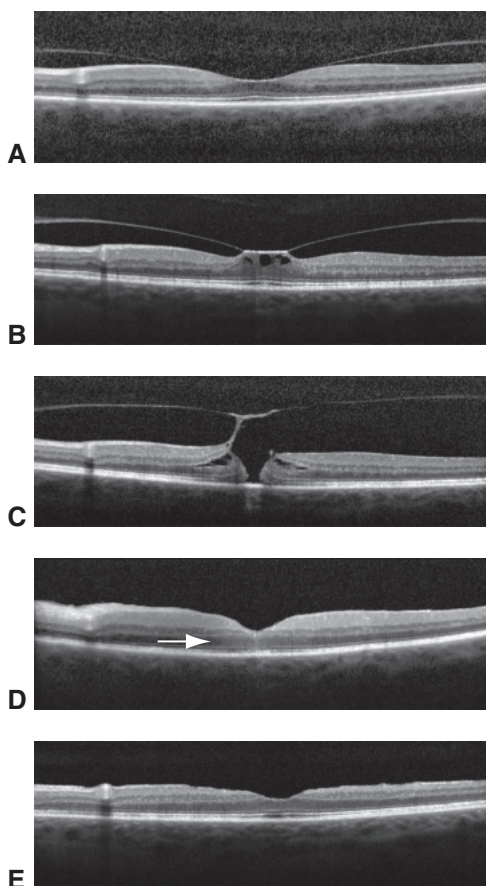
B-scans, volume rendering is computationally intensive. It is used in radiology but is not yet widely used in ophthalmology.

Some OCT scanners offer eye movement tracking. With the addition of this feature, ocular motion can be detected and corrected in the final image, improving the quality of the resulting scan. Tracking methods rely on recognizing fundus features and registering the scan pattern with the fundus image. This capability expands the utility of OCT; with it, scans interrupted by patient blinks still produce usable images. Also, it is possible to perform repeated scans of the same fundus location over time, enabling assessment of disease progression (Fig 2-4).

Optical Coherence Tomography Angiography

In a series of images taken at a sufficient interval, a moving object will appear at different positions on the successive images. When these images are compared pixel by pixel, nonmoving regions will show no change, while moving objects will produce areas that show high variance. If the color black is assigned to areas of low variance (ie, areas that do not move) and the color white is assigned to areas with high variance, the resulting image will highlight movement; this is called *motion contrast*. The retina has no moving parts, except for the flow of blood. If the images are high resolution, successive retinal images can show the movement of blood through

Figure 2-4 Evolution of a macular hole, visualized with OCT. **A**, Image from a patient with a perifoveal posterior vitreous detachment and no obvious traction on the macula. **B**, After 1 year, the patient experienced visual distortion; the image shows obvious traction with foveal tractional cavitations. **C**, Image taken 2 months later; note the full-thickness macular hole. **D**, Image taken 1 month after macular hole surgery; the hole is closed. Note the subtle area of increased reflectivity in the center. **E**, Image taken 3 months later shows the fovea with a nearly normal contour and laminar structure. (Courtesy of Richard F. Spaide, MD.)



the retina. Images taken with OCT are not only high resolution but also depth resolved. Therefore, data obtained from tissue at one point in time can be compared with data obtained from the same tissue at successive points in time. The result is a 3-dimensional visualization of movement within the retina, corresponding to blood flow in its various layers.

Unlike fluorescein angiography, which can visualize only the superficial capillary plexus, OCT angiography (OCTA) can image all capillary layers, including the superficial plexus, the radial peripapillary capillary network, and the deep capillary complex. This provides huge opportunities to advance our understanding of retinal diseases. Other advantages of OCTA over fluorescein angiography are that it is noninvasive and faster for imaging of the retinal circulation. However, OCTA cannot show vascular leakage, which fluorescein angiography can demonstrate in diseases such as retinal vasculitis (see the section “Fluorescein angiography” later in the chapter). En face OCTA offers another way to visualize flow information. En face imaging of flow in the retina is a useful technique because the resulting image of the retina is arranged in layers, as is its blood supply. In this method, a slab of the flow information corresponding to the expected position of a layer of vessels is selected. Next, the brightest pixel in each column of voxels is selected and displayed; this is called a *maximal intensity projection*. This projection creates a flat image from the data, which exists in 3 dimensions.

OCTA can visualize the retinal vasculature at a higher resolution than any other current imaging modality (Fig 2-5). However, OCTA is prone to artifacts. Understanding how these artifacts are created is key to understanding and interpreting the images produced. Motion results in bright areas in the image, but this motion does not necessarily come from blood flow. For example, if the patient’s eye moves during the examination, portions of the resulting image will contain motion artifacts. Multiple automatic scans with eye movement tracking and software repair can suppress most motion artifacts. Another type of defect, called a *projection artifact*, is created when light passes through a blood vessel and strikes a deeper reflective structure; over time, the light that reflects from that structure will change, mimicking the overlying blood vessel. The image created will have what appears to be 2 levels of the same vessel: the first at its actual location and the second at the level of the reflecting structure. Several mathematical approaches can remove projection artifacts. A third potential issue in OCTA is the appearance of dark areas on the image. Dark areas visualized in the fundus can be the result of a lack of blood flow, or at least blood flow too slow to be detected in successive scans at the interval time used. Often, however, it is too difficult to ascertain whether there is a true lack of flow, so the dark areas on the images are called *signal voids*.

Clinical OCTA devices have primarily imaged the macula, but technological advances have allowed wider-field OCTA imaging (see Fig 2-5E).

Spaide RF, Fujimoto JG, Waheed NK, Sadda SR, Staurengi G. Optical coherence tomography angiography. *Prog Retin Eye Res*. 2018;64:1–55. doi:10.1016/j.preteyeres.2017.11.003

Fundus Autofluorescence

Fundus autofluorescence (FAF) is a rapid, noncontact, noninvasive way to visualize fluorophores in the fundus. Intrinsic fluorophores in the retina include lipofuscin/bisretinoids and melanin. In FAF, the excitation light is introduced into the eye; fluorescence from

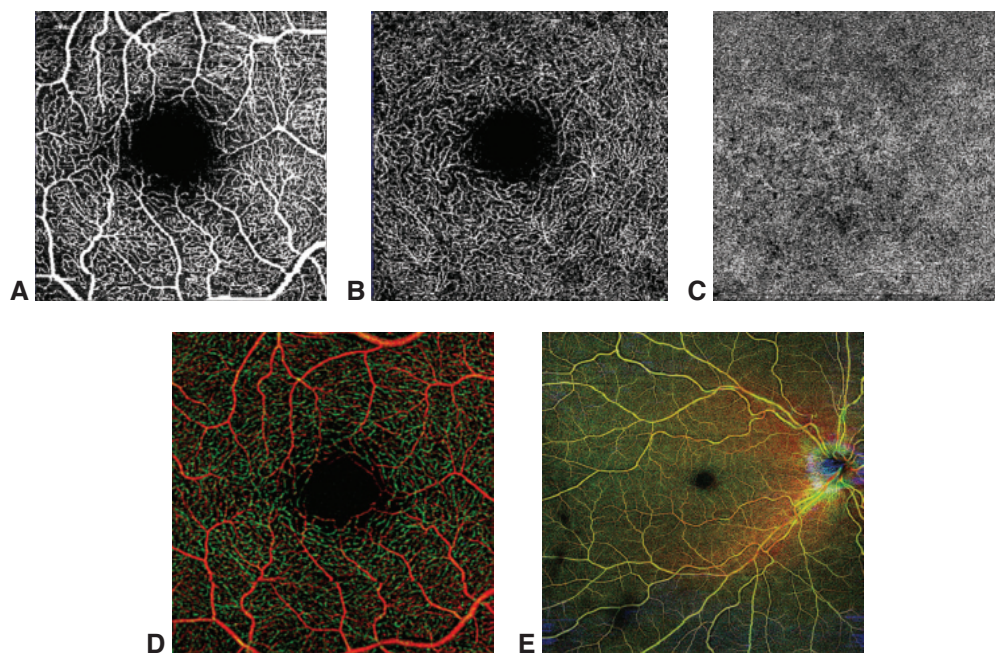


Figure 2-5 OCT angiography (OCTA) of a healthy eye (same eye in all parts). **A**, Superficial vascular plexus with fractal branching. **B**, Deep capillary plexus. Its vessels are small and do not show the same branching as the vessels of the superficial vascular plexus. **C**, Choriocapillaris. **D**, Color depth-encoded OCTA image of the macula. **E**, Color depth-encoded OCTA image. Wider-field fundus view shows the vessels at each layer delineated by a different color.

(Courtesy of Lucia Sobrin, MD.)

intrinsic fluorophores is detected by using a barrier filter to exclude that excitation light from the image (see Figure 2-6 for an example of FAF imaging in a healthy eye). For example, bisretinoids accumulate within the lysosomes of retinal pigment epithelium (RPE) cells as a normal part of the aging process; they are not necessarily harmful. When RPE cells die, the contained lipofuscin disperses, resulting in a loss of autofluorescence, so that these areas appear dark on FAF images. When there is a tear in the RPE, which is usually seen in patients with choroidal neovascularization (CNV), the scrolled RPE is hyperautofluorescent because of reduplication, while the bared area shows no autofluorescence signal (Fig 2-7). This mechanism of autofluorescence gain or loss is used to monitor the absence of RPE cells in a variety of diseases. Autofluorescence is particularly helpful for monitoring the rate of growth of geographic atrophy, characterized by areas of hypoautofluorescence, and for monitoring chorioretinal lesions in posterior uveitides; when these lesions are active, hyperautofluorescence is often seen at the lesions' borders on FAF.

Two main types of systems are used to image autofluorescence: fundus cameras and SLOs. For FAF with the fundus camera, special filters are used that are tuned to detect the signal generated by lipofuscin granules without being overcome by the interference of autofluorescence from the crystalline lens, which may be derived, in part, from tryptophan and by nonenzymatic glycosylation of lens proteins. These cameras use wavelengths that

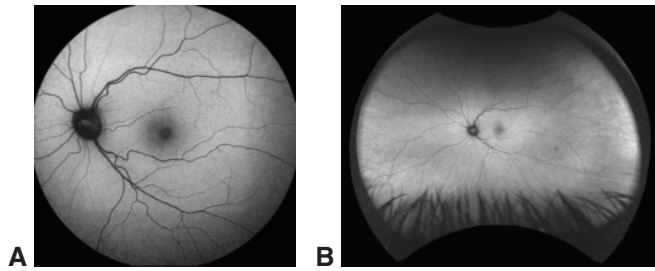


Figure 2-6 Fundus autofluorescence images of a healthy eye, acquired using scanning laser ophthalmoscopy. Two different devices were used, each with a different field of view: central (**A**) and ultra-wide-field (**B**). (Courtesy of Lucia Sobrin, MD.)

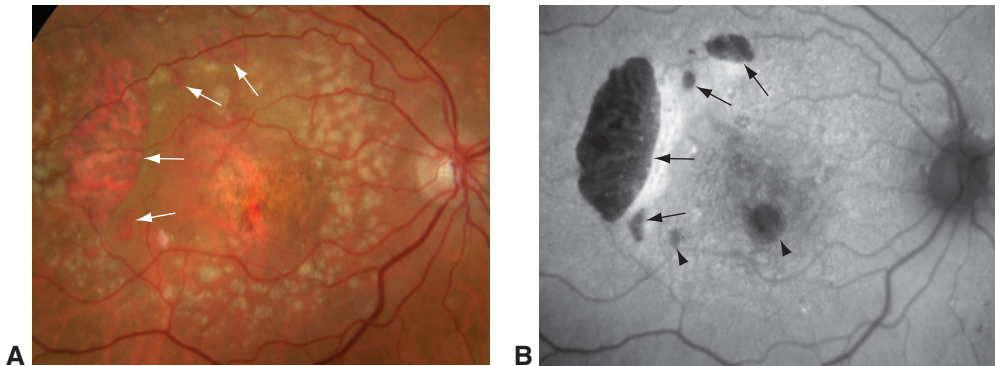


Figure 2-7 Tears in the retinal pigment epithelium (RPE). **A**, Fundus photograph from a patient with choroidal neovascularization (CNV) who was given an intravitreal injection of an anti-vascular endothelial growth factor agent and developed what appeared to be 4 RPE tears (arrows). **B**, FAF image reveals the absence of autofluorescence and an increased signal where the RPE appears to be scrolled, thus confirming the RPE tear (arrows). Small areas of atrophy are also revealed by the hypoautofluorescence (arrowheads). (Courtesy of Richard F. Spaide, MD.)

are in the green end of the spectrum, and the recorded autofluorescence begins closer to the orange wavelengths. The excitation wavelengths are not absorbed by macular pigment.

Commercial SLOs initially used blue excitation light to excite fluorescein, but these wavelengths were absorbed by macular pigment. Use of a green laser for excitation, the wavelengths of which are not absorbed by macular pigment, was later introduced and is still used today. By comparing the ratio of green light autofluorescence in 2 registered fundus images, it is possible to make a 2-dimensional map of macular pigment density.

Although lipofuscin in the RPE is the main source of autofluorescence from the fundus, accumulation of fluorophores in the subretinal space is another important signal source for the evaluation of some diseases, such as central serous chorioretinopathy. After the disease is present for a few months, the detachment becomes lighter in color and slightly more yellow, as well as hyperautofluorescent. This hyperautofluorescence is easier to detect with a fundus camera than with an SLO system for 2 main reasons. First, SLO systems are confocal; if the plane of focus is at the level of the RPE, the top of the detachment may not be in the confocal range. Second, the wavelengths used for FAF imaging

with the fundus camera are more closely tuned to the fluorescence wavelengths emitted by fluorophores in the retina. On OCT imaging, an accumulation of material has been found on the back surface of the retina in eyes with central serous chorioretinopathy with hyperautofluorescent detachments. It is thought that the photoreceptor outer segments typically are phagocytized and processed by the RPE, but if the retina has been physically elevated by fluid, the photoreceptors become separated from the RPE, thus impeding phagocytosis. This mechanism of disease pathophysiology may also be seen in vitelliform deposits in vitelliform macular dystrophy, adult vitelliform lesions, the yellow material that builds up under chronic retinal detachments caused by optic pit maculopathy, and the pockets of retained subretinal fluid after detachment surgery.

Near-infrared FAF imaging using 787-nm excitation and greater than 800-nm emission reveals fluorescence that was previously attributed to melanin from the RPE and the deeper layers of the choroid. However, lipofuscin can also fluoresce when excited at the wavelengths mentioned, and it appears that during lipofuscin processing, melanosomes are fused with lysosomes to produce melanolysosomes. The melanin may bind to some of the free radicals in lipofuscin, but in any case, molecular cross-linking occurs. The resulting melanolipofuscin also fluoresces in the selected ranges. Thus, it may be possible to detect differing molecular species with near-infrared FAF.

Time-resolved fluorescence imaging has shown that different molecules can fluoresce at the same wavelengths but at measurably different times after excitation. Using time-resolved imaging with a phasor approach allows in vivo identification of various molecular species, as well as measurement of the reduction–oxidation reaction state. Studies are being conducted on hyperspectral autofluorescence in which differing wavelengths of fluorescence are measured in order to better understand the formation of component molecules.

Adaptive Optics Imaging

Adaptive optics imaging is a collection of techniques that compensates for wavefront aberrations in real time. These techniques, which were developed for use in astronomical telescopes, can help compensate for changes induced by variations in tear film, among other sources of aberration. This compensation for aberrations allows visualization of individual retinal photoreceptors and RPE cells. However, this type of imaging is extremely time-consuming and requires expensive custom-built instruments to obtain satisfactory results. Significant adoption of adaptive optics imaging in eye clinics has been prevented by the time required, the complexity of the instrumentation, and the limited ability to image all patients (eg, patients with media opacities or intraocular lenses cannot be imaged).

Retinal Angiographic Techniques

Fluorescein angiography

Fluorescein angiography (FA) is a technique used to examine the retinal circulation. It involves rapid serial photography after intravenous injection of fluorescein (Fig 2-8). Traditionally, a fundus camera or an SLO with a field of view of up to about 50° has been used for FA imaging. More recently, wide-field systems that can image most of the fundus, including the periphery, have been increasingly used (Fig 2-9).

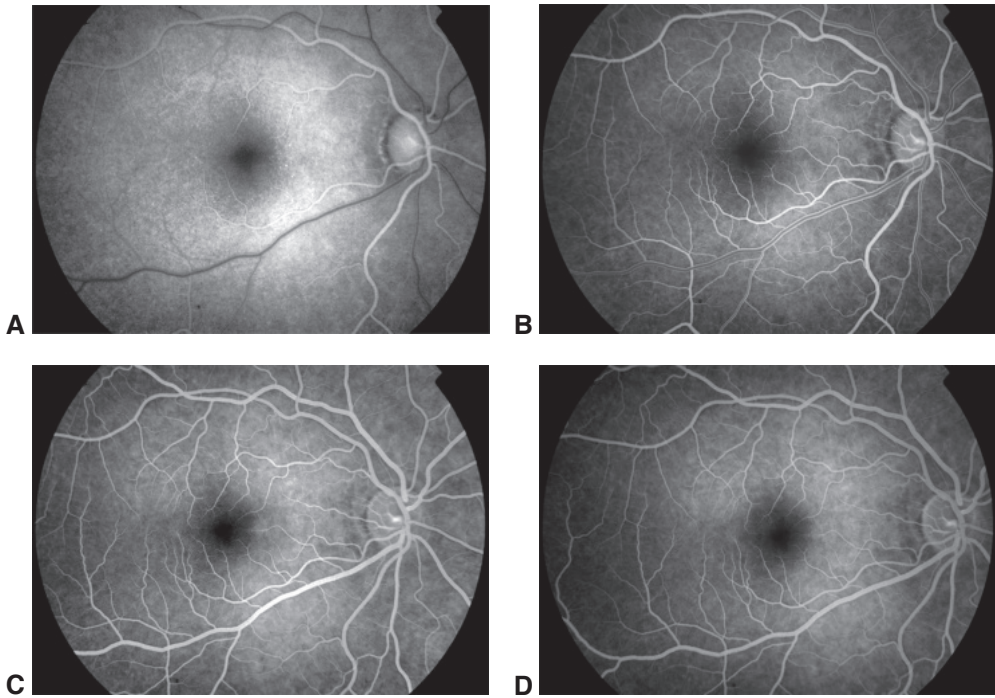


Figure 2-8 Fluorescein angiography of a healthy eye. **A**, The choroid fills approximately a half-second before the retina. The image shows the dye front beginning to enter the retinal arteries. **B**, Laminar filling after dye injection. **C**, Arteriovenous phase. **D**, In the late phase, the fluorescence decreases as the dye is removed from the bloodstream. (Courtesy of Richard F. Spaide, MD.)

Fluorescein ranges from yellow to orange-red in color, depending on its concentration. Fundus cameras equipped for FA have a matched pair of excitation and barrier filters. The excitation filter transmits blue-green light at 465–490 nm, the peak excitation range of fluorescein. The barrier filter transmits a narrow band of yellow light at 520–530 nm, fluorescein's peak emission range. The barrier filter effectively blocks all visible wavelengths except the specific color of fluorescein.

Fluorescein is approximately 80% protein-bound in circulation; the blood–retina barrier prevents it from diffusing into retinal tissue. However, leakage can show on FA in areas with new vessel growth, which lack a blood–ocular barrier, or regions with blood–ocular barrier defects induced by inflammation or ischemia. Fluorescein readily leaks from the choriocapillaris, staining the surrounding tissue. This rapid leakage, as well as the light absorption and scattering by the pigment in the RPE and choroid, prevents widespread use of fluorescein in choroidal imaging.

For the procedure, normally, 2–3 mL of a 25% sterile solution or 5 mL of a 10% sterile solution is injected in the antecubital vein. Typically, the dye is visible in the choroid within 8–12 seconds; filling of the retinal arterioles occurs 11–18 seconds after injection (*arterial phase*; see Fig 2-8A). Complete filling of the arteries and capillaries and the appearance of thin columns of dye along the walls of the larger veins (laminar flow; see Fig 2-8B) occur 1–3 seconds later (*arteriovenous phase*). Complete filling of the veins

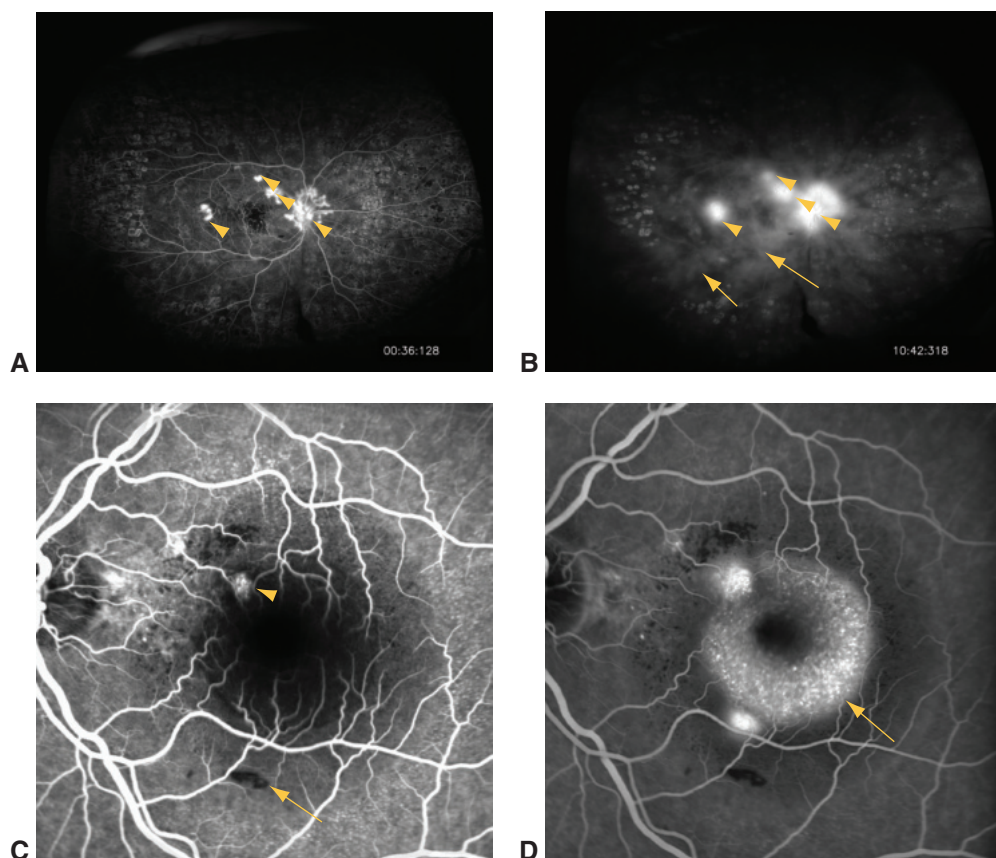


Figure 2-9 Examples of different patterns of hyperfluorescence and hypofluorescence in fluorescein angiography (FA). **A–B:** Wide-angle FA of an eye with posterior uveitis, retinal vasculitis, and retinal neovascularization. Retinal neovascularization of the optic nerve head and retina shows early leakage (*arrowheads, A*), which increases in the late frame (*arrowheads, B*). The early frame (**A**) shows macular nonperfusion, and the late frame (**B**) shows staining of laser scars in the periphery and inflammation-related deep multifocal leakage (*arrows*). **C–D:** FA of an eye with idiopathic polypoidal choroidopathy and drusen. The early frame (**C**) shows staining of the drusen, and both early and late (**D**) frames reveal leakage from the choroidal polyp (*arrowhead, C*). There is also blockage of fluorescence in the inferior macula in an area of hemorrhage (*arrow, C*). The late frame demonstrates pooling of fluorescein (*arrow, D*) under a serous retinal detachment centrally. Video 2-1 of initial dye-filling frames shows the onset of leakage from the polypoidal lesion in the superonasal macula. (Courtesy of Lucia Sobrin, MD.)

occurs over the subsequent 5–10 seconds (*venous phase*; see Fig 2-8C). The dye begins to recirculate 2–4 minutes after injection (*recirculation, or mid phase*). The *late phase*, occurring after 4–5 minutes (see Fig 2-8D), demonstrates the gradual elimination of dye from the retinal and choroidal vasculature.

The choroid may not fill uniformly. Any areas in the choroid that do not fill by the time the retinal circulation reaches the laminar flow stage are considered signs of abnormal choroidal filling. Once dye reaches the choriocapillaris, it leaks and stains Bruch membrane and the stroma, and details in the choroid are lost. Delay in the initial filling of the retinal vasculature is most commonly seen in patients with retinal vascular occlusions.

During FA, the fovea appears darker than the surrounding areas because of the presence of macular pigment; also, the RPE cells beneath the fovea are slightly taller and contain more melanin than peripheral RPE cells, and there are no retinal vessels.

Abnormalities observed with FA can be grouped into 2 main categories:

- hypofluorescence
- hyperfluorescence

In a fluorescein angiogram, reduction or absence of normal fluorescence is called *hypofluorescence* and is present in 2 major patterns:

- vascular filling defects
- blocked fluorescence

Vascular filling defects are abnormalities in which retinal or choroidal vessels fail to fill because of an intravascular obstruction that results in nonperfusion of an artery, vein, or capillary (see Fig 2-9A). These defects appear as either a delay in or complete absence of filling of the involved vessels. *Blocked fluorescence* occurs when excitation or visualization of the fluorescein is obstructed by fibrous tissue, pigment, or blood that blocks normal retinal or choroidal fluorescence in the area. The depth of a lesion can be easily determined by relating the level of the blocked fluorescence to details of the retinal circulation. For example, if lesions block the choroidal circulation but retinal vessels are present on top of this blocking defect, the lesions are located above the choroid and below the retinal vessels.

Hyperfluorescence refers to fluorescence that is abnormally excessive, typically extending beyond the borders of recognized structures. This manifests in several major patterns (Table 2-1; Video 2-1; see also Fig 2-9):

- leakage
- staining
- pooling
- transmission, or window, defect



VIDEO 2-1 Early-phase fluorescein angiogram.

Courtesy of Lucia Sobrin, MD.



Leakage is a gradual, marked increase in fluorescence over the course of the study and results from seepage of fluorescein molecules across the blood–retina barrier. When the outer blood–retina barrier is compromised, the dye traverses the RPE and enters the

Table 2-1 Hyperfluorescence Patterns: Differences in Fluorescence Brightness and Size as Fluorescein Angiography Progresses

Change Over Time	Leakage	Staining	Pooling	Window Defect
Brightness	Increase	Increase	Same/increase	Decrease
Size	Increase	No change, irregular shape	No change, regular shape (round or oval)	No change

subretinal space or neurosensory retina. When the inner blood–retina barrier is compromised, the dye leaks through vascular walls into the retinal parenchyma, fibrotic tissue, and cystoid spaces (Fig 2-10). Dye can also leak through the posterior blood–retina barrier (the RPE) and accumulate in the subretinal space, fibrotic tissue, or directly into the retina, if the external limiting membrane of the retina is compromised.

Staining refers to a pattern of hyperfluorescence in which the fluorescence increases in brightness through transit views and persists in late frames, but the borders remain intact throughout the study. Staining results from entry of fluorescein into a solid tissue or into material that retains the dye, such as a scar, drusen, blood vessel walls, optic nerve tissue, or sclera.

Pooling is the accumulation of fluorescein in a fluid-filled space in the retina or choroid (see Fig 2-9D). As fluorescein leaks into the space, the margins of the space trap the fluorescein and appear distinct, for example, as seen in an RPE detachment in central serous chorioretinopathy.

A *transmission defect*, or *window defect*, refers to a view of the normal choroidal fluorescence through a defect in the pigment of the RPE. In a transmission defect, hyperfluorescence occurs early, corresponding to filling of the choroidal circulation, and reaches its greatest brightness with the peak of choroidal filling. This fluorescence does not increase in brightness or size and usually fades in the late phases as the choroidal fluorescence becomes diluted by blood that does not contain fluorescein. The fluorescein remains in the choroid and does not enter the retina.

Multiple defects may be present in a diseased eye. For example, in an older adult patient with CNV, the choroid often shows segmental filling delays; hyperfluorescence is seen in the fovea because of the proliferation of vessels that leak; and there is late leakage from CNV (Fig 2-11).

Haug S, Fu AD, Johnson RN, et al. Fluorescein angiography: basic principles and interpretation.

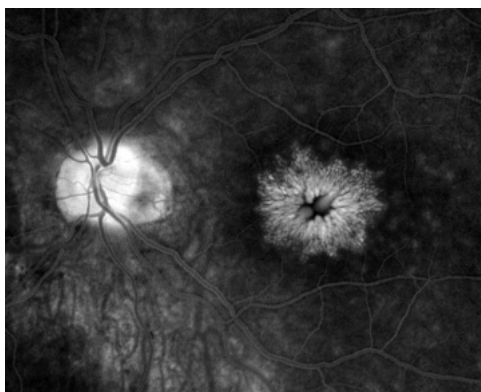
In: Schachat AP, Wilkinson CP, Hinton DR, Sadda SR, Wiedemann P, eds. *Ryan's Retina*.

6th ed. Vol 1. Elsevier; 2017:1–45.

Adverse effects of fluorescein angiography All patients injected with fluorescein experience a temporary yellowing of the skin and conjunctiva that lasts 6–12 hours. The most common adverse effects include nausea and vomiting (in approximately 5% of injections)

Figure 2-10 Fluorescein angiogram showing an eye with postsurgical cystoid macular edema. Fluorescein pools in the petaloid cystoid spaces within the central macula, and there is late staining of the optic nerve head.

(Courtesy of Richard F. Spaide, MD.)



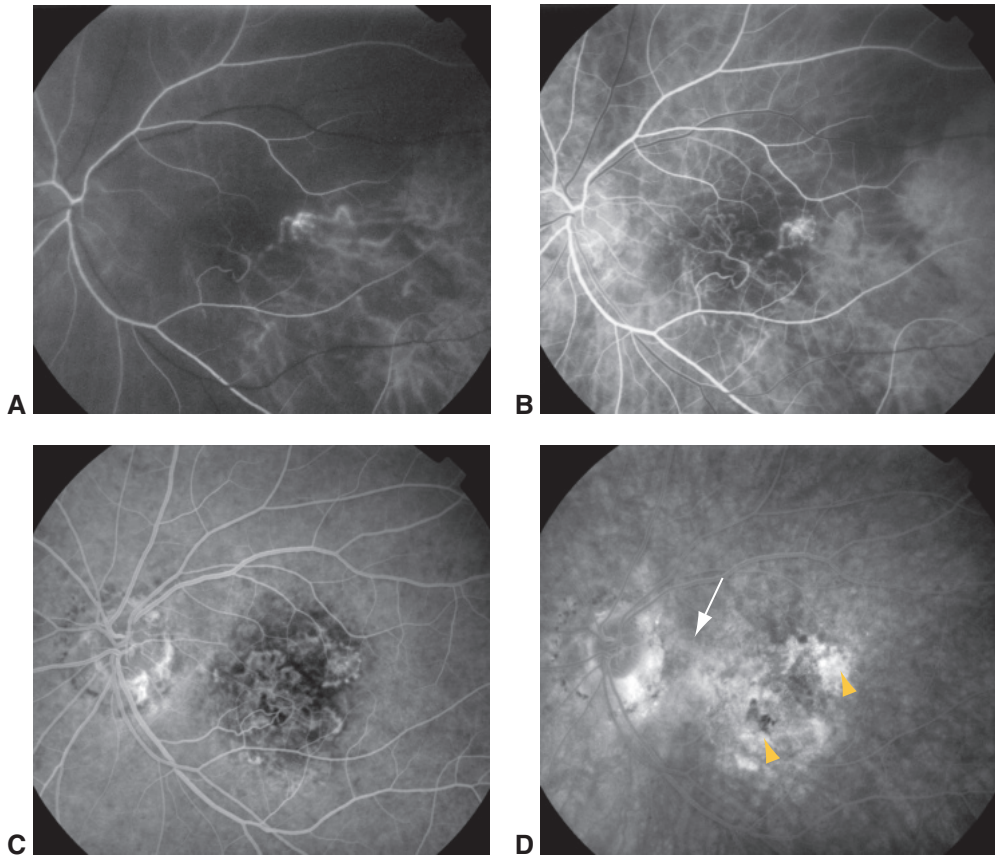


Figure 2-11 Fluorescein angiography of an eye with CNV. **A**, The choroid shows delayed filling. By the time dye reaches the central retinal artery, only a few choroidal vessels contain dye. **B**, In the early laminar-filling stage, a large portion of the choroid still shows poor filling. **C**, In the arteriovenous stage, the choriocapillaris appears uniformly filled. The clearly defined network of choroidal neovascular vessels is revealed in the central macula. **D**, The late-phase angiogram reveals leakage around the vessels with the earliest filling, an image consistent with classic CNV (*arrowheads*). There is also late staining and mild leakage from a poorly defined region (*arrow*), which is consistent with occult CNV. (*Courtesy of Richard F. Spaide, MD.*)

and the development of hives (also in approximately 5% of injections). The nausea passes in a few seconds without treatment. Hives, unless very mild, are usually treated with diphenhydramine. More serious adverse effects such as hypotension, shock, laryngeal spasm, or even death (approximately 1:222,000) have occurred, but only in rare instances. A physician should be on the premises when FA is occurring, and a crash cart should always be available. Prior urticarial reactions to fluorescein increase a patient's risk of having a similar reaction after subsequent injections; however, premedicating the individual with antihistamines, corticosteroids, or both appears to decrease the risk. Extravasation of the dye into the skin during injection can be painful, requiring application of ice-cold compresses to the affected area for 5–10 minutes. Close follow-up of the patient over hours or days until the edema, pain,

and redness resolve is advised. Although teratogenic effects have *not* been identified, many ophthalmologists avoid using FA in pregnant women in the first trimester unless absolutely necessary. In women who are lactating, fluorescein is transmitted to breast milk.

Indocyanine green angiography

Indocyanine green (ICG) is a water-soluble tricarbocyanine dye that is almost completely protein-bound (98%) after intravenous injection. Because the dye is protein-bound, diffusion through the small fenestrations of the choriocapillaris is limited. The intravascular retention of ICG, coupled with its low permeability, makes ICG angiography (ICGA) ideal for imaging choroidal vessels. ICG is metabolized in the liver and excreted into the bile. Both the excitation (790–805 nm) and emission peak (825–835 nm) are in the near-infrared range. See Figure 2-12 for an example of ICGA in a healthy eye.

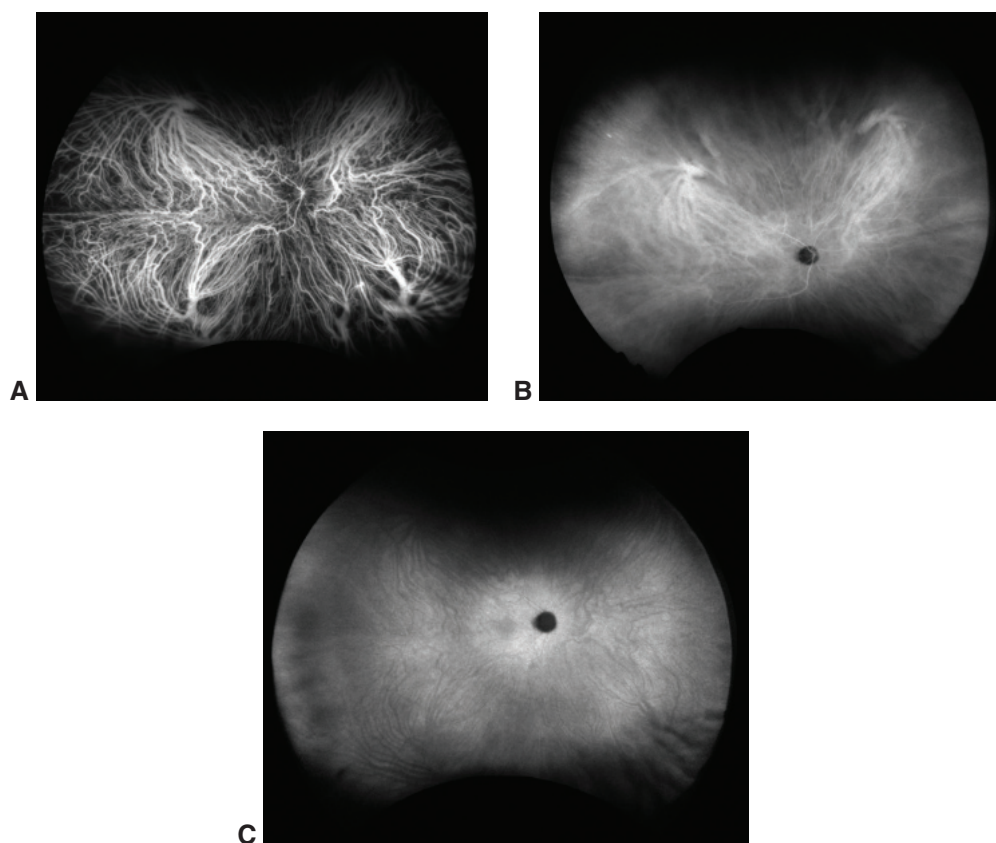


Figure 2-12 Wide-field indocyanine green angiography (ICGA) of a healthy eye. **A**, The early phase of ICGA is characterized by the first appearance of ICG dye in the choroidal circulation. Large choroidal arteries and veins and the retinal vasculature can be observed. **B**, Between 5 and 15 minutes after injection, the middle phase occurs; the choroidal veins become less distinct, and a diffuse homogeneous choroidal fluorescence is observed. Hyperfluorescence of the retinal blood vessels is diminished. **C**, In the late phase, which occurs approximately 15 minutes after injection, less retinal and choroidal vasculature detail is observed. (Courtesy of Lucia Sobrin, MD.)

ICGA is a valuable tool for identification of choroidal diseases (Video 2-2). It is used to image polypoidal choroidal vasculopathy, which is a common form of CNV (Fig 2-13), and to provide important information about the pathophysiology of type 3 neovascularization (also known as *retinal angiomatous proliferation*). With the use of ICGA, it was discovered that patients with drusen could have asymptomatic CNV. ICGA, particularly ultra-wide-field imaging, is helpful for diagnosing inflammatory diseases such as birdshot chorioretinopathy and multifocal choroiditis and panuveitis. Eyes with central serous chorioretinopathy show multifocal areas of choroidal vascular hyperpermeability when visualized with ICGA. However, use of this technique for diagnosing uveitis and central serous chorioretinopathy has been somewhat supplanted by autofluorescence imaging combined with EDI-OCT.



VIDEO 2-2 Early-phase indocyanine green angiogram.

Courtesy of Lucia Sobrin, MD.



Adverse effects of indocyanine green angiography Mild adverse events occur in fewer than 1% of patients. ICG is dissolved in a 5% sodium iodide solution (sodium iodide is an additive used in table salt). Although an iodine allergy is considered a relative contraindication to ICGA, there is no reason that a shellfish allergy should preclude the use of ICG. However, angiographic facilities should have emergency plans and establish protocols to manage complications associated with either fluorescein or ICG administration, including anaphylaxis. ICG may persist in the blood longer in patients with liver disease than in healthy patients.

Ultrasonography

Contact B-scan (also called *B-mode*) ultrasonography is the most common form of ultrasonography used in the clinic (Video 2-3). For the procedure, a 10-MHz probe is placed

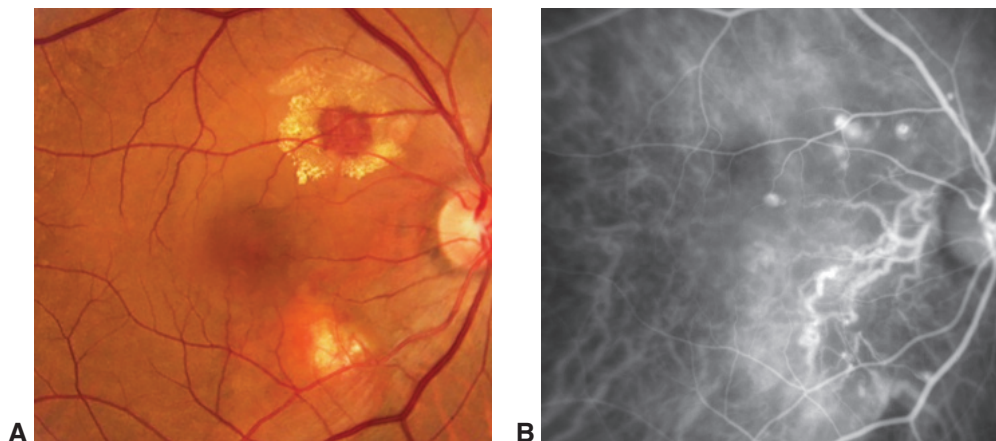


Figure 2-13 Polypoidal choroidal vasculopathy. **A**, Fundus photograph shows an area of lipid exudation surrounding a hemorrhage, large orange-colored vessels, and an area of decreased pigmentation inferotemporal to the optic nerve. **B**, The ICGA image clearly shows the sub-RPE vessels affected by polypoidal choroidal vasculopathy. (Courtesy of Richard F. Spaide, MD.)

on the patient's closed eyelid. A piezoelectric crystal within the transducer is used to send and receive sound waves for each A-scan. The ultrasound beam is approximately 1 mm wide at the level of the retina, which severely limits the lateral resolution. The axial resolution, which is the resolution along the axis of the ultrasound beam, is very different in the eye versus as measured with flat surfaces. This difference is due to the interaction of the eye's curved surfaces with the lateral summation of the signal.



VIDEO 2-3 Diagnostic B-scan ultrasonography: basic technique.

Courtesy of Patrick Lavalle, CDOS, and Lucia Sobrin, MD.



Contact B-scan ultrasonography is used to evaluate tumor thickness, detect foreign bodies, assess choroidal and retinal detachments, and analyze the vitreous (Figs 2-14, 2-15; Videos 2-4, 2-5). Optic disc drusen can be detected by observing small areas of bright reflection in the nerve that cause shadows. Careful ultrasonography allows retinal tears to be identified. Ultrasonography can also be used to image the eye during saccades, because imaging does not occur through the pupil. Information gained during dynamic examinations is helpful for examining the vitreous and for differentiating retinoschisis from true detachment. Contact B-scan ultrasonography can produce images through opaque media, although gases and silicone oil used for vitreoretinal surgery attenuate imaging substantially.



VIDEO 2-4 Contact B-scan ultrasonography showing choroidal effusions.

Courtesy of Patrick Lavalle, CDOS, and Lucia Sobrin, MD.



VIDEO 2-5 Contact B-scan ultrasonography showing a dislocated cataractous lens in the vitreous cavity.

Courtesy of Patrick Lavalle, CDOS, and Lucia Sobrin, MD.

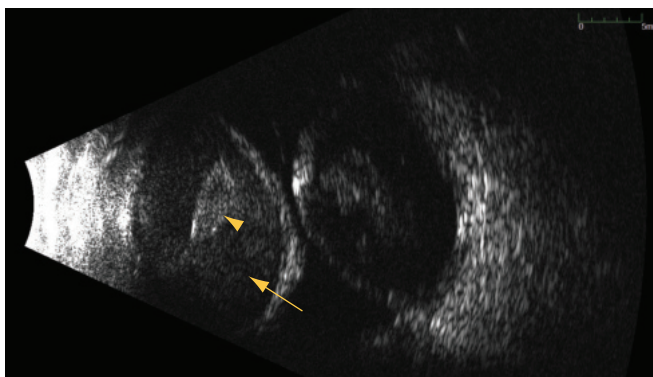


Figure 2-14 Contact B-scan ultrasonography shows massive choroidal effusions ("kissing choroidals," or appositional choroidal detachment) containing liquefied (*arrow*) and clotted (*arrowhead*) blood. The corresponding video (Video 2-4) shows the swirling of the blood and clot within the choroidals with eye movement. Dynamic evaluation of ocular contents during ultrasonography is a powerful tool. (*Courtesy of Patrick Lavalle, CDOS, and Lucia Sobrin, MD.*)

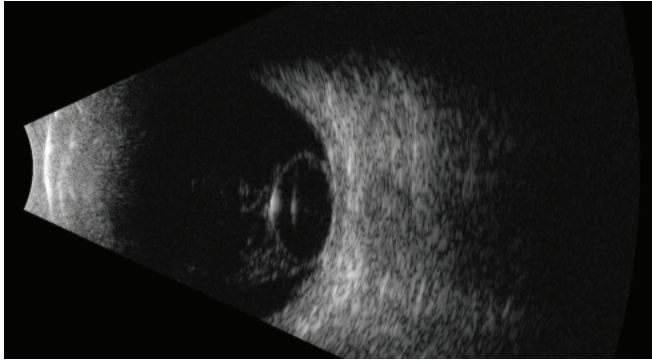


Figure 2-15 Dislocated cataractous lens in the vitreous cavity. B-scan view shows a strongly reflective ovoid lesion with moderately reflective internal signals consistent with a dislocated lens. The corresponding video (Video 2-5) shows the vitreous and lens and their interactions during eye movement. (Courtesy of Patrick Lavalle, CDOS, and Lucia Sobrin, MD.)

Ultrasound biomicroscopy (UBM) uses higher frequencies than B-scan ultrasonography and thus offers higher-resolution images but at the cost of decreased tissue penetration depth. The probe, typically 50 MHz, is contained inside a soft, water-filled bag that is placed against the patient's eye. UBM is used to evaluate the anterior chamber and ciliary body and can also be employed to visualize the vitreous insertion anteriorly. Typical uses in a retina practice include the evaluation of tumors, iris cysts, foreign bodies, anterior suprachoroidal effusions, cyclodialysis clefts, intraocular lens placement, and hyphemas.

Singh AD, Lorek BH. *Ophthalmic Ultrasonography*. Saunders; 2012.

CHAPTER 3

Retinal Physiology and Psychophysics



This chapter includes related videos. Go to www.aao.org/bcscvideo_section12 or scan the QR codes in the text to access this content.

Highlights

- Electrophysiologic testing provides objective measures of visual system function, which are interpreted in conjunction with structural imaging data; normal structure should not be assumed to mean normal function.
- Multifocal electroretinography (ERG) can produce a topographic ERG map of central retinal cone system function, which can help the clinician diagnose macular dysfunction and assess the extent of central retinal involvement in generalized retinal disease.
- The electro-oculogram assesses the health and function of the retinal pigment epithelium.
- Though nonspecific, visual evoked potentials can objectively demonstrate normal function in the presence of symptoms that suggest otherwise.
- Psychophysical tests can be highly sensitive, but they are subjective and do not provide information about specific levels of the visual system.

Electrophysiologic Testing

Most electrophysiologic tests use evoked potential techniques in which a controlled stimulus is used to evoke an electrophysiologic response. Different techniques can be used to assess the function of the majority of the visual system, extending from the retinal pigment epithelium (RPE) to the primary visual cortex (Table 3-1).

Electrophysiologic testing provides objective measures of visual system function, which are interpreted in conjunction with structural imaging data; normal structure should not be assumed to mean normal function. In order to accurately interpret the data obtained from electrophysiologic testing, the clinician needs to know the origin of the signals generated during testing. The test findings can then be correlated to the patient's underlying pathophysiology. In addition to diagnostic uses, electrophysiologic data are used in objective monitoring, either of disease progression or the efficacy of treatment,

Table 3-1 Electrophysiologic Testing

Electrophysiologic Test	Level of Visual System and Characteristic Tested
Full-field electroretinogram (ffERG)	Generalized retinal function under light- and dark-adapted conditions
Dark-adapted 0.01 (weak flash)	On-bipolar cells (inner nuclear layer) of rod system; the only test that selectively monitors rod system function
Dark-adapted 3.0 (standard flash)	Mixed rod-cone response (rod dominant)
Dark-adapted 10.0/30.0 (strong flash)	Mixed rod-cone response
Oscillatory potentials	Primarily amacrine cell signaling
Light-adapted 3.0 flash	Cones and bipolar cells
Light-adapted 3.0 30-Hz flicker	Generalized cone system function
Multifocal ERG (mfERG)	Measure of cone system function over central 40°–50° of the visual field
Pattern ERG (PERG)	Macular retinal ganglion cell function
Electro-oculogram (EOG)	Generalized retinal pigment epithelium function
Visual evoked potential (VEP)	Function of the entire visual pathway from the retina to area V1 of the visual cortex

and/or as both an outcome measure and an index of safety in the evaluation of novel therapeutic interventions.

A thorough patient history and careful ophthalmic examination help the clinician determine the most appropriate tests to employ; those tests should then be performed using standardized protocols. The International Society for Clinical Electrophysiology of Vision (ISCEV) publishes minimum standards for performing routine tests, thus enabling meaningful interlaboratory comparison and literature searches.

Brigell M, Bach M, Barber C, Moskowitz A, Robson J; Calibration Standard Committee of the International Society for Clinical Electrophysiology of Vision. Guidelines for calibration of stimulus and recording parameters used in clinical electrophysiology of vision. *Doc Ophthalmol*. 2003;107(2):185–193.

Standards, guidelines and extended protocols. International Society for Clinical Electrophysiology of Vision. Accessed January 17, 2022. <https://iscev.wildapricot.org/standards>

Electroretinography

The clinical electroretinogram (ERG) provides an objective measure of the electrical activity of the retina, usually evoked by a brief flash of light. ERGs are recorded with electrodes that contact the cornea or bulbar conjunctiva or with skin electrodes attached to the lower eyelids. Several types of corneal electrodes can be used, including contact lens, fiber, jet, and gold foil electrodes (Video 3-1). The 3 main types of electroretinography—full-field (Ganzfeld), multifocal, and pattern—are discussed in the following sections.



VIDEO 3-1 Performing electroretinography.
Courtesy of Shriji Patel, MD, MBA.



Full-Field (Ganzfeld) Electroretinography

In full-field electroretinography, a Ganzfeld bowl uniformly illuminates the entire retina with a full-field luminance stimulus; the Ganzfeld also provides a uniform background for photopic adaptation and photopic ERG recording. Regular calibration of flash strength is required for clinical accuracy. Figure 3-1 shows typical full-field ERG (ffERG) responses; however, normal values vary with recording techniques, and each laboratory must establish its own normative data (Video 3-2). Even with standardization, variations in the type of electrode and specific equipment used will affect the test results.



VIDEO 3-2 Interpreting an electroretinogram.
Courtesy of Milam A. Brantley, MD, PhD.



The pupils are dilated to maximize retinal illumination. In most laboratories, the patient is dark-adapted while the pupils are dilating, the electrodes are positioned under dim red light, and then stimulation commences by using an interstimulus interval sufficient to allow the retina to recover between flashes (from 2 seconds for low intensities up to 20 seconds for high intensities). Many laboratories record responses to a series of increasing stimulus strengths. The patient is then light-adapted (using standardized background intensity and adaptation time), and photopic testing is performed, in which the stimuli are delivered under rod-suppressing background illumination.

The ISCEV standard ffERG consists of 6 different responses (see Fig 3-1A). The nomenclature used for these is based on the flash strength as measured in candela-seconds per square meter and the adaptive state of the eye (ie, dark-adapted [DA] or light-adapted [LA]); older terms are given in parentheses in the following list. Measurement of the ERG focuses on the size and timing of the major components, as indicated in Figure 3-1.

1. *DA 0.01 (rod-specific)*: In this response, a b-wave arises in the on-bipolar cells (BPCs) (inner nuclear layer) of the rod system. A reduction in this response identifies dysfunction within the rod system, but because it arises at an inner retinal level, this response cannot differentiate between dysfunction at the level of the photoreceptor and inner retinal dysfunction. It therefore acts as a measure of rod system sensitivity.
2. *DA 3.0 (mixed rod-cone)*: This response consists of an a-wave and a b-wave. The a-wave at this flash strength usually has 2 peaks between approximately 15 and 21 milliseconds, either of which may be prominent. Because only approximately the first 8 milliseconds of the DA a-wave reflects photoreceptor hyperpolarization, the ISCEV standard includes additional brighter flash testing for better diagnostic specificity.
3. *DA 10.0/30.0*: At either of these flash strengths, the a-wave has an easily measurable peak, and most of the a-wave reflects photoreceptor function. Consequently, this response can localize dysfunction to either a photoreceptor or an inner retinal level. Thus, a reduced DA 0.01 response accompanied by marked reduction in the a-wave of the DA 10.0/30.0 response indicates photoreceptor dysfunction. However, if the a-wave amplitude is normal (see Fig 3-1A) or near normal and the b-wave amplitude is lower than that of the a-wave (known as a negative or electronegative ERG waveform), dysfunction occurs post-phototransduction, at an inner retinal level.

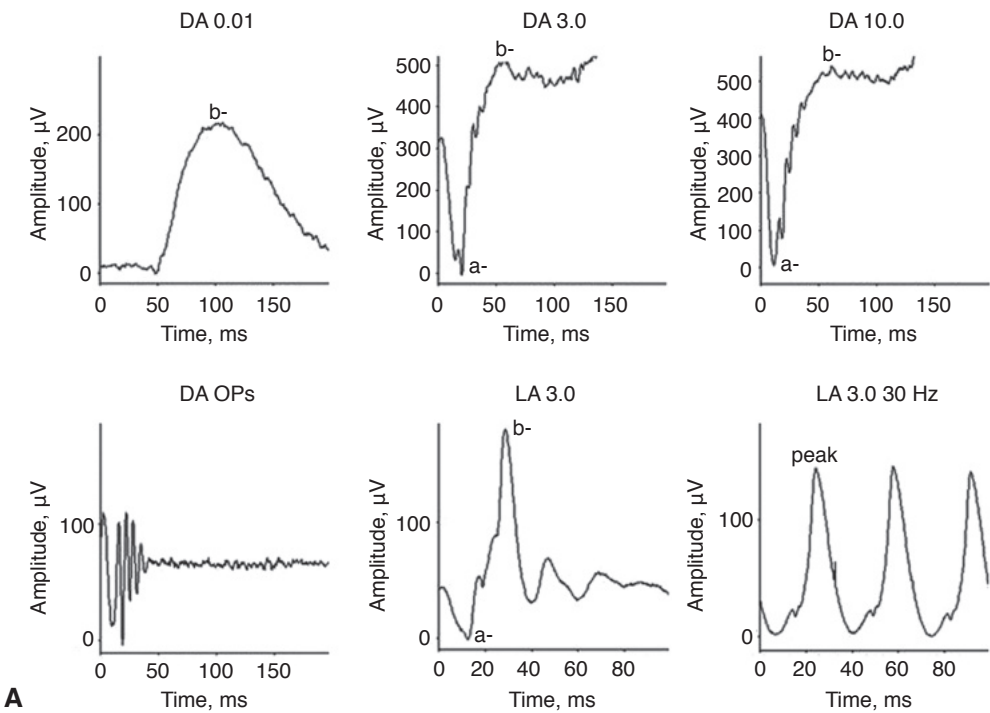


Figure 3-1 A, Basic full-field electroretinogram (ffERG) responses as defined by the International Society for Clinical Electrophysiology of Vision. The amplitude and peak times are typical, but normal values must be established for each laboratory using local techniques. a- = a-wave; b- = b-wave; DA = dark-adapted; LA = light-adapted; OPs = oscillatory potentials; numbers following abbreviations denote stimulus intensity (in candela-seconds per square meter). **B**, Standard ffERG setup. (Part A courtesy of Graham E. Holder, PhD; part B courtesy of Shriji Patel, MD, MBA, and Rocky Munn.)

4. *Oscillatory potentials*: These small oscillations on the ascending limb of the b-wave probably arise largely in the amacrine cells and can be made more visible by filtering. They are reduced in retinal ischemic states and in most cases of congenital stationary night blindness, but overall, they have limited diagnostic value.
5. *LA 3.0 (photopic single-flash)*: This ERG response is obtained by stimulating with a flash superimposed on a rod-suppressing background. The a-wave relates to function in the cone photoreceptors and off-BPCs. The b-wave arises as a synchronized component in on- and off-BPCs. This response thus enables some localization of cone system dysfunction.
6. *LA 3.0 30 Hz (photopic flicker)*: The temporal resolution of the rod system is poor, and this response arises in the cone system. It is the more sensitive measure of cone system dysfunction but allows no anatomical specificity. Both timing and amplitude are important parameters; delay in the flicker ERG response is a sensitive measure of generalized retinal cone system dysfunction, whereas reduced amplitude but normal peak time (see Fig 3-1A) usually indicates restricted loss of function.

Several factors influence the size and timing of a normal ERG response, one of which is pupil size; thus, pupil diameter should always be measured at the start of the test. Because ERG amplitude declines with age, age-related controls are necessary. Although newborns have smaller ERG responses with simplified waveforms, the responses mature rapidly, reaching adult values in the first year of life. The ERG is relatively insensitive to refractive error; highly myopic eyes have lower-amplitude ERGs but without the peak-time delay usually associated with inherited retinal degeneration. Similarly, ERG response is generally minimally affected by media opacity such as cataract or vitreous hemorrhage.

As a measure of a biological signal, ERGs have inherent noise. However, a reduction in amplitude of more than 25% over time is usually considered significant—even if the amplitudes remain within the reference range (“normal range”). For peak-time measures, a change greater than 3 milliseconds is regarded as significant for cone-derived response a- or b-waves and brighter-flash DA a-waves; a change greater than 6 milliseconds is significant for DA b-waves.

In general, ERG peak-time shift suggests generalized dysfunction, whereas simple amplitude reduction suggests restricted loss of function such as may occur in a partial retinal detachment (loss of function in the detached area of retina but normal function in the attached retina), branch vascular occlusion, regional uveitic damage, or restricted (“sector”) forms of retinitis pigmentosa (RP). Timing is often best assessed using the 30-Hz flicker ERG peak time. Generalized inflammatory disease, such as posterior uveitis, may be associated with delay but preservation of amplitude. Indeed, marked 30-Hz flicker delay with a high amplitude almost always indicates an inflammatory etiology.

Figure 3-2 presents examples of ERG patterns found in association with specific disorders. As the ffERG shows the mass response of the entire retina to flash stimuli, the responses will be normal when dysfunction is confined to the macula. Even though the central macula is cone dense, most retinal cones lie outside the macula; consequently, the macula contributes little to a ffERG. Because abnormal photopic ERG responses indicate cone dysfunction outside the macula, ERG testing can help the clinician distinguish between a macular dystrophy phenotype (normal ffERG response) and a cone or cone-rod dystrophy phenotype (abnormal ERG response), which may have more serious visual implications for the patient. For example, in some patients, *ABCA4* retinopathy (eg, Stargardt disease, fundus

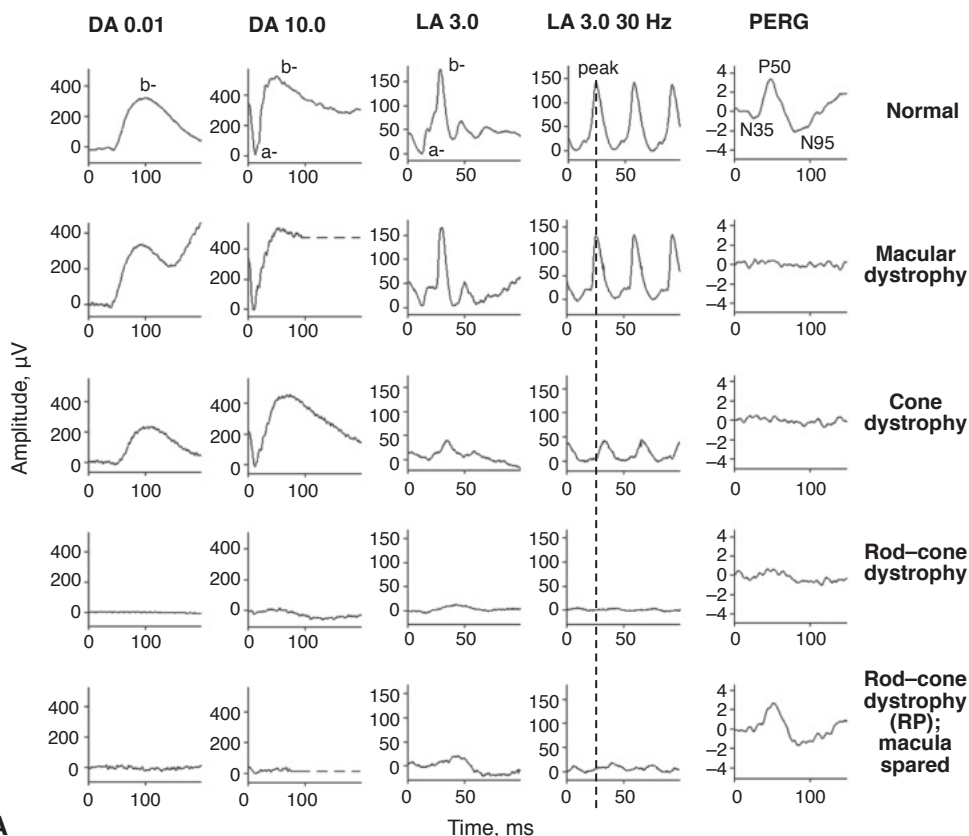


Figure 3-2 ERG findings in various disorders. **A, Normal:** Typical waveforms are shown at the top. The timing of the 30-Hz flicker ERG is shown by the vertical *dashed line*. For all responses, the flash occurs at time 0 ms. **Macular dystrophy:** Full-field ERG (ffERG) responses are all normal, but the pattern ERG (PERG) response is undetectable. **Cone dystrophy:** Dark-adapted (DA) 0.01 (rod-specific) and DA 10.0 ERG responses are normal; light-adapted (LA) 3.0 30-Hz (photopic flicker) and LA 3.0 (single-flash) ERG responses are reduced and delayed; the PERG response is subnormal, indicating macular involvement. **Rod-cone dystrophy:** Retinitis pigmentosa (RP) with macular involvement. All ERG responses are markedly subnormal, with rod ERGs more affected than cone ERGs; severe reduction of the DA 10.0 a-wave, indicating photoreceptor disease; and delayed 30-Hz and LA 3.0 cone ERGs, indicating generalized cone system dysfunction. Abnormal PERG response shows macular involvement. **Rod-cone dystrophy (RP); macula spared:** ffERGs show an abnormal rod-cone response pattern similar to that shown directly above, but a normal PERG response shows macular sparing.

(Continued)

flavimaculatus) can be associated with severe generalized cone and rod system dysfunction. If the ffERGs of these patients are normal at presentation, the dysfunction is confined to the macula and the ERGs have prognostic value: 80% of such patients will still have normal ffERG responses at 10-year follow up.

Fujinami K, Lois N, Davidson AE, et al. A longitudinal study of Stargardt disease: clinical and electrophysiologic assessment, progression, and genotype correlations. *Am J Ophthalmol.* 2013;155(6):1075–1088.

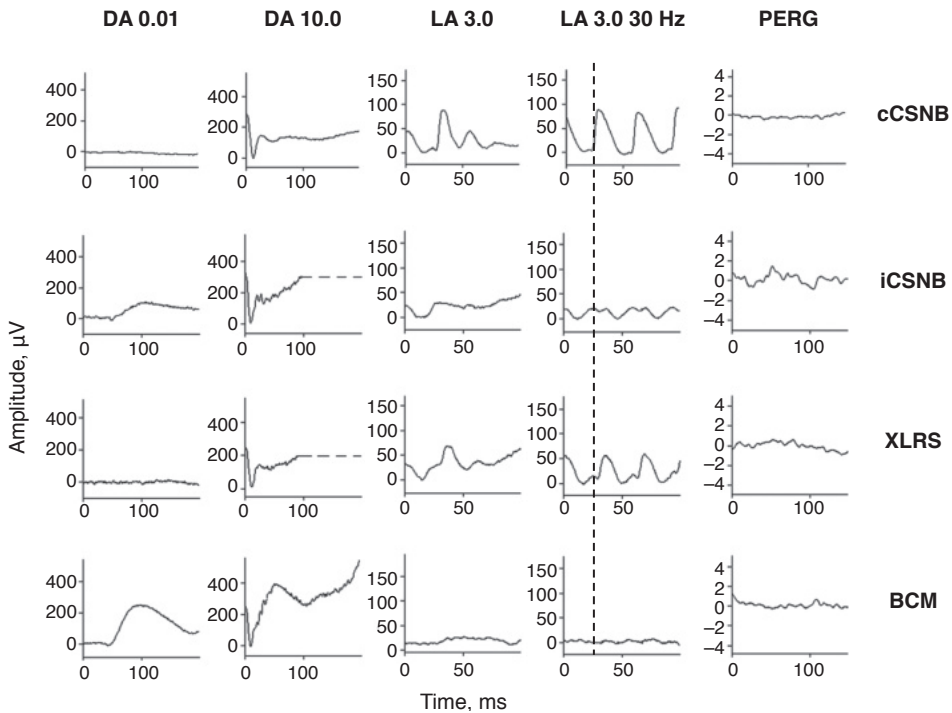


Figure 3-2 (continued) B, cCSNB ("complete" congenital stationary night blindness): Findings show loss of on-pathway function at a postreceptoral level. DA 0.01 response is undetectable; DA 10.0 response is profoundly electronegative, with the normal a-wave reflecting normal photoreceptor function and the relatively marked b-wave reduction indicating inner retinal disease; 30-Hz flicker ERG shows only minor changes in waveform and mild delay; LA 3.0 ERG shows changes diagnostic of loss of cone on-pathway function but sparing of the off-pathway. The a-wave commences normally but then shows a broadened trough. The b-wave rises sharply, with loss of the photopic oscillatory potentials, and marked reduction in the b-wave:a-wave ratio. The PERG response is markedly subnormal. **iCSNB** ("incomplete" CSNB): DA 0.01 response is subnormal but detectable; DA 10.0 response is markedly electronegative; 30-Hz flicker ERG response is markedly subnormal, showing delay and a characteristic triphasic waveform; LA 3.0 ERG shows a subnormal a-wave and a markedly subnormal b-wave, reflecting involvement of both on- and off-cone pathways; the PERG response is subnormal. **XLRS** (X-linked retinoschisis): DA 0.01 response is severely reduced; DA 10.0 response is profoundly electronegative; 30-Hz flicker ERG shows delay; LA 3.0 ERG shows delay and marked reduction in the b-wave:a-wave ratio; the PERG response is markedly subnormal. **BCM** (blue-cone [S-cone] monochromatism): DA 0.01 and DA 10.0 ERG responses are normal; 30-Hz flicker ERG response is virtually undetectable; LA 3.0 response shows only a small b-wave at approximately 50 ms, consistent with an S-cone origin; PERG response is undetectable. (Courtesy of Graham E. Holder, PhD.)

Multifocal Electroretinography

Multifocal electroretinography can produce a topographic ERG map of central retinal cone system function, which can help the clinician diagnose macular dysfunction and assess the extent of central retinal involvement in generalized retinal disease (Fig 3-3). The stimulus consists of multiple hexagons, smaller in the center than the periphery to reflect cone photoreceptor density, each of which flashes in a pseudorandom sequence.

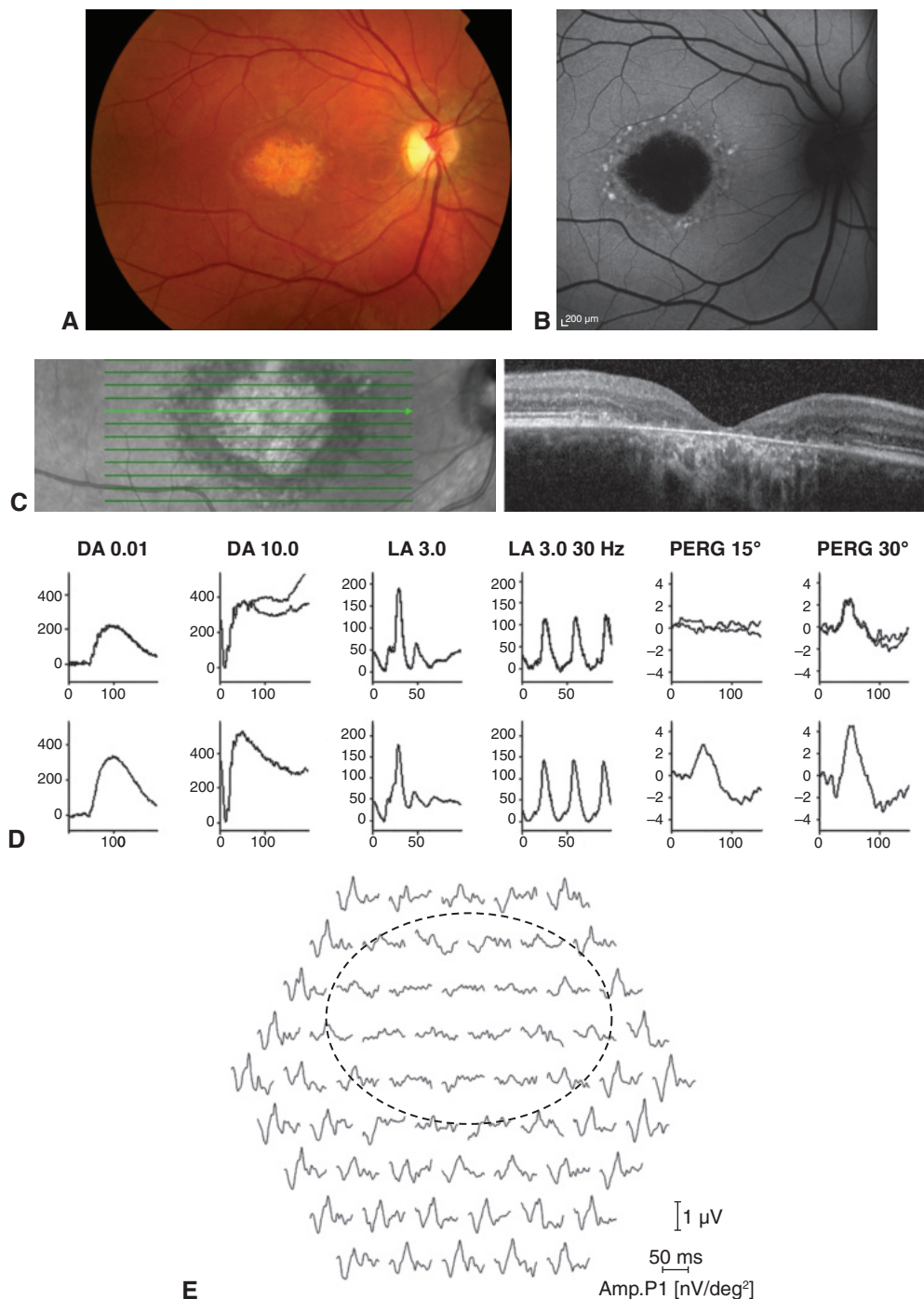


Figure 3-3 Multifocal ERG (mfERG), full-field ERG (ffERG), and pattern ERG (PERG) from a patient with *ABCA4* retinopathy (Stargardt disease; fundus flavimaculatus) show the importance of fixation in mfERG recording and interpretation. **A–C**: Macular atrophy centralized on the fovea. **A**, Fundus photograph. **B**, Fundus autofluorescence image. **C**, Near-infrared and spectral-domain optical coherence tomography (SD-OCT) images. **D**, ffERG responses are normal (see Fig 3-1 for explanation of abbreviations; x-axis = ms; y-axis = μV); PERG response to a 15° field is undetectable; however, PERG response to a 30° field is present but subnormal. **E**, mfERG shows an area of dysfunction that is localized but apparently not around the fovea, which simply reflects the eccentric fixation often present in a patient with a central scotoma. (Courtesy of Graham E. Holder, PhD.)

Cross-correlation techniques are used to calculate the small ERGs corresponding to each hexagon. The resulting multifocal ERG (mfERG) waveforms have an initial negative deflection (termed *N1*), followed by a positive peak (termed *P1*) and a second negative deflection (termed *N2*). The *N1* deflection derives from the same cells that contribute to the a-wave of the LA fERG (ie, cone photoreceptors and cone BPCs). The *P1* and *N2* deflections include contributions from the cells that lead to the LA b-wave and oscillatory potentials.

The overall stimulus field size is usually approximately 40°–50°. For patients with stable and accurate fixation (essential for obtaining technically satisfactory and clinically meaningful results), multifocal electroretinography can objectively determine the spatial distribution of macular dysfunction. The mfERG is less sensitive than the pattern ERG for disorders such as cystoid macular edema, in which primary photoreceptor dysfunction is not the main pathophysiologic feature; these 2 tests can provide complementary information.

Clinicians have increasingly used mfERGs in the diagnosis of hydroxychloroquine toxicity (Fig 3-4). In affected patients, there may be relative sparing of the response to the central foveal hexagon but loss of responses to the ring of surrounding hexagons; a ring analysis may be beneficial. However, it has been demonstrated that Asian patients may show an extramacular pattern of damage, which would not be detected by multifocal electroretinography.

Hoffmann MB, Bach M, Kondo M, et al. ISCEV standard for clinical multifocal electroretinography (mfERG) (2021 update). *Doc Ophthalmol*. 2021;142(1):5–16.

Marmor MF, Kellner U, Lai TY, Melles RB, Mieler WF; American Academy of Ophthalmology. Recommendations on screening for chloroquine and hydroxychloroquine retinopathy (2016 revision). *Ophthalmology*. 2016;123(6):1386–1394.

Pattern Electroretinography

The pattern ERG (PERG) captures the retinal response to an isoluminant pattern-reversing checkerboard stimulus presented to the macula; the stimulus is therefore primarily alternating contrast. The image must be in focus on the macula, and electrodes that spare the optics of the eye are used for recording; corneal/contact lens electrodes are not suitable. The responses are small, and signal averaging is needed. However, when technical factors are considered, PERG reliability is similar to that of fERG. There are 2 main components, P50 and N95, with most patients showing an earlier negative component, N35. N95 arises in the retinal ganglion cells (RGCs) and thus provides a direct measure of central RGC function. The P50 component depends on macular photoreceptor function, even though approximately 70% of it arises in the RGCs; the amplitude of P50 is clinically useful as an objective index of macular function. Because the PERG response is evoked by a stimulus similar to that used in recording the visual evoked potential (VEP; discussed later in this chapter), knowledge of a patient's PERG findings can help the clinician more accurately interpret abnormal VEP findings. The PERG is also useful in diagnosing primary ganglion cell disease such as dominantly inherited optic atrophy or Leber hereditary optic neuropathy.

Holder GE. Pattern electroretinography (PERG) and an integrated approach to visual pathway diagnosis. *Prog Retin Eye Res*. 2001;20(4):531–561.

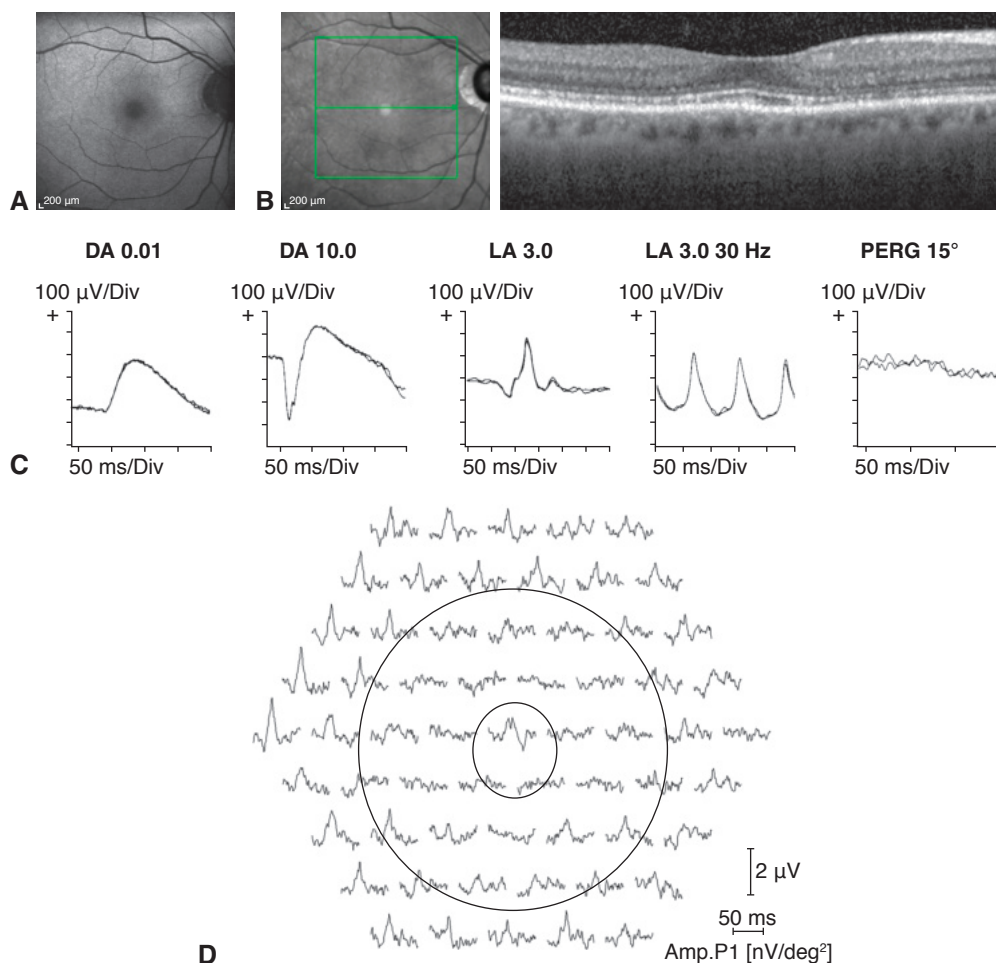


Figure 3-4 mfERG, ffERG, and PERG from a patient with hydroxychloroquine toxicity. **A**, Fundus autofluorescence image. **B**, Near-infrared and SD-OCT images. The changes shown on OCT are less marked, particularly temporal to the fovea, than may have been predicted by the degree of functional vision loss. **C**, ffERG responses are normal (see Fig 3-1 for explanation of abbreviations); PERG response to a 15° field is barely detectable. **D**, The mfERG shows marked abnormality with some sparing of the response to the central foveal hexagon (*inner circle*) but loss of parafoveal responses (*outer circle*). (Courtesy of Graham E. Holder, PhD.)

Clinical Considerations

The ERG provides objective data on retinal function and is therefore important in the diagnosis, management, and follow-up of retinal disease. Symptomatic indications include nyctalopia, which requires distinguishing between the potentially blinding rod-cone dystrophies and the relatively benign congenital stationary night blindness (CSNB). The dystrophies are associated with markedly abnormal a-waves in DA bright-flash ERGs; CSNB is usually associated with a normal a-wave and a negative ERG waveform (see Fig 3-2). Other symptomatic indications include photophobia, which indicates generalized cone dysfunction (as

in cone dystrophy), and photopsia or shimmering, which can sometimes signal the development of autoimmune retinopathy, possibly paraneoplastic. The ERG can be used in the assessment and monitoring of inflammatory disorders such as birdshot chorioretinopathy. The ERG facilitates an objective assessment of disease severity, with clinicians using the results in making decisions on when and how to treat; following treatment, the ERG provides a valuable measure of treatment effectiveness that is more sensitive than conventional clinical parameters. In addition, the ERG can be used to monitor for early drug-related retinal toxicity, as can occur with systemically administered chemotherapy.

ERGs must always be interpreted in a clinical context. Results are diagnostic (pathognomonic) for only 3 relatively rare inherited disorders: bradyopsia (mutation in *RGS9* or *R9AP*), enhanced S-cone syndrome (*NR2E3*), and “cone dystrophy with supernormal rod ERG” (*KCNV2*).

The ERG can be useful in assessing patients with vascular disease. In patients with central retinal artery occlusion, the ERG is characteristically negative (b-wave amplitude is smaller than the a-wave amplitude), reflecting the dual blood supply to the retina; the photoreceptors are supplied via the choroidal circulation, but the central retinal artery supplies the inner nuclear layer. Thus, the b-wave amplitude is reduced but the a-wave is relatively preserved. In eyes with central retinal vein occlusion, a negative ERG or delay in the 30-Hz flicker response suggests significant ischemia.

The ERG can also be helpful in determining the carrier state of individuals with X-linked disease. For example, carriers of X-linked RP usually have abnormal ERG findings that reflect lyonization, even with a healthy-appearing fundus. However, in choroideremia, carriers usually exhibit a normal ERG response despite an abnormal fundus appearance (also resulting from lyonization).

Electroretinography is suitable for use in children of all ages, providing objective functional data for patients who may not be able to describe their symptoms. Interpretation of pediatric ERGs involves special consideration, as adult ERG values are not reached until 6–9 months of age and general anesthesia, which may be necessary depending on the child’s age, can affect the sensitivity of the assessment.

Johnson MA, Marcus S, Elman MJ, McPhee TJ. Neovascularization in central retinal vein occlusion: electroretinographic findings. *Arch Ophthalmol*. 1988;106(3):348–352.

Vincent A, Robson AG, Holder GE. Pathognomonic (diagnostic) ERGs. A review and update. *Retina*. 2013;33(1):5–12.

Electro-oculography

Electro-oculography assesses the health of the RPE and its interaction with the photoreceptors by measuring the corneo-retinal standing potential during dark adaptation and light adaptation. The standing potential, which reflects the voltage differential across the RPE, is positive at the cornea. Estimates of trans-RPE potential range from 1 to 10 mV.

For the electro-oculographic (EOG) test, the patient makes fixed 30° lateral eye movements for approximately 10 seconds each minute during 15 minutes of dark adaptation, and again during a 12-minute period of light adaptation (Fig 3-5). The amplitude of the signal

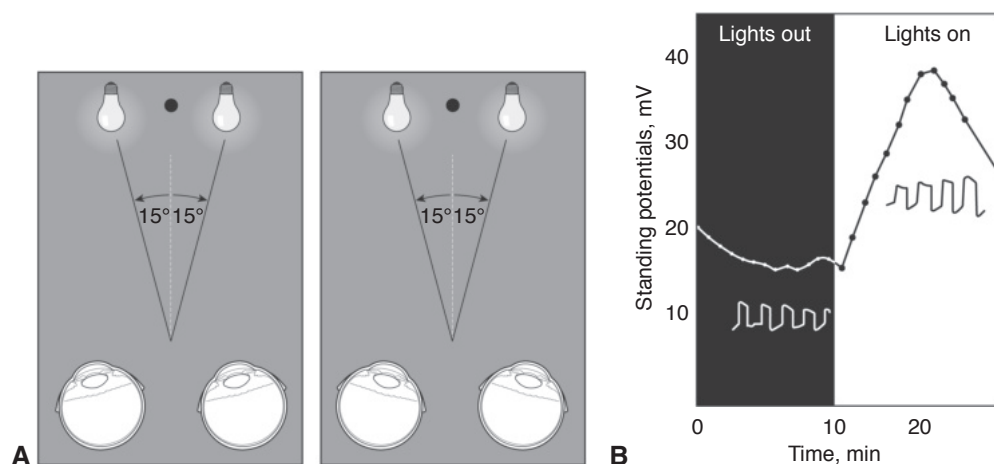


Figure 3-5 The clinical electro-oculogram (EOG). **A**, After electrodes are fixed to an area near the medial and lateral canthi, the patient is asked to alternate their gaze on 2 fixation targets (dimly lit lights), which are separated by a distance that results in a 30° horizontal eye movement. As each eye moves, the voltage between skin electrodes varies in proportion to the size of the standing potential of the eye (the voltage differential across the retinal pigment epithelium). **B**, Plot of the amplitude of the oscillations. As the eyes turn toward the cornea-positive electrodes, an increased potential is measured; thus, the slow back-and-forth motions result in the relatively square-looking voltage curve. During testing, the standing potential diminishes to a minimum in the dark (the *dark trough*) and then rises to a maximum after the light is turned on (the *light peak*). In clinical practice, the EOG result is usually reported as the ratio of the amplitude of the light peak to that of the dark trough expressed as a percentage, the *Arden index* or *ratio*. (Illustrations by Mark Miller.)

recorded between electrodes positioned near the medial and lateral canthi reaches a minimum after approximately 12 minutes of dark adaptation—the dark trough—and a maximum at approximately 8 minutes of light adaptation—the light peak. The ratio of the amplitude of the light peak to that of the dark trough is expressed as a percentage (the *Arden index* or *ratio*). A normal light rise will be greater than 170% and requires fully functioning photoreceptors in contact with a normally functioning RPE. The light peak reflects progressive depolarization of the RPE basal membrane via mechanisms that are not fully understood; however, the protein bestrophin is implicated in the final opening of chloride channels.

Any disorder of rod photoreceptor function will affect an EOG, and the light rise is typically severely reduced in an EOG of any widespread photoreceptor degeneration, including RP. However, the EOG is principally used in clinical practice in the diagnosis of acute zonal occult outer retinopathy (AZOOR) and diseases due to mutations in bestrophin 1 (*BEST1*) (see Chapter 12). In patients with Best disease, a dominantly inherited disorder caused by mutations in *BEST1*, a severely reduced or absent EOG light rise is accompanied by a normal fERG response. Severe loss of the EOG light rise is also seen in patients with autosomal recessive bestrophinopathy (ARB). ARB is a progressive retinal dystrophy and, unlike Best disease, requires biallelic mutation. Affected patients have fERG responses that are abnormal but not sufficiently so to explain the degree of EOG response abnormality. Also, unlike Best disease carriers, ARB carriers do not show an EOG response abnormality. In patients with adult vitelliform macular dystrophy, the EOG findings may be mildly subnormal but are not reduced as much as they are in Best disease (Fig 3-6).

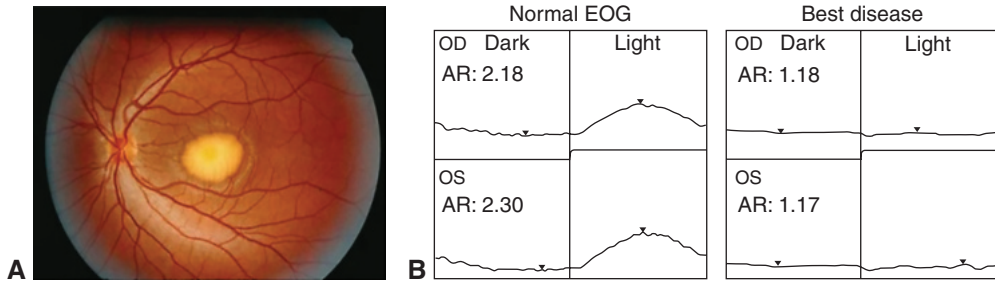


Figure 3-6 Best disease. **A**, Fundus photograph shows an egg yolk–like vitelliform macular lesion. **B**, The EOG demonstrates a reduced light peak to dark trough (Arden) ratio compared with a normal EOG. AR = Arden ratio. (From Gundogan FC, Yolcu U. *Clinical ocular electrophysiology*. In: Davey P, ed. *Ophthalmology: Current Clinical and Research Updates*. IntechOpen; 2014. doi:10.5772/57609)

Arden GB, Constable PA. The electro-oculogram. *Prog Retin Eye Res*. 2006;25(2):207–248.

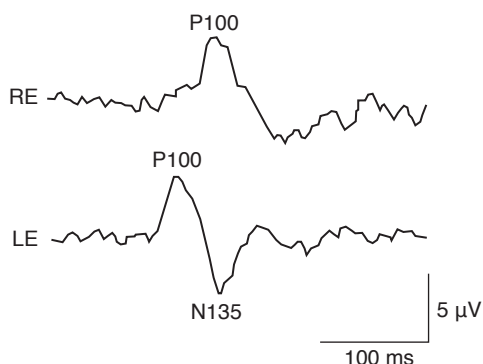
Burgess R, Millar ID, Leroy BP, et al. Biallelic mutation of *BEST1* causes a distinct retinopathy in humans. *Am J Hum Genet*. 2008;82(1):19–31.

Visual Evoked Potentials

Visual evoked potential (VEP; also called *visual evoked cortical potential [VECP]* or *response [VER]*) testing measures electrical signals produced in the brain in response to stimulation of the retina by either light flashes (*flash VEP*) or patterned stimuli, usually a pattern-reversing black-and-white checkerboard displayed on a monitor (*pattern-reversal VEP* or *pattern onset-offset VEP*). The signals are recorded via electrodes placed on the occipital scalp. The VEP is extracted from the larger background electroencephalogram by averaging the responses to multiple reversals or flashes. Pattern-reversal VEPs have a similar waveform across a population and a remarkably consistent timing; amplitudes show greater variability. Flash VEPs are far more variable across a population but can be useful when clinicians compare eyes or hemispheric responses in the same patient; hemispheric comparison requires multiple recording channels. A normal pattern-reversal VEP (Fig 3-7) contains a major positive component at approximately 100 milliseconds, P100. Measurement is usually taken of P100 amplitude and peak time (sometimes called *latency*).

In adults, VEPs are often used to demonstrate optic nerve conduction delay, particularly in patients with suspected multiple sclerosis; patients with demyelinating optic neuritis almost invariably show VEP delay even when vision recovers (see Fig 3-7). However, there can be subclinical delay in patients without any history or signs of optic neuropathy. In most optic nerve diseases, VEP delay is present, but a VEP abnormality can be confined to amplitude (interocular asymmetry), for example, as in patients with nonarteritic anterior ischemic optic neuropathy. It is important to note that a delayed VEP is not diagnostic of optic nerve disease. Macular dysfunction can cause similarly abnormal findings, and assessment of macular function with multifocal or pattern electroretinography enables improved VEP interpretation. In patients with medically unexplained vision loss, VEPs are crucial when the vision loss is suspected to be nonorganic. Though nonspecific, VEPs can objectively demonstrate normal function in the presence of symptoms that suggest otherwise.

Figure 3-7 Pattern-reversal visual evoked potential from a patient with a 4-month history of right eye (RE) optic neuritis and recovery of right visual acuity to 20/20. Left eye (LE) response is normal; RE P100 component shows profound delay with preservation of amplitude and waveform. (Courtesy of Graham E. Holder, PhD.)



VEPs are indispensable in examining children, particularly those who are preverbal, who have apparent vision loss or who present in infancy with roving eye movements or unexplained nystagmus.

Pattern-appearance stimulation—in which the stimulus appears from a uniformly gray background and then disappears, maintaining isoluminance throughout—can also be used to elicit VEPs. VEPs elicited in this manner are particularly useful in demonstrating the intracranial misrouting associated with ocular or oculocutaneous albinism (multiple recording channels are required) because they are less affected by nystagmus than are reversal VEPs. For babies and infants who cannot maintain adequate fixation on a pattern stimulus, flash stimulation is effective. If the check size and contrast levels are varied, pattern-appearance VEPs can also be used to objectively assess visual system resolution, providing a surrogate measure of visual acuity.

Microperimetry

Microperimetry is a visual field test that simultaneously integrates computer threshold perimetry with real-time retinal imaging. Microperimeters measure a patient's response to light stimuli at individual retinal points and then superimpose that data on an image captured by scanning laser ophthalmoscopy or fundus photography. This test can be used to accurately and reliably identify points of impaired retinal light sensitivity as well as assist in localization of functional defects. Retinal tracking allows real-time detection of retinal movement and correction for changes in fixation. This correction is particularly useful in assessing residual visual functioning in patients with significant vision loss due to macular disease. See also BCSC Section 3, *Clinical Optics and Vision Rehabilitation*.

Markowitz SN, Reyes SV. Microperimetry and clinical practice: an evidence-based review. *Can J Ophthalmol*. 2013;48(5):350–357.

Psychophysical Testing

Although electrophysiologic testing objectively assesses the functioning of cell layers and cell types in the visual pathway, it does not always provide localized responses and may

not be sensitive to small areas of localized dysfunction. Psychophysical tests can be highly sensitive, but they are subjective and do not provide information about specific levels of the visual system; perception represents an integration of information provided by different parts of the visual pathway. Psychophysical tests relevant to retinal disease include testing of

- visual acuity
- visual field
- color vision
- contrast sensitivity
- dark adaptation

Color vision, contrast sensitivity, and dark adaptation testing are discussed in this chapter. See BCSC Section 3, *Clinical Optics and Vision Rehabilitation*, for discussion of visual acuity and contrast sensitivity; Section 5, *Neuro-Ophthalmology*, for further discussion of contrast sensitivity; and Section 10, *Glaucoma*, for discussion of visual field testing.

Dingcai C. Color vision and night vision. In: Ryan SJ, Schachar AP, Wilkinson CP, Hinton DR, Sadda SR, Wiedemann P, eds. *Retina*. 5th ed. Elsevier/Saunders; 2013:285–299.

Color Vision

A healthy human retina has 3 cone types, each containing a different outer segment visual pigment: short-wavelength sensitive (S cone; formerly, *blue*), medium-wavelength sensitive (M cone; formerly, *green*), and long-wavelength sensitive (L cone; formerly, *red*). The integrative cells in the retina and higher visual centers are organized primarily to recognize *contrasts* between light or colors, and the receptive fields of color-sensitive cells typically have regions that compare the intensity of red versus green or blue versus yellow.

The classification and the testing of dysfunctional color vision are based on this contrast-recognition physiology. Red-green color deficiency, which is common in males through X-linked inheritance (5%–8% incidence), is traditionally separated into protan and deutan types, referring to absent or defective long-wavelength-sensitive or medium-wavelength-sensitive pigment, respectively. These distinctions have value in terms of patients' perception, even though individuals with normal color vision often have a duplication of pigment genes, and individuals with color vision deficiency may not have single or simple gene defects. Blue-yellow color deficiency is rarely inherited and can be an important early marker for acquired disease. Inherited color vision defects are described in Chapter 12.

Testing of color vision

The most accurate instrument for classifying congenital red-green color defects is the *anomaloscope*, but it is not widely used. In this test, the patient views a split screen and is asked to match the yellow appearance of one half by mixing varying proportions of red and green light in the other half. Individuals with red-green color deficiency use abnormal proportions of red and green to make the match.

The most common tests of color vision use colored tablets or diagrams. These tests must be performed in appropriate lighting, usually illumination that mimics sunlight.

Pseudoisochromatic plates, such as the *Ishihara* plates (which assess color discrimination along protan [red] and deutan [green] axes only) and *Hardy-Rand-Rittler* plates (which also assess the tritan [blue] axis), present colored numbers or figures against a background of colored dots (Fig 3-8). The colors of both figure and background are selected from hues that are difficult for a person with abnormal color vision to distinguish. Individuals with defective color vision see either no pattern at all or an alternative pattern based on brightness rather than hue. These tests are quick to perform and sensitive for screening for color vision abnormalities, but they are not effective in classifying the deficiency.

Panel tests, including the Farnsworth-Munsell 100 and the Farnsworth Panel D-15 hue tests, are more accurate in classifying color deficiency. The *Farnsworth-Munsell 100-hue test* is very sensitive because the difference in hues between adjacent tablets approximates the minimum that a typical observer can distinguish (1–4 nm). The spectrum is divided into 4 parts of 25 colored tablets each, and the patient is asked to discriminate between subtle shades of similar colors. Testing is tiring and time-consuming but is more sensitive in identifying difficulties with hue discrimination and color confusion.

Consisting of only 15 colored tablets, the *Farnsworth Panel D-15 test* (Fig 3-9) is quicker than the Farnsworth-Munsell 100 and more convenient for routine clinical use. The hues are more saturated, and they cover the spectrum so that patients will confuse colors for which they have deficient perception (such as red and green). The patient is asked to arrange the tablets in sequence, and errors can be quickly plotted to define the color deficiency. The D-15 test may miss mildly affected individuals, but it is still deemed useful because of its speed. The relative insensitivity may also be an asset in judging the practical significance of mild degrees of color deficiency. For example, individuals who fail the Ishihara plates but pass the D-15 test will probably not have color discrimination problems under most circumstances and in most occupations. Desaturated versions of the D-15 test, such as the L'Anthony D-15, which recognize more subtle degrees of color deficiency, are perhaps more clinically useful.

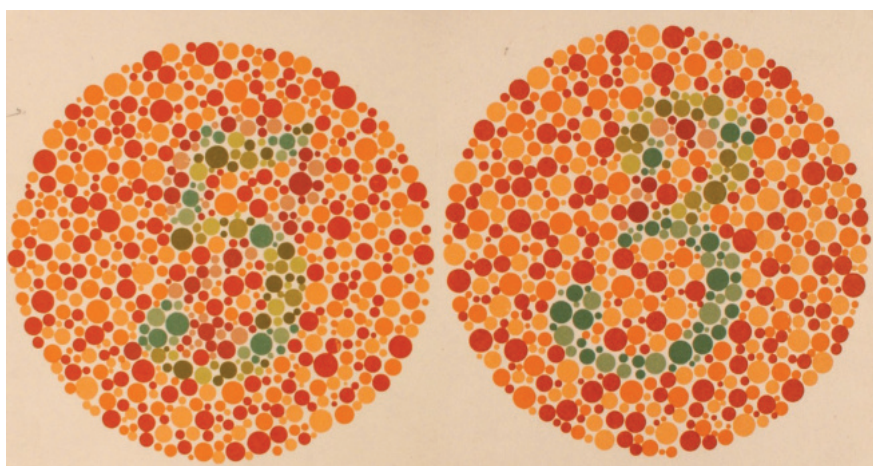


Figure 3-8 Pseudoisochromatic plates. (Courtesy of Carl Regillo, MD.)



Figure 3-9 Farnsworth Panel D-15 test. (© 2021 American Academy of Ophthalmology.)

Individuals with major congenital color deficiencies typically show a distinct protan or deutan pattern on the D-15 scoring graph, whereas those with acquired optic nerve or retinal disease show an irregular pattern of errors. Tritan axis errors (blue-yellow confusion), which usually signify acquired disease, are readily detected using the D-15 test. Enlarged versions (PV-16 tests) are available for testing patients with reduced visual acuity.

Neitz M, Green DG, Neitz J. Visual acuity, color vision, and adaptation. In: Albert DM, Miller JW, Azar DT, Blodi BA, eds. *Albert & Jakobiec's Principles and Practice of Ophthalmology*. 3rd ed. Saunders; 2008:chap 123.

Contrast Sensitivity

Contrast sensitivity (CS) is a very important concept to understand. The loss of CS often results in visual difficulties and dysfunction out of proportion to the patient's measured visual acuity. For example, patients with nonexudative macular degeneration or diabetic macular edema may have good measured visual acuity of 20/30 or better but have diminished CS that makes it difficult for them to perform routine visual tasks such as reading the newspaper or navigating stairways. Because a conventional Snellen visual acuity is based on high-contrast, achromatic, square-wave stimuli, it does not measure the patient's ability to perceive the subtleties of light. However, the visual system codes much of what is seen on the basis of contrast rather than spatial resolution, with subtleties of light and dark providing most of the richness of visual perception. For example, when dusk, fog, or smoke reduces contrast, it becomes very difficult for anyone to resolve ordinary objects. Similarly, when a patient becomes unable to perceive contrast under ordinary environmental conditions because of retinal disease or media opacity, visual function is adversely impacted.

Testing of contrast sensitivity

Several clinical tests of CS are available. Most relate CS to *spatial frequency*, which refers to the size of the light-dark cycles. Individuals are typically most sensitive to contrast for

objects that have a spatial frequency between 2 and 5 cycles per degree, but this sensitivity can change in patients with ophthalmic disease. Some tests use letters or optotypes of varying dimness and size to provide a more clinical context.

The *Pelli-Robson test* measures CS using a single, large letter size (20/60 optotype), with the contrast of the 3-letter groups decreasing from top to bottom of the chart and left to right within each line (Fig 3-10). Patients read the letters, starting with the highest contrast, and continue until they are unable to read 2 or 3 letters in a single group. The subject is assigned a score based on the contrast of the last group in which 2 or 3 letters were correctly read. The Pelli-Robson score is a logarithmic measure of the subject's CS. Thus, a score of 2 means that the subject could read at least 2 of the 3 letters with a contrast of 1% (CS = 100%, or $\log_{10} 2$). That is, a score of 2.0 indicates normal CS of 100%. A Pelli-Robson CS score less than 1.5 is consistent with visual impairment, and a score less than 1.0 represents visual disability.

See BCSC Section 3, *Clinical Optics and Vision Rehabilitation*, and Section 5, *Neuro-Ophthalmology*, for additional discussion of CS testing.

Owsley C. Contrast sensitivity. *Ophthalmol Clin North Am.* 2003;16(2):171–177.

Rubin GS. Visual acuity and contrast sensitivity. In: Ryan SJ, Schachat AP, Wilkinson CP,

Hinton DR, Sadda SR, Wiedemann P, eds. *Retina*. 5th ed. Elsevier/Saunders; 2013:300–306.



Figure 3-10 The top 5 of 8 lines of a standard Pelli-Robson contrast sensitivity chart. The top left 3-letter block has a log contrast value of 0.05; there is a log contrast change of 0.15 with each 3-letter block. In the full 8-line chart, the lowest contrast letters have a log value of 2.3; 2.0 represents normal contrast sensitivity. (Used with permission from Pelli DG, Robson JG, Wilkins AJ. The design of a new letter chart for measuring contrast sensitivity. *Clin Vision Sci.* 1988;2(3):187–199.)

Dark Adaptometry

The sensitivity of the human eye extends over a range of 10–11 \log_{10} units. Cones and rods adapt to different levels of background light through neural mechanisms and through the bleaching and regeneration of visual pigments. Clinical dark adaptometry primarily measures the absolute thresholds of cone and rod sensitivity.

Dark adaptation can be measured and quantified with the *Goldmann-Weekers (G-W) adaptometer*; however, it is neither widely available nor used. Although newer instruments have been introduced, they have yet to gain widespread acceptance, and most of the research literature is devoted to the G-W instrument.

Dark adaptometry is useful in assessing patients with nyctalopia. Although it is a subjective test, dark adaptometry can complement the ERG; as a *focal test* (relevant when interpreting results from patients with local rather than generalized retinal dysfunction), it can be a more sensitive indicator of pathology than the ERG, especially early in the disease process.

PART II

Diseases of the Retina and Vitreous

CHAPTER 4

Age-Related Macular Degeneration and Other Causes of Choroidal Neovascularization



This chapter includes a related activity. Go to www.aao.org/bcscactivity_section12 or scan the QR code in the text to access this content.

Highlights

- Age-related macular degeneration (AMD) is a leading cause of permanent vision loss worldwide. It has 2 late-stage manifestations, which may coexist: a nonneovascular form known as *geographic atrophy* and a neovascular form characterized by the presence of macular neovascularization, previously known as *choroidal neovascularization*.
- Risk factors for AMD may be nonmodifiable (eg, age) or modifiable (eg, cigarette smoking and low micronutrient intake).
- According to multiple genome-wide association studies, genetic factors account for at least 55% of total AMD risk, and the pathway most consistently implicated in AMD is the complement cascade.
- Anti-vascular endothelial growth factor agents are the mainstay of treatment for exudative AMD and are typically administered using 1 of 3 broad approaches: fixed-interval dosing, as-needed dosing, or treat-and-extend dosing.
- In addition to AMD, multiple retinal pathologies may lead to choroidal neovascularization; these distinct exudative diseases are also frequently managed with anti-vascular endothelial growth factor drugs.

Age-Related Macular Degeneration Studies

This glossary provides the abbreviated and full names of age-related macular degeneration studies referenced in this chapter. Only the short names are used in the text.

ANCHOR Anti-VEGF Antibody for the Treatment of Predominantly Classic Choroidal Neovascularization in AMD

AREDS Age-Related Eye Disease Study

AREDS2 Age-Related Eye Disease Study 2

CATT Comparison of Age-Related Macular Degeneration Treatments Trials

EXCITE Efficacy and Safety of Ranibizumab in Patients With Subfoveal Choroidal Neovascularization Secondary to AMD

HARBOR A Study of Ranibizumab Administered Monthly or on an As-Needed Basis in Patients With Subfoveal Neovascular AMD

HOME HOme Monitoring of the Eye (HOME) Study

HORIZON Open-label Extension Trial of Ranibizumab for Choroidal Neovascularization Secondary to AMD

MARINA Minimally Classic/Occult Trial of the Anti-VEGF Antibody Ranibizumab in the Treatment of Neovascular AMD

MESA Multi-Ethnic Study of Atherosclerosis

PIER Phase 3b, Multicenter, Randomized, Double-Masked, Sham Injection-Controlled Study of the Efficacy and Safety of Ranibizumab in Subjects With Subfoveal Choroidal Neovascularization With or Without Classic Choroidal Neovascularization Secondary to AMD

PLANET Aflibercept in Polypoidal Choroidal Vasculopathy study

SUSTAIN Study of Ranibizumab in Patients With Subfoveal Choroidal Neovascularization Secondary to AMD

TREND TReat and extEND

VIEW 1 and VIEW 2 VEGF Trap-Eye: Investigation of Efficacy and Safety in Wet AMD 1 and 2

Age-Related Macular Degeneration

Age-related macular degeneration (AMD) is a leading cause of irreversible vision loss worldwide among people older than 50 years. In the United States, it is the most common cause of legal blindness, affecting an estimated 2.07 million people in 2010 and projected to affect 3.7 million by 2030. An estimated 71,000 new cases of neovascular AMD develop each year in North America.

This complex disorder has 2 main clinical stages: an intermediate or earlier phase of nonexudative degeneration (often referred to collectively as *dry AMD*) and a late stage (also known as *advanced AMD*). Late-stage AMD is further subdivided into a nonneovascular form, known as *geographic atrophy*, and a neovascular form characterized by macular neovascularization (MNV). These 2 late stages often coexist in the same eye. Historically, the term *choroidal neovascularization (CNV)* or *CNV membrane (CNVM)*

was used to refer to the neovascular complex associated with AMD. However, the term *MNV* is now preferred because in some cases, the neovascularization arises from the retinal vasculature. The terms *neovascular AMD*, *exudative AMD*, and *wet AMD* are also used for the neovascular form.

Normal aging initiates a spectrum of changes in the macula that affect the outer retina, retinal pigment epithelium (RPE), Bruch membrane, and choriocapillaris (Fig 4-1):

- Photoreceptors, rods more than cones, are reduced in density and distribution.
- In the RPE, ultrastructural changes include loss of melanin granules, formation of lipofuscin granules, and accumulation of residual bodies.
- Basal laminar deposits accumulate between the plasma membrane of the RPE cell and the native RPE basement membrane in AMD; these deposits consist of extracellular matrix proteins, including widely spaced collagen fibers.
- Basal linear deposits accumulate and expand to soft drusen in AMD; this lipid-rich material is attributed to lipoprotein particles that accumulate between the basement membrane of the RPE and the inner collagenous layer of Bruch membrane.
- In the choriocapillaris, progressive involutional changes occur.

All of these changes represent aging and may not be part of AMD pathology.

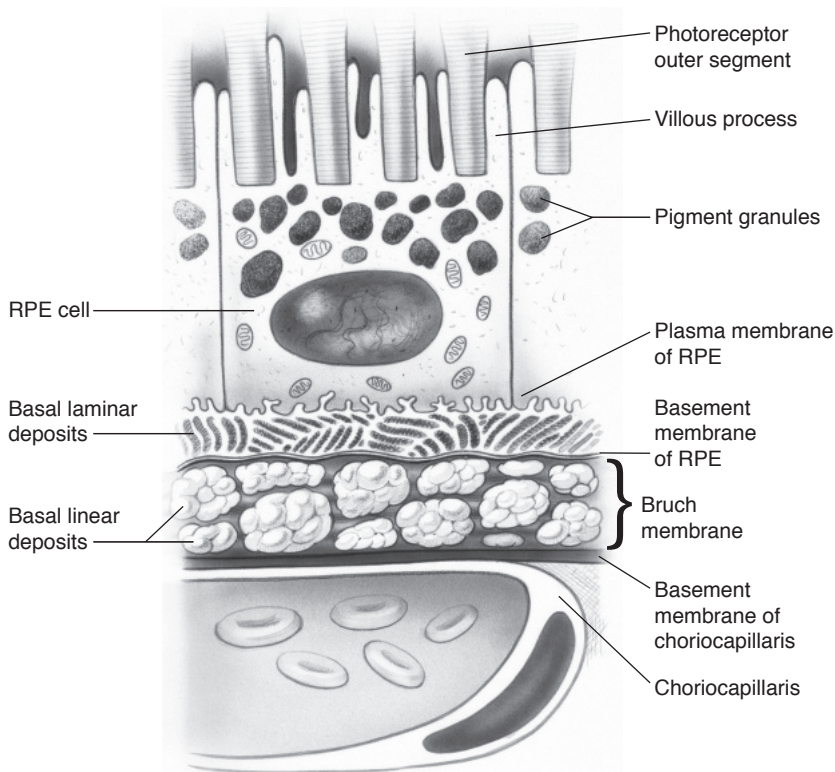


Figure 4-1 Schematic illustration of basal laminar deposits and basal linear deposits that result in a thickened inner collagenous layer of Bruch membrane. RPE = retinal pigment epithelium. (Illustration by Christine Gralapp.)

Abnormalities associated with AMD that are not related to normal aging may be classified as nonneovascular or neovascular.

Population-based studies have demonstrated that age is the foremost risk factor for AMD; in resource-rich countries, approximately 10% of individuals older than 65 years and 25% older than 75 years have AMD. In addition to age, other nonmodifiable risk factors for AMD include female sex, family history of AMD, hyperopia, light iris color, and race. MESA, a 10-year longitudinal study, found that the prevalence of AMD in the United States was highest in White participants (5.4%) and lowest in African American individuals (2.4%); among participants of Asian and Hispanic ethnicity, the prevalence was 4.6% and 4.2%, respectively.

The most common modifiable risk factor for AMD is cigarette smoking. Others include hypertension, hypercholesterolemia, cardiovascular disease, high waist-to-hip ratio in men, and elevated levels of C-reactive protein and other inflammatory markers.

Klein R, Klein BE, Knudtson MD, et al. Prevalence of age-related macular degeneration in 4 racial/ethnic groups in the Multi-Ethnic Study of Atherosclerosis. *Ophthalmology*. 2006;113(3):373–380.

Genetics and AMD

Although the exact etiology of AMD is poorly understood, its development appears to involve an interplay of extrinsic and intrinsic risk factors. Within this context, a genetic predisposition has emerged as one of the most important risk factors for the disorder. According to familial and population-based studies, genetic factors account for an estimated 55% or more of the total variability in AMD risk. Although the emerging association between AMD and genetics is strong, it is also complex. Human genome-wide association studies have identified more than 34 genetic loci for AMD on at least 19 chromosomes.

Although genetic studies have identified multiple biochemical pathways related to AMD pathophysiology, including lipid transport and metabolism (eg, *APOE*), modulation of the extracellular matrix (eg, *COL8A1*, *COL10A1*, *MMP9*, and *TIMP3*), clearance of all-*trans*-retinaldehyde from photoreceptors (*ABCA4*), and angiogenesis (eg, *VEGFA*), the pathway most consistently implicated in genetic studies of AMD is the complement cascade. The complement system is a complex, innate immune response that allows a host to clear damaged cells, regulate inflammation, and opsonize foreign cells; polymorphisms within certain complement components, including *CFD*, *CFH*, *CFI*, *C2/CFB*, *C3*, *C5*, and *C7*, have been strongly linked to AMD risk.

The 2 major susceptibility genes for AMD are *CFH* (1q31), which codes for complement factor H, and *ARMS2/HTRA1* (10q26). The *CFH* Y402H polymorphism confers a 4.6-fold increased risk for AMD when heterozygous and a 7.4-fold increased risk when homozygous. The A69S *ARMS2/HTRA1* polymorphism confers a 2.7-fold increased risk for AMD when heterozygous and an 8.2-fold increased risk when homozygous. When both genes are homozygous for the aforementioned mutations, the risk for AMD is increased 50-fold.

Although genetic testing is available for AMD, the American Academy of Ophthalmology's official recommendation is to defer this testing until replicable studies have confirmed its value for prognostication or response to therapy.

American Academy of Ophthalmology Preferred Practice Pattern Retina/Vitreous Committee, Hoskins Center for Quality Eye Care. Preferred Practice Pattern Guidelines. *Age-Related Macular Degeneration*. American Academy of Ophthalmology; 2015. www.aao.org/ppp
 Frisch LG, Igl W, Cooke Bailey JN, et al. A large genome-wide association study of age-related macular degeneration highlights contributions of rare and common variants. *Nat Genet*. 2016;48(2):134–143.

Nonneovascular AMD

In all stages of nonneovascular AMD, the defining lesion is the druse (plural, *drusen*). Because drusen variably affect overlying photoreceptors, they may be associated with mild to moderate vision loss, decreased contrast sensitivity and color vision, and impaired dark adaptation. Other indicators of nonneovascular AMD are abnormalities of the RPE, including hypopigmentation, hyperpigmentation, and atrophy.

Drusen

Clinically, drusen typically are round, yellow lesions located along the basal surface of the RPE, mostly in the postequatorial retina (Fig 4-2). Histologically, this material corresponds to the abnormal thickening of the inner aspect of Bruch membrane, shown in Figure 4-1. Ultrastructurally, basal laminar deposits (granular, lipid-rich material and widely spaced collagen fibers between the plasma membrane and basement membrane of

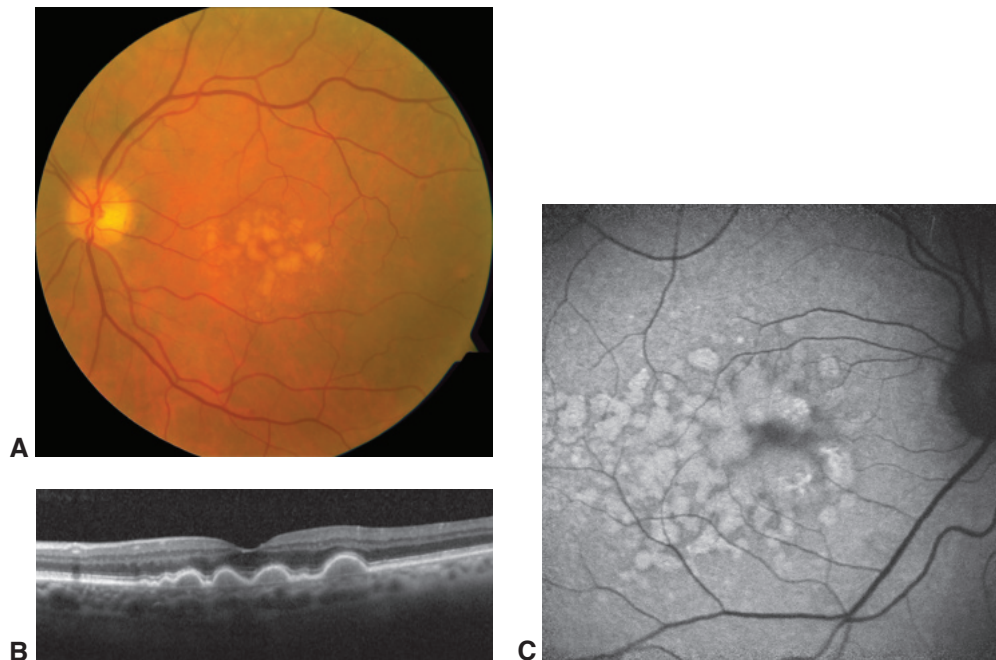


Figure 4-2 Drusen. **A**, Color fundus photograph shows large soft and confluent drusen in a patient with nonneovascular (dry) age-related macular degeneration (AMD). **B**, Corresponding spectral-domain optical coherence tomography (SD-OCT) image of the soft drusen. **C**, Auto-fluorescence image of an eye with areas of confluent drusen. (Courtesy of David Sarraf, MD.)

the RPE cell) and basal linear deposits (phospholipid vesicles and electron-dense granules within the inner collagenous zone of Bruch membrane) are observed.

The thickened inner aspect of Bruch membrane, along with the RPE, may separate from the rest of the membrane, resulting in a pigment epithelial detachment (PED). When small, such a detachment may be identified as a large or soft druse; when larger (ie, diameter $>350\text{ }\mu\text{m}$), it is recognizable as large confluent drusen that have coalesced into a PED, also known as a *drusenoid PED*.

Drusen are categorized by size as follows, with the typical diameter given within parentheses: small ($<63\text{ }\mu\text{m}$), intermediate ($63\text{--}124\text{ }\mu\text{m}$), and large ($\geq 125\text{ }\mu\text{m}$). Increasing size, number, and confluence of the drusen elevate the risk of progression to MNV or geographic atrophy (GA). In AREDS, among patients with early AMD (ie, with many small drusen or a few intermediate drusen, category 2), the risk of progression to category 4 AMD over a 5-year period was 1.3%. In contrast, for patients with nonsubfoveal GA, many intermediate drusen, or even a single large druse (category 3), the risk was 18%. Patients who progressed to MNV or subfoveal GA were considered to have advanced, or category 4, AMD. Patients with no AMD (a few small or no drusen without pigment changes, category 1) had 0% risk of progression to category 4 AMD.

Drusen are further distinguished by their boundaries: hard (discrete and well demarcated), soft (amorphous and poorly demarcated; see Fig 4-2A, B), or confluent (contiguous drusen without clear boundaries; see Fig 4-2C). Hard drusen are well-defined focal areas of lipidization or hyalinization of the RPE–Bruch membrane complex. Soft drusen are associated with diffuse thickening of the inner aspects of Bruch membrane (ie, basal linear deposits). An eye containing soft, and perhaps confluent, drusen is more likely to progress to atrophy or MNV than an eye containing only hard drusen; consistent with this, drusen volume has emerged as a possible biomarker for increased risk of late AMD development.

Reticular pseudodrusen or subretinal drusenoid deposits are similar in appearance to drusen; however, they are recognizable by their reticular-like network, best seen on fundus autofluorescence and near-infrared imaging (Fig 4-3). These lesions are typically smaller than soft drusen, are located on the apical surface of the RPE, and are commonly distributed in the superior macular region. Although they share some proteins with drusen (eg, apolipoprotein E, complement factor H, and vitronectin), they contain different lipids and do not contain shed disc remnants. Their presence has been associated with progressive atrophy of the photoreceptor layer, GA, and increased risk of MNV.

Fluorescein angiography of drusen On fluorescein angiography (FA), drusen appearance may vary. Typically, small hard drusen hyperfluoresce early in FA studies because of a window defect, whereas larger soft and confluent drusen and drusenoid PEDs slowly and homogeneously stain late because of pooling of the fluorescein dye in the sub-RPE compartment.

Optical coherence tomography of drusen Spectral-domain optical coherence tomography (SD-OCT) of small and large drusen typically reveals sub-RPE nodular elevations with a notable absence of intraretinal and subretinal fluid (see Fig 4-2). Reticular pseudodrusen are identified above the RPE and beneath the inner segment ellipsoid layer (see Fig 4-3).

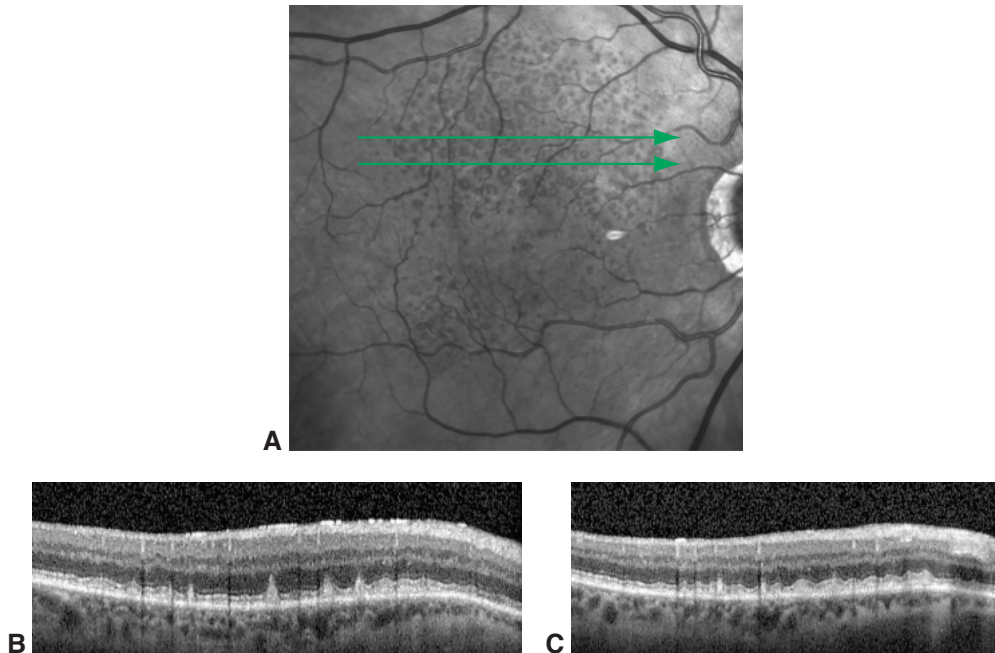


Figure 4-3 Reticular pseudodrusen. **A**, Near-infrared reflectance image shows the multifocal and typical netlike arrangement of pseudodrusen. *Green arrows mark locations of B (top arrow) and C (bottom arrow).* **B**, SD-OCT image demonstrates the location of typical peak-shaped reticular pseudodrusen above the RPE. **C**, SD-OCT image demonstrates the location of undulating reticular pseudodrusen above the RPE. (Courtesy of Charles C. Wykoff, MD, PhD.)

Enhanced depth imaging (EDI) OCT provides more details of choroidal architecture and a clearer definition of the choroidal-scleral interface, which is helpful in characterizing AMD. In eyes with AMD, choroidal thickness is often reduced.

Abnormalities of the retinal pigment epithelium

In patients with nonneovascular AMD, characteristic RPE abnormalities include focal hyperpigmentation or hypopigmentation, intraretinal pigment migration, focal atrophy, and GA. Focal RPE hyperpigmentation appears as increased pigmentation at the level of the outer retina. These areas typically block fluorescence on FA and appear as hyperreflective outer retinal foci on SD-OCT. Intraretinal pigment migration within the neurosensory retina may be visualized superficial to drusen or drusenoid PEDs. The incidence of these abnormalities increases with age, and their presence increases the risk of progression to more advanced forms of AMD.

Geographic atrophy In the eye, focal atrophy can appear clinically as areas of mottled pigmentation or depigmentation. When these lesions are contiguous and have a diameter greater than 175 μm , they are described as GA of the RPE. In areas of GA, absence or depigmentation of the RPE exposes the choroidal vessels. The overlying outer retina typically appears thin, and the underlying choriocapillaris is attenuated or atrophied. On FA, GA appears as well-circumscribed window defects of varying sizes corresponding to the

area of absent RPE. On SD-OCT, GA manifests as loss of the photoreceptors and RPE. Choriocapillaris loss may also be appreciated. On fundus autofluorescence (FAF), another useful noninvasive technique for monitoring disease progression (Fig 4-4), GA appears as well-demarcated areas of decreased signal intensity; multiple potential FAF patterns involving adjacent tissue have also been described.

GA often spares the fovea until late in the disease course, and affected patients may maintain good vision until then. Although GA was traditionally considered slowly progressive, multiple analyses have highlighted the severe functional impairment and consistent, inexorable rate of annual progression associated with the condition. The average rate of disease progression is approximately 1.79 mm²/year; however, this rate of longitudinal GA enlargement is highly variable and is influenced by multiple factors, including lesion size at baseline and adjacent FAF patterns. When the fovea becomes involved and visual

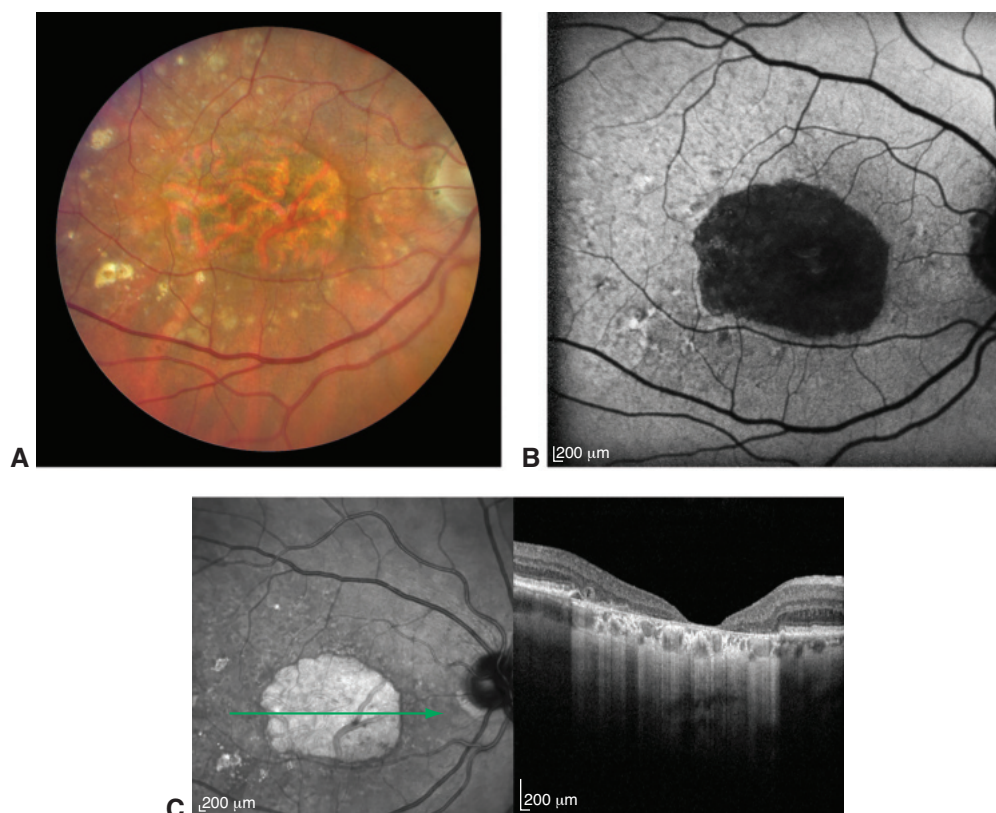


Figure 4-4 Geographic atrophy (GA). **A**, Color fundus photograph of right eye, demonstrating advanced GA. **B**, Corresponding fundus autofluorescence image from the same patient. The areas of RPE atrophy are hypoautofluorescent (*dark gray or black*), the areas of “sick” RPE are hyperautofluorescent (*brighter than background*), and the areas of healthy RPE are gray. **C**, Corresponding near-infrared reflectance image in the same patient (*left*). Large choroidal vessels are visible through the central area of GA. *Green arrow* marks the location seen in the SD-OCT image (*right*) showing complete atrophy of photoreceptors, RPE, and choriocapillaris. (Courtesy of Charles C. Wykoff, MD, PhD.)

acuity (VA) declines, patients are able to read and perform detailed visual tasks by relying on eccentric fixation using the noncentral retina. Among patients with GA, 12%–20% experience severe vision loss.

Although not all eyes with drusen will develop GA, the incidence of atrophy appears to increase with age. In addition, 10% of patients with AMD and a VA of 20/200 or less have GA. Decreased contrast sensitivity and reduced microperimetry sensitivity values reflect the presence of pseudodrusen before progression to GA.

Holekamp N, Wyckoff CC, Schmitz-Valckenberg S, et al. Natural history of geographic atrophy secondary to age-related macular degeneration: results from the Prospective Proxima A and B Clinical Trials. *Ophthalmology*. 2020;127(6):769–783.

Sadda SR, Guymer R, Holz FG, et al. Consensus definition for atrophy associated with age-related macular degeneration on OCT: classification of atrophy report 3. *Ophthalmology*. 2018;125(4):537–548. Published correction appears in *Ophthalmology*. 2019;126(1):177.

Other abnormalities As drusen resorb over time, atrophy of the RPE may develop. Dysrophic lipidization and calcification may also occur, resulting in the development of refractile or crystalline lesions in the macula (termed *refractile* or *calcific drusen*). Furthermore, pigment or pigment-laden cells (either RPE cells or macrophages that have ingested the pigment) may migrate to the photoreceptor level, causing focal clumps or a reticulated pattern of hyperpigmentation, a proposed prognosticator of progression to late-stage AMD. On OCT, areas of outer retinal tubulation may be misidentified as exudative fluid. These ovoid hyporeflective spaces with hyperreflective borders are located at the outer nuclear layer and represent degenerating photoreceptor rearrangement after retinal injury (Fig 4-5).

Differential diagnosis of nonneovascular AMD

Multiple disorders associated with RPE abnormalities are often misinterpreted as nonneovascular AMD. Central serous chorioretinopathy may produce changes in the RPE and PEDs similar to those in AMD (discussed in Chapter 9). However, in patients with central

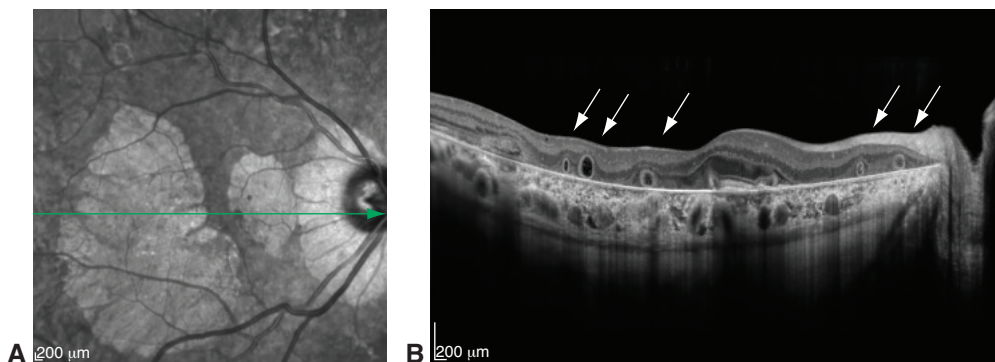


Figure 4-5 Outer retinal tubulation. **A**, Near-infrared reflectance image with *green arrow* marking the location of the SD-OCT image (**B**) showing multiple areas of outer retinal tubulation, indicated by *white arrows* in the context of extensive macular atrophy. (Courtesy of K. Bailey Freund, MD.)

serous chorioretinopathy, EDI-OCT reveals a thickened choroid in the affected and fellow eyes, as opposed to the normal or thin choroid often associated with AMD.

Other differential diagnoses include pattern dystrophies, a group of predominantly autosomal dominant diseases of the RPE that may present with reticular or butterfly-shaped hyperpigmentation of the macula in both eyes, which is often symmetric. Patients with adult-onset foveomacular vitelliform dystrophy (AOFVD) may present with unilateral or bilateral yellow subretinal lesions. On SD-OCT, this condition appears as a hyperreflective, dome-shaped central lesion between the photoreceptor layer and the RPE, often with subretinal fluid that is not responsive to anti-vascular endothelial growth factor (anti-VEGF) therapy (Fig 4-6). However, unlike in AMD, increased subfoveal choroidal thickness is frequently apparent in AOFVD. FAF typically shows decreased central autofluorescence corresponding to the lesion with annular hyperautofluorescence. On FA, early blocked fluorescence is seen, with a surrounding zone of hyperfluorescence; late staining of the vitelliform material may also occur.

Consideration of the patient's concurrent or past pharmaceutical exposure is critical in the differential diagnosis of AMD. For example, a history of drug ingestion and lack of large drusen may help differentiate RPE mottling and macular atrophy from AMD (see Chapter 14).

Management of nonneovascular AMD

Education and follow-up Although eyes in early- and intermediate-stage AMD are often minimally symptomatic, they may progress to late AMD with associated severe vision loss. Therefore, patients should be educated about modifiable risk factors, such as low micronutrient levels and tobacco use. Patients with nonneovascular AMD should also be educated about the symptoms of late-stage disease, including metamorphopsia or scotomata, and instructed to promptly seek ophthalmic care when they occur.

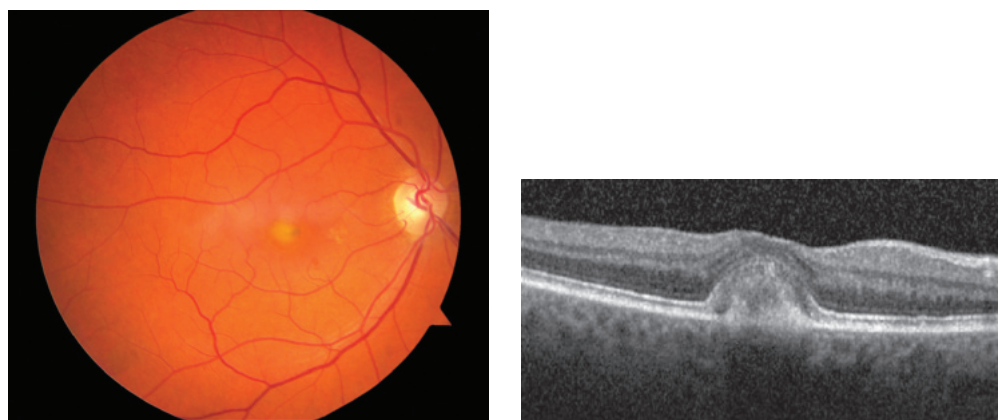


Figure 4-6 Color fundus photograph (*left*) and corresponding SD-OCT image (*right*) of adult-onset foveomacular vitelliform maculopathy. The foveal region has a yellowish discoloration resembling an egg yolk. OCT demonstrates that the lesion is elevated. (Courtesy of David Sarraf, MD.)

Micronutrients Ophthalmologists should counsel patients with nonneovascular AMD about epidemiologic studies demonstrating positive associations between the intake of certain micronutrients and decreased risk of the disease.

AREDS first established the benefits of vitamin and zinc supplementation in reducing vision loss in nonexudative AMD. In the study, patients with intermediate or advanced AMD who took antioxidant vitamins C (500 mg) and E (400 IU), beta carotene (15 mg), and the micronutrient zinc (80 mg zinc oxide and 2 mg cupric oxide to prevent zinc-induced anemia) had a 25% reduced risk of progression to more-advanced stages of AMD and a 19% reduced risk of moderate vision loss (≥ 3 lines of VA) at 5 years. The study defined intermediate (category 3) AMD as the presence of at least 1 large druse (≥ 125 μm), extensive intermediate drusen (diameter of 63–124 μm), or nonsubfoveal GA. Advanced (category 4) AMD was defined as vision loss due to neovascular AMD or subfoveal GA in only 1 eye. At 10 years, 44% of placebo recipients had advanced AMD compared with 34% of supplement recipients (a 23% risk reduction). In addition, mortality did not increase among patients taking the AREDS-recommended formula. However, among participants with no AMD or with only early-stage AMD (ie, a few small drusen), supplementation provided no measurable benefit.

AREDS investigators developed a simplified 5-step severity scale for classifying the severity of AMD and predicting the disease course based on the following findings:

- presence of 1 or more large (≥ 125 - μm diameter) drusen (1 point)
- presence of any pigment abnormalities (1 point)
- for patients with no large drusen, presence of bilateral intermediate (63- to 124- μm) drusen (1 point)
- presence of neovascular AMD (2 points)

In the study, risk factors were totaled across both eyes to reach a number between 0 and 4, which was used to estimate patients' 5- and 10-year risk of advanced AMD developing in 1 eye (Table 4-1).

AREDS2, a large, prospective, follow-up study, tested whether replacing beta carotene with xanthophylls (lutein and zeaxanthin) and adding omega-3 long-chain polyunsaturated fatty acids (LCPUFAs; docosahexaenoic acid and eicosapentaenoic acid) would further reduce AMD progression. The response of the 4000 participants confirmed the overall risk reduction found in the original AREDS study, leading the authors to conclude that lutein

Table 4-1 Five- and 10-Year Risks^a of Advanced AMD in 1 Eye

Number of Risk Factor Points	5-Year Risk, %	10-Year Risk, %
0	0.5	1
1	3	7
2	12	22
3	25	50
4	50	67

AMD = age-related macular degeneration.

^aRisks are based on the number of Age-Related Eye Disease Study (AREDS) risk factors (see chapter text).

and zeaxanthin had effects similar to those of beta carotene but without the increased risk of lung cancer reported in other studies in current and former smokers. It also confirmed that an 80-mg dose of zinc is appropriate for AMD prophylaxis. The addition of LCPUFAs at the dose studied did not decrease the rate of progression to advanced AMD.

The study's final recommendation was to modify the original AREDS supplement, replacing beta carotene with lutein and zeaxanthin (Table 4-2). Currently, patients with category 3 or 4 AMD are advised to take the AREDS2 supplement.

Age-Related Eye Disease Study 2 Research Group. Lutein + zeaxanthin and omega-3 fatty acids for age-related macular degeneration: the Age-Related Eye Disease Study 2 (AREDS2) randomized clinical trial. *JAMA*. 2013;309(19):2005–2015.

Ferris FL, Davis MD, Clemons TE, et al; Age-Related Eye Disease Study (AREDS) Research Group. A simplified severity scale for age-related macular degeneration: AREDS report no. 18. *Arch Ophthalmol*. 2005;123(11):1570–1574.

Lifestyle changes Smoking cessation, obesity reduction, and blood pressure control may reduce the development and progression of AMD. Evidence linking cataract surgery to AMD progression is inconsistent, and evidence linking ultraviolet (UVA or UVB) light exposure to disease progression is weak. In addition, no evidence has linked blue light emitted from electronic devices to increased risk of AMD.

Amsler grid testing Patients may use the Amsler grid at home to monitor for visual distortion due to AMD-related retinal architectural distortion, including the development of exudative AMD. The Amsler test card, which contains grid lines and a central dot for fixation, is commonly used to test the central 10° of vision. Each eye is tested individually with reading glasses and at reading distance to check for new or progressive metamorphopsia, scotoma, or other changes in central vision. Any changes noted by the patient should be evaluated promptly. Online and smartphone app versions of the Amsler grid may be more convenient than the test card.

Hyperacuity testing Vernier acuity measures a patient's ability to detect deviations in the alignment of visual objects, for example, 2 line segments. Hyperacuity, which helps the viewer discern deviations as small as a single point on a line, is extremely sensitive to any geometric shift in the outer retinal morphology, producing a perception of distortion. In

Table 4-2 AREDS2 Recommendations for Nutritional Supplementation^a

Nutrient	Daily Dose
Vitamin C	500 mg
Vitamin E	400 IU
Lutein	10 mg
Zeaxanthin	2 mg
Zinc	80 mg
Copper ^b	2 mg

AREDS2 = Age-Related Eye Disease Study 2.

^aRecommendations for nutritional supplementation are based on the AREDS2 study (see text).

^bAs cupric oxide; added to avoid zinc-related copper deficiency.

patients with intermediate AMD, preferential hyperacuity perimetry (PHP), which has been studied extensively, can detect recent-onset MNV with high sensitivity (82%) and high specificity (88%). The HOME study, a phase 3 randomized clinical trial with 1520 participants, demonstrated the efficacy and potential benefit of PHP in early detection of MNV.

Shape-discrimination hyperacuity uses a principle similar to that of PHP but instead tests for discrimination of shapes, such as the ability to discern a perfect circle from a distorted contour.

Chew EY, Clemons TE, Harrington M, et al; AREDS2-HOME Study Research Group.

Effectiveness of different monitoring modalities in the detection of neovascular age-related macular degeneration: the Home Study, report number 3. *Retina*. 2016;36(8):1542–1547.

Neovascular AMD

The presence of MNV is the defining characteristic of neovascular AMD. Degenerative changes in Bruch membrane (eg, the accumulation of drusen and progressive thickening of the membrane that characterize nonneovascular AMD) and possibly the choriocapillaris may lead to a proangiogenic environment, with pathologic neovascularization developing from the choriocapillaris or from the neurosensory retina itself. These new vessels, which may be accompanied by fibroblasts, may leak and bleed, disrupting the normal retinal architecture with a degenerate fibrovascular complex; when untreated, this complex ultimately produces a hypertrophic, fibrotic, disciform scar.

Signs and symptoms of neovascular AMD

Patients with neovascular AMD may describe a sudden decrease in vision, metamorphopsia, and/or paracentral scotomata. Amsler grid self-testing by patients is highly effective in detecting early exudative AMD. Clinical signs of MNV may include subretinal or intraretinal fluid (eg, cystoid macular edema [CME]), exudate and/or blood, a pigment ring or gray-green membrane, irregular elevation of the RPE or a PED, an RPE tear, and/or a sea fan pattern of subretinal vessels.

Anatomical classification of MNV

The 3 main subtypes of MNV are based on level of origin:

- In type 1 MNV, also called *occult CNV*, new vessels originating from the choriocapillaris grow through Bruch membrane into the sub-RPE space (Fig 4-7). Fluid leakage and bleeding may produce a vascularized serous or fibrovascular PED. These fibrovascular PEDs typically have an irregular surface contour.
- In type 2 MNV, also called *classic CNV*, new vessels extend into the space between the RPE and the neurosensory retina. On examination, this may appear as a lacy or gray-green lesion. Neovascularization that exists beneath both the neurosensory retina and the RPE is designated as mixed type 1 and type 2 MNV, also termed *minimally classic CNV*.
- In type 3 MNV, the pathologic vessels develop from the deep capillary plexus of the retina and grow downward toward the RPE. Because of their intraretinal origin,

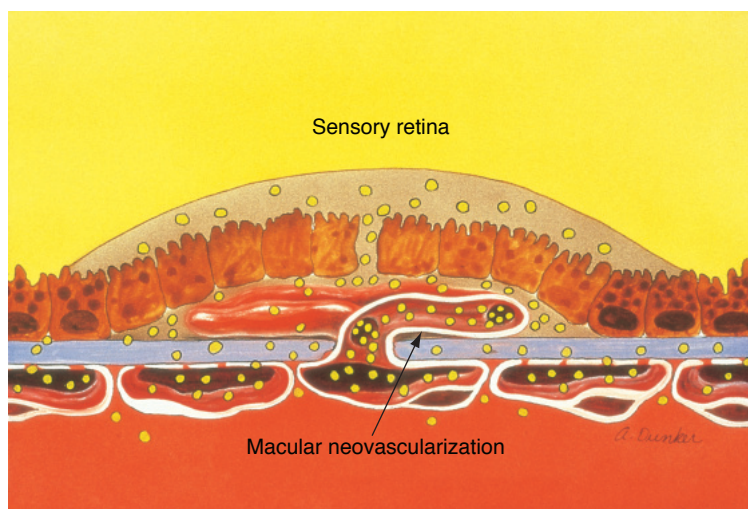


Figure 4-7 Schematic illustration of type 1 macular neovascularization (MNV) originating from the choriocapillaris, breaking through Bruch membrane (indicated by gray horizontal line bisected by MNV extending up from the choriocapillaris), and proliferating in the subretinal pigment epithelial space. (Modified with permission from Bressler NM, Bressler SB, Fine SL. Age-related macular degeneration. *Surv Ophthalmol.* 1988;32(6):375–413.)

these lesions were originally called *retinal angiomatous proliferations*; intraretinal pigment migration may occur before the development and maturation of this subtype of MNV. On examination, type 3 MNV often appears as a small area of red discoloration associated with retinal exudate or a bleb of subretinal fluid.

Nonexudative neovascular AMD

Type 1 MNV may manifest without the clinical signs of exudation; that is, MNV may be observed between Bruch membrane and the RPE without associated intraretinal fluid, subretinal fluid, or hemorrhage. This clinical scenario is called *nonexudative neovascular AMD*. These lesions, which have been reported in up to 14% of eyes with intermediate AMD or GA, can be identified with OCT angiography (OCTA) and/or indocyanine green angiography (ICGA). A less reliable finding—a double-layer sign on structural SD-OCT (ie, a low-lying, irregular PED)—may be misdiagnosed as an area of confluent drusen or a drusenoid PED. Clinical recognition of these lesions is relevant because they have been associated with a substantially increased risk of progression to exudative AMD (21%) at 1-year follow-up compared with eyes without these lesions (4%). There may also be a relationship between the presence of nonexudative neovascular AMD and GA progression; type 1 MNV has been hypothesized to be potentially protective against local GA development.

de Oliveira Dias JR, Zhang Q, Garcia JMB, et al. Natural history of subclinical neovascularization in nonexudative age-related macular degeneration using swept-source OCT angiography. *Ophthalmology.* 2018;125(2):255–266.

Imaging of MNV Several imaging techniques play an important role in describing, diagnosing, and/or classifying MNV.

FLUORESCEIN ANGIOGRAPHY OF MNV Before multimodal imaging-based classification with SD-OCT and OCTA, FA was instrumental in describing types of neovascularization, including classic, occult, and minimally classic patterns. As mentioned previously, *classic MNV* refers to a bright, lacy, and well-defined hyperfluorescent lesion that appears in the early phase of FA and progressively leaks by the late phases. *Occult MNV* refers to more diffuse hyperfluorescence that takes 1 of 2 forms: (1) PED, either fibrovascular PED or vascularized serous PED; or (2) late leakage from an undetermined source. *Minimally classic MNV* refers to a pattern of early hyperfluorescence with late leakage and surrounding stippled hyperfluorescence that also shows late leakage (Fig 4-8).

A fibrovascular PED is an irregular elevation of the RPE with progressive, stippled leakage on FA. Alternatively, the PED may pool dye rapidly in a homogeneous ground-glass pattern that is consistent with a serous PED but has a notch, or hot spot, due to a vascular component, hence the term *vascularized serous PED* (Fig 4-9).

Late leakage from an undetermined source describes fluorescence at the level of the RPE that is poorly defined in the early phases of FA, but better appreciated in the late phases.

The angiographic appearance of occult MNV is consistent with that of type 1 neovascularization, whereas the appearance of classic MNV is more often related to that of type 2 neovascularization; however, this is not a hard-and-fast rule. Type 3 neovascularization, or retinal angiomatous proliferations, may appear as a spot of retinal hemorrhage in the macula. It produces a focal hot spot on FA and ICGA with late CME or pooling into a PED.

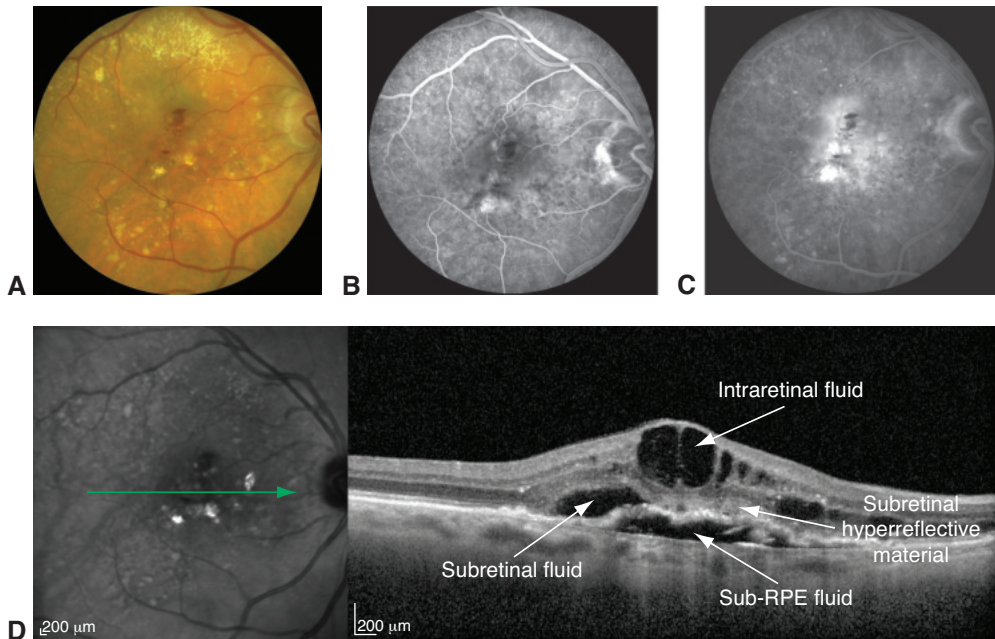


Figure 4-8 Treatment-naïve neovascular AMD. Color fundus photograph (A) with early (B) and late (C) frames of fluorescein angiogram of a minimally classic, fovea-involving, choroidal neovascular membrane. D, Near-infrared reflectance image (left) with green arrow marking the location seen in the SD-OCT image (right) showing intraretinal, subretinal, and sub-RPE fluid with subretinal hyperreflective material. (Courtesy of Charles C. Wykoff, MD, PhD.)

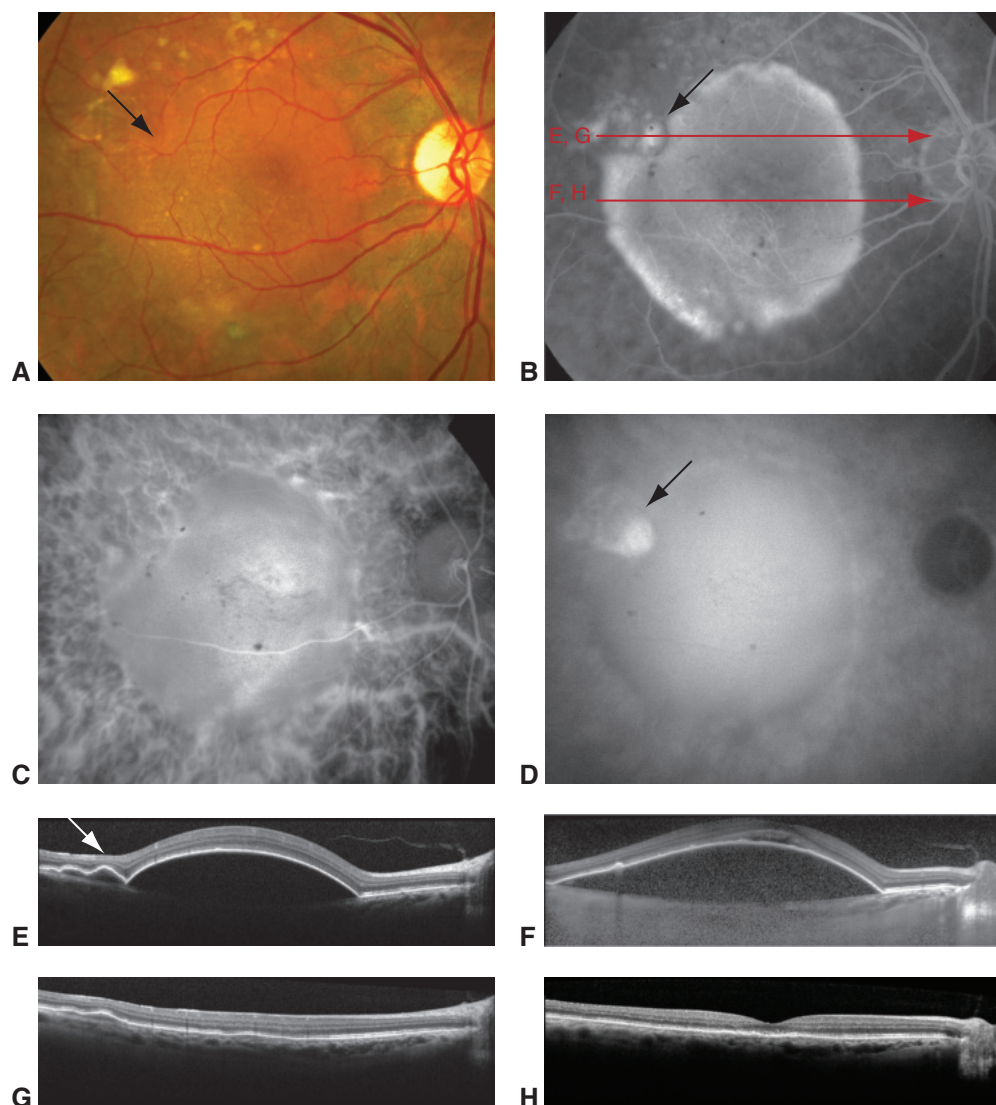


Figure 4-9 Vascularized serous pigment epithelial detachment (PED). **A**, Color fundus photograph of a vascularized serous PED with a notch (arrow) that corresponds to a hot spot on fluorescein angiography (black arrow in **B**). Red letters and arrows in **B** indicate the SD-OCT scan locations for parts **E** through **H**. Early (**C**) and late (**D**) indocyanine green (ICG) angiography images show pooling of the serous PED and hyperfluorescence of the hot spot (arrow in **D**). **E**, **F**, SD-OCT images of the large serous PED. Note the irregular portion of the PED (arrow in **E**), which corresponds to the hot spot and harbors the type 1 neovascular membrane. **G**, **H**, SD-OCT images show that the PED has resolved after therapy with anti-vascular endothelial growth factor. (Modified with permission from Mrejen S, Sarraf D, Mukkamala SK, Freund KB. Multimodal imaging of pigment epithelial detachment: a guide to evaluation. *Retina*. 2013;33(9):1735–1762.)

During angiography, thick blood, pigment, scar tissue, or a PED may block fluorescence and obscure an underlying MNV. ICGA, with its longer wavelength fluorescence in the infrared spectrum, may penetrate deeper through heme or pigment to reveal a hot spot that identifies MNV. Because it has 90% protein binding, ICGA may also be able to differentiate between scar tissue and serous RPE fluid to reveal an active vascular lesion.

SD-OCT OF MNV SD-OCT is noninvasive and is the most practical visualization technique for diagnosing and classifying MNV as well as monitoring response to treatment. For example, SD-OCT reveals the elevation of the RPE and PEDs produced by type 1 MNV. Serous PEDs appear as sharply elevated, dome-shaped lesions with hollow internal reflectivity and typically no associated subretinal or intraretinal fluid. Fibrovascular PEDs may or may not be sharply elevated and typically demonstrate lacy or polyplike hyperreflective lesions on the undersurface of the RPE, with or without signs of contraction (Fig 4-10; Activity 4-1). Chronic fibrovascular PEDs often have a multilayered appearance because of sub-RPE cholesterol crystal precipitation in an aqueous environment; this appearance has been called the *onion sign*. The fibrotic “bridge arch-shaped” serous PED may develop after anti-VEGF treatment and is associated with a poor visual outcome.



ACTIVITY 4-1 OCT Activity: OCT of subfoveal pigment epithelial detachment.

Courtesy of Colin A. McCannel, MD.



In eyes with MNV, subretinal hyperreflective material (SHRM) may be hyperreflective on SD-OCT. This morphological feature found between the retina and RPE is thought to be a heterogeneous mixture of fluid, fibrin, blood, MNV, and other material. SHRM may have an adverse effect on VA and may cause scarring when it persists. Complex fibrovascular

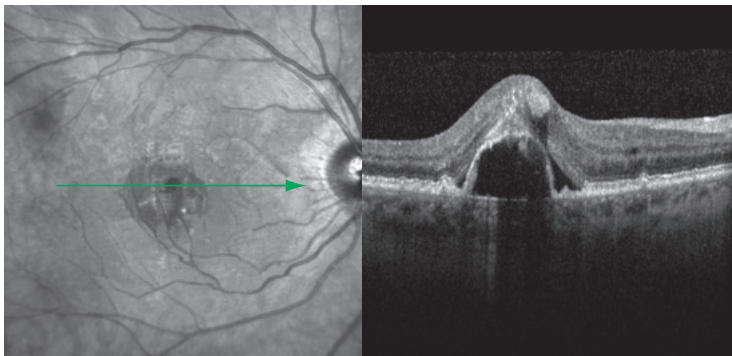


Figure 4-10 OCT image from a 61-year-old woman who reported progressively decreased vision and onset of waviness of straight lines in the right eye. OCT shows a subfoveal PED with associated subretinal fluid, intraretinal fluid, and intraretinal hyperreflective material. There is also an area of hyperreflective material on the underside of the RPE, likely representing a neovascular complex (see slices 13 and 14 in Activity 4-1). Scrolling through the macula in Activity 4-1 reveals the extent of the lesion, as well as RPE irregularities that resemble small PEDs (drusen). (*Courtesy of Colin A. McCannel, MD.*)

scarring may also be visualized in the sub-PED compartment, with or without associated subretinal and/or intraretinal fluid.

Recognition of MNV patterns on SD-OCT may be helpful for differential diagnosis and for predicting treatment outcomes. Type 1 MNV complexes start from the choroid and are limited to the sub-RPE space, visible as heterogeneous hyperreflective RPE elevations. Type 2 MNV appears as a hyperreflective band or plaque in the subneurosensory space, with associated subretinal and/or intraretinal fluid. Type 3 MNV presents on SD-OCT as hyperreflective foci emanating from the deep capillary plexus of the retina, with or without associated CME and PED.

Mrejen S, Sarraf D, Mukkamala SK, Freund KB. Multimodal imaging of pigment epithelial detachment: a guide to evaluation. *Retina*. 2013;33(9):1735–1762.

OCTA OF MNV The structural details of MNV can be revealed by OCTA. The fine details of the vascular architecture of each MNV type may be easily visualized, free of the blur caused by fluorescein leakage in FA (Figs 4-11, 4-12, 4-13). In type 1 MNV, OCTA shows abnormal vessels below the RPE. In type 2 MNV, the angiogenic complexes are seen above the RPE. Comparably, downgrowth of new vessels toward the RPE may be seen in type 3 MNV.

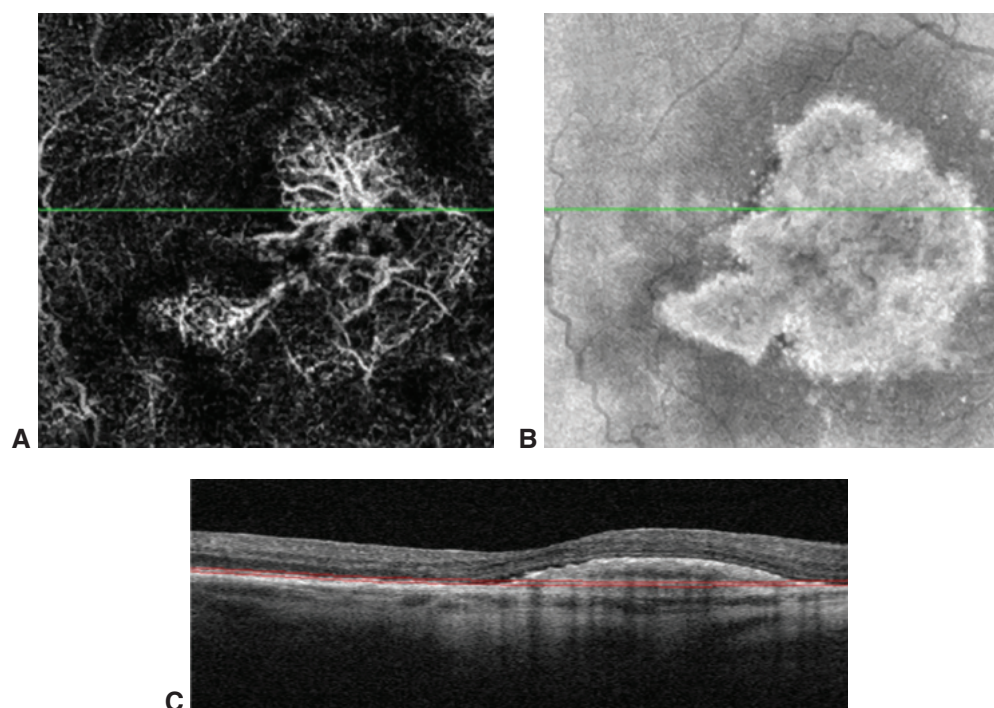


Figure 4-11 Type 1 MNV. **A**, OCT angiogram (OCTA) of type 1 MNV located beneath the RPE. The lesion has a “sea fan” configuration, with large feeder vessels and large caliber vessels. **B**, En face OCT structural image highlights the hyperreflective dome over the vessels. **C**, Cross-sectional B-scan OCT shows the distortion of the retinal profile caused by the MNV. (Courtesy of Richard B. Rosen, MD.)

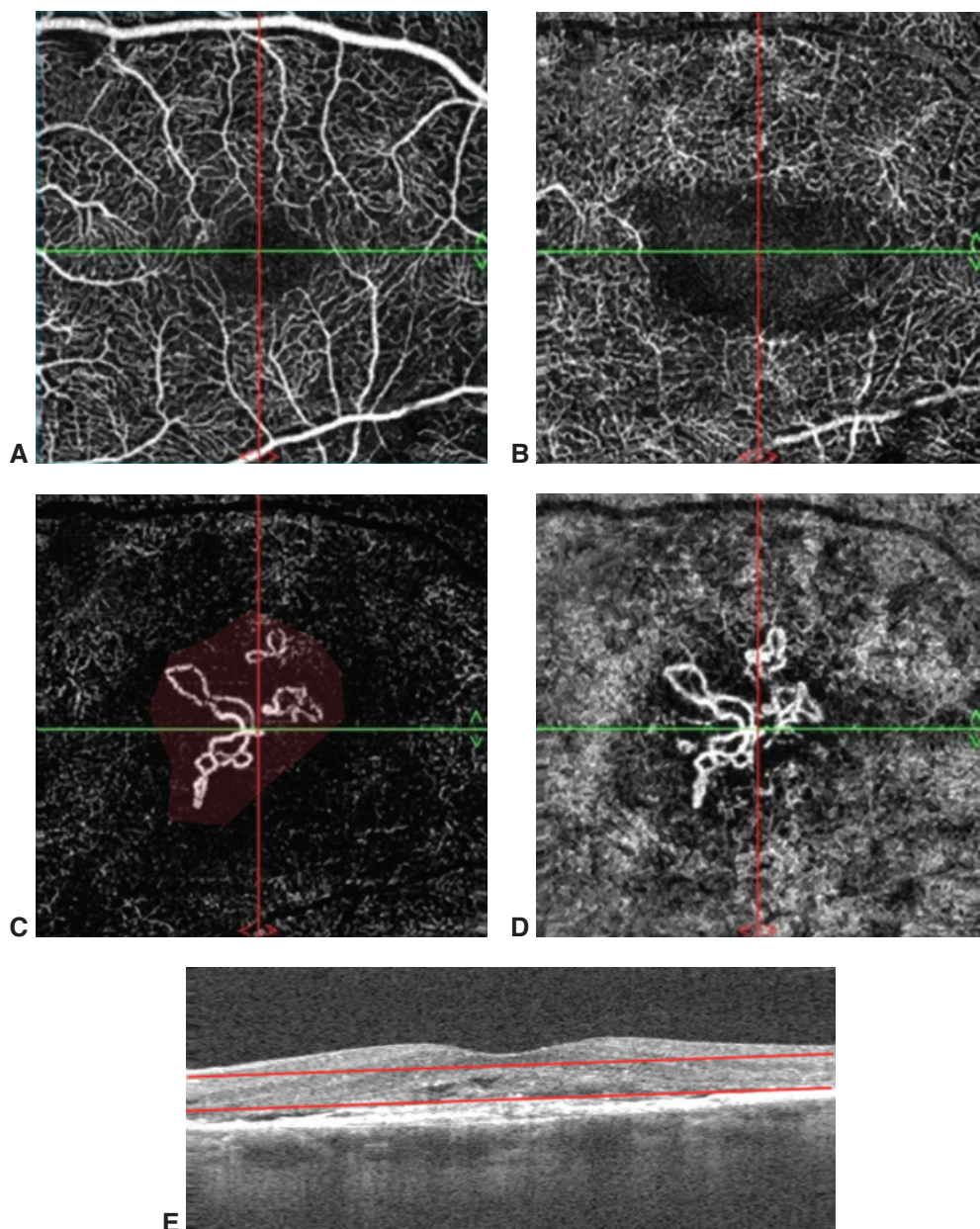


Figure 4-12 OCTA series of progressively deeper en face slices (**A–D**) of a type 2 MNV located above the RPE in the avascular zone of the retina. **A**, Superficial slab shows the superficial capillary plexus level and large retinal vessels. **B**, Deep capillary plexus level with an expanded foveal avascular zone caused by elevation of the underlying MNV. **C**, Avascular zone of the retina with MNV. **D**, Choriocapillaris level with MNV extending upward in the retina. **E**, Cross-sectional B-scan OCT shows disturbance in the RPE subretinal fluid and fibrosis. (Courtesy of Bruno Lumbroso.)

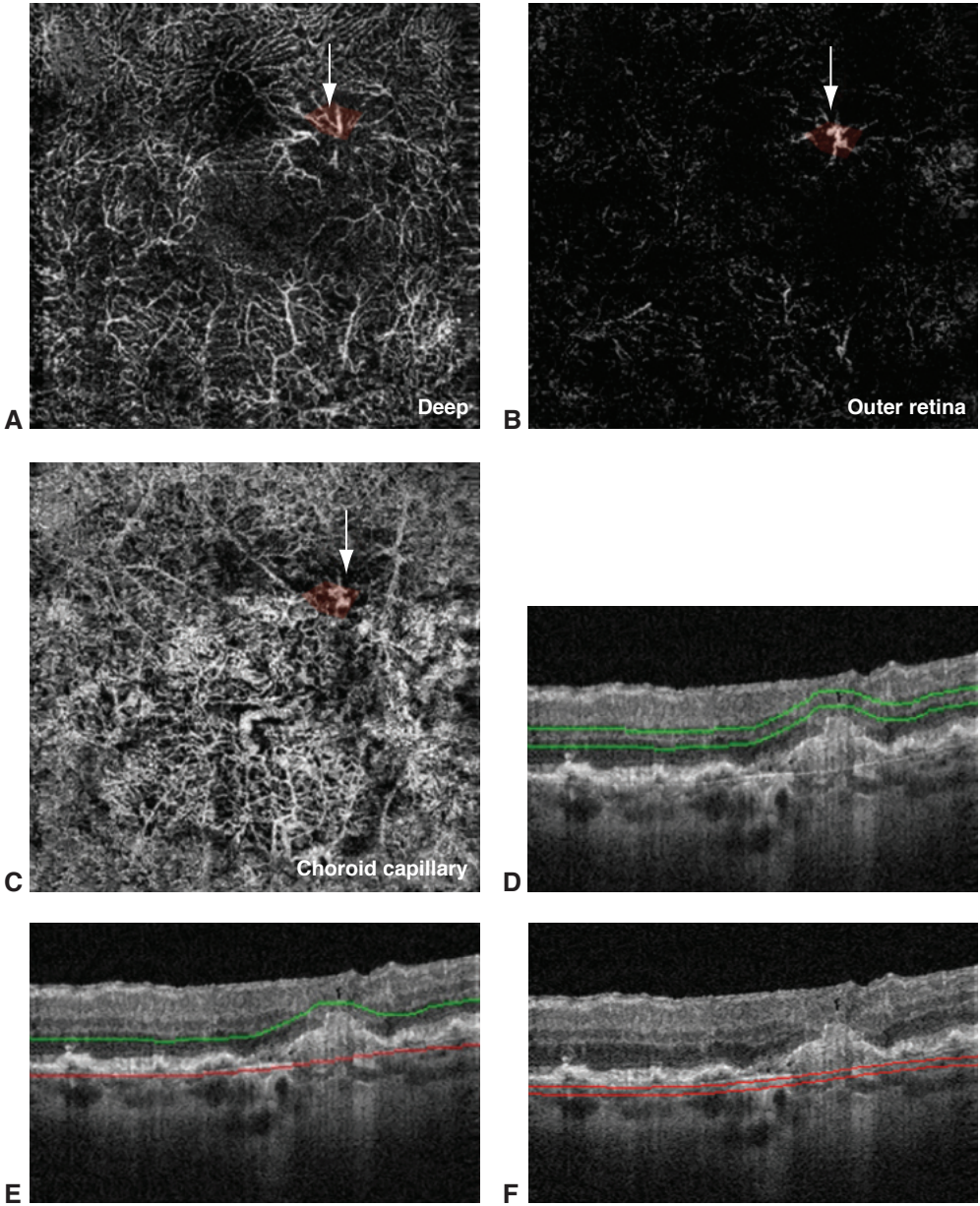


Figure 4-13 OCTA of type 3 MNV (retinal angiomatous proliferation lesion). **A**, Deep capillary plexus level reveals dilated blood vessels (*arrow*) wider than surrounding capillaries near the edge of the foveal avascular zone. **B**, Avascular zone level shows isolated MNV (*arrow*). **C**, Choriocapillaris level demonstrates interconnection of dilated deep capillary plexus vessels and choroidal vessels (*arrow*). **D**, Cross-sectional B-scan OCT shows segmentation of **A**. **E**, Cross-sectional B-scan OCT shows segmentation of **B**. **F**, Cross-sectional B-scan OCT shows segmentation of **C**. (Courtesy of Richard B. Rosen, MD.)

Spaide RF, Jaffe GJ, Sarraf D, et al. Consensus nomenclature for reporting neovascular age-related macular degeneration data: Consensus on Neovascular Age-Related Macular Degeneration Nomenclature Study Group. *Ophthalmology*. 2020;127(5):616–636. Published correction appears in *Ophthalmology*. 2020;127(10):1434–1435.

Polypoidal choroidal vasculopathy Polypoidal choroidal vasculopathy (PCV), initially called *posterior uveal bleeding syndrome*, is a variant of MNV (type 1) and presents with multiple, recurrent serosanguineous RPE detachments. A network of polyps is associated with feeder vessels that adhere to the RPE monolayer of the fibrovascular PED in a “string-of-pearls” configuration. Although PCV was first discovered in middle-aged African American or Asian American women with hypertension, it has since been identified in women and men of all races. In Asian individuals, however, 20%–50% of cases of neovascular AMD are PCV type, whereas in White people, less than 5% of cases of MNV are PCV type.

In PCV, associated serosanguineous detachments are often peripapillary and multifocal but may be peripheral, and there may be associated nodular, orange, subretinal lesions. Vitreous hemorrhage occurs more frequently in PCV AMD than in the non-PCV form. Soft drusen, typical in AMD, may or may not be present, whereas a thickened or so-called *pachychoroid* is often observed on EDI-OCT. ICGA, SD-OCT, and OCTA are all useful for identifying polyps.

Natural history and VA outcomes of PCV may be better than those of MNV associated with AMD, except in cases with severe subretinal hemorrhage (Figs 4-14, 4-15; see also Chapter 2, Fig 2-13). PCV is less responsive to anti-VEGF therapy than other types of MNV. Although the EVEREST studies demonstrated that photodynamic therapy with verteporfin with or without ranibizumab provided better response than ranibizumab alone for PCV, the PLANET study found that aflibercept monotherapy was noninferior to aflibercept plus photodynamic therapy with verteporfin for treatment of the disorder.

Koh A, Lai TYY, Takahashi K, et al; EVEREST II study group. Efficacy and safety of ranibizumab with or without verteporfin photodynamic therapy for polypoidal choroidal vasculopathy: a randomized clinical trial. *JAMA Ophthalmol*. 2017;135(11):1206–1213.

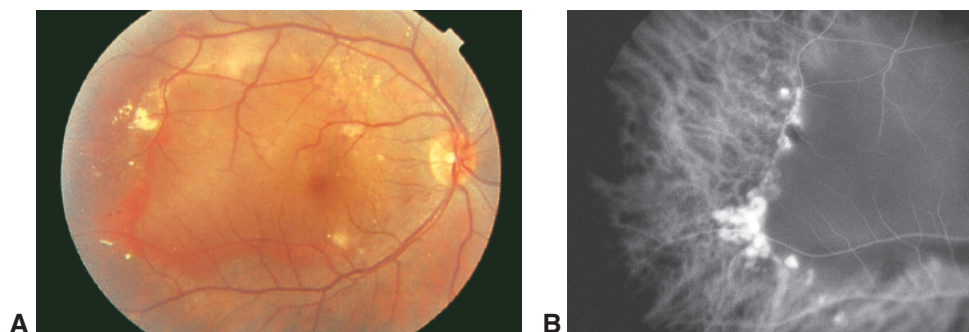


Figure 4-14 Polypoidal choroidal vasculopathy. **A**, Fundus photograph shows a large RPE detachment with multiple yellow-orange nodular lesions temporally. **B**, ICG angiogram demonstrates the characteristic polypoidal lesions temporally. (Courtesy of Lawrence A. Yannuzzi, MD.)

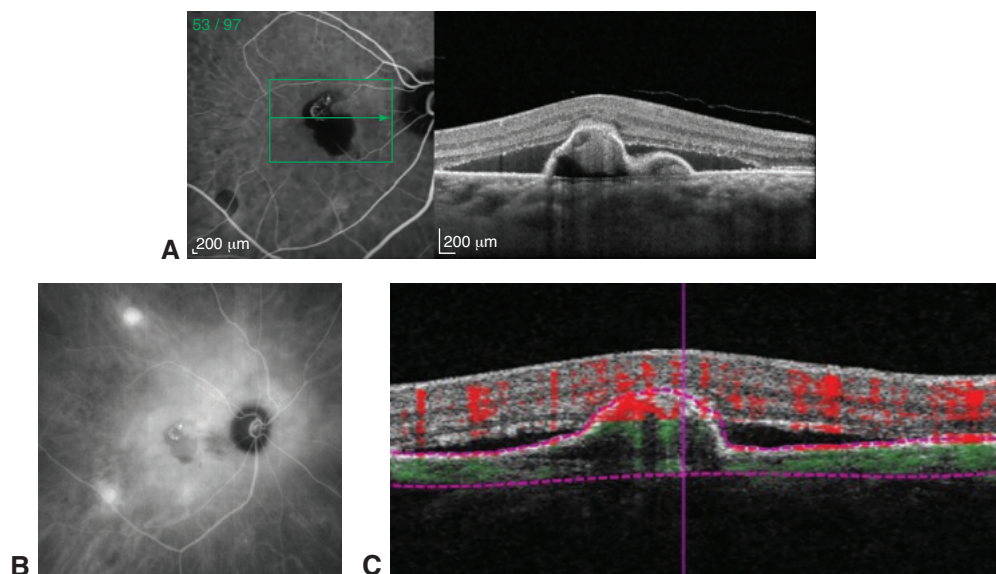


Figure 4-15 Polypoidal choroidal vasculopathy (PCV). **A**, Near-infrared reflectance image (left) showing ring-shaped PCV lesion within a retinal PED. Green arrow marks the location of the SD-OCT image (right) showing PED and subretinal fluid with PCV polyp visible just under the RPE monolayer. **B**, Corresponding wide-field ICG angiography. PCV complex is visible in the central macula with diffuse hyperpermeability in the macula and peripapillary regions. **C**, Corresponding OCTA. Red-highlighted area within the PED illustrates the polypoidal lesion with high vascular flow. (Courtesy of Gregg T. Kokame, MD.)

Lee WK, Iida T, Ogura Y, et al; PLANET Investigators. Efficacy and safety of intravitreal aflibercept for polypoidal choroidal vasculopathy in the PLANET study: a randomized clinical trial. *JAMA Ophthalmol.* 2018;136(7):786–793. Published correction appears in *JAMA Ophthalmol.* 2018;136(7):840.

Differential diagnosis of neovascular AMD

Many conditions associated with disruption of Bruch membrane complex and secondary CNV can mimic the MNV of AMD (see the section Other Causes of Choroidal Neovascularization later in this chapter). For example, central serous chorioretinopathy (CSC) may be confused with AMD, as subretinal fluid may be seen in both conditions; however, eyes with CSC typically do not have associated subretinal hemorrhage unless secondary CNV has developed. In addition, the choroidal layer, readily visualized using EDI-OCT, is frequently thick in eyes with CSC compared with the typical thin choroidal layer in eyes with AMD.

Macular telangiectasia, especially the most common variant type 2, may also be misdiagnosed as neovascular AMD (see Chapter 7).

Management of neovascular AMD

When neovascular AMD is suspected clinically, OCT can help establish the diagnosis and monitor response to therapy.

Laser photocoagulation (“thermal laser”) Thermal laser treatment is now used only in exceptionally rare instances of neovascular AMD because of poor outcomes from high recurrence rates, as revealed in the Macular Photocoagulation Study trials.

Photodynamic therapy (“cold laser”) Photodynamic therapy (PDT) was introduced in 2000 as a less-destructive phototherapy for treating MNV. Treatment involves intravenous administration of the photosensitizing drug verteporfin followed by the application of light of a specific wavelength. The light incites a localized photochemical reaction in the targeted area, resulting in MNV thrombosis. Although PDT slows progression, it does not prevent major vision loss in most eyes with MNV and has been shown to upregulate VEGF in the treatment area. Use of PDT to manage exudative AMD is now rare, except in eyes with PCV.

Antiangiogenic therapies Angiogenesis is the sprouting of new blood vessels from existing vessels. The first events in this complex cascade are vasodilation of existing vessels and increased vascular permeability. Next, degradation of the surrounding extracellular matrix occurs, facilitating migration and proliferation of endothelial cells. As endothelial cells join to create lumen, new capillaries develop and then mature, remodeling into stable vascular networks. To date, the most important activator of angiogenesis in retinal diseases is VEGF, originally known as vascular permeability factor.

VEGF is a homodimeric glycoprotein with a heparin-binding growth factor specificity for vascular endothelial cells. In addition to angiogenesis and vascular permeability, it induces lymphangiogenesis, and it acts as a survival factor for endothelial cells by preventing apoptosis. VEGF is actually a family of 5 distinct cytokines: VEGF-A, VEGF-B, VEGF-C, VEGF-D, and placental growth factor. Because the latter 4 were discovered after VEGF-A, VEGF-A is often referred to simply as *VEGF*.

Most anti-angiogenesis research has focused on the inhibition of VEGF-A (hereafter called VEGF unless specification is warranted), which has multiple isoforms. Elevated concentrations of VEGF in excised MNV and vitreous samples from patients with AMD have suggested a causal role for the glycoprotein in the pathologic neovascularization of AMD.

To date, 4 anti-VEGF pharmaceuticals given by intravitreal injection have been approved by the US Food and Drug Administration (FDA) for the treatment of exudative AMD; an additional drug is widely used but is not FDA approved for ophthalmic use. Overall, this class of therapeutics has been incredibly valuable, changing the epidemiology of blindness in some countries after its clinical introduction. In general, the earlier that conversion to exudative AMD is diagnosed and anti-VEGF therapy is initiated, the better the long-term outcomes.

Although antiangiogenic therapies are effective in AMD, the biggest challenge with their clinical application is the need for repeated doses to achieve optimal long-term outcomes. When exudative AMD is treated with anti-VEGF pharmacotherapy, a variety of clinical approaches may be used. Broadly, these include 1 of 3 strategies or a hybrid of them: (1) fixed dosing; (2) as-needed dosing, also referred to as *pro re nata* (PRN) dosing; and (3) treat-and-extend dosing, also referred to as *TAE*, *T&E*, or *TREX*. In the following subsections, these management approaches are discussed in the context of the pharmaceutical agent(s) used in key studies.

Pegaptanib In 2004, the FDA approved pegaptanib as the first intravitreal anti-VEGF therapy. Studies showed that pegaptanib, an RNA oligonucleotide ligand (or aptamer) that inhibits the human VEGF₁₆₅ isoform without inhibiting all VEGF isoforms, slowed vision loss; however, it has since been supplanted by more effective agents that inhibit all VEGF isoforms.

Ranibizumab Ranibizumab is a recombinant humanized antibody fragment that binds VEGF. Monthly ranibizumab dosing was assessed in 2 studies, MARINA and ANCHOR. At 12 months, a loss of fewer than 15 ETDRS (Early Treatment Diabetic Retinopathy Study) letters was reported in 95% of ranibizumab-treated patients compared with 62% of sham-treated patients and 64% of PDT-treated patients. In addition, VA improvement of 15 letters or more was reported in 30%–40% of ranibizumab-treated patients compared with 5% or less of control participants (Fig 4-16, Table 4-3). At 24 months, approximately 90% of ranibizumab-treated eyes had lost fewer than 15 ETDRS letters, and the VA gains achieved in the first year were maintained.

Multiple studies have analyzed less-frequent dosing of ranibizumab. VA improvements similar to those seen in the MARINA and ANCHOR studies over the first 3 months were also reported in the PIER and EXCITE studies. However, treatment effects declined in participants undergoing quarterly (ie, every 3 months) ranibizumab dosing as opposed to monthly dosing.

With PRN dosing, ranibizumab is administered until signs of exudation are resolved on OCT and clinical examination; after that, patients are followed up monthly, and treatment

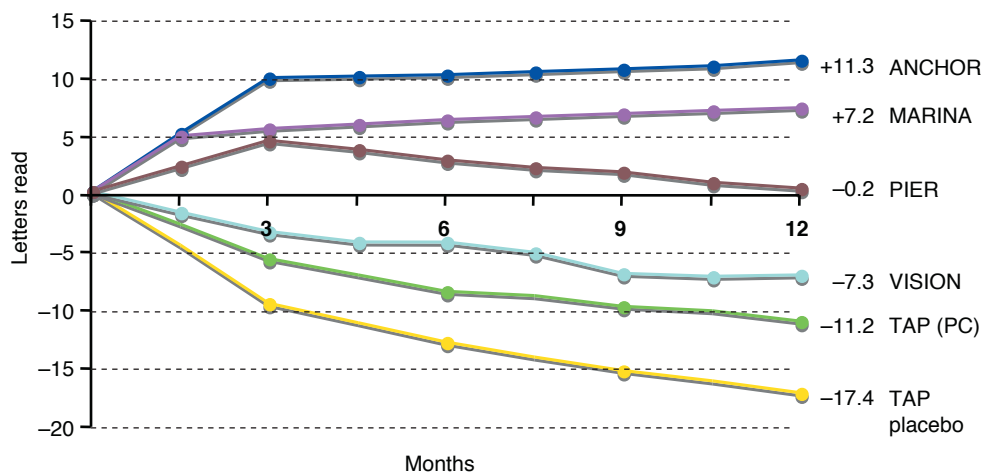


Figure 4-16 Graph illustrates the mean change in visual acuity (number of letters read) from several phase 3 clinical trials. Comparison of data between different trials should be interpreted with caution; the potentially different study inclusion criteria and baseline characteristics of eyes for different studies may affect the stated visual acuity gains. ANCHOR = Anti-VEGF Antibody for the Treatment of Predominantly Classic Choroidal Neovascularization in AMD; MARINA = Minimally Classic/Occult Trial of the Anti-VEGF Antibody Ranibizumab in the Treatment of Neovascular AMD; PC = predominantly classic; PIER = Phase 3b, Multicenter, Randomized, Double-Masked, Sham Injection-Controlled Study of the Efficacy and Safety of Ranibizumab in Subjects With Subfoveal Choroidal Neovascularization With or Without Classic Choroidal Neovascularization Secondary to AMD; TAP = Treatment of AMD with Photodynamic Therapy; VISION = VEGF Inhibition Study in Ocular Neovascularization. (Courtesy of Peter K. Kaiser, MD.)

Table 4-3 Selected Clinical Trials, Treatments, and Outcomes

Clinical Trial	Treatment	Outcome
ANCHOR	Ranibizumab monthly vs photodynamic therapy as needed quarterly	Increase of 11.3 letters in ranibizumab monthly group vs decrease of 9.5 letters in verteporfin group ($P < 0.001$ at 2 years)
MARINA	Ranibizumab monthly vs sham treatment	Increase of 7.2 letters in ranibizumab monthly group vs loss of 10.4 letters in sham group ($P < 0.001$ at 2 years)
VIEW 1	Ranibizumab monthly vs aflibercept monthly and bimonthly	Increase of 8.1 letters in ranibizumab monthly group (94.4% lost <15 letters) Increase of 10.9 letters in aflibercept monthly group (95.1% lost <15 letters) Increase of 7.9 letters in aflibercept bimonthly group (95.1% lost <15 letters)
VIEW 2	Ranibizumab monthly vs aflibercept monthly and bimonthly	Aflibercept deemed noninferior to ranibizumab Increase of 9.4 letters in ranibizumab monthly group (94.4% lost <15 letters) Increase of 7.6 letters in aflibercept monthly group (95.6% lost <15 letters) Increase of 8.9 letters in aflibercept bimonthly group (95.6% lost <15 letters) Aflibercept deemed noninferior to ranibizumab

Data from Rofagha S, Bhisitkul RB, Boyer DS, Sadda SR, Zhang K; SEVEN-UP Study Group. Seven-year outcomes in ranibizumab-treated patients in ANCHOR, MARINA, and HORIZON: a multicenter cohort study (SEVEN-UP). *Ophthalmology*. 2013;120(11):2292–2299.

is resumed only when there are signs of recurrent exudation. Several clinical trials have evaluated PRN approaches to anti-VEGF therapy: SUSTAIN, HORIZON, and HARBOR. In each of these studies, participants were administered 3 monthly injections of ranibizumab, followed by various as-needed treatment regimens according to clinical and OCT-guided criteria. In these studies, visual acuity improvements were comparable to or less favorable than those reported in MARINA and ANCHOR. In the HORIZON study, which involved patients enrolled in prior ranibizumab AMD trials, eyes that had gained 10.2 letters on the ETDRS eye chart after 2 years of monthly injections during ANCHOR or MARINA lost VA, ending with a mean letter gain of only 2.0 compared with baseline (ie, they lost nearly 8 letters once the regimen was switched from monthly injections to an as-needed protocol). HORIZON did not offer any re-treatment guidelines for investigators, resulting in a mean of only 3.6 ranibizumab injections in the 12 months of the extension trial. The phase 3 HARBOR study compared higher-dose (2.0 mg) with standard-dose (0.5 mg) ranibizumab using both monthly and PRN dosing with specific predefined re-treatment criteria. Subjects randomly assigned to PRN dosing were evaluated monthly to determine their need for re-treatment. Study authors reported no differences in VA or anatomical outcomes between the fixed monthly and PRN dosing and noted a very wide range of dosing needs among individual patients.

In patients with MNV, the goal of TAE management is to suppress exudative activity using as few re-treatments as possible. This typically involves 3 phases. First, monthly anti-VEGF therapy is administered until exudation is resolved. Second, treatment continues at

progressively increasing intervals, with intervals between doses often lengthened by 2-week increments, until recurrent exudation is identified. Third, a fixed-interval dosing strategy is initiated using an interval just less than the interval at which signs of exudation recurred. In the TREND study, 650 patients with exudative AMD were randomly assigned to either monthly or TAE management with ranibizumab. At 1 year, TAE management was associated with a mean of 8.7 injections and was found to be noninferior to monthly management, which was associated with a mean of 11.1 injections. In addition, TAE and monthly regimens were associated with mean gains of 6.6 and 7.9 ETDRS letters, respectively, and 62% of eyes managed with TAE were receiving injections at intervals of 8 weeks or longer.

Silva R, Berta A, Larsen M, Macfadden W, Feller C, Monés J; TREND Study Group. Treat-and-extend versus monthly regimen in neovascular age-related macular degeneration: results with ranibizumab from the TREND study. *Ophthalmology*. 2018;125(1):57–65.

Aflibercept Aflibercept is a soluble VEGF receptor decoy; it combines the ligand-binding elements of the extracellular domains of *VEGFR1* and *VEGFR2* and the constant region (Fc) of immunoglobulin G and binds VEGF-A, VEGF-B, and placental growth factor. In the paired VIEW 1 and VIEW 2 studies, patients received aflibercept monthly or every second month after 3 monthly loading doses, while a comparison group received monthly ranibizumab. Both aflibercept regimens demonstrated noninferiority to monthly ranibizumab, with each of the 6 arms gaining between 7.6 and 10.9 letters at 1 year (ie, primary endpoint; see Table 4-3). At 96 weeks, VA gains were maintained with both aflibercept dosing regimens; in addition, 3-line VA increases were seen in 30%–33% of patients in each arm, comparable to results with monthly ranibizumab. In addition, OCT-measured anatomical response was similar among the 3 randomized arms through 2 years, as were safety profiles for both aflibercept and ranibizumab. Among patients with persistent exudative disease activity through the first 3 monthly doses, transition to every-second-month dosing was associated with maintenance of the VA gains achieved during the 3 monthly doses; however, among these incomplete responders, continued monthly dosing appeared to achieve better visual and anatomical outcomes than every-second-month dosing.

Heier JS, Brown DM, Chong V, et al; VIEW 1 and VIEW 2 Study Groups. Intravitreal aflibercept (VEGF trap-eye) in wet age-related macular degeneration. *Ophthalmology*. 2012;119(12):2537–2548.

Jaffe GJ, Kaiser PK, Thompson D, et al. Differential response to anti-VEGF regimens in age-related macular degeneration patients with early persistent retinal fluid. *Ophthalmology*. 2016;123(9):1856–1864.

Bevacizumab Bevacizumab is a full-length monoclonal antibody against VEGF that is FDA approved for the intravenous treatment of multiple types of systemic cancer. It is also widely used “off-label” for the intravitreal treatment of exudative AMD. Ranibizumab is derived from bevacizumab, although there are key differences between the drugs. First, with 2 antigen-binding domains, bevacizumab is larger than ranibizumab, which has a single domain. Because full-length antibodies are not cleared as rapidly as antibody fragments, intravitreal injections of bevacizumab have a longer systemic half-life (as well as longer intravitreal half-life) than intravitreal injections of ranibizumab. Second, the repackaged bevacizumab used to treat exudative retinal diseases costs substantially less than ranibizumab.

Several large, prospective, randomized studies on neovascular AMD have demonstrated comparable efficacy between bevacizumab and ranibizumab (Table 4-4). CATT, a multicenter trial funded by the US National Eye Institute, studied 1208 patients and found that bevacizumab and ranibizumab had similar effects on VA over a 2-year period and that PRN treatment provided lower VA gains than fixed monthly dosing. Mean gains from baseline were 8.8 letters in the ranibizumab-monthly group, 7.8 letters in the bevacizumab-monthly group, 6.7 letters in the ranibizumab PRN group, and 5.0 letters in the bevacizumab PRN group. Although the proportion of patients with 1 or more systemic adverse events was significantly greater in the bevacizumab group (39.9%) than in the ranibizumab group (31.7%), death and arteriothrombotic events were not statistically different between the 2 drugs. At 5 years, vision gains in the first 2 years were not sustained, but 50% of eyes maintained VA of 20/40 or better.

Brolucizumab Brolucizumab is a single-chain antibody fragment with a molecular weight of 26 kDa, compared with 48 kDa for ranibizumab, 115 kDa for aflibercept, and 149 kDa for bevacizumab. In the HAWK and HARRIER paired trials, the largest phase 3 exudative AMD program to date, 2824 eyes were randomly assigned to aflibercept given every second month after 3 monthly doses or brolucizumab. Patients taking brolucizumab received 3 monthly doses and then transitioned to injections every 12 weeks, with dosing shortened to every 8 weeks when exudative disease activity worsened at multiple prespecified assessment visits. At 48 weeks, VA noninferiority between the drugs, the primary study endpoint, was achieved. At the final study visit at 96 weeks, fewer than half of patients receiving brolucizumab remained on quarterly dosing. Anatomically, brolucizumab appeared to be a statistically significant superior drying agent. However, during the phase 3 program, intraocular inflammation developed in 4.6% of brolucizumab-treated patients, with retinal vasculitis and/or vascular occlusion also developing in some of these patients; in contrast, intraocular inflammation developed in 1.1% of aflibercept-treated patients.

Dugel PU, Singh RP, Koh A, et al. HAWK and HARRIER: ninety-six-week outcomes from the phase 3 trials of brolucizumab for neovascular age-related macular degeneration. *Ophthalmology*. 2021;128(1):89–99.

Complications of intravitreal antiangiogenic therapy Intravitreal antiangiogenic therapy has been associated with a range of potential adverse effects. The rate of endophthalmitis is approximately 1 in 2000 patients who use anti-VEGF agents (see also Chapter 19). With or without anti-VEGF therapy, eyes with fibrovascular PEDs may be at increased risk for the development of an RPE tear, especially with PEDs greater than 600 μm in height. The mechanism of the tear is thought to be contraction of the underlying type 1 MNV, which may occur after anti-VEGF dosing. Use of bevacizumab to treat cancer has also increased the risk of hypertension; thromboembolic events, especially myocardial infarctions and cerebral vascular accidents; gastrointestinal perforations; and bleeding. However, evidence that intravitreal anti-VEGF agents increase the rate of systemic complications is conflicting.

Solomon SD, Lindsley K, Vedula SS, Krzystolik MG, Hawkins BS. Anti-vascular endothelial growth factor for neovascular age-related macular degeneration. *Cochrane Database Syst Rev*. 2014;8(8):CD005139.

Table 4-4 Clinical Trials Comparing Bevacizumab With Ranibizumab

Study Abbreviation	Study Name	Location	Patients Enrolled	Treatment Regimen	Major Outcome
BRAMD	Comparing the Effectiveness of Bevacizumab to Ranibizumab in Patients With Exudative Age-Related Macular Degeneration	The Netherlands	327	Fixed-interval dosing	Bevacizumab noninferior to ranibizumab with regard to visual acuity outcomes
CATT	Comparison of Age-Related Macular Degeneration Treatments Trials	United States	1208	As-needed, fixed-interval dosing	Bevacizumab noninferior to ranibizumab with regard to visual acuity outcomes
GEFAL	Groupe d'Evaluation Français Avastin vs Lucentis	France	501	As-needed dosing	No significant difference in outcomes between drugs
IVAN	Randomised Controlled Trial of Alternative Treatments to Inhibit VEGF in Age-Related Choroidal Neovascularisation	United Kingdom	610	As-needed, fixed-interval dosing	No statistically significant differences in visual or anatomical outcomes between drugs
LUCAS	Lucentis Compared to Avastin Study	Norway	432	Treat-and-extend dosing	No significant differences in outcomes between drugs
MANTA	A Randomized Observer and Subject Masked Trial Comparing the Visual Outcome After Treatment With Ranibizumab or Bevacizumab in Patients With Neovascular Age-Related Macular Degeneration Multicenter Anti-VEGF Trial in Austria	Austria	321	As-needed dosing	Groups had similar visual acuity and anatomical outcomes

Data from CATT Research Group; Martin DF, Maguire MG, Ying G, et al. Ranibizumab and bevacizumab for neovascular age-related macular degeneration. *N Engl J Med*. 2011;364(20):1897–1908; and from CATT Research Group; Martin DF, Maguire MG, Fine SL, et al. Ranibizumab and bevacizumab for treatment of neovascular age-related macular degeneration: two-year results. *Ophthalmology*. 2012;119(7):1388–1398.

Combination treatment To address the complex interactions between inflammation, angiogenesis, and fibrosis that are thought to play a role in exudative AMD pathogenesis, combinations of therapies have been explored. Trials have shown that combining PDT with ranibizumab may reduce re-treatment rates compared with ranibizumab monotherapy. Combination strategies may be particularly beneficial for patients with PCV that is refractive to anti-VEGF monotherapy. In those with exudative AMD, cytokines and molecular pathways beyond VEGF-A are also being evaluated to improve outcomes and reduce treatment frequency.

Lim TH, Lai TYY, Takahashi K, et al; EVEREST II Study Group. Comparison of ranibizumab with or without verteporfin photodynamic therapy for polypoidal choroidal vasculopathy: the EVEREST II randomized clinical trial. *JAMA Ophthalmol.* 2020;138(9):935–942.

Surgical treatments In cases of thick submacular hemorrhage, injection of intravitreal or subretinal tissue plasminogen activator with pneumatic displacement may be considered. In contrast, both submacular surgery, with removal of the MNV from beneath the fovea, and macular translocation surgery involve complex techniques developed before the introduction of anti-VEGF agents and have been abandoned.

Low-vision therapies and low-vision rehabilitation Despite the success of intravitreal anti-VEGF pharmacotherapy, a substantial number of patients with AMD will ultimately progress to bilateral central blindness. However, for some of these patients, the use of optical and non-optical devices may improve functional status and quality of life (see BCSC Section 3, *Clinical Optics and Vision Rehabilitation*). For example, an implantable miniature telescope can provide magnification up to a factor of 2.7, although corneal decompensation due to endothelial cell loss is a known risk of this technology. Even simple strategies such as magnification (eg, high-plus lenses, video magnifiers), optimal lighting, and contrast enhancement techniques may be beneficial and warrant discussion with patients.

Social determinants of neovascular AMD treatment A lack of caretakers and the financial burden of treatment may play a major role in patient nonadherence with treatment visits.

Other Causes of Choroidal Neovascularization

A number of conditions other than AMD can produce degenerative changes within the macula, with central vision loss caused by CNV, atrophy, or scarring. Although historically focused on laser therapies or PDT, CNV management now involves primarily the use of intravitreal anti-VEGF agents.

Ocular Histoplasmosis Syndrome

Histoplasma capsulatum fungus is endemic to the Mississippi and Ohio River valleys. Humans become infected by inhaling the yeast form of this fungus, which then disseminates throughout the bloodstream. Although the systemic infection eventually subsides, the individual may be left with chorioretinal scars that produce visual symptoms years later.

Ocular histoplasmosis syndrome (OHS), a disease associated with *H capsulatum* infection, is also referred to as *presumed* OHS because the causality has not been definitively confirmed. OHS is most prevalent among individuals with the greatest percentage of positive skin reactors; more than 90% of patients with the characteristic OHS fundus appearance react positively to the histoplasmin skin test. The organism has been identified histologically in the choroid of 5 patients with OHS. Nevertheless, other etiologies besides *H capsulatum* may produce a similar phenotype (see also the section “Multifocal choroiditis, including inner punctate choroiditis” in Chapter 11).

Clinically, OHS presents with small, atrophic, “punched-out” chorioretinal scars in the midperiphery and posterior pole (“histo spots”), linear peripheral atrophic tracks, and juxtapapillary chorioretinal scarring with or without CNV in the macula (Fig 4-17). Lesions are bilateral in more than 60% of patients, and characteristically, vitreous inflammation is

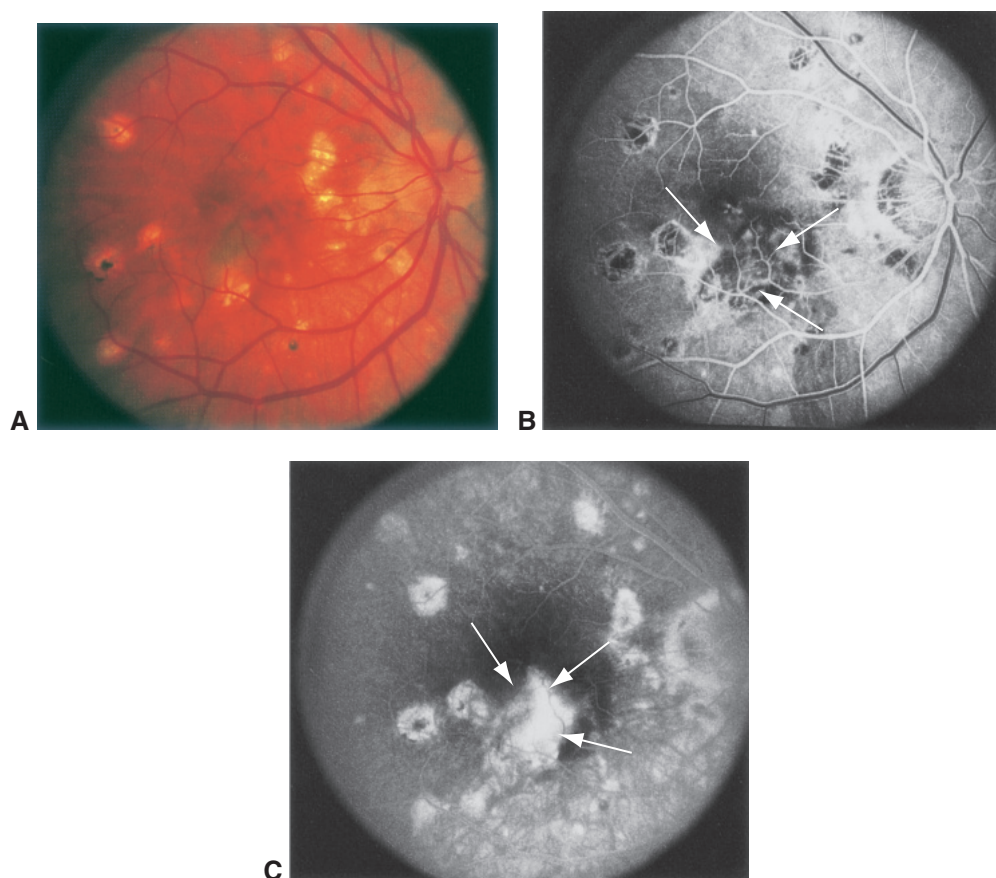


Figure 4-17 Ocular histoplasmosis syndrome with CNV. **A**, Fundus photograph shows peripapillary atrophy and numerous atrophic scars. **B**, Transit frame of the angiographic study reveals blocked fluorescence from blood and pigment as well as hyperfluorescence resulting from the CNV (arrows) and choroidal transmission in areas of atrophy. **C**, Leakage from the choroidal neovascular membrane (arrows) late in the study, as well as staining of the sclera beneath atrophic scars.

absent. Most patients with OHS are asymptomatic until the development of CNV, which may cause vision loss, metamorphopsia, and paracentral scotomata. Diseases with features similar to those of OHS include panuveitis and multifocal choroiditis; see also BCSC Section 9, *Uveitis and Ocular Inflammation*.

Angioid Streaks

Irregular dark red or brown lines radiating from a ring of peripapillary atrophy surrounding the optic nerve head are referred to as *angioid streaks* because they mimic the appearance of blood vessels. On FA, characteristic window defects with late staining are noted, resulting from dehiscences or cracks in the thickened and calcified Bruch membrane (Fig 4-18).

The systemic disease most commonly associated with angioid streaks is pseudoxanthoma elasticum (PXE), or Grönblad-Strandberg syndrome, a predominantly autosomal recessive disorder inherited through mutation in the *ABCC6* gene, which is located on band 16p13.11. Additional fundus findings associated with PXE include optic disc drusen, peripheral round atrophic scars with a “comet” sign, and a mottled RPE appearance referred to as *peau d’orange* (“skin of an orange”). Paget disease of bone, β -thalassemia, sickle cell anemia, and Ehlers-Danlos syndrome may also be associated with angioid streaks. When the ophthalmologist establishes a new diagnosis of angioid streaks and the patient has none of the aforementioned conditions, the patient should be referred for evaluation and management of possible underlying systemic diseases.

Unless they are subfoveal, angioid streaks usually are asymptomatic. Visual disturbances may develop owing to submacular hemorrhage resulting from trauma, but these disturbances may resolve spontaneously when there is no CNV. The most relevant visual complication is the development of CNV. Safety glasses are an advisable precaution for patients with angioid streaks, who may be highly susceptible to choroidal rupture after even

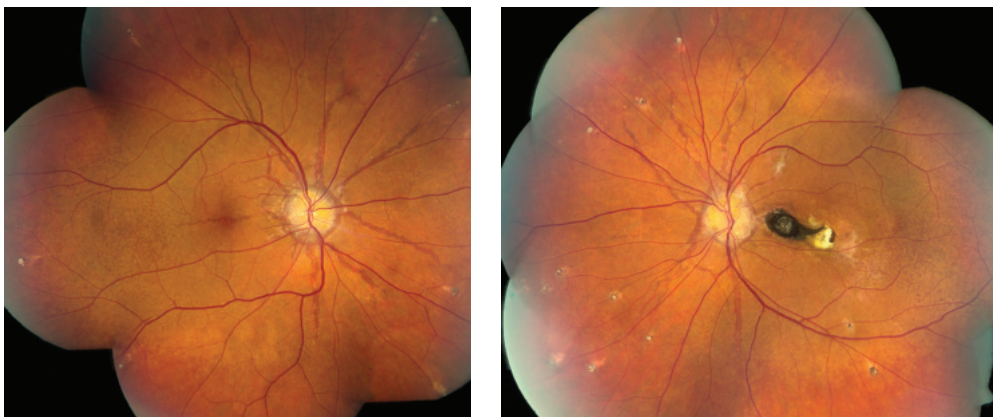


Figure 4-18 Color montages of fundus photographs from a patient with pseudoxanthoma elasticum showing, in both eyes, angioid streaks radiating from the optic nerve head; a “peau d’orange” appearance of the fundus temporal to the macula; optic disc drusen; midperipheral comet lesions; and in the left eye, an old, inactive CNV. (Courtesy of Stephen J. Kim, MD.)

minor blunt injury. Medical consultation is indicated to evaluate for systemic manifestations of PXE, including benign features such as “plucked chicken” skin appearance and more serious life-threatening findings such as calcific arteriosclerosis of coronary arteries and gastrointestinal and cerebrovascular bleeding.

Pathologic Myopia

Choroidal neovascularization may develop in 5%–10% of adult eyes with an axial length of 26.5 mm or more, with or without lacquer cracks or widespread chorioretinal degeneration (Fig 4-19; see also Chapter 10). Laser therapy is typically not used because of the risk of laser scar expansion through the foveal center over time (so-called *atrophic creep*). Although PDT has been shown to be beneficial, the mainstay of treatment currently is intravitreal anti-VEGF therapy. Several studies have demonstrated sustained regression of myopic CNV after anti-VEGF treatment, with stabilization or improvement of VA after as

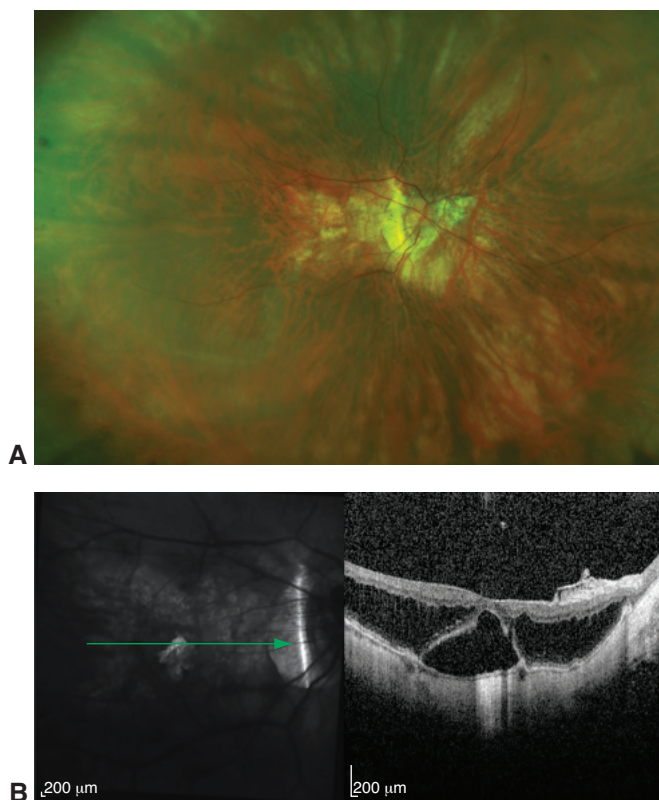


Figure 4-19 Pathologic myopia. **A**, Color fundus photograph of the right eye demonstrating myopic macular degeneration with a posterior staphyloma, prominent peripapillary atrophy of the RPE, and extensive pigment mottling centrally. **B**, Near-infrared reflectance image (*left*) with *green arrow* marking the location of the SD-OCT image (*right*) showing extensive intraretinal fluid with myopic macular schisis as well as central subretinal fluid and a mild epiretinal membrane. (Courtesy of Charles C. Wykoff, MD, PhD.)

Table 4-5 Conditions Associated With Choroidal Neovascularization

Degenerative	Neoplastic
Age-related macular degeneration	Choroidal hemangioma
Angioid streaks	Choroidal nevus
Myopic degeneration	Hamartoma of the RPE
Heredodegenerative	Metastatic choroidal tumors
Fundus flavimaculatus	Traumatic
Optic disc drusen	Choroidal rupture
Vitelliform maculopathy	Intense photocoagulation
Inflammatory	Idiopathic
Behçet disease	
Multifocal choroiditis	
Ocular histoplasmosis syndrome	
Rubella	
Serpiginous-like choroiditis (also called <i>multifocal serpiginoid choroiditis</i>)	
Sympathetic ophthalmia	
Toxocariasis	
Toxoplasmosis	
Vogt-Koyanagi-Harada syndrome	

RPE = retinal pigment epithelium.

few as 1 or 2 injections and no need for ongoing repeated injections in many patients, in contrast to management of exudative AMD.

Wolf S, Balciuniene VJ, Laganovska G, et al; RADIANCE Study Group. RADIANCE: a randomized controlled study of ranibizumab in patients with choroidal neovascularization secondary to pathologic myopia. *Ophthalmology*. 2014;121(3):682–692.e2.

Idiopathic CNV and Miscellaneous Causes of CNV

Choroidal neovascularization may complicate any of the conditions known to damage Bruch membrane, including inflammatory chorioretinopathies, choroidal neoplasms, traumatic choroidal rupture, and optic nerve head abnormalities (Table 4-5). It may also develop in eyes with no apparent risk factors or predisposing lesions (eg, idiopathic CNV).

Heier JS, Brown D, Ciulla T, et al. Ranibizumab for choroidal neovascularization secondary to causes other than age-related macular degeneration: a phase I clinical trial. *Ophthalmology*. 2011;118(1):111–118.

CHAPTER 5

Diabetic Retinopathy



This chapter includes a related activity. Go to www.aao.org/bcscactivity_section12 or scan the QR code in the text to access this content.

Highlights

- Systemic control of hyperglycemia, hypertension, and hyperlipidemia is the foundation of care for all diabetic eye diseases.
- For treating proliferative diabetic retinopathy, both panretinal photocoagulation and intravitreal anti-VEGF therapy are effective. Panretinal photocoagulation may also be considered for eyes with severe nonproliferative diabetic retinopathy, especially in patients with type 2 diabetes. Anti-vascular endothelial growth factor (anti-VEGF) agents frequently reduce the severity of diabetic retinopathy and the risk of vision-threatening complications in eyes with nonproliferative disease but may not improve long-term visual outcomes.
- Intravitreal anti-VEGF is first-line therapy for most eyes with center-involved diabetic macular edema and vision loss. In contrast, treatment can generally be deferred in eyes with good vision despite center-involved diabetic macular edema.
- When anti-VEGF treatment is inappropriate or ineffective for diabetic macular edema, intravitreal corticosteroid therapy and macular focal/grid laser photocoagulation may be used as alternative or adjunctive therapy.

Introduction

Diabetic retinopathy is a leading cause of vision loss worldwide among patients aged 25–74 years, especially in resource-rich countries such as the United States. This chapter provides a foundation for the evaluation and treatment of diabetic retinopathy. See BCSC Section 1, *Update on General Medicine*, for discussion of diabetes mellitus. The following glossary provides the abbreviated and full names of diabetic retinopathy and diabetic and macular edema studies referenced in this chapter. Only the short names are used in the text.

Diabetic Retinopathy and Diabetic Macular Edema Studies

ACCORD Action to Control Cardiovascular Risk in Diabetes

ACCORDION ACCORD Follow-On Study

CLARITY Clinical Efficacy and Mechanistic Evaluation of Aflibercept for Proliferative Diabetic Retinopathy

DCCT Diabetes Control and Complications Trial

DRS Diabetic Retinopathy Study

DRVS Diabetic Retinopathy Vitrectomy Study

ETDRS Early Treatment Diabetic Retinopathy Study

FIELD Fenofibrate Intervention and Event Lowering in Diabetes

PANORAMA Study of the Efficacy and Safety of Intravitreal Aflibercept for the Improvement of Moderately Severe to Severe Nonproliferative Diabetic Retinopathy

RIDE and RISE Ranibizumab Injection in Subjects with CSME With Center Involvement Secondary to Diabetes Mellitus

UKPDS United Kingdom Prospective Diabetes Study

VISTA Study of Intravitreal Aflibercept Injection in Patients with Diabetic Macular Edema

VIVID Intravitreal Aflibercept Injection in Vision Impairment Due to Diabetic Macular Edema

WESDR Wisconsin Epidemiologic Study of Diabetic Retinopathy

Terminology and Classification

Diabetes Terminology

The American Diabetes Association classifies diabetes mellitus as type 1 diabetes (formerly, *insulin-dependent diabetes mellitus*) or type 2 diabetes (formerly, *non-insulin-dependent diabetes mellitus*). Type 1 diabetes results from the idiopathic or immune-mediated destruction of pancreatic β cells, which usually leads to absolute insulin deficiency. Type 2 diabetes is characterized by insulin resistance with or without insulin deficiency. Other classifications of diabetes mellitus recognized by the American Diabetes Association include a genetically mediated form secondary to endocrinopathy and drug- or chemical-induced diabetes.

Diabetic Retinopathy Terminology

Diabetic retinopathy is classified according to the severity and extent of hallmark diabetic lesions found within an eye. In *nonproliferative diabetic retinopathy (NPDR)*, intraretinal

vascular changes are present, but extraretinal fibrovascular tissue does not develop. NPDR is staged across a spectrum of severity levels as mild, moderate, or severe. (Of note, although NPDR has been referred to as *background diabetic retinopathy*, this term is no longer used.) *Proliferative diabetic retinopathy (PDR)* is defined as the presence of retinal neovascularization due to diabetes-induced ischemia. It represents the most advanced level of diabetic retinopathy and may develop after an eye has progressed through the sequential stages of NPDR. Clinically, PDR is staged as either early disease or PDR with high-risk characteristics.

Diabetic macular edema (DME), or swelling of the central retina, results from abnormal vascular permeability and may develop in patients with diabetic retinopathy of any severity. DME is classified as *center-involved* (or *central-involved*) when the central 1-mm-diameter retinal subfield is thickened on optical coherence tomography (OCT); it is classified as *non-center-involved DME* when retinal thickening occurs only outside the central retinal subfield. *Clinically significant diabetic macular edema (CSME)* is an older term from the ETDRS that describes DME that meets certain severity criteria for size and location. However, this classification is no longer routinely used to determine the need for treatment.

In this chapter, research results are reported using terminology from the respective study being discussed, even though it may not conform to current usage.

Epidemiology of Diabetic Retinopathy

Diabetes mellitus is a growing global epidemic, projected to affect 700 million people by 2045, with a corresponding increase in the prevalence of diabetic retinopathy worldwide. Approximately one-third of the global population with diabetes mellitus also has diabetic retinopathy; of this group, one-third has a vision-threatening form of retinopathy.

Important long-term data on disease rates and progression, including a direct association between longer duration of both type 1 and type 2 diabetes and increased prevalence of diabetic retinopathy, were provided by the WESDR. Among WESDR participants with a 20-year history of diabetes mellitus, nearly 99% of those with type 1 disease and 60% of those with type 2 disease had some degree of diabetic retinopathy. PDR was also reported in 50% of patients with a 20-year history of type 1 diabetes and in 25% of those with a 25-year history of type 2 diabetes. In addition, a visual acuity of 20/200 or worse was observed in 3.6% of patients with younger-onset disease (ie, aged <30 years at diagnosis) and 1.6% of patients with older-onset disease (ie, aged 30 years or older at diagnosis). This vision loss was attributed to diabetic retinopathy in 86% of the younger-onset group and 33% of the older-onset group.

Of note, epidemiologic data from the WESDR study, first published in the 1980s, were drawn largely from White patients of northern European descent and therefore are not entirely applicable to other racial groups. Also, social determinants of health are increasingly recognized for their contributions to the increasing incidence of diabetes in the United States and the disproportionate effect of this disease on racial and ethnic minority groups and low-income adult populations. In 2011, data from the US Centers for Disease Control and Prevention indicated that the age-adjusted percentages of adults with a diagnosis of diabetes mellitus who reported visual impairment were 20.7%, 17.1%, and 15.6% among Black, White, and Hispanic participants, respectively. More recent studies indicate

that rates of diabetic retinopathy progression and vision loss have fallen with improvements in both systemic control of diabetes and treatments.

About diabetes: diabetes facts and figures. International Diabetes Federation Web site.

Updated December 2, 2020. Accessed January 18, 2022. www.idf.org/aboutdiabetes/what-is-diabetes/facts-figures.html.

Centers for Disease Control and Prevention. *National Diabetes Statistics Report 2020*. US Dept of Health and Human Services, Centers for Disease Control and Prevention; 2020. Accessed January 18, 2022. <https://www.cdc.gov/diabetes/pdfs/data/statistics/national-diabetes-statistics-report.pdf>

Klein R, Lee KE, Knudtson MD, Gangnon RE, Klein BE. Changes in visual impairment prevalence by period of diagnosis of diabetes: the Wisconsin Epidemiologic Study of Diabetic Retinopathy. *Ophthalmology*. 2009;116(10):1937–1942.

Yau JW, Rogers SL, Kawasaki R, et al; Meta-Analysis for Eye Disease (META-EYE) Study Group. Global prevalence and major risk factors of diabetic retinopathy. *Diabetes Care*. 2012;35(3):556–564.

Pathogenesis of Diabetic Retinopathy

Although the primary cause of diabetic microvascular disease remains poorly understood, exposure to hyperglycemia over time is known to adversely alter biochemical and molecular pathways. Changes include increases in inflammatory oxidative stress, advanced glycation end products, and plasma kallikrein and protein kinase C pathways, which ultimately cause endothelial damage and pericyte loss. Concomitant systemic factors, such as hypertension and hyperlipidemia, may exacerbate diabetic pathology. In addition, numerous hematologic abnormalities are associated with the onset and progression of retinopathy, including increased platelet adhesion, increased erythrocyte aggregation, and defective fibrinolysis. Diabetic neural pathology includes inner retinal layer thinning before development of clinically visible vascular lesions and perturbations in neural retinal function, as well as disorganization of neural retinal tissue in late-stage disease. However, the precise role of these abnormalities in the pathogenesis of retinopathy—individually or in combination—is not well defined.

Over time, changes in retinal capillaries, such as basement membrane thickening and selective loss of pericytes, lead to capillary occlusion and retinal nonperfusion. High-resolution imaging of the retinal vasculature, available through OCT angiography (OCTA) and adaptive optics scanning laser ophthalmoscopy, often reveals areas of vascular remodeling even in eyes with clinically mild diabetic retinopathy. These vascular abnormalities occur in both the superficial and deeper retinal capillary plexuses and worsen with increasing severity of diabetic retinopathy (Fig 5-1). In addition, endothelial barrier decompensation leads to serum leakage and retinal edema. In late stages of the disease, retinal neovascularization occurs in response to increased levels of intraocular VEGF, which is produced by ischemic retinal tissue.

Duh EJ, Sun JK, Stitt AW. Diabetic retinopathy: current understanding, mechanisms, and treatment strategies. *JCI Insight*. 2017;2(14):e93751.

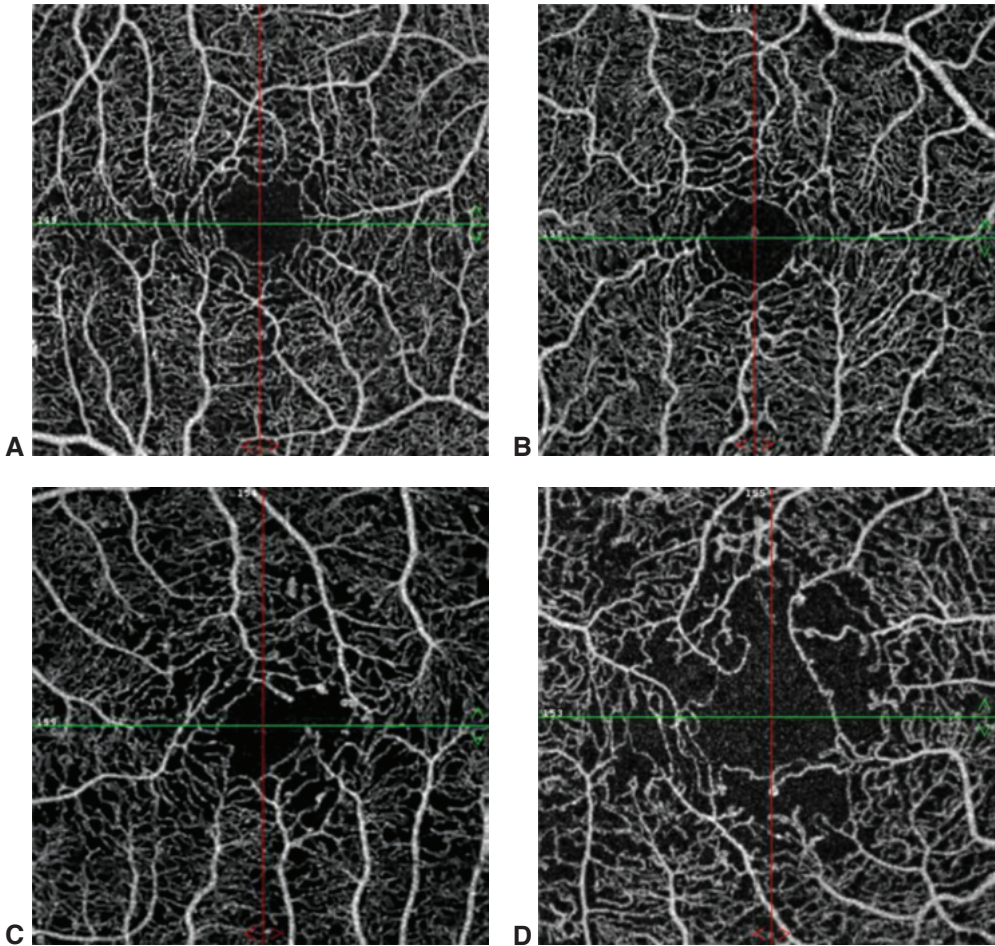


Figure 5-1 Optical coherence tomography angiography images demonstrate macular capillary nonperfusion and vascular tortuosity in diabetic eyes. The foveal avascular zone diameters in these images increase with worsening diabetic retinopathy severity level. **A**, Nondiabetic eye. **B**, Mild nonproliferative diabetic retinopathy (NPDR). **C**, Moderate NPDR. **D**, Proliferative diabetic retinopathy. (Courtesy of Jennifer K. Sun, MD, MPH.)

Recommended Diabetes Mellitus–Related Ophthalmic Examinations

In the first 5 years after a diagnosis of type 1 diabetes, advanced retinopathy is rare. In contrast, at initial diagnosis of type 2 diabetes, which may postdate the advent of hyperglycemia by years, a larger percentage of patients already have retinopathy and require concomitant ophthalmic examination.

Because pregnancy is associated with progression of diabetic retinopathy, pregnant women with diabetes mellitus may require more frequent retinal evaluations than the general population. An eye examination is recommended soon after conception and early

Table 5-1 Recommended Eye Examination Schedule for Patients With Diabetes Mellitus

Diabetes Type	Recommended Time of First Eye Examination	Routine Minimum Follow-up Interval
Type 1	5 years after diagnosis	Annually
Type 2	Upon diagnosis	Annually
Pregnant patients (type 1 or 2)	Soon after conception and early in the first trimester	For patients with no retinopathy to mild or moderate NPDR: every 3–12 months For patients with severe NPDR or worse: every 1–3 months

NPDR = nonproliferative diabetic retinopathy.

Modified from American Academy of Ophthalmology Retina/Vitreous Panel. Preferred Practice Pattern Guidelines. *Diabetic Retinopathy*. American Academy of Ophthalmology; 2019. aao.org/preferred-practice-pattern/diabetic-retinopathy-ppp

in the first trimester and at the discretion of the ophthalmologist thereafter (Table 5-1). Vision loss in pregnant women may occur from DME or from the complications of PDR. Although retinopathy may regress after delivery, high-risk PDR that develops just before or during pregnancy generally requires photocoagulation treatment. The frequency of follow-up visits during pregnancy depends on the severity of the retinopathy, history of blood glucose levels, and blood pressure control, as well as the need to identify worsening disease while it can still be treated in a timely fashion to prevent vision loss.

To help detect diabetic retinopathy and triage patients with the disorder, effective and efficient telemedicine screening approaches are needed globally to supplement in-person clinical examinations (Table 5-2). In recent years, artificial intelligence algorithms have successfully identified clinically referable cases of diabetic eye disease. Two of these systems, IDx-DR (Digital Diagnostics) and EyeArt (Eyenuk), are currently cleared by the US Food and Drug Administration for diabetic retinopathy screening, and the role of artificial intelligence in ocular telehealth systems is expected to grow. See BCSC Section 2, *Fundamentals and Principles of Ophthalmology*, for further discussion of artificial intelligence.

Abràmoff MD, Lavin PT, Birch M, Shah N, Folk JC. Pivotal trial of an autonomous AI-based diagnostic system for detection of diabetic retinopathy in primary care offices. *NPJ Digit Med*. 2018;1:39.

American Academy of Ophthalmology Retina/Vitreous Preferred Practice Pattern Panel. *Diabetic Retinopathy Preferred Practice Pattern*. American Academy of Ophthalmology; 2019. <https://www.aao.org/preferred-practice-pattern/diabetic-retinopathy-ppp>

Horton MB, Brady CJ, Cavallerano J, et al. Practice guidelines for ocular telehealth-diabetic retinopathy, third edition. *Telemed J E Health*. 2020;26(4):495–543.

Systemic Medical Management of Diabetic Retinopathy

Optimal glycemic control is by far the most important factor in the systemic management of diabetic retinopathy, as demonstrated by both the DCCT and the UKPDS (Table 5-3). In these studies, intensive glycemic control was associated with a reduced risk of new-onset

Table 5-2 Recommended Eye Examination Schedule Based on Diabetic Retinopathy Severity

Diabetic Retinopathy Severity	Presence of Macular Edema	Suggested Follow-up Interval (months)
Normal or minimal NPDR	No	12
Mild NPDR	No	12
	Non-CI DME	3–6
	CI DME ^a	1
Moderate NPDR	No	6–12
	Non-CI DME	3–6
	CI DME ^a	1
Severe NPDR ^b	No	3–4
	Non-CI DME	2–4
	CI DME ^a	1
Non-high-risk PDR ^c	No	3–4
	Non-CI DME	2–4
	CI DME ^a	1
High-risk PDR ^c	No	2–4
	Non-CI DME	2–4
	CI DME ^a	1
Inactive/involved PDR	No	6–12
	Non-CI DME	3–4
	CI DME ^a	1

CI DME = center-involved diabetic macular edema; non-CI DME = non-center-involved diabetic macular edema; NPDR = nonproliferative diabetic retinopathy; PDR = proliferative diabetic retinopathy.

^a Consider intravitreal anti-vascular endothelial growth factor injection.

^b Consider panretinal scatter laser surgery, especially in patients with type 2 diabetes.

^c Consider panretinal scatter laser surgery or intravitreal anti-vascular endothelial growth factor injection.

Modified from American Academy of Ophthalmology Retina/Vitreous Panel. Preferred Practice Pattern Guidelines. *Diabetic Retinopathy*. American Academy of Ophthalmology; 2019. aao.org/preferred-practice-pattern/diabetic-retinopathy-ppp

retinopathy and with reduced progression of existing retinopathy in people with diabetes mellitus (type 1 in the DCCT and type 2 in the UKPDS). In addition, the DCCT showed that intensive glycemic control reduced progression to severe NPDR and PDR, the incidence of DME, and the need for panretinal and focal photocoagulation compared with conventional treatment. Even small but sustained changes in hemoglobin A_{1c} (HbA_{1c}) levels had a substantial effect on progression of diabetic retinopathy. Indeed, the delay in retinopathy onset and the reduction in disease progression and need for ocular surgery with intensive glycemic control were sustained over at least 2 decades, a “metabolic memory” that persisted even after the DCCT study ended and HbA_{1c} levels between the original randomization groups converged.

On the basis of the DCCT and UKPDS results, most patients with diabetes are now advised to achieve an HbA_{1c} level of less than 7.0%. The ACCORD trial and its follow-up, ACCORDION, found that further reduction in HbA_{1c} levels to less than 6.0% slowed diabetic retinopathy progression in patients with type 2 diabetes; however, this intensive regimen is not generally recommended because it is also associated with a greater mortality rate.

Effective management of comorbidities such as hypertension and hyperlipidemia can also reduce the risk of diabetic retinopathy worsening. When poorly controlled over many years, hypertension is associated with an increased risk of progression of diabetic retinopathy

Table 5-3 Seminal Trials in Diabetic Retinopathy Management

Study	Major Study Question(s)	Study Cohort	Randomization	Primary Results
Diabetes Control and Complications Trial (DCCT)	<i>Primary prevention study:</i> Will intensive control of blood glucose level slow development and subsequent progression of diabetic retinopathy (neuropathy and nephropathy)?	<i>Primary prevention study:</i> 726 patients with type 1 diabetes (1–5 years' duration) and no diabetic retinopathy.	Intensive control of blood glucose level (multiple daily insulin injections or insulin pump) vs conventional management.	In the primary prevention cohort, intensive control reduced the risk of developing retinopathy by 76%, and in the secondary intervention cohort, it slowed progression of retinopathy by 54%. In the 2 cohorts combined, intensive control reduced the risk of clinical neuropathy by 60% and albuminuria (nephropathy) by 54%.
	<i>Secondary intervention study:</i> Will intensive control of blood glucose level slow progression of diabetic retinopathy (neuropathy and nephropathy)?	<i>Secondary intervention study:</i> 715 patients with type 1 diabetes (1–15 years' duration) and mild to moderate diabetic retinopathy.		
United Kingdom Prospective Diabetes Study (UKPDS)	1. Will intensive control of blood glucose level in patients with type 2 diabetes reduce the risk of microvascular complications of diabetes, including the risk of retinopathy progression?	1. 4209 patients with newly diagnosed type 2 diabetes. 2. 1148 patients with hypertension and newly diagnosed type 2 diabetes.	1. Conventional policy starting with diet (1138 patients) vs an intensive policy starting with sulfonylurea—chlorpropamide (788 patients), glibenclamide (615 patients), or glipizide (170 patients) treatment—or treatment with insulin (1156 patients). If overweight and in the intensive group, patients were assigned to start treatment with metformin (342 patients).	1. Intensive control of blood glucose level slowed progression of retinopathy and reduced the risk of other microvascular complications of diabetes mellitus. Sulfonylureas did not increase the risk of cardiovascular disease. 2. Intensive control of blood pressure slowed progression of retinopathy and reduced the risk of other microvascular and macrovascular complications of diabetes mellitus. No clinically or statistically significant difference was found in retinopathy outcomes when comparing blood pressure reduction with ACE inhibitors versus beta-blockers.
	2. Will intensive control of blood pressure in patients with type 2 diabetes and elevated blood pressure reduce the risk of microvascular complications of diabetes, including the risk of retinopathy progression?		2. Tight control of blood pressure (400 with ACE inhibitor and 398 with beta-blockers) vs less tight control (390 patients).	

Study	Major Study Question(s)	Study Cohort	Randomization	Primary Results
Diabetic Retinopathy Study (DRS)	Is photocoagulation (argon or xenon arc) effective for treating diabetic retinopathy?	1742 participants with PDR or bilateral severe NPDR, with visual acuity of 20/100 or better in each eye.	1 eye randomly assigned to photocoagulation (argon or xenon arc) and 1 eye assigned to no photocoagulation.	At 5 years of follow-up, eyes treated with PRP had a reduction of 50% or more in rates of SVL compared with untreated control eyes. Thus, photocoagulation (argon or xenon arc) reduces the risk of SVL compared with no treatment. Treated eyes with high-risk PDR achieved the greatest benefit (see Fig 5-9). In the DRS, complications of argon laser PRP were generally mild but included a decrease in visual acuity by 1 or more lines in 11% of eyes and visual field loss in 5%.
Early Treatment Diabetic Retinopathy Study (ETDRS)	1. Is photocoagulation effective for treating DME? 2. Is photocoagulation effective for treating diabetic retinopathy? 3. Is aspirin effective in preventing progression of diabetic retinopathy?	3711 participants with mild NPDR through early PDR, with visual acuity of 20/200 or better in each eye.	1 eye randomly assigned to photocoagulation (scatter and/or focal) and 1 eye assigned to no photocoagulation; patients randomly assigned to 650 mg/day aspirin or placebo.	<p><i>Macular edema results:</i></p> <p>Focal photocoagulation for DME decreased risk of moderate vision loss (doubling of initial visual angle), increased chance of moderate vision gain (halving of initial visual angle), and reduced retinal thickening.</p> <p><i>Early scatter photocoagulation results:</i></p> <p>Early scatter photocoagulation resulted in a small reduction in the risk of severe vision loss (<5/200 for at least 4 months), but is not indicated for eyes with mild to moderate diabetic retinopathy. Early scatter photocoagulation may be most effective in patients with type 2 diabetes.</p> <p><i>Aspirin use results:</i></p> <p>Aspirin use did not alter progression of diabetic retinopathy, increase risk of vitreous hemorrhage, or adversely affect vision. Aspirin use reduced risk of cardiovascular morbidity and mortality.</p>

ACE = angiotensin-converting enzyme; DME = diabetic macular edema; DRCR = Diabetic Retinopathy Clinical Research; NPDR = nonproliferative diabetic retinopathy; PDR = proliferative diabetic retinopathy; PRP = panretinal photocoagulation; SVL = severe vision loss.

and DME. In contrast, the UKPDS showed that control of hypertension reduced progression of retinopathy and vision loss in patients with type 2 diabetes. Abnormally high lipid levels are associated with increased risk of vision loss from DME-associated hard exudates. Because hard exudates can resolve over time and with therapy, a fasting lipid panel should be checked in patients with extensive macular lipid deposits and treatment of hyperlipidemia initiated. Severe carotid artery occlusive disease may result in advanced PDR as part of ocular ischemic syndrome, whereas advanced diabetic nephropathy and anemia may exacerbate diabetic retinopathy.

Aiello LP, Sun W, Das A, et al; DCCT/EDIC Research Group. Intensive diabetes therapy and ocular surgery in type 1 diabetes. *N Engl J Med*. 2015;372(18):1722–1733.

Chew EY, Mills JL, Metzger BE, et al. Metabolic control and progression of retinopathy: The Diabetes in Early Pregnancy Study. National Institute of Child Health and Human Development Diabetes in Early Pregnancy Study. *Diabetes Care*. 1995;18(5):631–637.

Diabetes Control and Complications Trial Research Group. Progression of retinopathy with intensive versus conventional treatment in the Diabetes Control and Complications Trial. *Ophthalmology*. 1995;102(4):647–661.

UK Prospective Diabetes Study Group. Intensive blood-glucose control with sulphonylureas or insulin compared with conventional treatment and risk of complications in patients with type 2 diabetes (UKPDS 33). *Lancet*. 1998;352(9131):837–853.

UK Prospective Diabetes Study Group. Tight blood pressure control and risk of macrovascular and microvascular complications in type 2 diabetes: UKPDS 38. *BMJ*. 1998;317(7160):703–713.

CLINICAL PEARL

In patients with diabetic retinopathy, vision loss is commonly associated with the following abnormalities:

- capillary leakage (DME)
- capillary occlusion (macular ischemia)
- sequelae from retinal ischemia (retinal neovascularization, vitreous hemorrhage, traction retinal detachment, neovascular glaucoma)

Nonproliferative Diabetic Retinopathy

In NPDR, retinal microvascular changes are limited to the retina and do not extend beyond the internal limiting membrane (ILM). Characteristic findings include intraretinal hemorrhages, microaneurysms, cotton-wool spots, intraretinal microvascular abnormalities (IRMAs), and dilation and beading of retinal veins. NPDR is generally graded as mild, moderate, or severe according to the extent and degree of clinical findings compared with standard photographs from the ETDRS (the photographs are discussed later in this section). More severe ETDRS retinopathy level at baseline has been associated with higher rates of progression to PDR.

To help clinicians identify patients at greatest risk of progression to PDR and high-risk PDR, the ETDRS investigators developed the 4:2:1 rule, which is based largely on

results from ETDRS Report Number 9 (see Table 5-3). According to this rule, severe NPDR manifests with any 1 of the following features:

- severe intraretinal hemorrhages (typically estimated as >20 intraretinal hemorrhages) and microaneurysms in 4 quadrants (Fig 5-2)
- definite venous beading in 2 or more quadrants (Fig 5-3)
- moderate IRMA in 1 or more quadrants (Fig 5-4)

In the ETDRS, patients with severe NPDR had 15% and 60% chances of progression to high-risk PDR within 1 and 3 years, respectively. In patients with *very severe NPDR*, which was defined as having 2 or more of the features in the preceding list, the chance of progression to high-risk PDR within 1 year increased to 45%.

The ETDRS severity scale has been the reference standard for classifying diabetic retinopathy for several decades. To use it, clinicians need to acquire and interpret standardized photographic fields that cover approximately 90° of the patient's posterior retina (eg, with ultra-wide-field imaging, >80% of the retina can now be visualized in a single 200° image). Peripheral diabetic retinopathy lesions are often present outside the standard ETDRS fields; in approximately 10% of eyes, these lesions suggest more severe diabetic retinopathy. Preliminary studies also suggest that a predominance of peripheral diabetic retinopathy lesions increases the risk of diabetic retinopathy progression. This association is being evaluated in the ongoing DRCR Retina Network (DRCR.net) Protocol AA study.

In more advanced cases of NPDR, retinal capillary nonperfusion is a common finding. Closure of retinal arterioles may expand areas of nonperfusion and progressive ischemia. In addition, the foveal avascular zone may appear increasingly irregular on fluorescein angiography (FA) or OCTA as well as enlarged when the innermost capillaries become nonperfused. With increasing retinopathy severity, macular vessel density decreases in the superficial and deep capillary plexuses. Peripheral nonperfusion is also frequently seen on ultra-wide-field FA (Fig 5-5), even in eyes with mild NPDR.

When NPDR leads to loss of visual function, 1 of 2 mechanisms is typically implicated: (1) increased intraretinal vascular permeability, resulting in macular edema (see

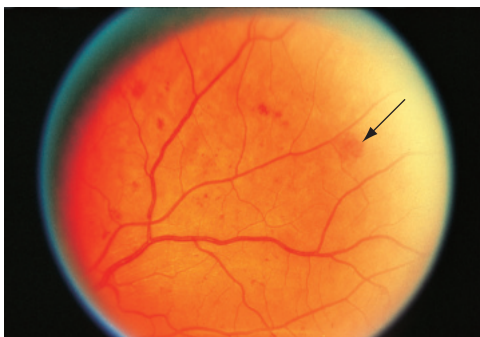


Figure 5-2 Fundus photograph shows diffuse intraretinal hemorrhages (arrow) and microaneurysms in an eye with NPDR. (Standard photograph 2A, courtesy of the Early Treatment Diabetic Study [ETDRS].)



Figure 5-3 Fundus photograph shows venous beading (arrows) in an eye with NPDR. (Standard photograph 6B, courtesy of the ETDRS.)

Figure 5-4 Fundus photograph demonstrates intraretinal microvascular abnormalities (IRMAs) (arrows) in an eye with NPDR. (Courtesy of Jennifer K. Sun, MD, MPH.)

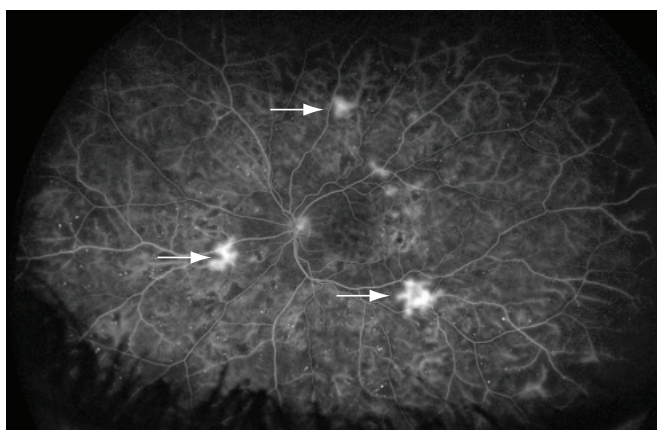
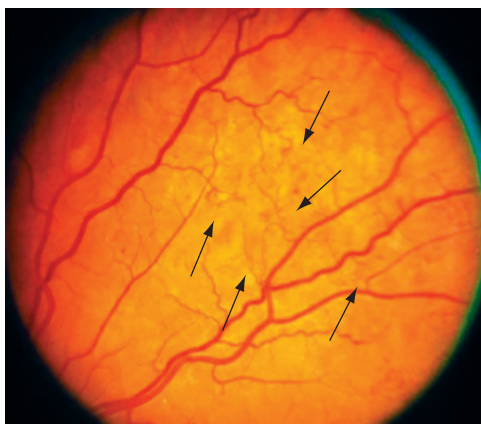


Figure 5-5 Ultra-wide-field fluorescein angiogram with focal areas of hyperfluorescence (arrows) representing leakage from retinal neovascularization along the vascular arcades. There are also patchy areas of hypofluorescence due to nonperfusion. (Courtesy of Jennifer K. Sun, MD, MPH.)

the section Diabetic Macular Edema later in this chapter); and (2) variable degrees of intraretinal capillary closure, resulting in macular ischemia.

Ashraf M, Sampani K, Clermont A, et al. Vascular density of deep, intermediate and superficial vascular plexuses are differentially affected by diabetic retinopathy severity. *Invest Ophthalmol Vis Sci.* 2020;61(10):53.

Early Treatment Diabetic Retinopathy Study Research Group. Early photocoagulation for diabetic retinopathy. ETDRS report number 9. *Ophthalmology.* 1991;98(5 Suppl):766–785.

Early Treatment Diabetic Retinopathy Study Research Group. Grading diabetic retinopathy from stereoscopic color fundus photographs—an extension of the modified Airlie House classification. ETDRS report number 10. *Ophthalmology.* 1991;98(5 Suppl):786–806.

Silva PS, Cavallerano JD, Haddad NM, et al. Peripheral lesions identified on ultrawide field imaging predict increased risk of diabetic retinopathy progression over 4 years. *Ophthalmology.* 2015;122(5):949–956.

Treatment of Nonproliferative Diabetic Retinopathy

For eyes with NPDR without DME, there is no clear treatment mandate aside from systemic control of blood glucose, lipid, and hypertension levels. For patients with severe NPDR or worse, especially if they have type 2 diabetes or are unlikely to adhere to recommendations for follow-up or systemic control, early treatment with panretinal photocoagulation (PRP) should be considered. In eyes at all levels of NPDR, anti-VEGF therapy can reduce rates of vision-threatening complications and improve diabetic retinopathy severity. In addition, the DRCR Retina Network Protocol W study (Table 5-4) found that the cumulative probability of developing either center-involved DME with vision loss or PDR was reduced nearly threefold after 2 years of treatment with aflibercept versus sham injections. The PANORAMA trial, which also randomly assigned eyes to aflibercept versus sham treatment, showed that approximately 50% to 60% of eyes with moderately severe to severe NPDR at baseline improved by 2 or more levels on the ETDRS disease severity scale with aflibercept treatment. Despite improvements in anatomical outcomes in cohorts of eyes with good vision at baseline, neither Protocol W nor PANORAMA demonstrated gains in visual acuity with aflibercept treatment at 2 years. Both aflibercept and ranibizumab have been approved by the US Food and Drug Administration for use in diabetic retinopathy, including NPDR without DME; however, it is unclear at this time whether routine early treatment of eyes with NPDR is warranted given the lack of a clear long-term visual benefit.

Additional methods may improve diabetic retinopathy severity and slow the progression of diabetic retinal disease. For example, intravitreal steroid therapy for DME has been shown to reduce diabetic retinopathy severity. Similarly, in the ACCORD and FIELD studies, diabetic retinopathy progression was slowed in patients with type 2 diabetes after fenofibrate treatment, most likely independent of the drug's effects on blood lipid levels.

Bressler SB, Qin H, Melia M, et al; Diabetic Retinopathy Clinical Research Network. Exploratory analysis of the effect of intravitreal ranibizumab or triamcinolone on worsening of diabetic retinopathy in a randomized clinical trial. *JAMA Ophthalmol.* 2013;131(8):1033–1040.

Chew EY, Ambrosius WT, Davis MD, et al; ACCORD Study Group; ACCORD Eye Study Group. Effects of medical therapies on retinopathy progression in type 2 diabetes. *N Engl J Med.* 2010;363(3):233–244.

Ferris F. Early photocoagulation in patients with either type I or type II diabetes. *Trans Am Ophthalmol Soc.* 1996;94:505–537.

Maturi RK, Glassman AR, Josic K, et al; DRCR Retina Network. Effect of intravitreal anti-vascular endothelial growth factor vs sham treatment for prevention of vision-threatening complications of diabetic retinopathy: the Protocol W Randomized Clinical Trial. *JAMA Ophthalmol.* 2021;139(7):701–712.

Proliferative Diabetic Retinopathy

As retinopathy progresses, capillary damage and nonperfusion increase. Worsening retinal ischemia leads to release of vasoproliferative factors and the subsequent development of retinal neovascularization. VEGF, a major proangiogenic factor isolated from the vitreous of patients with PDR, may stimulate neovascularization of the retina, optic nerve head, or anterior segment.

Table 5-4 Selected DRCR Retina Network Studies

Protocol	Study Name	End Date	Study Conclusions
B	A Randomized Trial Comparing Intravitreal Triamcinolone Acetonide and Laser Photocoagulation for Diabetic Macular Edema	10/03/2008	At 2 years, focal/grid laser photocoagulation for center-involved DME was more effective and had fewer adverse effects than 1-mg or 4-mg doses of preservative-free intravitreal triamcinolone.
D	Evaluation of Vitrectomy for Diabetic Macular Edema Study	02/26/2009	Vitrectomy reduced retinal thickening in most eyes with DME and vitreomacular traction. Although VA outcomes improved by 10 or more letters in 38% of eyes, 22% lost 10 or more letters after vitrectomy.
I	Intravitreal Ranibizumab or Triamcinolone Acetonide in Combination with Laser Photocoagulation for Diabetic Macular Edema	12/31/2013	At 2 years, intravitreal ranibizumab with prompt or deferred (≥ 24 weeks) focal/grid laser photocoagulation was more effective in increasing VA than focal/grid laser treatment alone or intravitreal triamcinolone with laser photocoagulation for the treatment of center-involved DME. In eyes with center-involved DME with vision impairment, focal/grid laser treatment at the initiation of intravitreal ranibizumab was no better, and was possibly worse, for vision outcomes than deferring laser treatment for 24 weeks or longer. This small observational study of eyes with DME undergoing cataract surgery revealed that only a small percentage of eyes experienced substantial VA loss or definitive worsening of DME after surgery.
P	A Pilot Study in Individuals with Center-Involved DME Undergoing Cataract Surgery	11/12/2010	A history of DME treatment and presence of non-center-involved DME are risk factors for development of center-involved DME after cataract surgery in eyes with diabetic retinopathy and no center-involved DME before surgery. Ranibizumab injections are an effective alternative to PRP in treating PDR.
Q	An Observational Study in Individuals with Diabetic Retinopathy without Center-Involved DME Undergoing Cataract Surgery	05/19/2011	At 2 and 5 years, VA outcomes with ranibizumab were noninferior to outcomes with PRP, whereas average VA over the 2-year (but not the 5-year) period was better with ranibizumab. Over 5 years, ranibizumab was associated with less peripheral field loss, reduced rates of DME onset, and fewer eyes requiring vitrectomy.
S	Prompt Panretinal Photocoagulation versus Intravitreal Ranibizumab with Deferred Panretinal Photocoagulation for Proliferative Diabetic Retinopathy	02/05/2018	The 2-year clinical trial compared 3 drugs used to treat DME and found that gains in vision were greater for participants receiving aflibercept than for those receiving bevacizumab, but only among participants starting treatment with VA of 20/50 or worse. At 1 year, aflibercept showed superior gains compared with ranibizumab in this vision subgroup; however, a difference could not be identified at 2 years. The 3 drugs yielded similar gains in vision for patients with a VA of 20/32 or 20/40 at the start of treatment.
T	A Comparative Effectiveness Study of Intravitreal Aflibercept, Bevacizumab and Ranibizumab for Diabetic Macular Edema	10/18/2018	

Protocol	Study Name	End Date	Study Conclusions
Tx	A Comparative Effectiveness Study of Intravitreal Afibercept, Bevacizumab and Ranibizumab for Diabetic Macular Edema – Follow-up Extension Study	04/18/2019	Approximately two-thirds of eligible Protocol T participants completed a 5-year visit after study enrollment (2 years of study participation and 3 years of standard clinical care). Average vision at 5 years was better than the baseline value by 7.4 letters, but mean vision declined by nearly 5 letters between 2 and 5 years. Average OCT central subfield thickness remained stable from 2 to 5 years.
U	Short-term Evaluation of Combination Corticosteroid + Anti-VEGF Treatment for Persistent Central-Involved Diabetic Macular Edema Following Anti-VEGF Therapy	6/01/2017	In eyes with persistent DME and visual impairment despite previous anti-VEGF therapy, the dexamethasone + ranibizumab group experienced greater reduction of DME than the sham + ranibizumab group but no greater improvement in vision over 6 months.
V	Treatment for Central-Involved Diabetic Macular Edema in Eyes with Very Good Visual Acuity	09/11/2018	Eyes with good vision (20/25 or better) despite center-involved DME had similar rates of vision loss (ie, 5 or more letters lost) over 2 years whether they initially received intravitreal aflibercept, laser therapy, or observation (aflibercept was given to patients in the laser and observation groups who experienced vision loss during follow-up). At 2 years, all 3 groups had a mean VA of 20/20.
W	Intravitreal Anti-VEGF Treatment for Prevention of Vision-Threatening Diabetic Retinopathy in Eyes at High Risk	Anticipated 01/04/2022	Among eyes with moderate to severe NPDR, the proportion that developed PDR or center-involved DME with vision loss was lower with periodic aflibercept treatment than with sham treatment through at least 2 years. However, compared with aflibercept initiated after development of PDR or DME, preventive treatment with aflibercept did not confer visual benefits at 2 years.
AB	Intravitreal Anti-VEGF vs. Prompt Vitrectomy for Vitreous Hemorrhage from Proliferative Diabetic Retinopathy	01/09/2020	Eyes with vitreous hemorrhage from PDR that were randomly assigned to vitrectomy or intravitreal aflibercept had similar visual outcomes at 6 months and 2 years. On average, vitrectomy-treated eyes had faster early visual recovery. Approximately one-third of eyes in each group received the alternative treatment for PDR during the 2 years of the study.

DME = diabetic macular edema; DRCR = Diabetic Retinopathy Clinical Research; NPDR = nonproliferative diabetic retinopathy; OCT = optical coherence tomography; PDR = proliferative diabetic retinopathy; PRP = panretinal photocoagulation; VA = visual acuity; VEGF = vascular endothelial growth factor.

Data from JAEB Center for Health Research. Diabetic Retinopathy Clinical Research Network (DRCR.net) website. Accessed September 5, 2021. www.drcr.net.

Extraretinal fibrovascular proliferation, which defines PDR, progresses through 3 stages:

1. Fine new vessels with minimal fibrous tissue cross and extend beyond the ILM, often using the posterior hyaloid as a scaffold.
2. The new vessels grow in size and extent, developing an increased fibrous component.
3. The new vessels regress, leaving residual fibrovascular tissue that may be tethered within the posterior hyaloid.

In PDR, neovascular proliferation is categorized by its location: either on or within a disc diameter of the optic nerve head (neovascularization of the disc [NVD]) or elsewhere (neovascularization elsewhere [NVE]).

Patients may receive treatment at any stage of PDR. However, treatment is usually considered mandatory once an eye has developed high-risk characteristics, and it has been shown to dramatically reduce rates of severe vision loss. PDR with high-risk characteristics is defined as the presence of any of the following findings:

- any NVD with vitreous or preretinal hemorrhage
- extent of NVD greater than or equal to one-fourth the disc area, with or without vitreous or preretinal hemorrhage (ie, greater than or equal to the extent shown in ETDRS standard photograph 10A) (Fig 5-6)
- extent of NVE greater than or equal to one-half the disc area, with vitreous or preretinal hemorrhage (Fig 5-7)

In eyes that have not developed high-risk characteristics, treatment may be deferred. Treatment may also be deferred in eyes that have peripheral neovascularization outside the seven 30° photographic fields comprising the standard protocol for diabetic retinopathy

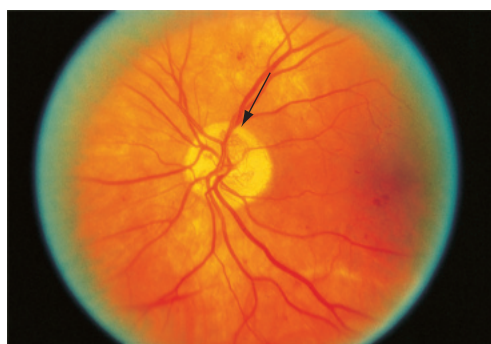


Figure 5-6 Fundus photograph of a left eye shows neovascularization of the disc (NVD, arrow) with a small amount of vitreous hemorrhage. Even without vitreous hemorrhage, this degree of neovascularization is the lower limit of moderate NVD and is considered high-risk proliferative diabetic retinopathy. (Standard photograph 10A, courtesy of the Diabetic Retinopathy Study.)

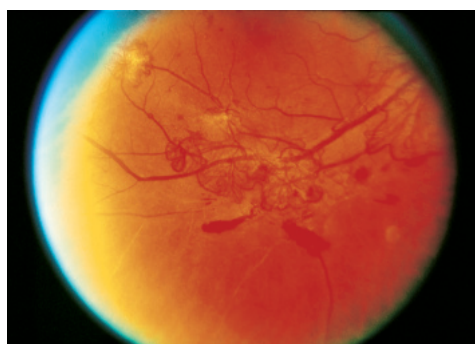


Figure 5-7 Fundus photograph of a right eye shows cotton-wool spots and moderate neovascularization elsewhere with preretinal hemorrhage. (Standard photograph 7, courtesy of the Diabetic Retinopathy Study.)

imaging set by the ETDRS, but that do not have accompanying intraocular hemorrhage. However, patients at especially high risk for diabetic retinopathy progression because of nonadherence or poor systemic control should be treated promptly.

Management of Proliferative Diabetic Retinopathy and Its Complications

The goals of PDR treatment are to control ischemia and reduce ocular VEGF levels so that neovascularization can involute or regress and the incidence of vitreous hemorrhage is reduced. This can be accomplished with either intravitreal administration of anti-VEGF drugs or ablation of ischemic retina via laser photocoagulation. Because of the contraction of fibrovascular tissue that can occur with either anti-VEGF therapy or PRP, treatment may be followed by increased vitreoretinal traction, recurring vitreous hemorrhage, traction (also called *tractional*) retinal detachment, and/or combined traction and rhegmatogenous retinal detachment. When appropriate, complications from PDR or its treatment (eg, vitreous hemorrhage and traction retinal detachment) may be addressed with vitreoretinal surgery.

Pharmacologic management of proliferative diabetic retinopathy

Anti-VEGF and steroid drugs Multiple studies of anti-VEGF drugs, including phase 3 trials for the treatment of DME, have shown that intravitreal administration (see the section Intravitreal Injections in Chapter 19 of this volume for a discussion of the injection procedure) of these agents is highly effective at regressing retinal neovascularization in eyes with PDR. This regression has been observed in both newly diagnosed cases and chronic, refractory disease. Potential complications from the use of anti-VEGF drugs to manage PDR include traction retinal detachments, retinal tears, and as mentioned previously, combined traction and rhegmatogenous retinal detachments related to the induced rapid contracture of fibrovascular tissue, sometimes referred to as the “crunch” phenomenon.

Because of its effectiveness in regressing intraocular neovascularization and its generally favorable safety profile, anti-VEGF therapy is a reasonable alternative or adjunctive therapy to PRP for many eyes with PDR. In the DRCR.net Protocol S study, eyes with active PDR were randomly assigned to treatment with either prompt PRP (ie, standard care) or intravitreal ranibizumab and deferred PRP (see Figure 5-8 for a simplified flowchart of the DRCR.net anti-VEGF treatment algorithm for PDR). At 2 and 5 years, visual outcomes were equivalent between treatment groups. However, ranibizumab did show some benefits over PRP, including better average vision over the first 2 years of treatment. In addition, over 5 years, the ranibizumab-treated group had less peripheral visual field loss, reduced rates of vitrectomy surgery, and fewer cases of DME onset with visual impairment. No substantial differences in rates of major cardiovascular adverse events were found between the treatment groups, and most eyes in the ranibizumab group were still receiving injections at 5 years. (For more information on DRCR.net studies, see the sidebar Selected DRCR Retina Network Studies.) Similarly, the CLARITY study reported superior visual outcomes after 1 year of aflibercept therapy versus PRP in patients with PDR.

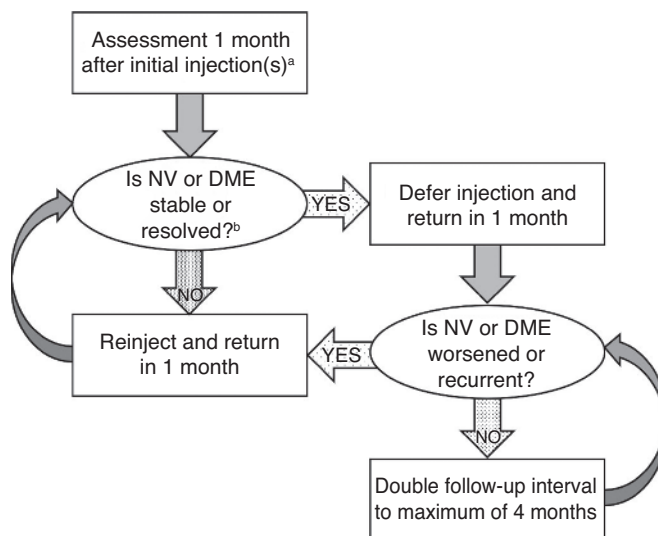


Figure 5-8 Simplified flowchart of the DRCR Retina Network anti-VEGF treatment algorithm for proliferative diabetic retinopathy and diabetic macular edema. DME = diabetic macular edema; NV = neovascularization; OCT = optical coherence tomography; PDR = proliferative diabetic retinopathy; VEGF = vascular endothelial growth factor.

^aIn DRCR.net studies, an initial series of monthly injections was given for PDR or DME.

^bPDR is considered stable once there is no improvement or worsening in NV over 2 injection visits. Resolved PDR is defined as the absence of any NV, including fibrous proliferation. DME is considered stable once there is no improvement or worsening in either visual acuity of 5 letters or more or OCT central subfield thickness of 10% or more over 2 injection visits. Resolved DME is defined as a normal central subfield thickness on OCT with visual acuity of 20/20 or better.

(Courtesy of Jennifer K. Sun, MD, MPH.)

SELECTED DRCR RETINA NETWORK STUDIES

The DRCR Retina Network (DRCR.net, formerly known as the *Diabetic Retinopathy Clinical Research Network*) conducts clinical research on diabetic eye disease, initiatives that typically involve community practices as well as academic centers. Since its inception in 2002, DRCR.net has conducted many of the studies underpinning current standard care practices for diabetic retinopathy and DME. See Table 5-4 earlier in this chapter and eTable 5-1, which provides an additional list of DRCR.net studies with primary results reported. Visit www.aao.org/bcscsupplement_section12 to view the eTable.

Anti-VEGF drugs can also cause beneficial involution of anterior segment neovascularization and can be successfully used to treat neovascular glaucoma, although long-term control is better achieved with PRP. In addition, when administered preoperatively, anti-VEGF drugs may be an adjunct to vitrectomy to manage complications of PDR. Of note, anti-VEGF injections should be given within a week of surgery to minimize the risk of vision-impairing traction retinal detachment.

Although anti-VEGF therapy is effective for PDR and offers some advantages over PRP, the decision to use these agents should be made on an individual basis. Once anti-VEGF therapy is selected, patients should adhere to near-monthly follow-up visits throughout the first 1–2 years of treatment. When the recommended follow-up intervals are ignored, recurrent and unchecked retinal neovascularization may occur, resulting in irreversible vision loss. For patients with medical instability or other limitations that may hinder adherence, treatment with PRP is more appropriate, as its effects may last for decades. In clinical practice, some physicians combine anti-VEGF and PRP treatments to take advantage of the respective advantages of each.

Although steroid agents are not used for primary treatment of PDR, they do reduce PDR-related outcomes in diabetic eyes. Combined rates of vitreous hemorrhage, need for PRP, and development of neovascularization (as viewed on fundus photographs or during a clinical examination) have decreased in eyes receiving intravitreal steroid therapy for non-PDR indications, such as DME.

Aiello LP, Avery RL, Arrigg PG, et al. Vascular endothelial growth factor in ocular fluid of patients with diabetic retinopathy and other retinal disorders. *N Engl J Med*. 1994;331(22):1480–1487.

Gross JG, Glassman AR, Liu D, et al. Five-year outcomes of panretinal photocoagulation vs intravitreal ranibizumab for proliferative diabetic retinopathy: a randomized clinical trial. *JAMA Ophthalmol*. 2018;136(10):1138–1148.

Sivaprasad S, Prevost AT, Vasconcelos JC, et al; CLARITY Study Group. Clinical efficacy of intravitreal aflibercept versus panretinal photocoagulation for best corrected visual acuity in patients with proliferative diabetic retinopathy at 52 weeks (CLARITY): a multicentre, single-blinded, randomised, controlled, phase 2b, non-inferiority trial. *Lancet*. 2017;389(10085):2193–2203.

Nonpharmacologic management of proliferative diabetic retinopathy

Laser treatment Over the last 4 decades (ie, until the recent advent of anti-VEGF therapy), the mainstay of treatment for PDR was thermal laser photocoagulation in a panretinal pattern to induce regression of neovascularization. Indications for photocoagulation are still largely based on findings from the DRS (Fig 5-9; see Table 5-3). For patients with high-risk PDR who are not already receiving anti-VEGF therapy, PRP treatment is almost always recommended. PRP destroys ischemic retina, thus reducing production of growth factors that promote disease progression, such as VEGF. PRP also increases oxygen tension in the eye via 2 mechanisms: (1) decreased oxygen consumption overall as a result of purposeful retinal destruction; and (2) increased diffusion of oxygen from the choroid in the areas of the photocoagulation scars. Collectively, these changes cause regression of existing neovascular tissue and prevent progressive neovascularization.

Laser treatment may be accomplished in a single session or over multiple sessions. The DRCR.net Protocol F study found no long-term vision benefits with multiple-session versus single-session laser administration. After the initial PRP, additional therapy may be applied incrementally in an attempt to achieve complete regression of persistent or recurrent neovascularization. As mentioned previously, some clinicians combine anti-VEGF therapy with PRP based on the premise that initial anti-VEGF therapy will regress neovascularization quickly and reduce onset or worsening of DME, whereas the effect of the PRP will endure for years, without the need for long-term intravitreal injections.

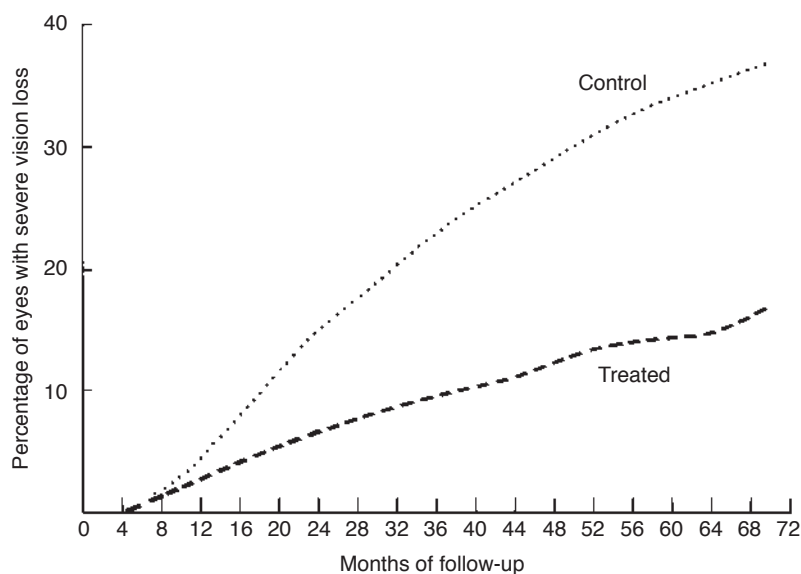


Figure 5-9 Comparison of argon laser and xenon arc treatment groups combined versus control groups in the Diabetic Retinopathy Study shows cumulative percentage of eyes that experienced severe vision loss during the follow-up period. (Reprinted from *Diabetic Retinopathy Study Research Group. Photocoagulation treatment of proliferative diabetic retinopathy. Clinical application of DRS findings, DRS report number 8. Ophthalmology. 1981;88(7):583–600. ©1981, with permission from Elsevier.*)

Full PRP, as used in the DRS and ETDRS (see Table 5-3), included 1200 or more 500- μ m burns created by using argon green or blue-green lasers, separated by one-half burn width (Fig 5-10). Although use of automated pattern scan lasers has increased in recent years, uncontrolled studies suggest that these treatments do not have equivalent effects in a burn-for-burn comparison.

Adverse effects of scatter PRP include choroidal detachment as well as decreases in peripheral field vision, night vision, color vision, contrast sensitivity, and in rare cases, pupillary dilation. After treatment, some patients may experience a transient loss of 1 or 2 lines of visual acuity or increased glare. Other transient adverse effects include loss of accommodation, loss of corneal sensitivity, and photopsias. Macular edema may also be precipitated or worsened by PRP. Sparing the horizontal meridians (ie, the path of the long ciliary vessels and nerves) protects accommodation, pupillary function, and corneal innervation. When necessary, heavy treatment should be performed in areas of the retina where vision loss is less noticed by patients (ie, the inferior retina) or in areas that are associated with a low likelihood of morbidity. Great care must be taken to avoid foveal photocoagulation, especially when image-inverting lenses are used.

Chew EY, Ferris FL III, Csaky KG, et al. The long-term effects of laser photocoagulation treatment in patients with diabetic retinopathy: the early treatment diabetic retinopathy follow-up study. *Ophthalmology*. 2003;110(9):1683–1689.

Diabetic Retinopathy Study Research Group. Photocoagulation treatment of proliferative diabetic retinopathy. Clinical application of Diabetic Retinopathy Study (DRS) findings, DRS report number 8. *Ophthalmology*. 1981;88(7):583–600.

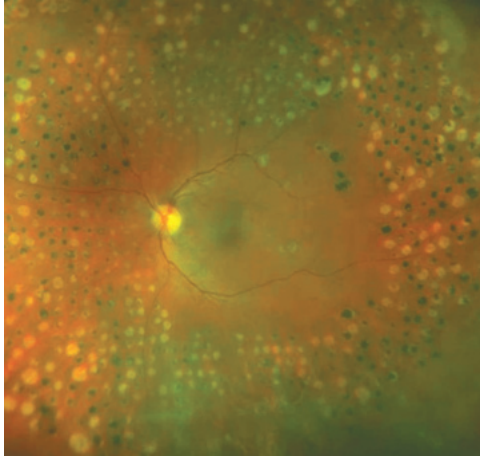


Figure 5-10 Fundus photograph shows an eye that has undergone panretinal photocoagulation treatment. Laser scars are characterized by either chorioretinal and retinal pigment epithelium (RPE) atrophy or RPE hyperpigmentation. (Courtesy of Jennifer K. Sun, MD, MPH.)

Vitrectomy In patients with PDR, indications for pars plana vitrectomy are

- nonclearing vitreous hemorrhage
- substantial recurring vitreous hemorrhage, despite use of maximal PRP
- dense premacular subhyaloid hemorrhage
- traction retinal detachment involving or threatening the macula
- combined traction and rhegmatogenous retinal detachment
- red blood cell-induced (erythroclastic) glaucoma and ghost cell glaucoma
- anterior segment neovascularization with media opacities preventing PRP

A more extensive discussion of the surgical management of PDR appears in the section Vitrectomy for Complications of Diabetic Retinopathy in Chapter 19 of this volume.

Recchia FM, Scott IU, Brown GC, Brown MM, Ho AC, Ip MS. Small-gauge pars plana vitrectomy: a report by the American Academy of Ophthalmology. *Ophthalmology*. 2010;117(9):1851–1857.

Additional Vision-Threatening Complications of Diabetic Retinopathy

Neovascularization of the iris or anterior chamber angle

Small, isolated tufts of neovascularization at the pupillary border are relatively common in patients with diabetes mellitus. Treatment may be withheld in these eyes in favor of careful monitoring, with relatively short intervals between slit-lamp and gonioscopic examinations. However, treatment should be considered for eyes that have contiguous neovascularization of the pupil and iris collarette, with or without inclusion of the anterior chamber angle, and when wide-field FA reveals widespread nonperfusion or peripheral neovascularization. Treatment is usually PRP; intravitreal injection of anti-VEGF drugs may be used as a temporizing measure to reduce neovascularization until definitive PRP is administered. Development of peripheral anterior synechiae despite treatment with PRP or anti-VEGF may require glaucoma surgery.

Vitreous hemorrhage

The DRVS was a prospective randomized clinical trial published in 1985 that investigated the role of vitrectomy in the management of eyes with severe PDR. Benefits of early (1–6 months after onset of vitreous hemorrhage) versus late (1 year after onset) vitrectomy were evaluated. Eyes of patients with type 1 diabetes and severe vitreous hemorrhage clearly showed a benefit from earlier vitrectomy, whereas eyes of patients with type 2 or mixed diabetes did not.

In patients with PDR and no history of PRP, earlier intervention should be considered. In contrast, patients with previous, well-placed, complete PRP who have vitreous hemorrhage secondary to PDR may be observed for a longer period before intervention is initiated. In patients with dense, nonclearing vitreous hemorrhages, frequent ultrasonography studies are necessary to monitor for retinal detachment. When retinal detachment is discovered, the timing for the vitrectomy depends on the characteristics of the detachment. Patients with bilateral severe vitreous hemorrhage should undergo vitrectomy in 1 eye as soon as possible for vision rehabilitation. Recent advances in vitreoretinal surgery, including smaller-gauge instrumentation that shortens operating times and decreases complications, allow earlier intervention for nonclearing vitreous hemorrhage.

In the DRCR.net Protocol AB study, patients with vitreous hemorrhage from PDR were randomly assigned to vitrectomy versus intravitreal anti-VEGF therapy with aflibercept. Visual outcomes at 6 months and 2 years were similar between the groups. However, eyes treated with vitrectomy, especially those with worse baseline vision, recovered vision more quickly than eyes treated with anti-VEGF over the first 4–12 weeks.

Traction retinal detachment

Complications from PDR may be exacerbated by vitreous attachment to and traction on fibrovascular proliferative tissue, causing secondary traction retinal detachments. Partial posterior vitreous detachment frequently develops in eyes with fibrovascular proliferation, resulting in traction on the new vessels and vitreous or preretinal hemorrhage. Tractional complications such as vitreous hemorrhage, retinal schisis, retinal detachment, or macular heterotopia may ensue, as well as progressive fibrovascular proliferation. In addition, contraction of the fibrovascular proliferation and vitreous may result in retinal breaks and subsequent combined traction and rhegmatogenous retinal detachment.

Traction retinal detachment that does not involve the macula may remain stable for many years even when left untreated. However, when the macula becomes involved or is threatened, prompt vitrectomy is generally recommended.

Diabetic papillopathy

Unilateral or bilateral optic nerve head edema may occur in patients with diabetes, sometimes in association with DME from increased vascular leakage. Risk factors for diabetic papillopathy include a small cup–disc ratio or rapid reduction of glycemia; however, it can develop at any severity stage of diabetic retinopathy or level of glycemic control. Although there is no proven therapy for diabetic papillopathy, this condition generally has a good prognosis.

Diabetic Macular Edema

Diabetic macular edema results from a hyperglycemia-induced breakdown of the blood–retina barrier, which leads to fluid extravasation from retinal vessels into the surrounding neural retina (Fig 5-11). A diagnosis of DME is made when retinal thickening involves the macula. DME may be associated with hard exudates, which are precipitates of plasma lipoproteins that may persist after DME resolution.

In patients with diabetes, central subfield–involved DME that affects the fovea is a common cause of vision loss. In contrast, non–center-involved DME is unlikely to affect vision unless it progresses to center involvement. Although DME is increasingly common

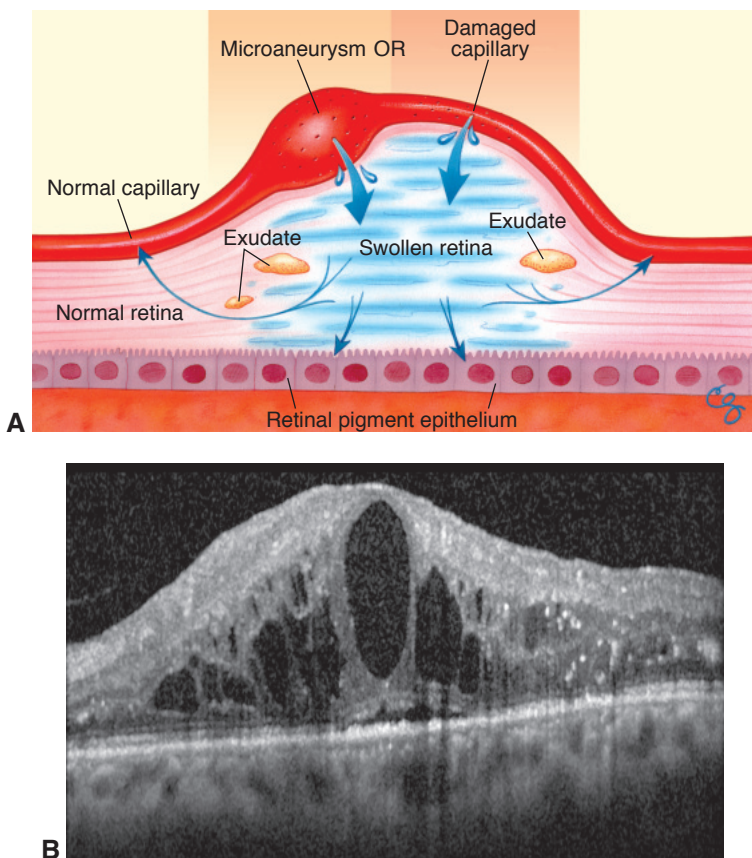


Figure 5-11 Diabetic macular edema (DME). **A**, Artist's rendering of the mechanism of DME, demonstrating development of retinal thickening from a breakdown of the blood–retina barrier. **B**, Spectral-domain OCT scan of DME. Although there are extensive cystic changes in the outer plexiform and outer nuclear layers, the external limiting membrane line appears intact across the extent of the scan, with the exception of shadowing artifacts from more superficial hyperreflective lesions. Note the foveal detachment. (Part A from Ginsburg LH, Aiello LM. *Diabetic retinopathy: classification, progression, and management*. Focal Points: Clinical Modules for Ophthalmologists. American Academy of Ophthalmology; 1993, module 7. Illustration by Christine Galapp. Part B courtesy of Colin A. McCannel, MD.)

among eyes with more advanced diabetic retinopathy, DME may occur with diabetic retinopathy of any severity. Even patients with mild NPDR may experience substantial vision loss from highly thickened retinas.

Imaging studies are useful for diagnosing DME. FA depicts the breakdown of the blood–retina barrier by showing local areas of retinal capillary leakage. However, leakage may also be observed on an angiogram in the absence of macular retinal thickening. OCT and slit-lamp biomicroscopy are the most appropriate studies for detecting macular thickening (Fig 5-12; Activity 5-1).



ACTIVITY 5-1 OCT Activity: OCT of diabetic macular edema.
Courtesy of Colin A. McCannel, MD.



Classification of Diabetic Macular Edema

Diabetic macular edema is classified as center involved or non-center involved (Fig 5-13) by using algorithms based on a simple, OCT-related definition. Quantitative thresholds for abnormal thickening of the 1-mm-diameter OCT central subfield vary according to machine type and, on average, are thicker in men than in women (see Fig 5-12).

The prospective, randomized ETDRS was the first study to establish standard treatment paradigms for managing DME in patients with diabetes and non-high-risk PDR (see Table 5-3). It defined *clinically significant diabetic macular edema (CSME)* with the following features as an indication for focal laser photocoagulation treatment:

- retinal thickening located at or within 500 μm of the center of the macula
- hard exudates at or within 500 μm of the center if associated with thickening of adjacent retina
- a zone of thickening larger than 1 disc area that is located within 1 disc diameter of the center of the macula

As mentioned previously, CSME is an older term that predates use of OCT to diagnose DME. Now that anti-VEGF treatment has supplanted macular laser photocoagulation as first-line therapy for DME, the CSME diagnosis, which is made clinically, is less relevant.

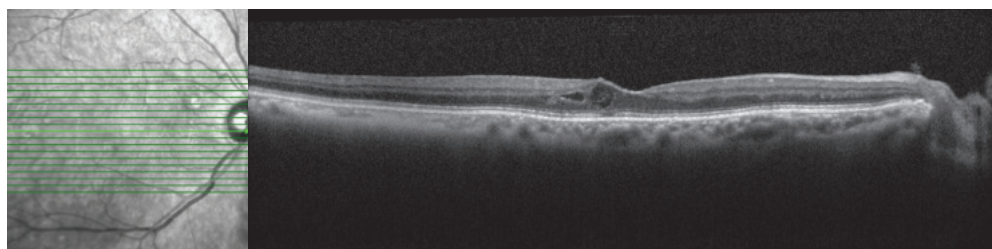


Figure 5-12 OCT volume scan of an eye with DME from a 75-year-old Hispanic man with a long history of poorly controlled type 2 diabetes (hemoglobin A_{1c} levels typically in the 9–9.6 range). The right eye has moderate NPDR. The patient previously underwent treatment with bevacizumab and aflibercept, but there is persistent center-involved DME. The cystic changes involving the temporal and inferior foveal regions are most noticeable in slices 10 through 7 in Activity 5-1. (Courtesy of Colin A. McCannel, MD.)

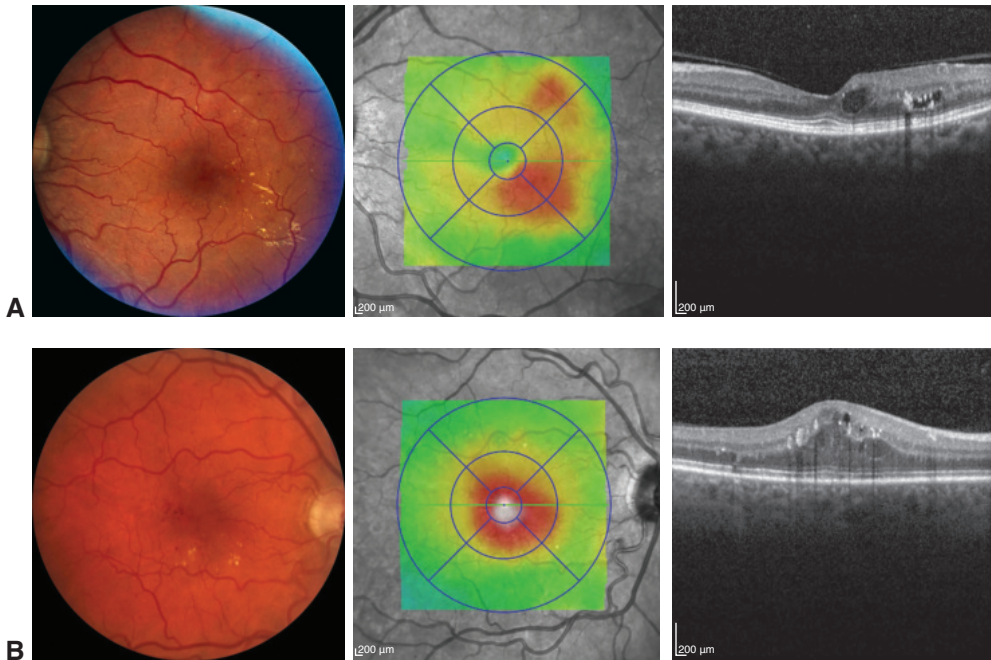


Figure 5-13 Imaging of eyes with DME on fundus photography and OCT. **A**, Eye with non–center-involved DME. **B**, Eye with center-involved DME. (Courtesy of Jennifer K. Sun, MD, MPH.)

Whether it is center involved or non–center involved, DME may manifest as focal or diffuse retinal thickening. Focal macular edema is characterized by areas of local fluorescein leakage from specific capillary lesions, such as microaneurysms. Diffuse macular edema is characterized by extensive retinal capillary leakage and widespread breakdown of the blood–retina barrier, often accumulating in a cystoid configuration in the perifoveal macula (ie, cystoid macular edema). Studies have shown no differences in treatment response based on pattern of macular edema, whether focal, diffuse, or a combination of these.

Management of Diabetic Macular Edema

To maximize visual function and prevent progressive vision loss in eyes with DME, ocular therapies should be considered in parallel with medical management and optimization of patient health habits. When macular edema is center involved and affects visual acuity, treatment is typically indicated. When patients are asymptomatic or have normal visual acuity, the decision to treat DME becomes more complex, as the condition may resolve spontaneously. In general, treatment may be safely deferred in eyes with good visual acuity despite center-involved DME as long as patients are followed up closely and therapy is instituted when vision worsens. Factors for consideration include the proximity of exudates or thickening to the fovea; the status and course of the fellow eye; any anticipated cataract surgery; the presence of high-risk PDR; treatment risks; any systemic conditions or medications (eg, thiazolidinediones) that may exacerbate or cause edema; and systemic control

of glycemia, hypertension, and hyperlipidemia. Ideally, DME treatment is initiated before scatter photocoagulation and cataract surgery are performed to reduce the risk of DME from these interventions.

Pharmacologic management of diabetic macular edema

Anti-VEGF drugs are first-line therapy for most eyes with center-involved DME, especially those with visual impairment caused by the DME. Corticosteroids are alternative agents for eyes that are not candidates for anti-VEGF therapy or in some eyes that were incompletely responsive to previous anti-VEGF treatment.

Anti-VEGF drugs Clinical trials have shown that anti-VEGF treatment is generally beneficial for eyes with DME. The DRCR.net Protocol I study was the first phase 3 trial to demonstrate that visual acuity outcomes with intravitreal anti-VEGF therapy were superior to outcomes with laser treatment for center-involved DME. This study revealed that intravitreal ranibizumab combined with prompt or deferred (≥ 24 weeks) focal/grid laser treatment was more effective in increasing visual acuity than focal/grid laser treatment alone or in combination with triamcinolone acetonide injections at both 1- and 2-year follow-up. After 1 year of treatment, eyes in the ranibizumab-treated groups gained an average of 8 or 9 letters of visual acuity versus those in the laser monotherapy group, which gained an average of only 3 letters. Through 5 years of follow-up, eyes in the ranibizumab treatment groups maintained the vision gains accrued in the first year of therapy, despite a progressively decreasing number of injections (Fig 5-14). Results from this study also suggest that for DME, adding focal/grid laser treatment at the initiation of intravitreal ranibizumab is no better, and is possibly worse, for vision outcomes than deferring laser treatment for 24 weeks or more.

RISE and RIDE, 2 additional parallel phase 3 trials with identical study designs, indicated that compared with sham injections, ranibizumab rapidly and sustainably improved vision, reduced the risk of further vision loss, and improved macular edema in patients with DME, with low rates of complications. According to pooled data from these studies, the proportions of patients who gained 15 or more letters of visual acuity from baseline to 36 months were 41% and 44% in the 0.3-mg and 0.5-mg ranibizumab-treated groups, respectively.

Phase 3 trials have also demonstrated excellent efficacy of aflibercept for treatment of DME. In the VIVID and VISTA trials, an initial phase of 5 monthly injections of aflibercept followed by 148 weeks of either monthly or bimonthly therapy provided substantial visual acuity gains compared with laser photocoagulation therapy.

Although all available anti-VEGF agents are effective in treating DME, results from the DRCR.net Protocol T study demonstrated the superiority of aflibercept over bevacizumab in improving ETDRS visual acuity after both 1 and 2 years of treatment (see Figure 5-8 for a simplified flowchart of the DRCR.net anti-VEGF treatment algorithm for DME). Aflibercept was also superior to ranibizumab at 1-year follow-up but was statistically similar to ranibizumab at 2 years. The differences between the agents were due to the effects of these agents in eyes with worse (ie, $\leq 20/50$) baseline vision. In eyes with milder visual impairment (ie, 20/32 to 20/40), results were equivalent for all 3 treatments at both 1 and 2 years. At 2 years, visual acuity improvements of 10 or more letters were

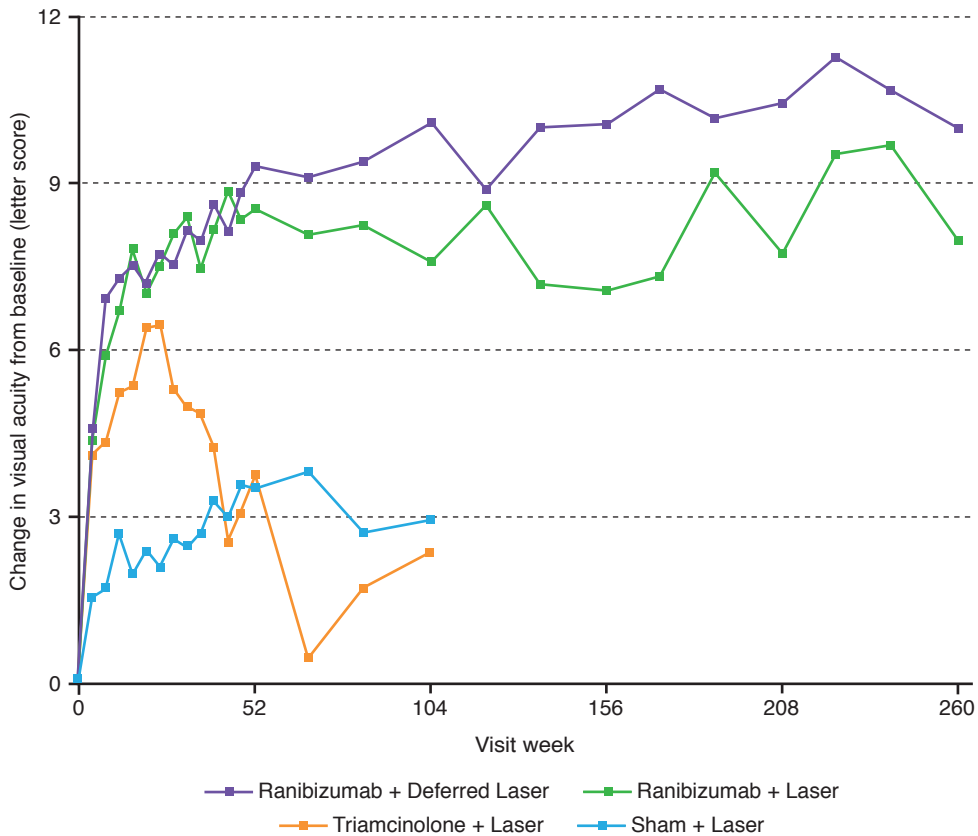


Figure 5-14 Results of the DRCR.net Protocol I study through 5 years demonstrating the superior visual acuity outcomes of treatment with ranibizumab with either prompt or deferred laser treatment compared with laser alone or in combination with triamcinolone through 2 years. Starting in the third year, only patients originally assigned to the ranibizumab groups were followed up. Results from years 3 to 5 suggest that treatment with ranibizumab plus prompt laser therapy is no better than ranibizumab with deferred laser treatment. (Reprinted from *Diabetic Retinopathy Clinical Research Network; Elman MJ, Qin H, Aiello LP, et al. Intravitreal ranibizumab for diabetic macular edema with prompt versus deferred laser treatment: three-year randomized trial results. Ophthalmology. 2012;119(11):2312–2318. © 2012, with permission from Elsevier.*)

observed in 50%, 41%, and 46% of the aflibercept, bevacizumab, and ranibizumab groups, respectively. In contrast, in eyes with worse visual impairment, 2-year improvement of 10 or more letters was observed in 76%, 66%, and 71% of aflibercept, bevacizumab, and ranibizumab groups, respectively. Rates of substantial vision loss were low in all 3 treatment groups.

In general, anti-VEGF agents are well tolerated. Serious intraocular events such as endophthalmitis are rare, with a prevalence of approximately 1 in 1000 injections. Although systemic thromboembolic events are known to be associated with systemic anti-VEGF administration, they have not been shown to be more common among patients who receive intraocular anti-VEGF treatment.

Although anti-VEGF therapy is indicated for most eyes with center-involved DME and visual impairment of 20/32 or worse, in eyes with DME and better vision, a strategy of initial observation with treatment only when vision worsens is generally safe. In the DRCR.net Protocol V study, eyes with visual acuity of 20/25 or better despite center-involved DME were randomly assigned to aflibercept therapy, macular laser treatment, or initial observation. Eyes in the laser and observation groups were given aflibercept if visual acuity worsened during study follow-up. At 2 years, rates of 1 line or greater vision loss (ie, decrease of 5 or more letters) were not significantly different between the groups, and all groups had mean visual acuity of 20/20. In the observation and laser groups, two-thirds and three-fourths of eyes, respectively, did not require aflibercept over the course of the study.

Corticosteroids Corticosteroids are generally used as second-line agents for DME because of studies that have demonstrated inferiority of visual outcomes with steroids versus other therapies and because of the high proportion of eyes that develop adverse effects with continued steroid use. At 2 years in the DRCR.net Protocol B trial, treatment of DME with focal/grid laser photocoagulation was more effective and caused fewer adverse effects than 1-mg or 4-mg doses of preservative-free intravitreal triamcinolone acetonide. Similarly, the DRCR.net Protocol I trial showed that at 2 years, treatment with intravitreal triamcinolone acetonide combined with laser therapy was inferior to treatment with ranibizumab with or without laser therapy as well as to laser treatment alone. A number of small studies initially suggested that intravitreal triamcinolone acetonide benefited patients with refractory DME. However, the DRCR.net Protocol U study, which evaluated eyes with persistent center-involved DME and visual impairment despite at least 6 prior injections of anti-VEGF agents, demonstrated that combination therapy with continued anti-VEGF treatment and a dexamethasone implant did not provide superior vision gains compared with continued anti-VEGF treatment alone. Eyes in the combination group did show greater improvements in retinal thickening over the 6-month study period, but this anatomical benefit was not associated with functional gains. Rates of cataracts and glaucoma are also higher in steroid-treated eyes than in anti-VEGF-treated eyes.

Nonetheless, corticosteroids are beneficial in some patients with DME. Studies of 2 types of sustained-release steroid implants, one made of dexamethasone and the other made of fluocinolone acetonide, reported improved visual acuity of 3 or more lines in eyes with DME. In patients with DME who have already undergone cataract surgery, steroid treatment may be a reasonable alternative to anti-VEGF therapy. In the DRCR.net Protocol I, visual acuity results in steroid-treated eyes that were pseudophakic at baseline (ie, they could not develop cataracts as a result of steroid treatment) were similar to those in anti-VEGF-treated eyes and were superior to results in the laser-treated group.

Baker CW, Glassman AR, Beaulieu WT, et al. Effect of initial management with aflibercept vs laser photocoagulation vs observation on vision loss among patients with diabetic macular edema involving the center of the macula and good visual acuity: a randomized clinical trial. *JAMA*. 2019;321(19):1880–1894.

Boyer DS, Yoon YH, Belfort R Jr, et al; Ozurdex MEAD Study Group. Three-year, randomized, sham-controlled trial of dexamethasone intravitreal implant in patients with diabetic macular edema. *Ophthalmology*. 2014;121(10):1904–1914.

- Campochiaro PA, Brown DM, Pearson A, et al; FAME Study Group. Long-term benefit of sustained-delivery fluocinolone acetonide vitreous inserts for diabetic macular edema. *Ophthalmology*. 2011;118(4):626–635.e2.
- Elman MJ, Ayala A, Bressler NM, et al; Diabetic Retinopathy Clinical Research Network. Intravitreal ranibizumab for diabetic macular edema with prompt versus deferred laser treatment: 5-year randomized trial results. *Ophthalmology*. 2015;122(2):375–381.
- Wells JA, Glassman AR, Ayala AR, et al; Diabetic Retinopathy Clinical Research Network. Aflibercept, bevacizumab, or ranibizumab for diabetic macular edema. *N Engl J Med*. 2015;372(13):1193–1203.

Nonpharmacologic management of diabetic macular edema

There are 2 nonpharmacologic interventions for DME: laser treatment and surgery. Macular focal/grid laser photocoagulation retains an important role as adjunctive treatment in eyes that are resistant to anti-VEGF agents; it is also an occasional first-line treatment in eyes with DME resulting from non-central focal leakage, which can be easily targeted by the laser. In addition, laser therapy may be a useful first-line treatment for patients who are not good candidates for anti-VEGF therapy because they are medically unstable or who are unable to adhere to near-monthly anti-VEGF treatment, especially in the first year. Pars plana vitrectomy, with or without ILM peeling, is often effective in improving retinal thickening in eyes with DME, especially when there is traction from the vitreous or an overlying epiretinal membrane; however, it does not always improve vision. Furthermore, definitive studies are needed to clearly define the role of vitrectomy in DME treatment.

Laser treatment Although anti-VEGF therapy has largely supplanted laser photocoagulation in the treatment of DME, laser therapy is well proven and causes minimal adverse events. Compared with observation alone in the ETDRS, macular focal/grid laser photocoagulation treatment of CSME reduced the risk of moderate vision loss, increased the chance of vision improvement, and was associated with only minor visual field loss. In contrast, eyes with DME that did not meet the criteria for CSME showed no benefit with laser treatment over the control group at 2 years.

Potential adverse effects of macular laser therapy include paracentral scotomata, transient increases of edema and/or decreases in vision, laser scar expansion, subretinal fibrosis, choroidal neovascularization, and inadvertent foveal burns. Clinical features associated with poorer visual acuity outcomes after photocoagulation treatment for DME include macular ischemia (extensive perifoveal capillary nonperfusion) and hard exudates in the fovea.

During treatment of DME, FA, along with an OCT thickness map, may be used to guide the laser. The laser parameters differ from those used in PRP and typically include spot sizes of 50–100 μm and burn durations of 0.1 second or less. For focal leakage, direct laser treatment using green or yellow wavelengths is applied to all leaking microaneurysms between 500 μm and 3000 μm from the center of the macula. For diffuse leakage or zones of capillary nonperfusion in the macula, a light-intensity grid pattern may be applied. Burns are typically separated by 1 burn width, and a green- or yellow-wavelength laser is used. Treatment should include areas of diffuse leakage more than 500 μm from the center of the macula and 500 μm from the temporal margin of the optic nerve head. Laser

sessions are repeated as often as every 16 weeks until retinal thickening has resolved or all leaking microaneurysms have been adequately treated.

Some studies suggest that micropulse therapy, or subthreshold intensity burns, is as effective as standard macular laser treatment while reducing damage to the retinal pigment epithelium and outer retinal layers. In eyes with DME, treatment of peripheral non-perfusion as visualized on ultra-wide-field FA with scatter photocoagulation does not improve vision or retinal thickening.

Early Treatment Diabetic Retinopathy Study Research Group. Treatment techniques and clinical guidelines for photocoagulation of diabetic macular edema: Early Treatment Diabetic Retinopathy Study report number 2. *Ophthalmology*. 1987;94(7):761–774.

Vitrectomy When posterior hyaloidal traction or an associated epiretinal membrane leading to mechanical traction is present, creation of a posterior vitreous detachment and possible ILM or epiretinal membrane peeling can help reduce retinal thickening. The use of vitrectomy as first-line therapy for DME without vitreomacular traction is uncommon in the United States; however, it is more prevalent internationally.

Although vitrectomy generally improves retinal thickening in eyes with DME, multiple studies have reported inconsistent effects of the procedure on visual acuity in eyes with DME, despite consistent improvements in edema. In the DRCR.net Protocol D study, a prospective observational case series, retinal thickening was reduced in most eyes after vitrectomy; however, median visual acuity remained unchanged over the 6-month follow-up period.

Haller JA, Qin H, Apte RS, et al; Diabetic Retinopathy Clinical Research Network Writing Committee. Vitrectomy outcomes in eyes with diabetic macular edema and vitreomacular traction. *Ophthalmology*. 2010;117(6):1087–1093.e3.

Jackson TL, Nicod E, Angelis A, Grimaccia F, Pringle E, Kanavos P. Pars plana vitrectomy for diabetic macular edema: a systematic review, meta-analysis, and synthesis of safety literature. *Retina*. 2017;37(5):886–895.

Cataract Surgery in Patients With Diabetes Mellitus

Various studies suggest that the severity of both diabetic retinopathy and DME may worsen after cataract surgery. In the DRCR.net Protocol Q trial, patients with NPDR but no preoperative center-involved DME were more likely to develop postoperative DME after cataract surgery if they had non-center-involved DME or a history of DME treatment before surgery. In the Protocol P study, which enrolled patients with preexisting DME, a small percentage of eyes had substantial visual acuity loss or definitive progression in central retinal thickening after cataract surgery. Therefore, in clinical practice, a preoperative anti-VEGF or steroid injection is typically given to patients with center-involved DME who are about to undergo cataract surgery. In addition, control of systemic factors should be optimized as much as possible before surgery.

In patients with severe NPDR or PDR, scatter photocoagulation should be considered before cataract removal if the ocular media are sufficiently clear to allow for treatment. When the density of the cataract precludes adequate evaluation of the retina or treatment, prompt

postoperative retinal evaluation and treatment are recommended. In general, all patients with preexisting diabetic retinopathy should be reevaluated after cataract surgery.

Cataract surgeons should be mindful of the need for regular retinal evaluations postoperatively and possible surgical interventions in the future. They should perform an adequate capsulorrhexis to prevent anterior capsular phimosis and should avoid the use of silicone lenses in diabetic eyes, as these lenses may fog with condensation during subsequent vitrectomies. The use of multifocal lenses may also complicate future surgical approaches and may result in unsatisfactory visual outcomes in patients with macular disease. BCSC Section 11, *Lens and Cataract*, briefly discusses issues that should be considered by the cataract surgeon when treating patients with diabetes mellitus.

Baker CW, Almukhtar T, Bressler NM, et al; Diabetic Retinopathy Clinical Research Network Authors/Writing Committee. Macular edema after cataract surgery in eyes without preoperative central-involved diabetic macular edema. *JAMA Ophthalmol.* 2013;131(7):870–879.

Bressler SB, Baker CW, Almukhtar T, et al; Diabetic Retinopathy Clinical Research Network Authors/Writing Committee. Pilot study of individuals with diabetic macular edema undergoing cataract surgery. *JAMA Ophthalmol.* 2014;132(2):224–226.

CHAPTER 6

Retinal Vascular Diseases Associated With Cardiovascular Disease



This chapter includes related activities. Go to www.aao.org/bcscactivity_section12 or scan the QR codes in the text to access this content.

Highlights

- Retinal venous and arterial occlusions are frequently associated with systemic disease and represent a unique opportunity for the ophthalmologist to contribute to a patient's general medical care. The most common associations are hypertension, diabetes, and atherosclerosis; but inflammatory, infectious, or hematologic disorders can also be identified.
- Retinal artery occlusion is a medical emergency that must be regarded as a “stroke equivalent,” requiring immediate evaluation for carotid and cardiac disease.
- Pharmacologic therapy is presently the standard of care for macular edema associated with retinal vein occlusion. Intravitreal injection of anti-vascular endothelial growth factor (anti-VEGF) agents is the first-line treatment, and intravitreal corticosteroid may be helpful as a second-line or adjunctive treatment in recalcitrant cases.
- Cases of artery occlusion without obvious emboli must be evaluated for giant cell arteritis, which can result in bilateral blindness if not treated promptly and correctly.

Systemic Arterial Hypertension and Associated Ocular Diseases

Elevated blood pressure (BP) is defined as systolic BP of 120–129 mm Hg *and* diastolic BP less than 80 mm Hg. Stage 1 hypertension is defined as 130–139 mm Hg systolic *or* 80–89 mm Hg diastolic. Ocular effects of hypertension can be observed in the retina, choroid, and optic nerve. Retinal changes can be described and classified with the use of ophthalmoscopy and angiography. An ophthalmologist's recognition of posterior segment vascular changes may prompt the initial diagnosis of hypertension. BCSC Section 1, *Update on General Medicine*, discusses hypertension in more detail.

Hypertensive Retinopathy

Hypertension affects arterioles and capillaries, the anatomical loci of both autoregulation and nonperfusion. An acute hypertensive episode may produce focal intraretinal periarteriolar transudates (FIPTs) at the precapillary level. The presence of infarctions of the nerve fiber layer (NFL), or *cotton-wool spots* (also called *soft exudates*), indicates ischemia of the retinal NFL (Fig 6-1). Uncontrolled systemic hypertension leads to nonperfusion at various retinal levels as well as neuronal loss and associated scotomata (Fig 6-2). Other, more chronic, hypertensive retinal lesions include microaneurysms, intraretinal microvascular abnormalities (IRMAs), blot hemorrhages, lipid exudates (also called *hard exudates*), venous beading, and neovascularization.

The relationship between hypertensive vascular changes and arteriosclerotic vascular disease is complex, with wide variation related to the duration and severity of the hypertension, the presence of diabetic retinopathy, the severity of any dyslipidemia, the patient's age, and a history of smoking. Hence, it is difficult to classify which retinal vascular changes were caused strictly by hypertension; the often-cited features of focal arteriolar narrowing and arteriovenous nicking have been shown to have little predictive value for severity of hypertension. Nonetheless, 1 well-known historical classification of mostly arteriosclerotic retinopathy is the Modified Scheie Classification of Hypertensive Retinopathy:

- Grade 0: No changes
- Grade 1: Barely detectable arterial narrowing
- Grade 2: Obvious arterial narrowing with focal irregularities
- Grade 3: Grade 2 plus retinal hemorrhages and/or exudates
- Grade 4: Grade 3 plus optic nerve head swelling

Hypertension may be complicated by branch retinal artery occlusion, branch retinal vein occlusion, central retinal vein occlusion, or retinal arterial macroaneurysms (all

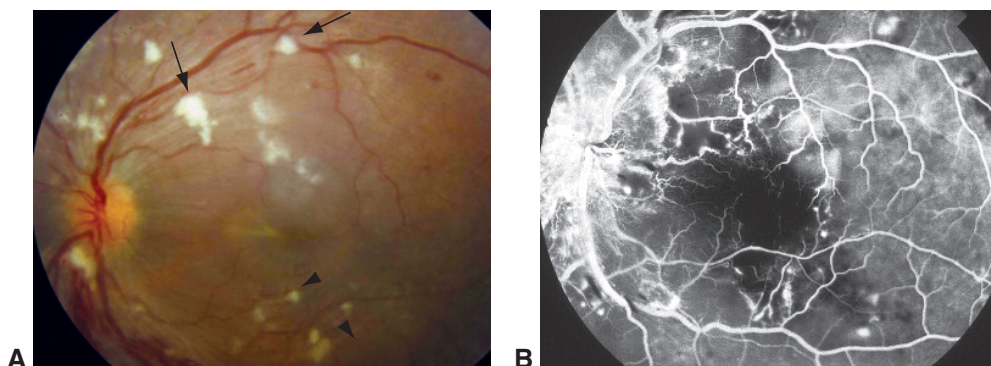


Figure 6-1 Severe hypertensive retinopathy. **A**, Fundus photograph from a 25-year-old man with renal hypertension shows large, superficial, white cotton-wool spots (*arrows*) contrasting with small, deep, tan focal intraretinal periarteriolar transudates (FIPTs, *arrowheads*). **B**, Angiography image shows areas of nonperfusion corresponding to the cotton-wool spots and punctate hyperfluorescence corresponding to the FIPTs. (Courtesy of Hermann D. Schubert, MD.)



Figure 6-2 Acute hypertensive episode. This 40-year-old patient presented with several weeks of blurred vision and headache. Blood pressure at presentation was 245/150 mm Hg. **A, B**, Fundus photographs of the right and left eyes, respectively, show elements of both retinopathy and optic neuropathy: optic nerve head edema, dilated capillaries on the nerve head, flame-shaped nerve fiber layer (NFL) hemorrhages, cotton-wool spots, macular exudates, and subretinal fluid. **C**, Optical coherence tomography (OCT) of the right macula shows fluid in the NFL, retina, and subretinal space. **D**, Photograph of the left fundus 3 months later, after initiation of systemic antihypertensive medications, shows resolution of optic nerve head edema and reduction in retinal exudation and hemorrhage. Blood pressure at this visit was 197/99 mm Hg. (Parts A and B courtesy of Jeremy Anderson, OD, and parts C and D courtesy of Franco M. Recchia, MD.)

discussed later in this chapter). In addition, the coexistence of hypertension and diabetes results in more severe retinopathy.

Cheung CYL, Wong TY. Hypertension. In: Schachat AP, Wilkinson CP, Hinton DR, Sadda SR, Wiedemann P, eds. *Ryan's Retina*. 6th ed. Elsevier/Saunders; 2018:chap 52.

Wong TY, Mitchell P. The eye in hypertension. *Lancet*. 2007;369(9559):425–435.

Hypertensive Choroidopathy

Hypertensive choroidopathy typically occurs in young patients who have experienced an episode of acute, severe hypertension, often associated with preeclampsia, eclampsia, pheochromocytoma, or renal hypertension (see Chapter 9 for more on choroidal disease). Lobular nonperfusion of the choriocapillaris may occur, initially resulting in tan,

lobule-shaped patches that, in time, become hyperpigmented and surrounded by margins of hypopigmentation; these lesions are known as *Elschnig spots*). Linear configurations of similar-appearing hyperpigmentation, known as *Siegrist streaks*, follow the meridional course of choroidal arteries. Fluorescein angiography shows focal choroidal hypoperfusion in the early phases and multiple subretinal areas of leakage in the late phases. Focal retinal pigment epithelium detachments may occur, and in severe cases, extensive bilateral exudative retinal detachments may develop.

Hypertensive Optic Neuropathy

Patients with optic neuropathy secondary to severe hypertension may exhibit linear peripapillary flame-shaped hemorrhages, blurring of the optic nerve head (ONH) margins, florid ONH edema with secondary retinal venous stasis, and macular exudates (see Fig 6-2). The differential diagnosis for patients with this clinical appearance includes central retinal vein occlusion, anterior ischemic optic neuropathy, diabetic papillopathy, radiation papillopathy, neuroretinitis, and retrobulbar tumor.

Retinal Venous Occlusion

Overview of Retinal Venous Occlusion

Retinal venous occlusion (RVO) is the second most common retinal vascular disorder, following diabetic retinopathy. It is caused by a thrombus located at any point along the venous circulation and is named according to the site of the occlusion. A *branch retinal vein occlusion (BRVO)* produces a sectoral (typically quadrantic) area of damage due to thrombosis in 1 of the branches of the intraretinal portion of the venous tree. A *central retinal vein occlusion (CRVO)* arises from thrombosis in the retrolaminar portion and, thus, affects the entire retina. *Hemicentral retinal vein occlusion (HRVO)* occurs in eyes with a persistent vestigial bifurcation in the retrolaminar portion of the central retinal vein, affecting either the superior or the inferior half of the retina.

Clinical presentation and pathogenesis of RVO

Patients typically present with acute decline in central vision and/or a paracentral or peripheral scotoma. The classic ophthalmoscopic findings are dilated, tortuous retinal veins and intraretinal hemorrhages in the areas affected by the occlusion. In BRVO, this is most commonly seen in the superotemporal quadrant (Fig 6-3); the occlusion may also be restricted to the macula, termed a *macular BRVO* (Fig 6-4). In CRVO, all 4 retinal quadrants are involved (Fig 6-5). HRVO may involve either the superior or the inferior half of the retina (Fig 6-6). Cotton-wool spots and ONH edema occur in more severe cases of RVO. Varying degrees of macular edema, macular ischemia, and foveal hemorrhage may be seen. Macular edema is best assessed and quantified with spectral-domain optical coherence tomography (SD-OCT), whereas ischemia is best detected using fluorescein angiography or OCT angiography.

The pathogenesis of RVO mirrors Virchow's triad for thrombosis: endothelial injury, venous stasis, and hypercoagulability. Normally, retinal arteries and veins share a common adventitial sheath. Progressive arteriolosclerosis (as occurs in normal aging

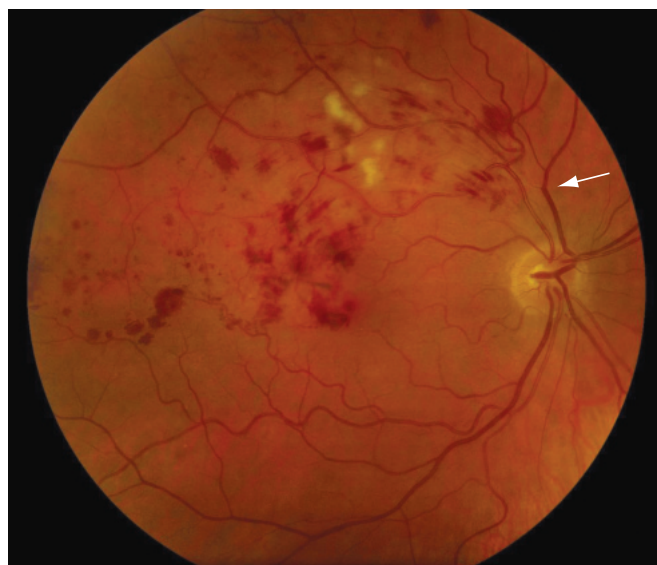


Figure 6-3 Typical findings of a major branch retinal vein occlusion (BRVO): moderate dilation and tortuosity of veins, intraretinal hemorrhages, and cotton-wool spots. Note that the hemorrhages are restricted to the superotemporal quadrant. The presumed site of obstruction is designated by the arrow. (Courtesy of Franco M. Recchia, MD.)

and hypertension) leads to thickening of the arterial wall, which in turn leads to compression and inelasticity of the venous wall. These changes to the venous wall (endothelial damage) may produce turbulent blood flow and venous stasis, which predispose to venous thrombosis.

At the cellular level, retinal ischemia caused by impairment of normal retinal circulation leads to the local upregulation and release of hypoxia-related factors into the retina and into the eye. The most salient of these are vascular endothelial growth factor (VEGF) and various mediators of inflammation. VEGF has 2 profound effects on the retinal vasculature: (1) increased vessel-wall permeability, leading to macular edema; and (2) growth of new blood vessels (*neovascularization*). Pro-inflammatory factors may worsen vascular leakage and macular edema.

Risk factors and causes of RVO

Retinal vein occlusion is most commonly associated with increasing age (90% of patients are >50 years old) and hypertension. Every patient with RVO should undergo medical evaluation in addition to a comprehensive ocular examination. In the absence of known cardiovascular disease, a search for other causative or predisposing systemic conditions should be considered, especially in patients younger than 50 years or in patients with simultaneous bilateral CRVO. The Eye Disease Case-Control Study and other studies have enumerated risk factors associated with BRVO and CRVO:

- increasing age
- systemic arterial hypertension
- cigarette smoking

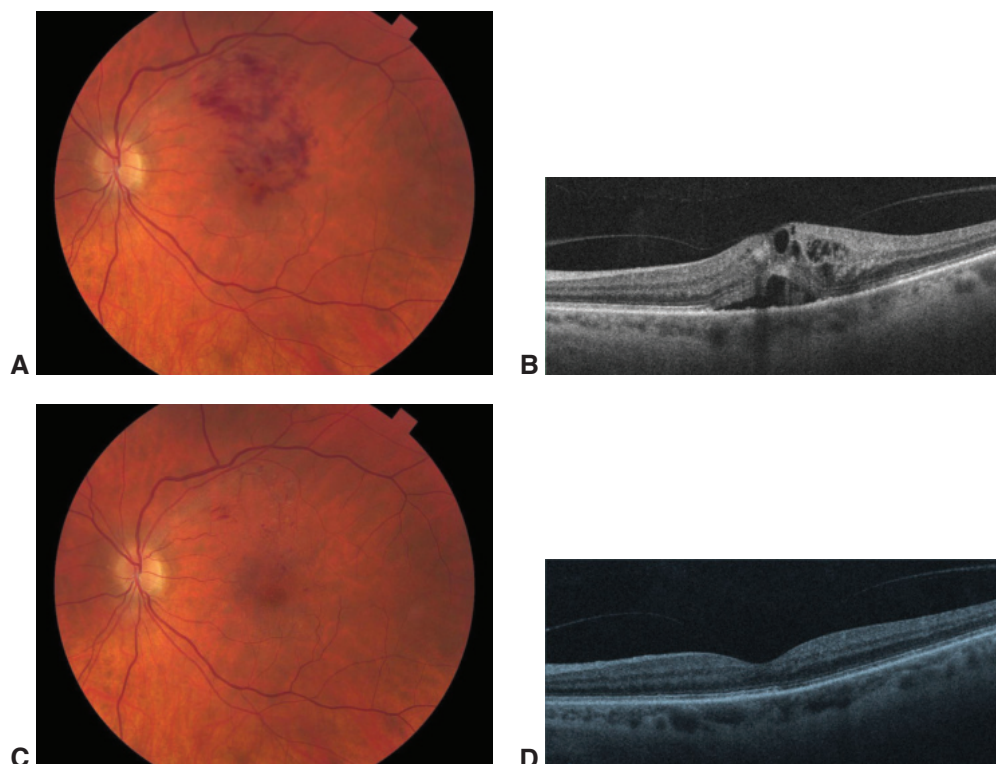


Figure 6-4 **A**, Fundus photograph of a macular BRVO. At presentation, corrected distance visual acuity (CDVA; also called *best-corrected visual acuity*) was 20/40. Intraretinal hemorrhages are confined to the superior macula and involve the fovea. **B**, OCT shows intraretinal and subretinal edema and an incidental finding of vitreofoveal adhesion. After 3 intravitreal injections of aflibercept, VA had improved to 20/20⁻², with improvement in retinal hemorrhages (**C**) and resolution of macular edema (**D**). (Courtesy of Franco M. Recchia, MD.)

- open-angle glaucoma
- diabetes mellitus
- hyperlipidemia
- hypercoagulability
- hypothyroidism

Although rare, predisposing hypercoagulable and inflammatory conditions may be present. However, when CRVO occurs in patients older than 50 years or patients with known cardiovascular risk factors, an extensive systemic workup is generally unnecessary.

American Academy of Ophthalmology Retina/Vitreous Panel. Preferred Practice Pattern Guidelines. *Retinal Vein Occlusions*. American Academy of Ophthalmology; 2019. www.aao.org/preferred-practice-pattern/retinal-vein-occlusions-ppp
 Goldman DR, Shah CP, Morley MG, Heier JS. Venous occlusive disease of the retina. In: Yanoff M, Duker JS, eds. *Ophthalmology*. 4th ed. Elsevier/Saunders; 2014:526–534.
 Hayreh SS. Retinal vein occlusion. *Indian J Ophthalmol*. 1994;42(3):109–132.



Figure 6-5 Typical findings of a central retinal vein occlusion (CRVO): dilation and tortuosity of veins and intraretinal hemorrhages involving all 4 retinal quadrants, edema of the optic nerve head, and scattered cotton-wool spots. (Courtesy of Franco M. Recchia, MD.)

Risk factors for branch retinal vein occlusion. The Eye Disease Case-Control Study Group.

Am J Ophthalmol. 1993;116(3):286–296.

Risk factors for central retinal vein occlusion. The Eye Disease Case-Control Study Group.

Arch Ophthalmol. 1996;114(5):545–554.

Complications of RVO

The most common complications of RVO are intraocular neovascularization and the sequelae thereof. Neovascularization is driven by VEGF, the levels of which are correlated with the extent of retinal ischemia. In BRVO, neovascularization occurs most commonly at the border between the affected ischemic retina and normal perfused retina; it is seen less frequently at the ONH and, in rare instances, in the anterior segment. In CRVO, neovascularization occurs most commonly in the anterior segment and can also occur within the retina or at the ONH.

Spontaneous resolution of RVO can occur and is usually associated with the development of alternative paths of venous outflow (*collateral vessels*). In BRVO, capillaries extending across the median raphe dilate, helping to compensate for the compromised venous drainage. In CRVO, small vessels that normally connect the retinal circulation to the choroidal circulation near the ONH expand, resulting in the undulating appearance of optociliary shunt vessels (Fig 6-7). These mechanisms redirect venous drainage to the choroid, vortex veins, and superior and inferior ophthalmic veins in the orbit, bypassing the occluded central retinal vein. The presence of collateral vessels, however, does not

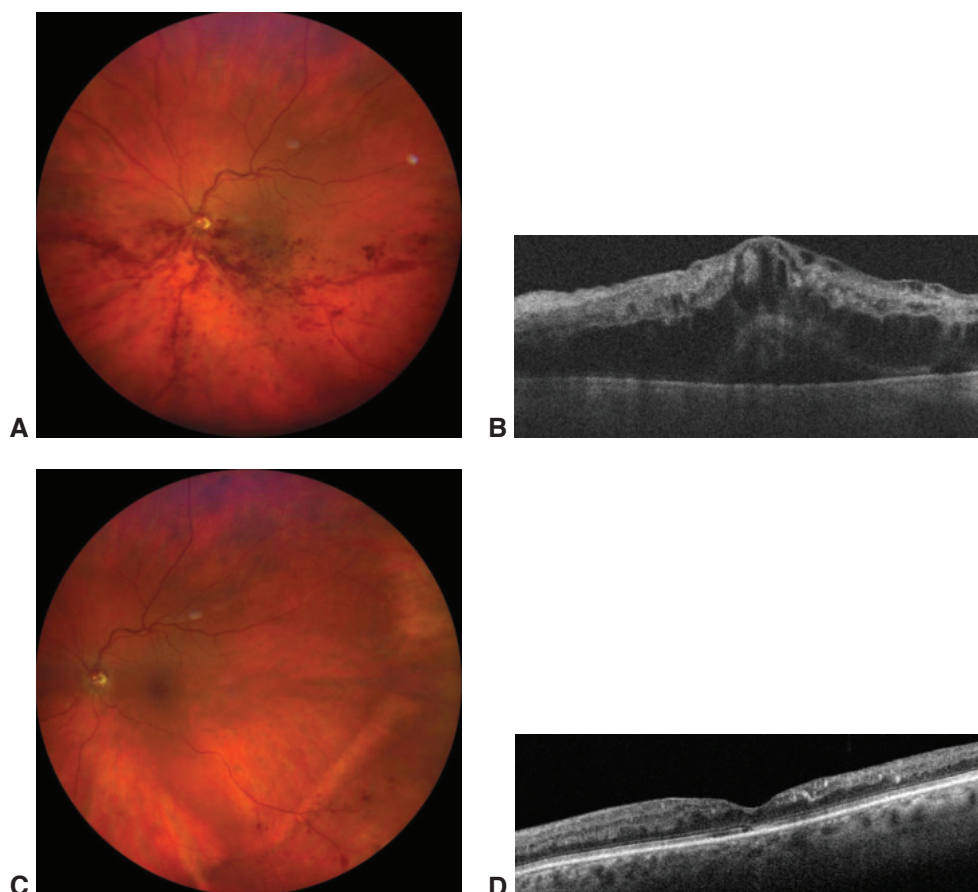


Figure 6-6 Typical findings of a hemicentral retinal vein occlusion (HRVO). **A**, Fundus photograph at presentation shows dilation and tortuosity of veins and intraretinal hemorrhages confined to the 2 inferior retinal quadrants. **B**, OCT at presentation shows inner hyporeflectivity consistent with intraretinal edema and outer hyporeflectivity consistent with subfoveal fluid. Fundus photograph (**C**) and OCT (**D**) taken 10 months after presentation show diminution of retinal hemorrhage and resolution of macular edema after 6 treatments with intravitreal aflibercept. Thinning of the inner retina and discontinuity of the ellipsoid zone are demonstrated on OCT; these anatomical changes will likely limit the degree of visual recovery. (Courtesy of Franco M. Recchia, MD.)

consistently equate with functional improvement. Chronic, untreated venous occlusive disease commonly leads to the development of retinal microvascular changes characterized by microaneurysms, telangiectasias, and macular edema.

Pharmacologic management of RVO

Anti-VEGF drugs have become the first-line treatment for macular edema associated with RVO because of their excellent efficacy and safety profiles. Improvement and maintenance of visual acuity are optimized by administering anti-VEGF treatment immediately upon diagnosis of RVO-related macular edema and continuing treatment long enough to

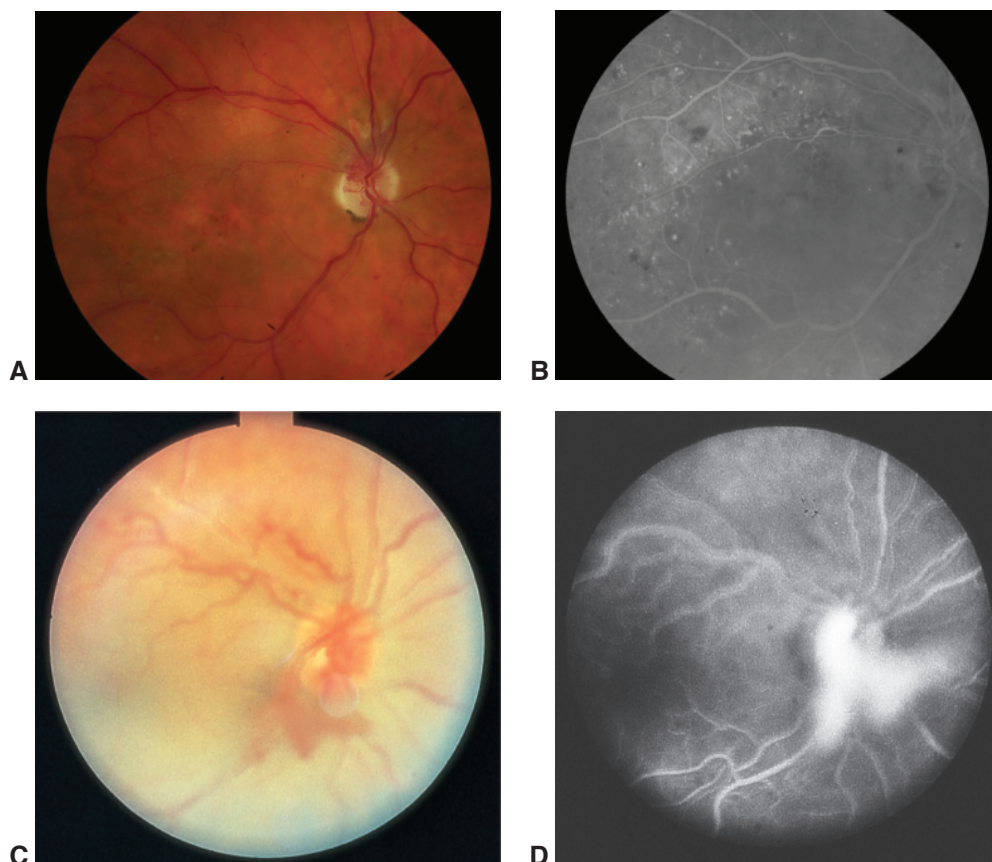


Figure 6-7 Characteristic retinal changes seen in a chronic retinal vein occlusion (RVO). **A**, Color photograph shows collateral vessels (specifically optociliary shunt vessels) on the superior optic nerve head, macular atrophy, and epiretinal membrane. **B**, Corresponding fluorescein angiogram shows areas of nonperfusion, telangiectasias, and mild macular edema. The collateral optic nerve head vessels can be contrasted with neovascularization of the disc shown in **C** and **D**. (Parts A and B courtesy of Franco M. Recchia, MD; parts C and D courtesy of Gary C. Brown, MD.)

prevent recurrence of macular edema. Intraocular corticosteroids are also effective at reducing macular edema. Because studies are increasingly not separating BRVO and CRVO when evaluating pharmacologic treatment of macular edema secondary to retinal venous occlusive disease, they are discussed together in this section.

Laser photocoagulation, pars plana vitrectomy, and other surgical techniques are also used in selected cases of BRVO and CRVO. See the discussions of surgical management in the specific sections for those entities.

Table 6-1 summarizes the major clinical trials that inform contemporary management of RVO and their salient findings. Because the study acronyms are generally more familiar to readers than are the study titles, the acronyms are used in the chapter text; for the complete titles, please refer to the table.

Table 6-1 Clinical Trials for Retinal Vein Occlusion

Study Acronym, Title (Year Completed)	Outcome Measure(s)	Number of Patients	Treatment Arms	Main Conclusions
Trials Evaluating Laser				
CVOS , Central Vein Occlusion Study (1994)	Visual acuity at 3 y	155	1. Grid macular laser q4mo PRN 2. Observation	Laser reduced angiographic macular edema but did not improve visual acuity.
	Incidence of anterior segment neovascularization	181	1. Prompt PRP 2. PRP deferred until appearance of NVI or NVA	PRP is recommended when at least 2 clock-hours of NVI or any degree of NVA is observed.
BVOS , Branch Vein Occlusion Study (1984)	Visual acuity at final study visit (mean 3.1 y)	139	1. Grid macular laser q4mo PRN 2. Observation	In patients with macular edema of >3 mo and BCVA \leq 20/40, grid laser improved BCVA.
	Development of retinal NV and vitreous hemorrhage (mean 2.8 y)	319	1. Scatter peripheral laser q4mo PRN 2. Observation	Patients in whom retinal NV develops should be treated with scatter laser photocoagulation to the involved retinal sector. Risk of posterior segment NV correlates with extent of retinal ischemia.
Trials Evaluating Corticosteroid				
SCORE , The Standard Care vs Corticosteroid for Retinal Vein Occlusion, for BRVO (2008)	Gain in >15 letters of BCVA at 12 mo	352 with BRVO, 59 with hemi-CRVO	1. Intravitreal triamcinolone, 1 mg q4mo if re-treatment criteria were met 2. Intravitreal triamcinolone, 4 mg q4mo if re-treatment criteria were met 3. Grid macular laser photocoagulation	Early visual acuity gains with steroid treatment were not sustained. Cataract progression and need for IOP-lowering medications were greater following steroid treatment and were dose dependent.

Study Acronym, Title (Year Completed)	Outcome Measure(s)	Number of Patients	Treatment Arms	Main Conclusions
SCORE , The Standard Care vs Corticosteroid for Retinal Vein Occlusion Study (2008)	Gain in >15 letters of BCVA at 12 mo	271 with CRVO	1. Intravitreal triamcinolone, 1 mg q4mo 2. Intravitreal triamcinolone, 4 mg q4mo 3. Observation	Intravitreal corticosteroid was more likely to produce gains in visual acuity. Cataract progression and/or ocular hypertension occurred in one-third of eyes by 12 mo.
GENEVA , Global Evaluation of Implantable Dexamethasone in Retinal Vein Occlusion With Macular Edema (2008)	Time to achieve gain of >15 letters in BCVA	830 with BRVO, 437 with CRVO	1. Single intravitreal dexamethasone implant, 0.7 mg 2. Single intravitreal dexamethasone implant, 0.35 mg 3. Sham injection	Improvement in BCVA was greatest with dexamethasone implant at 60 d, but effectiveness waned by 6 mo. Risk of ocular hypertension was 16% after 1 dexamethasone injection.
COMRADE C , Clinical Efficacy and Safety of Ranibizumab Versus Dexamethasone for Central Retinal Vein Occlusion: A European Label Study (2014)	Mean change in BCVA at 6 mo	144	1. Single intravitreal dexamethasone implant, 0.7 mg 2. Intravitreal ranibizumab, 0.5 mg (monthly x3, then PRN)	Ranibizumab (monthly loading, then PRN) was superior to a single injection of dexamethasone (mean BCVA gain of 16 letters vs 9 letters, respectively).
FDA Registration Trials for Anti-VEGF Medications				
BRAVO , Ranibizumab for Macular Edema Following Branch Retinal Vein Occlusion (2008)	Mean change in BCVA at 6 mo	397	1. Monthly intravitreal ranibizumab, 0.3 mg 2. Monthly intravitreal ranibizumab, 0.5 mg 3. Sham injection	Monthly treatment with ranibizumab is superior to sham treatment. Mean gains of 16 and 18 letters for the 0.3-mg and 0.5-mg ranibizumab groups, respectively, compared with 7 letters for sham group; 61% of eyes treated with 0.5-mg ranibizumab gained at least 15 letters.

(Continued)

Table 6-1 (continued)

Study Acronym, Title (Year Completed)	Outcome Measure(s)	Number of Patients	Treatment Arms	Main Conclusions
CRUISE , Ranibizumab for Macular Edema Following Central Retinal Vein Occlusion (2008)	Mean change in BCVA at 6 mo	392	1. Monthly intravitreal ranibizumab, 0.3 mg 2. Monthly intravitreal ranibizumab, 0.5 mg 3. Sham injection	Monthly treatment with ranibizumab is superior to sham treatment. Mean gains of 13 and 15 letters for the 0.3-mg and 0.5-mg ranibizumab groups, respectively, compared with 0.8 letters for sham group; 48% of eyes treated with 0.5-mg ranibizumab gained at least 15 letters.
VIBRANT , Intravitreal Aflibercept for Macular Edema Following Branch Retinal Vein Occlusion (2012)	Gain in >15 letters of BCVA at 6 mo	183	1. Monthly intravitreal aflibercept, 2 mg 2. Macular laser photocoagulation	Monthly treatment with aflibercept is superior to laser. 53% of eyes treated with aflibercept gained ≥15 letters vs 28% of eyes treated with laser.
GALILEO/COPERNICUS , Vascular Endothelial Growth Factor Trap-Eye for Macular Edema Secondary to Central Retinal Vein Occlusion (2010)	Gain in >15 letters of BCVA at 6 mo	189	1. Monthly intravitreal aflibercept, 2 mg 2. Sham injection	Monthly treatment with aflibercept is superior to sham treatment. 56% of eyes treated with aflibercept gained ≥15 letters vs 12% in the sham group.
Trials Comparing Pharmacologic Treatments				
SCORE2 , Effect of Bevacizumab vs Aflibercept on Visual Acuity Among Patients With Macular Edema Due to Central Retinal Vein Occlusion (2016)	Mean change in BCVA at 6 mo	305 with CRVO, 57 with hemi-CRVO	1. Intravitreal bevacizumab, 1.25 mg 2. Intravitreal aflibercept, 2 mg	Bevacizumab was noninferior to aflibercept (mean gain of 18 letters in each group).

Study Acronym, Title (Year Completed)	Outcome Measure(s)	Number of Patients	Treatment Arms	Main Conclusions
CRAVE , Bevacizumab Versus Ranibizumab in the Treatment of Macular Edema Due to Retinal Vein Occlusion (2015)	Change in central foveal thickness at 6 mo	98	1. Monthly intravitreal bevacizumab, 1.25 mg 2. Monthly intravitreal ranibizumab, 0.5 mg	Both bevacizumab and ranibizumab reduced mean retinal thickness and improved visual acuity.
LEAVO , Clinical Effectiveness of Intravitreal Therapy With Ranibizumab vs Aflibercept vs Bevacizumab for Macular Edema Secondary to Central Retinal Vein Occlusion (2016)	Change in visual acuity at 100 wk	463	1. Intravitreal bevacizumab, 1.25 mg 2. Intravitreal ranibizumab, 0.5 mg 3. Intravitreal aflibercept, 2 mg Doses were monthly for the first 3 months, then given as needed if re-treatment criteria were met.	Mean gain of 12.5 ETDRS letters for ranibizumab, 15.1 letters for aflibercept, and 9.8 letters for bevacizumab. Visual results may be worse with bevacizumab when compared with other 2 agents.
MARVEL , A Randomised, Double-Masked, Controlled Study of the Efficacy and Safety of Intravitreal Bevacizumab Versus Ranibizumab in the Treatment of Macular Oedema due to Branch Retinal Vein Occlusion (2015)	Change in BCVA at 6 mo	75	1. Intravitreal bevacizumab, 1.25 mg 2. Intravitreal ranibizumab, 0.5 mg	Mean BCVA gain was similar between bevacizumab (18 letters) and ranibizumab (15.6 letters).

BCVA = best-corrected visual acuity; BRVO = branch retinal vein occlusion; CRVO = central retinal vein occlusion; d = day(s); ETDRS = Early Treatment Diabetic Retinopathy Study; IOP = intraocular pressure; mo = month(s); NV = neovascularization; NVA = neovascularization of the anterior chamber angle; NVI = neovascularization of the iris; PRN = pro re nata (as needed); PRP = panretinal photocoagulation; q4mo = every 4 months; VEGF = vascular endothelial growth factor; wk = week(s); y = year(s).

Intravitreal anti-VEGF therapy The initial studies of anti-VEGF therapy for macular edema caused by RVO were the BRAVO and CRUISE trials. In these studies, monthly injection of either 0.5 mg or 0.3 mg of ranibizumab was superior to sham injection for improving visual acuity. Similar results were achieved with intravitreal aflibercept (also called VEGF Trap-Eye) in the VIBRANT, COPENICUS, and GALILEO studies (see Figs 6-4 and 6-6). The benefits were maintained during the second 6 months of these aflibercept studies, during which as-needed treatment was administered.

Bevacizumab, which is commonly used off label for retinal disease, has also demonstrated efficacy in the management of cystoid macular edema (CME) secondary to RVO (Fig 6-8). In SCORE2, bevacizumab was shown to be noninferior to (not worse than) aflibercept in the treatment of macular edema secondary to CRVO.

More recently, in the LEAVO study, the 3 most commonly used anti-VEGF agents were compared in a prospective multicenter noninferiority trial in the United Kingdom. Aflibercept treatment was noninferior to ranibizumab treatment at 100 weeks. However, bevacizumab was *not* noninferior to ranibizumab and, by post hoc analysis, was not noninferior to aflibercept. In other words, change in visual acuity may be worse with the use of bevacizumab than with the use of ranibizumab or aflibercept.

In current clinical practice, anti-VEGF regimens for RVO include fixed monthly dosing, as-needed treatment, and treat-and-extend approaches. Clinical trials have shown no additive benefit of macular grid or peripheral scatter laser photocoagulation for BRVO in patients treated with anti-VEGF agents.

Brown DM, Campochiaro PA, Bhisitkul RB, et al. Sustained benefits from ranibizumab for macular edema following branch retinal vein occlusion: 12-month outcomes of a phase III study. *Ophthalmology*. 2011;118(8):1594–1602.

Campochiaro PA, Brown DM, Awh CC, et al. Sustained benefits from ranibizumab for macular edema following central retinal vein occlusion: twelve-month outcomes of a phase III study. *Ophthalmology*. 2011;118(10):2041–2049.

Hykin P, Prevost AT, Vasconcelos JC, et al. Clinical effectiveness of intravitreal therapy with ranibizumab vs aflibercept vs bevacizumab for macular edema secondary to central retinal vein occlusion: a randomized clinical trial. *JAMA Ophthalmol*. 2019;137(11):1256–1264.

Scott IU, VanVeldhuisen PC, Ip MS, et al; SCORE2 Investigator Group. Effect of bevacizumab vs aflibercept on visual acuity among patients with macular edema due to central retinal vein occlusion: the SCORE2 randomized clinical trial. *JAMA*. 2017;317(20):2072–2087.

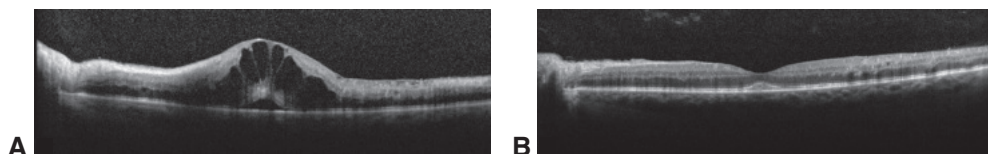


Figure 6-8 Cystoid macular edema (CME) secondary to CRVO, before and after treatment. **A**, Spectral-domain OCT (SD-OCT) scan shows severe CME with foveal detachment in a patient with a nonischemic CRVO. VA was 20/200. **B**, One month after intravitreal injection of bevacizumab 1.25 mg, the cystic changes and foveal detachment resolved, and VA was 20/25.

(Courtesy of Colin A. McCannel, MD.)

Intravitreal corticosteroids Intravitreal corticosteroids are efficacious for RVO, but their risks include cataract formation and steroid-induced elevation of intraocular pressure (IOP) (in 20%–65% of individuals). The SCORE trial found that intravitreal triamcinolone injection in eyes with BRVO was comparable in efficacy to macular grid laser treatment in terms of visual acuity gain of 3 or more lines; however, because eyes receiving triamcinolone were more likely to develop a cataract or experience elevated IOP, macular grid laser therapy was recommended. In the CRVO arm of the SCORE study, intravitreal steroid was associated with improved visual acuity.

The GENEVA study explored the use of a 0.7-mg dexamethasone intravitreal implant to treat macular edema secondary to RVO. The dexamethasone implant (Ozurdex, Allergan, Inc) is a small, biodegradable pellet injected into the vitreous cavity. Visual improvement was noted between 30 and 90 days, with the greatest response at day 60. The COMRADE study compared the dexamethasone implant against monthly ranibizumab treatment. The efficacy of the 2 treatments was similar early, but at months 4–6, the eyes treated with ranibizumab had significantly better visual acuity.

Haller JA, Bandello F, Belfort R Jr, et al; OZURDEX GENEVA Study Group. Randomized, sham-controlled trial of dexamethasone intravitreal implant in patients with macular edema due to retinal vein occlusion. *Ophthalmology*. 2010;117(6):1134–1146.e3.

Hoerauf H, Feltgen N, Weiss C, et al; COMRADE-C Study Group. Clinical efficacy and safety of ranibizumab versus dexamethasone for central retinal vein occlusion (COMRADE C): a European label study. *Am J Ophthalmol*. 2016;169:258–267.

Scott IU, Ip MS, VanVeldhuisen PC, et al; SCORE Study Research Group. A randomized trial comparing the efficacy and safety of intravitreal triamcinolone with standard care to treat vision loss associated with macular edema secondary to branch retinal vein occlusion: the Standard Care vs Corticosteroid for Retinal Vein Occlusion (SCORE) study report 6. *Arch Ophthalmol*. 2009;127(9):1115–1128. Published correction appears in *Arch Ophthalmol*. 2009;127(12):1655.

Systemic anticoagulation Systemic anticoagulation is not recommended for the treatment of RVO. Case series suggest that patients may experience worse outcomes as a result of increased bleeding in the retina.

Branch Retinal Vein Occlusion

In BRVO, venous thrombosis and obstruction occur most commonly at an arteriovenous crossing in the superotemporal quadrant. When the occlusion does not occur at an arteriovenous crossing, other inflammatory and infectious causes should be considered.

Prognosis for patients with BRVO

In acute disease, the presence or absence of macular or foveal involvement determines the visual prognosis. Before the availability of pharmacologic intervention, the BVOS found that the incidence of neovascularization from the retina or optic nerve was 36% in eyes with extensive retinal ischemia; extensive ischemia was defined as an area of at least 5 disc diameters in size (Fig 6-9). Vitreous hemorrhage developed in 60%–90% of such eyes if laser photocoagulation was not performed.

Over the long term, permanent vision loss may be related to macular ischemia, lipid residues (hard exudates) in the fovea, pigmentary macular disturbances, subretinal

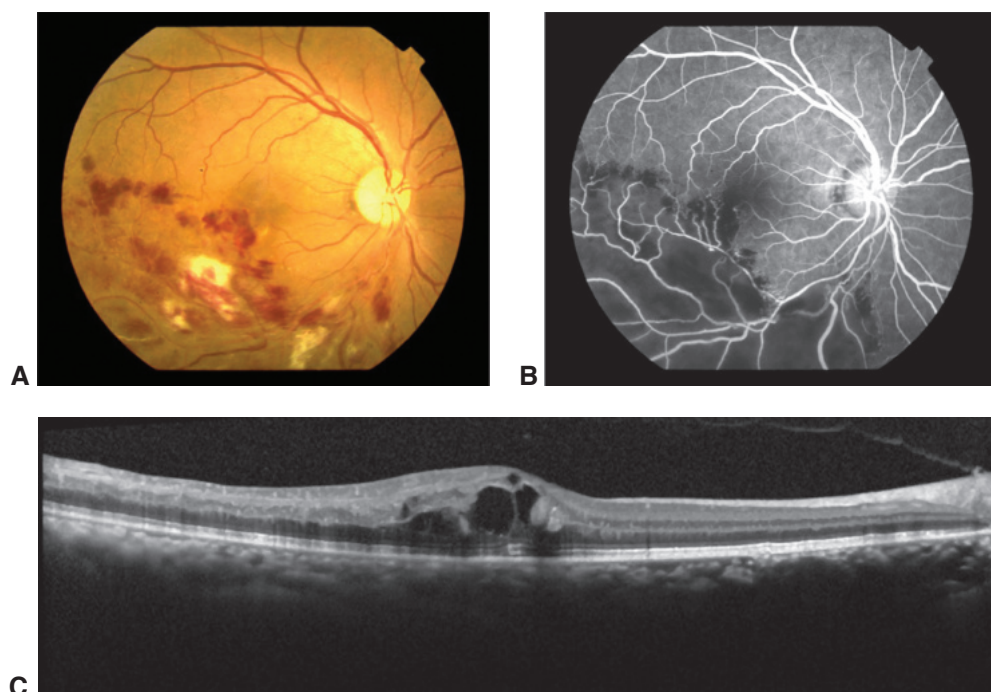


Figure 6-9 Branch retinal vein occlusion (BRVO) with ischemia. **A**, Fundus photograph shows inferotemporal BRVO. **B**, Fluorescein angiography image corresponding to **A** reveals pronounced retinal capillary nonperfusion in the distribution of the retina drained by the obstructed vein. **C**, SD-OCT image of the same eye reveals CME. (Courtesy of Neal H. Atebara, MD.)

fibrosis, CME, and epiretinal membrane formation. The last 2 conditions can be treated, and treatment may restore some visual function. Less common treatable causes of vision loss include vitreous hemorrhage, traction (also called *tractional*) retinal detachment, and rhegmatogenous retinal detachment. Traction retinal detachment typically arises from fibrosis and contraction of prior retinal neovascularization. Rhegmatogenous retinal detachment typically develops following a retinal break induced by vitreous traction in areas adjacent to or beneath the retinal neovascularization and fibrosis.

Treatment of BRVO

Pharmacologic management Pharmacologic management is currently the mainstay of BRVO management. See the earlier section “Pharmacologic management of RVO” for more detail.

Ehlers JP, Kim SJ, Yeh S, et al. Therapies for macular edema associated with branch retinal vein occlusion: a report by the American Academy of Ophthalmology. *Ophthalmology*. 2017;124(9):1412–1423.

Surgical management of BRVO In BRVO, macular laser photocoagulation and scatter panretinal photocoagulation may address macular edema and retinal neovascularization, respectively, by local destruction of ischemic retina and reduction in local pro-inflammatory and proangiogenic factors.

MACULAR LASER SURGERY Grid laser photocoagulation may be applied to areas of macular edema caused by the obstructed vein (Fig 6-10). The BVOS found that laser-treated eyes with intact foveal vasculature, macular edema, and visual acuity in the 20/40–20/200 range were more likely to gain 2 lines of visual acuity (65%) than untreated eyes (37%). At 3-year follow-up, treated eyes were more likely to have 20/40 or better visual acuity than untreated eyes (60% vs 34%, respectively), with a mean visual acuity improvement of 1.3 ETDRS (Early Treatment Diabetic Retinopathy Study) lines versus 0.2 line, respectively. In the BVOS, laser treatment of macular edema was delayed for at least 3 months to permit the maximum spontaneous resolution of intraretinal blood and edema. Although this practice may still be appropriate for macular laser therapy, treatment with pharmacologic agents should commence immediately upon diagnosis of BRVO.

SCATTER PHOTOCOAGULATION The BVOS showed that scatter photocoagulation to the area of retinal capillary nonperfusion is effective in causing regression of the new vessels in eyes with

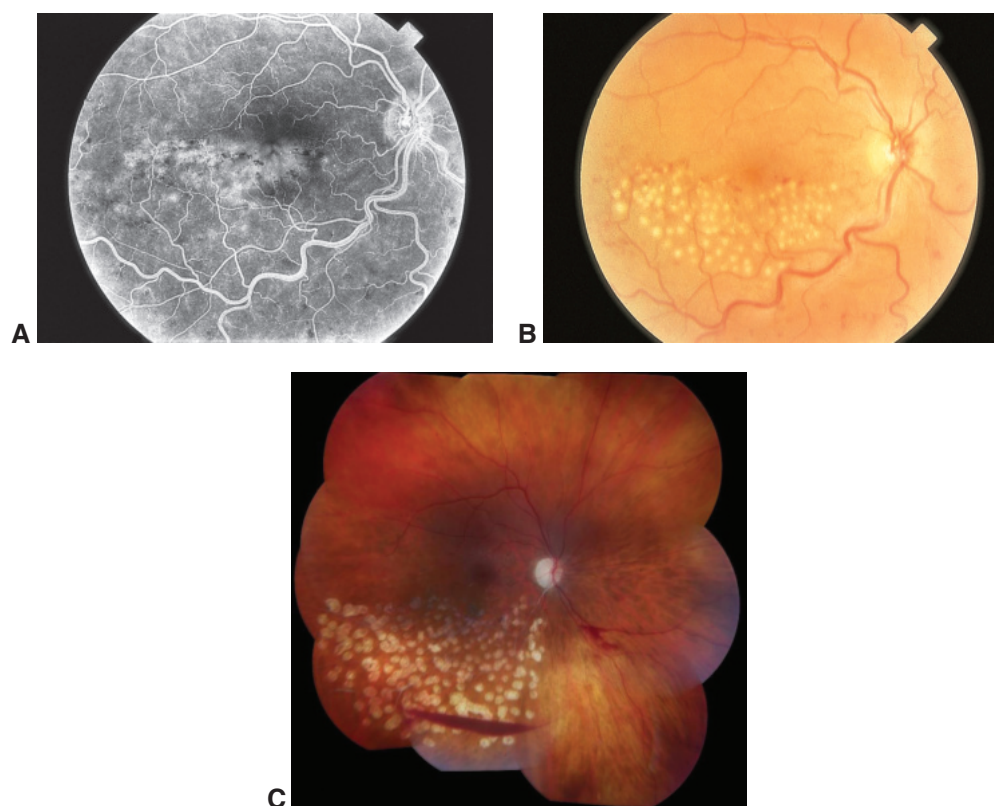


Figure 6-10 Two examples of laser photocoagulation for BRVO. **A**, Grid treatment for macular edema. The area of treatment corresponds to the area of leakage, as demonstrated by hyperfluorescence on fluorescein angiography. **B**, The laser spots spare the fovea. **C**, Peripheral scatter laser to an area of inferotemporal retinal ischemia (note the sclerotic vessels) as treatment for neovascularization of the disc and vitreous hemorrhage. Residual preretinal hemorrhage is seen inferiorly, but the neovascularization has regressed. (Parts A and B courtesy of Gary C. Brown, MD; part C courtesy of Franco M. Recchia, MD.)

retinal, ONH, or iris neovascularization (see Fig 6-9); it also reduced the risk of vitreous hemorrhage from 60% to 30%. Although the BVOS found that patients with large areas of nonperfusion were at significant risk of developing neovascularization, the study concluded that ischemia alone was not an indication for treatment, provided that follow-up could be maintained.

Neovascularization of the iris occurs in approximately 2% of eyes with BRVO. In these cases, scatter laser photocoagulation in the distribution of the occluded vein should be considered to prevent the development of neovascular glaucoma.

PARS PLANA VITRECTOMY Vitrectomy may be indicated for eyes that develop vitreous hemorrhage or retinal detachment (also see Chapters 16 and 19).

Central Retinal Vein Occlusion

In CRVO, vision loss is most commonly sudden and painless, with presenting visual acuity ranging from 20/20 to hand motions. Less commonly, patients may experience premonitory symptoms of transient obscuration of vision before overt retinal manifestations appear. Histologic studies suggest that most forms of CRVO arise from thrombosis of the central retinal vein at or posterior to the level of the lamina cribrosa. When thrombosis is more anterior, fewer collaterals are available, resulting in greater ischemia.

The CVOS was a multicenter prospective clinical study conducted in the early 1990s that elucidated the natural history of CRVO, the incidence of neovascular complications, and the utility of laser photocoagulation, as well as developing precise definitions of ischemic and nonischemic CRVO.

Nonischemic (perfused) CRVO is characterized by visual acuity of 20/200 or better, minimal or no afferent pupillary defect, and mild visual field changes. Ophthalmoscopy shows some dilation and tortuosity of all branches of the central retinal vein as well as dot- and flame-shaped hemorrhages in all quadrants of the retina (Fig 6-11). Macular edema and slight ONH swelling may be present (Activity 6-1). Fluorescein angiography usually demonstrates prolongation of the retinal circulation time with breakdown of capillary permeability but minimal areas of nonperfusion (<10 disc areas on standardized 7-field photography). Anterior segment neovascularization is rare in mild CRVO.



ACTIVITY 6-1 OCT Activity: Macular OCT of an eye with CRVO, severe CME, and foveal detachment.
Courtesy of Colin A. McCannel, MD.



Ischemic (nonperfused) CRVO is defined as at least 10 disc areas of retinal capillary nonperfusion on fluorescein angiography. Ischemic cases are usually associated with poor vision (worse than 20/200), an afferent pupillary defect, dense central scotoma, and peripheral visual field constriction. Marked venous dilation, more extensive hemorrhage, retinal edema, and variable numbers of cotton-wool spots are more frequent than in nonischemic CRVO (Fig 6-12). Fluorescein angiography demonstrates prolonged arteriovenous circulation time and widespread capillary nonperfusion. Because of inner retinal dysfunction due to ischemia, the b-wave to a-wave amplitude ratio is decreased in electroretinographic bright-flash dark-adapted testing. The CVOS showed that the natural history of ischemic CRVO is generally poor; only approximately 10% of eyes achieve vision better than

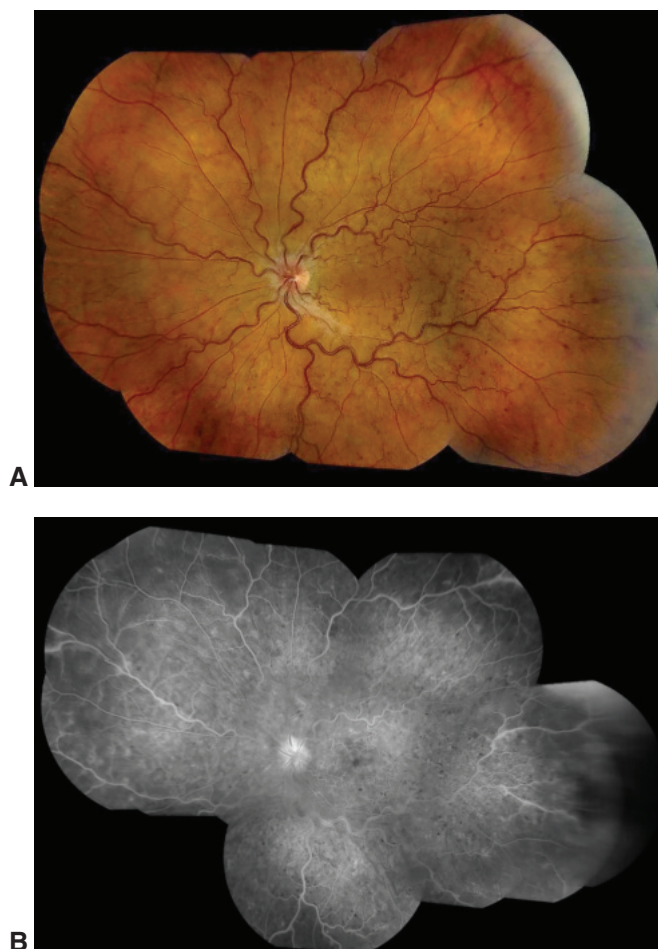


Figure 6-11 Perfused CRVO. A 38-year-old woman with a history of migraines presented with VA of 20/80. **A**, Montage of color fundus images shows prominent dilation and tortuosity of veins in all 4 retinal quadrants. **B**, Corresponding fluorescein angiography shows peripheral capillary nonperfusion, but this eye would be classified as perfused, according to Central Vein Occlusion Study criteria, on the basis of the intact perfusion in the postequatorial retina. (Courtesy of Franco M. Recchia, MD.)

20/400. With anti-VEGF treatment, however, the prognosis may now be somewhat better in all but the most severe cases.

Iris neovascularization in CRVO

Among eyes with severely ischemic CRVO, the incidence of anterior segment neovascularization (of the iris or angle) approaches 60%. Neovascularization of the iris (NVI) can occur as early as 2 weeks and as late as 6 months after the onset of symptoms, with the peak at approximately 2 months after presentation. The CVOS found that poor visual acuity is the risk factor most predictive of NVI. Other risk factors include large areas of retinal capillary nonperfusion and intraretinal blood. If NVI is not detected and treated promptly, neovascular glaucoma may develop.

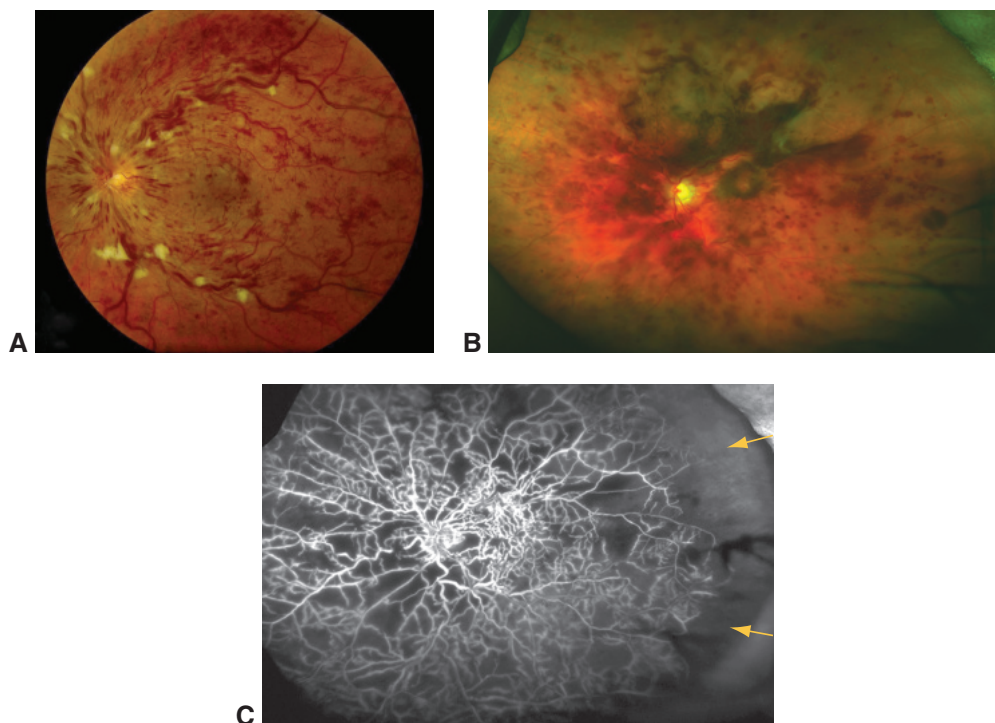


Figure 6-12 Two examples of a nonperfused (ischemic) CRVO. **A**, Fundus photograph of a nonperfused CRVO; patient's VA is counting fingers. There are diffuse retinal hemorrhages, numerous cotton-wool spots, and blurring of optic nerve head margins. Poor VA at presentation along with these clinical findings is consistent with severe nonperfusion. **B**, Ultra-wide-field fundus photograph of severe ischemic CRVO in an eye with VA of hand motions. The veins are dilated, and extensive retinal hemorrhages are present. **C**, Ultra-wide-field fluorescein angiography image corresponding to **B** taken 40 seconds after injection reveals widespread retinal capillary nonperfusion (arrows). (Part A courtesy of Franco M. Recchia, MD; parts B and C courtesy of Colin A. McCannel, MD.)

Baseline and early natural history report. The Central Vein Occlusion Study. *Arch Ophthalmol.* 1993;111(8):1087–1095.

Klein R, Moss SE, Meuer SM, Klein BE. The 15-year cumulative incidence of retinal vein occlusion: the Beaver Dam Eye Study. *Arch Ophthalmol.* 2008;126(4):513–518.

Differential diagnosis of CRVO

Hyperviscosity retinopathy can mimic the appearance of CRVO. However, the retinal findings in hyperviscosity retinopathy are generally bilateral. Blood hyperviscosity is usually related to dysproteinemia (eg, associated with Waldenström macroglobulinemia or multiple myeloma) or blood dyscrasias (eg, polycythemia vera). In many cases, the hyperviscosity can be reversed by treating the underlying condition. Diagnostic testing may include complete blood count, serum protein electrophoresis, and measurement of whole-blood viscosity. *Ocular ischemic syndrome* (discussed later in the chapter) can also resemble CRVO, but hemorrhages in this syndrome are limited to the deeper retinal layers, and vascular tortuosity is absent.

American Academy of Ophthalmology Retina/Vitreous Panel. Preferred Practice Pattern Guidelines. *Retinal Vein Occlusions*. American Academy of Ophthalmology; 2019. www.aao.org/preferred-practice-pattern/retinal-vein-occlusions-ppp

Natural history and clinical management of central retinal vein occlusion. The Central Vein Occlusion Study Group. *Arch Ophthalmol*. 1997;115(4):486–491. Published correction appears in *Arch Ophthalmol*. 1997;115(10):1275.

Evaluation and management of CRVO

Visual acuity, visual field, and relative afferent defect testing and dilated ophthalmoscopy can be useful in determining whether the vein occlusion is nonischemic or ischemic. Fluorescein angiography and OCT provide valuable additional data. It is important to perform gonioscopy at presentation and during follow-up to check for angle neovascularization. Eyes that initially appear perfused sometimes develop progressive ischemia. In the CVOS, 16% and 34% of CRVOs initially classified as nonischemic converted to ischemic by 4 months and 36 months, respectively. Patients presenting with CRVO may also have elevated IOP or frank open-angle glaucoma, either in the affected eye alone or in both eyes.

Follow-up In the absence of treatment, patients with CRVO should be monitored monthly during the first 6 months for evidence of progression and development of macular edema, anterior segment neovascularization, or neovascular glaucoma. Patients treated with intravitreal anti-VEGF agents may need to be observed even longer after discontinuation of treatment.

Stem MS, Talwar N, Comer GM, Stein JD. A longitudinal analysis of risk factors associated with central retinal vein occlusion. *Ophthalmology*. 2013;120(2):362–370.

Treatment of CRVO

Pharmacologic management Pharmacologic management is currently the mainstay of CRVO management. See the earlier section “Pharmacologic management of RVO” for more detail.

Yeh S, Kim SJ, Ho AC, et al. Therapies for macular edema associated with central retinal vein occlusion: a report by the American Academy of Ophthalmology. *Ophthalmology*. 2015;122(4):769–778.

Surgical management of CRVO Laser therapy does not appear to provide benefit in CRVO, although other surgical techniques may be useful in select cases.

MACULAR LASER SURGERY The CVOS showed that grid laser photocoagulation in CRVO with macular edema does not improve visual acuity, and therefore it is no longer recommended.

PANRETINAL PHOTOCOAGULATION The CVOS found that immediate prophylactic panretinal photocoagulation (PRP) did not result in a statistically significant decrease in the incidence of NVI; in fact, NVI developed in 20% of participants who received the prophylactic PRP. Although the CVOS investigators recommended delaying laser therapy until at least 2 clock-hours of NVI are present, PRP is often performed at the first sign of NVI.

A randomized clinical trial of early panretinal photocoagulation for ischemic central vein occlusion. The Central Vein Occlusion Study Group N report. *Ophthalmology*. 1995;102(10):1434–1444.

PARS PLANA VITRECTOMY CRVOs complicated by vitreous hemorrhage may benefit from pars plana vitrectomy to improve vision or to accomplish retinal ablative treatment in the management of anterior segment neovascularization. If neovascular glaucoma is present, a glaucoma drainage implant may be placed concurrently.

OTHER SURGICAL APPROACHES Several surgical approaches have been investigated over the last 3 decades. These approaches include creation of a peripheral laser anastomosis between a retinal vein and the choroidal circulation, radial relaxing incision of the optic nerve scleral ring to decompress the central retinal vein, and retinal vein cannulation with infusion of tissue plasminogen activator. These approaches are not recommended because of their lack of efficacy and/or high complication rates.

Ocular Ischemic Syndrome and Retinopathy of Carotid Occlusive Disease

Ocular ischemic syndrome (OIS) comprises the ocular symptoms and signs attributable to chronic severe ocular hypoperfusion caused by ipsilateral carotid obstruction or ophthalmic artery obstruction.

Symptoms and Signs of OIS

Symptoms of OIS typically include gradual vision loss that develops over a period of weeks to months, aching pain that is localized to the orbital area of the affected eye and is worse in upright position, and prolonged recovery of vision after exposure to bright light. Anterior segment signs include NVI in two-thirds of eyes and an anterior chamber cellular response in about one-fifth of eyes (Fig 6-13). Although iris and angle neovascularization are common,

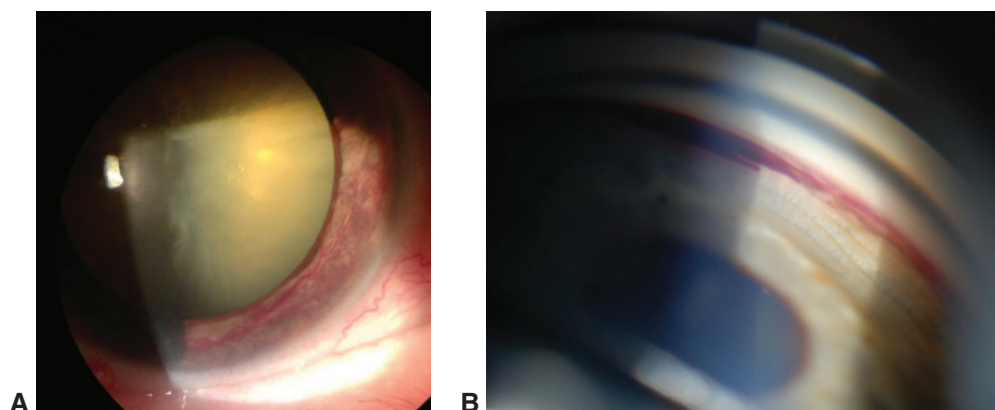


Figure 6-13 Anterior segment neovascularization in ocular ischemic syndrome (OIS). **A**, Slit-lamp photograph of diffuse neovascularization of the iris. **B**, Gonio photograph shows neovascularization of the anterior chamber angle (right part of image) as well as fresh blood in the angle and on the iris (left part of image). (Images originally published on the Retina Image Bank website. © American Society of Retina Specialists. Part A: Pauline Merrill, Illinois Retina Associates, NVI; 2012, image number 2096. Part B: Jason S. Calhoun, Dept. of Ophthalmology, Mayo Clinic Jacksonville; 2013, image number 7327.)

only one-half of eyes with this condition show an increase in IOP; low or normal IOP in the other eyes is most likely the result of impaired aqueous production.

OIS can cause a retinopathy similar in appearance to that of a partial occlusion of the central retinal vein; thus, it was originally called *venous stasis retinopathy*. Typical retinal findings include narrowed arteries; dilated but not tortuous veins; hemorrhages; microaneurysms; and neovascularization of the ONH, retina, or both (Fig 6-14). A helpful method for differentiating between OIS and CRVO is to measure the retinal artery pressure with an ophthalmodynamometer. An eye with CRVO will have normal artery pressure, whereas one with carotid occlusive disease will have low artery pressure, and the artery will collapse easily.

Fluorescein angiography reveals delayed choroidal filling in 60% of eyes, prolonged arteriovenous transit time in 95% of eyes, and prominent vascular staining (particularly of the arteries) in 85% of eyes. Electroretinography (ERG) demonstrates global decreased amplitude, reflecting damage caused by impaired blood supply to both the photoreceptors and the inner retina. An electronegative ERG occurs when the blood supply to the inner retina is compromised (as in CRVO or central retinal artery occlusion) while the supply to the photoreceptors is preserved. In cases of suspected OIS, urgent referral for carotid evaluation is needed.

Etiology and Course of OIS

The most common etiology of OIS is atherosclerosis. Typically, a 90% or greater ipsilateral obstruction is necessary to cause OIS. Other causes include Eisenmenger syndrome, carotid artery dissection, giant cell arteritis, and other inflammatory conditions. Most patients are older than 55 years. Approximately 20% of cases involve both eyes.

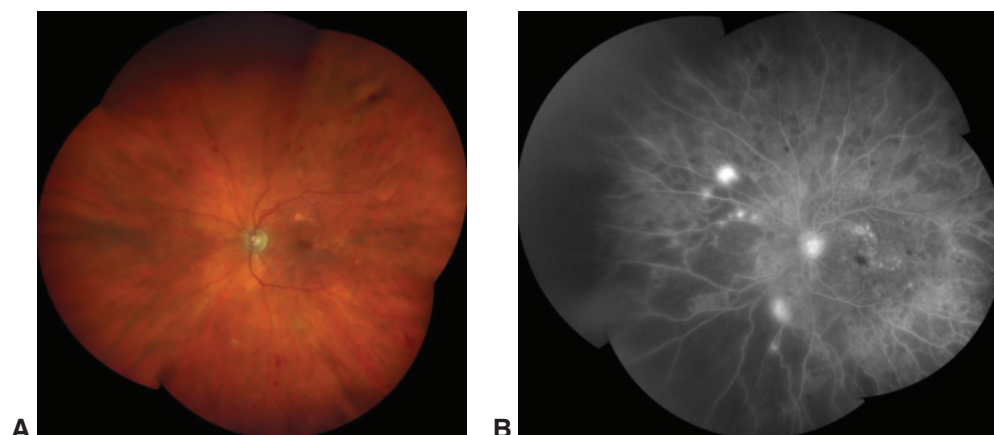


Figure 6-14 Retinal findings in OIS. An 80-year-old man with a history of coronary artery disease and diabetes mellitus presented with 2 weeks of aching pain and photosensitivity in his left eye. **A**, Fundus photograph shows dilated retinal veins without tortuosity and scattered blot (round, deep) retinal hemorrhages in the equatorial area. Retinal scars from previous focal macular laser treatment for diabetic macular edema are also present. **B**, Fluorescein angiography revealed delayed arterial perfusion (not shown), hypofluorescence consistent with diffuse capillary nonperfusion, and focal hyperfluorescence and leakage consistent with retinal neovascularization. (Courtesy of Franco M. Recchia, MD.)

When rubeosis iridis is present in OIS, visual acuity will decline to 20/200 or worse in more than 90% of cases within 1 year after diagnosis. Approximately one-half of patients with OIS also have ischemic cardiovascular disease; the stroke rate in these patients is higher than that of the general population, and the 5-year mortality is approximately 40%, mostly resulting from complications of cardiovascular disease.

Treatment of OIS

The most definitive treatment for OIS appears to be carotid artery stenting and endarterectomy. Unfortunately, these procedures are ineffective when there is 100% obstruction. In eyes with iris neovascularization and low or normal IOP as a result of impaired ciliary body perfusion and decreased aqueous formation, carotid reperfusion can lead to increased aqueous formation and a severe rise in IOP. Full-scatter PRP results in regression of anterior segment neovascularization in approximately two-thirds of cases. Anti-VEGF therapy has also been shown to cause regression of anterior segment neovascularization in patients with OIS.

Brown GC, Sharma S. Ocular ischemic syndrome. In: Schachat AP, Wilkinson CP, Hinton DR, Sadda SR, Wiedemann P, eds. *Ryan's Retina*. 6th ed. Elsevier/Saunders; 2018:chap 62.

Arterial Occlusive Disease

The blood supply to the inner layers of the retina is derived entirely from the central retinal artery unless a cilioretinal artery is present. Retinal ischemia results from disease processes that affect the vessels anywhere from the common carotid artery to the intraretinal arterioles. The signs and symptoms of arterial obstruction depend on the vessel involved: occlusion of a peripheral arteriole may be asymptomatic, whereas an ophthalmic artery occlusion can cause total blindness.

Cotton-Wool Spots

Acute obstruction in the distribution of the radial peripapillary capillary net leads to the formation of an NFL infarct, or *cotton-wool spot*, which causes impaired axoplasmic transport in the NFL (Fig 6-15). These inner retinal ischemic spots are superficial, white, and typically one-fourth disc area or less in size. They usually fade in 5–7 weeks, although spots present in association with diabetic retinopathy often remain longer. A subtle retinal depression caused by inner retinal ischemic atrophy may develop in an area of prior ischemia. The effect on visual function, including visual acuity loss and visual field defects, is related to the size and location of the occluded area.

The most common cause of cotton-wool spots is diabetic retinopathy (discussed in Chapter 5). Other causes, which should be investigated, are listed in Table 6-2. If even 1 cotton-wool spot is discovered in the fundus of an otherwise apparently healthy eye, the clinician should initiate a workup for the most likely underlying etiologies.

Brown GC, Brown MM, Hiller T, Fischer D, Benson WE, Magargal LE. Cotton-wool spots. *Retina*. 1985;5(4):206–214.

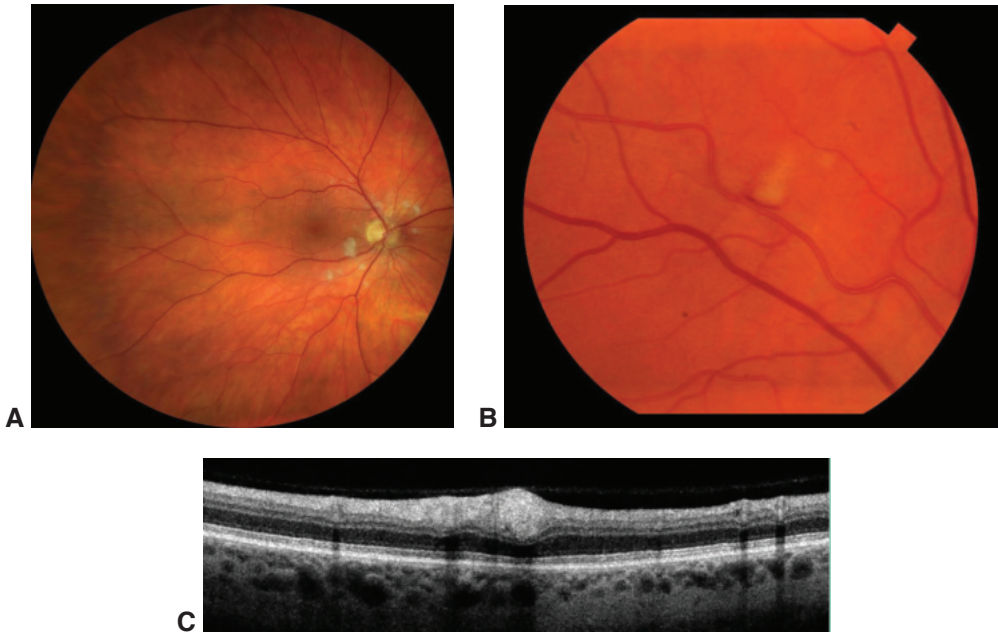


Figure 6-15 Examples of cotton-wool spots. **A**, Wide-field color fundus photograph of the right eye shows multiple fluffy, ill-defined white parapapillary lesions consistent with cotton-wool spots. Their superficial location is demonstrated by the obscuration of retinal vessels by some of the larger lesions. **B**, Fundus photograph shows an isolated cotton-wool spot just outside the superotemporal macula of the right eye. **C**, OCT through the lesion in **B** shows hyperreflectivity in the inner retina. (Courtesy of Franco M. Recchia, MD.)

Table 6-2 Causes of Cotton-Wool Spots	
	Diabetic retinopathy
	Systemic arterial hypertension
	HIV-associated retinopathy
	Anemia (severe)
	Radiation retinopathy
	Sickle cell retinopathy
	Cardiac embolic disease
	Carotid artery obstructive disease
	Vasculitis
	Collagen vascular disease
	Leukemia
	Putrscher and Putrscher-like retinopathy
	Giant cell arteritis

Branch Retinal Artery Occlusion

Although an acute branch retinal artery occlusion (BRAO) may be subtle and unapparent on initial ophthalmoscopic examination, within hours to days it can lead to edematous opacification caused by infarction of the inner retina in the distribution of the affected vessel (Fig 6-16). In time, the occluded vessel recanalizes, perfusion returns, and the

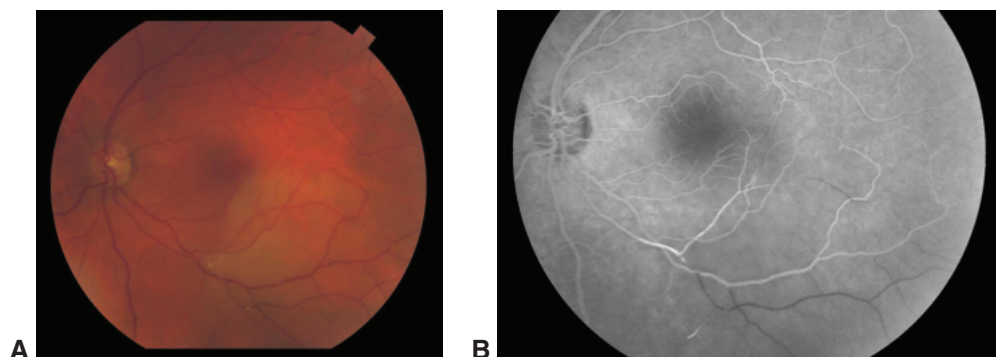


Figure 6-16 Branch retinal artery occlusion (BRAO). **A**, Fundus photograph shows a BRAO associated with 2 intra-arterial emboli: 1 at the first bifurcation of the inferotemporal arteriole, and 1 at its second bifurcation. Retinal whitening distal to these sites of occlusion signals acute retinal edema in response to retinal ischemia. **B**, In the corresponding fluorescein angiogram, blood flow is absent in the arterioles distal to the emboli, and the retina appears darker because of lack of capillary blood flow. (Courtesy of Franco M. Recchia, MD.)

edema resolves; however, a permanent visual field defect remains. A retinal arterial occlusion that occurs outside the posterior pole may be clinically asymptomatic.

Occlusion at any point along the arterial tree can be caused by embolization of the affected vessel. There are 3 main types of emboli:

- cholesterol emboli (so-called *Hollenhorst plaques*) arising in the carotid arteries (see Fig 6-16)
- platelet-fibrin emboli associated with large-vessel arteriosclerosis (Fig 6-17)
- calcific emboli arising from diseased cardiac valves

In rare cases, emboli might be caused by cardiac myxoma, long-bone fractures (*fat emboli*), infective endocarditis (*septic emboli*), and intravenous drug use (*talc emboli*). Although the occurrence is rare, migraine can cause ocular arterial occlusions in patients younger than 40 years.

Conditions other than embolic events, including infectious, inflammatory, and thrombophilic causes, can lead to retinal artery occlusion, especially in younger patients with no cardiovascular comorbidity (Table 6-3). Diagnosis can be facilitated by a detailed history and review of systems and complete ophthalmologic examination.

Initial management is directed toward determining the underlying systemic disorder. Patients with retinal arterial occlusion should be referred *urgently* to an emergency department or stroke center for evaluation of cerebrovascular disease and cardiac valvular disease. No specific ocular therapy has been found to be consistently effective in improving visual acuity.

Hayreh SS, Podhajsky PA, Zimmerman MB. Branch retinal artery occlusion: natural history of visual outcome. *Ophthalmology*. 2009;116(6):1188–1194.e944.

Wang JJ, Cugati S, Knudtson MD, et al. Retinal arteriolar emboli and long-term mortality: pooled data analysis from two older populations. *Stroke*. 2006;37(7):1833–1836.

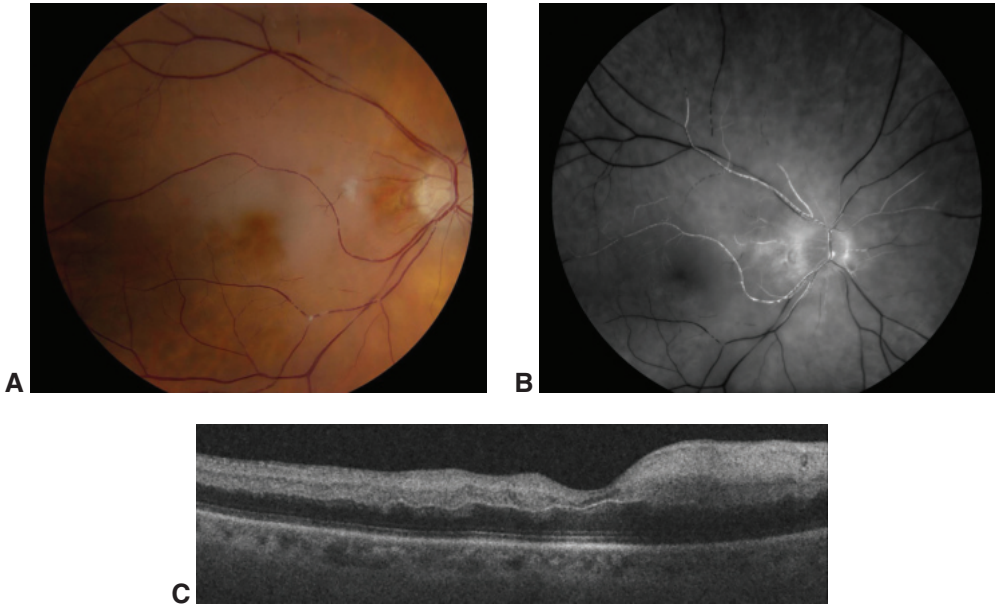


Figure 6-17 Central retinal artery occlusion (CRAO) caused by multiple emboli. **A**, The right eye shows diffuse retinal whitening, a cotton-wool spot, arteriolar attenuation, and multiple intra-arterial refractile lesions in both superior and inferior arterial distributions. **B**, Fluorescein angiography shows markedly delayed arterial filling and “boxcarring” of blood flow within retinal arterioles. Subsequent computed tomography revealed an ulcerative atherosclerotic plaque in the right internal carotid artery. **C**, Simultaneous OCT shows inner retinal hyperreflectivity due to retinal edema with corresponding hyporeflectivity of the outer retina. (Courtesy of Franco M. Recchia, MD.)

Table 6-3 Nonembolic Conditions Associated With Retinal Artery Occlusion

Infectious

- Acute retinal necrosis
- Bartonellosis (cat-scratch disease)
- Endocarditis
- Endogenous endophthalmitis
- HIV
- Ocular or neurosyphilis
- Ocular toxoplasmosis
- Orbital cellulitis/subperiosteal abscess
- Systemic COVID-19 disease

Inflammatory

- Behçet syndrome
- Churg-Strauss syndrome (eosinophilic granulomatosis)
- Crohn disease
- Granulomatosis with polyangiitis (formerly called *Wegener’s granulomatosis*)
- Neurosarcoidosis
- Susac syndrome
- Systemic lupus erythematosus

Thrombophilic

- Antiphospholipid syndrome
- Genetic polymorphisms or deficiencies in various clotting factors
- Lupus anticoagulant antibodies
- Pregnancy

Central Retinal Artery Occlusion

Sudden, complete, and painless loss of vision in 1 eye is characteristic of central retinal artery occlusion (CRAO). Three-fourths of patients present with visual acuity in the range of counting fingers. The retina becomes opaque and edematous, particularly in the posterior pole, where the nerve fiber and ganglion cell layers are thickest (Fig 6-18; see also Fig 6-17). The orange reflex from the intact choroidal vasculature beneath the foveola thus stands out in contrast to the surrounding opaque neural retina, producing a *cherry-red spot*. Even before the cherry-red spot appears, OCT imaging reveals a normal macular profile with diffuse hyperreflectivity and loss of internal layer definition (Fig 6-19, Activity 6-2; see also Fig 6-18). A cilioretinal artery may preserve some degree of macular vision (see Chapter 1, Fig 1-8).



ACTIVITY 6-2 OCT Activity: SD-OCT scan of an eye with CRAO and cilioretinal artery sparing.
Courtesy of Colin A. McCannel, MD.

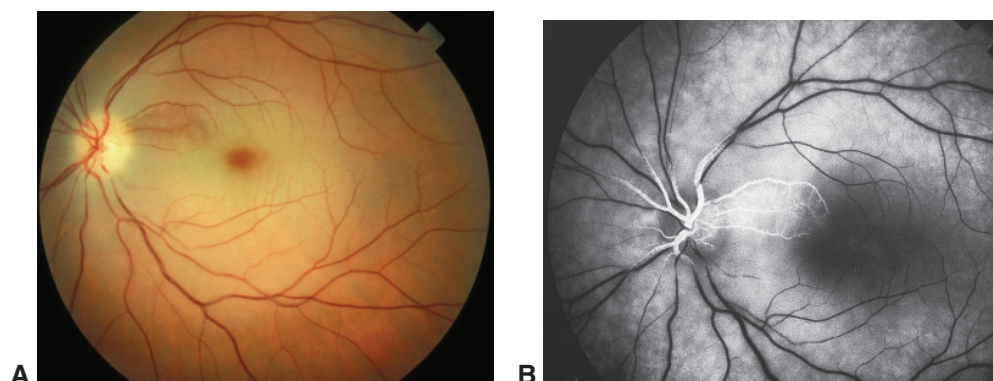


Figure 6-18 CRAO. **A**, Fundus photograph shows superficial macular opacification and a cherry-red spot in the foveola. **B**, Angiography image reveals preservation of a sector of superonasal macula related to cilioretinal vessels, which are perfused in this image. The patient had hand motions VA. (Courtesy of Hermann D. Schubert, MD.)

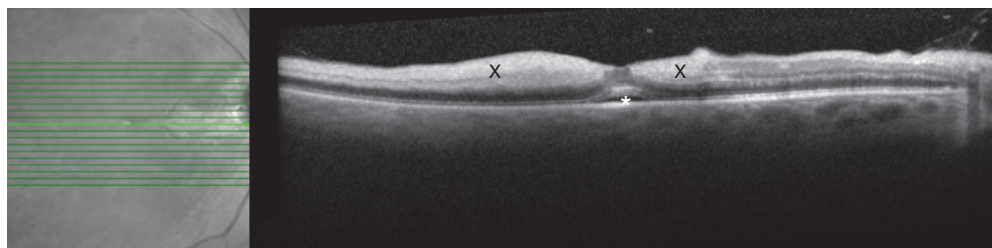


Figure 6-19 SD-OCT scan of a case of CRAO (similar to that seen in Figure 6-18) with cilioretinal artery sparing shows hyperreflectivity in the area of clinical opacification of the inner two-thirds of the retina in the affected areas (X). All retinal layers are identifiable in the area of retina perfused by the cilioretinal artery, adjacent to the optic nerve head. The foveal retina is spared from opacification, resulting in the appearance of a cherry-red spot on examination. Subfoveal fluid (asterisk) is variably present in these cases. (Courtesy of Colin A. McCannel, MD.)

With time, the central retinal artery reopens or recanalizes, and the retinal edema clears; however, the effect on visual acuity is usually permanent because the inner retina has been infarcted. In one study, 66% of eyes had final visual acuity worse than 20/400, and 18% of eyes had 20/40 or better. Most eyes in which visual acuity recovers to 20/40 or better have a patent cilioretinal artery. Vaso-occlusive vision loss to the level of no light perception is usually caused by choroidal vascular insufficiency from partial or complete ophthalmic artery occlusion or occlusions of the parent ciliary arteries in conjunction with occlusion of the central retinal artery (Fig 6-20). Studies in nonhuman primates have suggested that irreversible damage to the sensory retina begins after 90 minutes of complete CRAO. Nevertheless, clinical return of vision can occur in some instances even if the obstruction has persisted for many hours.

CRAO is most often caused by emboli originating anywhere between the heart and the ophthalmic artery or by atherosclerosis-related thrombosis occurring at the level of the lamina cribrosa. Emboli within the carotid distribution can cause transient ischemic attacks, amaurosis fugax, or both. Bright cholesterol emboli (Hollenhorst plaques), typically located at retinal artery bifurcations, suggest a carotid atheromatous origin and may be an indication for endarterectomy if accompanied by relevant symptoms and findings. Systemic etiologic considerations, such as those listed earlier in this chapter for BRAO, are important and require evaluation.

Giant cell arteritis (GCA) accounts for approximately 1%–2% of CRAO cases. When an embolus is not readily visible in an eye with CRAO, a thorough evaluation for GCA should be considered. The risk of GCA increases with advancing age, starting at 55 years. The erythrocyte sedimentation rate (ESR), C-reactive protein level, and fibrinogen levels, all of which are

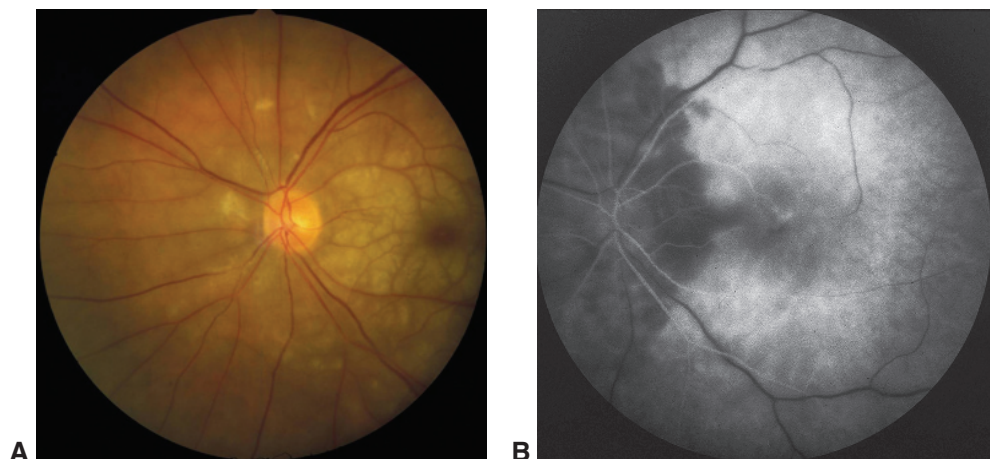


Figure 6-20 Central retinal and parent short ciliary artery occlusion. **A**, Fundus photograph of acute central retinal and short ciliary artery obstruction. Severe retinal opacification is present. The patient's VA was no light perception. **B**, Fluorescein angiography image taken 3 minutes after injection reveals hypofluorescence of the retinal vessels, the nasal choroid, and the optic nerve head, corresponding to an occlusion of the central retinal artery and nasal parent ciliary artery. Occlusion of the latter results in ischemia in the distribution of the short posterior ciliary arteries, with a vertical watershed of choroidal perfusion. (Courtesy of Hermann D. Schubert, MD.)

markers of inflammation, are usually elevated. A complete blood count may detect an elevated platelet count, which is suggestive of GCA; the blood count also aids in the interpretation of the ESR. If GCA is suspected, high-dose systemic corticosteroid therapy should be instituted promptly because the second eye can become involved by ischemia within hours to days after the first. In addition, a temporal artery biopsy should be performed within 14 days to confirm the diagnosis and determine the need for prolonged corticosteroid treatment. See BCSC Section 5, *Neuro-Ophthalmology*, for further discussion of GCA.

Ahn SJ, Woo SJ, Park KH, Jung C, Hong JH, Han MK. Retinal and choroidal changes and visual outcome in central retinal artery occlusion: an optical coherence tomography study. *Am J Ophthalmol*. 2015;159(4):667–676.

Atkins EJ, Bruce BB, Newman NJ, Bioussé V. Translation of clinical studies to clinical practice: survey on the treatment of central retinal artery occlusion. *Am J Ophthalmol*. 2009;148(1):172–173.

Callizo J, Feltgen N, Pantenburg S, et al; European Assessment Group for Lysis in the Eye. Cardiovascular risk factors in central retinal artery occlusion: results of a prospective and standardized medical examination. *Ophthalmology*. 2015;122(9):1881–1888.

Falkenberry SM, Ip MS, Blodi BA, Gunther JB. Optical coherence tomography findings in central retinal artery occlusion. *Ophthalmic Surg Lasers Imaging*. 2006;37(6):502–505.

Park SJ, Choi NK, Yang BR, et al. Risk and risk periods for stroke and acute myocardial infarction in patients with central retinal artery occlusion. *Ophthalmology*. 2015;122(11):2336–2343.e2.

Management of CRAO

The most important step in initial management is identification of the underlying systemic etiologic factors and an *urgent* referral to an emergency department for a stroke workup. In 2011 and 2013, the National Stroke Association and the American Heart Association included “retinal cell death” in their consensus statement defining central nervous system infarction (stroke). The leading cause of death in patients with retinal arterial obstruction is cardiovascular disease, with an elevated risk of myocardial infarction within the first 7 days after onset of the obstruction. Studies have reported that as many as 78% of patients may have undiagnosed risk factors.

Patients should preferably undergo neuroimaging evaluation within 24 hours of symptom onset and be evaluated at an emergency department associated with a stroke center. Carotid ultrasonography is useful as a first-line screening test, but it depends on the availability of an experienced ultrasonographer and can image only the extracranial portion of the carotid tree. Computed tomography angiography or magnetic resonance angiography is therefore recommended for a more definitive imaging study.

In addition to a stroke workup, patients with isolated acute retinal ischemia should undergo brain imaging, ideally brain magnetic resonance imaging with diffusion-weighted imaging, analogous to the management of patients with acute cerebral ischemia. Multiple small cerebral infarctions are seen on diffusion-weighted magnetic resonance imaging of the brain in up to 31% of patients with acute RAO. The presence of these silent (asymptomatic) cerebral infarctions is associated with a higher chance of identifying an embolic cause for the acute retinal ischemia (Fig 6-21).

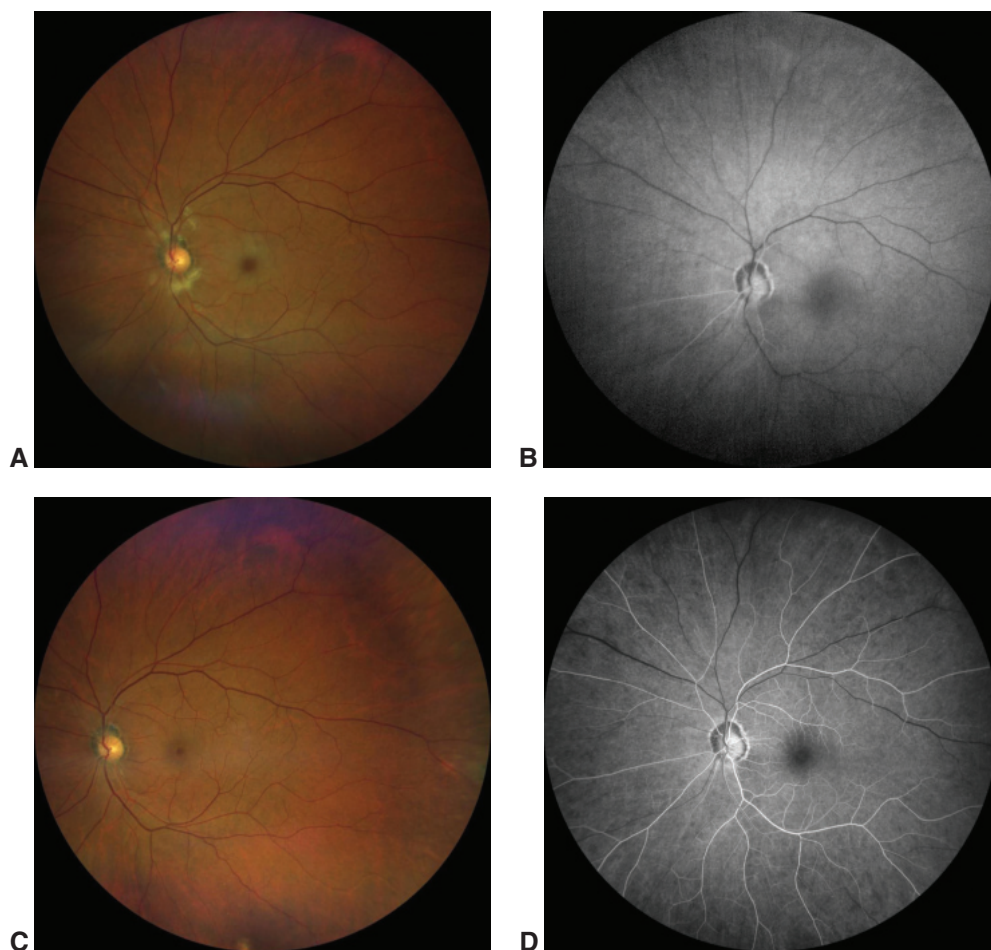


Figure 6-21 Acute retinal ischemia. This 64-year-old man with diabetes, hypertension, hyperlipidemia, and coronary artery disease presented with a 3-day history of a central blind spot in his left eye and VA of counting fingers. **A**, Fundus photograph shows parapapillary cotton-wool spots, macular whitening, and a cherry-red spot. **B**, Fluorescein angiography shows arterial filling beginning at 1 minute 19 seconds after dye injection. Stroke workup was performed immediately and revealed 90% carotid occlusion, which was treated with carotid endarterectomy (CEA). Three weeks after CEA, VA had improved to 20/40. **C**, There was resolution of retinal whitening and improvement in retinal perfusion. **D**, Dye appearance at 33 seconds after infusion demonstrates the improved perfusion. (Courtesy of Franco M. Recchia, MD.)

At present, there is no proven treatment for symptomatic RAO. Case reports and uncontrolled studies have suggested the utility of digital massage of the affected eye, anterior chamber paracentesis, vasodilation, breathing into a paper bag, carbogen therapy (a mixture of 95% oxygen and 5% carbon dioxide), topical IOP-lowering medications, hyperbaric oxygen, and transvitreal Nd:YAG embolysis. However, there are no level I data to support any specific therapy. Treatment with antifibrinolytic agents (typically, tissue plasminogen activator [tPA])

can be considered in select circumstances. In a recent white paper based on meta-analysis and literature review, the American Heart Association recommends the following:

- intravenous tPA for patients without systemic contraindication and who are evaluated within 4.5 hours of onset of visual symptoms; or
- intra-arterial tPA, through superselective catheterization of the ipsilateral ophthalmic artery, for patients who are not candidates for intravenous therapy and who are evaluated within 6 hours of onset of visual symptoms.

NVI develops in approximately 18% of eyes within 1–12 weeks after acute CRAO (mean interval, approximately 4 weeks). Treatment of NVI is highly effective in avoiding neovascular glaucoma. Full-scatter PRP results in regression of anterior segment neovascularization in approximately two-thirds of cases. Anti-VEGF therapy, either alone or in conjunction with PRP, is also effective. The current American Academy of Ophthalmology recommendations for acute management of RAO can be found at www.aao.org/preferred-practice-pattern/retinal-ophthalmic-artery-occlusions-ppp.

Patients in whom RAO is diagnosed incidentally as a chronic or remote event should still be evaluated for cerebrovascular disease and for modifiable vascular risk factors. However, unlike the procedures for acute RAO, such evaluation likely does not need to be immediate.

Biousse V, Nahab F, Newman NJ. Management of acute retinal ischemia: follow the guidelines! *Ophthalmology*. 2018;125(10):1597–1607.

Hayreh SS, Podhajsky PA, Zimmerman MB. Retinal artery occlusion: associated systemic and ophthalmic abnormalities. *Ophthalmology*. 2009;116(10):1928–1936.

Mac Grory B, Schrag M, Biousse V, et al. Management of central retinal artery occlusion: a scientific statement from the American Heart Association. *Stroke*. 2021;52(6):e282–e294. Published correction appears in *Stroke*. 2021;52(6):e309.

Cilioretinal Artery Occlusion

A distinct clinical entity is the occlusion of the cilioretinal artery, which arises from the short posterior ciliary vessels rather than the central retinal artery. These vessels, which are present in approximately 18%–32% of eyes, usually contribute to some portion of the macular circulation. Most commonly, their occlusion occurs in patients with a CRVO; it is postulated that the increased hydrostatic pressure associated with CRVO can reduce blood flow in the cilioretinal artery to the point of stagnation (Fig 6-22). When cilioretinal artery occlusion occurs in isolation, GCA should be considered.

Hayreh SS, Fraterrigo L, Jonas J. Central retinal vein occlusion associated with cilioretinal artery occlusion. *Retina*. 2008;28(4):581–594.

Ophthalmic Artery Occlusion

Ophthalmic artery occlusion is very rare. Clinically, the disorder typically produces vision loss to the level of light perception or no light perception because simultaneous nonperfusion of the choroid and retina results in ischemia of all retinal layers. Both the inner retina

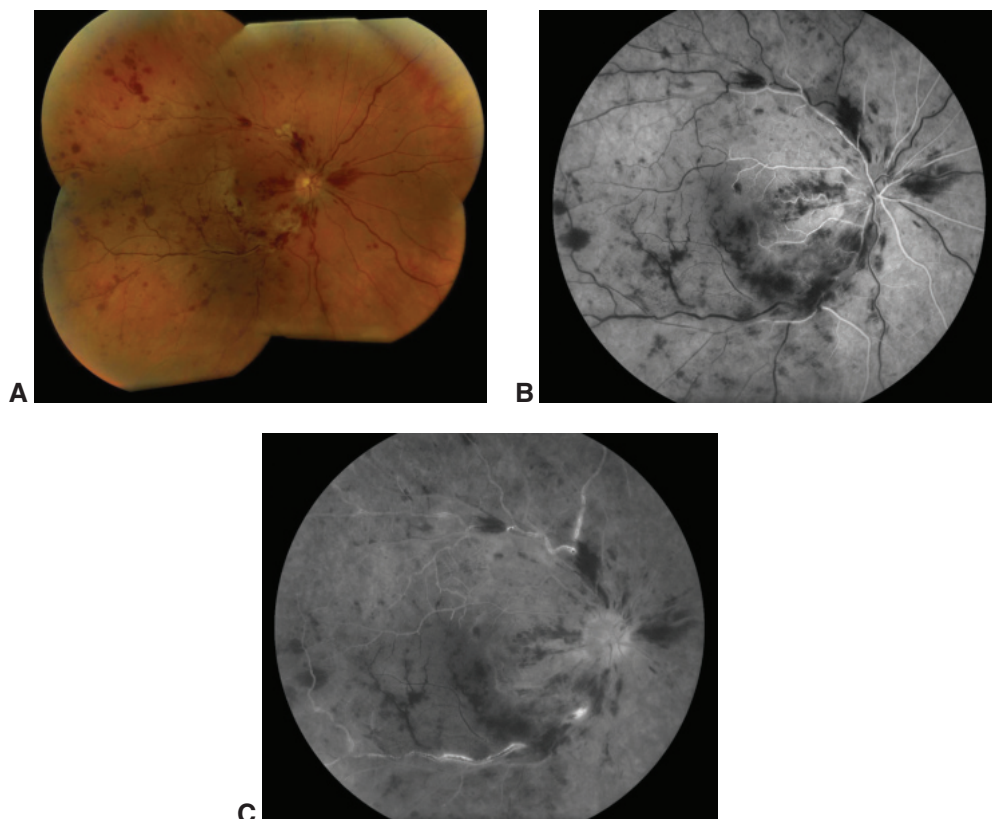


Figure 6-22 Cilioretinal artery occlusion. This 53-year-old woman presented with acutely decreased VA of 20/400 in her right eye. Medical history was notable for 2 first-trimester spontaneous abortions, and systemic workup ultimately revealed high levels of circulating anticardiolipin antibodies. **A**, Montage of color fundus photographs shows elements of both RVO (venous dilation and tortuosity, intraretinal hemorrhages at various layers, and cotton-wool spots) and cilioretinal artery occlusion (whitening in the temporal macula). **B**, Fluorescein angiography in the early arteriovenous phase shows multiple areas of arterial occlusion and peripheral nonperfusion. Note that in this case, the occlusions do *not* occur at arteriolar bifurcations, as would be expected in embolic occlusive disease. **C**, Angiogram taken in the late recirculation phase shows staining of the retinal veins, persistent arteriolar occlusion (notably, in branches of the inferotemporal arcade), and leakage consistent with macular edema. (Courtesy of Franco M. Recchia, MD.)

and outer retina become opacified from the infarction; thus, a cherry-red spot may not be present because there is a lack of contrast between the foveal and perifoveal retina.

Ophthalmic artery occlusion may be caused by internal carotid artery dissection, orbital mucormycosis, or embolization. A growing number of ophthalmic artery occlusions caused by cosmetic facial-filler injections, particularly into the periocular and brow area, have been reported as the popularity of such procedures has increased (Fig 6-23). In autopsy studies of patients who died during active GCA, up to 76% had some degree of vasculitis affecting the ophthalmic artery; clinically, however, ophthalmic artery occlusion is rare in GCA.



Figure 6-23 Ophthalmic artery occlusion. Fundus photograph montage of the left eye of a 44-year-old woman after ipsilateral injection of synthetic calcium hydroxyapatite gel into her left lateral lower eyelid for cosmetic purposes. Sudden loss of vision ensued to the level of no light perception. An ophthalmic artery occlusion occurred from presumed retrograde flow of the cosmetic filler into the ophthalmic artery by way of anastomotic arteries in the orbit bridging the internal and external carotid circulations. The white filler material is visible in the retinal circulation and choroidal blood vessels. (Courtesy of Kathryn Sun, MD, PhD; Thomas F. Essman, MD; and Brenda Schoenauer, CDOS.)

Paracentral Acute Middle Maculopathy

Paracentral acute middle maculopathy (PAMM) refers to macular lesions with changes in the inner nuclear layer on SD-OCT. The primary etiology in PAMM may be ischemia of the deep capillary system, which is responsible for blood supply to the middle retina.

The typical presentation is acute onset of diminished central visual acuity (although Snellen measurement of 20/20 is possible) or paracentral scotoma. Ophthalmoscopically, the lesions may appear only as subtle parafoveal gray-white spots or wedges. Compared with cotton-wool spots, the retinal whitening associated with PAMM lesions is more distinct, duller gray-white, less opaque, and deeper in the retina; also, it is not distributed along the NFL. However, these lesions are evanescent and may resolve before clinical examination takes place. In such cases, the characteristic hyperreflective bands on SD-OCT should still be detectable (Fig 6-24). Over time, PAMM lesions typically resolve with thinning of the inner nuclear layer, resulting in persistent paracentral scotomata.

PAMM is primarily a disease of retinal ischemia and often seen in association with retinal vascular occlusion. Evaluation in suspected cases includes imaging and systemic workup for cardiovascular risk factors and sickle cell disease.

Chu S, Nesper PL, Soetikno BT, Bakri SJ, Fawzi AA. Projection-resolved OCT angiography of microvascular changes in paracentral acute middle maculopathy and acute macular neuroretinopathy. *Invest Ophthalmol Vis Sci*. 2018;59(7):2913–2922.

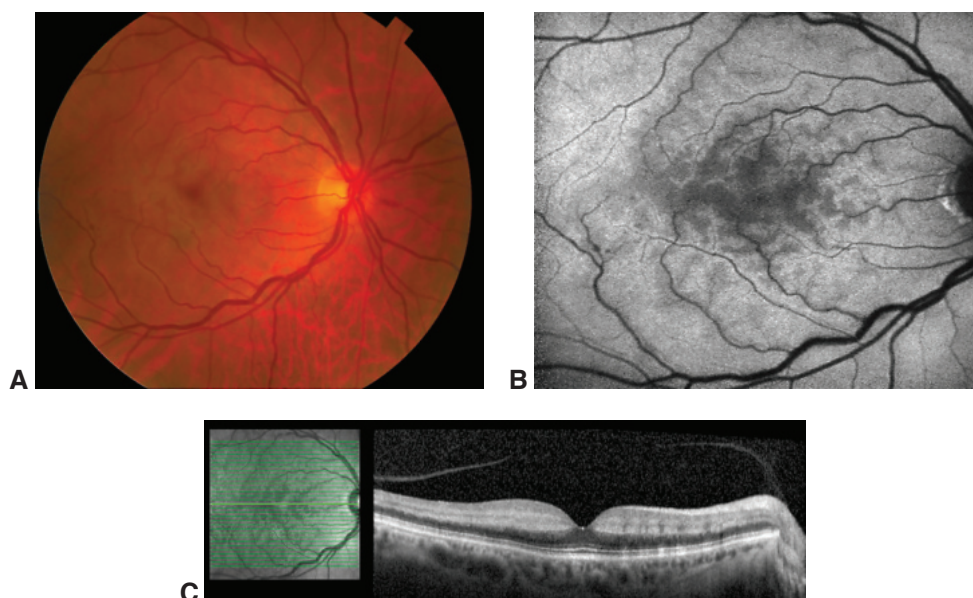


Figure 6-24 Paracentral acute middle maculopathy (PAMM). A 57-year-old woman presented with acute visual defects that she described as “lacy patterns” in her vision. **A**, Fundus photograph shows ill-defined grayish lesions in the macula, corresponding to intraretinal opacification. **B**, Fundus autofluorescence highlights the blocking defect of the perivenular retinal opacification. **C**, SD-OCT shows hyperreflectivity of the inner nuclear layer, more patchy nasally and more continuous temporally. These clinical and imaging findings are consistent with PAMM. (Courtesy of Amani Fawzi, MD.)

Arterial Macroaneurysms

Retinal arterial macroaneurysms are acquired ectasias of the first 3 orders of retinal arterioles. Large macroaneurysms can actually traverse the full thickness of the retina. Vision loss may occur from embolic or thrombotic occlusion of the end arteriole (*white infarct*) or from hemorrhage in any retinal layer. Other retinal findings may include capillary telangiectasia and remodeling, as well as retinal edema and exudate involving the macula (Fig 6-25). Often, there are multiple arterial macroaneurysms, although only 10% of cases are bilateral. Arterial macroaneurysms are associated with systemic arterial hypertension in approximately two-thirds of cases and may occur in the area of previous vascular occlusions. Systemic blood pressure should be measured at the time of diagnosis, and the patient should be referred for further evaluation.

Typically, the macroaneurysm closes and scleroses spontaneously, with accompanying resorption of related hemorrhage. Reopening of the macroaneurysm and rebleeding are rare. Thus, initial management is usually observation. Laser photocoagulation treatment may be considered if increasing edema in the macula threatens central vision. In most instances, closure can be achieved with moderate-intensity laser treatment of the retina, performed immediately adjacent to the macroaneurysm, using 2–3 rows of large-spot-size (200–500 μm) applications. Some specialists prefer direct treatment. Caution

Figure 6-25 Fundus photograph of a retinal arterial macroaneurysm with some exudate in the superior macula, resulting from leakage of the lesion, and mild hemorrhage. (Courtesy of Colin A. McCannel, MD.)



should be used when treating macroaneurysms that occur in macular arterioles because thrombosis with retinal arterial obstruction distal to the macroaneurysm may result.

Lee EK, Woo SJ, Ahn J, Park KH. Morphologic characteristics of retinal arterial macroaneurysm and its regression pattern on spectral-domain optical coherence tomography. *Retina*. 2011;31(10):2095–2101.

Pitkänen L, Tommila P, Kaarniranta K, Jääskeläinen JE, Kinnunen K. Retinal arterial macroaneurysms. *Acta Ophthalmol*. 2014;92(2):101–104.

Other Retinal Vascular Diseases

Highlights

- Proliferative sickle cell retinopathy occurs most commonly with sickle cell–hemoglobin C disease.
- All Black patients presenting with a traumatic hyphema should be screened for a sickling hemoglobinopathy.
- Cerebellar hemangioblastoma and renal cell carcinoma are the leading causes of death in patients with von Hippel–Lindau syndrome.

Sickle Cell Disease and Retinopathy

Sickle Cell Disease

Sickle cell anemia is the most common inherited blood disorder in the United States. The sickle cell hemoglobinopathies of greatest ocular importance are those in which mutant hemoglobins S, C, or both are inherited instead of hemoglobin A, which is normally predominant in adults (see Part III, Genetics, in BCSC Section 2, *Fundamentals and Principles of Ophthalmology*). Sickle cell hemoglobinopathies are most prevalent in the Black population and affect approximately 10% of African American people (Table 7-1). Thalassaemia, in which the α - or β -polypeptide chain is defective, is rare but frequently causes retinopathy.

Table 7-1 Incidence of Sickle Cell Hemoglobinopathies in North America

Hemoglobinopathy	Incidence in Population, %	Incidence of Proliferative Retinopathy in Subgroups
Any sickle hemoglobin	10	—
Sickle cell trait (HbAS)	8	Uncommon
Hemoglobin C trait (HbAC)	2	Uncommon
Homozygous sickle cell (HbSS)	0.4	3% ^a
Sickle cell–hemoglobin C (HbSC)	0.2	33% ^a
Sickle cell–thalassaemia (S β Thal)	0.03	14% ^a
Homozygous C (HbCC)	0.016	Unknown

^aApproximate.

Reproduced with permission from Fekrat S, Goldberg MF. Sickle retinopathy. In: Regillo CD, Brown GC, Flynn HW Jr, eds. *Vitreoretinal Disease: The Essentials*. Thieme; 1999:333. www.Thieme.com

Although sickling and solubility tests (sickle cell preparations) are reliable indicators of the presence of hemoglobin S and therefore are excellent for sickle cell anemia screening, these tests do not distinguish between heterozygous and homozygous states in the hemoglobinopathies. Patients who test positive on sickle cell preparations should also undergo hemoglobin electrophoresis testing. See BCSC Section 1, *Update on General Medicine*, for further discussion of sickle cell disease.

Scott AW, Luty GA, Goldberg MF. Hemoglobinopathies. In: Schachat AP, Wilkinson CP, Hinton DR, Sadda SR, Wiedemann P, eds. *Ryan's Retina*. Vol 1. 6th ed. Elsevier/Saunders; 2018:chap 60.

Stages of Sickle Cell Retinopathy

Sickle cell retinopathy has been classified into 5 stages based on the following pathogenic sequence (stages 1 through 3 are depicted in Fig 7-1):

- peripheral arteriolar occlusions (*stage 1*) leading to
- peripheral nonperfusion and peripheral arteriovenular anastomoses (*stage 2*), which are dilated, preexisting capillary channels
- peripheral sea fan neovascularization (*stage 3*), which may occur at the posterior border of areas of nonperfusion and lead to
- vitreous hemorrhage (*stage 4*) and
- traction (also called *tractional*) retinal detachment (*stage 5*)

Nonproliferative Sickle Cell Retinopathy

The retinal changes in nonproliferative sickle cell retinopathy are caused by arteriolar and capillary occlusion. Anastomosis and remodeling occur in the periphery, as does the resorption of blood around the infarct (see Fig 7-1). Salmon-patch hemorrhages represent areas of intraretinal hemorrhage that occur after a peripheral retinal arteriolar occlusion (Fig 7-2A). Refractile spots are old, resorbed hemorrhages with hemosiderin deposition within the inner retina just beneath the internal limiting membrane (ILM) (Fig 7-2B). Black “sunburst” lesions are localized areas of retinal pigment epithelial hypertrophy, hyperplasia, and pigment migration in the peripheral retina, probably caused by hemorrhage.

Occlusion of parafoveal capillaries and arterioles is one cause of decreased vision in patients with sickle cell retinopathy (Fig 7-3). These changes can be detected on angiography, particularly with optical coherence tomography angiography (OCTA), and may be subtle (Fig 7-4) or catastrophic (Fig 7-5). Spontaneous occlusion of the central retinal artery may also develop in patients with sickle cell hemoglobinopathies.

Proliferative Sickle Cell Retinopathy

Proliferative sickle cell retinopathy (PSR) occurs most commonly with sickle cell–hemoglobin C (also called *HbSC*) disease, with an incidence of approximately 33% (see Table 7-1). It occurs less commonly with sickle cell–thalassemia (S α Thal), the incidence of which is approximately 14%. Homozygous sickle cell disease (also called *HbSS disease*) results in more systemic complications than the other types of sickle cell disease but has a

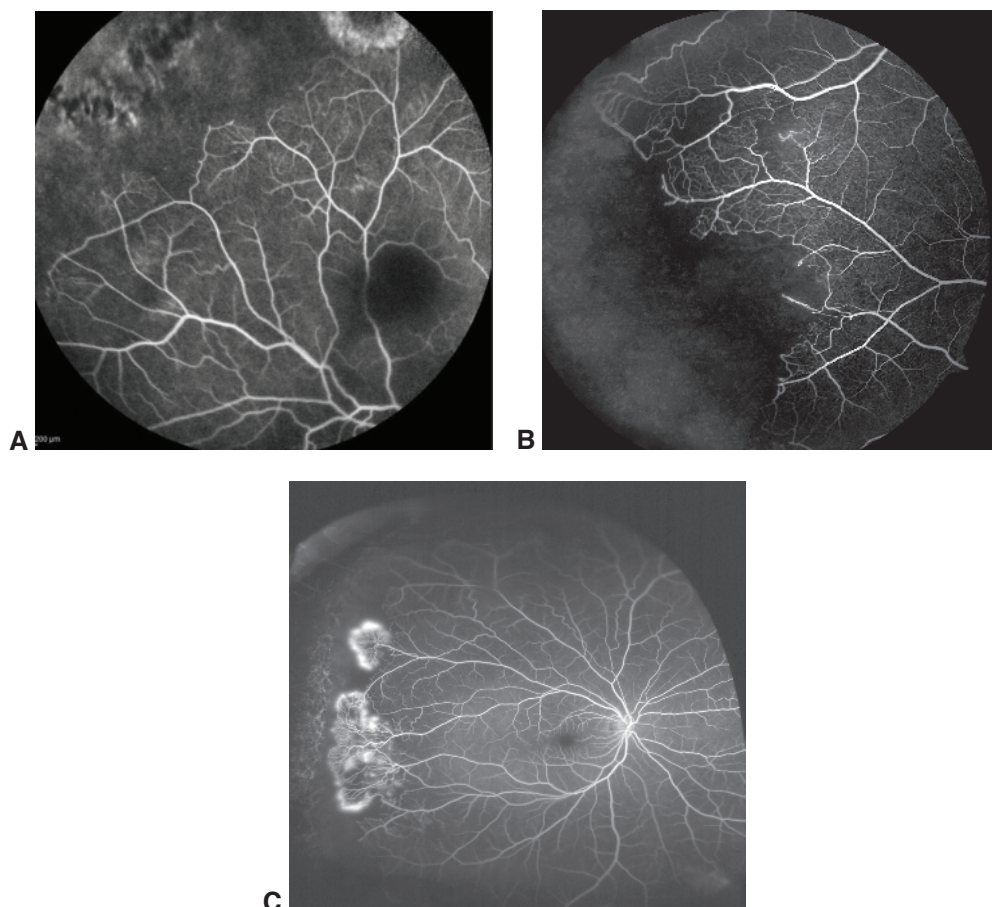


Figure 7-1 Fluorescein angiograms (FAs) showing the first 3 stages of sickle cell retinopathy. **A**, Stage 1: The image shows normal vessels posteriorly but severe capillary dropout throughout the periphery. **B**, Stage 2: FA shows peripheral nonperfusion and dilated arteriovenular anastomosis. **C**, Stage 3: The image shows peripheral retinal neovascularization, consistent with proliferative sickle cell retinopathy. (These images were originally published in the *Retina Image Bank*. Part A: Thomas A. Ciulla, MD, MBA. Photograph by Thomas Steele. *Sickle Cell Retinopathy*. *Retina Image Bank*, 2015; image number 2566. Parts B and C: Michael P. Kelly, FOPS. *Sickle Cell Retinopathy*. *Retina Image Bank*, 2012; image numbers 949, 721. © American Society of Retina Specialists.)

very low incidence of proliferative retinopathy at approximately 3%. Proliferative retinopathy is rare with sickle cell trait (also called *HbAS*). The ocular complications result from ischemia secondary to infarction of the retinal tissue by means of arteriolar, precapillary arteriolar, capillary, or venular occlusions; they include retinal neovascularization, preretinal or vitreous hemorrhage, and traction retinal detachment.

PSR is one of many retinal vascular diseases in which extraretinal fibrovascular proliferation occurs in response to retinal ischemia. While the neovascularization in eyes with proliferative diabetic retinopathy (PDR) generally begins postequatorially, the neovascularization in PSR is located more peripherally (Fig 7-6). Another way in which PSR

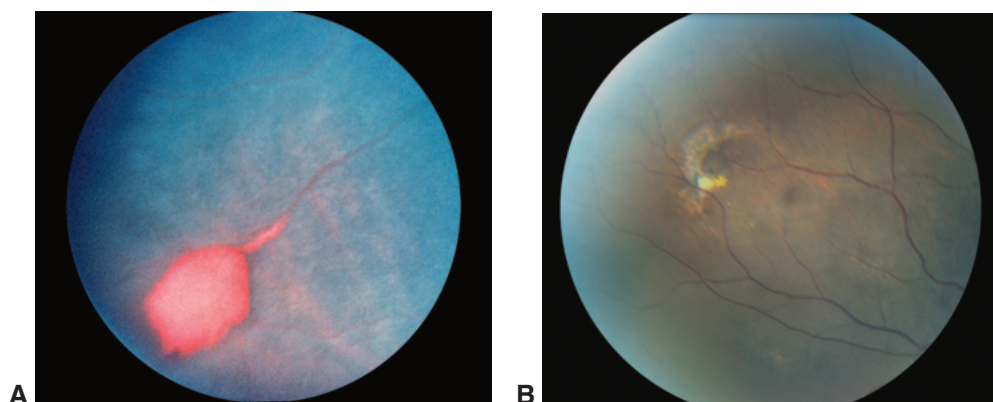


Figure 7-2 Salmon-patch hemorrhage in sickle cell retinopathy. **A**, Peripheral fundus photograph from a patient with sickle cell disease shows a retinal hemorrhage unrelated to proliferation; instead, it is the result of infarction of the retina from a vascular occlusion—a *salmon patch*. **B**, Peripheral fundus photograph of an iridescent, or refractile, patch that represents an area of previous, now resorbed, retinal hemorrhage (salmon patch). (Part A: This image was originally published in the Retina Image Bank. Larry Halperin, MD. Sickle Salmon-Patch Hemorrhage. Retina Image Bank, 2012; image number 1789. © American Society of Retina Specialists. Part B courtesy of G. Baker Hubbard III, MD.)

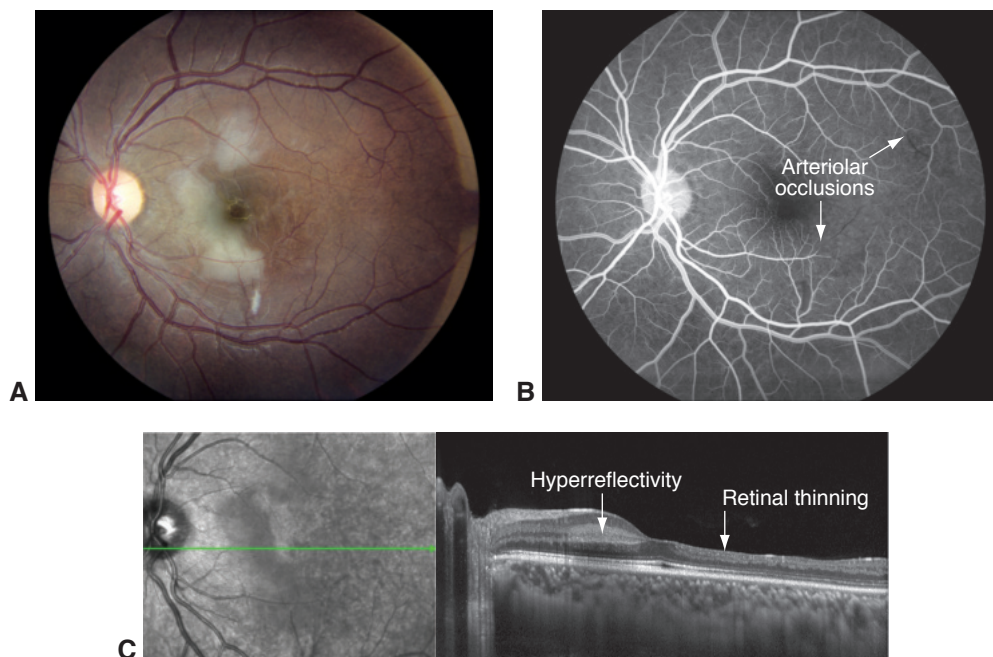


Figure 7-3 Retinal arteriolar occlusions in nonproliferative sickle cell retinopathy. **A**, Fundus photograph of patchy, creamy parafoveal retinal infarctions in the left eye of a 21-year-old woman with sickle cell (HbSS) disease; the sickling crisis was dehydration induced. **B**, FA demonstrates occlusion of multiple small retinal arterioles (arrows); however, none correspond to the areas of opacified retina. Similar findings were present in the other eye. Note that unlike embolic events, these occlusions do not occur at a bifurcation. The patient maintained good central visual function. **C**, Optical coherence tomography (OCT) demonstrates *hyperreflectivity* in the middle retina corresponding to an area of creamy retinal infarction, suggesting ischemia of the deep capillary plexus. There is temporal *retinal thinning* with loss of the inner retinal layers, indicating previous infarctions in that area. (Courtesy of Michael Dollin, MD.)

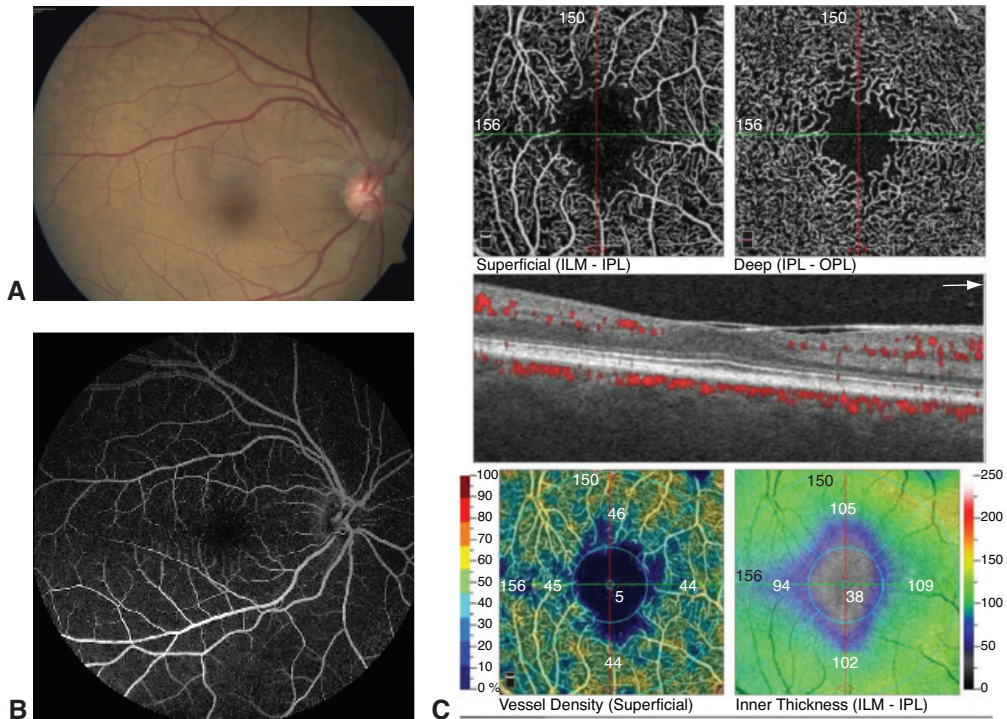


Figure 7-4 **A**, Fundus photograph of the right eye of a 47-year-old woman with sickle cell-hemoglobin C (HbSC) disease and 20/20 vision. **B**, FA is unremarkable. **C**, *Top row*: OCT angiography (OCTA) of the superficial and deep capillary plexus shows an enlarged foveal avascular zone (FAZ) that is especially prominent in the superficial, pruned capillaries. *Middle row*: Cross-sectional OCT with flow overlay, showing widened foveal depression, vitreomacular adhesion, and expanded vascular FAZ boundaries. *Bottom row*: Superficial vessel density (*right*) and inner retinal thickness (*left*) maps. *Left image* shows central thinning consistent with an enlarged FAZ, while the capillary density map highlights decreased density in areas outside the FAZ (pseudocolored in deeper shades of blue). (Courtesy of Jennifer Irene Lim, MD.)

can be differentiated from PDR is that in PSR, spontaneous regression of the peripheral neovascularization by autoinfarction frequently occurs, resulting in a white sea fan neovascularization (Fig 7-7). Table 7-2 presents a differential diagnosis for peripheral retinal neovascularization.

Elagouz M, Jyothi S, Gupta B, Sivaprasad S. Sickle cell disease and the eye: old and new concepts. *Surv Ophthalmol.* 2010;55(4):359–377.

Other Ocular Abnormalities in Sickle Cell Hemoglobinopathies

Many patients with HbSS or HbSC disease exhibit segmentation of blood in the conjunctival blood vessels. Numerous comma-shaped thrombi dilate and occlude capillaries, most often in the inferior bulbar conjunctiva and fornix (referred to as the *comma sign*). Similarly, small vessels on the surface of the optic nerve head can exhibit intravascular occlusions, manifested as dark red spots (called *the nerve head sign of sickling*). Angioid streaks

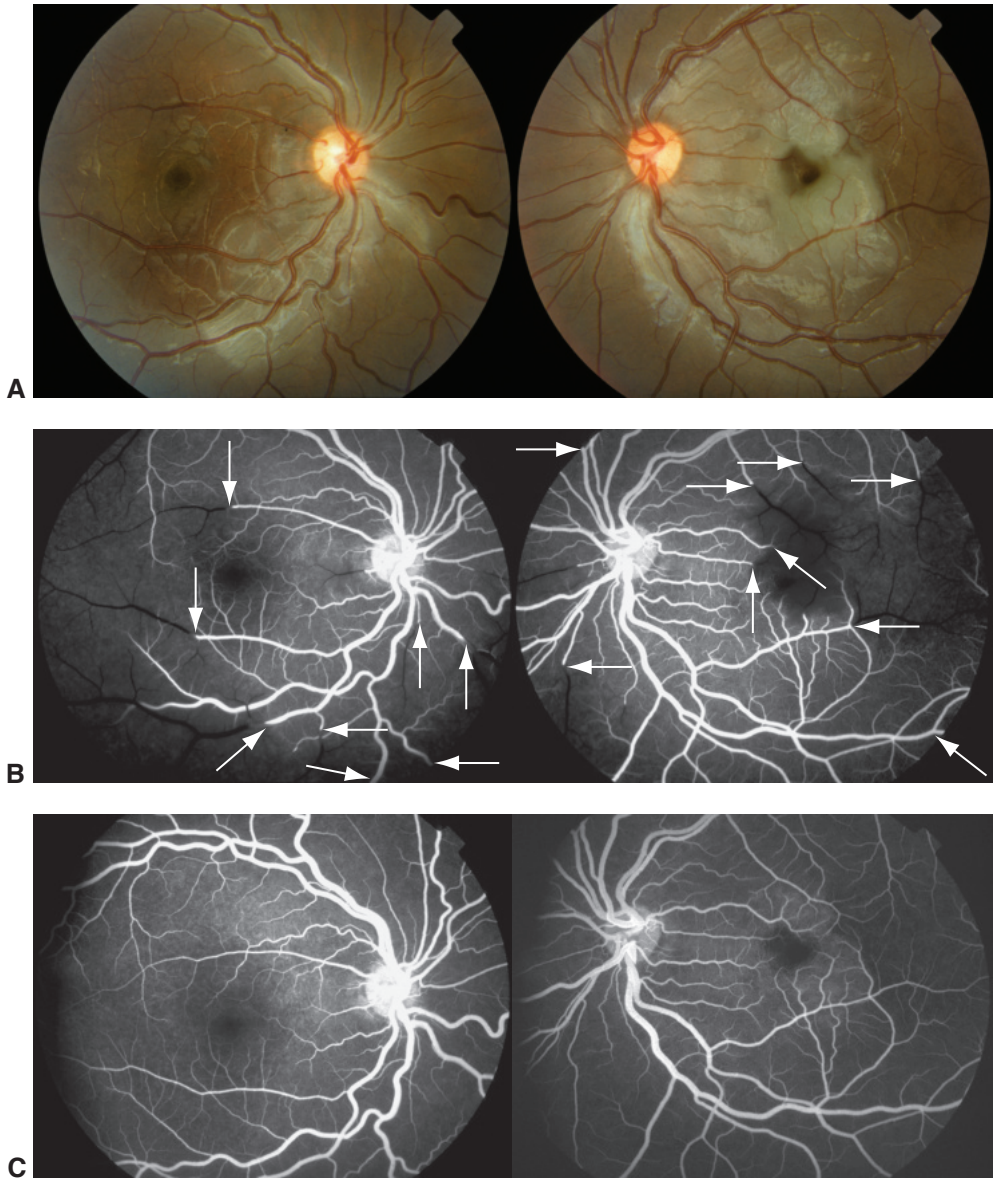


Figure 7-5 Bilateral, multiple branch retinal artery occlusions (BRAOs) in nonproliferative sickle cell retinopathy. **A**, Fundus photographs from a 5½-year-old boy with HbSS disease (sickle cell anemia) show multiple acute BRAOs during a massive sickling episode. **B**, FA images show numerous medium and large arteriolar vessel occlusions (*arrows*), notably not located at bifurcations. **C**, The patient was treated promptly following a hypertransfusion protocol, which resulted in dramatic reperfusion of the retina. However, the corrected distance visual acuity did not improve beyond 20/200 in either eye. (Courtesy of Brian Leonard, MD.)

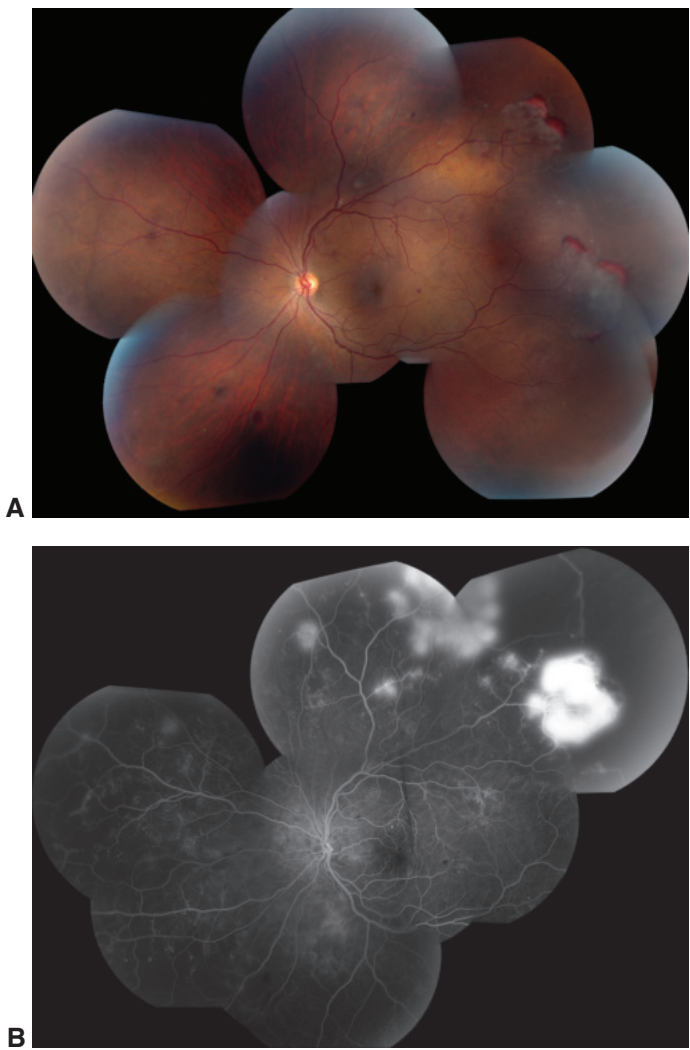


Figure 7-6 Wide-field fundus image montages of the left eye of a 26-year-old African American man with a history of HbSC disease. **A**, Hemorrhaging has occurred at the anterior border of the proliferative lesions. **B**, FA imaging shows leakage from the sea fan lesions in the periphery and peripheral nonperfusion anterior to the sea fans. (Courtesy of Asheesh Tewari, MD.)



Figure 7-7 Fundus photograph of peripheral neovascularization (sea fan neovascularization) with autoinfarction, as illustrated by the white atrophic vessels. (Courtesy of Harry W. Flynn Jr, MD.)

Table 7-2 Differential Diagnosis of Peripheral Retinal Neovascularization**Vascular diseases with ischemia**

Aortic arch syndromes/ocular ischemic syndromes
 Branch retinal artery occlusion (BRAO)
 Branch retinal vein occlusion (BRVO)
 Carotid-cavernous fistula
 Central retinal artery occlusion
 Central retinal vein occlusion
 Coats disease
 Eales disease
 Familial exudative vitreoretinopathy (FEVR)
 Hyperviscosity syndromes (eg, chronic myelogenous leukemia)
 Idiopathic retinal vasculitis, aneurysms, and neuroretinitis (IRVAN)
 Proliferative diabetic retinopathy (PDR)
 Retinal embolization (eg, talc emboli)
 Retinopathy of prematurity (ROP)
 Sickling hemoglobinopathies (eg, SC, SS) and
 other hemoglobinopathies (eg, HbAC, HbAS)

Inflammatory diseases with possible ischemia

Birdshot chorioretinopathy
 Multiple sclerosis
 Retinal vasculitis (eg, systemic lupus erythematosus)
 Sarcoidosis
 Susac syndrome
 Toxoplasmosis
 Uveitis, including pars planitis

Miscellaneous conditions

Choroidal melanoma
 Chronic retinal detachment
 Incontinentia pigmenti
 Radiation retinopathy
 Retinitis pigmentosa
 Retinoschisis

Modified with permission from Elsevier. Jampol LM, Ebroon DA, Goldbaum MH. Peripheral proliferative retinopathies: an update on angiogenesis, etiologies, and management. *Surv Ophthalmol.* 1994;38(6): 519–540.

have been reported clinically in up to 6% of cases of HbSS disease and in persons with sickle cell trait (HbAS).

Management of Sickle Cell Retinopathy and Its Complications

Traumatic hyphema

All Black patients presenting with a traumatic hyphema should be screened for a sickling hemoglobinopathy (including HbAS) because of the increased risk of rigid sickled erythrocytes inducing high intraocular pressure (IOP). For patients with hyphema and increased IOP, early anterior chamber washout is recommended in order to control the IOP and prevent corneal blood staining. In general, carbonic anhydrase inhibitors should be avoided in patients with sickle cell disease as these drugs may worsen sickling through the production of systemic acidosis.

CLINICAL PEARL

Always remember to test for sickle cell disease in patients with traumatic hyphema (especially in Black patients).

McLeod DS, Merges C, Fukushima A, Goldberg MF, Luty GA. Histopathologic features of neovascularization in sickle cell retinopathy. *Am J Ophthalmol.* 1997;124(4):455–472.

Proliferative sickle cell retinopathy: photocoagulation

Peripheral scatter photocoagulation applied to the ischemic peripheral retina generally causes regression of neovascular fronds and thus decreases the risk of vitreous hemorrhage. The decision to treat PSR with scatter photocoagulation should be made cautiously, however, because retinal tears can occur and do so more commonly after such treatment in PSR than in PDR.

Proliferative sickle cell retinopathy: vitreoretinal surgery

Surgery may be indicated for nonclearing vitreous hemorrhage and for rhegmatogenous, traction, schisis, or combined retinal detachment. Retinal detachment usually begins in the ischemic peripheral retina. The tears typically occur at the base of sea fans and can be precipitated by photocoagulation treatment. Anterior segment ischemia or necrosis has been reported in association with 360° scleral buckling procedures, particularly when combined with extensive diathermy or cryopexy.

Vasculitis

Retinal vasculitis from any cause may progress through the stages of inflammation, ischemia, neovascularization, and subsequent hemorrhagic and tractional complications. The early clinical manifestations are generally nonspecific, consisting of perivascular infiltrates and sheathing of the retinal vessels (vascular wall thickening with vessel involution; Fig 7-8). Veins tend to become inflamed earlier and more frequently than arterioles, but involvement of both arteries and veins is the rule. A variety of inflammatory uveitides may cause retinal vasculitis; see Table 5-5 in BCSC Section 9, *Uveitis and Ocular Inflammation*. Masquerade



Figure 7-8 Fundus photograph of retinal vasculitis in an eye of a patient with Crohn disease. Retinal hemorrhages and edema are present, as is prominent sheathing of the retinal vessels. (Courtesy of Gary C. Brown, MD.)

syndromes should also be considered as possible causes. See Section 9 for further discussion of most of these conditions and Section 5, *Neuro-Ophthalmology*, for discussion of multiple sclerosis and giant cell arteritis.

A primary occlusive retinal vasculopathy for which no cause can be found is termed *Eales disease*. This condition usually involves the peripheral retina of both eyes and often results in extraretinal neovascularization with vitreous hemorrhage. It typically occurs in males and may be associated with tuberculin hypersensitivity. There is also a possible association between tuberculosis and Eales disease.

Susac syndrome is characterized by multiple branch retinal artery occlusions and can be associated with hearing loss and, in rare cases, with strokes. It is most commonly diagnosed in women in their third decade of life, and there is no known cause. Treatment of Susac syndrome includes corticosteroids and generally requires long-term immunosuppression.

Chronic embolism or thrombosis without inflammation may result in a clinical picture that is indistinguishable from previous retinal vasculitis. Evaluation includes a search for possible causes: cardiac valvular disease, cardiac arrhythmias, ulcerated atheromatous disease of the carotid vessels, and hemoglobinopathies.

Idiopathic retinal vasculitis, aneurysms, and neuroretinitis (IRVAN) describes a syndrome characterized by the presence of retinal vasculitis, multiple macroaneurysms, neuroretinitis, and peripheral capillary nonperfusion. Systemic investigations are generally noncontributory, and oral prednisone has demonstrated little benefit. Capillary nonperfusion is often sufficiently severe to warrant panretinal photocoagulation.

Cystoid Macular Edema

Cystoid macular edema (CME) is characterized by intraretinal edema contained in honeycomb-like cystoid spaces. The source of the edema is abnormal perifoveal retinal capillary permeability, which in many cases is visible on fluorescein angiography (FA) as multiple small focal leaks and late pooling of the dye in extracellular cystoid spaces. OCT findings in CME include diffuse retinal thickening with cystoid areas that are more prominent in the inner nuclear and outer plexiform layers. On occasion, a nonreflective cavity that is consistent with subretinal fluid accumulation is present beneath the neurosensory retina (see Chapter 5, Fig 5-11B, and Chapter 6, Fig 6-8A). Because of the radial foveal arrangement of both the glia and Henle inner fibers, this pooling classically forms a “flower petal” (petaloid) pattern (Fig 7-9).

Etiologies of CME

Abnormal permeability of the perifoveal retinal capillaries may occur in a wide variety of conditions, including diabetic retinopathy, central retinal vein occlusion, branch retinal vein occlusion, any type of uveitis, and retinitis pigmentosa (RP). CME can also be triggered or worsened by drugs. In addition, CME may occur after any ocular surgery. Cataract surgery is one of the most common etiologies of CME from any cause and is discussed in detail in BCSC Section 11, *Lens and Cataract*. CME occurring after cataract extraction is called *Irvine-Gass syndrome*. There is no uniform definition of pseudophakic CME, the reported

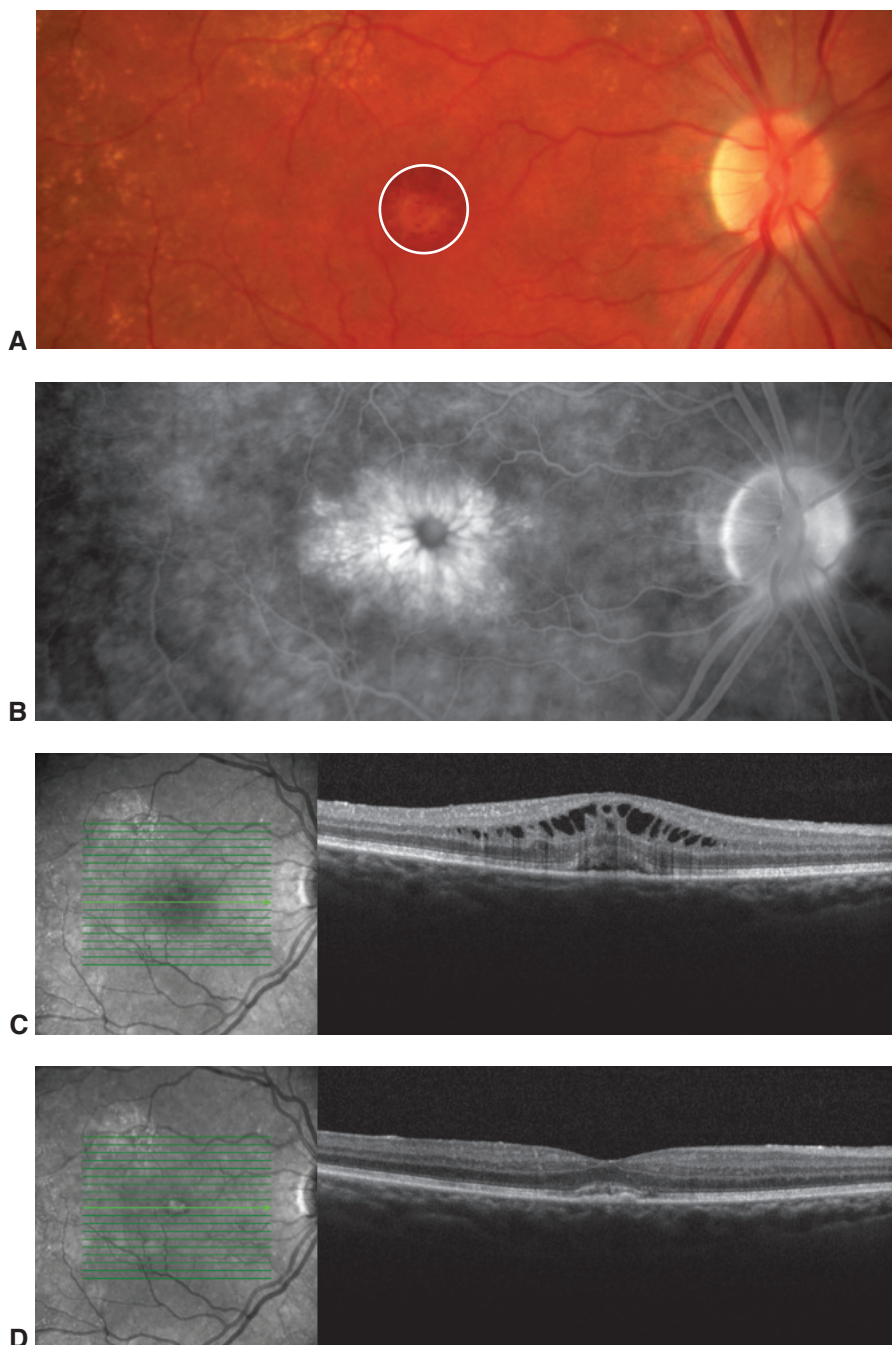


Figure 7-9 Pseudophakic cystoid macular edema (CME). **A**, Fundus photograph of an optic nerve head and macula 3 months after complex cataract surgery. A small incidental grayish-yellow adult vitelliform dystrophy lesion is present in the subfoveal region (*circled*). **B**, A mid-phase FA image demonstrates cystoid hyperfluorescence, with a classic petaloid pattern. As is typical in eyes with pseudophakic CME, there is mild hyperfluorescence of the nasal portion of the optic nerve head. **C**, OCT image shows cystoid retinal thickening and a subfoveal vitelliform lesion. **D**, After 8 weeks of topical steroidal and nonsteroidal anti-inflammatory therapy, OCT shows that the CME has fully resolved. (*Courtesy of Brian Leonard, MD.*)

incidence of which ranges from approximately 1% to over 30% following extracapsular cataract extraction. The incidence of clinically relevant pseudophakic CME, which includes reduced vision in the presence of CME, is 1%–2%. The differential diagnosis of CME in which FA fails to show leakage includes conditions such as X-linked hereditary retinoschisis, Goldmann-Favre disease, and RP. Angiographically silent CME may also occur as an adverse effect of treatment with nicotinic acid and taxanes (see also Chapter 14 in this volume).

Johnson MW. Etiology and treatment of macular edema. *Am J Ophthalmol.* 2009;147(1):11–21.

Treatment of CME

Treatment of CME is generally directed toward the underlying etiology (eg, branch retinal vein occlusion, uveitis). To reduce the risk of postoperative pseudophakic CME, a combination of topical corticosteroids and nonsteroidal anti-inflammatory drugs is commonly used as prophylactic treatment. If CME is severe or refractory to topical therapy, periocular (eg, posterior sub-Tenon triamcinolone acetonide) or intraocular injection of steroid preparations is an appropriate escalation of therapy. Oral and/or topical acetazolamide may be successful for treatment of CME, especially in chronic cases (eg, associated with RP).

If CME is associated with vitreous adhesions to the iris or a corneoscleral wound, vitrectomy or Nd:YAG laser treatment to interrupt the vitreous strands may be helpful. In cases of CME caused by epiretinal membranes or vitreomacular traction, surgical intervention may be appropriate (see Chapter 19).

Kim SJ, Schoenberger SD, Thorne JE, Ehlers JP, Yeh S, Bakri SJ. Topical nonsteroidal anti-inflammatory drugs and cataract surgery: a report by the American Academy of Ophthalmology. *Ophthalmology.* 2015;122(11):2159–2168.

Coats Disease

Coats disease is characterized by the presence of vascular abnormalities (retinal telangiectasia), including ectatic arterioles, microaneurysms, venous dilatations (phlebectasias), and fusiform capillary dilatations, which are frequently associated with exudative retinal detachment. Age at onset is 6–8 years, usually only 1 eye is involved, and there is a marked male predominance (85% of cases). To date, researchers have not identified an associated gene or chromosome or any hereditary pattern, and no association between Coats disease and systemic disease has been found.

In an eye with Coats disease, the abnormal vessels are compromised, resulting in the leakage of serum and other blood components, which accumulate in and under the retina. Any portion of the peripheral and macular capillary system may be involved. Although angiography demonstrates the presence of retinal capillary nonperfusion, posterior segment neovascularization is unusual. The clinical findings vary widely, ranging from mild retinal vascular abnormalities and minimal exudation to extensive areas of retinal telangiectasia associated with massive leakage and exudative retinal detachment. The severity and rate of progression appear greater in children younger than 4 years, in whom massive exudative retinal detachment with the retina juxtaposed to the lens may simulate retinoblastoma or other causes of leukocoria (called *Coats reaction*; Fig 7-10) or xanthocoria (yellow pupil). See BCSC Section 6, *Pediatric Ophthalmology and Strabismus*, for the differential diagnosis of leukocoria.

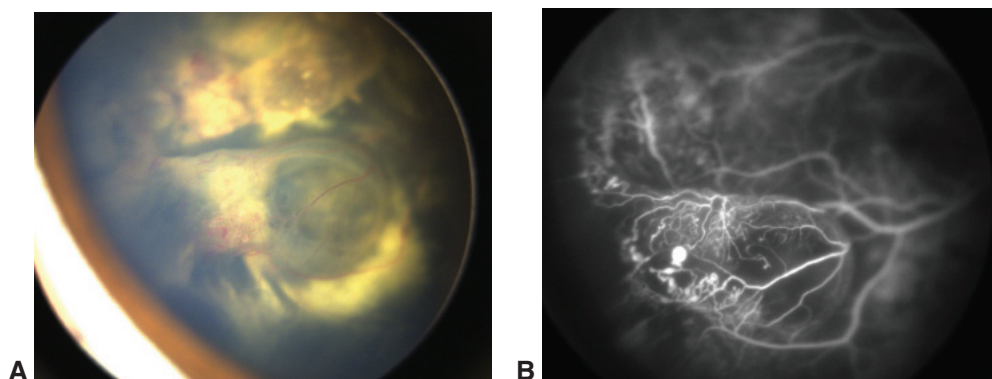


Figure 7-10 Photograph (A) and FA image (B) from a boy who presented with unilateral leukocoria. The patient had extensive vascular changes, telangiectatic vessels, and an exudative retinal detachment with extensive lipid deposition characteristic of Coats disease. FA highlights the peripheral telangiectasias and characteristic aneurysms. (Courtesy of Safa Rahmani, MD.)

Pediatric patients with peripheral involvement typically present with lipid deposition in an otherwise angiographically normal macula, because hard exudate tends to accumulate in the macula. Similar findings in adults probably represent late decompensation of preexisting vascular anomalies. Occasionally, the initial finding is a submacular lipogranuloma or subretinal fibrosis. The differential diagnosis for Coats disease may include

- dominant (familial) exudative vitreoretinopathy
- facioscapulohumeral muscular dystrophy
- retinopathy of prematurity (ROP)
- retinal hemangioblastomas (von Hippel–Lindau syndrome)

For milder cases of lipid exudation, additional considerations are diabetic retinopathy, branch retinal vein occlusion, juxtafoveal retinal telangiectasia, and radiation retinopathy.

Treatment of Coats disease generally consists of direct ablation of the vascular anomalies with photocoagulation or cryotherapy and, in severe cases, retinal reattachment surgery. Intravitreal anti-vascular endothelial growth factor (VEGF) therapy may be a useful adjunctive treatment for cases that are resistant to ablative therapy alone.

Coats-like Reaction in Other Retinal Conditions

Certain forms of RP may be associated with a “Coats-like” reaction, characterized by telangiectatic, dilated vessels and extensive lipid exudation. Most well documented among these forms is *CRB1*-associated RP1 (preserved para-arteriolar retinal pigment epithelium phenotype). Other retinopathies that may present with a unilateral Coats-like phenotype include retinal vasoproliferative tumor (VPT; also known as *reactive retinal astrocytic tumor*), which is distinguished by a preretinal fibrotic mass, disorganized vasculature, and isolated temporal location.

Sigler EJ, Randolph JC, Calzada JI, Wilson MW, Haik BG. Current management of Coats disease. *Surv Ophthalmol*. 2014;59(1):30–46.

Macular Telangiectasia

Macular telangiectasia is divided into 3 general types:

- type 1: unilateral parafoveal telangiectasia, congenital or acquired
- type 2: bilateral parafoveal telangiectasia
- type 3: bilateral parafoveal telangiectasia with retinal capillary obliteration

Macular Telangiectasia Type 1

Macular telangiectasia type 1 (MacTel 1; also called *aneurysmal telangiectasia*), typically occurs unilaterally, predominantly in young males, and with characteristic aneurysmal dilatations of the temporal macular vasculature with surrounding CME and yellowish exudates. MacTel 1 is considered a macular variant of Coats disease. Peripheral vascular changes may also occur. Anti-VEGF therapy is generally ineffective.

Macular Telangiectasia Type 2

Macular telangiectasia type 2 (MacTel 2; also called *juxtafoveal telangiectasis*), the most common form of macular telangiectasis, is a rare, progressive bilateral idiopathic neurodegenerative disease of the macular, parafoveal, retina. Characteristic findings begin to appear in affected individuals in the fifth to seventh decades of life and include a reduced foveolar reflex, loss of retinal transparency (retinal graying), superficial retinal crystalline deposits, mildly ectatic capillaries, slightly dilated blunted venules, progression to pigment hyperplasia, and foveal atrophy (Fig 7-11). Subretinal neovascularization may occur during the natural disease course and can be difficult to differentiate from the anomalous vasculature, requiring multimodal imaging and clinical suspicion. Many of the clinical features of MacTel 2 are characterized by dysfunction of both neural and vascular retinal elements, suggesting that a macular Müller cell defect plays an essential role in the pathogenesis of this disease (see Fig 7-11).

The telangiectatic vessels are readily apparent on FA and usually leak. OCT imaging typically shows a thinned central macular retina, including the fovea; within the inner foveal layers, oblong cavitations are present in which the long axis is parallel to the retinal surface (Fig 7-12; also see Fig 7-11). OCTA visualizes the deep capillary plexus changes of MacTel 2 (Fig 7-13).

To date, there is no FDA-approved, effective treatment of MacTel 2. Intravitreal anti-VEGF therapy is used for the management of active subretinal neovascularization with associated hemorrhage or exudation. The MacTel Project (www.lmri.net/mactel/the-mactel-project/) is an important ongoing international collaboration that aims to better understand MacTel 2 and find new therapeutic targets and therapies.

Chew EY, Clemons TE, Jaffe GJ, et al. Effect of ciliary neurotrophic factor on retinal neurodegeneration in patients with macular telangiectasia type 2: a randomized clinical trial. *Ophthalmology*. 2019;126(4):540–549.

Clemons TE, Gillies MC, Chew EY, et al; MacTel Research Group. Baseline characteristics of participants in the natural history study of macular telangiectasia (MacTel). MacTel Project report no. 2. *Ophthalmic Epidemiol*. 2010;17(1):66–73.

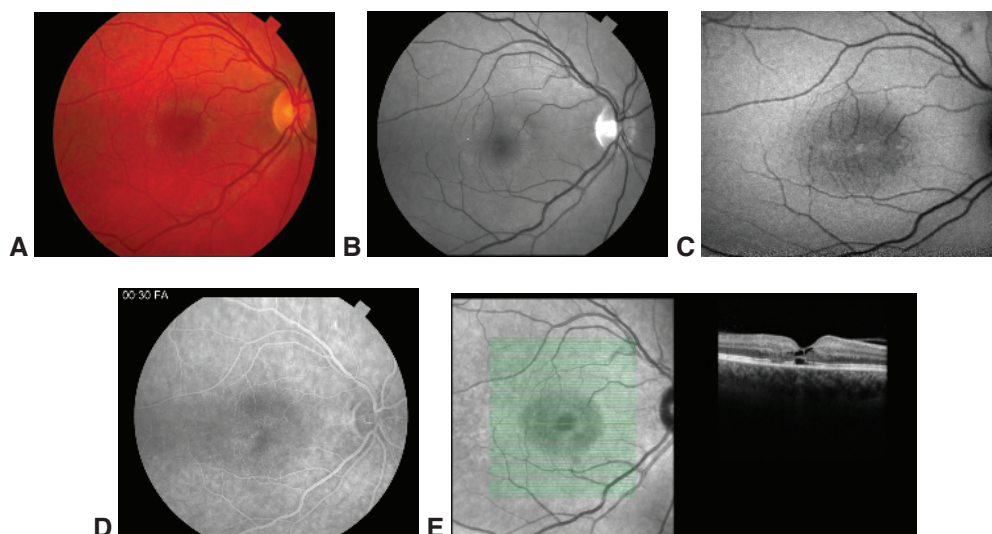


Figure 7-11 Early MacTel 2. **A**, Color photograph shows a subtle parafoveal halo and a few crystals in the temporal parafovea, highlighted in the red-free image (**B**). **C**, Fundus autofluorescence (488 nm) shows loss of foveal pigment, apparent as a hyperautofluorescent signal. **D**, Early frames of FA show the telangiectatic vessels around the FAZ. **E**, OCT (*right*) shows characteristic central cavitory lesions in the inner retina and loss of the ellipsoid zone in the fovea and temporally. Corresponding infrared image (*left*) highlights the parafoveal halo. (Courtesy of Amani Fawzi, MD.)

Gantner ML, Eade K, Wallace M, et al. Serine and lipid metabolism in macular disease and peripheral neuropathy. *N Engl J Med*. 2019;381(15):1422–1433. doi:10.1056/NEJMoa1815111
 Yannuzzi LA, Bardal AM, Freund KB, Chen KJ, Eandi CM, Blodi B. Idiopathic macular telangiectasia. *Arch Ophthalmol*. 2006;124(4):450–460.

Macular Telangiectasia Type 3

Macular telangiectasia type 3 is an extremely rare vasocclusive process that affects the parafoveal region and is distinct from macular telangiectasia types 1 and 2.

Phakomatoses

Conventionally, many of the syndromes referred to as phakomatoses (“mother spot”) are grouped loosely by the common features of ocular and extraocular or systemic involvement of a congenital nature. Most, but not all, are hereditary. Except for Sturge-Weber syndrome, the phakomatoses involve the neuroretina and its circulation. The phakomatoses discussed in this chapter are those most commonly associated with retinal vascular disease. For further discussion of the phakomatoses, see BCSC Section 5, *Neuro-Ophthalmology*, and Section 6, *Pediatric Ophthalmology and Strabismus*.

Von Hippel–Lindau Syndrome

Von Hippel–Lindau (VHL) syndrome (also called *familial cerebelloretinal angiomatosis*, among other names) is caused by a tumor suppressor gene mutation on the short arm of

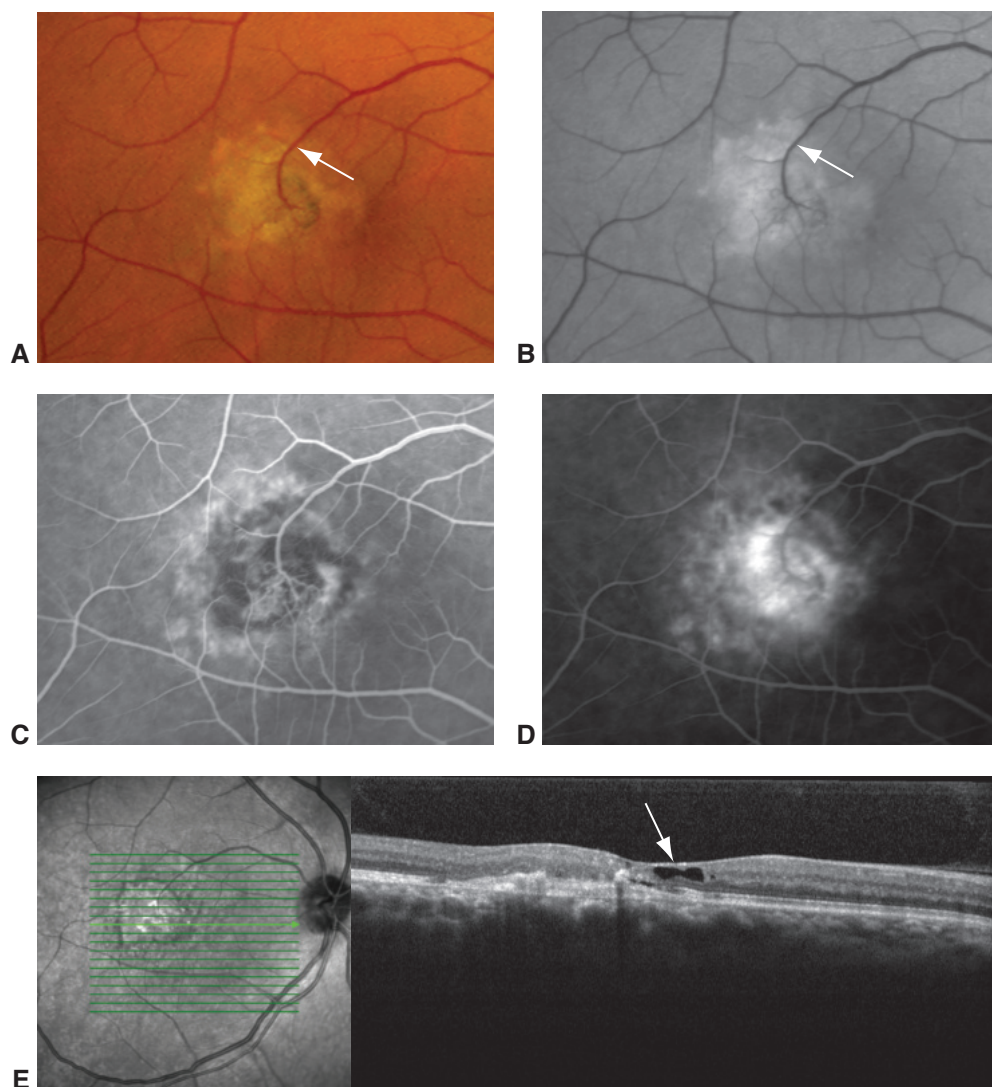


Figure 7-12 Advanced MacTel 2. **A**, Fundus photograph of the right eye shows the chorioretinal venous shunt vessel (*arrow*). This patient receives recurring intravitreal anti-vascular endothelial growth factor (VEGF) treatments for a subretinal neovascular membrane. **B**, Red-free image of the eye shown in **A**. **C**, Mid-phase FA image demonstrates subretinal neovascularization with superficial and deep components. **D**, Later-phase FA image shows late staining of the neovascular membrane complex. **E**, OCT demonstrates the neovascular membrane complex and MacTel 2-like hyporefective cavities within the inner foveal layers (*arrow*). (Courtesy of Brian Leonard, MD.)

chromosome 3 (3p26–p25), the inheritance of which is autosomal dominant with incomplete penetrance and variable expression. The disease is characterized by retinal and central nervous system hemangioblastomas and visceral manifestations (see BCSC Section 6, *Pediatric Ophthalmology and Strabismus*). Central nervous system tumors include hemangioblastomas of the cerebellum, medulla, pons, and spinal cord in 20% of patients with VHL syndrome. Systemic manifestations include renal cell carcinoma; pheochromocytomas;

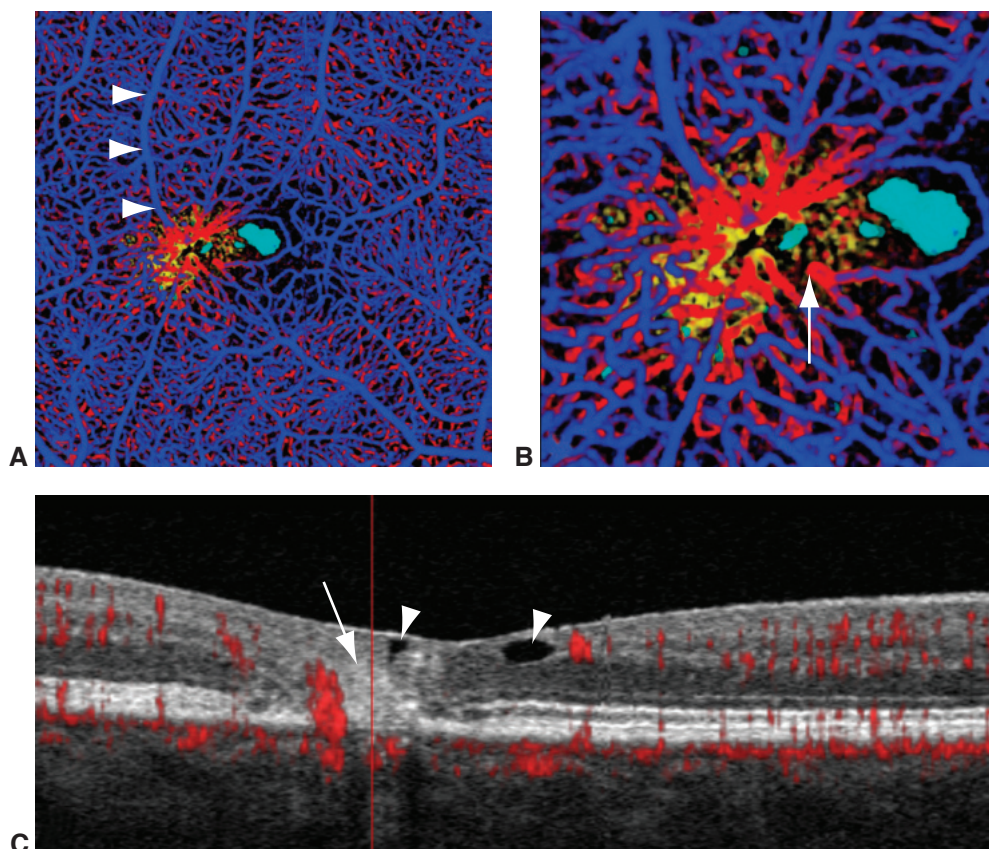


Figure 7-13 MacTel 2 OCT and OCTA imaging. OCTA images do not show leakage and thus can better reveal the complex vascular pathology. **A**, Volume-rendered OCTA image of a right eye. At the level of the superficial vascular plexus, the vessels are *blue*; at the deep plexus they are *red*; and external to the deep plexus, they are *yellow*. Retinal cavitations are *cyan*. A contraction in the temporal juxtafoveal region causes a dragging of the perifoveal capillary ring temporally. Note the dragging of vessels such as the large retinal vein (*arrowheads*), producing an appearance of a right-angle vein. **B**, OCTA image shows enlargement of the area of contracture in the temporal juxtafoveal macula. Note the angled capillary segments (*arrow*) that point toward the epicenter of the contracture. **C**, This B-scan structural OCT shows a flow overlay in red. The scan was taken at the fovea. The hyperreflective material extends nearly the full thickness of the retina (*arrow*). Note the considerable flow (*red color*) on the temporal side, which is suggestive of retinochoroidal anastomotic vessels. Nasal to the hyperreflective region are cavitations (*arrowheads*). Over time, cavitations may change in size, shape, and number. (Courtesy of Richard F. Spaide, MD.)

endolymphatic sac tumors; cysts of the kidney, pancreas, and liver; and bilateral papillary cystadenomas of the epididymis (men) or broad ligament of the uterus (women). Diagnosis of a retinal hemangioblastoma warrants a systemic workup and genetic testing, the results of which can confirm the diagnosis of VHL syndrome. Cerebellar hemangioblastoma and renal cell carcinoma are the leading causes of death in patients with VHL syndrome.

A fully developed retinal lesion is a spherical orange-red tumor fed by a dilated, tortuous retinal artery and drained by an engorged vein (Fig 7-14). Hemangioblastomas of the optic nerve head and peripapillary region are often flat and difficult to recognize.

Multiple hemangioblastomas may be present in the same eye, and bilateral involvement occurs in 50% of patients. Leakage from a hemangioblastoma may cause decreased vision from macular exudates (Fig 7-15) with or without exudative retinal detachment. Vitreous hemorrhage or traction detachment may also occur.

Ocular management includes destructive treatment of all identified retinal hemangioblastomas with careful follow-up to detect recurrence or the development of new lesions. Successful treatment is facilitated by early diagnosis, because the lesions usually enlarge with time and require repeated sessions for complete ablation. Laser photocoagulation or cryotherapy is used to treat and destroy the angiomatous lesions directly, with an end point of blanching of the vascular structure. Photodynamic therapy with verteporfin can also be used (Fig 7-16). Successful treatment results in shrinkage of the hemangioblastoma,

Figure 7-14 Fundus photograph from a patient with von Hippel-Lindau syndrome shows a peripheral retinal hemangioblastoma with surrounding exudate and retinal detachment. The feeder arteriole and draining venule are dilated.

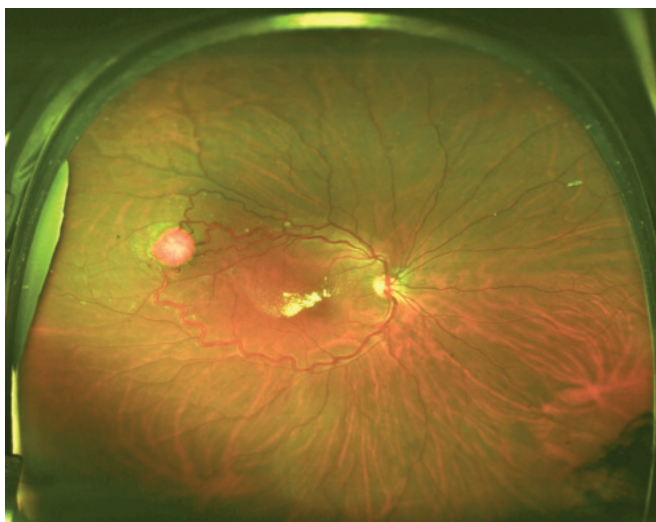
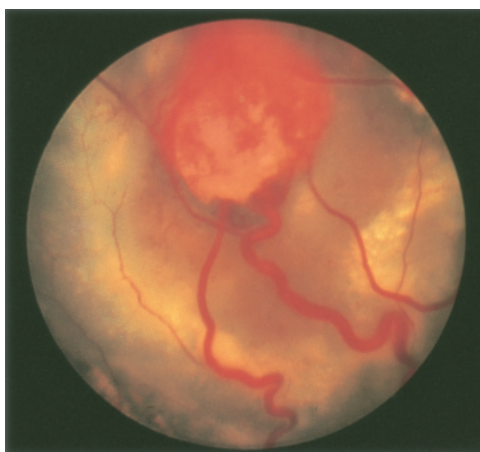


Figure 7-15 Ultra-wide-field fundus photograph from a patient with von Hippel-Lindau syndrome, showing a retinal hemangioblastoma in the near periphery and associated exudative maculopathy. (Courtesy of Colin A. McCannel, MD.)

attenuation of the afferent vessels, and resorption of the subretinal fluid. Cryotherapy may be used to treat larger, especially more peripheral, lesions but can cause a temporary and marked increase in the amount of exudation and sometimes exudative retinal detachment. Anti-VEGF therapy does not usually result in a meaningful, long-term treatment effect.

Retinal hemangioblastomas may also occur sporadically without systemic involvement; these have been called *von Hippel lesions*. Another form of retinal lesions, VPTs (discussed earlier in the chapter), are thought to be reactive astrocytic in nature and may present as a large peripheral vascular mass with surrounding exudation/Coats-like reaction. These acquired lesions do not have the dilated feeder and draining vessels seen with hemangioblastomas. Generally, vasoproliferative lesions are idiopathic and isolated; in rare cases, they may be present as a late complication of ROP, RP, uveitis, or other conditions.

Gaudric A, Krivosic V, Duquid G, Massin P, Giraud S, Richard S. Vitreoretinal surgery for severe retinal capillary hemangiomas in von Hippel–Lindau disease. *Ophthalmology*. 2011;118(1):142–149.

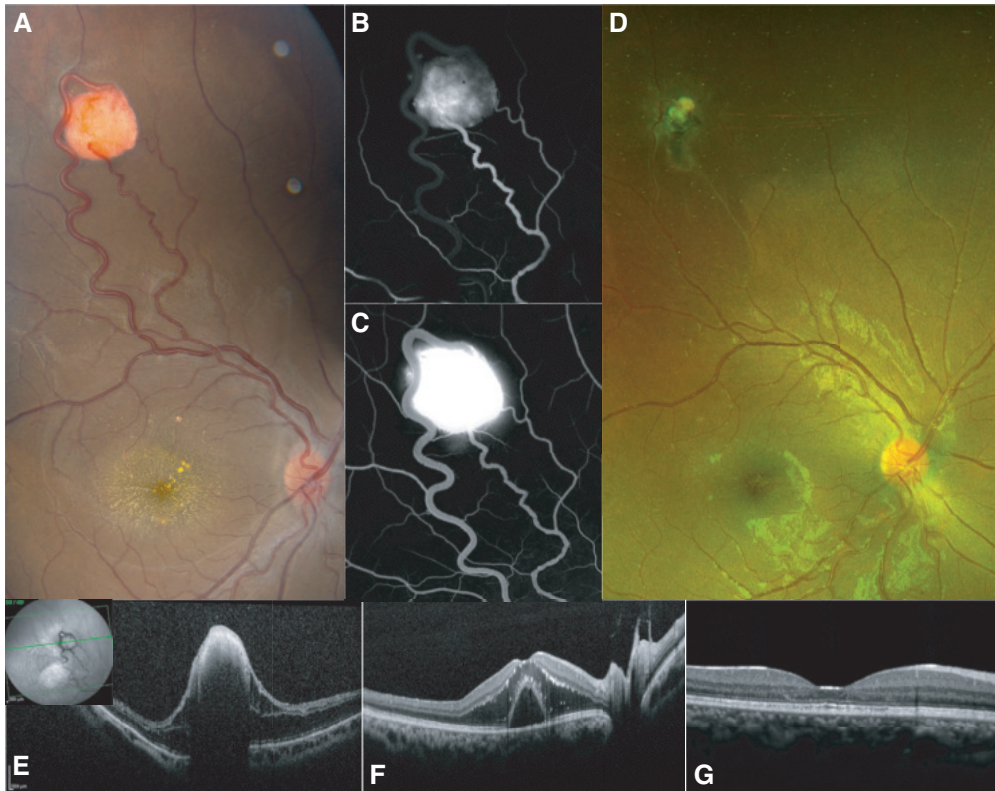


Figure 7-16 Retinal hemangioblastoma (RH). **A**, Classic appearance with dilated feeder vessels, along with hard exudates. Note the large area of fluid in the macula. Classic early-phase (**B**) and late-phase (**C**) FA images showing RH leakage. **D**, Appearance of this tumor after a single photodynamic therapy (PDT) session. Note that the vessel caliber and tortuosity normalize after treatment. **E**, OCT of the tumor itself (*inset* depicts the location of the OCT slice). **F**, Intraretinal and subretinal fluid in the macula at presentation. **G**, Resorption of the fluid following PDT. (Courtesy of Anthony B. Daniels, MD, MSc.)

Wyburn-Mason Syndrome

In Wyburn-Mason syndrome, congenital retinal arteriovenous malformations occur in conjunction with similar ipsilateral vascular malformations in the brain, face, orbit, and mandible. The lesions are composed of blood vessels without an intervening capillary bed (racemose hemangioma). The abnormalities may range from a single arteriovenous communication to a complex anastomotic system. In the eye, the lesions are usually located in the retina and optic nerve and are unilateral and asymptomatic. Typically, they do not show leakage on FA. Intraosseous vascular malformations that may occur in the maxilla and mandible can lead to unexpected hemorrhaging during dental extractions. Most commonly, racemose hemangiomas in the retina are isolated and are not part of the full syndrome (Fig 7-17).

Retinal Cavernous Hemangioma

Although most cases of cavernous hemangioma are sporadic and restricted to the retina or optic nerve head, they may occur in a familial (autosomal dominant) pattern and may be associated with intracranial and skin hemangiomas. For this reason, cavernous hemangioma may be considered one of the phakomatoses.

Retinal cavernous hemangioma is characterized by the formation of grapelike clusters of thin-walled saccular angiomatous lesions in the inner retina or on the optic nerve head (Fig 7-18). The blood flow in these lesions is derived from the retinal circulation and is relatively stagnant, producing a characteristic picture on FA. These dilated saccular lesions fill slowly during angiography, and the sluggish blood flow results in plasma-erythrocyte layering, which is pathognomonic. Fluorescein leakage is characteristically absent, correlating with the absence of subretinal fluid and exudate in the retinal cavernous hemangioma and serving to differentiate the condition from retinal telangiectasia, retinal hemangioblastomas, and racemose hemangioma of the retina.

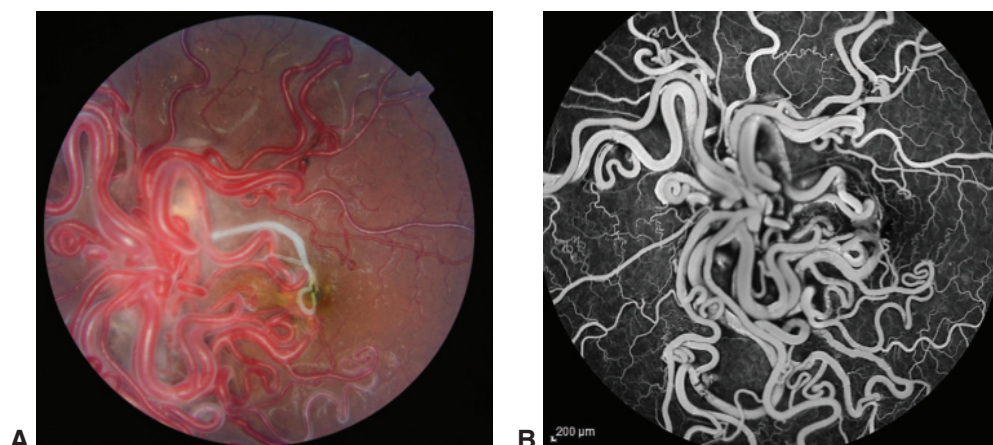


Figure 7-17 **A**, Fundus photograph from a 16-year-old female patient with poor vision in one eye demonstrates racemose angiomas as seen in Wyburn-Mason syndrome. **B**, FA highlights the vascular lesion without fluorescein leakage. (These images were originally published in the *Retina Image Bank*. Caesar K. Luo, MD. Photographs by Joseph Trabucchi. Wyburn Mason. *Retina Image Bank*, 2018; image numbers 28305, 28304. © American Society of Retina Specialists.)

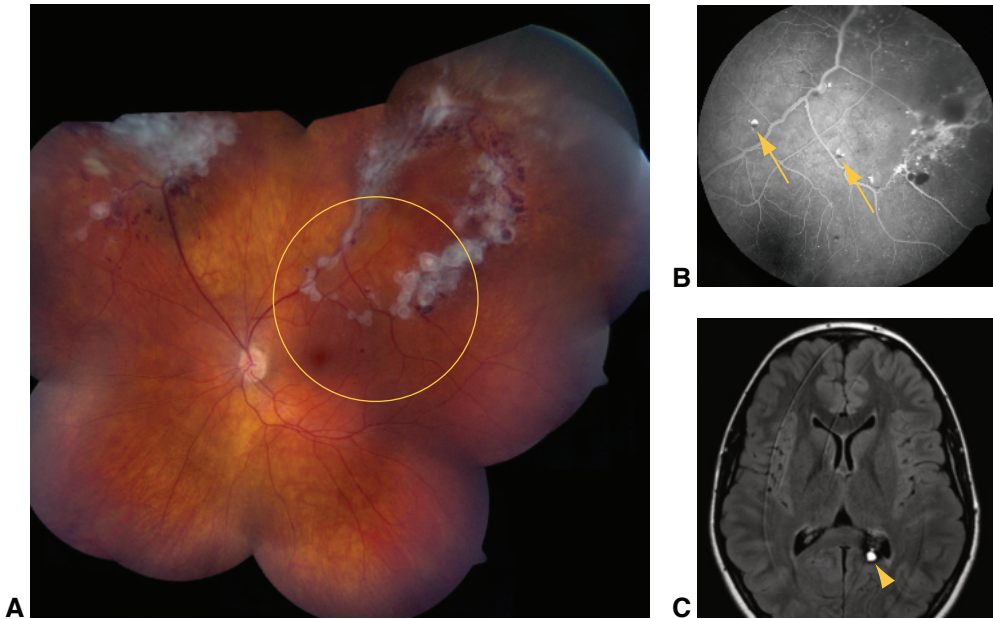


Figure 7-18 Retinal cavernous hemangioma in a 13-year-old girl. **A**, Color fundus image montage of the left eye (right eye was normal) shows superficial gliosis and grapelike clusters of thin-walled saccular angiomatous lesions in the inner retina. **B**, FA (of the area circled in **A**) shows characteristic findings of dilated saccular lesions and plasma-erythrocyte layering (*arrows*) but no leaking because of stagnant blood flow. **C**, Magnetic resonance image (T2 fluid-attenuated inversion recovery) demonstrates an associated left-sided cerebral cavernous hemangioma (*arrowhead*). The patient underwent stereotactic image-guided resection to reduce the risk of intracranial hemorrhage. (Courtesy of Kenneth Taubenslag, MD, and Stephen J. Kim, MD.)

These hemangiomas usually remain asymptomatic but may bleed into the vitreous in rare instances. Treatment of retinal cavernous hemangiomas is usually not indicated unless vitreous hemorrhage recurs, in which case photocoagulation or cryotherapy may be effective. Intracranial hemangiomas may lead to seizures, intracranial hemorrhages, and even death (see Fig 7-18). Neuroimaging should always be done to rule out intracranial involvement. See also BCSC Section 4, *Ophthalmic Pathology and Intraocular Tumors*.

Radiation Retinopathy

Exposure to ionizing radiation can damage the retinal vasculature. Radiation retinopathy typically has a delayed onset, is slowly progressive, and causes microangiopathic changes that clinically resemble diabetic retinopathy. The development of radiation retinopathy depends on dose fractionation and can occur after either external beam or local plaque brachytherapy, typically within months to years after radiation treatment. In general, radiation retinopathy is noted around 18 months after treatment with external beam radiation and earlier after treatment with brachytherapy. Because radiation retinopathy appears very similar to other vascular diseases, eliciting a history of radiation treatment is important in establishing the diagnosis. An exposure to doses of 30–35 grays (Gy) or more is usually

necessary to induce clinical symptoms; occasionally, however, retinopathy may develop after as little as 15 Gy of external beam radiation. Studies have shown retinal damage in 50% of patients receiving 60 Gy and in 85%–95% of patients receiving 70–80 Gy. The total dose, volume of retina irradiated, and fractionation scheme are important in determining the threshold dose for radiation retinopathy. See BCSC Section 4, *Ophthalmic Pathology and Intraocular Tumors*, for further discussion of external beam radiation and brachytherapy.

CLINICAL PEARL

Remember to inquire about previous radiation treatment in patients who present with microvascular changes that mimic diabetic retinopathy.

Clinically, affected patients may be asymptomatic or may describe decreased vision. Ophthalmic examination may reveal signs of retinal vascular disease, including cotton-wool spots, which are foci of axoplasmic stasis in the nerve fiber layer (Fig 7-19); retinal hemorrhages; microaneurysms; perivascular sheathing; capillary telangiectasis; macular edema; and optic nerve head edema. Capillary nonperfusion, documented by FA, is commonly present, and extensive retinal ischemia can lead to neovascularization of the retina, iris, or optic nerve head. Other possible complications include optic atrophy, central retinal artery occlusion, central retinal vein occlusion, choroidal neovascularization, vitreous hemorrhage, neovascular glaucoma, and traction retinal detachment. Visual outcome is primarily related to the extent of the macular involvement with CME, exudative maculopathy, or capillary nonperfusion. Occasionally, vision loss may be caused by acute optic neuropathy.



Figure 7-19 Radiation retinopathy following plaque brachytherapy for choroidal melanoma. Progression of retinopathy over time. **A**, Image shows intraretinal hemorrhages and cotton-wool spots. Compared with other entities (such as diabetes) that can cause intraretinal hemorrhages and cotton-wool spots, radiation retinopathy causes many more of these spots relative to the extent of the hemorrhages. **B**, Eight months later, there is substantial progression of the retinopathy, with increased exudation and subretinal and intraretinal fluid in the macula. Visual acuity declined in the interim. (Courtesy of Anthony B. Daniels, MD, MSc.)

Anti-VEGF agents or steroids may be effective (off-label) treatments for radiation retinopathy. Laser photocoagulation is less effective because it results in retinal atrophy and laser scar expansion.

Patel SJ, Schachat AP. Radiation retinopathy. In: Albert DM, Miller JW, Azar DT, Blodi BA, eds. *Albert & Jakobiec's Principles and Practice of Ophthalmology*. 3rd ed. Saunders; 2008:chap 175.

Valsalva Retinopathy

A sudden rise in intrathoracic or intra-abdominal pressure (eg, as during coughing, vomiting, lifting, or straining for a bowel movement) may increase intraocular venous pressure sufficiently to rupture small superficial capillaries in the macula. The hemorrhage is typically located under the ILM, where it may create a hemorrhagic detachment of the ILM (Fig 7-20), but patients can present with hemorrhage in any layer of the retina. Vitreous hemorrhage

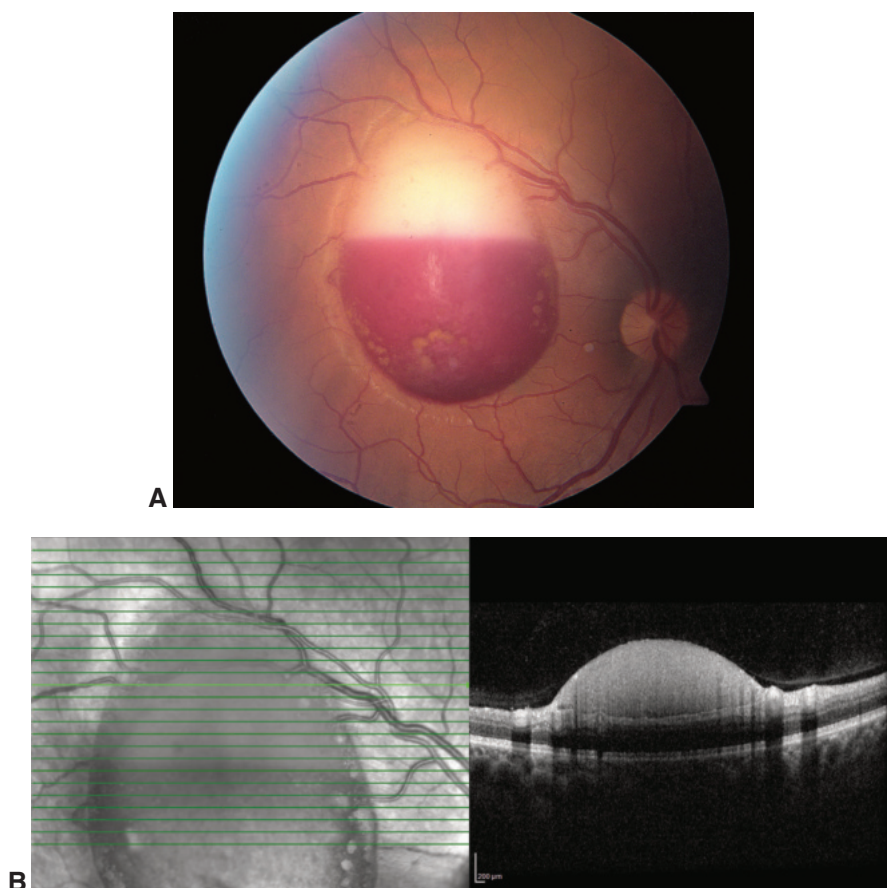


Figure 7-20 Valsalva retinopathy. **A**, Fundus photograph from a 30-year-old man who experienced sudden vision loss after receiving the Heimlich maneuver. **B**, Spectral-domain OCT demonstrates classic hemorrhagic detachment of the internal limiting membrane with corresponding shadowing effect. (Courtesy of Kenneth Taubenslag, MD, and Edward Cherney, MD.)

and subretinal hemorrhage may be present. Vision is usually only mildly reduced, and the prognosis is excellent, with spontaneous resolution usually occurring within months after onset. The differential diagnosis of Valsalva retinopathy includes posterior vitreous separation, which may cause an identical hemorrhage or a macroaneurysm. Therefore, in all cases, a peripheral retinal tear or an aneurysm along an arteriole must be ruled out.

Purtscher Retinopathy and Purtscher-like Retinopathy

After acute compression injuries to the thorax or head, a patient may experience vision loss associated with Purtscher retinopathy in 1 or both eyes (Table 7-3). This retinopathy is characterized by cotton-wool spots, polygonal areas of retinal whitening (Purtscher flecken), hemorrhages, and retinal edema, which are found most commonly surrounding the optic nerve head. FA reveals evidence of arteriolar obstruction and leakage. Occasionally, patients present with optic nerve head edema and an afferent pupillary defect. Vision may be permanently lost from infarction, and optic atrophy may develop.

Purtscher retinopathy is thought to be a result of injury-induced complement activation, which causes granulocyte aggregation and leukoembolization. This process in turn can occlude small arterioles. When the occlusion of a precapillary arteriole affects the radial peripapillary capillary network, cotton-wool spots develop; these areas of retinal whitening have indistinct borders and can obscure or partially overlie retinal blood vessels. When capillaries in lamina deeper than the radial peripapillary network are blocked, the ophthalmoscopic correlate is instead Purtscher flecken, which manifest as intraretinal whitening with a clear zone on either side of the retinal arterioles, venules, and precapillary arterioles.

Various other conditions may activate complement and produce a similar fundus appearance. Purtscher's original description involved trauma; cases not involving trauma but with similar fundus findings are therefore termed *Purtscher-like retinopathy* (Fig 7-21; see Table 7-3).

Table 7-3 Conditions Associated With Purtscher or Purtscher-like Retinopathy

Acute pancreatitis
Amniotic fluid embolism
Autoimmune diseases
Chest compression
Chronic renal failure
Dermatomyositis
Early postpartum state
Head injury
Long-bone fractures (fat embolism syndrome)
Orbital steroid injection
Retrobulbar anesthesia
Scleroderma
Sjögren syndrome
Systemic lupus erythematosus
Thrombotic thrombocytopenic purpura
Trauma

Modified with permission from Regillo CD. Posterior segment manifestations of systemic trauma. In: Regillo CD, Brown GC, Flynn HW Jr, eds. *Vitreoretinal Disease: The Essentials*. Thieme; 1999:538. www.Thieme.com

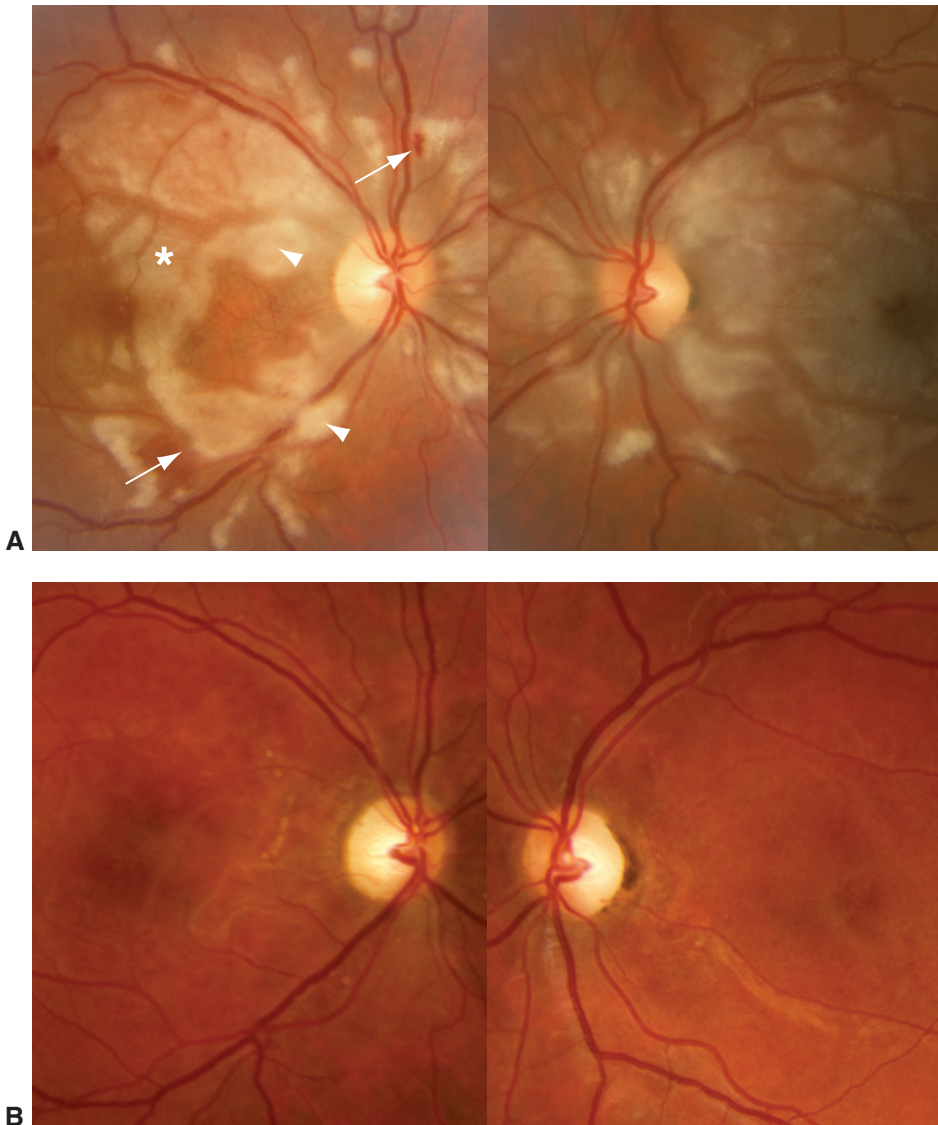


Figure 7-21 Purtscher-like retinopathy. **A**, Fundus photographs from a 20-year-old woman were taken 1 day after an uncomplicated delivery of a healthy baby. The patient had noted profound, persistent bilateral vision loss beginning 1 hour after parturition. Intraretinal hemorrhages (*arrows*) and bright, superficial cotton-wool spots (*arrowheads*) were present, in addition to extensive areas of well-demarcated Purtscher flecken (*asterisk*) with characteristic sparing of the perivascular retina. The flecken are likely the result of occlusion of the precapillary arterioles. The location of these flecken and cotton-wool spots surrounding the optic nerve head is characteristic and distinguishes this entity from other ischemic conditions. **B**, Corresponding fundus photographs taken 4 years later demonstrate optic atrophy and deep macular pigmentary atrophy. Visual acuity was 20/200 OD and 20/800 OS. (Courtesy of Brian Leonard, MD.)

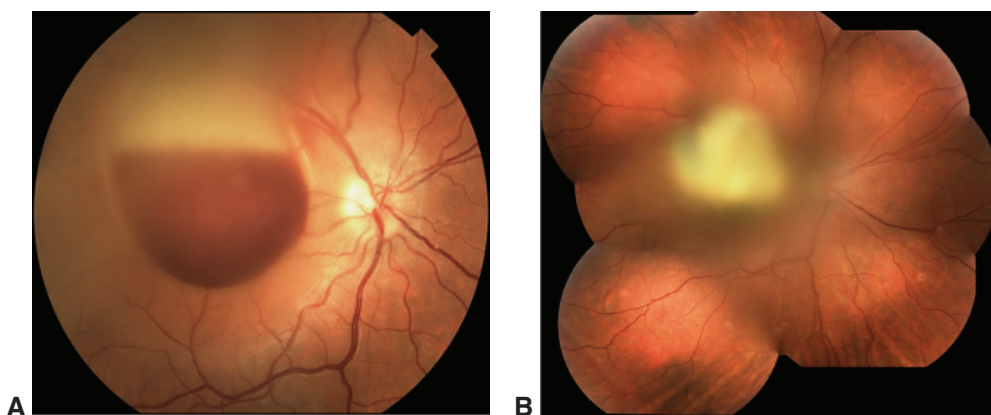


Figure 7-22 Fundus photographs from an 18-year-old male who presented with central blurred vision in his right eye after traumatic brain injury (due to a skateboarding accident), occipital skull fracture, and right-sided subdural and epidural hematoma. **A**, Image from the initial presentation shows a premacular (subhyaloid) hemorrhage. **B**, Over the following 3 weeks, the hemorrhage dispersed into the vitreous cavity. (Courtesy of Brian C. Joondeph, MD, MPS.)

For example, the retinopathy associated with acute pancreatitis, which appears identical to traumatic Purtscher retinopathy, is probably also caused by complement-mediated leuko-embolization. Other conditions that may cause these changes include collagen vascular diseases (such as systemic lupus erythematosus), early postpartum state, and amniotic fluid embolism. Fat embolism following crush injuries or long-bone fractures may cause similar retinal findings.

Terson Syndrome

Terson syndrome is recognized as a vitreous and sub-ILM or subhyaloid hemorrhage caused by an abrupt intracranial hemorrhage (Fig 7-22). Although the exact mechanism is not known, it is suspected that the acute intracranial hemorrhage causes an acute rise in the intraocular venous pressure, resulting in a rupture of peripapillary and retinal vessels. Approximately one-third of patients with subarachnoid or subdural hemorrhage have associated intraocular hemorrhage, which may include intraretinal and subretinal bleeding. In most cases, visual function is unaffected once the hemorrhage clears. Spontaneous improvement generally occurs, although vitrectomy is occasionally required to clear the ocular media.

Agarwal A. *Gass' Atlas of Macular Diseases*. 5th ed. Saunders; 2012:724–726.

CHAPTER 8

Retinopathy of Prematurity



This chapter includes related videos. Go to www.aaopt.org/bcscvideo_section12 or scan the QR codes in the text to access this content.



This chapter also includes a related activity. Go to www.aaopt.org/bcscactivity_section12 or scan the QR code in the text to access this content.

Highlights

- Retinopathy of prematurity (ROP) is the arrest of normal retinal vascular development in the preterm infant, with compensatory mechanisms that produce aberrant vascularization of the retina.
- In most infants, ROP follows a predictable course of onset, progression, and resolution that is closely tied to gestational age, not postnatal (also called *chronologic*) age.
- The level of ROP for which treatment is recommended is currently termed *type 1 ROP*.

Introduction

Retinopathy of prematurity is a complex disease process in preterm infants initiated in part by incomplete or abnormal retinal vascularization. When normal vascular growth (ie, *vasculogenesis*) is disturbed, new vessels proliferate (ie, *angiogenesis*) into the vitreous cavity at the border of the vascular and avascular retina. Left untreated, ROP culminates in the development of a dense, white, fibrovascular plaque behind the lens and complete traction retinal detachment (this end stage is reflected in the former name for ROP, *retrolental fibroplasia*).

The main risk factors for ROP are prematurity and low birth weight. See BCSC Section 6, *Pediatric Ophthalmology and Strabismus*, for additional discussion of ROP.

Epidemiology

Premature birth is defined as any delivery before 37 weeks of gestation, whereas delivery before 32 weeks of gestation is generally associated with the development of retinal disease. In the United States, according to the National Institutes of Health, approximately 80,000 infants are at risk for ROP each year, and approximately 1100–1500 have disease that is severe enough to require treatment. Among these infants, 400–600 will never achieve visual acuity better than 20/200. Globally, an estimated 50,000 children younger

than 15 years are blind because of complications of ROP. The prevalence is highest in the poorest countries of Latin America, southeast Asia, and Africa. In these resource-limited regions, the rise in cases of ROP corresponds to increased survival rates among at-risk preterm infants.

In a study by the Cryotherapy for Retinopathy of Prematurity Cooperative Group, some signs of ROP were present in 66% of infants with a birth weight of ≤ 1250 g and in 82% of infants with a birth weight of < 1000 g. Progression to treatment-requiring ROP occurred in approximately 10% of infants with a birth weight of ≤ 1250 g, but up to 50% of infants with a birth weight of ≤ 500 g.

Palmer EA, Flynn JT, Hardy RJ, et al. Incidence and early course of retinopathy of prematurity. The Cryotherapy for Retinopathy of Prematurity Cooperative Group. *Ophthalmology*. 1991;98(11):1628–1640.

Classification, Terminology, and Clinical Features

Normal retinal vascularization begins at approximately week 16 of gestation, with vessel growth proceeding from the optic nerve head to the periphery. Vascularization is completed nasally by approximately 36 weeks' gestation and temporally by 40 weeks' gestation. Thus, a child born prematurely (typically before 32 weeks of gestation) is at risk for ROP.

To formalize discussion of the clinical aspects of ROP and to standardize and support research into ROP, a necessary lexicon of clinical descriptors was developed. This lexicon, the International Classification of ROP (ICROP), was introduced in 1984 and revised in 2005 and most recently in 2021. The original ICROP group introduced 4 defining concepts for ROP: the *location*, or *zone*, of involvement; the *extent* of disease (measured in clock-hours); the disease *severity*, or stage; and the presence or absence of *plus disease*, which is defined as the presence of dilatation and tortuosity of vessels in zone I (see Table 8-1 and accompanying Figs 8-1 through 8-8).

As an extension of these concepts, the following diagnostic terminology can be used to further classify ROP, which can help clinicians optimize management and treatment decisions (Table 8-2):

- The term *threshold ROP* was coined in the mid-1980s by investigators in the Cryotherapy for ROP (CRYO-ROP) study to define disease with equal chances of spontaneous regression or progression to an unfavorable outcome. Threshold disease is characterized by at least 5 contiguous clock-hours of extraretinal neovascularization or 8 cumulative clock-hours of extraretinal neovascularization with plus disease as well as retinal vessels ending in zone I or II.
- The term *prethreshold disease* was introduced in the early 2000s with the Early Treatment for Retinopathy of Prematurity (ETROP) study. Prethreshold disease is further divided into high-risk prethreshold, or type 1, ROP and lower-risk prethreshold, or type 2, ROP (see Table 8-2 for a detailed description). In current practice, type 1 ROP is the point at which treatment is indicated (Activity 8-1).

Table 8-1 Classification of Acute Retinopathy of Prematurity**Location**

Zone I: posterior retina within a circle (the radius of which is twice the estimated distance between the optic nerve head center and foveal center) centered on the optic nerve

Zone II: annulus centered on the nerve extending from zone I to the nasal ora serrata

Zone III: remaining crescent of temporal peripheral retina

Extent: number of clock-hours involved (from 1 to 12)

Severity

Stage 0: immature retinal vasculature without pathologic changes (see Fig 8-1)

Stage 1: a flat, thin, white *demarcation line* between vascularized and avascular retina (see Fig 8-2); abnormal branching or dilatation of the retinal vessels may lead up to the line

Stage 2: a demarcation line that has height, width, and volume (*ridge*); small, isolated tufts of neovascular tissue lying on the surface of the retina, commonly called *popcorn*, may be seen posterior to the ridge (see Fig 8-3)

Stage 3: a ridge with extraretinal fibrovascular proliferation infiltrating the vitreous (see Fig 8-4)

Stage 4: a partial retinal detachment (see Fig 8-5)

A: extrafoveal

B: retinal detachment including the fovea

Stage 5: total retinal detachment (see Fig 8-6)

A: optic nerve head is visible by ophthalmoscopy (suggesting open-funnel configuration of retinal detachment)

B: optic nerve head is not visible by ophthalmoscopy (due to retrolental fibrosis or a closed-funnel retinal detachment)

C: abnormalities of the anterior segment accompanying stage 5B

Plus disease: vascular dilatation (venous) and tortuosity (arteriolar or venous) of the retinal vessels within zone I; iris vascular dilatation and vitreous haze may be present (see Fig 8-7; see also Fig 8-4B)

Aggressive ROP (also referred to as *Rush disease* and *aggressive posterior ROP*): a rapidly progressive, severe form of ROP often (but not always) characterized by posterior location, prominent plus disease, and sometimes iris rubeosis; the peripheral retinopathy may be ill-defined (see Fig 8-8)

ROP = retinopathy of prematurity.

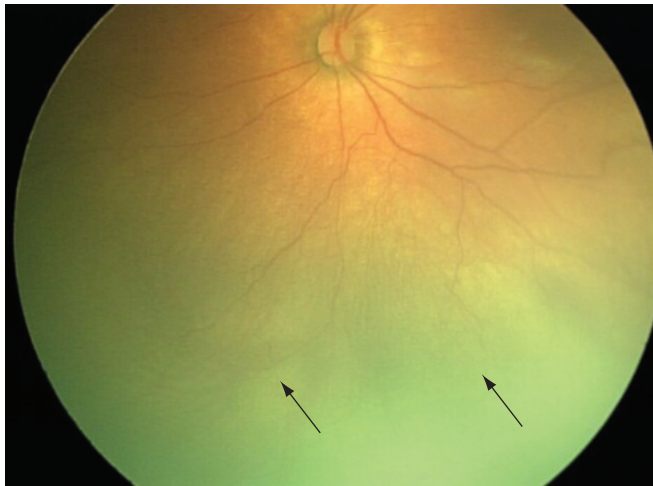


Figure 8-1 Fundus photograph demonstrating immature retinal vascularization (stage 0 ROP). Note the progressive tapering and eventual disappearance of retinal vessels (*arrows*) as they course peripherally. ROP = retinopathy of prematurity. (Courtesy of Franco M. Recchia, MD.)



Figure 8-2 Stage 1 ROP. Fundus photograph reveals a faint white demarcation line temporally (*arrows*). Arborizing, dilated vessels approach the line, and a choroidal vessel is seen extending to the periphery (*arrowheads*). (Courtesy of Franco M. Recchia, MD.)

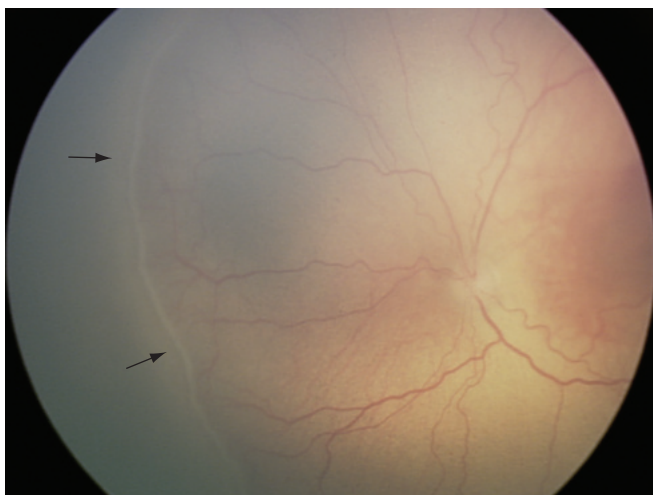


Figure 8-3 Stage 2 ROP. Fundus photograph shows an elevated gray-white ridge (*arrows*) at the border of the vascularized (*rosy*) and avascular (*grayish*) retina. (Courtesy of Franco M. Recchia, MD.)

- **Aggressive ROP (A-ROP;** previously referred to as *Rush disease* and *aggressive posterior ROP [AP-ROP]*) is characterized by the rapid development of pathologic neovascularization and severe plus disease without progression through the typical stages of ROP. Hemorrhages at the junction of the vascular and avascular retina, as well as iris rubeosis, may be seen (see Fig 8-8). The vascular-avascular junction

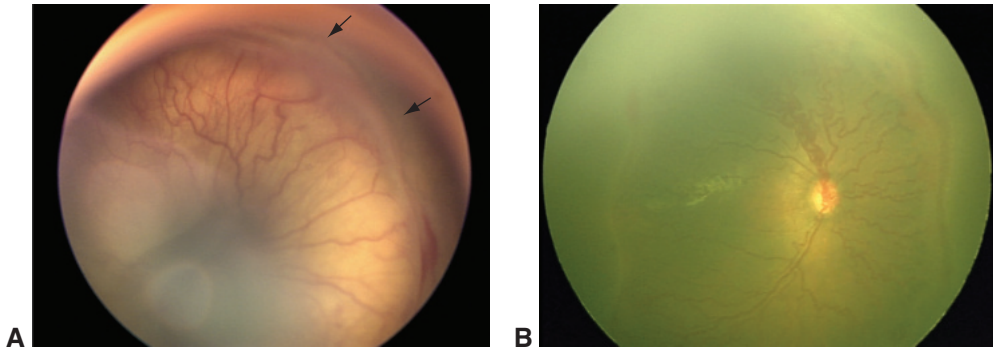


Figure 8-4 Stage 3 ROP. **A**, Fundus photograph shows fibrovascular tissue (arrows) extending from the surface of the retina into the vitreous and preretinal hemorrhage (lower right). **B**, Fundus photograph shows an elevated circumferential fibrovascular ridge and marked plus disease (dilation and tortuosity of all posterior vessels). (Part A courtesy of Colin A. McCannel, MD; part B courtesy of Franco M. Recchia, MD.)

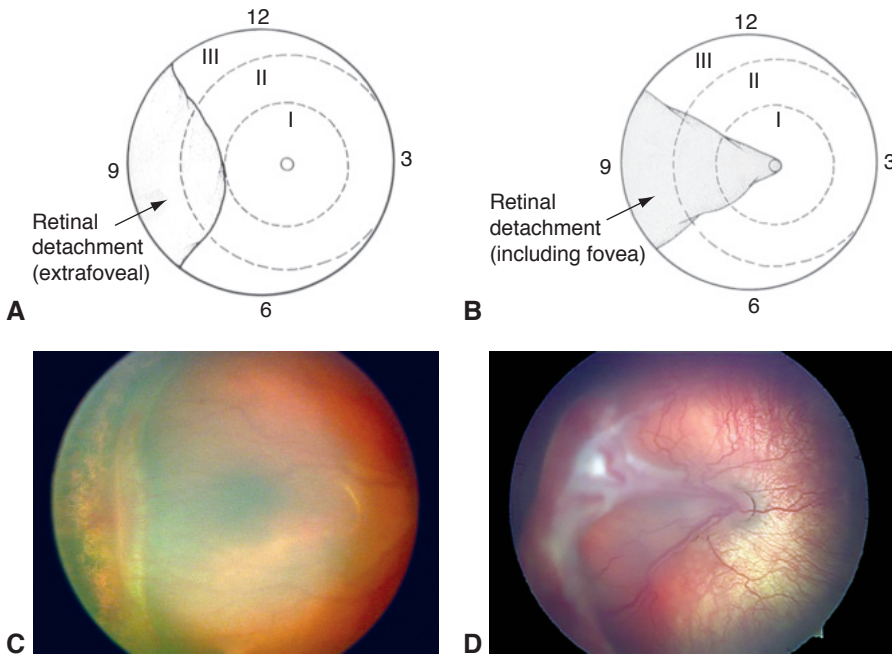


Figure 8-5 Stage 4 ROP. Schematic representations show stage 4A (**A**) and stage 4B (**B**). The roman numerals in each circle indicate the zones, per the international classification, and the arabic numerals indicate clock-hours. Wide-angle clinical photographs of stage 4A (**C**) and stage 4B (**D**) correspond to the schematic diagrams. (Parts A and B courtesy of J. Arch McNamara, MD; parts C and D courtesy of Audina Berrocal, MD.)

may be deceptively featureless, with neovascularization appearing only as a flat network of fine vessels that may be confused with underlying choroid (Fig 8-9). This phenomenon is not restricted to the posterior retina or to the smallest infants, as originally thought.

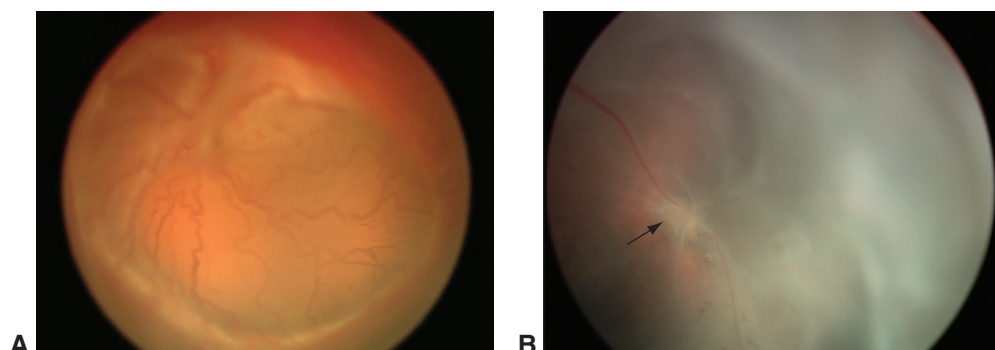


Figure 8-6 Stage 5 ROP. Wide-angle fundus photographs show total ROP retinal detachment (RD). **A**, Total RD with visible optic nerve head is now defined as stage 5A. Persistent vascular activity accompanies the preretinal fibrovascular ridge that contracts circumferentially, acting like a purse string. **B**, Eventually, the vascular activity subsides, and the fibrosis starts to close the funnel anteriorly (evolution into stage 5B). The arrow denotes the optic nerve head, which is almost completely obscured. (Part A courtesy of Audina Berrocal, MD; part B courtesy of Franco M. Recchia, MD.)

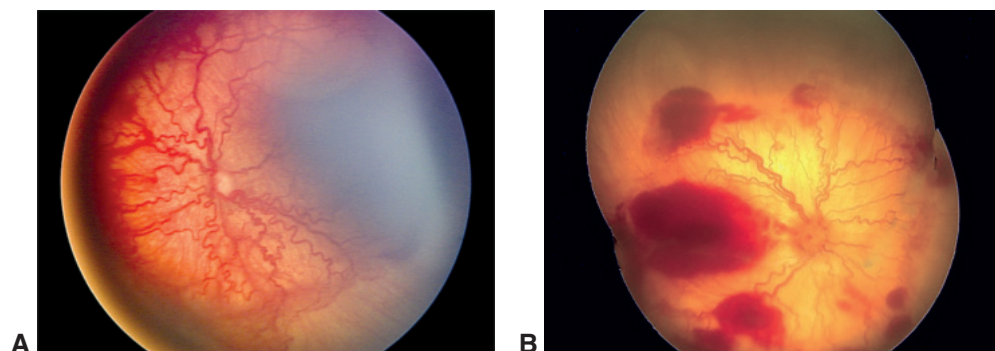


Figure 8-7 Fundus photographs show pronounced plus disease in eyes with ROP. The retinal arteries and veins are dilated and tortuous. **A**, The avascular retina and preretinal proliferations can be seen inferiorly and inferotemporally (*bottom right*). **B**, Preretinal hemorrhages are visible, originating from the proliferative disease. (Part A courtesy of Colin A. McCannel, MD; part B courtesy of Audina Berrocal, MD.)

According to the ICROP, an eye is classified on the basis of the most advanced disease noted. However, documentation should reflect all affected zones and stages observed, including their relative extent.



ACTIVITY 8-1 Interactive schematic for type 1 ROP.

Developed by Franco M. Recchia, MD.



Chiang MF, Quinn GE, Fielder AR, et al. International Classification of Retinopathy of Prematurity, 3rd ed [epub ahead of print, July 8, 2021]. *Ophthalmology*. 2021;128(10):e51–e68. doi:10.1016/j.opthta.2021.05.031

Early Treatment for Retinopathy of Prematurity Cooperative Group. Revised indications for the treatment of retinopathy of prematurity: results of the Early Treatment for Retinopathy of Prematurity randomized trial. *Arch Ophthalmol*. 2003;121(12):1684–1694.

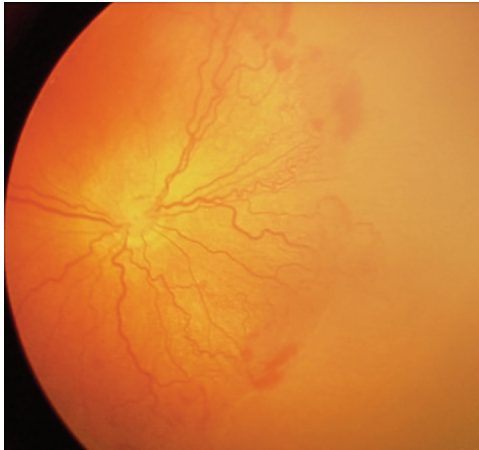


Figure 8-8 Aggressive ROP (A-ROP). Fundus photograph shows prominent plus disease and ill-defined retinopathy in zone I, accompanied by blot hemorrhages. (Courtesy of Franco M. Recchia, MD.)

Table 8-2 Common Terms Used in Clinical Trials to Describe Acute Retinopathy of Prematurity (ROP)

Threshold disease (all 3 features must be present)

Extraretinal neovascularization (stage 3 disease): EITHER 5 contiguous clock-hours
OR 8 cumulative clock-hours
Retinal vessels ending within zone I or zone II
Plus disease

Prethreshold disease

All zone I and zone II changes, except zone II stage 1 and zone II stage 2 without plus disease, that do not meet threshold treatment criteria; subdivided into type 1 and type 2 disease

Type 1 ROP

Zone I, any stage ROP with plus disease, or
Zone I, stage 3 ROP without plus disease, or
Zone II, stage 2 or 3 ROP with plus disease

Type 2 ROP

Zone I, stage 1 or 2 ROP without plus disease, or
Zone II, stage 3 ROP without plus disease

International Committee for the Classification of Retinopathy of Prematurity. The International Classification of Retinopathy of Prematurity revisited. *Arch Ophthalmol.* 2005; 123(7):991–999.

Pathophysiology of ROP

A link between excessively exuberant perinatal oxygen supplementation and severe ROP was well recognized by the 1950s. After substantial reductions in oxygen use in neonatal intensive care units (NICUs), the incidence of ROP decreased dramatically. However, many infants experienced adverse neurologic outcomes as an unintended consequence of that oxygen restriction, and infant death rates rose. Once oxygen was again used more liberally, neurologic outcomes and survival improved, with the consequence of a resurgence of ROP.

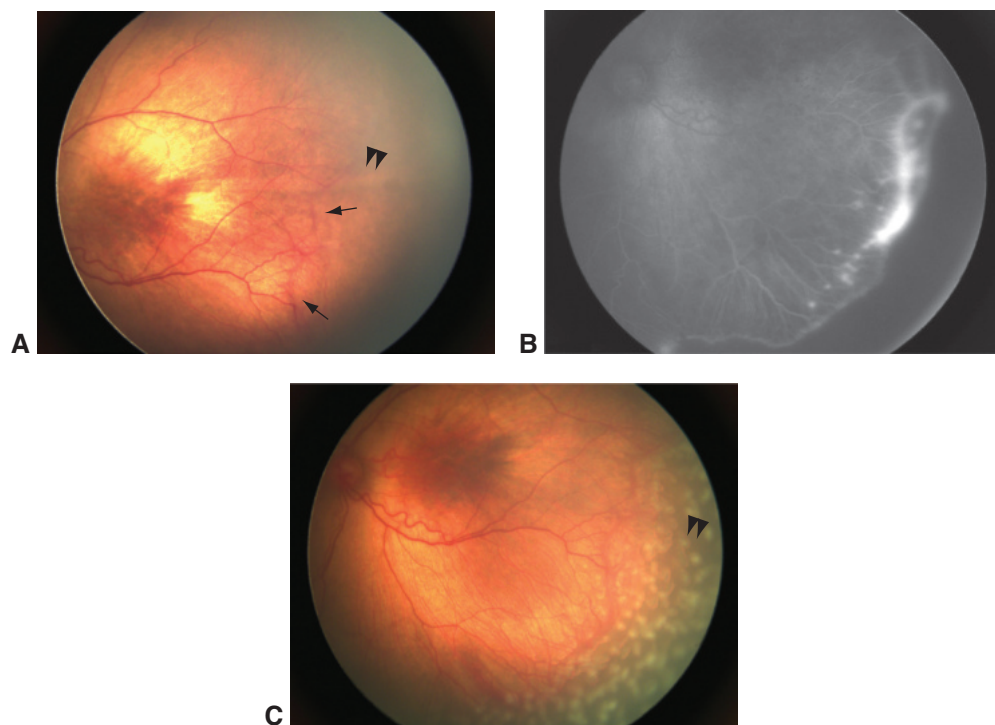


Figure 8-9 Type 1 ROP (stage 3, zone II) treated with peripheral laser photocoagulation. **A**, Color fundus photograph shows the long posterior ciliary nerve (*arrowheads*) and flat neovascularization in posterior zone II temporally (*arrows*), which is identified definitively by the areas of leakage on the corresponding fluorescein angiogram (**B**). **C**, Color photograph taken immediately after laser treatment. Note that treatment abuts the ridge and is intentionally more sparse in the region of the long posterior ciliary nerve (*arrowheads*) to minimize damage to the nerve. (Courtesy of Franco M. Recchia, MD.)

Since then, converging lines of experimental and clinical evidence suggest that the disease proceeds in 2 phases linked in large part to fluctuations in retinal oxygenation:

- *Phase 1* of ROP occurs from birth until approximately 31 weeks of gestational age, when there is relative hyperoxia compared with the typical intrauterine environment. The relative hyperoxia leads to a lower demand for retinal oxygenation and a subsequent arrest in retinal blood vessel growth. This cessation in vessel growth is largely due to a decrease in the levels of hormones and growth factors that govern normal vascular development in the eye, such as vascular endothelial growth factor (VEGF) and insulin-like growth factor 1 (IGF-1).
- *Phase 2* of ROP begins over the ensuing weeks (typically by 32–34 weeks' gestational age). Increased metabolic demands in the retina coupled with insufficient oxygenation (due to the suppression of vessel growth in phase 1) lead to relative hypoxia, which then induces increased retinal production of growth factors (particularly VEGF). This leads to the proliferation of abnormal blood vessels, and oxidative damage to endothelial cells, which leads to disorganized vascular growth.

The onset of phase 2 corresponds to the clinical appearance of ROP on ophthalmoscopy and is closely correlated with the infant's gestational age, rather than his or her postnatal age. Initially, this process causes the formation of visible flat or raised whitish tissue (ROP stages 1 [flat line] and 2 [ridge]). As the disease progresses, vascular growth proliferates into the vitreous cavity (ROP stage 3). In this vasoproliferative phase, new vessels varying widely in size and extent arise from retinal vessels just posterior to the peripheral ridge. These abnormal new vessels easily bleed, leading to vitreous hemorrhage, and may induce contracture of the firmly attached vitreous gel. Eventually, growth factor and hormonal changes cause involution and fibrosis of the blood vessels with cicatricial contraction that may lead to traction (also called *tractional*) retinal detachment (ROP stages 4 and 5).

Hartnett ME, Penn JS. Mechanisms and management of retinopathy of prematurity. *N Engl J Med*. 2012;367(26):2515–2526.

Natural Course

Although the precise systemic and/or local tissue factors that influence progression and regression of ROP are not known, the time course is predictable. ROP is typically a transient disease that regresses spontaneously in most infants, particularly those with heavier birth weights (closer to 1500 g) and older gestational age (closer to 32 weeks) at birth. In general, eyes with ROP in zone III have a good visual prognosis. In contrast, the more posterior the zone at the time of diagnosis, the greater the area of nonperfused retina and thus the more worrisome the prognosis.

Screening Recommendations

Screening for ROP consists of a dilated fundus examination using binocular indirect ophthalmoscopy. Use of a topical anesthetic and an eyelid speculum facilitates examination. The pupils should be examined for failure to dilate and the iris inspected for vessel engorgement or frank rubeosis, as these may be signs of aggressive disease. In addition, the optic nerve should be evaluated for plus disease and the periphery examined with scleral depression to establish the extent of vessel growth.

Alternatively, telemedicine (ie, photographic) screening approaches may replace the indirect ophthalmoscopic examination (see the section Fundus Photographic Screening of ROP). However, clinicians should be aware that telemedicine screening criteria developed in one country may not apply in another country, especially when the level or quality of available medical or perinatal care is not comparable.

Screening Criteria

All infants with a birth weight <1500 g or a gestational age of ≤30 weeks should be screened for ROP. Infants with a birth weight between 1500 and 2000 g or a gestational age >30 weeks who have an unstable clinical course and are considered by their attending pediatrician or neonatologist to be at high risk for the disease should also be screened. The

first examination is generally performed at a postnatal age of between 4 and 6 weeks or, alternatively, between 31 and 33 weeks' gestational or postmenstrual age, whichever is later.

Newer neonatal algorithms, such as WINROP (Weight, Insulin-like growth factor-I, Neonatal, ROP), can identify infants at highest risk for ROP as early as 6 weeks before the onset of clinical findings of ROP through a calculation using birth weight, rate of postnatal weight gain, levels of IGF-1 and IGF-binding proteins, and other factors. Conversely, they may also predict which infants will not develop ROP and may not require examination despite meeting the conventional screening criteria. These algorithms are a useful adjunct to standard screening criteria and are being used with increasing frequency worldwide.

Screening Intervals

After each patient evaluation for ROP, disease features dictate the follow-up interval (eg, more severe disease indicates a shorter follow-up interval).

Follow up in 1 week or less

- zone I: immature vascularization only (stage 0);
- zone I: stage 1 or stage 2 ROP;
- immature retina (stage 0) extending into posterior zone II, near the boundary of zone I and zone II;
- suspected A-ROP; and
- stage 3 ROP: zone I requires treatment not observation

Follow up in 1–2 weeks

- posterior zone II: immature vascularization (stage 0);
- zone II: stage 2 ROP; and
- zone I: unequivocally regressing ROP

Follow up in 2 weeks

- zone II: stage 1 ROP;
- zone II: immature vascularization (stage 0); and
- zone II: unequivocally regressing ROP

Follow up in 2–3 weeks

- zone III: stage 1 or 2 ROP; and
- zone III: regressing ROP

Retinal screening examinations are usually discontinued when any one of the following criteria is met:

- full retinal vascularization (ie, vascularization ending within 1 disc-diameter of the ora serrata; this criterion should be used for all patients with ROP treated with intravitreal anti-VEGF medications alone)
- zone III retinal vascularization attained without previous zone I or II ROP
- postmenstrual age of 45 weeks and no type 1 ROP (ie, as stage 3 ROP in zone II or any ROP in zone I) or more severe ROP

- postmenstrual age of at least 65 weeks in patients for whom intravitreal anti-VEGF medications caused regression of ROP (ie, this treatment alters the natural history of the disease); because very late recurrences of proliferative ROP have been reported, clinical judgment and caution should be used on a case-by-case basis to determine when surveillance can be safely terminated in these patients
- regression of ROP (care must be taken to confirm the absence of abnormal vascular tissue that could reactivate)

Fierson WM; American Academy of Pediatrics Section on Ophthalmology; American Academy of Ophthalmology; American Association for Pediatric Ophthalmology and Strabismus; American Association of Certified Orthoptists. Screening examination of premature infants for retinopathy of prematurity. *Pediatrics*. 2018;142(6). doi:10.1542/peds.2018-3061 [Published correction appears in *Pediatrics*. 2019;143(3):320183810.]

Fundus Photographic Screening of ROP

Ultra-wide-angle (120°) fundus photography is useful for documenting disease in premature infant eyes, for assessing disease progression, and for screening. Given shortages of willing examiners skilled in indirect ophthalmoscopy and ROP screening, remote screening of photographic fundus images (ie, telemedicine) has efficiently and cost-effectively improved access to eye care for premature infants at high risk for ROP, providing real-time diagnosis and improving documentation. For detection of plus disease and disease requiring treatment, photoscreening by experienced personnel is comparable to binocular indirect ophthalmoscopy, which is considered the gold standard for ROP screening examinations.

To help identify patients who require an in-person examination after photoscreening, the Photographic Screening for Retinopathy of Prematurity (Photo-ROP) Cooperative Group established a definition of *clinically significant ROP* based on features detectable by photography:

- zone I, any ROP without plus disease
- zone II, stage 2 with no plus disease or up to 1 quadrant of plus disease
- zone II, stage 3 with no plus disease or up to 1 quadrant of plus disease

In addition, more advanced approaches to interpretation of fundus photographs, such as electronic image recognition and deep learning algorithms, are under study.

Daniel E, Quinn GE, Hildebrand PL, et al; e-ROP Cooperative Group. Validated system for centralized grading of retinopathy of prematurity: telemedicine approaches to Evaluating Acute-Phase Retinopathy of Prematurity (e-ROP) study. *JAMA Ophthalmol*. 2015;133(6):675–682.

Prevention and Risk Factors

Preventing ROP begins with preventing prematurity through optimal prenatal, perinatal, and postnatal care. During the postnatal clinical course, factors that appear to increase the risk of severe ROP include sepsis, blood transfusion, intraventricular hemorrhage, necrotizing enterocolitis, and slow weight gain.

Alteration of oxygenation levels as the infant grows is thought to modify the course of ROP. In keeping with the two-phase pathophysiology of ROP (discussed earlier), some researchers have suggested that oxygen saturation should be decreased during phase 1 ROP, when the infant's oxygen requirements are lower, whereas oxygenation should be increased during phase 2 to meet the infant's growing demands. Aggressive parenteral nutrition has reduced the risk of less severe ROP but not severe ROP. Supplementation with vitamins A and E, inositol, or breast milk also appears to reduce the incidence of ROP but only in observational studies, whereas use of transfusion guidelines, erythropoietin, and antifungal agents showed no benefit.

Fang JL, Sorita A, Carey WA, Colby CE, Murad MH, Alahdab F. Interventions to prevent retinopathy of prematurity: a meta-analysis. *Pediatrics*. 2016;137(4):e20153387. doi:10.1542/peds.2015-3387

Kim SJ, Port AD, Swan R, Campbell JP, Chan RVP, Chiang MF. Retinopathy of prematurity: a review of risk factors and their clinical significance. *Surv Ophthalmol*. 2018;63(5):618–637.

Treatment of Acute ROP

In 1988, the multicenter CRYO-ROP study demonstrated that ablation of the avascular anterior retina reduced the incidence of unfavorable outcomes by approximately one-half in eyes with threshold ROP (Table 8-3). Although this finding represented a major advance, nearly one-fourth of eyes still experienced unfavorable outcomes with treatment; eyes with posterior disease had the worst outcomes. Also in the late 1980s, the introduction of portable laser units coupled with an indirect ophthalmoscope offered a promising alternative for treating the peripheral retina with photocoagulation.

To examine whether early ablation of the avascular retina improves visual and structural outcomes in infants with bilateral, high-risk, prethreshold ROP, the ETROP trial randomly assigned 1 eye to early laser photocoagulation and the fellow (ie, control) eye to conventional management per the CRYO-ROP study. High-risk disease was determined using a computational model based on the natural history cohort of the CRYO-ROP study. The ETROP group determined that in infants with high-risk prethreshold ROP, earlier treatment was associated with reduced rates of unfavorable functional and structural outcomes. For risk assessment of prethreshold eyes, the study also determined that clinical categorization of eyes as having either type 1 or type 2 ROP achieved results very similar to those of the computational model. The authors concluded that treatment should be initiated in eyes with the following retinal findings characteristic of type 1 ROP:

- zone I ROP: any stage with plus disease;
- zone I ROP: stage 3, no plus disease; and
- zone II ROP: stage 2 or 3 with plus disease

The authors also suggested that eyes meeting the criteria for type 1 ROP should be considered for peripheral retinal laser treatment, whereas those meeting the criteria for type 2 ROP may be monitored at short intervals. When eyes with type 2 ROP progress to type 1 ROP or to threshold ROP, laser ablative treatment may be considered.

Table 8-3 Summary of Multicenter Clinical Trials That Guide Current Treatment of Acute ROP

Study Name (Year Enrollment Completed)	Outcome Measure(s)	Number of Eyes Assessed for Primary Outcome	Trials of Peripheral Retinal Ablation			Main Conclusions	Comments
			Randomization Point	Treatment Arms			
Cryotherapy for Retinopathy of Prematurity; CRYO-ROP (1987)	(1) Unfavorable structural outcome at 1 year (defined as the presence of a macular fold, RD involving zone I, or obscuration of the posterior pole by cataract or retrolental fibrosis)	291	Threshold disease	(a) Observation (b) Peripheral cryotherapy	Unfavorable structural outcomes occurred in 48% of observed eyes vs 26% of treated eyes. Unfavorable functional outcomes occurred in 56% of observed eyes vs 35% of treated eyes.	Findings were consistent through 15 years of follow-up. Long-term risk of RD increased in all eyes throughout follow-up.	
	(2) Unfavorable functional outcome at 1 year (Snellen equivalent of 20/200 or worse)						
The Early Treatment for Retinopathy of Prematurity Study; ETROP (2002)	(1) Unfavorable functional outcome at 9 months	657 (718 randomized enrolled)	High-risk prethreshold disease ^a	(a) Immediate laser photocoagulation to peripheral retina (361 eyes) (b) Conventional treatment (delay of laser until reaching threshold disease) (357 eyes)	Earlier treatment was associated with a reduction in unfavorable visual acuity outcomes (from 19.5% to 14.5%) and a reduction in unfavorable structural outcomes (from 15.6% to 9.1%).	The rate of cardiopulmonary complications was higher among infants treated earlier, but there was no difference in mortality between the two groups. The greatest benefit from early treatment was seen in eyes with zone I disease.	
	(2) Unfavorable structural outcome at 9 months						

(Continued)

Table 8-3 (continued)

Study Name (Year Enrollment Completed)	Outcome Measure(s)	Number of Eyes Assessed for Primary Outcome	Trials of Intravitreal Anti-VEGF Agents			Main Conclusions	Comments
			Randomization Point	Treatment Arms			
Bevacizumab Eliminates the Angiogenic Threat for Retinopathy of Prematurity; BEAT-ROP (2010)	Recurrence of ROP requiring re-treatment by 54 weeks of postconceptional age	143 (150 enrolled)	Stage 3+ ROP in zone I or posterior zone II	(a) Laser retinal ablation (b) Intravitreal bevacizumab, 0.625 mg in 0.025 mL	Recurrence of ROP was significantly higher in zone I eyes treated with laser than in eyes treated with bevacizumab (42% vs 6%, respectively). The difference for zone II eyes was not statistically significant (12% vs 5%, respectively).	The recurrence rate in the laser arm was higher than rates in previous studies. Two-thirds of study sites were in Texas. Median time to recurrent ROP was 16 weeks after injection and 6 weeks after laser therapy.	
Ranibizumab Compared With Laser Therapy for the Treatment of Infants Born Prematurely With Retinopathy of Prematurity study; RAINBOW (2017)	Treatment success was defined as no active retinopathy, no unfavorable structural outcomes, and no need for a different treatment modality by 24 weeks after therapy.	214 (225 enrolled)	Bilateral ROP as follows: Zone I, stage 1+, 2+, 3, or 3+ ROP Zone II, stage 3+ AP-ROP	(a) Laser retinal ablation (b) Bilateral intravitreal ranibizumab, 0.1 mg (c) Bilateral intravitreal ranibizumab, 0.2 mg	Treatment was successful in 80% of eyes receiving ranibizumab 0.2 mg, 75% of eyes receiving ranibizumab 0.1 mg, and 66% of eyes undergoing laser therapy.	The RAINBOW study cohort was not identical to the BEAT-ROP study cohort. Inclusion criteria were closer to the clinical profile of eyes typically treated in modern practice. There was no reduction in circulating serum levels of VEGF in any of the groups.	

AP-ROP = aggressive posterior retinopathy of prematurity; RD = retinal detachment; ROP = retinopathy of prematurity; VEGF = vascular endothelial growth factor.

^aThe term *high-risk prethreshold*, which was coined by the ETROP investigators, required 2 findings: (1) clinical evidence of prethreshold ROP; AND (2) >15% computed risk of progression to unfavorable outcome if untreated. This risk was calculated using an algorithm incorporating demographic and clinical variables from the natural history arm of the CRYO-ROP study.

Early Treatment for Retinopathy of Prematurity Cooperative Group. Revised indications for the treatment of retinopathy of prematurity: results of the Early Treatment for Retinopathy of Prematurity randomized trial. *Arch Ophthalmol*. 2003;121(12):1684–1694.

Shulman JP, Hobbs R, Hartnett ME. Retinopathy of prematurity: evolving concepts in diagnosis and management. *Focal Points: Clinical Modules for Ophthalmologists*. American Academy of Ophthalmology; 2015, module 1.

Laser and Cryoablation Surgery

Ablation of ROP should be performed with a laser rather than cryoablation because laser surgery is associated with less treatment-related morbidity. A diode red (810-nm) laser is preferred, as its energy will not be absorbed by prominent iris vessels or a persistent tunica vasculosa lentis. The conventional treatment pattern is best described as nearly confluent, with burns placed 0.5- to 1-burn width apart starting at the ridge and proceeding anteriorly to the ora serrata for 360° to treat all avascular retina (see Fig 8-9 earlier in the chapter). In the horizontal meridians, laser treatment should be applied in a lighter pattern to avoid damaging the long ciliary vessels and nerves, as damage to these structures may cause severe anterior segment ischemia. Although retinal cryoablation surgery is now rare in the United States, the technique may still be used when laser or intravitreal therapy is unavailable. Because respiratory or cardiorespiratory arrest occurs in up to 5% of infants treated with cryotherapy, treatment should be performed in conjunction with systemic monitoring. To minimize stress and risk to the infant, use of systemic analgesia may be considered. Some neonatologists prefer that infants undergo treatment with general anesthesia in an operating room.

Follow-up is recommended at 1 week after laser treatment. At that time, some reduction in the level of plus disease, but not necessarily regression of neovascularization, is expected. The primary purpose of this follow-up visit is to confirm that the disease has not worsened. By 1 month after laser therapy, obvious improvement, and even complete regression, of peripheral disease is expected.

Simpson JL, Melia M, Yang MB, Buffenn AN, Chiang MF, Lambert SR. Current role of cryotherapy in retinopathy of prematurity: a report by the American Academy of Ophthalmology. *Ophthalmology*. 2012;119(4):873–877.

Anti-VEGF Drugs

Intravitreal bevacizumab monotherapy for zone I or posterior zone II stage 3 ROP with plus disease was studied by the Bevacizumab Eliminates the Angiogenic Threat for Retinopathy of Prematurity (BEAT-ROP) group. In eyes with zone I ROP, recurrent neovascularization was observed significantly less often with bevacizumab treatment than with laser therapy by 54 weeks' gestational age. In contrast, in eyes with zone II disease, outcomes were similar with either treatment. Interestingly, normal peripheral retinal vascularization continued after treatment with intravitreal bevacizumab, though at gestational ages several months older than normally seen. Recurrence of ROP requiring treatment was noted in 6% of all infants treated with bevacizumab, at a median interval of 16 weeks after injection. On average, ROP recurred sooner in eyes with zone II disease than in eyes with zone I disease.

The authors concluded that the sample size was too small and the follow-up period too short to allow proper evaluation of the systemic safety of intravitreal bevacizumab or to assess the true incidence of late recurrence of ROP.

In the international prospective study RANibizumab Compared With Laser Therapy for the Treatment of INfants BOrn Prematurely With Retinopathy of Prematurity (RAINBOW), investigators compared the efficacy and safety of intravitreal ranibizumab with that of laser therapy for ROP and concluded that ranibizumab 0.2 mg may be superior for the treatment of very low-birth-weight infants with ROP. However, 15% of eyes treated with ranibizumab 0.2 mg still required at least 1 retreatment within 6 months.

VanderVeen DK, Melia M, Yang MB, Hutchinson AK, Wilson LB, Lambert SR. Anti-vascular endothelial growth factor therapy for primary treatment of type 1 retinopathy of prematurity: a report by the American Academy of Ophthalmology. *Ophthalmology*. 2017;124(5):619-633.

Indications

For most cases of type I ROP, laser therapy remains the mainstay of treatment, given its proven safety, efficacy, predictable outcomes, and high probability of long-term success. Nevertheless, anti-VEGF treatment may be preferred in cases of iris rubeosis with poor dilation and very posterior disease and in infants who cannot tolerate the anesthesia associated with laser treatment.

Intravitreal injection technique

Intravitreal injections may be performed in the NICU (Video 8-1). A topical anesthetic and 5% betadine solution are applied first, and a sterile eyelid speculum is used to retract the eyelids. The injection site should be no more than 1.5 mm posterior to the corneal limbus, through the pars plicata. Given that infants have a proportionally larger crystalline lens than adults, the direction of the injection should be parallel to, rather than oblique to, the visual axis. Injection volume is typically 0.03 mL or less (approximately half the volume used in adults). Risks associated with the injection include ocular hypertension, cataract, endophthalmitis, bleeding, and retinal detachment.



VIDEO 8-1 Intravitreal injection in an infant.
Courtesy of Franco M. Recchia, MD.



Follow-up

Follow-up is recommended within 1 week of injection to assess therapeutic response and to determine the need for additional treatment. Because late reactivation of major proliferative disease is possible in infants whose ROP was treated with an intravitreal injection of bevacizumab or ranibizumab alone, continued close follow-up is crucial. This is particularly important between 2 and 4 months after injection, when the risk of ROP reactivation is highest.

In addition, special caution is urged before suspending regular retinal examinations in infants receiving anti-VEGF medications for ROP. Initial ROP regression (as with laser treatment) or achievement of 45 weeks' postmenstrual age (as with untreated type 2 ROP) is not sufficient to discontinue monitoring. Although full retinal vascularization is the

only clear criterion for terminating examinations, full retinal vascularization is not always achieved in infants treated with anti-VEGF monotherapy. Thus, many experts recommend definitive treatment with peripheral retinal laser photocoagulation before these patients are discharged from the NICU.

Safety profile

The results of the BEAT-ROP, RAINBOW, and other studies have dramatically changed how zone I ROP, and probably all ROP, is treated. However, substantive long-term data on systemic safety are limited.

Mintz-Hittner HA, Kennedy KA, Chuang AZ; BEAT-ROP Cooperative Group. Efficacy of intravitreal bevacizumab for stage 3⁺ retinopathy of prematurity. *N Engl J Med*. 2011;364(7):603–615.

Stahl A, Lepore D, Fielder A, et al. Ranibizumab versus laser therapy for the treatment of very low birthweight infants with retinopathy of prematurity (RAINBOW): an open-label randomised controlled trial. *Lancet*. 2019;394(10208):1551–1559.

Vitrectomy and Scleral Buckling Surgery

Eyes with stage 4 ROP (ie, progressive, active-phase ROP) require surgical intervention using scleral buckling or a lens-sparing vitrectomy to alleviate the vitreoretinal traction causing retinal detachment. Eyes undergoing surgical intervention at stage 4A have more favorable outcomes than those undergoing surgery at later stage 4B or 5; in addition, lens-sparing vitrectomy at stage 4A ROP may reduce progression to stage 4B and 5 disease. Given the improved visual outcome, this is the preferred approach.

In one study of infants with stage 5 ROP, vitrectomy combined with dissection of the fibrovascular membranes and adherent vitreous resulted in full or partial reattachment of the retina in approximately 30% of eyes (Video 8-2). Nevertheless, only 25% of retinas in eyes with initial partial or total reattachment after surgery remained fully attached at a median follow-up of 5 years. When a drainage retinotomy is performed or an iatrogenic retinal break occurs during a vitrectomy for ROP, the prognosis for that eye is uniformly poor.



VIDEO 8-2 Stage 5 ROP surgery.

Courtesy of Audina M. Berrocal, MD.



Capone A Jr, Trese MT. Lens-sparing vitreous surgery for tractional stage 4A retinopathy of prematurity retinal detachments. *Ophthalmology*. 2001;108(11):2068–2070.

Quinn GE, Dobson V, Barr CC, et al. Visual acuity of eyes after vitrectomy for retinopathy of prematurity: follow-up at 5 1/2 years. The Cryotherapy for Retinopathy of Prematurity Cooperative Group. *Ophthalmology*. 1996;103(4):595–600.

Associated Conditions and Late Sequelae of ROP

Following resolution of the acute phase of ROP, the infant should be examined by a pediatric ophthalmologist (typically within 6–12 months) for myopia, strabismus, and amblyopia.

In the ETROP study, high myopia (minus 5 diopters or greater) among children receiving laser treatment for ROP was observed in approximately one-fourth within 1 year of age and one-half by 6 years of age.

Conditions that are more likely to occur over time in eyes with regressed ROP include

- myopia with astigmatism
- anisometropia
- strabismus
- amblyopia
- cataract
- glaucoma
- macular dragging (Fig 8-10)
- retinal pigmentary changes
- retinal tears
- abnormal vitreoretinal interface/adhesions
- retinal detachment (rhegmatogenous, traction, and/or exudative) (Figs 8-11, 8-12, 8-13, respectively)
- anomalous foveal anatomy (Fig 8-14)

Figure 8-10 Montage color fundus photograph from an adult who had untreated ROP as an infant, showing severe dragging of retinal vessels and a macular fold extending to the temporal periphery. Diffuse pigmentary changes are also visible. (Courtesy of Franco M. Recchia, MD.)

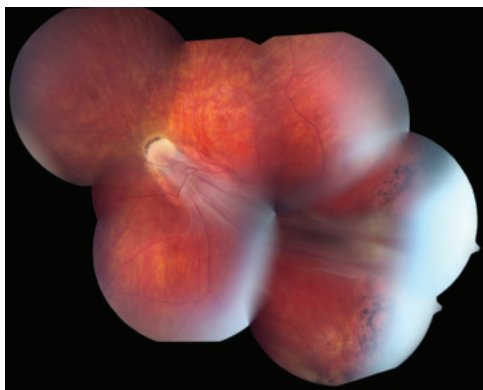


Figure 8-11 Rhegmatogenous retinal detachment in a 16-year-old male who was born at 26 weeks of gestational age. Avascular retina with numerous atrophic retinal holes (arrows) are seen peripheral to an old demarcation line in the temporal periphery. Subretinal fluid extends into the temporal macula. (Courtesy of Franco M. Recchia, MD.)





Figure 8-12 Traction retinal detachment in a 19-year-old male with a history of severe prematurity. Circumferential contraction of the posterior hyaloid has led to superior traction detachment. Scattered old laser photocoagulation scars are seen in the periphery. (Courtesy of Franco M. Recchia, MD.)



Figure 8-13 Montage of color fundus photographs showing exudative (also termed *Coats-like*) retinopathy in the right eye of a 22-year-old woman who was born at 24 weeks of gestation. Dense lipid exudate and subretinal fluid are present in the inferior and temporal pre-equatorial retina. Macular dragging and residual white fibrotic ridge tissue are also present in the superotemporal quadrant. (Courtesy of Franco M. Recchia, MD.)

Medicolegal Aspects of ROP

Several unique aspects of ROP care contribute to the risk of liability. The protracted hospital stay of premature infants requires complex coordination of multiple services, practitioners, caregivers, and specialists, of whom the ophthalmologist is just one of many and may be forgotten. Miscommunication between care coordinators and the ophthalmologist may delay scheduling or performance of eye examinations. If the narrow treatment window is missed, adverse outcomes may result. In addition, given the shortage of

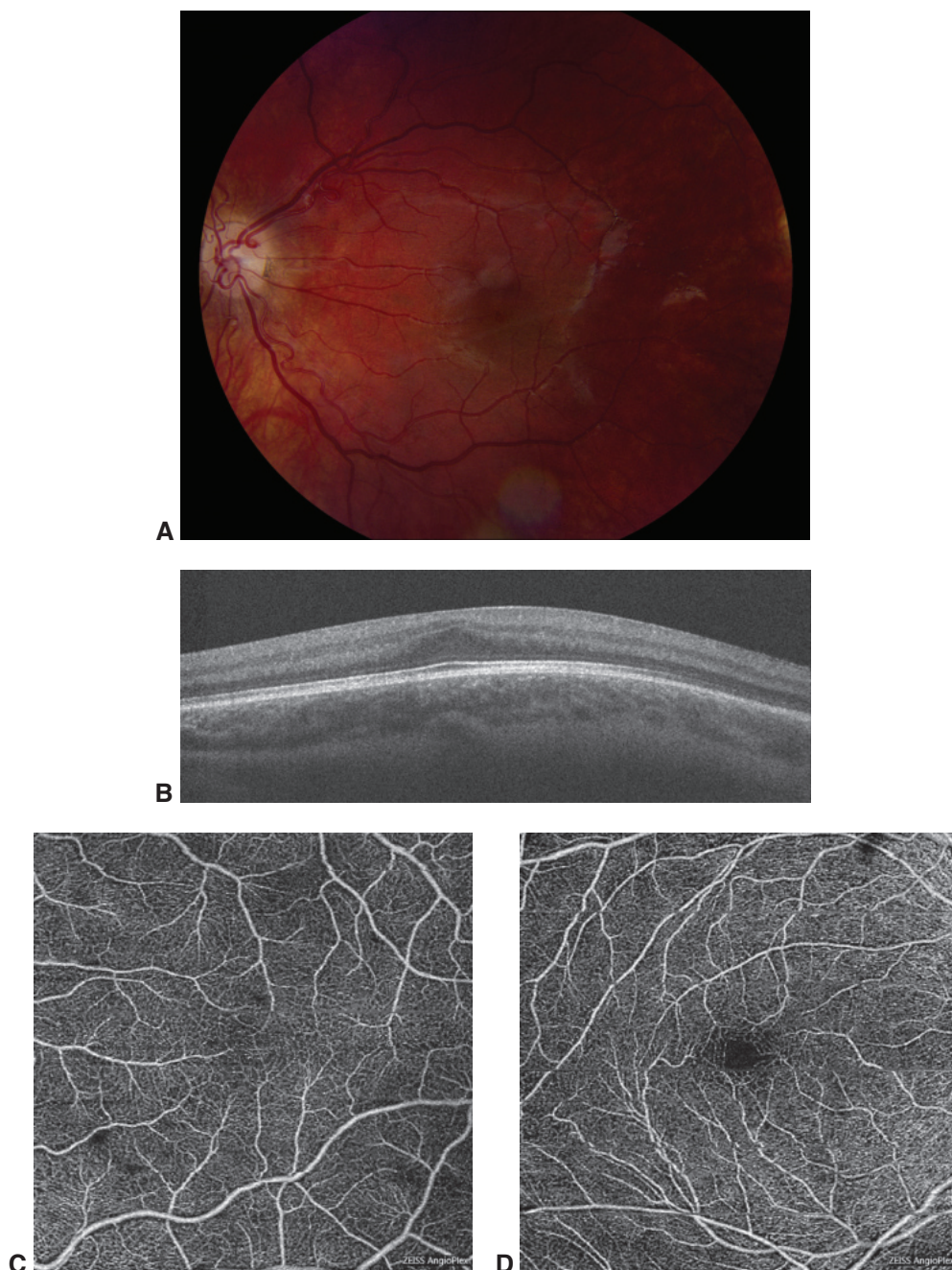


Figure 8-14 A–C: Images from a 10-year-old boy who was referred for evaluation because visual acuity was correctable only to 20/40. Pertinent medical history was his birth at 28 weeks' gestation. Color photograph (**A**) shows macular dragging and a blood vessel entering the foveal area. Optical coherence tomography (OCT) (**B**) through the anatomical center of the macula shows absence of a foveal depression and persistence of all retinal layers. OCT angiography (OCTA) (**C**) shows absence of a foveal avascular zone. **D**, OCTA from a 10-year-old child born at full term is shown for comparison. The finding of a blunted or absent foveal depression (also termed *fovea plana*) is a biomarker of premature birth. Normally, the foveal depression forms embryologically by a patterned centrifugal regression of inner retinal layers by the 30th week of gestation. Although the finding of foveal dysplasia or fovea plana, as seen here, indicates a premature birth, it is still compatible with good vision. (Courtesy of Eric W. Schneider, MD.)

experienced ROP screeners, management of ROP in some hospitals becomes the responsibility of ophthalmologists who may be uncomfortable or unfamiliar with the nuances and complexities of ROP care.

Poor outcomes from ROP may be perceived as medical malpractice and therefore pose a risk for litigation by patients or their families. Malpractice claims alleging mismanagement of ROP rank among the highest in ophthalmology and indeed all of medicine. Indemnity payments have exceeded 20 million dollars and are rationalized by the young age of the plaintiff and the lifelong duration of irreversible vision loss.

Patient safety can be promoted and liability minimized through implementation of an “ROP safety net,” offered through the Ophthalmic Mutual Insurance Company (OMIC). See the following reference for toolkits that detail every step in the care process.

Menke AM. ROP Safety Net: Risk Analysis. Version 8/15/18. Ophthalmic Mutual Insurance Company; 2018. <https://www.omic.com/rop-safety-net/>

Choroidal Disease

Highlights

- Pachychoroid is an entity with an evolving definition but is generally thought of as abnormally dilated choroidal vessels abutting the retinal pigment epithelium (with or without choroidal thickening).
- Fluorescein angiography can contribute to the diagnosis of arteritic anterior ischemic optic neuropathy.
- Hypertensive choroidopathy can be diagnosed by means of multimodal imaging because of its unique characteristics on optical coherence tomography and fundus autofluorescence.

Scope of Chapter

This chapter describes noninflammatory choroidal diseases that also involve the retina. Inflammatory disorders of the retina and choroid are discussed in Chapter 11. See also BCSC Section 9, *Uveitis and Ocular Inflammation*. Intraocular tumors such as melanoma are covered in BCSC Section 4, *Ophthalmic Pathology and Intraocular Tumors*.

Central Serous Chorioretinopathy

Central serous chorioretinopathy (CSC; also called central serous retinopathy [CSR]) causes an idiopathic serous detachment of the retina related to leakage at the level of the retinal pigment epithelium (RPE) secondary to hyperpermeability of the choriocapillaris, as seen on indocyanine green angiography (ICGA). While the condition was originally described in 1866 by von Graefe as recurrent central retinitis, it was Maumenee who first performed fluorescein angiography on patients with CSC and found a leak at the level of the RPE, not from retinal vessels (the previously hypothesized source of leakage). Gass subsequently described the findings seen on fluorescein angiography (FA) and suggested that laser photocoagulation could be used to treat affected patients. Gass also stated that the disease was secondary to hyperpermeability of the choriocapillaris, a hypothesis that was confirmed decades later via ICGA.

Demographics and Features

Central serous chorioretinopathy occurs primarily in persons between the ages of 35 and 55 years, with a male-to-female ratio of 3:1; at present, there are no reliable statistics

suggesting any association with race. Patients describe a variety of symptoms, including sudden onset of blurred or dim vision, micropsia, metamorphopsia, paracentral scotomata, decreased color vision, and prolonged afterimages. Visual acuity ranges from 20/20 to 20/200, but in most patients, it is better than 20/30. Decreased visual acuity can often be improved with a small hyperopic correction.

CSC has several clinical variations. In an acute manifestation, the retina has a round or oval elevation in the macular region; it often involves the fovea. FA shows leaks from the RPE that may appear early in the angiographic sequence as a dot (the *dot* form) or as a tree-shaped movement of dye in the subretinal space (the *smokestack* form) (Fig 9-1). In some circumstances, vigorous leaks can cause deposition of a grayish-white, feathered-edge subretinal material that is generally believed to be fibrin. In chronic CSC, the RPE

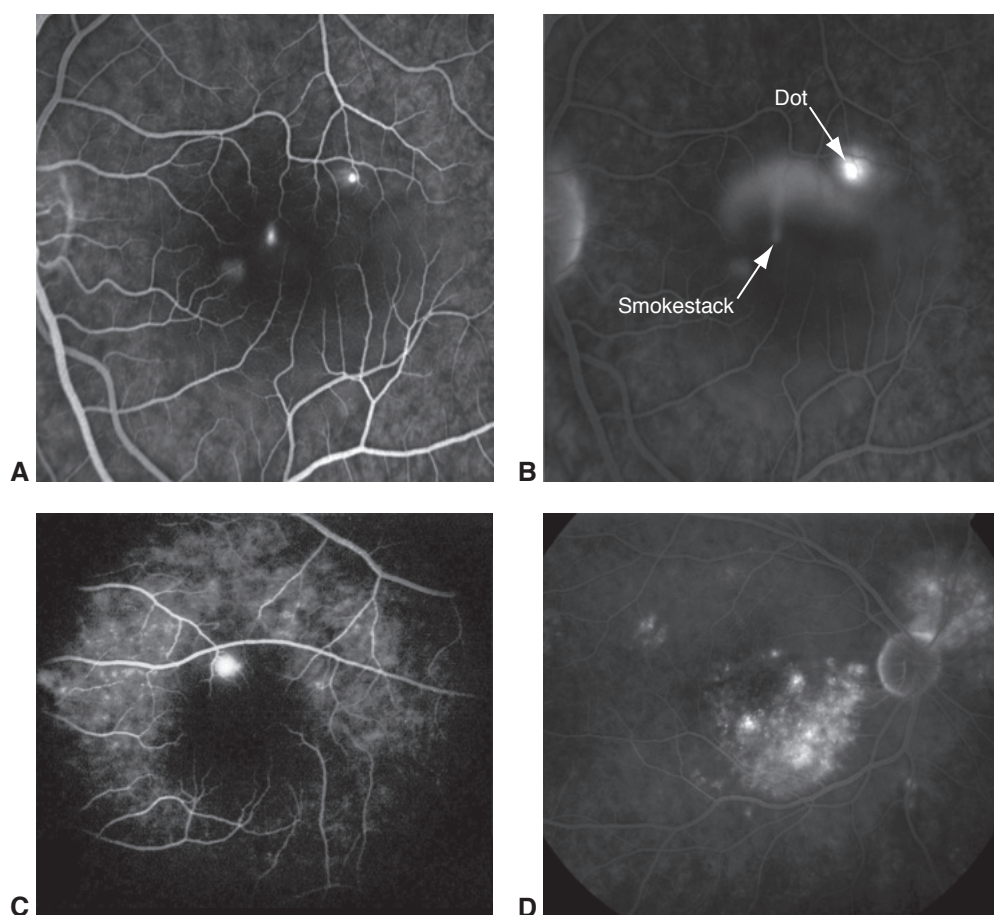


Figure 9-1 Fluorescein angiographic (FA) patterns of the leaks in central serous chorioretinopathy (CSC). **A**, In the early phase, the patient was seen to have 2 main leaks. **B**, Later in the angiogram, the leaks show 2 different morphologies: the *smokestack* and the *dot* varieties. **C**, Acute CSC generally presents with 1 leak or a few leaks. **D**, Chronic forms of CSC exhibit many small leaks, as demonstrated in this image from a different patient. (Courtesy of Richard F. Spaide, MD.)

shows granular pigmentation; FA reveals many small, sometimes inconspicuous leaks; and there is widespread shallow detachment with areas of atrophy of the photoreceptors (see Fig 9-1D).

CLINICAL PEARL

Retinal pigment epithelial changes on optical coherence tomography (OCT) or fundus autofluorescence (FAF) may suggest previous episodes of CSC and resolved subretinal fluid.

Systemic Associations

Central serous chorioretinopathy is associated with stress and with a tense, driven personality. Systemic associations include endogenous hypercortisolism (Cushing syndrome), hypertension, sleep apnea, use of psychopharmacologic medications, and pregnancy. Use of systemic corticosteroids, which may be administered through intramuscular, topical, inhalational, epidural, or even intra-articular routes, is associated with CSC; but, curiously, use of intraocular corticosteroids does not appear to be associated with the condition. Organ transplant recipients and patients with autoimmune disease requiring long-standing, high-dose steroids are particularly vulnerable to the more severe and chronic variants.

Fawzi AA, Holland GN, Kreiger AE, Heckenlively JR, Arroyo JG, Cunningham ET Jr. Central serous chorioretinopathy after solid organ transplantation. *Ophthalmology*. 2006;113(5):805–813.e5.

Mrejen S, Balaratnasingam C, Kaden TR, et al. Long-term visual outcomes and causes of vision loss in chronic central serous chorioretinopathy. *Ophthalmology*. 2019;126(4):576–588.

Imaging

The extent of the detachment can be documented with color fundus photographs. FAF imaging shows the accumulation of shed photoreceptor outer segments in the subretinal space, as well as distributed defects of the RPE. It has been theorized that the white dots seen under the retina are macrophages with fluorophores from phagocytized outer segments (Fig 9-2). Eyes with chronic CSC can display descending tracts during both FA and FAF imaging (Fig 9-3). Enhanced depth imaging OCT (EDI-OCT) shows thickening of the choroid and, in areas where thickening is most prominent, posterior loculation of fluid in the deep choroid. Figure 9-4 shows the internal structure of a healthy choroid, and Figure 9-5 shows the choroid in 1 healthy eye and in 3 eyes with CSC.

Although ICGA can reveal choroidal vascular hyperpermeability (Fig 9-6), it has largely been supplanted by OCT, even for detecting possible coexisting choroidal neovascularization (CNV), which may be present in up to 20% of cases in individuals older than 50 years. OCT angiography seems to be adept at detecting secondary CNV that may develop in these patients.

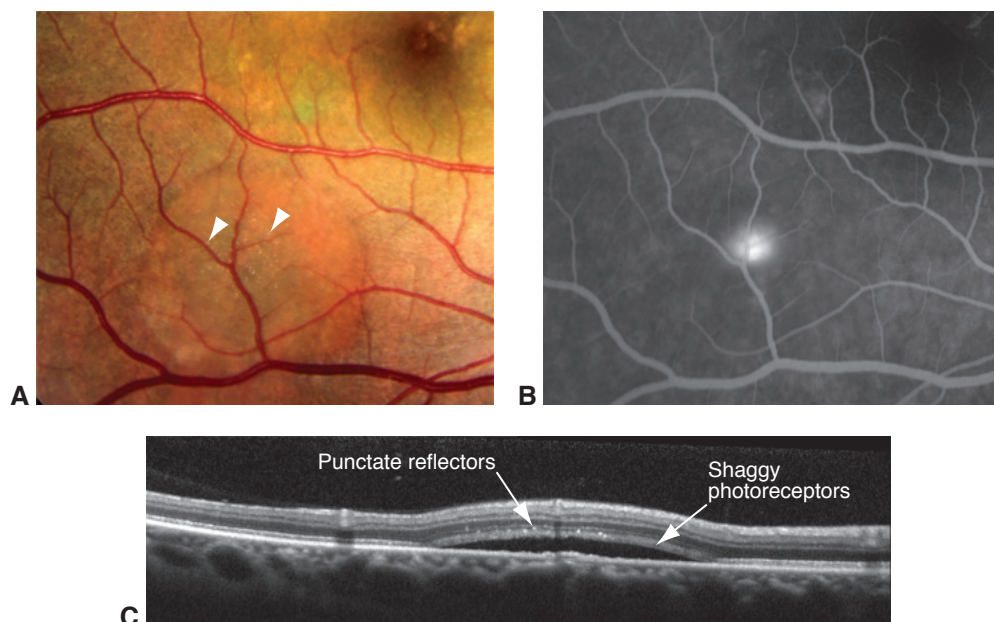


Figure 9-2 Central serous chorioretinopathy with white dots. **A**, Fundus photograph shows an ovoid elevation of the retina with white dots on the undersurface (*arrowheads*). **B**, FA reveals a single leakage point. **C**, The elevated retina, seen in cross section, has a thick coat on its inner surface that has autofluorescent characteristics consistent with retinal outer segment–derived fluorophores. These fluorophores are therefore considered to be derived from the outer segments that could not be phagocytized by the retinal pigment epithelium (RPE) because of the physical separation, caused by the fluid, between the retina and RPE. The region of shaggy photoreceptors contains punctate dots that are highly reflective; it has been theorized that these dots are macrophages. (Courtesy of Richard F. Spaide, MD.)

Imamura Y, Fujiwara T, Margolis R, Spaide RF. Enhanced depth imaging optical coherence tomography of the choroid in central serous chorioretinopathy. *Retina*. 2009;29(10):1469–1473.

Spaide RF, Klancnik JM Jr. Fundus autofluorescence and central serous chorioretinopathy. *Ophthalmology*. 2005;112(5):825–833.

Differential Diagnosis

Other entities that may be considered in the differential diagnosis of CSC include type 1 CNV and polypoidal choroidal vasculopathy (PCV; see Chapter 4), which is a variant of type 1 CNV. The FA findings can overlap significantly; both entities show leakage of fluorescein, and the visualization of the structures underlying the RPE is poor. If CNV is present, OCT demonstrates an irregular wavy, shallow elevation of the RPE by a layer of material with heterogeneous reflectivity. The neovascularization seen in association with CSC is generally easy to detect with OCT angiography. What complicates the issue, particularly regarding treatment, is that type 1 CNV and PCV appear to be associated with CSC; they may be its sequelae.

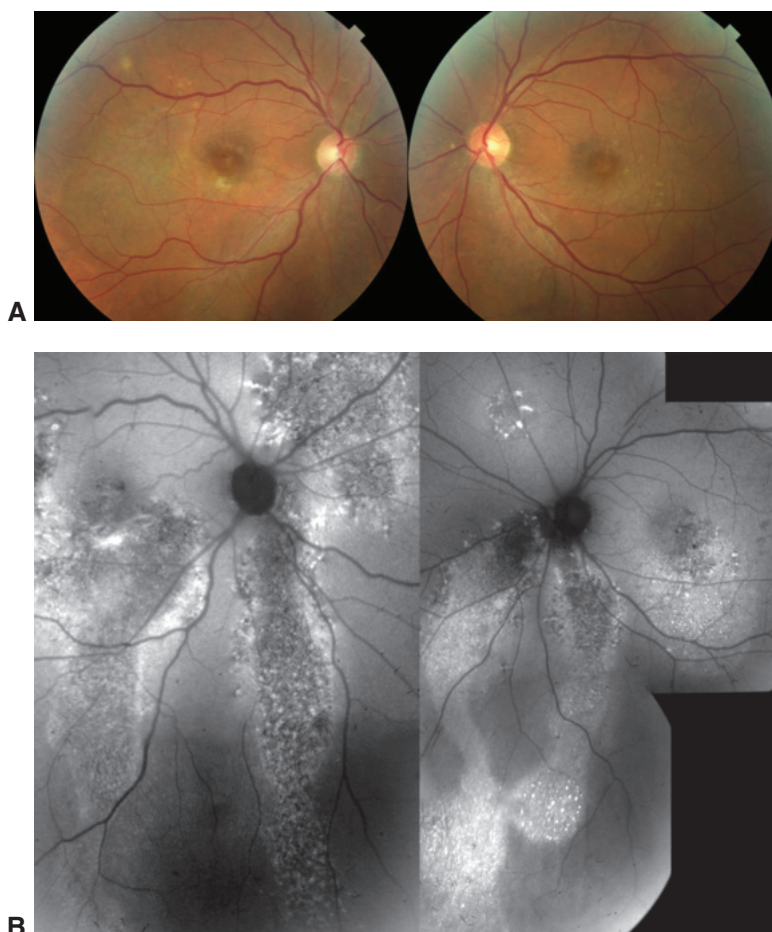


Figure 9-3 Autofluorescence abnormalities in CSC. **A**, Fundus photographs show the right and left eyes of a patient with CSC. Although subtle pigmentary changes are visible, it can be difficult to discern where fluid has accumulated. **B**, Autofluorescent images show widespread abnormalities induced by the presence of subretinal fluid, particularly the descending tracts created by the fluid. (Reproduced with permission from Elsevier. Imamura Y, Fujiwara T, Spaide RF. Fundus autofluorescence and visual acuity in central serous chorioretinopathy. *Ophthalmology*. 2011;118(4):700–705. Copyright 2011.)

Pachychoroid spectrum and its evolving nomenclature

The widespread utilization of EDI-OCT has facilitated quantitative evaluation of the choroid and, with it, the recognition of a thick, or *pachy*, choroid phenotype, which is commonly seen in CSC. The spectrum of disease encompassed in this entity ranges from pigment epithelial changes in the setting of thick, poorly tessellated choroid (*pachychoroid pigment epitheliopathy*) to *pachyvessels*, which on cross-sectional OCT appear to compress and obliterate the overlying choriocapillaris, to PCV (see Chapter 4 for further discussion). Ophthalmologists have recently recognized that increased choroidal thickness may not be universally present in these eyes and have moved toward a more pathogenesis-based definition, with the understanding that these pachyvessels are actually dilated anastomotic

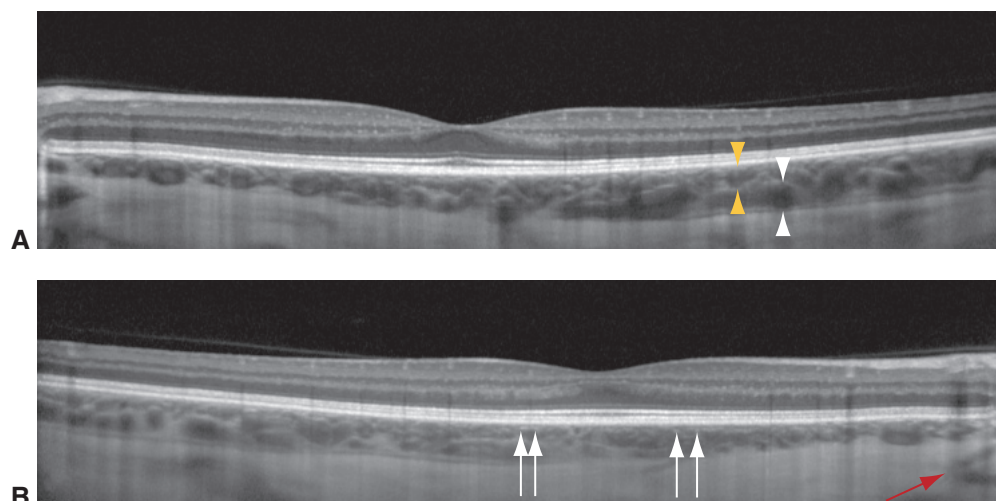


Figure 9-4 The internal structure of the healthy choroid, depicted on enhanced depth imaging optical coherence tomography (EDI-OCT). The choroidal vessels decrease in diameter from the outer to the inner choroid. **A**, The larger vessels (*white arrowheads*) are dark in the center with a thick hyperreflective wall. The medium-sized vessels (*yellow arrowheads*) have a smaller hyporeflective area in the center and a hyperreflective wall. **B**, As vessel diameter decreases, the central hyporeflective area decreases until it is not visible. At that size, the vessel appears as a white hyperreflective structure (*white arrows*). Note the delineation of the hyporeflective line near the junction with the inner sclera, which appears to be in the suprachoroidal space. The *red arrow* points to a vessel coursing through the sclera. (Reproduced with permission from Elsevier. Mrejen S, Spaide RF. Optical coherence tomography: imaging of the choroid and beyond. *Surv Ophthalmol*. 2013;58(5):387–429. Copyright 2013.)

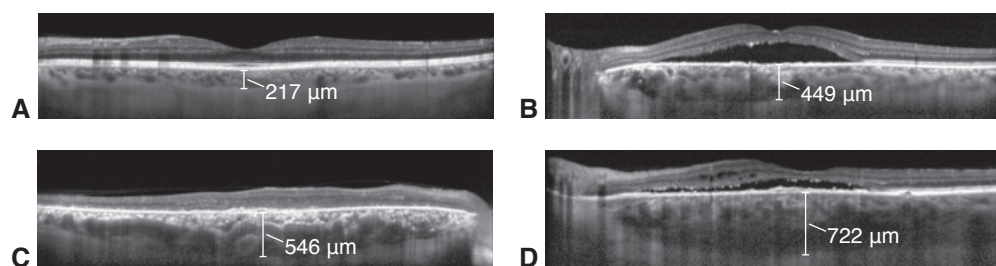


Figure 9-5 The choroid is seen in cross section using EDI-OCT. Subfoveal choroidal thickness was measured vertically from the outer border of the RPE to the inner border of the sclera (*brackets*) in a healthy eye in a 55-year-old man (**A**) and in 3 representative eyes with CSC: in a 44-year-old man (**B**), a 57-year-old man (**C**), and a 63-year-old man (**D**). (Reproduced with permission from Imamura Y, Fujiwara T, Margolis R, Spaide RF. Enhanced depth imaging optical coherence tomography of the choroid in central serous chorioretinopathy. *Retina*. 2009;29(10):1469–1473. doi:10.1097/IAE.0b013e3181be0a83)

venous channels that run across the choroidal watershed zones, traversing the macula. These observations signal choroidal venous insufficiency as the potential unifying underlying pathogenesis of these entities.

Cheung CMG, Lee WK, Koizumi H, Dansingani K, Lai TYY, Freund KB. Pachychoroid disease. *Eye (Lond)*. 2019;33(1):14–33.

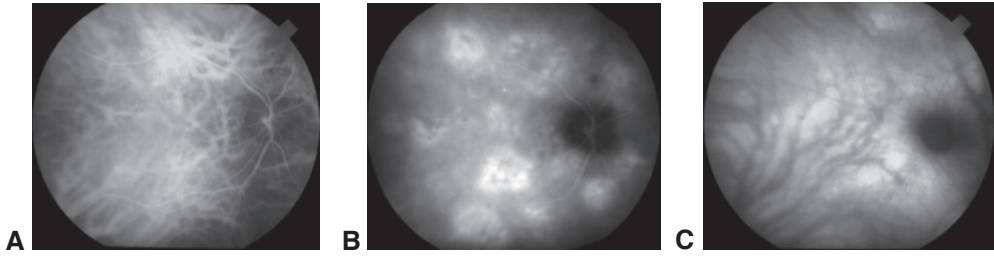


Figure 9-6 Stages of indocyanine green angiography (ICGA) in CSC. **A**, Early after injection, the dye can be seen within the choroidal vessels. **B**, During the middle phase of the angiogram, choriocapillaris hyperpermeability results in the appearance of multiple hyperfluorescent clouds. **C**, Later in the angiogram, the dye has largely been removed from the choroidal vessels. Dye that has leaked into the stroma has diffused posteriorly, silhouetting the larger choroidal vessels. (Reproduced with permission from Spaide RF, Hall L, Haas A, et al. Indocyanine green videoangiography of older patients with central serous chorioretinopathy. *Retina*. 1996;16(3):203–213. doi:10.1097/00006982-199616030-00004)

Matsumoto H, Hoshino J, Mukai R, et al. Vortex vein anastomosis at the watershed in pachy-choroid spectrum diseases. *Ophthalmol Retina*. 2020;4(9):938–945.
 Warrow DJ, Hoang QV, Freund KB. Pachychoroid pigment epitheliopathy. *Retina*. 2013;33(8):1659–1672.

Treatment

Central serous chorioretinopathy is generally self-limited and resolves spontaneously, with the majority of patients attaining excellent visual results. However, it can be destructive in some chronic cases, causing visually significant scotomata. *Verteporfin photodynamic therapy (PDT)*, whether at full fluence or, more commonly, reduced fluence, has been shown to decrease or eliminate subretinal fluid, decreases choroidal thickness, and reduces choroidal vascular hyperpermeability. Treatment is guided by either FA or ICGA, and a sufficiently large spot size is used to cover the main leakage point(s) with a surrounding safety margin of 1000 μm . This therapy (at full fluence, in studies of age-related macular degeneration) is associated with a 4% risk of vision decrease. CSC may recur after successful PDT, and therapy can be repeated safely, especially if lower fluence is used and the lesion is extrafoveal.

Laser photocoagulation therapy is no longer preferred for CSC, as secondary CNV occurred in the immediate postoperative period in up to 2% of eyes treated with this modality. Moreover, unlike PDT, photocoagulation has no effect on choroidal thickness.

Use of mineralocorticoid receptor antagonists (eplerenone or spironolactone) has shown some benefit in anecdotal reports. However, a recent randomized placebo-controlled trial using eplerenone in chronic CSC demonstrated no benefit with the medication (25 mg/day for 1 week, increasing to 50 mg/day for up to 12 months).

Lotery A, Sivaprasad S, O'Connell A, et al. Eplerenone for chronic central serous chorioretinopathy in patients with active, previously untreated disease for more than 4 months (VICI): a randomised, double-blind, placebo-controlled trial. *Lancet*. 2020;395(10220):294–303.
 Maruko I, Iida T, Sugano Y, Ojima A, Ogasawara M, Spaide RF. Subfoveal choroidal thickness after treatment of central serous chorioretinopathy. *Ophthalmology*. 2010;117(9):1792–1799.

Choroidal Perfusion Abnormalities

The choroid receives its arterial supply from approximately 20 short posterior ciliary arteries and 2 anterior ciliary arteries. A network of branching arterioles distributes the blood throughout the choroid in a segmental fashion, ultimately leading to the choriocapillaris, and helps reduce the blood pressure as well. Although the vessels in the choriocapillaris exhibit relatively uniform patterns in any given region of the eye, the pressure gradients imposed by the feeding arterioles and draining venules establish a lobular perfusion pattern. Abnormalities in choroidal blood flow can be divided into several main categories based on the underlying disease process.

Arteritic Disease

In arteritic diseases such as *giant cell arteritis* (Figs 9-7, 9-8) or *granulomatosis with polyangiitis* (formerly called *Wegener granulomatosis*; Fig 9-9), inflammatory occlusion can cause sectoral areas of nonperfusion. FA or ICGA is typically performed in cases in which an arteritic cause of vision loss is suspected; flow defects in the choroid are often undetected by ophthalmoscopy alone. Patchy and delayed choroidal filling, especially around the optic nerve, is characteristic of arteritic ischemic optic neuropathy (see Fig 9-7).

Nonarteritic Disease

Nonarteritic problems with blood flow can occur as a result of embolic or systemic disease or as a manifestation of severe hypertension. Emboli from the heart, injection of corticosteroids or calcium hydroxylapatite, and intravascular coagulation all have the potential to occlude choroidal vessels. Vascular occlusion can also occur in patients with lupus anticoagulants.

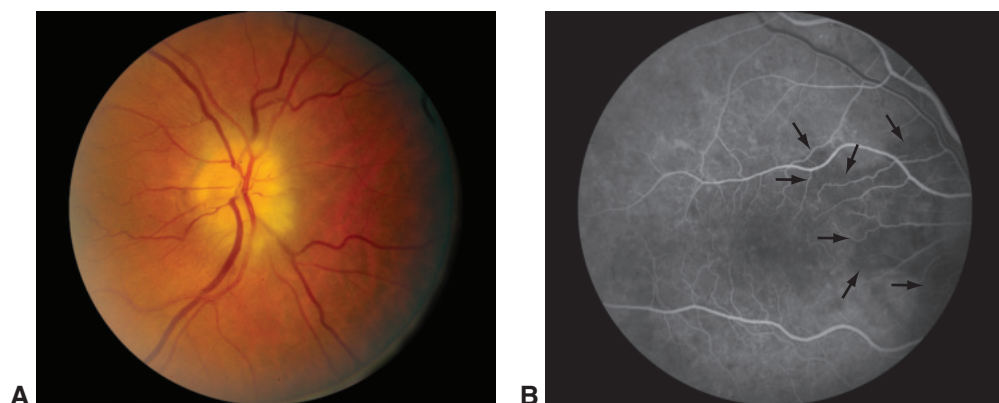


Figure 9-7 Arteritic anterior ischemic optic neuropathy with delayed choroidal filling. **A**, Color fundus photograph showing pallid edema of the right optic nerve head. **B**, Early venous phase of the angiogram showing incomplete filling of the choroidal lobule surrounding the optic nerve (arrows). Normally, choroidal filling is complete by the early venous to mid-venous phase. (Courtesy of Nicholas J. Volpe, MD.)

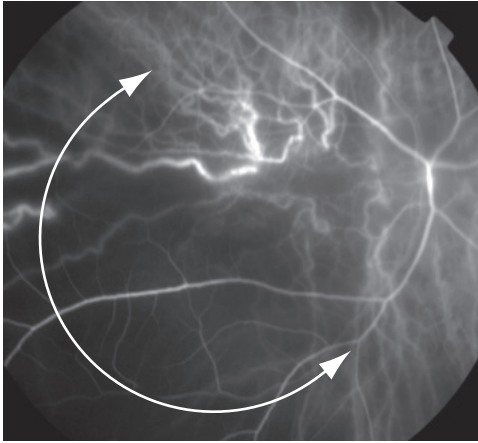


Figure 9-8 Giant cell arteritis. ICGA image taken 1 day after this patient had severe vision loss secondary to arteritic anterior ischemic optic neuropathy. A wedge-shaped area of choroidal nonperfusion is apparent (*curved arrow*). The apex of the wedge of nonperfusion points toward the area of the occluded short posterior ciliary artery. (Courtesy of Richard F. Spaide, MD.)

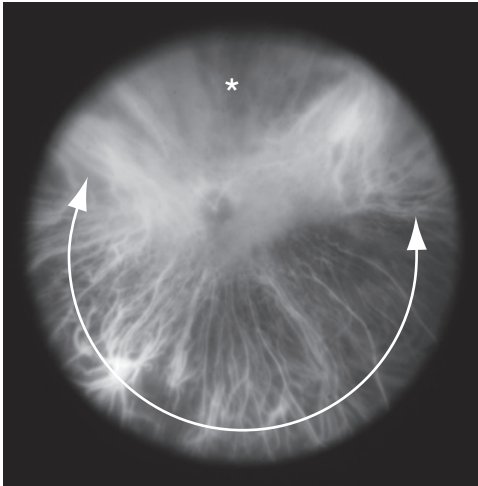


Figure 9-9 Granulomatosis with polyangiitis (formerly, Wegener granulomatosis). The early phase of wide-angle ICGA of the left eye reveals a widespread filling defect of the arterioles and choriocapillaris in the inferior fundus (*curved arrow*) and in a segmental area of the superior fundus (*asterisk*). (Reproduced with permission from Elsevier. Iida T, Spaide RF, Kantor J. Retinal and choroidal arterial occlusion in Wegener's granulomatosis. *Am J Ophthalmol.* 2002;133(1):151–152. Copyright 2002.)

Thrombotic thrombocytopenic purpura causes a classic pentad of findings: (1) microangiopathic hemolytic anemia, (2) thrombocytopenia, (3) fever, (4) neurologic dysfunction, and (5) renal dysfunction. Patients with this condition may have multifocal yellow placoid areas and associated serous detachment of the retina. Similar fundus findings may occur in patients with *disseminated intravascular coagulation*, in which consumption of coagulation proteins, involvement of cellular elements, and release of fibrin degradation products lead to hemorrhage from multiple sites and ischemia from microthrombi.

Similar fundus findings also occur in patients with acute hypertension, such as malignant hypertension or eclampsia. In addition to causing retinal and optic nerve head abnormalities, these disorders commonly lead to serous detachment of the retina associated with areas of yellow placoid discoloration of the RPE (Fig 9-10). The perfusion

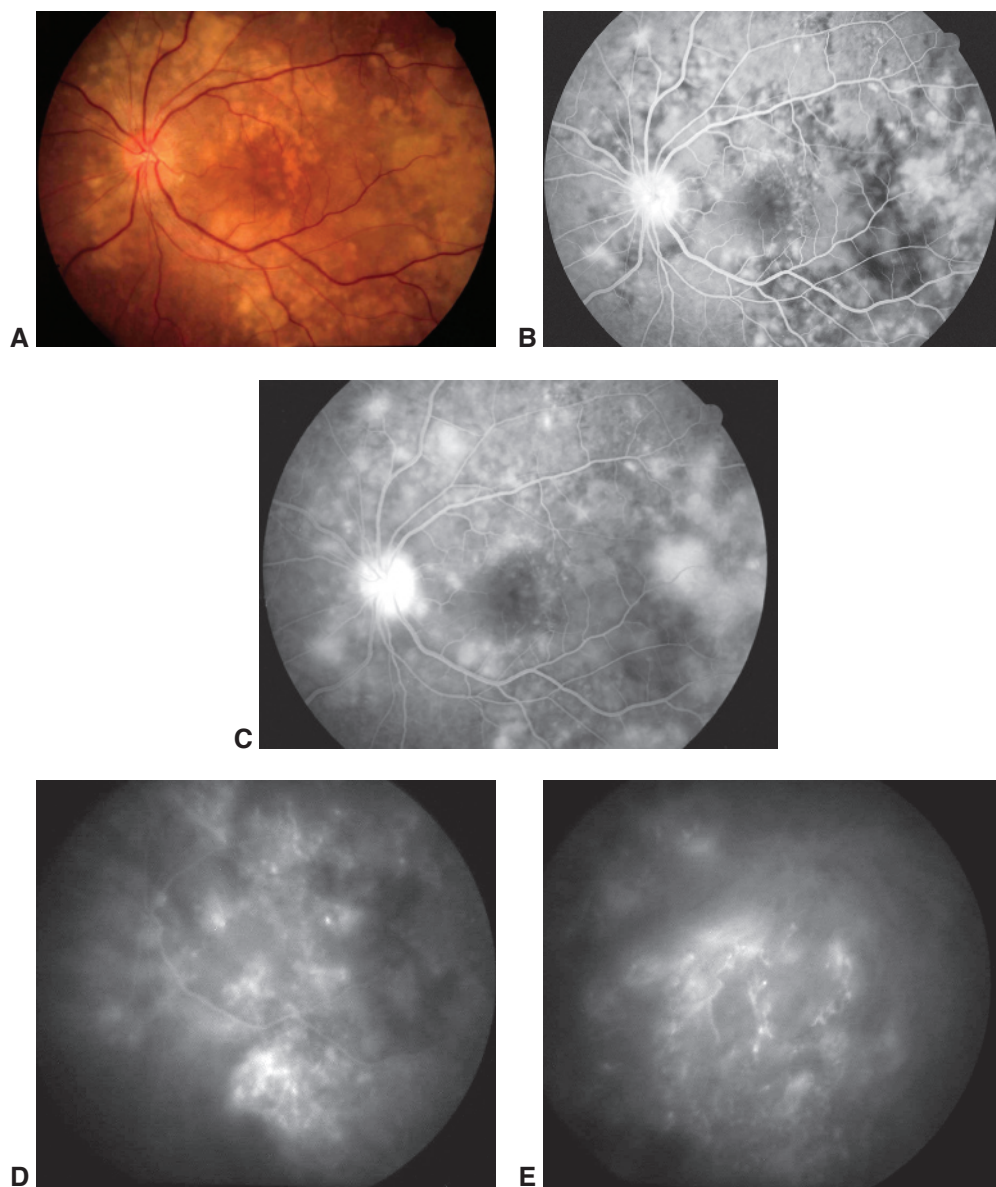


Figure 9-10 Preeclampsia with hemolysis, elevated liver enzymes, and low platelet count (HELLP) syndrome. **A**, Fundus photograph reveals a serous detachment of the retina and multiple yellowish placoid areas at the level of the RPE and inner choroid. **B**, Early-phase FA image shows reticular patterns of decreased choroidal perfusion bordering areas of hyperfluorescence. Early leakage from the level of the RPE is evident and becomes more apparent in the later phases of the study (**C**). There is also staining of and leakage from the optic nerve. **D**, ICGA image shows profound choroidal vascular filling defects alternating with areas of abnormal vessel leakage and staining, a rare finding. **E**, In the late phase, numerous arterioles show staining of their walls, indicating severe vascular damage. (Reproduced with permission from Spaide RF, Goldbaum M, Wong DW, Tang KC, Iida T. Serous detachment of the retina. *Retina*. 2003;23(6):820–846.)

abnormalities may range from focal infarction of the choriocapillaris to fibrinoid necrosis of larger arterioles. Resolution of smaller infarcts, which initially appear tan in color, produces small patches of atrophy and pigmentary hyperplasia called *Elschnig spots* (Fig 9-11). Infarction of an arteriole can lead to *Siegrist streaks*, which are hyperpigmented flecks arranged linearly along choroidal vessels. Posterior ciliary artery occlusions can result in wedge-shaped zones of choroidal infarction called *Amalric triangles*.

Choriocapillaris Blood Flow Abnormalities

Choroidal blood flow defects affect lobule-sized areas of the choroid or areas supplied by arterioles and therefore affect 1 to several choroidal lobules. Many ocular diseases (eg, acute

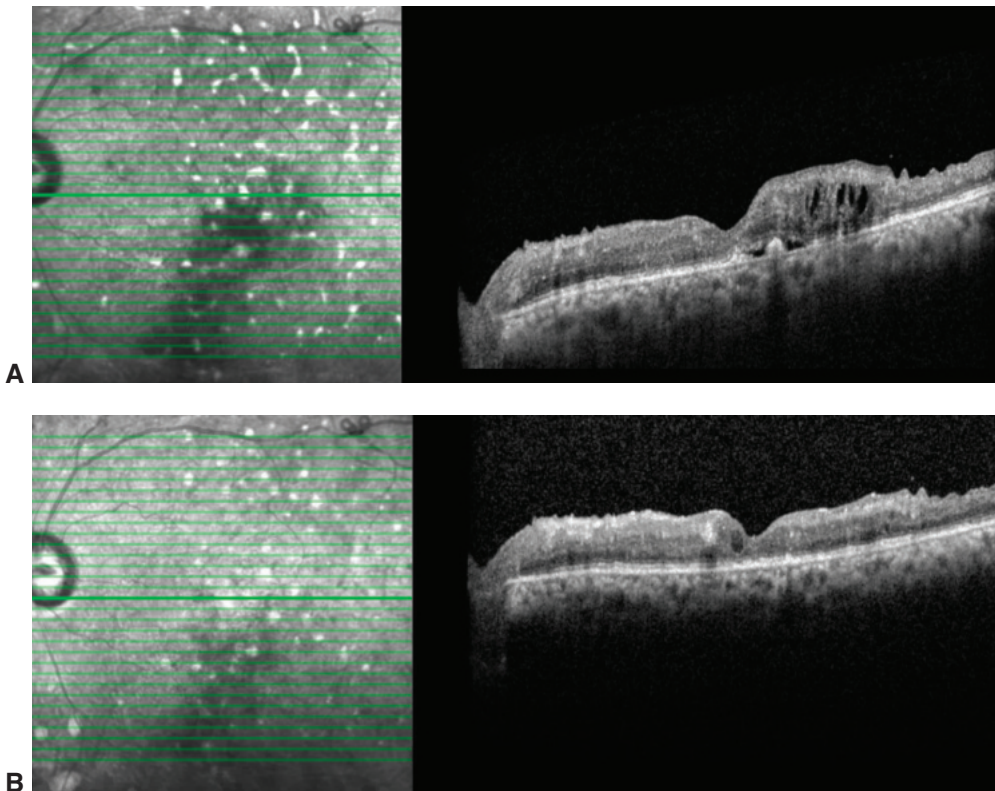


Figure 9-11 OCT images from a 43-year-old man with a history of hypertension, type 2 diabetes, chronic kidney disease, and proliferative diabetic retinopathy who had previously undergone vitrectomy for bilateral traction retinal detachment. He presented to the emergency department with a hypertensive urgency requiring admission and initiation of dialysis for acute renal failure. **A**, Imaging performed 2 months after these events. Notably, hyperreflective lesions on the infrared (IR) image (*to the right of the OCT image*) were new and not present at prior ophthalmologic visits. OCT shows sub-RPE deposits and subretinal and intraretinal fluid, consistent with hypertensive choroidopathy, and Elschnig spots. The patient was observed without retinal intervention while blood pressure and renal issues resolved. **B**, Vision stabilized and fluid resolved without further ocular intervention, with some fading of the IR hyperreflective lesions and inner retinal thinning over the following 18 months. (Courtesy of Amani Fawzi, MD.)

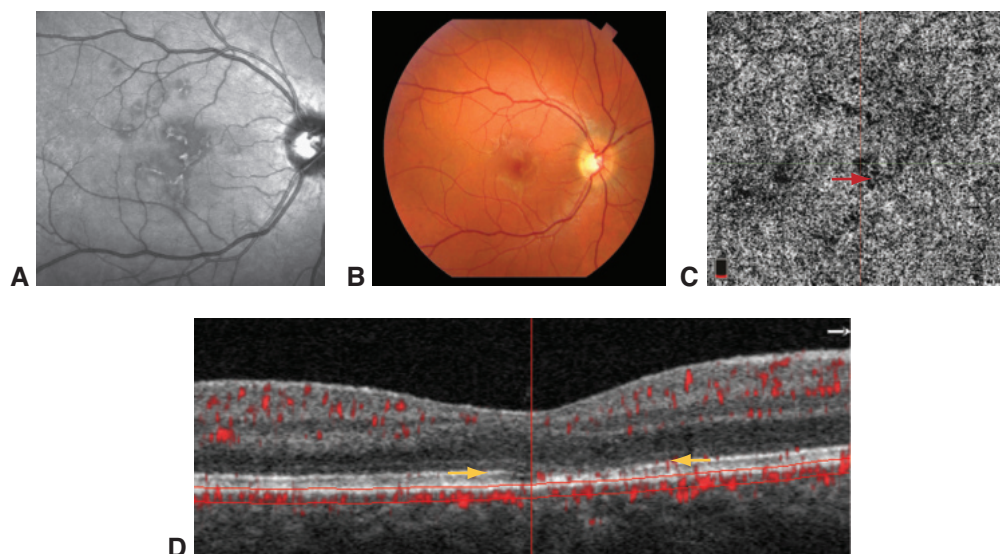


Figure 9-12 Resolving case of acute posterior multifocal placoid pigment epitheliopathy (APMPPE). **A**, Infrared image shows the hallmark jigsaw pattern pigmentary changes. **B**, These changes are visible as hyporeflective lesions on the fundus photograph. **C**, OCT angiography focused on the choriocapillaris shows focal flow deficit (arrow). **D**, Corresponding outer retinal lesion on OCT is seen as thinning and disruption of the ellipsoid zone (between arrows). (Courtesy of Amani Fawzi, MD.)

posterior multifocal placoid pigment epitheliopathy; Fig 9-12) characteristically produce lesions that are the putative size of a choroidal lobule. On OCT angiography at the level of the choriocapillaris, multiple areas of signal voids are frequently seen and are consistent with decreased perfusion, which is best depicted by this modality. These areas increase in size and number with age; they are also larger and more numerous in patients with hypertension, pseudodrusen, or, interestingly, late age-related macular degeneration in the *fellow* eye. These characteristic OCT angiographic findings are consistent with histologic studies showing a growing number of ghost vessels in the choriocapillaris (a sign of vessel death), basal linear deposits, and subretinal drusenoid deposits with increasing age. Some diseases are known to be associated with both RPE atrophy and geographic atrophy; they include pseudoxanthoma elasticum and maternally inherited diabetes mellitus and deafness. Even in the absence of RPE atrophy, patients with these diseases can exhibit remarkable loss of the choriocapillaris (Fig 9-13).

Hayreh SS. Posterior ciliary artery circulation in health and disease: the Weisenfeld lecture. *Invest Ophthalmol Vis Sci.* 2004;45(3):749–757; 748.

Increased Venous Pressure

In rare cases, choroidal blood flow abnormalities may be related to venous outflow problems, including those caused by *dural arteriovenous malformations* or *carotid-cavernous*

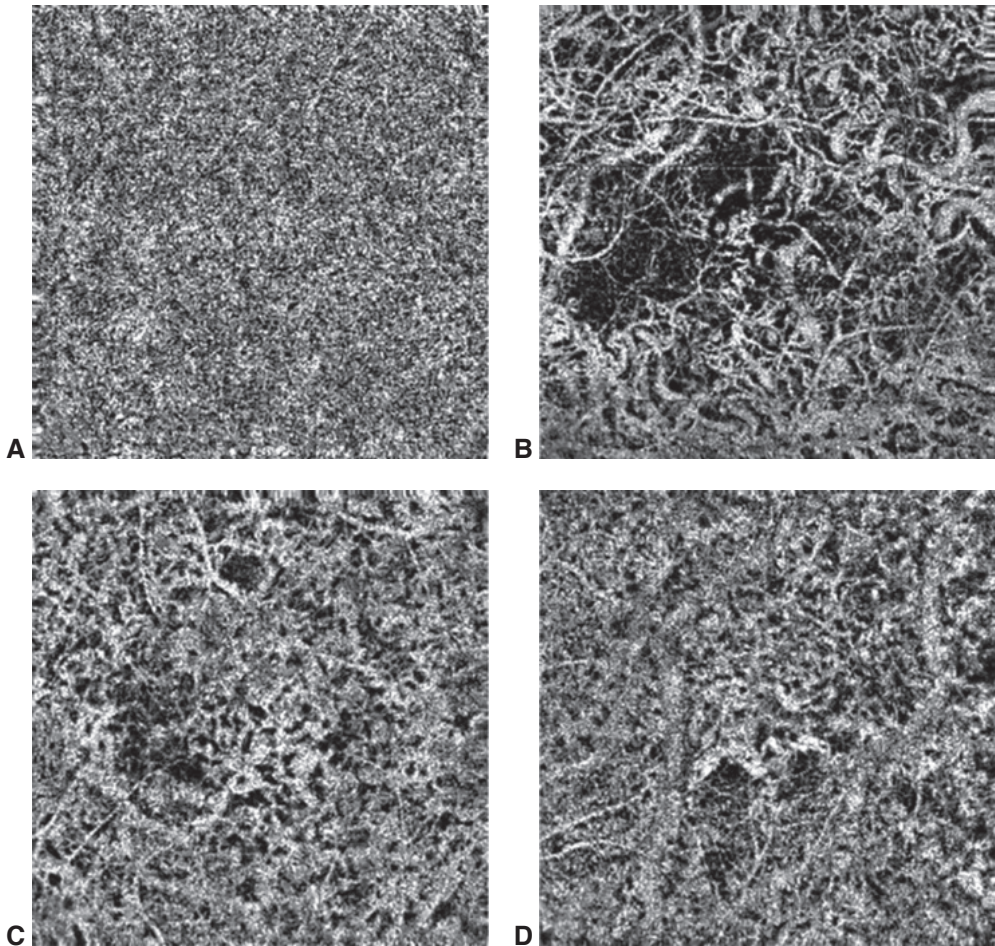


Figure 9-13 OCT angiography images of the choriocapillaris in a healthy patient and in patients with pseudoxanthoma elasticum (PXE). **A**, Healthy 63-year-old patient with no ocular disease. **B–D**: Three different patients with PXE: a 55-year-old patient (**B**) and two 63-year-old patients (**C**, **D**). The eyes with PXE show no evidence of RPE atrophy but have remarkable loss of the choriocapillaris. (Reproduced with permission from Spaide RF. Choriocapillaris signal voids in maternally inherited diabetes and deafness and in pseudoxanthoma elasticum. *Retina*. 2017;37(11):2008–2014. doi:10.1097/IAE.0000000000001497)

fistulas (Fig 9-14). Diagnosis of choroidal blood flow abnormalities often requires dye-based angiography and occasionally a stethoscope (to detect a bruit). These patients should be referred for appropriate medical evaluation.

Age-Related Choroidal Atrophy

The thickness of the choroid decreases with higher levels of myopia and increasing age. In some older patients, the choroid is much thinner than expected. The eyes of these

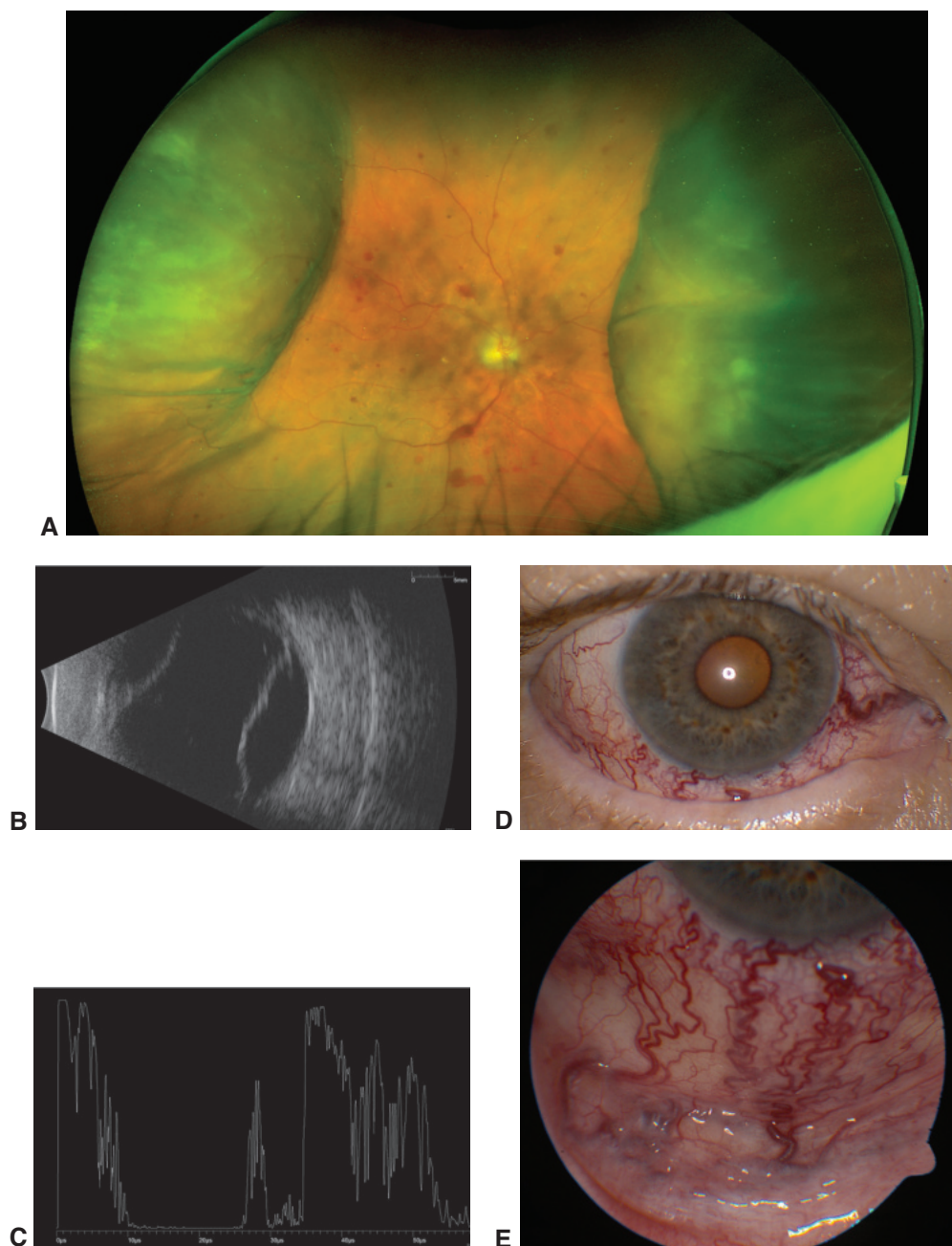


Figure 9-14 Constellation of classic findings with carotid-cavernous fistulas. **A**, Wide-angle color photograph from an older adult patient who was referred for “multiple choroidal melanomas” found incidentally on examination. **B**, B-scan shows large choroids. **C**, Diagnostic A-scan shows very low internal reflectivity, consistent with serous choroids rather than tumor masses. **D, E**, The patient was noted to have a red eye. On very specific questioning, he revealed that he had fallen and hit his head approximately 9 months earlier, and the eye began to turn red approximately 1–2 months after the fall. The patient was hypertensive. These images show classic corkscrew vessels. Patients with a carotid-cavernous fistula can also have a hyporeactive pupil from anterior segment ischemia, as was the case with this patient. (Courtesy of Anthony B. Daniels, MD, MSc.)

individuals tend to have *pseudodrusen*, which resemble drusen in appearance but are caused by collections of subretinal drusenoid deposits above the RPE. Like eyes with drusen, eyes with subretinal drusenoid deposits have an increased risk of CNV, particularly types 2 and 3, and geographic atrophy. More than 90% of eyes with geographic atrophy also have pseudodrusen. In contrast with patients with drusen, patients with subretinal drusenoid deposits perform more poorly on microperimetry, and dark adaptation is markedly prolonged in this group (Figs 9-15, 9-16).

Spaide RF. Disease expression in nonexudative age-related macular degeneration varies with choroidal thickness. *Retina*. 2018;38(4):708–716.

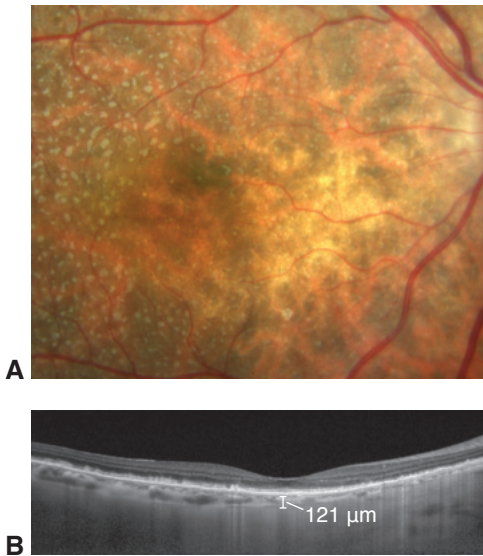


Figure 9-15 Pseudodrusen and the choroid. **A**, Fundus photograph shows an eye with prominent pseudodrusen. **B**, The true nature of the pseudodrusen is seen as subretinal drusenoid deposits. The subfoveal choroidal thickness is 121 μm. The choroid is thinner in eyes with pseudodrusen than in those with drusen. (Reproduced with permission from Spaide RF. Disease expression in nonexudative age-related macular degeneration varies with choroidal thickness. *Retina*. 2018;38(4):708–716. doi:10.1097/IAE.0000000000001689)

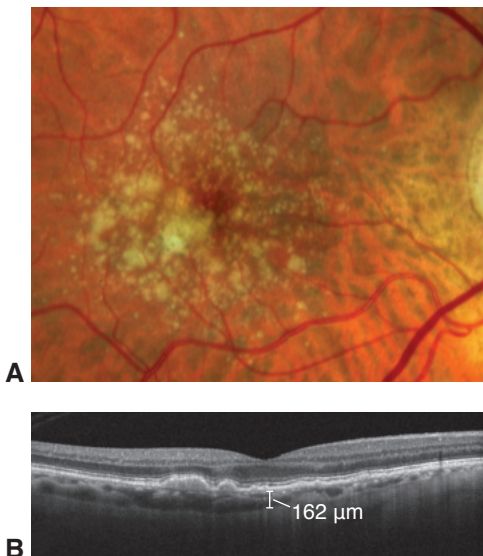


Figure 9-16 Drusen and the choroid. **A**, An eye with typical soft drusen. **B**, The subfoveal choroidal thickness is 162 μm. (Reproduced with permission from Spaide RF. Disease expression in nonexudative age-related macular degeneration varies with choroidal thickness. *Retina*. 2018;38(4):708–716. doi:10.1097/IAE.0000000000001689)

Choroidal Folds

Folds in the choroid, sometimes called *chorioretinal folds*, occur for various reasons, including secondary to disease. Forces external to the eye, such as an indenting tumor or thyroid eye disease, can cause choroidal folds. The sclera may be thickened by posterior scleritis, thereby crowding the choroid (Fig 9-17). A relatively common phenomenon, which is poorly characterized, is the development of choroidal folds in middle-aged adults, with acquired hyperopia occurring in some of these individuals. Engorgement of the choroid causes an expansion of the tissue, which is limited by the sclera. Reduced intraocular pressure, occurring most commonly as a postoperative complication, can cause ciliochoroidal effusions and curvilinear choroidal folds in the posterior pole, a condition known as *hypotony maculopathy*. Use of medications such as topiramate can cause idiopathic swelling of the choroid resulting in chorioretinal folds and ciliochoroidal effusions without hypotony. Increased intracranial pressure can cause papilledema resulting in fine folds that course circumferentially around the optic nerve head; these folds are called *Patton lines*. Localized choroidal folds can be seen in association with CNV, choroidal neoplasms, and scleral buckles (Table 9-1).

Spaide RF, Goldbaum M, Wong DW, Tang KC, Iida T. Serous detachment of the retina. *Retina*. 2003;23(6):820–846.

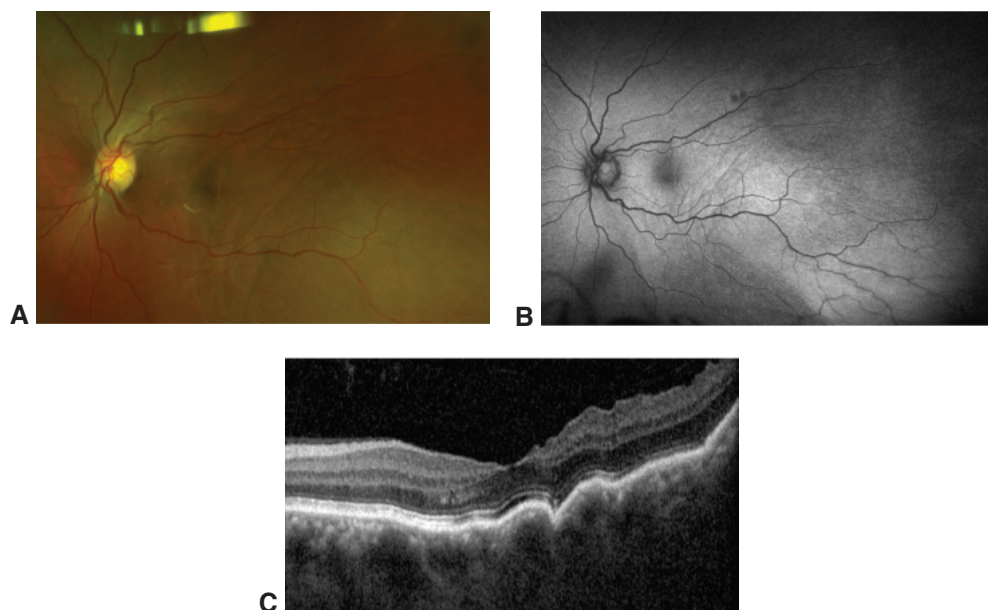


Figure 9-17 Choroidal folds in a patient with nodular posterior scleritis. **A**, Fundus photograph shows subtle striae associated with choroidal folds extending through the temporal macula. **B**, Fundus autofluorescence highlights the striae of folds with alternating hyper- and hypoauto-fluorescent changes emanating from the inferotemporal area of posterior nodular scleritis. **C**, Spectral-domain OCT shows characteristic undulations of RPE consistent with choroidal folds and a thickening choroid consistent with posterior scleritis. (Courtesy of Avni P. Finn, MD, MBA.)

Table 9-1 Differential Diagnosis of Choroidal Folds

Etiology of Choroidal Folds	Characteristic
Focal choroidal mass/neovascularization	Usually radiating from center of the lesion
Hyperopia	Usually horizontal in posterior pole/papillomacular bundle; extreme example in posterior microphthalmia
Hypotony	Ciliochoroidal effusions and curvilinear choroidal folds in the posterior pole
Idiopathic; theories include scleral calcification and/or inflammation	Oblique, along the insertion of the oblique muscles
Medications (eg, topiramate)	Ciliochoroidal effusions without hypotony
Papilledema	Patton lines, concentric with optic nerve head
Retrobulbar mass/orbital hardware	Varies according to indent location
Thyroid eye disease	Nonspecific

Choroidal Hemangiomas

Isolated choroidal hemangiomas are reddish-orange, well-circumscribed tumors of varying thickness that can affect the macula either directly or through subretinal fluid (Fig 9-18). Circumscribed hemangiomas transilluminate readily and exhibit highly echographic patterns on ultrasonography. During dye-based angiography, hemangiomas show very early filling of large vessels.

Sturge-Weber syndrome (encephalofacial hemangiomatosis) causes a diffuse hemangioma that, in children, may present first as glaucoma or amblyopia. The areas corresponding to the hemangioma typically appear reddish orange on ophthalmoscopy, a pattern referred to as “tomato ketchup fundus”; the underlying choroidal markings are not visible. The choroidal hemangiomas in Sturge-Weber syndrome are sometimes overlooked because they are diffuse and may blend imperceptibly into adjacent normal choroid. An ipsilateral facial nevus flammeus (port-wine birthmark) is also typically present in patients with this syndrome. See BCSC Section 4, *Ophthalmic Pathology and Intraocular Tumors*, and Section 6, *Pediatric Ophthalmology and Strabismus*, for further discussion.

Hemangiomas have been treated with laser photocoagulation, cryopexy, external beam and plaque radiation, and PDT.

Blasi MA, Tiberti AC, Scupola A, et al. Photodynamic therapy with verteporfin for symptomatic circumscribed choroidal hemangioma: five-year outcomes. *Ophthalmology*. 2010;117(8):1630–1637.

Madreperla SA, Hungerford JL, Plowman PN, Laganowski HC, Gregory PT. Choroidal hemangiomas: visual and anatomic results of treatment by photocoagulation or radiation therapy. *Ophthalmology*. 1997;104(11):1773–1778.

Uveal Effusion Syndrome

Uveal effusion syndrome is a rare condition in which abnormal scleral composition or thickness reduces transscleral aqueous outflow, inhibiting net fluid movement through

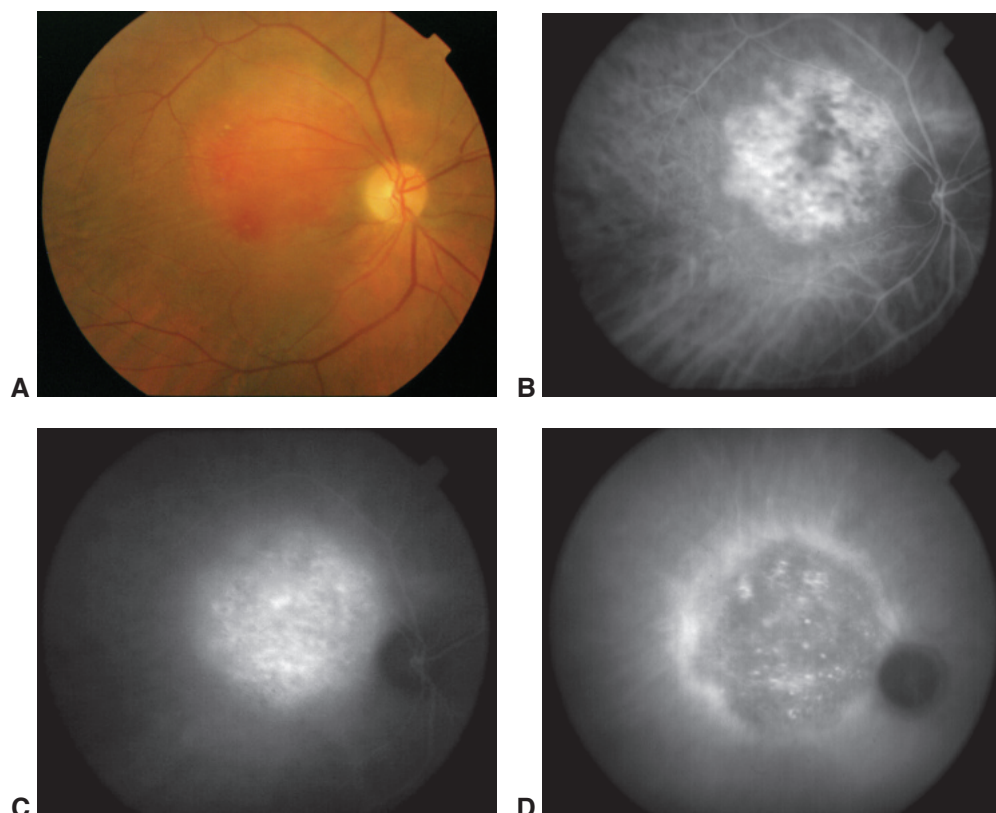


Figure 9-18 Choroidal hemangioma. **A**, Fundus photograph of the typical reddish-orange elevation of a circumscribed choroidal hemangioma. **B**, Soon after injection of ICG dye, the vascular composition of the hemangioma is revealed. **C**, Hyperfluorescence of the tumor occurs in the middle phase of the angiographic study from a combination of dye within and leakage from the vessels of the hemangioma. **D**, In the late phase of the study, the dye “washes out” of the lesion, leaving hyperfluorescent staining in the adjacent tissues. (Reproduced with permission from Spaide RF, Goldbaum M, Wong DW, Tang KC, Iida T. Serous detachment of the retina. *Retina*. 2003;23(6):820–846.)

the posterior eye wall. Choroidal and ciliary body thickening, RPE alterations, and exudative retinal detachment may occur. The choroid is often so thick that OCT imaging is not possible, but the gross thickening can be imaged with ultrasonography. FA usually shows a leopard-spot pattern of hypofluorescence without focal leakage (Fig 9-19). Uveal effusion syndrome is a diagnosis of exclusion, usually made after ruling out all of the more common entities, such as posterior scleritis, and other etiologies of exudative detachments. A high index of suspicion for uveal effusion syndrome should be maintained for young patients with hyperopia. Scleral window surgery may yield anatomical restoration.

Elagouz M, Stanescu-Segall D, Jackson TL. Uveal effusion syndrome. *Surv Ophthalmol*. 2010;55(2):134–145.

Johnson MW, Gass JD. Surgical management of the idiopathic uveal effusion syndrome. *Ophthalmology*. 1990;97(6):778–785.

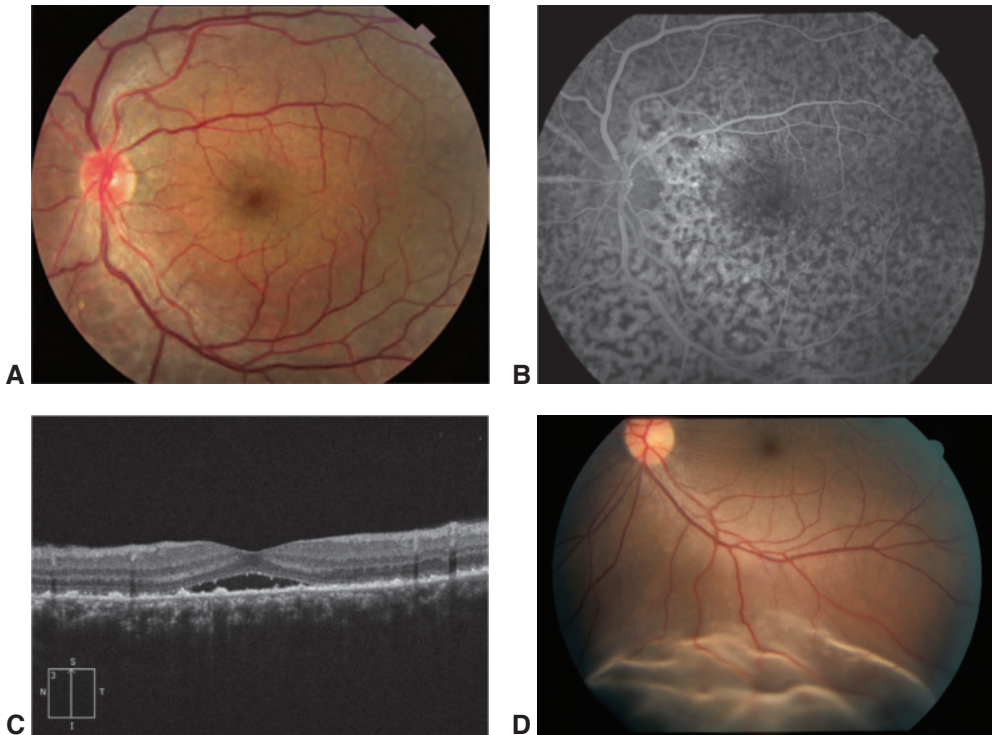


Figure 9-19 Idiopathic uveal effusion syndrome. **A–C:** In this patient’s left eye, visual acuity was reduced to 20/70, and results of the systemic workup were negative. **A,** Fundus photograph demonstrates a blunted foveal reflex and irregular, subtle subretinal deposits. **B,** Corresponding FA image reveals a diffuse leopard-spot pattern of blocking with intervening window defects involving the entire posterior pole. **C,** OCT scan reveals a small amount of subfoveal fluid and outer retinal deposits. Not shown is a peripheral serous retinal detachment. **D,** Fundus photograph from a different patient with recent-onset uveal effusion shows the typical appearance of serous retinal detachment syndrome as well as an underlying choroidal detachment, which is common for this condition. (Parts A–C courtesy of Ronald C. Gentile, MD; part D courtesy of Colin A. McCannel, MD.)

Bilateral Diffuse Uveal Melanocytic Proliferation

A rare paraneoplastic disorder affecting the choroid, *bilateral diffuse uveal melanocytic proliferation (BDUMP)* causes diffuse thickening of the choroid, “giraffe skin” reddish or brownish choroidal discoloration, serous retinal detachment, and cataracts (Fig 9-20). The bilateral proliferation of benign melanocytes is usually associated with or often heralds systemic cancer. These proliferations can look like large nevi.

Most patients with BDUMP also exhibit nummular loss of the RPE, an anatomical change that differs distinctly from large nevi or thickening of the choroid. These areas of RPE loss are hypoautofluorescent during FAF but hyperfluorescent during FA. OCT shows mounds of residual material, presumed to be persistent RPE cells, between areas of loss. Tumors commonly associated with BDUMP are cancers of the ovary, uterus, and

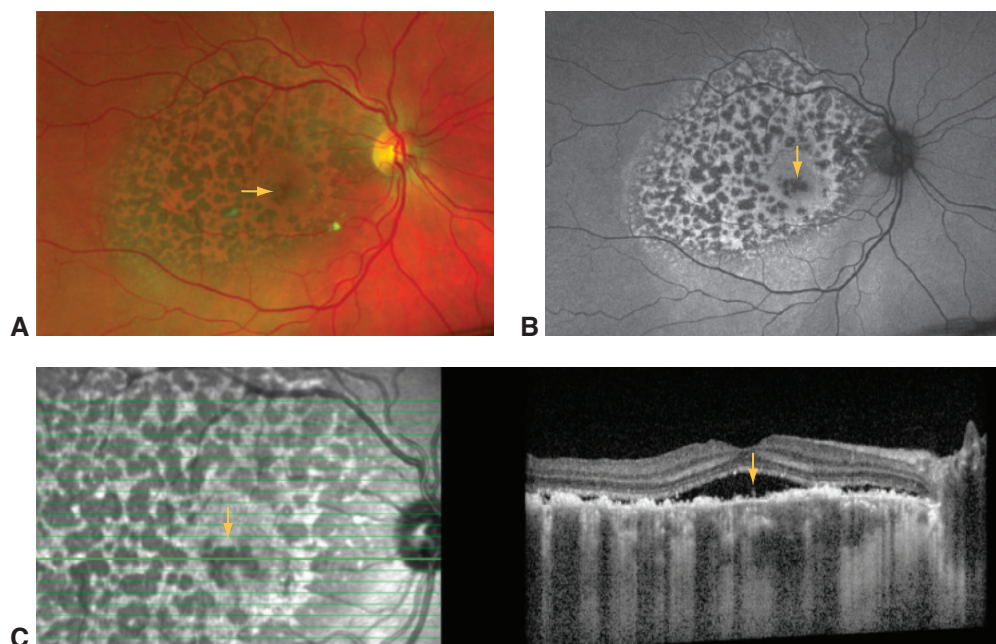


Figure 9-20 Multimodal imaging of bilateral diffuse uveal melanocytic proliferation (BDUMP). **A**, Pseudocolor image (Optos) shows the “giraffe skin” pattern of hypopigmentation and hyperpigmentation (*arrow*). **B**, Autofluorescence (530 nm) shows that the hyperpigmented areas (*arrow*) correspond to hypoautofluorescence (green autofluorescence) and hyporeflectivity on IR imaging (**C**, *left*). These areas correspond to attenuation of the RPE on OCT (**C**, *right*). In addition, the hyperautofluorescent areas around the attenuation correspond to the hypopigmented areas on the color photograph. **C**, The OCT image highlights the thickened, disorganized choroidal architecture and the thickened RPE (thickened RPE corresponds to the hypopigmented, hyperautofluorescent, and hyperreflective areas on the color, autofluorescence, and IR images, respectively). (Courtesy of Amani Fawzi, MD.)

lung, although BDUMP may also occur with cancers of the kidney, colon, pancreas, gallbladder, breast, and esophagus.

Gass JD, Gieser RG, Wilkinson CP, Beahm DE, Pautler SE. Bilateral diffuse uveal melanocytic proliferation in patients with occult carcinoma. *Arch Ophthalmol*. 1990;108(4):527–533.

Wu S, Slakter JS, Shields JA, Spaide RF. Cancer-associated nummular loss of the pigment epithelium. *Am J Ophthalmol*. 2005;139(5):933–935.

Myopia and Pathologic Myopia

Highlights

- Pathologic myopia and its consequences are increasingly among the most common causes of vision loss and blindness throughout the world.
- Posterior segment manifestations of pathologic myopia include macular schisis, choroidal neovascularization, staphyloma, and retinal detachment.
- Retinal and scleral thinning are important posterior segment surgical considerations in patients with pathologic myopia.

Definition, Prevalence, and Epidemiology

There has been a dramatic increase in the prevalence of myopia around the world. Although the more severe manifestations of myopia, variously termed *pathologic myopia* or *high myopia*, are found in a small proportion of the population, this subset accounts for many of the vision problems that occur in eyes with myopia. Moreover, pathologic myopia and its consequences rank at or near the top of the list of causes of vision decrease or blindness in many countries (Table 10-1). Pathologic myopia may be defined as the development of the pathologic changes associated with myopia. However, most studies use a myopic refractive error of -6.00 diopters (D) or greater or an axial length of 26.5 mm or more as the threshold for pathologic myopia. Currently, pathologic myopia is found in 1%–2% of individuals in the United States; approximately 5%, in Italy; 5%–8%, in Japan; 15%, in Singapore; and 38% of university students in Taiwan, China.

Many factors may contribute to the occurrence of myopia, but determining a cause has proved difficult as findings from one study have not necessarily been replicated in other studies. A genetic association with the occurrence of pathologic myopia has also been difficult to prove. Common factors among patients with pathologic myopia include a lack of outdoor activities at a young age and concentrated near work.

Prevention of Pathologic Myopia

Prevention of pathologic myopia is a complex and evolving topic. Participation in outdoor activities is thought to be a contributing factor in reducing the incidence of myopia. This finding is supported by experimental animal model data showing that periods of blue light

Table 10-1 Classic Findings Associated With Pathologic Myopia

Lattice degeneration
Vitreous degeneration
Retinal tear/hole/detachment
Retinal thinning
Retinal vascular traction
Macular schisis/hole
Lacquer crack
Choroidal neovascularization
Choroidal thinning
Fundus tessellation
Peripapillary intrachoroidal cavitation
Chorioretinal atrophy
Scleral thinning
Staphyloma
Inferior staphyloma syndrome, or tilted disc syndrome
Glaucoma
Dome-shaped macula (anterior bowing of the macula associated with posterior staphyloma; see Fig 10-8B)

exposure decrease the amount of myopia that develops. Some theories posit chromatic aberration in the eye as a cause of myopia; red light is focused at a deeper level than blue light.

McBrien and colleagues demonstrated that atropine could slow the development of form-deprivation myopia via a mechanism that was independent of accommodation. Numerous studies have been conducted using atropine eyedrops, including eyedrops at very low concentrations, and suggest a decrease in the amount of myopia progression but a possible rebound in myopia progression after discontinuation of treatment.

Chia A, Chua WH, Cheung YB, et al. Atropine for the treatment of childhood myopia: safety and efficacy of 0.5%, 0.1%, and 0.01% doses (Atropine for the Treatment of Myopia 2).

Ophthalmology. 2012;119(2):347–354.

Chia A, Lu QS, Tan D. Five-year clinical trial on atropine for the treatment of myopia 2: myopia control with atropine 0.01% eyedrops. *Ophthalmology*. 2016;123(2):391–399.

McBrien NA, Moghaddam HO, Reeder AP. Atropine reduces experimental myopia and eye enlargement via a nonaccommodative mechanism. *Invest Ophthalmol Vis Sci*. 1993;34(1):205–215.

Pineles SL, Kraker RT, VanderVeen DK, et al. Atropine for the prevention of myopia progression in children: a report by the American Academy of Ophthalmology. *Ophthalmology*. 2017;124(12):1857–1866. doi:10.1016/j.ophtha.2017.05.032

The Retina and Choroid

The Retina

In the central macula, the retinal thickness in eyes with pathologic myopia is not substantially different from that in emmetropic eyes, particularly in younger individuals. In older persons with marked thinning of the choroid, there may be loss of the outer retinal bands and apparent thinning of the central macula (Fig 10-1). Outside the macula, the

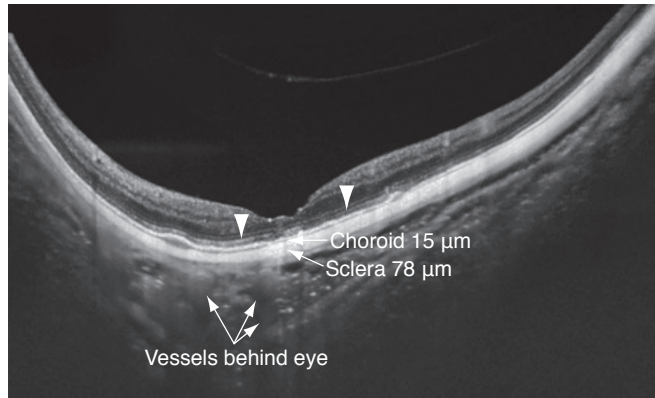


Figure 10-1 Swept-source optical coherence tomography (SS-OCT) image demonstrates some of the many abnormalities that can be present in a highly myopic eye. The magnitude and thickness of the reflection from the ellipsoid layer (*arrowheads*) show a rough correlation to the thickness of the underlying choroid but do vary with the location in the image because of a number of factors, including defocus of the illumination beam and astigmatism. The subfoveal choroid is 15 μm thick; the subfoveal sclera, 78 μm thick. Both measurements are less than 10% of their expected values. The layers of this eye are so thin that it is possible to image structures in the orbit behind the eye, including blood vessels. Note the unusual shape of the eye, which is due to the presence of a staphyloma. (Courtesy of Richard F. Spaide, MD.)

retinal thickness in eyes with pathologic myopia is reduced compared with that in emmetropic eyes.

Lattice degeneration is more commonly found in myopic eyes than in emmetropic eyes. With increasing age, the vitreous starts to detach, with small areas of detachment bordering areas of attachment; this occurs in all eyes, including those with myopia. Vitreous traction in areas of persistent attachment can cause retinal tears and then retinal detachment or may cause subretinal fluid to occur in association with small atrophic holes in lattice degeneration. The proportion of retinal detachment secondary to holes increases with higher degrees of myopia, as compared with that secondary to retinal tears. In patients with high myopia, repair of retinal detachment may be more difficult because of the thinner retina, the higher prevalence of lattice degeneration, the thinner sclera (which can complicate buckle placement), the more posterior location of retinal breaks, and the possibility of multiple retinal defects.

In eyes with larger amounts of myopia, traction on the retina can affect broader areas of the retina, independent of vitreous attachment. However, the posterior portion of the retina can remain attached to the retinal pigment epithelium (RPE) despite broad areas of traction. Retinal thickness increases because of the fluid accumulation within the retina and distention of the cellular elements in the retina.

Myopic macular schisis most commonly involves Henle fiber layer but can also involve the inner nuclear layer, the ganglion cell layer, and the region underneath the internal limiting membrane (ILM). The traction can be related to vitreous traction from attached vitreous, but eyes with myopic macular schisis can still have vitreous traction with posterior vitreous detachment (Fig 10-2). After posterior vitreous detachment, a

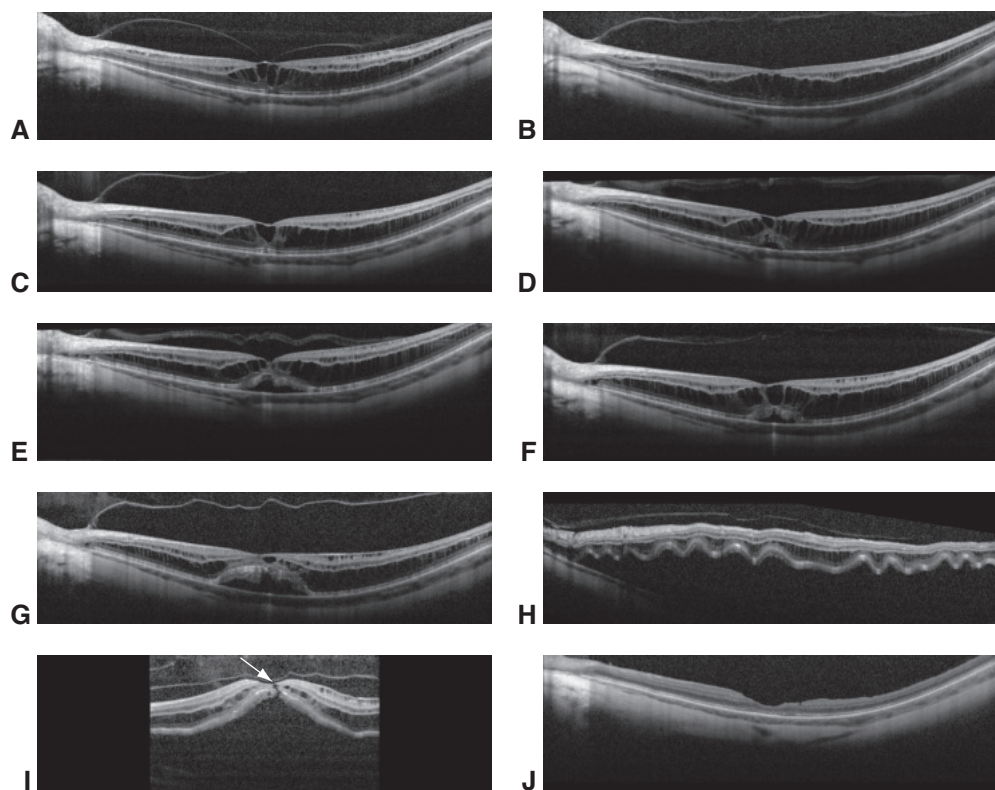


Figure 10-2 Successive OCT examinations of a female patient with myopic macular schisis. At presentation, the patient had a perifoveal vitreous detachment (**A**) that separated (**B**). **C**, Four months later, a larger foveal cavitation developed. **D**, One month after that, a localized detachment of the fovea occurred. **E–F**: One month after the image in **D** was taken, the detachment was slightly larger (**E**) and persisted (**F**). **G**, At 4-month follow-up, the macular detachment had increased in size. **H**, One month later, she returned with a substantial loss of central vision. Imaging revealed a large retinal detachment with edematous folding of the outer retina. **I**, A small macular hole caused the larger detachment (*arrow*). **J**, The macular hole was repaired by vitrectomy with internal limiting membrane removal, which resulted in resolution of the retinal detachment and the myopic macular schisis. (Courtesy of Richard F. Spaide, MD.)

skim coat of vitreous remains on the surface of the retina and appears to cause traction. Varying amounts of epiretinal membrane may also contribute to the traction. Peeling of the ILM results in resolution of the schisis, typically near the area where the ILM was peeled; this has led to the conclusion that the ILM may be altered in eyes with myopic macular schisis. Another possibility is that many of these eyes have progressive myopia with continued ocular expansion. The ILM may not necessarily be remodeled, and therefore it may not expand like the outer retina.

More advanced tractional changes can lead to retinal detachment over staphylomas and to myopic macular holes. For macular holes, the rate of successful repair is lower in eyes with high myopia than in emmetropic eyes. Also, macular holes in high myopia frequently require use of the inverted ILM technique, in which the ILM is folded over the hole prior to fluid gas exchange. In addition, in eyes with high myopia, macular holes

may lead to extensive or complete retinal detachment (see Chapter 16, Fig 16-20). Fovea-sparing ILM peeling may result in better visual outcomes when treating foveal retinal detachments caused by myopic traction maculopathy.

Traction appears to affect the retinal vessels in pathologic myopia. These vessels, particularly the maculopapillary bundle, can straighten, with occasional microaneurysm formation, and slight elevation of the arcade vessels is possible. Paravascular cavitations and lamellar holes may also be found, but these defects do not appear to have any clinically meaningful effect.

Bruch Membrane

Located between the RPE and the choriocapillaris, Bruch membrane forms early in the development of the eye and appears to undergo varying amounts of remodeling over time. However, this may not be true in eyes with higher degrees of myopia. In these eyes, the Bruch membrane opening shifts so that the nasal portion of the optic nerve head is undermined by Bruch membrane. The nerve fibers must course around the nasal portion of the Bruch membrane opening; this has been referred to as “supertraction” or “supertraction crescent.” Corresponding temporal displacement of the posterior part of the Bruch membrane opening is related to the myopic macular crescent, which is typically located on the temporal side of the optic nerve. The lack of choroidal circulation in this region gives it a white appearance due to visualization of the sclera.

Ocular expansion in pathologic myopia puts stress on Bruch membrane, potentially leading to fine ruptures called *lacquer cracks*. The outer lamella of Bruch membrane is the basement membrane of the choriocapillaris. The cracks not only disrupt the avascular membrane but may also rupture the capillaries in the choriocapillaris, resulting in subretinal hemorrhages. These hemorrhages can be difficult to differentiate from those caused by choroidal neovascularization (CNV; discussed in the following section). Lacquer cracks offer a region of ingress for CNV (Fig 10-3). Extension of lacquer cracks through the center of the fovea can cause distortion and loss of visual acuity. If many lacquer cracks develop, a region of pigmentary granularity can form. In late-stage myopic degeneration, large dehiscences in Bruch membrane may occur.

Choroidal Neovascularization

Early manifestations of CNV in pathologic myopia include decreased or distorted vision. The clinical findings include subretinal hemorrhage, elevation and infiltration of the outer retina by vascular invasion, accumulation of subretinal fluid, and a localized area of pigmentary change. In highly myopic eyes, the findings can easily be overlooked on ophthalmoscopy.

Myopic CNV is often seen in close association with lacquer cracks (see the previous section), or it may occur as an extension from a region of chorioretinal atrophy. In the United States, it is not uncommon to find CNV in young women with myopia who show signs of multifocal choroiditis either concurrently or later. These eyes may develop damage from the CNV, from inflammation, or from both; each component requires careful treatment.

Myopic CNV was first treated with thermal laser photocoagulation; later, photodynamic therapy was used, but both approaches were suboptimal. The advent of injections

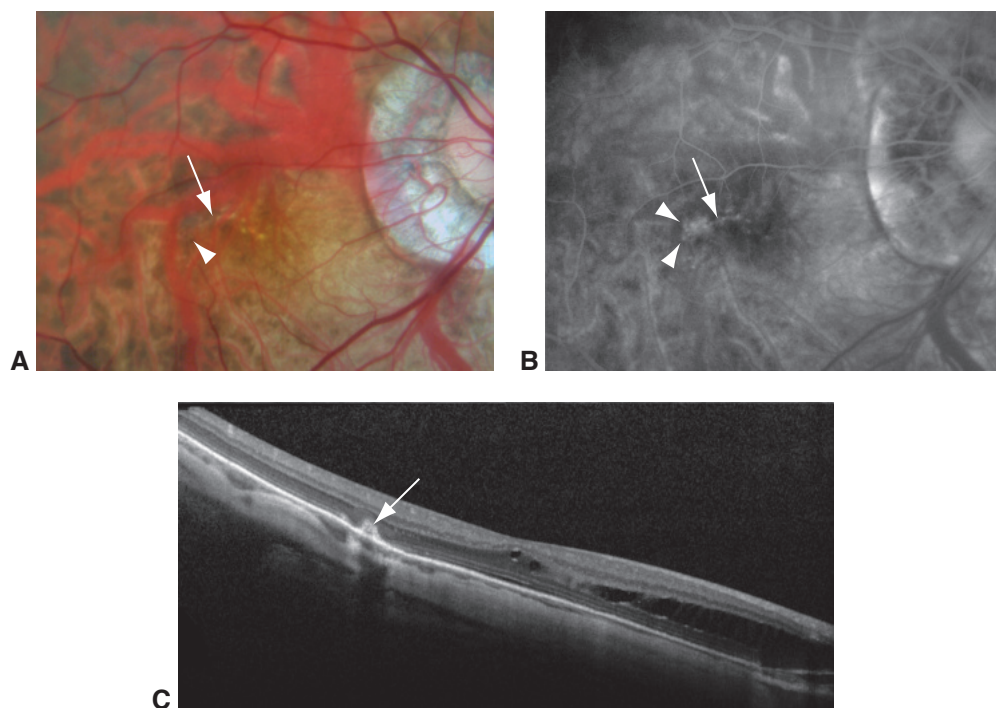


Figure 10-3 Myopic choroidal neovascularization (CNV) emanating from a lacquer crack. **A**, In a patient with -16.00 diopter myopia, a small scotoma developed near the center of the visual field. Note the lacquer cracks (arrow) and associated pigmentary changes (arrowhead). **B**, Fluorescein angiography image shows hyperfluorescent leakage (arrowheads) consistent with CNV and the window defect of the lacquer crack (arrow). **C**, OCT scan shows a small elevated lesion (arrow) and also nonassociated macular schisis. (Reproduced with permission from Springer Nature. Spaide RF. Pathologic Myopia. Copyright 2014.)

of anti-vascular endothelial growth factor (anti-VEGF) agents, which allow regression of neovascularization without causing immediate collateral damage, was a major advancement (Fig 10-4). To control the CNV, episodic reinjection of medications may be necessary. Compared with CNV secondary to age-related macular degeneration, myopic CNV generally requires fewer injections. With or without treatment, CNV in pathologic myopia may become hyperpigmented (known as a *Fuchs spot*). With longer follow-up, areas of atrophy often develop at or adjacent to the pigmented lesions, and the atrophy eventually encompasses the central macula.

The Choroid

The choroidal circulation accounts for more than 80% of the total blood flow in the eye. The innermost layer of the choroid, the choriocapillaris, supplies the RPE and the outer retina. In addition, the choroid serves as a heat sink, absorbing stray light, participating in immune response and host defense, and playing an integral part in the process of emmetropization. Thinning of the choroid can impair function. Even small decreases in atmospheric oxygen tension can result in suboptimal visual function. Optical coherence tomography (OCT),

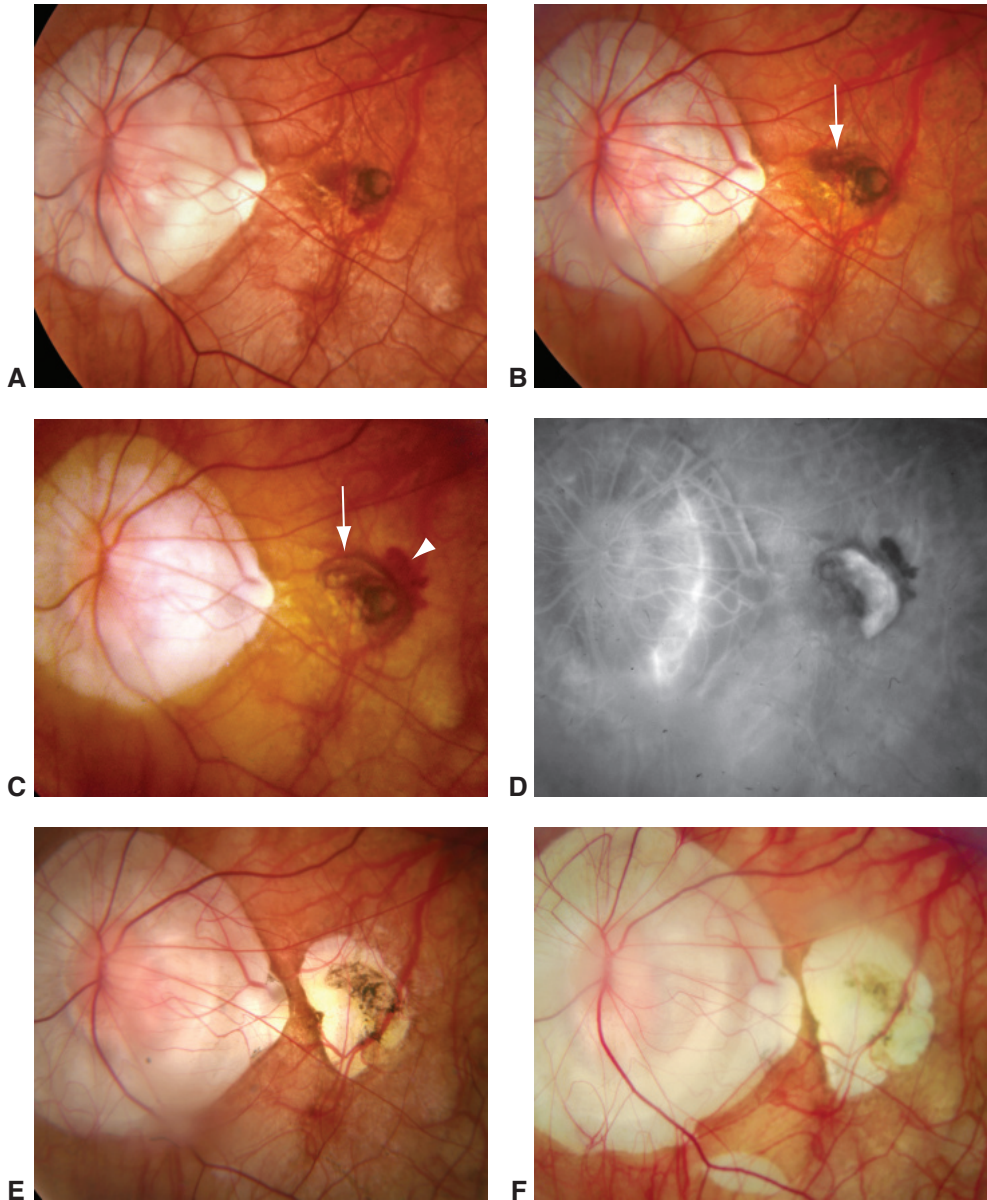


Figure 10-4 Expansion of CNV after treatment with photodynamic therapy (PDT) followed by bevacizumab. **A**, This patient was treated with PDT for myopic CNV with leakage. Note the rings of pigment centrally, indicating successive expansions of the lesion. **B**, After treatment, the lesion expanded even more. Note the increased pigment (*arrow*). **C**, After several PDT treatments, the lesion expanded further (*arrow*), and a hemorrhage developed (*arrowhead*). Visual acuity was 20/80. **D**, Fluorescein angiography image reveals the extent of the neovascularization. The patient was given an injection of intravitreal bevacizumab 1.25 mg. **E**, The patient received 2 additional injections over time. Six years after first being treated with bevacizumab, the patient had some residual hyperpigmentation, but also a wide area of pigmentary loss. Visual acuity was 20/60. **F**, Nearly 10 years after injection, the atrophy continued to expand.

(Courtesy of Richard F. Spaide, MD.)

particularly either swept-source OCT or enhanced depth imaging using spectral-domain OCT, can image the full thickness of the choroid in myopic eyes.

With increasing age, the choroid becomes thinner. One study found that the mean subfoveal choroidal thickness in children aged 11–12 years was 369 ± 81 μm in girls and 348 ± 72 μm in boys. In contrast, the typical subfoveal choroidal thickness in an emmetropic 60-year-old is approximately 220–260 μm . Eyes with myopia, particularly with myopia progressing into the range of pathologic myopia, undergo expansion starting in late childhood, and this expansion is also associated with choroidal thinning (Fig 10-5). In another study, a group of myopic patients with a mean age of 59.7 years had a mean refractive error of -11.9 D and a mean subfoveal choroidal thickness of 93 μm , with a relatively large standard deviation of 63 μm . The thinning of the choroid per decade of life is approximately the same in myopic and nonmyopic eyes. Thus, older individuals, and individuals with higher amounts of myopia, may have remarkably thin choroids. The most significant predictor of visual acuity in highly myopic eyes with no macular pathology is subfoveal choroidal thickness. In patients with pathologic myopia, visual acuity is lost for many reasons, some of which are dramatic, such as retinal detachment. However, in comparison, a greater number of older individuals with high myopia have smaller amounts of visual acuity loss associated with decreased choroidal thickness.

When the choroid becomes very thin, the pigmentation of the RPE often becomes granular. The larger choroidal vessels are easily visible. The choroid may show a repeating pattern of pigmentation, blood vessel, pigmentation, blood vessel, referred to as *tessellation*. Eventually, the choroid may become so thin that the choroidal tissue and the overlying RPE are no longer supported (Fig 10-6). This produces ovoid areas of white, called

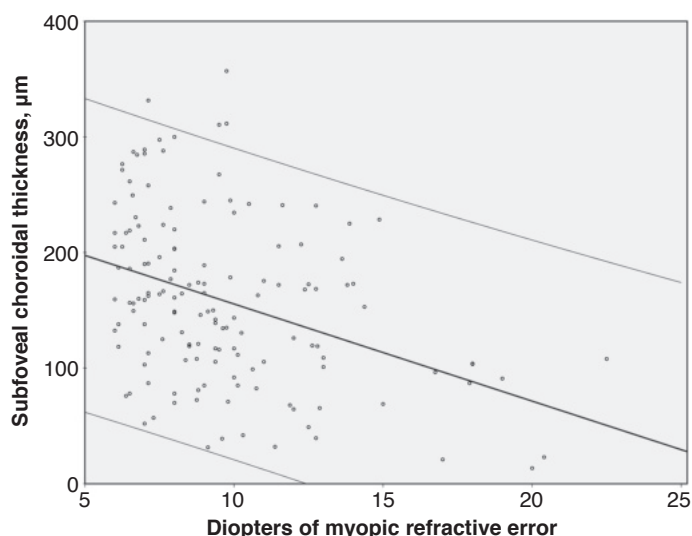


Figure 10-5 Subfoveal choroidal thickness versus myopic refractive error in a group of 145 highly myopic eyes with no macular pathology. The trend line demonstrates the decrease in choroidal thickness with increasing refractive error, and the thinner bordering lines show the 95% confidence interval of the trend line. (Data from Nishida Y, Fujiwara T, Imamura Y, Lima LH, Kurosaka D, Spaide RF. Choroidal thickness and visual acuity in highly myopic eyes. *Retina*. 2012;32(7):1229–1236.)

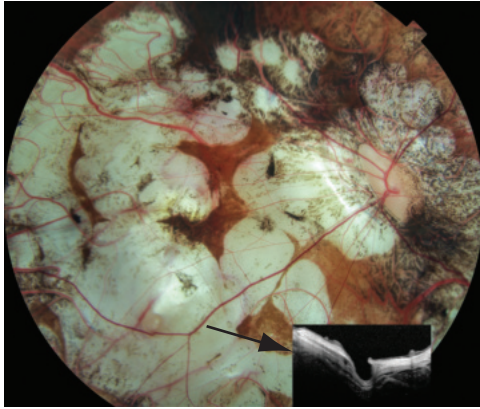


Figure 10-6 End-stage chorioretinal atrophy in pathologic myopia. Note the patches of full-thickness tissue loss; these appear white because of direct visualization of the sclera. The emissary openings in the sclera become enlarged. *Inset:* OCT image, taken at the origin of the arrow, demonstrates remarkable thinning of the sclera and near absence of scleral tissue in the emissary opening itself. (Courtesy of Richard F. Spaide, MD.)

patchy atrophy, in which the underlying sclera is visible. If the central macula is involved, the patient's vision will be poor. In eyes with larger areas of atrophy, even Bruch membrane can rupture, leaving a truly bare sclera.

Around the optic nerve, between 5% and 10% of highly myopic eyes have a yellow-orange pocket, which at one time was thought to be a localized retinal detachment, but more refined OCT imaging revealed it to be an acquired cavitation in the choroid (Fig 10-7). Therefore, these lesions are called *peripapillary intrachoroidal cavitations*. Enhanced depth imaging OCT demonstrated that these cavitations are associated with a posterior bowing of the sclera around the nerve.

Li XQ, Jeppesen P, Larsen M, Munch IC. Subfoveal choroidal thickness in 1323 children aged 11 to 12 years and association with puberty: the Copenhagen Child Cohort 2000 Eye Study. *Invest Ophthalmol Vis Sci.* 2014;55(1):550–555.

Nickla DL, Wallman J. The multifunctional choroid. *Prog Retin Eye Res.* 2010;29(2):144–168.

Ohno-Matsui K, Jonas JB, Spaide RF. Macular Bruch membrane holes in highly myopic patchy chorioretinal atrophy. *Am J Ophthalmol.* 2016;166:22–28.

Spaide RF, Akiba M, Ohno-Matsui K. Evaluation of peripapillary intrachoroidal cavitation with swept source and enhanced depth imaging optical coherence tomography. *Retina.* 2012;32(6):1037–1044.

The Sclera

The thickness of the sclera in a nonmyopic eye varies considerably with location; the thickest area, which is around the optic nerve, can be slightly more than 1 mm, whereas the area immediately under the rectus muscle insertions may be as thin as 0.3 mm. When ocular expansion related to myopia begins, the eye elongates, but the amount of material that makes up the sclera does not increase (see Fig 10-1). The collagen fibers become thinner, the typical gradient in fiber thickness in the sclera is lost, and the amount of extracellular matrix decreases. Over time, the sclera in a myopic eye shows more elasticity and greater viscoelastic creep than the sclera in a nonmyopic eye. These factors appear to be necessary to allow the myopic eye to expand, but why it expands is unknown.

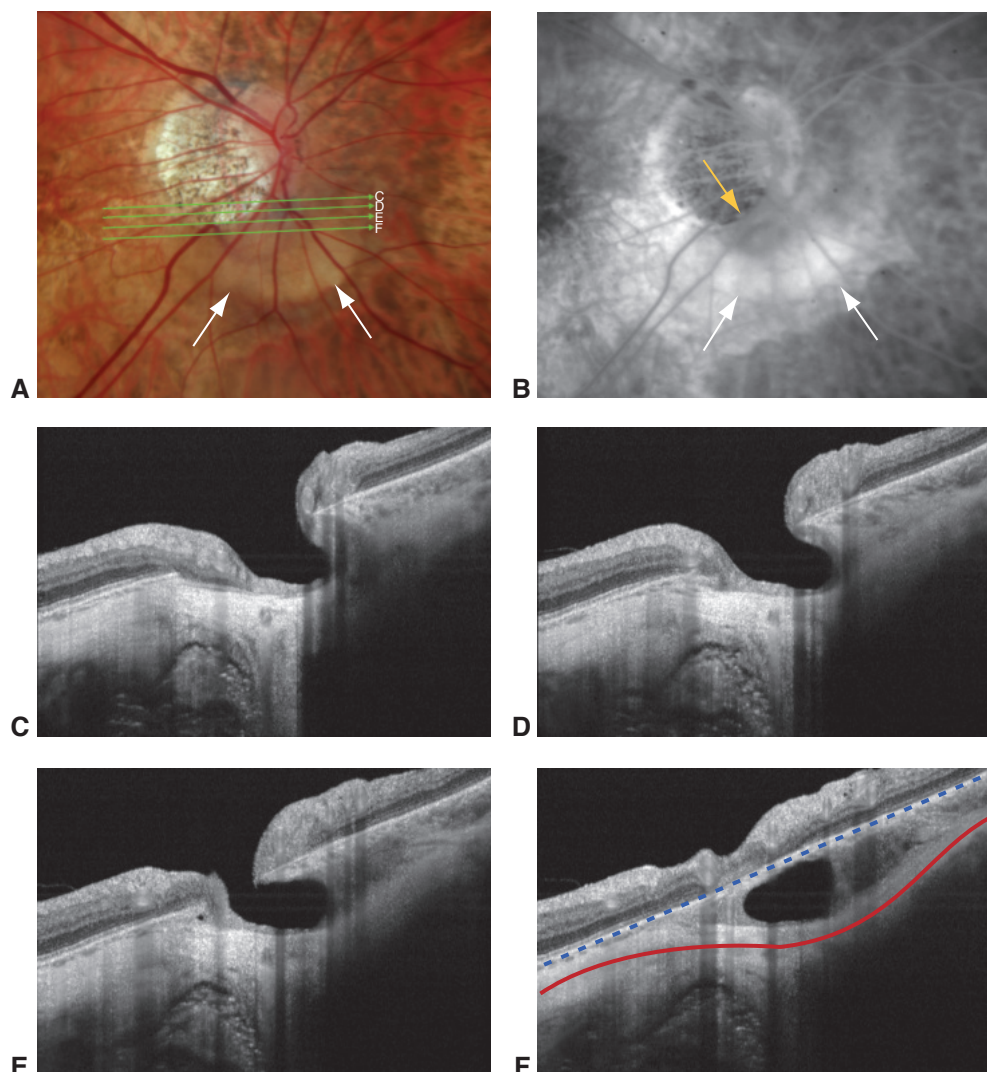


Figure 10-7 Peripapillary intrachoroidal cavitation. **A**, Color fundus photograph shows the yellow-orange region of the intrachoroidal cavitation (*white arrows*). The *green arrows* show the locations of subsequent OCT sections. **B**, Fluorescein angiography image shows a modest late collection of dye within the cavity (*white arrows*). Note the upper edge of the cavity is sharply demarcated (*yellow arrow*). The edge of the retinal defect is more clearly evident than in the color photograph. **C–F**: Successive serial sections taken using SS-OCT show the inner retinal defect and the extension of the cavitation into the choroid. A veil of tissue extends through the thickness of the choroid at the border of the cavitation. In **F**, the hyperreflective band that corresponds to the retinal pigment epithelium is nearly straight, as illustrated by the *blue dashed line*. The *red line* follows a posterior bowing at the center-point thickness in the sclera. (Used with permission from Spaide RF, Akiba M, Ohno-Matsui K. Evaluation of peripapillary intrachoroidal cavitation with swept source and enhanced depth imaging optical coherence tomography. *Retina*. 2012;32(6):1037–1044. doi:10.1097/IAE.0b013e318242b9c0)

In animal models, form deprivation and lens-induced defocus result in abnormal changes in axial length. Neither optic nerve sectioning nor the destruction of the ciliary nerve prevents the development of experimental myopia. Form deprivation of a hemifield results in expansion of the eye that is conjugate with that hemifield, even if the optic nerve is sectioned. These findings support the hypothesis that remodeling of the eye results from local effects within the eye, beginning with signaling that originates in the retina and choroid and eventually affects the sclera. Connection to the brain does not appear to be necessary. Eyes that develop axial myopia lengthen, but in comparison to the posterior pole, the periphery becomes relatively hyperopic. Peripheral hyperopia can induce myopia in animal models, and curiously myopia can develop in eyes with peripheral hyperopia even if the posterior portion of the retina has been destroyed.

Ocular expansion can vary regionally, inducing formation of areas of the sclera that have differing radii of curvature. Bulging of the sclera and adherent uveal tissue in an area of thin sclera, or *staphyloma*, can result from regional expansion of the eye. These protrusions typically involve 3 general areas of the eye: (1) the area around the nerve; (2) the macular region, which leads to exaggerated thinning of the choroid and possibly myopic traction maculopathy; and (3) the inferior or inferotemporal portion of the eye (Fig 10-8). The superior portion of the eye has one radius of curvature, the inferior portion has another, and there is a visible border between these 2 curves. If the border occurs above the optic nerve, the optic nerve head will appear grossly tilted and rotated. If the border bisects the fovea, several alterations may be seen. In later life, there may be atrophy along the border that affects the RPE under the fovea, and either subretinal fluid without CNV or frank CNV may also develop in these eyes. Because a staphyloma involving the inferior or inferotemporal eye may be accompanied by a set of possible ocular manifestations, it has been referred to as *inferior staphyloma syndrome* or *tilted disc syndrome*.

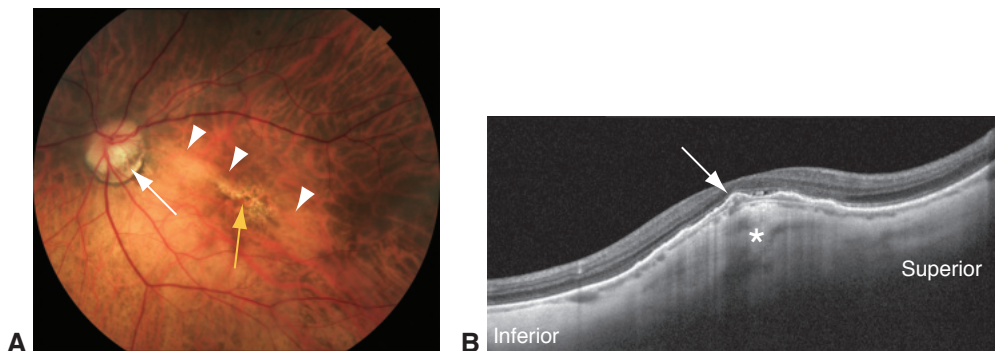


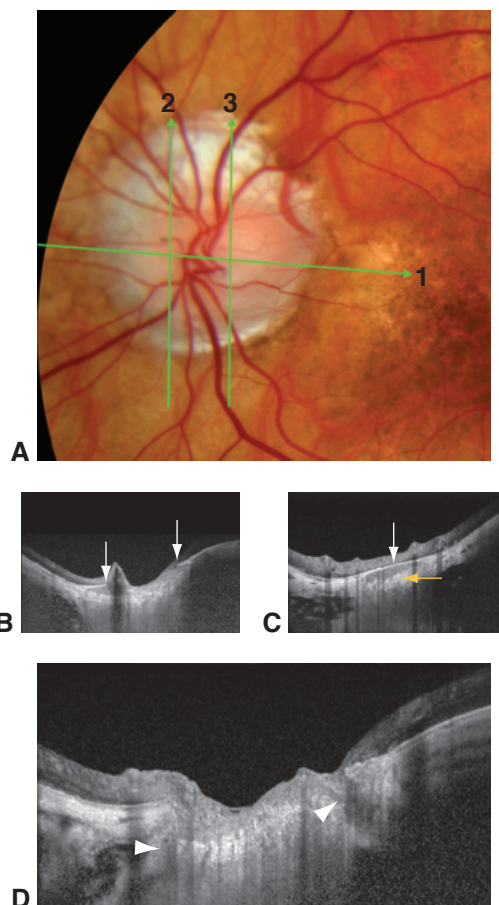
Figure 10-8 Inferior staphyloma syndrome, also known as *tilted disc syndrome*. **A**, Fundus photograph shows that the superior fundus is darker than the staphylomatous inferior fundus. At the border between the 2 regions (*arrowheads*) there is a pigmentary change in the macula (*yellow arrow*). Because this border runs through the superior border of the optic nerve head, the patient has a tilted disc (*white arrow*). **B**, Dome-shaped macula. Vertical OCT image taken through the fovea shows the 2 curves. At the ridge between them, there is CNV (*arrow*) associated with a small amount of submacular fluid. The sclera is typically thicker at the border zone (*asterisk*) than anywhere in the neighboring areas. (Courtesy of Richard F. Spaide, MD.)

- Diether S, Schaeffel F. Local changes in eye growth induced by imposed local refractive error despite active accommodation. *Vision Res.* 1997;37(6):659–668.
- Smith EL 3rd, Hung LF, Huang J, Blasdel TL, Humbird TL, Bockhorst KH. Effects of optical defocus on refractive development in monkeys: evidence for local, regionally selective mechanisms. *Invest Ophthalmol Vis Sci.* 2010;51(8):3864–3873.
- Smith EL 3rd, Ramamirtham R, Qiao-Grider Y, et al. Effects of foveal ablation on emmetropization and form-deprivation myopia. *Invest Ophthalmol Vis Sci.* 2007;48(9):3914–3922.
- Wildsoet CF, Schmid KL. Optical correction of form deprivation myopia inhibits refractive recovery in chick eyes with intact or sectioned optic nerves. *Vision Res.* 2000;40(23):3273–3282.

The Optic Nerve

In eyes with pathologic myopia, the optic nerve head is undercut by a shifted Bruch membrane opening (Fig 10-9), the scleral canal may be stretched and tilted, the circle of Zinn-Haller is greatly enlarged, and the optic nerve may appear stretched and pallorous.

Figure 10-9 Optic nerve changes in pathologic myopia. **A**, The optic nerve head seen in the color fundus photograph does not accurately show the size of the Bruch membrane opening. **B**, Enhanced depth imaging OCT shows the actual Bruch membrane opening (*arrows*). Note how far Bruch membrane extends into what appears to be the nerve (*left arrow*). **C**, A vertical section through 2 in the color photograph shows the extent of Bruch membrane. The *white arrow* shows Bruch membrane extending into the nerve tissue. The nerve fibers have to arch nasally under Bruch membrane to reach the lamina cribrosa (*yellow arrow*). **D**, A vertical section through 3 in the color photograph shows 2 dehiscences (*arrowheads*) in the lamina cribrosa. Although this is a common finding in both glaucoma and pathologic myopia, it is not known whether every patient with a lamina defect in high myopia also has glaucoma. When an eye with glaucoma develops a Drance hemorrhage, typically a lamina cribrosa dehiscence is apparent. However, in pathologic myopia, dehiscences in the lamina are not typically found to have any associated hemorrhage. (Courtesy of Richard F. Spaide, MD.)



Glaucoma is much more common in highly myopic eyes than in emmetropic eyes and frequently goes undetected. Measuring the retinal nerve fiber layer with OCT is problematic not only because of the varying shape of the eye and the potential for schisis, but also because normative databases were developed for eyes that are not pathologically myopic. Visual field tests may show defects because of the shape of the eye, some of which can be “fixed” by using a refractive correction for that portion of the eye. Dehiscences in the lamina cribrosa are common in eyes with high myopia (see Fig 10-9D).

Ohno-Matsui K, Akiba M, Moriyama M, et al. Acquired optic nerve and peripapillary pits in pathologic myopia. *Ophthalmology*. 2012;119(8):1685–1692.

Focal and Diffuse Retinal and Choroidal Inflammation

Highlights

- The most important step in managing chorioretinal inflammation is distinguishing between noninfectious and infectious etiologies.
- Noninfectious forms of chorioretinal inflammation, particularly the white dot syndromes, have characteristic features that can be useful in identifying these entities, for which the workup, treatments, and prognoses vary substantially.
- A good history and high index of suspicion are necessary to obtain the appropriate laboratory tests for patients with infectious forms of chorioretinal inflammation.
- Primary vitreoretinal lymphoma can masquerade as uveitis.

Overview

A variety of inflammatory diseases are associated with yellow-white lesions of the retina and choroid. This chapter highlights various focal and diffuse retinal and choroidal inflammatory diseases that can cause such lesions. When the term *standard treatment* is used to describe therapy, options for inflammatory eye disease include corticosteroids in the acute phase and immunosuppressive agents for longer-term therapy. Choice of immunosuppressive therapy can vary widely. Other therapies or disease-specific treatment options are also outlined as appropriate. See BCSC Section 9, *Uveitis and Ocular Inflammation*, for more in-depth information on these diseases, further detail on treatment approaches, and additional illustrations.

Agarwal A. *Gass' Atlas of Macular Diseases*. 2 vols. 5th ed. Saunders; 2012:805–1064.

Albert DM, Miller JW, Azar DT, Young LH. Intermediate and Posterior Uveitis section.

Albert and Jakobiec's Principles and Practice of Ophthalmology. 4th ed. Springer; 2022:4025–4363.

Foster CS, Vitale AT, Jakobiec FA. *Diagnosis and Treatment of Uveitis*. 2nd ed. Jaypee Brothers Medical Publishers; 2013.

Freund KB, Sarraf D, Mieler WF, Yannuzzi LA. *The Retina Atlas*. 2nd ed. Saunders; 2017:399–492.

Noninfectious Retinal and Choroidal Inflammation

White Dot Syndromes

The term *white dot syndromes* has been used to refer to the following conditions (Table 11-1):

- acute posterior multifocal placoid pigment epitheliopathy
- serpiginous choroiditis
- multiple evanescent white dot syndrome
- birdshot chorioretinopathy
- multifocal choroiditis (MFC)
- multifocal choroiditis and panuveitis syndrome
- punctate inner choroiditis or choroidopathy (PIC)

Many authorities now believe that MFC and PIC are part of a spectrum of the same condition. Acute zonal occult outer retinopathy, acute macular neuroretinopathy, and acute idiopathic maculopathy are often included in discussions of the more classic white dot syndromes listed previously because of their presumed inflammatory etiology and the frequently shared symptoms of decreased vision, scotomata, and photopsias; thus, in this chapter, they are discussed under White Dot Syndromes.

Acute posterior multifocal placoid pigment epitheliopathy

Acute posterior multifocal placoid pigment epitheliopathy (APMPPE; also known as *AMPPPE* or *AMPPE*) is an uncommon, bilateral inflammatory disease characterized by the acute onset of blurred vision, scotomata, and in some patients, photopsias. Approximately one-third of patients describe an antecedent flulike illness. Men and women are affected equally; onset usually occurs in early adulthood to middle age. Mild anterior chamber and vitreous inflammation may be present. The lesions, which are typically multiple, yellow-white, placoid, and variable in size, occur at the level of the outer retina (retinal pigment epithelium, RPE) and inner choroid (choriocapillaris) (Fig 11-1). Recurrences are uncommon. The etiology is unknown, although the condition is characterized by hypoperfusion of the choriocapillaris that results in injury to the overlying RPE. Systemic involvement—especially cerebral vasculitis—may occur in rare cases, and neurologic symptoms should prompt urgent neuroimaging. APMPPE-like lesions may be present in patients with sarcoidosis, syphilis, and tuberculosis; therefore, testing to exclude these conditions should be considered.

In the acute stage, fluorescein angiography (FA) of active lesions shows early blockage followed by progressive late leakage and staining. Indocyanine green angiography (ICGA) shows early and late (persistent) hypofluorescence, corresponding to and often extending beyond those lesions identified clinically and on FA. Optical coherence tomography (OCT) through active lesions reveals outer retinal lesions associated with disruption of the outer retinal hyperreflective bands. Autofluorescence in and around active lesions varies over time and may be either increased or decreased at presentation; it tends to decrease as disease activity subsides. With time, hypoautofluorescence develops in areas of RPE disruption. The fundus appearance and visual symptoms typically improve within weeks.

There is no definitive evidence that treatment with corticosteroids is beneficial in altering the outcome for APMPPE, but systemic corticosteroids are required in cases with

Table 11-1 White Dot Syndromes: Comparative Findings, Course, and Treatment

Disease	Laterality	Age	Sex	Notable Findings	Course	Treatment
APMPPE	Bilateral	Early adulthood to middle age	M = F	Early blockage (hypofluorescence) and late staining (hyperfluorescence) on fluorescein angiogram Cerebral vasculitis in rare cases No vitritis	Spontaneous resolution with good visual prognosis; recurrences rare	No proven treatment Evaluate for cerebral vasculitis if indicated; when it is present, systemic corticosteroids required
Serpiginous choroiditis	Bilateral	Young to middle age	M = F	Angiogram findings similar to those in acute APMPE; presence of vitritis should raise suspicion for tubercular serpiginous-like choroiditis	Central vision loss due to scarring; chronic, progressive	Standard autoimmune disease treatment
MEWDS	Unilateral	Young to middle age	F > M	Central foveal granularity on clinical examination with surrounding hyperfluorescent lesions in wreathlike pattern on FA; usually no vitritis	Spontaneous resolution with good visual prognosis; recurrences rare	No proven treatment
Birdshot chorioretinopathy	Bilateral	Late middle age	F > M	Strong association with HLA-A29 Vitritis Possible nyctalopia, diminished contrast sensitivity, and decreased color vision	Vision loss due to CME, CNV, epiretinal membrane formation, and/or outer retinal atrophy; chronic, progressive	Standard autoimmune disease treatment
MFC	Bilateral	Young	F > M	Chorioretinal lesions evolve to burnt-out or punched-out scars; usually minimal or no vitritis, but some cases can have moderate vitritis	Central vision loss due to direct central macular involvement or CNV; chronic, progressive	Standard autoimmune disease treatment
PIC	Bilateral	Young	F > M	Subtype of MFC distinguished by lack of vitritis and smaller (100–300 µm), round, yellow lesions that are usually confined to the posterior pole	Central vision loss due to CNV; self-limited or chronic, progressive	Standard autoimmune disease treatment

APMPPE = acute posterior multifocal placoid pigment epitheliopathy; CME = cystoid macular edema; CNV = choroidal neovascularization; HLA = human leukocyte antigen; MEWDS = multiple evanescent white dot syndrome; MFC = multifocal choroiditis; PIC = punctate inner choroiditis/chorioidopathy.

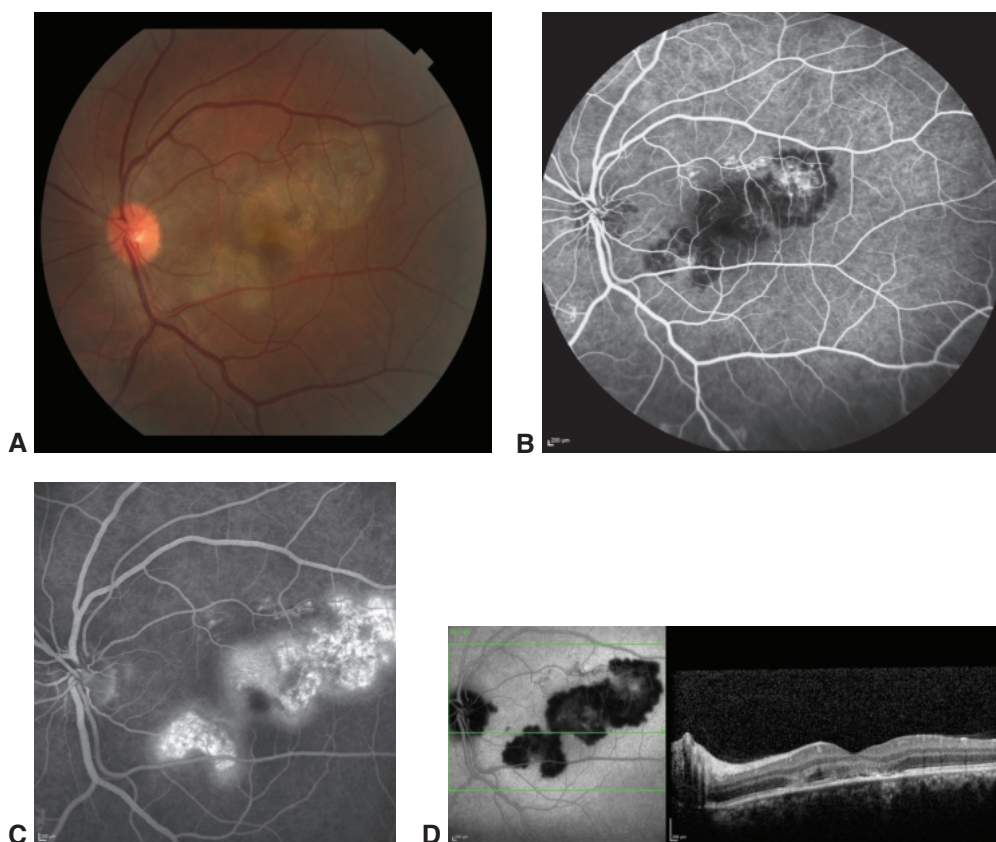


Figure 11-1 Acute posterior multifocal placoid pigment epitheliopathy (APMPPE). **A**, Color fundus photograph of the left eye of a 23-year-old male patient shows confluent yellowish placoid lesions in the posterior pole. The right eye (not pictured) was also involved. Early (**B**) and late-phase (**C**) fluorescein angiography (FA) demonstrates hypofluorescence (due to decreased choriocapillaris perfusion and/or thickening of the retinal pigment epithelium [RPE]), and hyperfluorescence, respectively. **D**, Indocyanine green angiography (ICGA; *left*) shows hypofluorescence of the lesions, and the optical coherence tomography (OCT) scan (*right*) demonstrates outer retinal involvement in the areas of lesions. (Courtesy of Lucia Sobrin, MD.)

cerebral vasculitis. Severe APMPPE may be difficult to distinguish from serpiginous choroiditis (discussed in the following section); this difficulty led to the introduction of the term *ampiginous* to characterize the APMPPE–serpiginous choroiditis disease continuum. Other entities in this placoid disorder continuum include *persistent placoid maculopathy*, which is characterized by central macular involvement, a longer healing time, and a high risk of choroidal neovascularization (CNV); and *relentless placoid chorioretinitis*, which is characterized by the frequent occurrence of smaller, geographically distributed lesions that typically require immunosuppressive treatment.

Marchese A, Agarwal AK, Erba S, et al. Placoid lesions of the retina: progress in multimodal imaging and clinical perspective. *Br J Ophthalmol.* 2022;106(1):14–25.

Serpiginous choroiditis

Serpiginous choroiditis, also known as *geographic choroiditis* or *helicoid peripapillary chorioidopathy*, is an uncommon, often vision-threatening, recurring inflammatory disease involving the outer retina, RPE, and inner choroid (the choriocapillaris). Serpiginous choroiditis tends to affect men and women equally; onset typically occurs in middle age. Persistent scotomata and decreased central vision are common symptoms. Classically, lesions first appear at or near the optic nerve head and extend centrifugally in a serpentine pattern. With numerous recurrences, a serpiginous (pseudopodial) or geographic (maplike) pattern of chorioretinal scarring develops (Fig 11-2). Findings on clinical examination and through multimodal imaging of active serpiginous lesions resemble those of severe APMPE. Lesions tend to occur near or adjacent to inactive scars from prior episodes of inflammation. Recent, active inflammation can be detected noninvasively as hyperautofluorescence on fundus autofluorescence (FAF) (see Fig 11-2). CNV can occur at the edge of the chorioretinal scars.

In endemic areas, such as India, tuberculosis is recognized as producing serpiginous-like lesions, leading some clinicians to describe such lesions as tubercular serpiginous-like choroiditis. In patients with serpiginous-like lesions, evaluation for tuberculosis, sarcoidosis, and syphilis should be considered.

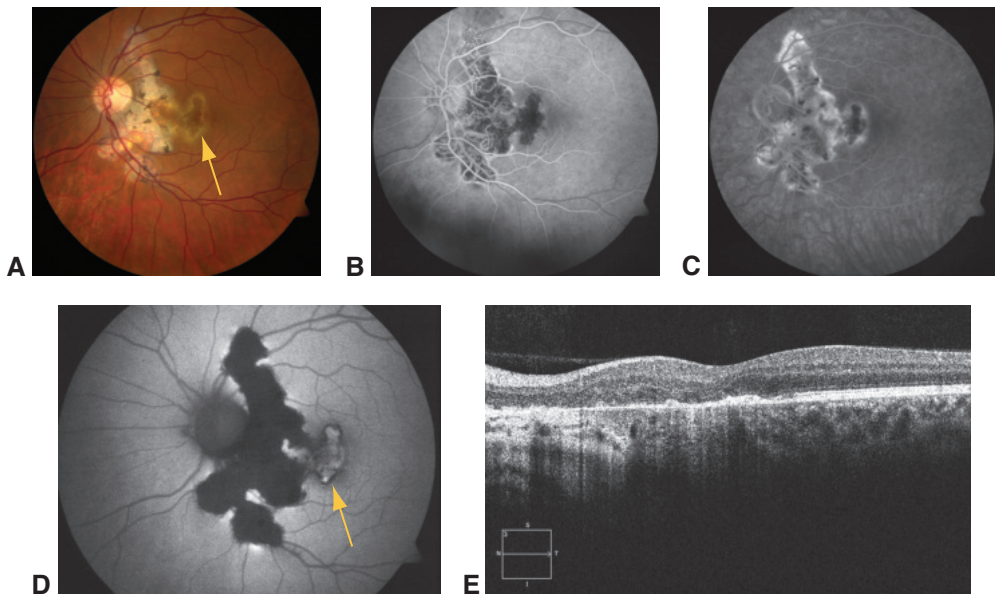


Figure 11-2 Serpiginous choroiditis. **A**, Color fundus photograph shows an old peripapillary chorioretinal scar with an active serpentine lesion (*arrow*) extending centrifugally into the fovea. **B**, Early-phase FA demonstrates classic hypofluorescence, with hyperfluorescence of the edge of the older peripapillary chorioretinal scar. **C**, Late-phase angiogram demonstrates hyperfluorescence of involved areas. **D**, Fundus autofluorescence (FAF) image demonstrates a complete absence of autofluorescence in the area of older chorioretinal scarring, but not in the area of active extension (*arrow*). **E**, OCT image demonstrates disorganization of outer retinal layers and choroid nasal to and underneath the fovea, which corresponds to the involved areas.

(Courtesy of Stephen J. Kim, MD.)

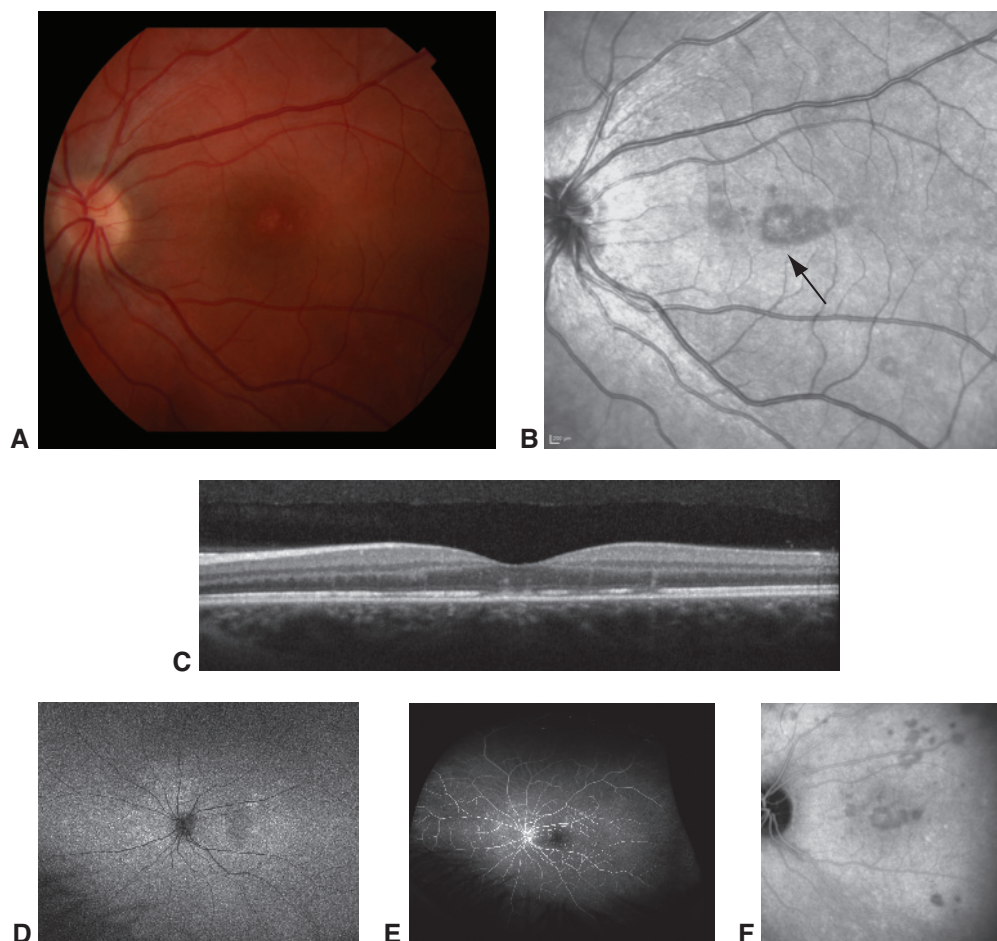


Figure 11-3 Multiple evanescent white dot syndrome (MEWDS). **A**, Color fundus photograph demonstrates foveal granularity. **B**, In the red-free image, the lesions (*arrow*) are more readily apparent than they are on the fundus photograph. **C**, OCT image demonstrates disruption of the outer retinal hyperreflective bands and RPE. **D**, FAF image shows hyperautofluorescence of the lesions. **E**, FA demonstrates hyperfluorescent lesions. **F**, ICGA shows hypofluorescence of the lesions. (Courtesy of Lucia Sobrin, MD.)

Multiple evanescent white dot syndrome

Multiple evanescent white dot syndrome (MEWDS) is an acute-onset syndrome characterized by multiple small gray, white, or yellow-white dots at the level of the outer retina in and around the posterior pole (Fig 11-3). Affected individuals are typically young to middle aged; women are affected more often than men. The etiology of MEWDS is unknown, although one-third of patients describe a flulike prodrome. Symptoms tend to be unilateral and include decreased vision, scotomata, and sometimes photopsias. In some patients, an unusual transient foveal granularity consisting of tiny yellow-orange flecks at the level of the RPE also develops; this is highly suggestive of the condition. Abnormalities on ICGA suggest simultaneous choroidal involvement. Mild anterior chamber cell reaction or vitritis may be present

but is more commonly absent. Temporal visual field abnormalities and an enlarged blind spot are common, and an afferent pupillary defect is often present.

FA reveals multiple punctate, hyperfluorescent lesions associated with the dots observed clinically, typically in a wreathlike configuration. Mild, late leakage and staining of the optic nerve head are often observed. ICGA shows hypofluorescence around the optic nerve head as well as multiple hypofluorescent dots, which are typically more numerous than those observed either clinically or on FA. OCT taken through active lesions reveals dome-shaped outer retinal lesions associated with disruption of the outer retinal hyperreflective bands. FAF imaging often shows focal hyperautofluorescence in the area of the white dots. On electroretinographic (ERG) testing, some patients show delayed light-adapted (LA) (photopic flicker) responses and decreased bright-flash, dark-adapted a-wave amplitudes. In most patients, the symptoms and fundus findings start to improve in 2–6 weeks without treatment.

Birdshot chorioretinopathy

Birdshot chorioretinopathy, previously called *vitiliginous chorioretinitis*, is bilateral and affects women more often than men, typically in late middle age. Most patients with birdshot chorioretinopathy are White, and in more than 90% of patients, test results are positive for human leukocyte antigen (HLA)–A29; birdshot chorioretinopathy has the strongest association documented between a disease and HLA class I. Early symptoms include floaters and blurred or decreased vision. Later in the course of disease, nyctalopia, diminished contrast sensitivity, and decreased color vision may occur as photoreceptors degenerate from ongoing inflammation. Examination reveals vitreous inflammation, which is typically mild and is associated with multiple yellow-white choroiditis spots that are often most prominent nasal to the optic nerve head (Fig 11-4). FA often shows leakage from the retinal vessels and optic nerve head, frequently producing cystoid macular edema (CME). Variable amounts of outer retinal atrophy can also be present, resulting in window defects. Choroidal lesions are best visualized using ICGA. OCT and FAF can be used to assess the extent of outer retinal atrophy.

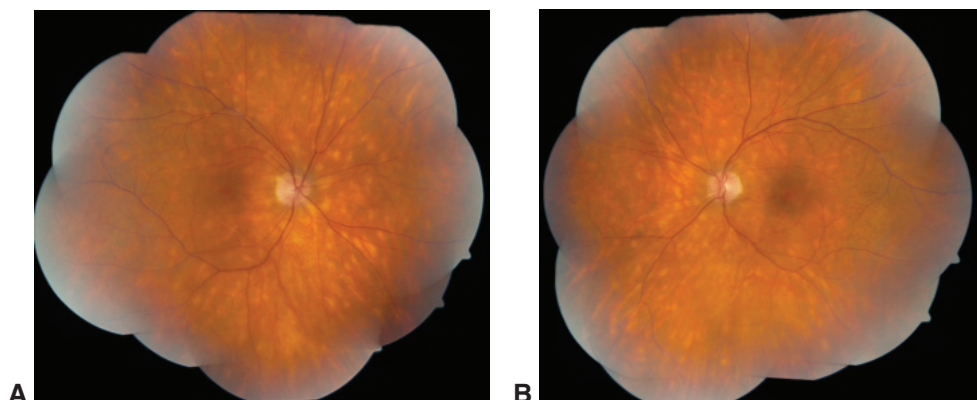


Figure 11-4 Color fundus photograph montage of the right (**A**) and left (**B**) eyes of a patient with birdshot chorioretinopathy demonstrates multiple creamy, yellow-white choroiditis lesions scattered around the posterior pole and midperiphery. The images are slightly hazy due to vitritis. (Courtesy of Stephen J. Kim, MD.)

The disease is chronic, progressive, and prone to recurrent episodes of inflammation. Vision loss may be caused by CNV, CME, epiretinal membrane formation, and/or outer retinal atrophy, which can be extensive and is associated with optic atrophy in advanced cases. Disease activity and progression may be assessed in the office using multimodal imaging (FA, ICGA, spectral-domain OCT, enhanced depth OCT, and FAF) and through periodic electrophysiologic (ERG), color vision, retinal nerve fiber layer OCT, and visual field testing—each of which may show a degree of dysfunction far greater than that suggested by Snellen visual acuity assessments. Common ERG abnormalities include prolonged LA implicit times and decreased b-wave amplitudes.

Multifocal choroiditis, including punctate inner choroiditis

Use of the terms *idiopathic multifocal choroiditis*, *multifocal choroiditis and panuveitis* (MFCPU), *recurrent multifocal choroiditis* (RMC), *punctate inner choroiditis* or *choroidopathy* (PIC), *pseudo-presumed ocular histoplasmosis syndrome* (pseudo-POHS), and *subretinal fibrosis and uveitis syndrome*, among others, is both inconsistent and confusing in the literature. Current recommendations suggest that only the term *multifocal choroiditis* (MFC) should be used to refer to the occurrence of discrete chorioretinitis lesions in the absence of an identifiable underlying infection (such as tuberculosis or histoplasmosis) or systemic inflammation (such as sarcoidosis). In MFC, lesions are commonly clustered in the macula and around the optic nerve head, although they can also occur in the mid- and far periphery and are frequently aligned in a curvilinear manner—configurations sometimes referred to as *Schlaegel lines* (Fig 11-5). Blurred or decreased vision and scotomata are the most common symptoms. Affected individuals are typically young, myopic, and female. Clinical examination usually reveals little or no anterior chamber or vitreous inflammation, although patients may have mild to moderate vitreous inflammation—a presentation some clinicians mean when using the term *MFCPU*. Decreased central vision

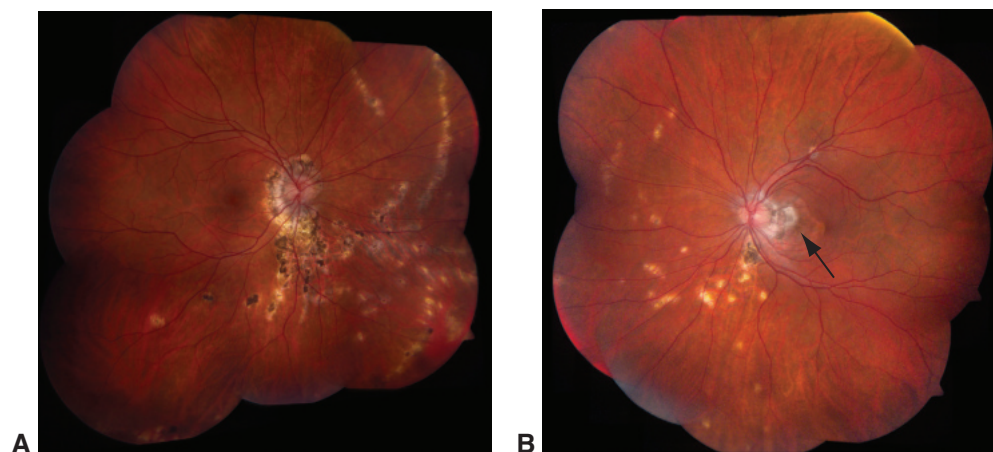


Figure 11-5 Multifocal choroiditis. Color fundus photograph montage of the right (A) and left (B) eyes showing multifocal chorioretinal scars, some with a punched-out appearance clustered in the macula and around the optic nerve. Note the curvilinear pattern of lesions nasally (more evident in the right), referred to as *Schlaegel lines*. The patient was a young female with myopia and 20/200 vision in the left eye due to previous choroidal neovascularization (CNV; arrow). (Courtesy of Stephen J. Kim, MD.)

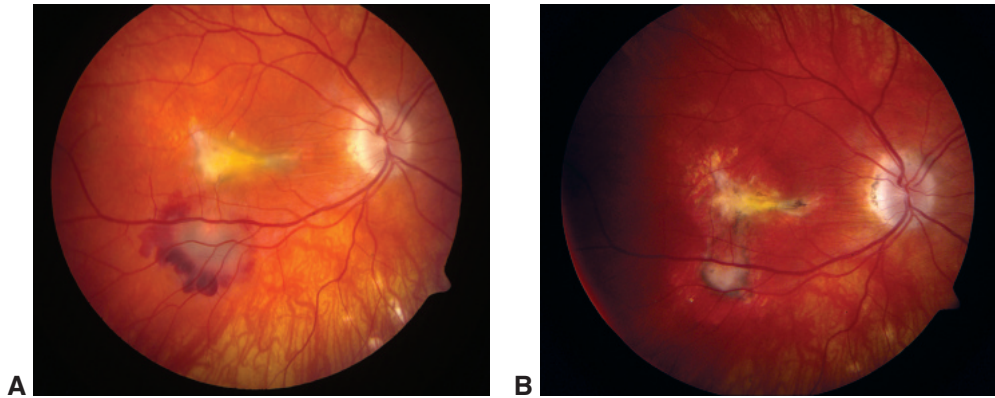


Figure 11-6 Choroidal neovascularization (CNV). **A**, Fundus photograph from a patient with multifocal choroiditis with central subfoveal fibrosis and CNV with adjacent subretinal hemorrhage inferiorly. **B**, After CNV resolves, subretinal fibrosis occurs at the site of previous CNV inferiorly. (Courtesy of Stephen J. Kim, MD.)

results most frequently from direct central macular involvement or from CNV, which occurs in one-third of patients (Fig 11-6). Subretinal fibrosis may occur in and around lesions and, when the central macula is involved, can also limit vision.

Acute zonal occult outer retinopathy

Acute zonal occult outer retinopathy (AZOOR), a presumed inflammatory disease, damages broad zones of the outer retina in 1 or both eyes. AZOOR typically occurs in young women with myopia, and onset is acute and unilateral. Three-fourths of cases progress to bilateral involvement. Initial symptoms include photopsia, nasal visual field loss, and sometimes an enlarged blind spot; visual acuity is affected in rare instances. On initial presentation, the fundus may appear normal or show evidence of mild vitritis. Nearly 25% of patients have an afferent pupillary defect. Angiographic findings may include retinal and optic nerve head capillary leakage, especially in patients with evidence of vitritis. On ERG, a delayed LA response is common; multifocal ERG shows decreased responses in areas of the visual field defect. Visual field testing may show scotomata, which can enlarge over weeks or months.

Some patients recover from AZOOR, whereas others have persistent, large visual field defects, which tend to stabilize over 6 months. Permanent visual field loss is often associated with late development of fundus changes. Depigmentation of large zones of RPE usually corresponds to scotomata (Fig 11-7); narrowed retinal vessels may be visible within these areas. In some patients, the late fundus appearance may resemble cancer-associated retinopathy or retinitis pigmentosa.

Mrejen S, Khan S, Gallego-Pinazo R, Jampol LM, Yannuzzi LA. Acute zonal occult outer retinopathy: a classification based on multimodal imaging. *JAMA Ophthalmol*. 2014;132(9):1089–1098.

Acute macular neuroretinopathy

Acute macular neuroretinopathy (AMN) is a rare condition characterized by the acute onset of paracentral scotomata in 1 or both eyes in young, otherwise healthy patients. The pathogenesis of AMN is unclear. Women outnumber men nearly 6 to 1 in this condition.

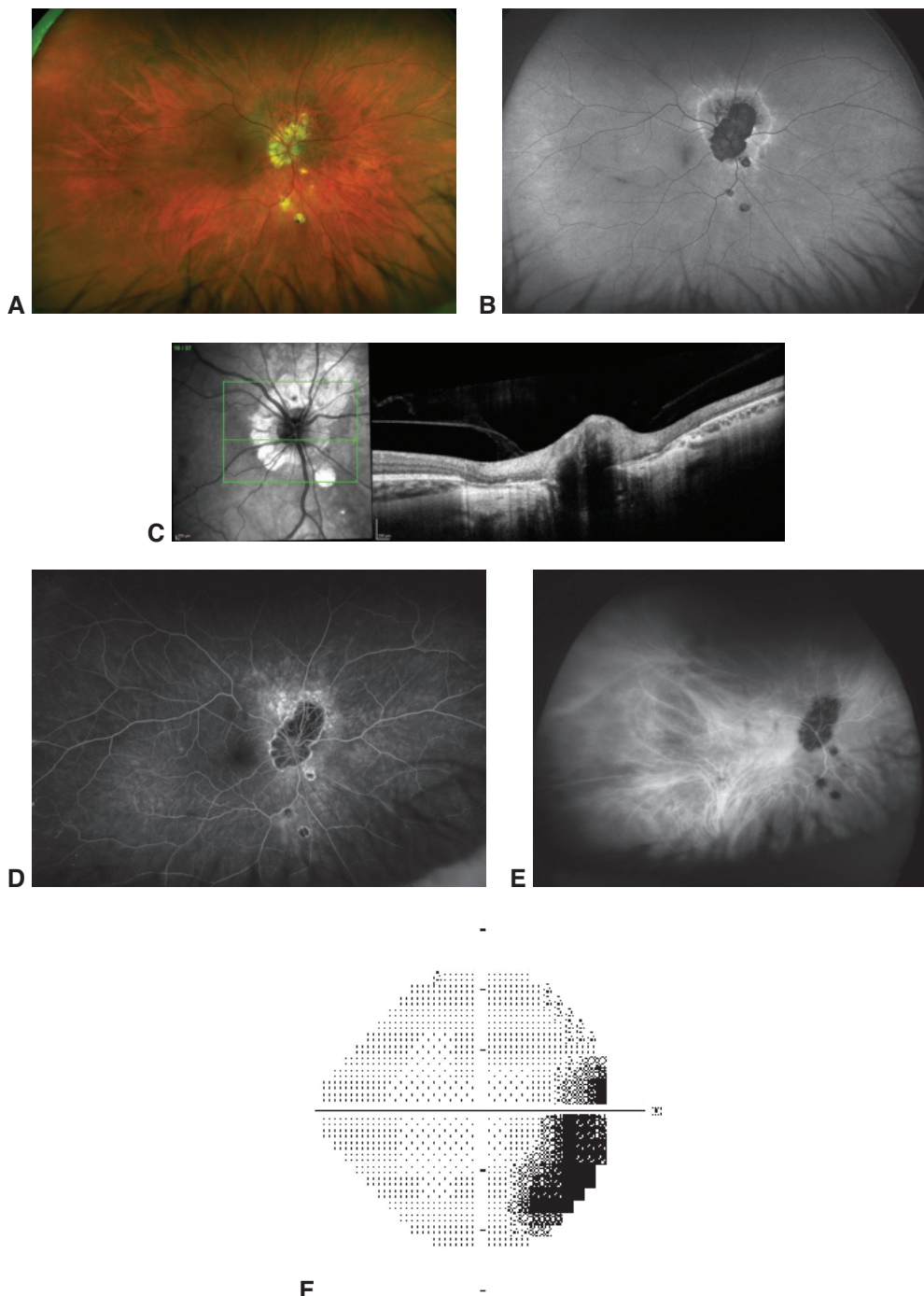


Figure 11-7 Acute zonal occult outer retinopathy (AZOOR). **A**, Annular depigmentation of the RPE can be seen around the optic nerve. **B**, FAF demonstrates a trizonal pattern of changes extending from the optic nerve: hypoautofluorescence adjacent to the nerve, an intermediate area of hyperautofluorescence, and normal autofluorescence. **C**, OCT image demonstrates outer retinal atrophy in the involved area. **D**, FA shows hypofluorescence in the area of peripapillary atrophy surrounded by staining. **E**, ICGA shows hypofluorescence of the peripapillary lesion. **F**, Humphrey 24-2 visual field shows enlargement of the blind spot. (Courtesy of Lucia Sobrin, MD.)

Clinically, reddish-brown teardrop or wedge-shaped lesions are observed around the fovea. The tips of these lesions point centrally; the lesions correspond in size and location to the subjective paracentral scotomata. The lesions can be difficult to see on fundus examination or with traditional color photography but are apparent on near-infrared imaging and multicolor images. The retinal vessels and optic nerve are unaffected, and there is no vitreous inflammation. High-resolution OCT is particularly helpful for visualizing the lesions, which characteristically involve the outer retina—including both the outer nuclear layer and the hyperreflective bands associated with the photoreceptors of the ellipsoid zone (Fig 11-8). These OCT changes are believed to result from ischemia of the deep capillary plexus of the central retina. AMN lesions can be distinguished from paracentral acute middle maculopathy (PAMM) lesions, which present with hyperreflectivity of the inner plexiform layer and inner nuclear layer (INL) and progress to INL thinning without outer retinal involvement (see Chapter 6).

Fawzi AA, Pappuru RR, Sarraf D, et al. Acute macular neuroretinopathy: long-term insights revealed by multimodal imaging. *Retina*. 2012;32(8):1500–1513.

Acute idiopathic maculopathy

Acute idiopathic maculopathy (AIM) is a rare disorder that presents with sudden, severe central or paracentral vision loss, typically in younger individuals following a flulike illness.

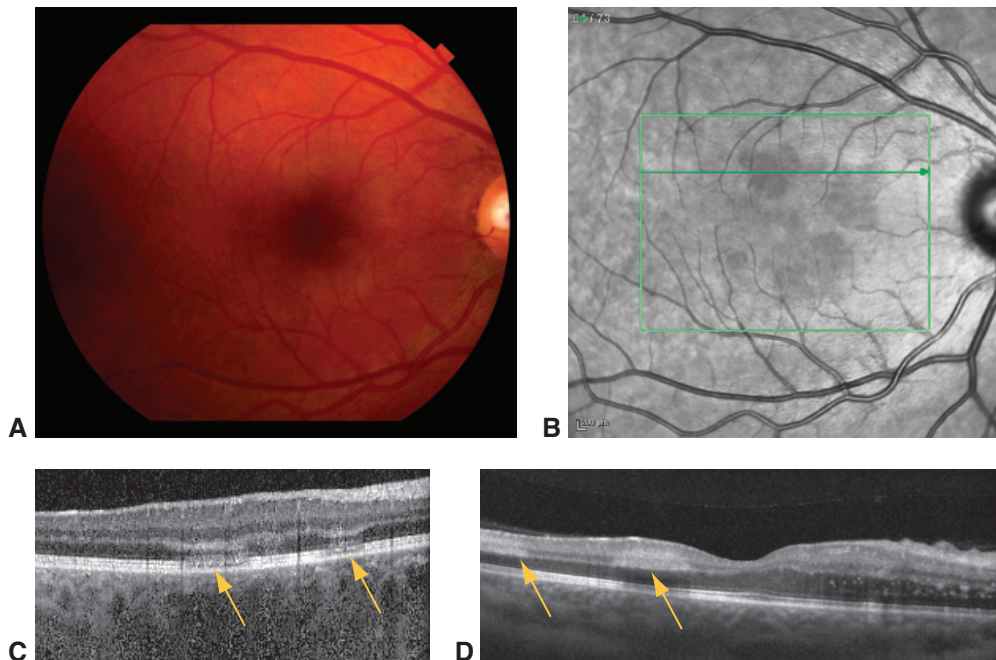


Figure 11-8 Acute macular neuroretinopathy (AMN). Reddish-brown lesions in the macula are difficult to see in a color fundus photograph (**A**), but they are apparent in a near-infrared image (**B**). **C**, OCT image demonstrates involvement of the outer nuclear layer, external limiting membrane, and ellipsoid zone (arrows). **D**, OCT image from a patient with ischemic retinal vasculitis shows involvement of the inner nuclear layer (arrows), which distinguishes paracentral acute middle maculopathy (PAMM) from AMN. (Courtesy of Lucia Sobrin, MD.)

Men and women are affected equally. The cause is unknown, although isolated cases have been associated with coxsackievirus infection. Initially, only central unilateral lesions were described, but both bilateral and eccentric macular lesions have since been added to the disease spectrum. The main clinical finding is an exudative neurosensory macular detachment with little or no vitreous inflammation and variable discoloration of the underlying RPE (Fig 11-9). Mild optic nerve head swelling, retinal hemorrhages, vasculitis, and subretinal infiltrates occur infrequently. FA typically shows progressive irregular hyperfluorescence at the level of the RPE, followed in the late stages by pooling in the detachment space. High-resolution OCT imaging documents the size and extent of the detachment space and shows loss of the hyperreflective outer retinal bands associated with the photoreceptors and RPE. The lesions resolve spontaneously but leave a bull's-eye pattern of RPE alteration. Typically near-complete recovery of vision occurs over weeks to months.

Freund KB, Yannuzzi LA, Barile GR, Spaide RF, Milewski SA, Guyer DR. The expanding clinical spectrum of unilateral acute idiopathic maculopathy. *Arch Ophthalmol.* 1996;114(5):555–559.

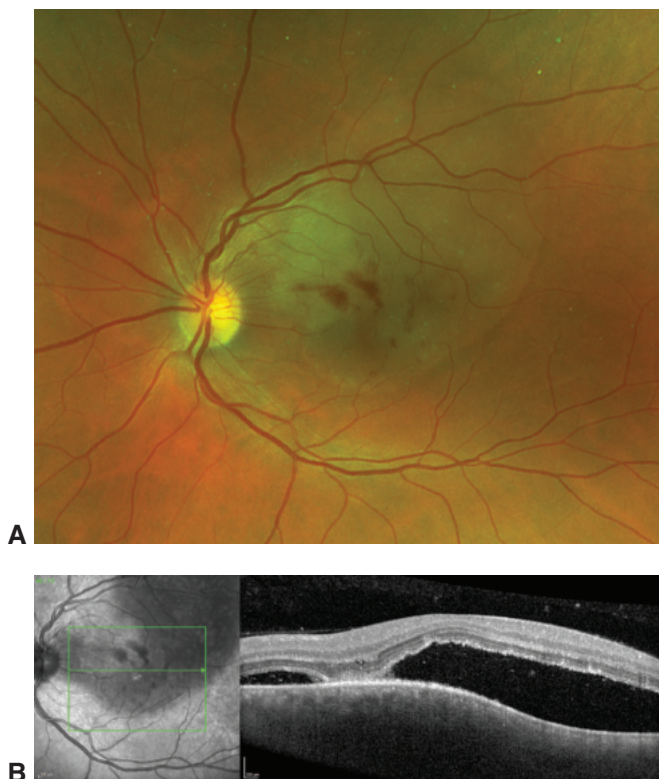


Figure 11-9 Acute idiopathic maculopathy. **A**, Retinal hemorrhages and an exudative neurosensory macular detachment with underlying yellowish discoloration. **B**, OCT through the lesion shows subretinal fluid with hyperreflective debris and loss of the outer retinal bands. (Courtesy of Lucia Sobrin, MD.)

Chorioretinal Autoimmune Conditions

The following sections detail selected autoimmune diseases that affect the retina and choroid. These conditions are generally treated using standard autoimmune treatment options. Specific treatment considerations are mentioned when applicable.

Inflammatory vasculitis

See BCSC Section 9, *Uveitis and Ocular Inflammation*, Chapter 5 for a full list of causes of inflammatory vasculitis.

Behçet disease Behçet disease is a complex systemic disorder characterized by recurrent attacks of inflammation and vascular occlusion involving multiple organ systems. The disease tends to affect men more than women and is particularly common in regions along the Silk Road trading routes: Japan, Southeast Asia, the Middle East, and the Mediterranean. The etiology is unknown.

There are no specific tests to confirm a diagnosis of Behçet disease, but it is associated with the major histocompatibility complex HLA-B5 allele, and more specifically with HLA-B51 (the predominant split antigen). The diagnosis is based on clinical criteria (Table 11-2). Recurrent oral ulceration affects nearly all patients, and genital ulcers and cutaneous lesions such as erythema nodosum are common. Central nervous system involvement may develop in more than 50% of patients and should be suspected in any patient with neurologic signs. Other systemic manifestations include arthritis, epididymitis, and intestinal ulcers.

Uveitis is common in patients with this disorder and may be anterior, posterior, or diffuse (panuveitis). Posterior segment involvement may include vitritis, an occlusive retinal vasculitis, intraretinal hemorrhages, macular edema, focal areas of retinal necrosis, and ischemic optic neuropathy. Recurring episodes of retinal vasculitis may lead to severe ischemia and retinal neovascularization, which is often treated with panretinal photocoagulation. Despite treatment, the visual prognosis is often poor because of progressive retinal ischemia from recurring episodes of occlusive vasculitis. Treatment with azathioprine and cyclosporine has been shown to reduce ocular manifestations in prospective trials. Biologic agents, such as inhibitors of tumor necrosis factor α , as well as interferon, are also quite effective.

Tugal-Tutkun I, Ozdal PC, Oray M, Onal S. Review for diagnostics of the year: multimodal imaging in Behçet uveitis. *Ocul Immunol Inflamm*. 2017;25(1):7–19.

Table 11-2 International Clinical Criteria for Diagnosis of Behçet Disease

Recurrent oral ulceration (aphthous or herpetiform) at least 3 times in 1 year in addition to 2 of the following:

- recurring genital ulcerations
 - ocular inflammation
 - skin lesions (erythema nodosum, pseudofolliculitis, papulopustular lesions, acneiform nodules)
 - positive pathergy test
-

Adapted from the International Study Group for Behçet's Disease. Criteria for diagnosis of Behçet's disease. *Lancet*. 1990;335(8697):1078–1080.

Lupus vasculitis Systemic lupus erythematosus (SLE) is a systemic autoimmune disorder that most commonly affects women of childbearing age. Black and Hispanic women are at higher risk than White women. As a multisystem disease, SLE can involve almost every ocular and periocular structure. Approximately 3%–10% of patients with SLE have retinal findings ranging from asymptomatic cotton-wool spots and intraretinal hemorrhages to macular infarction with severe central vision loss (Fig 11-10). Lupus choroidopathy is less common and presents as multifocal serous retinal detachments. The retinal and choroidal pathology is vascular and thought to be autoimmune in nature.

The presence of retinal vascular occlusion, including cotton-wool spots, is indicative of active systemic inflammation and should prompt treatment. Sarcoidosis can also cause retinal vasculitis and should be considered in the differential diagnosis (see BCSC Section 9, *Uveitis and Ocular Inflammation*, Chapter 9).

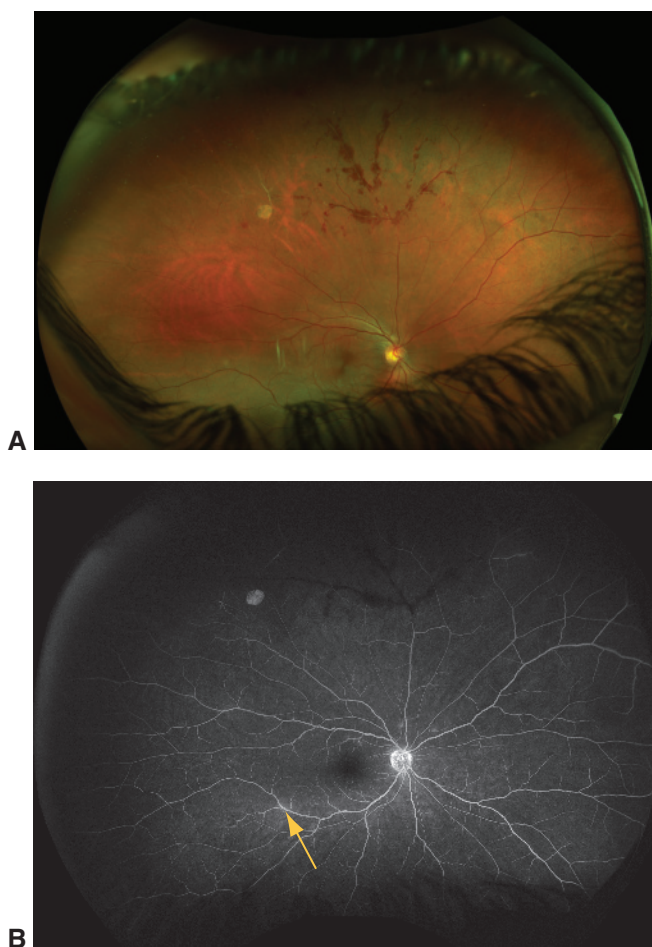


Figure 11-10 Vasculitis secondary to systemic lupus erythematosus. **A**, Fundus photograph shows perivascular exudate and perivascular hemorrhages superiorly. **B**, Late-phase FA image reveals retinal nonperfusion superiorly and mild perivascular leakage along the inferior arcade (arrow). (Courtesy of Lucia Sobrin, MD.)

Vogt-Koyanagi-Harada disease

Vogt-Koyanagi-Harada (VKH) disease (or syndrome) is a systemic autoimmune disorder in which T lymphocytes are directed against melanocytes in the eye, auditory system, meninges, and skin. VKH disease most commonly affects people of Asian, American Indian, Asian Indian, Mediterranean, and Middle Eastern descent. Ocular findings are typically bilateral and include vitreous inflammation associated with serous retinal detachment. Optic nerve head hyperemia and edema are common. FA studies can be particularly helpful in monitoring disease activity and often show multiple RPE leaks in the areas of detachment, a finding referred to as the “starry sky” or “Milky Way” sign (Fig 11-11). Depigmentation of the choroid results in the classic orange-red fundus discoloration, or “sunset glow” fundus appearance, as the uveitis subsides.

A diagnosis of VKH disease should be made only in patients who have not had a penetrating ocular injury or ocular surgery in either eye, to help distinguish this disease from sympathetic ophthalmia. VKH disease is called *probable* when characteristic ocular inflammation occurs in the absence of skin or neurologic findings; it is called *incomplete* when either skin or neurologic findings but not both are present; and it is called *complete* when both skin and neurologic findings develop.

The clinical course of VKH disease can be divided into 3 phases:

1. *prodromal phase*: characterized by a flulike illness with symptoms that can include headache, meningismus, tinnitus, and dysacusis
2. *acute uveitic phase*: closely follows the prodromal phase; characterized by pain, photophobia, and vision loss accompanied by the onset of bilateral panuveitis with serous retinal detachments
3. *chronic (convalescent) phase*: the uveitis subsides, but depigmentation of the skin (vitiligo), eyelashes (poliosis), and uvea can occur; ocular depigmentation may develop at the limbus (“Sugiura” sign), the trabecular meshwork (“Ohno” sign), or the choroid (“sunset glow” fundus appearance)

Sympathetic Ophthalmia

Sympathetic ophthalmia, a rare condition that occurs after penetrating ocular injury or ocular surgery, is caused by exposure of the immune system to sequestered uveal antigens (see BCSC Section 9, *Uveitis and Ocular Inflammation*). The ocular findings in sympathetic ophthalmia are clinically and histologically indistinguishable from those in VKH disease. Inflammation of the exciting (injured or operated) and sympathizing (fellow) eye may occur days to decades after the initial insult. As in VKH disease, the inflammation is bilateral and is characterized by the presence of panuveitis, often associated with areas of serous retinal detachment and yellowish white midperipheral choroidal lesions (Dalen-Fuchs nodules). Nonocular complications, such as vitiligo or poliosis, can occur but are much less common than in VKH disease. Moreover, in the rare instances when sympathetic ophthalmia does follow either injury or surgery, standard treatments almost always control the inflammation. Therefore, enucleation or evisceration of an injured eye to minimize risk of sympathetic ophthalmia is rarely practiced.



Figure 11-11 Vogt-Koyanagi-Harada (VKH) disease. **A**, Fundus photograph (left eye) taken during an acute uveitic phase in a patient with multiple serous detachments (*arrows*). **B**, OCT shows vitreous cells, subretinal fluid, and subretinal inflammatory debris and septae (*arrow*). **C**, Early-phase FA shows multifocal pinpoint RPE leakage, or the “starry sky” appearance. **D**, Late-phase FA shows pooling of fluid in the subretinal space. **E**, Three months after presentation, the patient noted that vitiligo had developed on the dorsum of his hand. (Courtesy of Lucia Sobrin, MD.)

Uveitis Masquerade: Intraocular Lymphoma

Primary vitreoretinal lymphoma (PVRL; previously called *primary intraocular lymphoma* PIOL), is a non-Hodgkin diffuse large B-cell lymphoma and is considered the most aggressive of the ocular lymphomas. Half of all cases of PVRL occur in patients older than 60 years. In most patients with PVRL, central nervous system (CNS) involvement will develop. Conversely, of patients who present with CNS involvement, approximately 20% will have intraocular involvement. HIV infection is associated with an increased risk of

lymphoma that ranges from 50-fold (with potent antiretroviral therapy) to more than 500-fold (prior to—or without access to—potent antiretroviral therapy).

Diagnosis of PVRL may be challenging, as PVRL often masquerades as posterior uveitis. Clinical features suggestive of PVRL include

- incomplete or transient response to corticosteroid treatment
- presence of atypical large vitreous cells, which may be uncharacteristically white and/or align along a single vitreous fibril (“string of pearls” pattern; Fig 11-12) or appear as a sheet formed by multiple, aligned vitreous fibrils (aurora borealis effect)
- presence of subretinal and/or sub-RPE infiltrates, which may be transient and/or shift location over time (Fig 11-13)

Optic nerve head edema and serous retinal detachment may also occur.

Patients with suspected PVRL should undergo magnetic resonance imaging of the brain with contrast material as well as a lumbar puncture for cytologic studies to evaluate for CNS involvement. A confirmatory CNS or vitreoretinal biopsy is usually performed. Best results are obtained when the vitreoretinal biopsy specimen is obtained as part of a surgical vitrectomy (as opposed to a vitreous tap) and both undiluted and diluted samples are taken. It is notoriously difficult to arrive at a diagnosis on the basis of tests of a vitreous specimen because of the low cell concentrations and the propensity of lymphoma cells to undergo autolysis. Because corticosteroids will also reduce cell count, it is best to stop any corticosteroid treatments for a period of weeks before a planned biopsy. Best results are achieved with rapid test processing and analysis by cytopathology, immunoglobulin or T-cell receptor gene rearrangement studies, flow cytometry, cytokine analyses (IL-10:IL-6 ratio >1.0), and *MYD88* mutation detection. Current management practices involve both chemotherapy and radiation treatment. Intravitreal injection of methotrexate and rituximab can be effective at controlling intraocular disease, but the recurrence rate is high and the long-term prognosis guarded.

In contrast with PVRL, uveal lymphoma is usually more indolent and is associated with systemic lymphoma in up to one-third of cases. Characteristic clinical findings include uveal thickening, which often produces a birdshot uveitis–like fundus appearance,

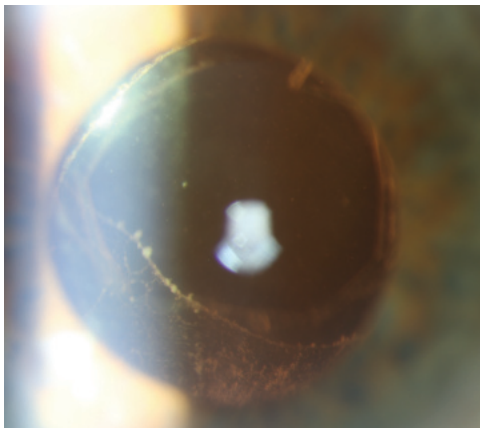


Figure 11-12 Classic “string of pearls” pattern, consisting of large lymphoma cells connected by vitreous fibrils, in an eye with primary vitreoretinal lymphoma (PVRL). Vitreous cells are larger and less abundant in PVRL than in typical vitritis and tend to aggregate. Note the distinct differences when compared to the string of pearls pattern seen in *Candida* endophthalmitis (see Fig 11-20). (Courtesy of Anthony B. Daniels, MD, MSc.)

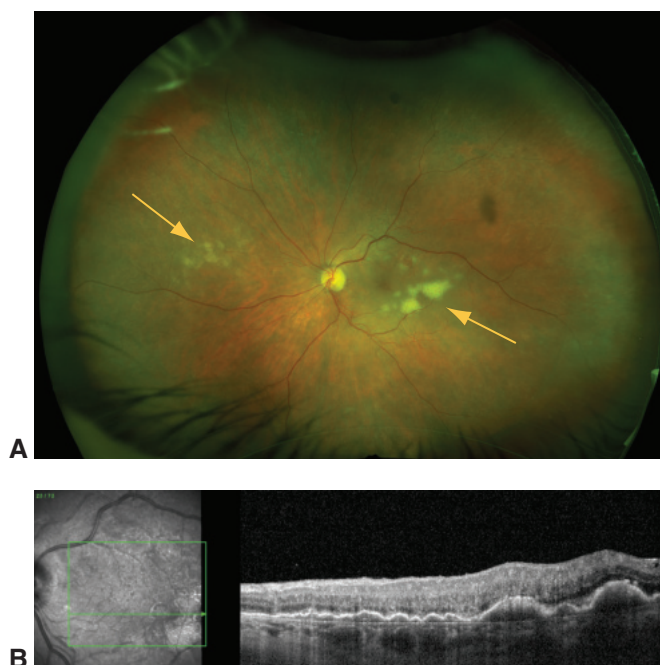


Figure 11-13 Primary vitreoretinal lymphoma. **A**, Fundus photograph shows sub-RPE infiltrates (arrows) in a patient with known central nervous system B-cell lymphoma. **B**, OCT shows diffuse sub-RPE hyperreflective material. (Courtesy of Lucia Sobrin, MD.)

with or without serous retinal detachment (Fig 11-14). Episcleral involvement may manifest anteriorly as salmon-colored conjunctival infiltration or posteriorly as a juxtascleral mass on ultrasonography. Biopsy of affected tissues can confirm the diagnosis. Evaluation

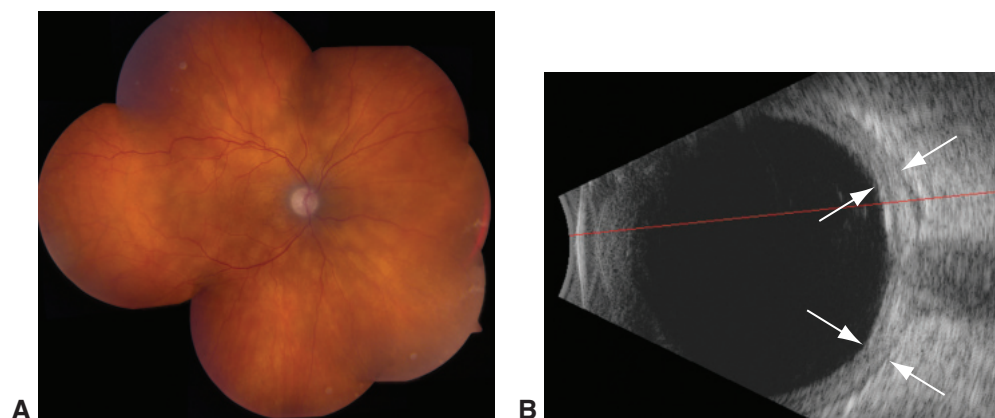


Figure 11-14 Uveal lymphoma. **A**, Fundus photograph demonstrates birdshot uveitis-like fundus appearance. **B**, B-scan ultrasonography reveals characteristic uveal thickening (arrows). (Courtesy of Stephen J. Kim, MD.)

for systemic involvement includes use of computed tomography (CT) or combined CT and positron emission tomography (PET) imaging of the thorax, abdomen, and pelvis.

Chan CC, Sen HN. Current concepts in diagnosing and managing primary vitreoretinal (intraocular) lymphoma. *Discov Med*. 2013;15(81):93–100.

Infectious Retinal and Choroidal Inflammation

The following sections briefly describe selected infectious diseases that can cause retinal and choroidal inflammation.

Cytomegalovirus Retinitis

Cytomegalovirus (CMV) causes the most common infectious congenital syndrome worldwide and can result in congenital CMV retinitis (see BCSC Section 6, *Pediatric Ophthalmology and Strabismus*, Chapter 27 for additional discussion). CMV retinitis is also the most common ocular opportunistic infection in adult patients with advanced AIDS and usually occurs when CD4⁺ T-cell counts are less than 50/ μ L. Patients with CMV retinitis typically present with floaters or decreased vision. Clinically, CMV retinitis has a characteristic appearance that consists of opacification of the necrotic retina, typically along retinal vessels and often with areas of hemorrhage (Fig 11-15). Periphlebitis and “frosted branch” angiitis—florid, dense, perivascular exudation that often obliterates visualization of the retinal vessels—may be prominent features. The degree of vitreous inflammation is highly variable but often minimal in immunocompromised patients. Early CMV retinitis may resemble the cotton-wool spots associated with HIV-related retinopathy. Although the diagnosis is often made clinically, polymerase chain reaction (PCR)-based analysis of ocular fluids may be diagnostic in unclear cases.

CMV retinitis can be treated with oral valganciclovir, or with ganciclovir or foscarnet, administered systemically or intravitreally. High-dose induction therapy is typically given for 2–3 weeks, after which maintenance therapy is continued until immune reconstitution

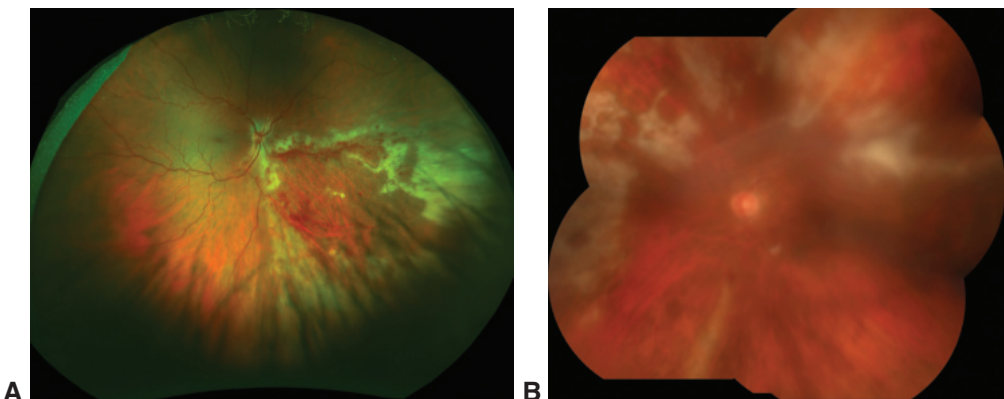


Figure 11-15 Cytomegalovirus retinitis. **A**, Retinitis with a hemorrhagic component in a patient with AIDS. **B**, Granular appearance of retinitis in a patient after renal transplant. (Courtesy of Lucia Sobrin, MD.)

results in restoration of anti-CMV T-cell immunity—usually at CD4⁺ T-cell counts greater than 200/ μ L. Immune recovery uveitis and its complications, most notably CME and epiretinal membrane formation, occur in approximately 20% of HIV-seropositive patients following immune reconstitution. Up to 50% of eyes with CMV retinitis eventually develop a rhegmatogenous retinal detachment.

CMV retinitis can occur in the absence of HIV infection/AIDS. This scenario almost always is associated with relative immunosuppression, such as that which occurs in organ transplant recipients and in other patients with use of systemic corticosteroids, steroid-sparing immunosuppressive agents, or chemotherapeutics.

Non-CMV Necrotizing Herpetic Retinitis

Both varicella-zoster virus (VZV) and herpes simplex virus (HSV) infection can cause necrotizing retinitis in patients, whether or not they are immunocompromised. Unlike CMV infection, these infections can progress rapidly and therefore should be treated aggressively. Two distinct clinical syndromes have been described: *acute retinal necrosis (ARN)* and *progressive outer retinal necrosis (PORN)*.

Characteristic features of ARN include the presence of 1 or more foci of retinitis, which usually occur in the periphery and are associated with occlusive retinal vasculitis and moderate to severe anterior chamber and vitreous inflammation (Fig 11-16).

PORN occurs in patients who are severely immunocompromised and consists of rapidly progressive, multifocal necrotizing retinitis with little or no anterior chamber or vitreous inflammation. PORN is rare because it occurs only with more severe immunosuppression in which the immune system is unable to mount any significant response to infection. Compared with ARN, PORN is associated with more rapid progression (Fig 11-17).

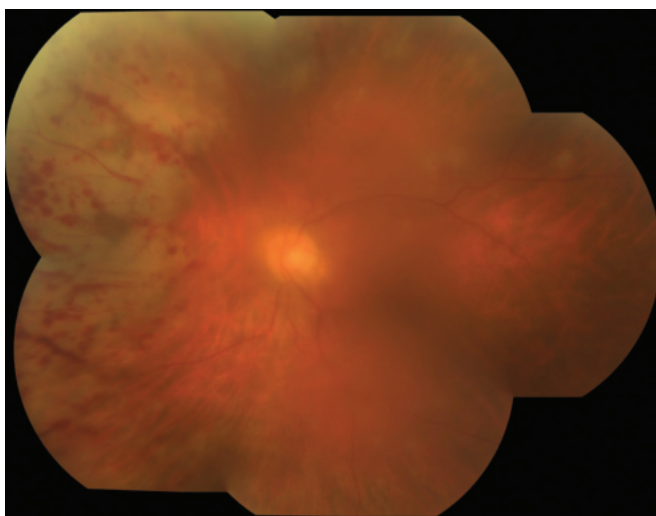


Figure 11-16 Peripheral necrotizing herpetic retinitis (acute retinal necrosis). Color fundus photograph montage shows intraretinal hemorrhage and full-thickness opacification of the retina. (Courtesy of Lucia Sobrin, MD.)

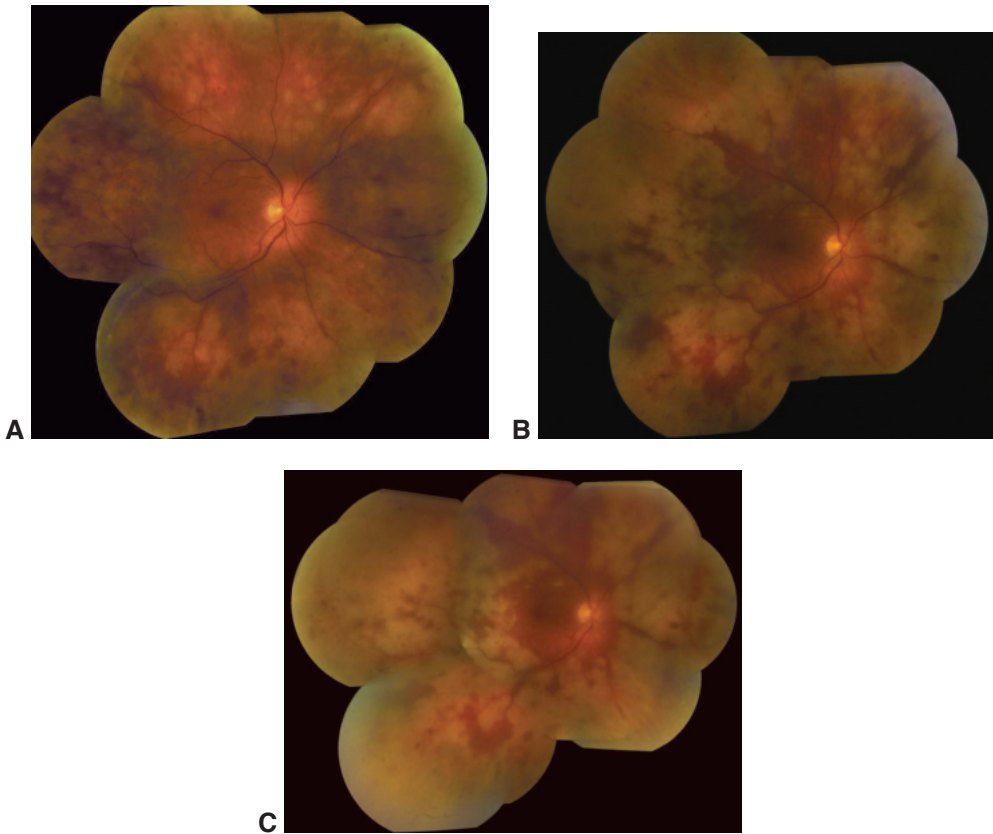


Figure 11-17 Progressive outer retinal necrosis (PORN) syndrome in a patient severely immunocompromised from high-dose chemotherapy for mantle cell lymphoma. The color fundus photograph montages show the rapid progression of retinitis and coalescence of lesions in the absence of vitreous inflammation from initial presentation (**A**), day 3 (**B**), and day 6 (**C**). An aqueous biopsy specimen was positive for varicella-zoster virus on polymerase chain reaction (PCR) testing. (Courtesy of Daniel F. Martin, MD, and Stephen J. Kim, MD.)

Evaluation should include serologic testing for syphilis as well as intraocular fluid aspiration for use in PCR analysis for VZV, HSV, CMV, and *Toxoplasma gondii*. VZV infection is the most commonly identified cause of both ARN and PORN. Because ARN and PORN progress rapidly, treatment should commence immediately upon suspicion of either (Table 11-3). Some specialists initiate therapy with intraocular injection of ganciclovir or foscarnet, particularly when the macula or optic nerve is threatened. High-dose antiviral therapy, using either intravenous acyclovir or oral valacyclovir (2 g, 3 times daily), should be administered initially. Thereafter, immunocompetent patients should be treated with oral suppressive therapy; treatment duration can vary from several months to long-term, even lifelong treatment. Patients with HIV infection/AIDS should be treated at least until the CD4⁺ cell count exceeds 200/ μ L, or perhaps indefinitely. Once antiviral therapy is initiated, systemic corticosteroids may be added in nonimmunocompromised patients and then tapered over several weeks. Retinal detachment is a common complication of

Table 11-3 Treatment Options for Herpetic Retinitis Caused by Cytomegalovirus (CMV), Varicella-Zoster Virus (VZV), or Herpes Simplex Virus (HSV) Infection

Intraocular Treatment			
Causative Virus	Drug	Dose	Maintenance/Suppression
CMV, VZV, HSV	Ganciclovir	2 mg	The implant was designed to release the drug over a 5- to 8-month period.
	Foscarnet	1.2–2.4 mg	
CMV only	Ganciclovir intraocular implant ^a	4.5 mg	
Systemic Treatment			
Causative Virus	Drug	Induction/High Dose	Maintenance/Suppression
CMV	Valganciclovir	900 mg twice daily	900 mg once daily
	Ganciclovir ^b	5 mg/kg, intravenously, every 12 hours for 2 weeks	
		Foscarnet ^{b,c}	90 mg/kg, intravenously, every 12 hours for 2 weeks
VZV/HSV	Acyclovir ^b	10 mg/kg, intravenously, every 8 hours	800 mg, orally, 5 times daily
	Valacyclovir ^b	2 g, orally, 3 times daily	1 g, orally, 3 times daily
	Prednisone (optional)	0.5 mg/kg/day for 3–6 weeks ^d	

^aNo longer clinically available.

^bStandard adult dosages. Monitoring of kidney function is required, as kidney toxicity can occur. Note that ganciclovir-resistant CMV strains exist; thus, after initiation of ganciclovir, close monitoring for response is required.

^cMonitoring of bone marrow function is required, as suppression can occur.

^dAfter antiviral therapy is initiated.

necrotizing retinitis, occurring in up to 70%–75% of cases, and reattachment surgery often is complex and requires silicone oil placement.

Schoenberger SD, Kim SJ, Thorne JE, et al. Diagnosis and treatment of acute retinal necrosis: a report by the American Academy of Ophthalmology. *Ophthalmology*. 2017;124(3):382–392.

Endogenous Bacterial Endophthalmitis

Endogenous bacterial endophthalmitis results from hematogenous seeding of the eye, typically during transient bacteremia. A wide range of bacteria can cause endogenous bacterial endophthalmitis. In North America, 40% of cases occur in patients with endocarditis, most typically caused by infection with either *Staphylococcus* or *Streptococcus* species. In contrast, 60% of endogenous endophthalmitis cases in Asia occur in patients with liver abscesses caused by *Klebsiella pneumoniae* infection. Nearly one-third of cases occur in patients who have urinary tract infections, most often caused by *Escherichia coli*. Other

cases can be associated with intravenous drug use or with procedures known to produce bacteremia, particularly placement of indwelling catheters.

Clinical presentation can vary and depends on both the size of the inoculum and the virulence of the organism; it ranges from a focal chorioretinitis (Fig 11-18) with little vitreous inflammation to a dense panophthalmitis that obscures the view of the posterior segment. Although decreased vision and eye pain are common symptoms, many patients do not have any constitutional symptoms. The patient should undergo systemic evaluation for the source of infection, and treatment with systemic antibiotics should be initiated. In addition, intravitreal injection of broad-spectrum antibiotics should be considered.

Fungal Endophthalmitis

Endophthalmitis caused by fungal infections may be either endogenous or exogenous. *Exogenous fungal endophthalmitis* is uncommon in North America and Europe. In contrast, in tropical regions such as India, fungi account for up to one-fifth of culture-positive cases following surgery or trauma. *Endogenous fungal endophthalmitis* is rare regardless of setting and typically occurs in either severely immunocompromised patients with persistent fungemia or otherwise healthy persons who inject drugs following transient fungemia.

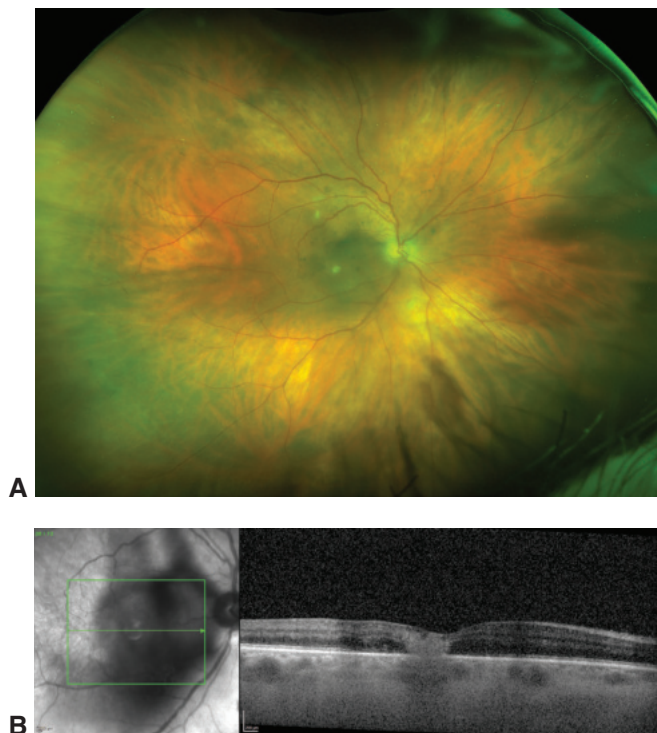
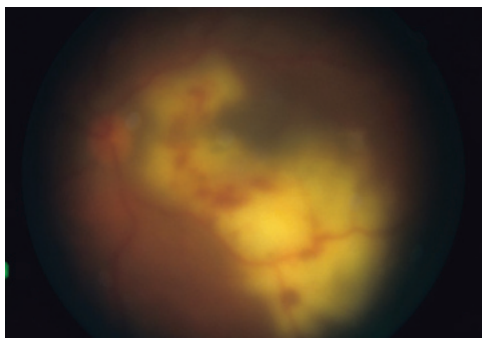


Figure 11-18 Endogenous bacterial endophthalmitis. **A**, Fundus photograph from a patient with *Streptococcus mitis* endocarditis shows 3 focal yellow chorioretinal infiltrates, as well as vitritis concentrated over the macula. **B**, OCT demonstrates the full-thickness hyperreflectivity of the macular chorioretinal lesion. (Courtesy of Lucia Sobrin, MD.)

Figure 11-19 Fundus photograph of endophthalmitis caused by infection with *Aspergillus* species. Features present include vitritis, a diffuse macular chorioretinal lesion with subretinal infiltration, and intraretinal hemorrhage. (Courtesy of Dean Elliott, MD.)



The clinical presentation is often subacute, and the diagnosis is typically delayed for weeks. *Aspergillus* (Fig 11-19) and *Fusarium* are the most commonly identified pathogens. Fungal keratitis may also progress to endophthalmitis, most typically when caused by *Fusarium*. Treatment is frequently difficult and typically involves vitrectomy, intravitreal injection of amphotericin B (5 µg/0.1 mL) and/or voriconazole (0.1 mg/0.1 mL), and systemic antifungal therapy. Two-thirds of patients with fungal endophthalmitis lose useful vision.

Endogenous yeast endophthalmitis is most frequently caused by *Candida* species. Affected patients frequently have previously used illicit intravenous drugs or indwelling catheters or have undergone long-term antibiotic treatment or immunosuppressive therapy. Many also have a history of hyperalimentation, recent abdominal surgery, or diabetes mellitus. The initial intraocular inflammation is usually mild to moderate, and yellow-white choroidal or chorioretinal lesions may be single or multiple (Fig 11-20). Subretinal infiltrates may coalesce into a mushroom-shaped white nodule that projects through the retina into the vitreous. Exogenous *Candida* endophthalmitis is rare.

The diagnosis of *Candida* endophthalmitis is usually made according to the history, clinical setting, and presence of characteristic fundus features. Intraocular culture specimens are best obtained during pars plana vitrectomy.

If the macula is not involved, the visual prognosis after treatment is generally good. Chorioretinal lesions are often successfully treated with systemic medications alone, for example, intravenous fluconazole or voriconazole, which penetrates the eye well.

Durand ML. Bacterial and fungal endophthalmitis. *Clin Microbiol Rev.* 2017;30(3):597–613.

Ocular Tuberculosis

Even though one-third of the world's population has been exposed to *Mycobacterium tuberculosis*, active *M tuberculosis* uveitis is uncommon, even in endemic areas. Suggestive clinical findings include solitary (Fig 11-21) or MFC, serpiginous-like chorioretinitis, and Eales disease–like peripheral nonperfusion in association with uveitis. Patients suspected of having tuberculous uveitis should undergo testing for prior *M tuberculosis* exposure, including a chest x-ray and a blood-based interferon-gamma release assay.

Once the diagnosis of ocular tuberculosis is either confirmed or strongly suggested, the patient should be treated for extrapulmonary tuberculosis as recommended by either the US Centers for Disease Control and Prevention (CDC) or the World Health Organization.

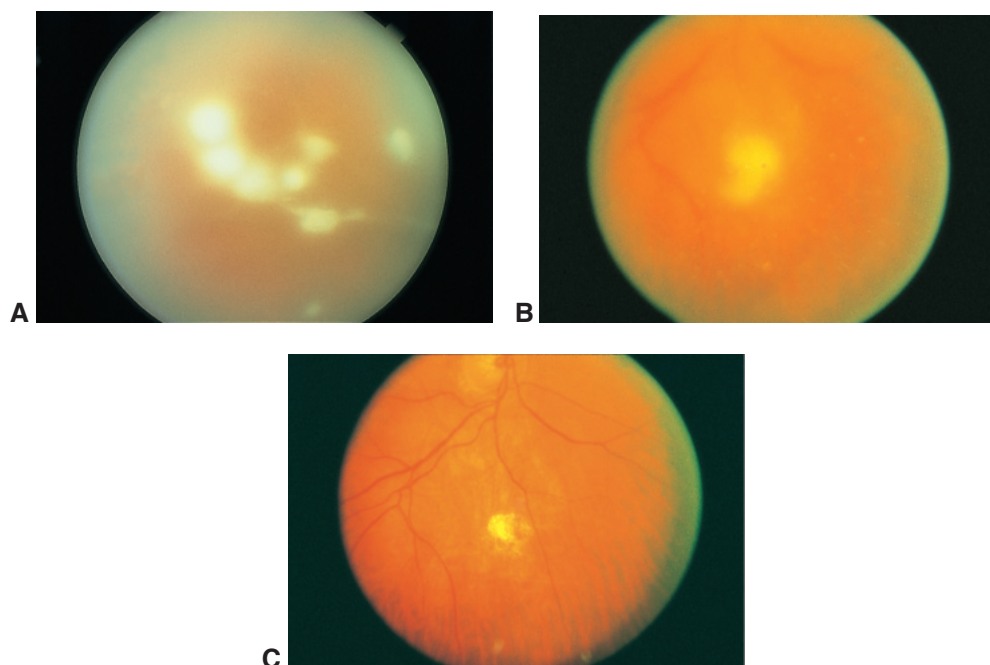


Figure 11-20 Fundus photographs of endogenous yeast (*Candida*) endophthalmitis. **A**, Note the vitreous infiltrates in a “string of pearls” configuration. **B**, Photograph from a patient with endogenous endophthalmitis before treatment. **C**, After treatment with vitrectomy and intravitreal amphotericin B, the endogenous endophthalmitis shown in **B** was resolved. (Courtesy of Harry W. Flynn, Jr, MD.)



Figure 11-21 Ocular tuberculosis. Fundus photograph shows a choroidal granuloma superotemporal to the optic nerve head. The inflammation can be localized to the choroid as the overlying retina and retinal vessels are relatively spared. (Courtesy of Janet L. Davis, MD.)

Ethambutol hydrochloride, a medication commonly used in the treatment of tuberculosis, can cause optic neuropathy; patients taking ethambutol need close monitoring for this treatment complication.

Agrawal R, Testi I, Mahajan S, et al; Collaborative Ocular Tuberculosis Study Consensus Group. Collaborative Ocular Tuberculosis Study consensus guidelines on the management of tubercular uveitis—report 1: guidelines for initiating antitubercular therapy in tubercular choroiditis. *Ophthalmology*. 2021;128(2):266–276.

Syphilitic Retinochoroiditis

Uveitis is often the presenting sign of syphilis but can occur at any stage of the infection. Syphilitic uveitis is confirmed through serologic testing. The traditional screening algorithm for syphilis uses a nontreponemal assay (eg, the nonspecific but quantitative VDRL or rapid plasma reagin [RPR] test) for primary evaluation and if the test is reactive, a treponemal assay (eg, fluorescent treponemal antibody absorption [FTA-ABS] test, *Treponema pallidum* particle agglutination assay [TP-PA], microhemagglutination assay for *T pallidum* antibodies [MHA-TP]) for confirmation. More recently, laboratories have reversed the order in which treponemal and nontreponemal tests are performed, leading to the development of the reverse sequence syphilis screening (RSSH) algorithm. Although the CDC currently continues to recommend the traditional testing approach, it provides a recommended algorithm for the use of RSSS. Briefly, initial testing is done with a treponemal assay, followed by a quantitative nontreponemal test for confirmation. Discordant samples are resolved on the basis of a second treponemal assay.

For patients with uveitis whose serologic test results are positive for syphilis, cerebrospinal fluid (CSF-) VDRL titers should be assessed before and, if the CSF-VDRL results are positive, after completion of treatment in order to document a complete response.

Many patients with syphilitic uveitis present with a nondescript panuveitis, which supports the need for routine syphilis testing in all sexually active patients with uveitis. Specifically suggestive clinical findings include inflammatory ocular hypertensive syndrome, iris roseola, and retinochoroiditis. The retinochoroiditis is often diaphanous—appearing less opaque than either herpetic or toxoplasmic retinitis—and is accompanied by overlying inflammatory accumulations called *retinal precipitates*. A distinctive form of syphilitic outer retinitis termed *acute syphilitic posterior placoid chorioretinitis* (ASPPC) is characterized by the presence of a placoid, round or oval, yellow lesion that involves or is near the macula (Fig 11-22). Because coinfection is common, all patients with syphilis should be tested for HIV. Patients with syphilitic uveitis should be treated for neurosyphilis.

Begaj T, Sobrin L. Ophthalmic consequences of syphilis. *Int Ophthalmol Clinics*. Forthcoming 2022.

Ocular Bartonellosis

Cat-scratch disease, caused by *Bartonella*, is associated with 2 ocular syndromes: Parinaud oculoglandular syndrome, which consists of conjunctival inflammation with preauricular adenopathy; and Leber stellate neuroretinitis, which includes macular star formation and optic nerve head swelling, often associated with a peripapillary serous macular detachment (Fig 11-23). Cat-scratch disease is the most common cause of neuroretinitis with stellate maculopathy, but several other infectious diseases can have this presentation, including toxoplasmosis, ehrlichiosis, and syphilis. Small, focal areas of retinitis or chorioretinitis are frequently noted in patients with *Bartonella* neuroretinitis. In rare cases, an optic nerve head angiomatous lesion can develop. Treatment with antibiotics is necessary in immunocompromised adults or in patients with persistent infection.

Toxoplasmic Chorioretinitis

Toxoplasmosis is the most common cause of posterior segment infectious disease worldwide. The causative organism, *Toxoplasma gondii*, is an obligate intracellular parasite.

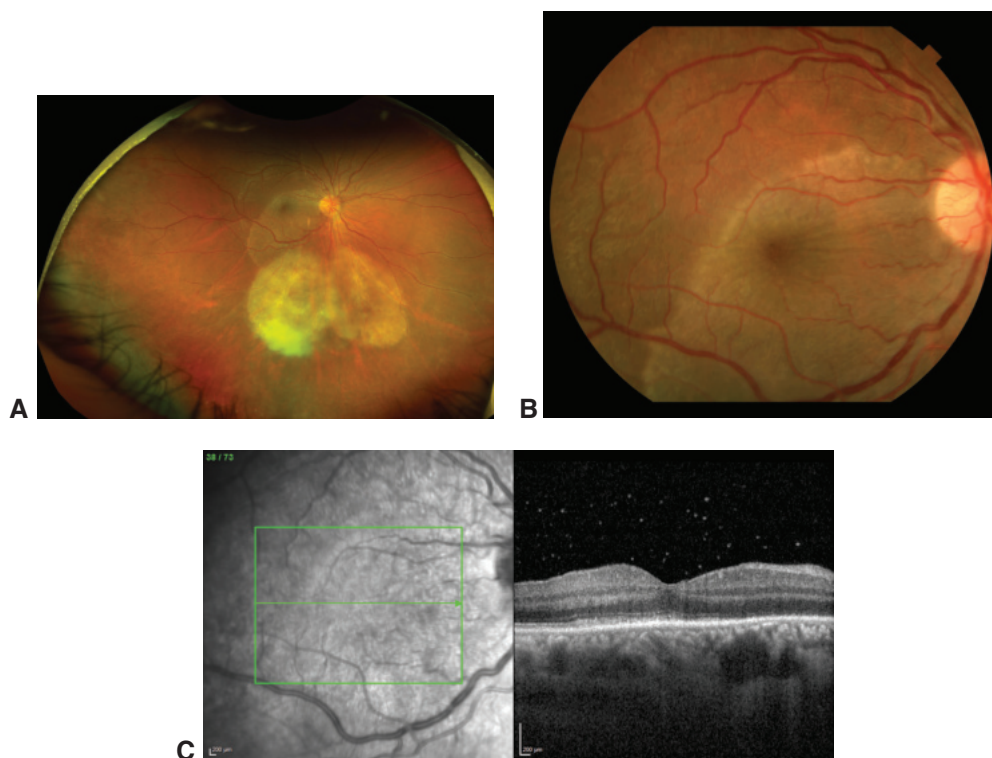


Figure 11-22 Syphilitic retinochoroiditis. **A**, Ultra-wide-field fundus photograph montage shows a right eye with a large placoid yellow lesion in the macula consistent with acute syphilitic posterior placoid chorioretinitis (ASPPC). In the inferior midperiphery are 2 other large areas of retinitis with overlying retinal precipitates. **B**, Fundus photograph shows a magnified view of ASPPC. **C**, OCT image demonstrates disruption of outer retinal layers with hyperreflective deposits in the area of ASPPC. (Courtesy of Lucia Sobrin, MD.)

Because seropositivity for *T gondii* is very common, seropositivity alone does not confirm that uveitis is related to toxoplasmosis. Congenital disease occurs via transplacental infection; a pregnant woman acquires the organism through exposure to tissue cysts or oocytes in uncooked meat or substances contaminated with cat feces (see also BCSC Section 6, *Pediatric Ophthalmology and Strabismus*, Chapter 25). The typical ocular finding in congenital toxoplasmosis is a chorioretinal scar, usually in the macula and often bilateral.

Most cases of toxoplasmosis are currently assumed to be acquired postnatally, although proving this assumption can be difficult. A positive serologic test result for immunoglobulin (Ig) M anti-*T gondii* antibodies supports the diagnosis of acquired disease. PCR analysis of ocular fluids for *T gondii* DNA and determining the Goldmann-Witmer coefficient to compare the IgG level in ocular fluid with that in serum can also assist in confirming the diagnosis. Of note, PCR analysis of ocular fluid for *Toxoplasma* is not as sensitive or specific as PCR analysis of ocular fluid for herpes virus (see BCSC Section 9, *Uveitis and Ocular Inflammation*, Chapter 5).

Decreased vision and floaters are the most common presenting symptoms of toxoplasmic chorioretinitis. Clinically, the condition consists of a focal area of intense, necrotizing

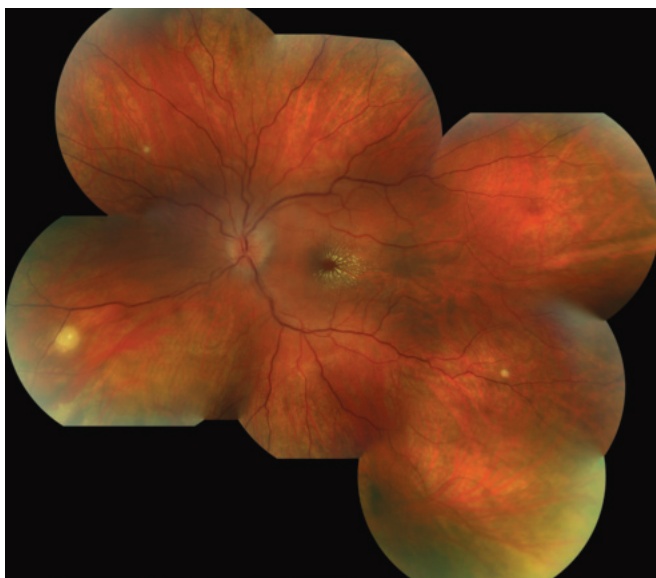


Figure 11-23 Color fundus photograph montage of neuroretinitis shows optic nerve head swelling and a macular star formation resulting from cat-scratch disease (*Bartonella henselae* infection). In the inferonasal periphery, a small focal area of chorioretinitis is visible. Two smaller foci are visible in the inferotemporal and superotemporal periphery. (Courtesy of Lucia Sobrin, MD.)

chorioretinitis, typically with moderate to severe overlying vitreous inflammation (Fig 11-24). Recurring disease is indicated by an adjacent or nearby chorioretinal scar. Multiple active lesions are rare and should prompt HIV testing and inquiry for other possible causes of immunosuppression. HIV-seropositive patients with ocular toxoplasmosis have a high risk of CNS involvement and thus should undergo magnetic resonance imaging with contrast material. Older adult patients may present with more aggressive disease because of their relative immunosuppression.

Active ocular toxoplasmosis is commonly treated with antibiotics, despite the lack of well-designed randomized controlled trials. The simplest approach is treatment with trimethoprim-sulfamethoxazole. Classic therapy uses sulfadiazine with pyrimethamine and prednisone (prescribed with folinic acid and accompanied by regular monitoring of blood cell counts); the addition of clindamycin results in so-called quadruple therapy. Atovaquone and azithromycin are also commonly used in clinical practice. None of these approaches has been shown to be superior to another for the final visual outcome, lesion size, or recurrence rate. Treatment typically lasts 4–6 weeks, and complete healing of active lesions occurs over 4–6 months. When used, systemic corticosteroids should be given under antibiotic cover. Use of long-acting, depot periocular or intraocular corticosteroid injections should be avoided. Long-term maintenance treatment with trimethoprim-sulfamethoxazole has been used to decrease the attack rate in patients experiencing frequent recurrences or in severely immunosuppressed patients. Intravitreal clindamycin with or without dexamethasone has been used to treat vision-threatening lesions or for patients who are intolerant of or who do not respond to systemic therapy.

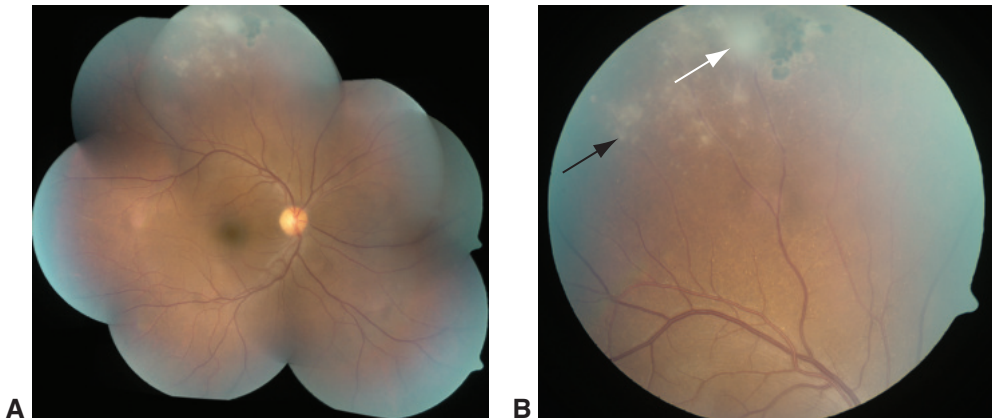


Figure 11-24 Toxoplasmic chorioretinitis. **A**, Color fundus photograph montage from a patient with recurring toxoplasmic chorioretinitis. **B**, Color fundus photograph shows white focal retinitis (white arrow) with overlying vitreous inflammation, which creates a “headlight in the fog” appearance, with an adjacent pigmented chorioretinal scar. Accompanying perivasculitis and nonspecific exudates are present, in addition to distinct lobular periaarteriolar collections of cells (black arrow) called *Kyrieleis* plaques. (Courtesy of Stephen J. Kim, MD.)

Fernandes Felix JP, Cavalcanti Lira RP, Grupenmacher AT, et al. Long-term results of trimethoprim-sulfamethoxazole versus placebo to reduce the risk of recurrent *Toxoplasma gondii* retinochoroiditis. *Am J Ophthalmol.* 2020;213:195–202.

Kim SJ, Scott IU, Brown GC, et al. Interventions for *Toxoplasma* retinochoroiditis: a report by the American Academy of Ophthalmology. *Ophthalmology.* 2013;120(2):371–378.

Toxocariasis

Toxocariasis is a parasitic infection caused by 1 of 2 roundworms, *Toxocara canis* or *Toxocara cati*, which are common intestinal parasites of dogs and cats, respectively. Humans are most commonly infected following ingestion of soil or vegetables contaminated by the *Toxocara* eggs. Although ocular toxocariasis is part of a systemic infestation by the nematode, systemic manifestations such as visceral larva migrans, fever, and eosinophilia are relatively uncommon. Children and young adults are affected disproportionately. Common ocular symptoms include decreased vision and floaters. The condition is unilateral in most cases and typically has 1 of 3 presentations:

- peripheral granuloma, which often produces a traction band that extends toward the macula (Fig 11-25) and occasionally mimics unilateral intermediate uveitis with snowbank formation
- posterior pole granuloma, which can decrease vision dramatically when the central macula is involved
- moderate to severe panuveitis that can mimic endogenous endophthalmitis

Enzyme-linked immunosorbent assay (ELISA) analysis of serum or intraocular fluids can help establish the diagnosis in these cases but is relatively insensitive. Vitreous inflammation, CME, and traction retinal detachment are the most common causes of vision

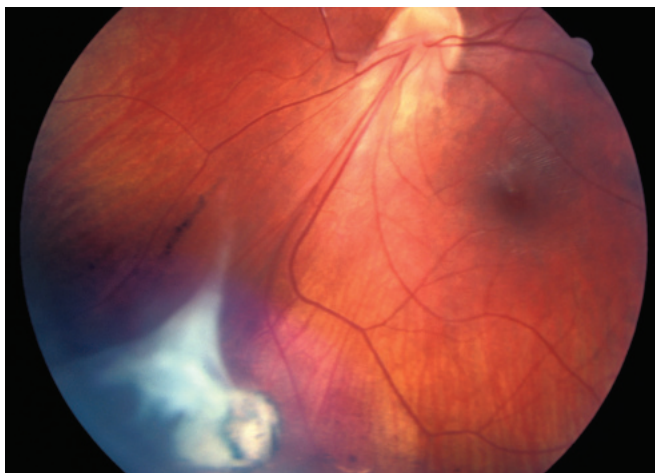


Figure 11-25 Fundus photograph from a 6-year-old boy with reduced and distorted vision. The image shows a peripheral toxocariasis cyst with associated fibrosis (*bottom left*). The fibrosis results in considerable traction, and the macula is dragged inferiorly and distorted. (Courtesy of Colin A. McCannel, MD.)

loss. Most specialists assume that the uveitis of toxocariasis represents an immune response to antigens released from a dead or dying worm. Thus, treatment typically involves use of local or systemic corticosteroids, and anthelmintic therapy has little or no therapeutic role.

Woodhall D, Starr MC, Montgomery SP, et al. Ocular toxocariasis: epidemiologic, anatomic, and therapeutic variations based on a survey of ophthalmic subspecialists. *Ophthalmology*. 2012;119(6):1211–1217.

Ocular Lyme Borreliosis

Lyme disease is caused by the spirochete *Borrelia burgdorferi*, which is transmitted to humans through the bite of infected ticks. Following the tick bite, the disease usually occurs in 3 stages. In stages 1 and 2, systemic manifestations consist of myalgias, arthralgias, fever, headache, malaise, and a characteristic skin lesion known as *erythema chronicum migrans* (bull's-eye rash), which consists of an annulus of erythema surrounding an area of central clearing. In stage 3, as neurologic or musculoskeletal findings manifest, ocular inflammation may develop but is uncommon. Lyme disease–related ocular findings include keratitis, scleritis, and uveitis, which may include anterior chamber or vitreous inflammation, retinal vasculitis, papillitis, or optic neuritis. Chronic uveitis in patients who reside in or have traveled to an endemic area or who have had a recent tick bite or an erythema migrans–like skin lesion should suggest the possibility of Lyme disease.

Initial serologic testing is performed using a sensitive ELISA. If an ELISA is positive or equivocal, separate IgM immunoblotting (if symptoms have been present for fewer than 30 days) and IgG immunoblotting should be performed on the same blood sample. A diagnosis of Lyme disease is supported only when results of both tests are positive. The 2 tests are designed to be used together; thus, the initial ELISA test should not be skipped.

Treatment for early disease consists of tetracycline, doxycycline, or penicillin. Advanced disease may require intravenous ceftriaxone or penicillin.

Raja H, Starr MR, Bakri SJ. Ocular manifestations of tick-borne diseases. *Surv Ophthalmol.* 2016;61(6):726–744.

Diffuse Unilateral Subacute Neuroretinitis

Diffuse unilateral subacute neuroretinitis (DUSN) is a rare condition that typically occurs in otherwise healthy, young patients and is caused by the presence of a mobile subretinal nematode. The causative nematodes in DUSN have yet to be definitively established, although *Toxocara* species, *Baylisascaris procyonis*, and *Ancylostoma caninum* have all been implicated. Prompt diagnosis and treatment of the condition can help prevent vision loss, which may be severe. The clinical findings in DUSN can be divided into acute and end-stage manifestations. In the acute phase, patients frequently have decreased visual acuity, vitritis, papillitis, and clusters of gray-white or yellow-white outer retinal and choroidal lesions. The clustering of the lesions is important because it often helps localize the mobile nematode. The degree of vision loss is often greater than might be expected from clinical examination findings. If DUSN is left untreated, late sequelae ultimately develop and include optic atrophy, retinal arterial narrowing, and diffuse RPE disruption with severe vision loss. The late findings may be misinterpreted as unilateral retinitis pigmentosa.

If the nematode can be visualized, it should be destroyed using laser photocoagulation (Fig 11-26).

de Amorim Garcia Filho CA, Gomes AH, de A Garcia Soares AC, de Amorim Garcia CA. Clinical features of 121 patients with diffuse unilateral subacute neuroretinitis. *Am J Ophthalmol.* 2012;153(4):743–749.

West Nile Virus Chorioretinitis

West Nile virus infection is transmitted to humans through the bite of an infected mosquito of the genus *Culex*, with birds serving as the primary reservoir. Human infection is most often subclinical, although a febrile illness occurs in approximately 20% of cases. Neurologic disease (meningitis or encephalitis) is common, frequently found in association with diabetes mellitus and advanced age. Ocular manifestations occur primarily in diabetic patients with encephalitis. The eye manifestation most commonly noted with West Nile virus infection is a multifocal chorioretinitis that is usually bilateral and includes lesions arranged in distinctive linear clusters that often follow the course of retinal nerve fibers (Fig 11-27). Vision typically remains good unless the lesions involve the central macula.

Zika Virus Chorioretinitis

Zika virus (ZIKV) is a member of the family Flaviviridae and is related to yellow fever virus, dengue virus, and West Nile virus. ZIKV is spread primarily by the female *Aedes aegypti* mosquito. Infection in adults is often asymptomatic or results in only mild symptoms. Infection during pregnancy, however, can result in severe microcephaly and other

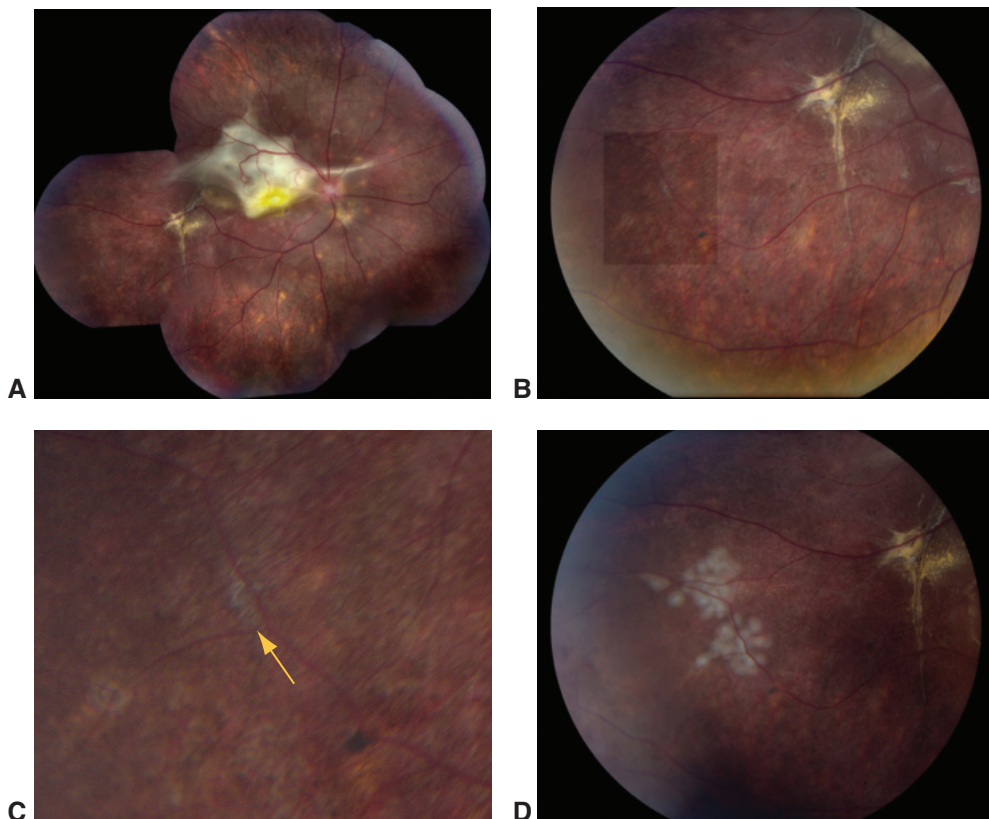


Figure 11-26 Diffuse unilateral subacute neuroretinitis. An 11-year-old boy presented with decreased vision in the right eye. Examination findings included moderate vitritis and a relative afferent pupillary defect in addition to multiple chorioretinal lesions and submacular fibrosis. A worm was not found, and the patient was treated with albendazole. **A**, Once vitreous inflammation had decreased, multifocal areas of chorioretinal scarring in the periphery as well as submacular fibrosis were visible. **B**, In the inferotemporal periphery, a worm was identified. **C**, With higher magnification, the small grayish worm (*arrow*) was visible. **D**, Laser spots were applied directly to the worm. The patient's vision subjectively improved, and no further lesions or inflammation was seen. (Courtesy of Jaclyn Kovach, MD.)

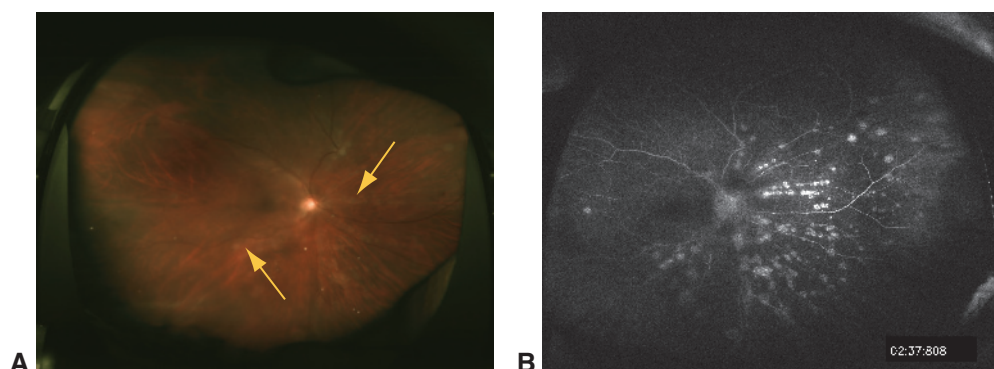


Figure 11-27 West Nile virus chorioretinitis. **A**, Fundus photograph shows chorioretinal lesions in a linear configuration (*arrows*). **B**, FA image shows staining of lesions that are characteristically arranged in a linear configuration in some areas. (Courtesy of Dean Elliott, MD.)

brain malformations in some infants. Macular and optic nerve abnormalities as well as chorioretinal lesions have been reported in some patients with ZIKV infection.

Ebola Virus Panuveitis

Ebola virus causes a severe and fatal hemorrhagic fever in humans; the mortality rate is as high as 90%. The virus is transmitted by direct contact with infected blood or other body fluids. Among survivors, uveitis has been described. There has been 1 report of severe panuveitis that occurred after the patient experienced a complete systemic recovery but still had persistent viral replication in the aqueous humor.

Chikungunya Virus Retinitis

Chikungunya virus (CHIKV) is a species of the genus *Alphavirus*. Typically, the virus is transmitted to humans by a mosquito bite. The most common symptoms of CHIKV infection are fever and joint pain. Several ocular findings have been reported, including retinitis and optic neuritis, but anterior uveitis may be the most common presentation.

Hereditary Retinal and Choroidal Disease

Highlights

- Congenital color vision defects are stationary and usually affect both eyes equally. When hereditary, they are most frequently X-linked recessive red-green abnormalities.
- Patients with retinal dystrophies should be monitored regularly for treatable causes of vision loss associated with their condition: cataract, macular edema, glaucoma, and retinal exudation.
- Drusen are not only seen in older-adult eyes; macular dystrophies affecting young adults typically include drusenlike deposits and may lead to choroidal neovascularization.
- Patients with minimal signs of ocular pathology who present with unexplained vision loss or are suspected of malingering may in fact have early stages of retinal dystrophy.
- Genetic screening can assist in confirming a diagnosis of retinal degeneration, establishing the inheritance pattern, informing at-risk relatives, and identifying candidates for gene therapies.

Color Vision Abnormalities

Defects in color vision, termed *dyschromatopsias*, are caused by abnormalities of the cone system. Dyschromatopsia can be either static (stationary) or progressive. Stable dyschromatopsia is usually, although not always, congenital. Congenital color vision defects are stationary and usually affect both eyes equally, whereas acquired color vision defects may be progressive and/or uniocular. This chapter describes the nonprogressive forms of color vision loss. For further discussion of optic neuropathies that may lead to acquired vision loss, refer to BCSC Section 5, *Neuro-Ophthalmology*.

Congenital Color Deficiency

Congenital color vision defects are traditionally classified by an individual's performance on color-matching tests. A person with normal color vision (*trichromatism*, or *trichromacy*) can match any colored light by varying a mixture of the 3 primary colors (eg, a long-wavelength red, middle-wavelength green, and short-wavelength blue light).

Individuals with anomalous trichromatism, who make up the largest group of color-deficient persons, can also use 3 primary colors to match a given color. However, because

1 of their cone photopigments has an abnormal absorption spectrum, they use different proportions of colors than those used by persons with normal color vision. Some individuals have only a mild abnormality. Others have poor color discrimination and may appear to have dichromatism on some of the color vision tests.

Hereditary congenital color vision defects are most frequently X-linked recessive red-green abnormalities; they affect 5%–8% of males and 0.5% of females. Acquired defects are more frequently of the blue-yellow, or *tritan*, variety and affect males and females equally. Table 12-1 shows the traditional classification of color vision deficits based on color-matching test results.

Individuals who need only 2 primary colors to make a color match have *dichromatism* (also called *dichromacy*). It is assumed that such individuals lack 1 of the cone photopigments. Approximately 2% of males have dichromatism.

An absence of color discrimination, or *achromatopsia*, means that any spectral color can be matched with any other solely by intensity adjustments. The congenital achromatopsias are disorders of photoreceptor function. Essentially, there are 2 forms of achromatopsia: rod monochromatism and blue-cone (S-cone) monochromatism. Both disorders typically present with infantile nystagmus syndrome (congenital nystagmus), poor vision, and photophobia. Electroretinography (ERG) testing helps differentiate achromatopsia from infantile nystagmus syndrome or ocular albinism, both of which are associated with normal cone ERGs (see Chapter 3, Fig 3-2).

Rod monochromatism (complete achromatopsia) is the most severe form; affected individuals have normal rod function but no detectable cone function and thus see the world in shades of gray. Patients may have partial to full expression of the disorder, with visual acuity

Table 12-1 Classification and Male-Population Incidence of Color Vision Defects

Color Vision	Inheritance	Incidence in Male Population, %
Hereditary		
<i>Trichromatism</i>		
Normal	–	92.0
Deuteranomalous ^a	XR	5.0
Protanomalous ^b	XR	1.0
Tritanomalous ^c	AD	0.0001
<i>Dichromatism</i>		
Deuteranomalous	XR	1.0
Protanomalous	XR	1.0
Tritanomalous	AD	0.001
<i>Achromatopsia (monochromatism)</i>		
Typical (rod monochromatism)	AR	0.0001
Atypical (blue-cone monochromatism)	XR	Unknown
Acquired		
Protanomalous-deuteranomalous (red-green)	Unknown	Unknown
Tritanomalous (blue-yellow)	Unknown	Unknown

AD = autosomal dominant; AR = autosomal recessive; XR = X-linked recessive.

^aDeuteranomalous means reduced sensitivity to green light.

^bProtanomalous means reduced sensitivity to red light.

^cTritanomalous means reduced sensitivity to blue light.

ranging from 20/80 to 20/200. Nystagmus is usually present in childhood and may improve with age. Characteristically, the ERG pattern in patients with rod monochromatism shows an absence of cone-derived responses and normal rod responses. Dark adaptometry shows no cone plateau and no cone-rod break. The disorder has autosomal recessive inheritance.

In *blue-cone (S-cone) monochromatism*, the function of rods and S cones is normal, but L- and M-cone function is absent. (“S” refers to short wavelength.) The condition is usually X-linked and can be difficult to distinguish clinically from rod monochromatism in the absence of a family history or results from specialized color or ERG testing. Individuals with blue-cone monochromatism exhibit preserved S-cone ERG responses, severely reduced light-adapted (LA) 3.0 30-Hz responses, and normal rod ERGs. These individuals typically have a visual acuity of approximately 20/80, which is better than the visual acuity of individuals with typical rod monochromatism.

Night Vision Abnormalities

Deficiencies in night vision, termed *nyctalopia*, are caused by abnormalities of the rod system. These are typically static (stationary) and associated with normal visual acuity.

Congenital Night-Blinding Disorders With Normal Fundi

Congenital stationary night blindness (CSNB) is a nonprogressive disorder of night vision. CSNB has 3 genetic subtypes:

- X-linked (most common)
- autosomal recessive
- autosomal dominant (rare)

Snellen visual acuities of patients with CSNB range from normal to occasionally as poor as 20/200, but most cases of decreased vision are associated with significant myopia. The appearance of the fundus is usually normal, except for myopic changes in some cases. Patients commonly present with difficulty with night vision, nystagmus, and reduced visual acuity. Some patients may have a paradoxical pupillary response, in which the pupil initially constricts when the ambient light dims. Dark-adaptometry curves reveal markedly reduced responses.

Electroretinography is important in the diagnosis of CSNB. The most common ERG pattern seen in patients with CSNB is the *negative* ERG (the Schubert-Bornschein form of CSNB), in which the 10.0/30.0 response has a normal (or near-normal) a-wave but a markedly reduced b-wave. The normal a-wave excludes significant rod photoreceptor dysfunction, and this result helps to differentiate CSNB from the potentially blinding disorder retinitis pigmentosa (see Chapter 3 for discussion of electrophysiologic testing). The differential diagnosis of CSNB includes other conditions with a negative ERG, such as X-linked juvenile retinoschisis, central retinal artery occlusion, birdshot chorioretinopathy, and melanoma-associated retinopathy; the latter demonstrates an ERG pattern identical to that of CSNB but usually presents with acquired nyctalopia (night blindness) and shimmering photopsias.

X-linked CSNB has been categorized into 2 types: complete and incomplete. Patients with *complete CSNB* have an undetectable dark-adapted (DA) 0.01 (rod-specific) ERG response and psychophysical thresholds that are mediated by cones (see Chapter 3, Fig 3-2B). Patients with *incomplete CSNB* have some detectable rod function on ERG and an elevated dark-adaptation final threshold (Fig 12-1). Mutations in the *NYX* and *CACNA1F* genes, which encode proteins involved in the transmission of signals between photoreceptors and bipolar cells, are responsible for complete and incomplete CSNB, respectively.

Congenital Night-Blinding Disorders With Fundus Abnormality

Fundus albipunctatus results from a mutation in *RDH5* (12q13–q14). *RDH5* encodes 11-*cis*-retinol dehydrogenase, a microsomal enzyme in the retinal pigment epithelium (RPE) that is involved in the regeneration of rhodopsin. Patients with fundus albipunctatus have very delayed rhodopsin regeneration; and although levels eventually normalize, the process may require many hours in the dark. Affected individuals have night blindness from birth and usually exhibit yellow-white dots in the posterior pole that extend into the midperiphery but spare the fovea (Fig 12-2). ERG responses commonly show a cone-isolated retina pattern, with undetectable DA 0.01 ERG response, and a severely reduced

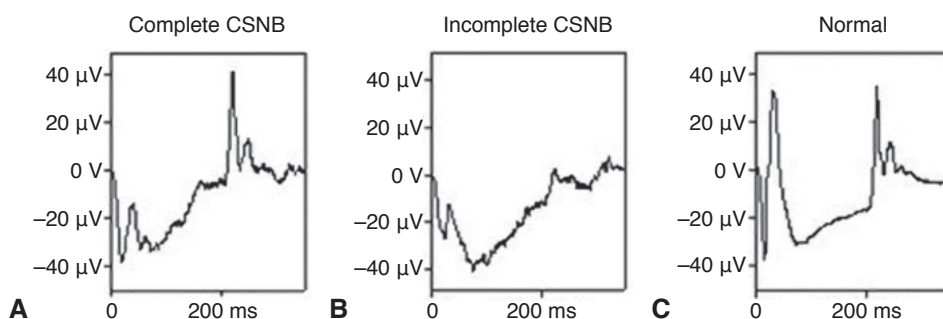


Figure 12-1 Electrophoretograms (ERG) patterns of on- and off-responses in congenital stationary night blindness (CSNB). The stimulus has a 200-millisecond (ms) duration to enable independent recording of the ERG responses to onset and offset. **A**, The pattern of a patient with complete CSNB shows a negative-waveform on-response but a normal off-response. **B**, The pattern of a patient with incomplete CSNB shows both on- and off-response abnormalities. **C**, Pattern of a subject with normal responses. (Courtesy of Graham E. Holder, PhD.)

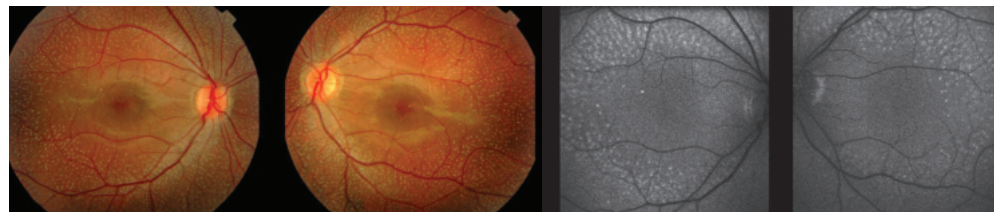


Figure 12-2 Fundus photographs and fundus autofluorescence (FAF) images from a patient with fundus albipunctatus, showing multiple spots of unknown material scattered primarily throughout the deep retina. (Reproduced from Sergouniotis PI, Sohn EH, Li Z, et al. Phenotypic variability in *RDH5* retinopathy (fundus albipunctatus). Ophthalmology. 2011;118(8):1661–1670, with permission from Elsevier.)

DA 10.0/30.0 response (arising in dark-adapted cones) that normalizes with sufficiently extended dark adaptation (Fig 12-3).

The differential diagnosis of fundus albipunctatus includes *retinitis punctata albes-cens*, a disorder related to mutation in *RLBP1*, which encodes cellular retinaldehyde-binding protein. In this condition, which is a progressive rod-cone dystrophy, the white dots may be finer than those of fundus albipunctatus, and the retinal vessels may be attenuated (Fig 12-4). ERG responses are usually very subnormal: although they show some recovery with extended dark adaptation, they do not normalize.

Patients with *Oguchi disease* also are night blind from birth. This condition is due to a mutation either in *SAG* (2q37), which encodes arrestin, or in *GRK1* (13q34), which encodes rhodopsin kinase. This very rare disorder is most common in Japanese patients. The fundus in eyes with Oguchi disease is normal after dark adaptation but shows a peculiar yellow iridescent sheen after even brief exposure to light (the *Mizuo-Nakamura phenomenon*; Fig 12-5).

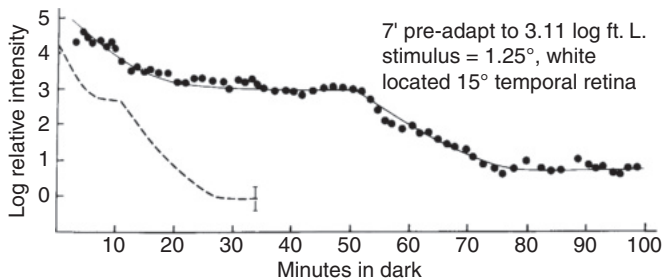


Figure 12-3 Dark-adaptometry curve in stationary night blindness. The dark-adaptometry curve of this patient (*dotted curve*) with good vision and nyctalopia and clinical findings of fundus albipunctatus shows no rod adaptation. *Dashed curve* indicates normal response. (Reproduced from Margolis S, Siegel IM, Ripps H. Variable expressivity in fundus albipunctatus. *Ophthalmology*. 1987;94(11):1416–1422. Copyright 1987, with permission from Elsevier.)

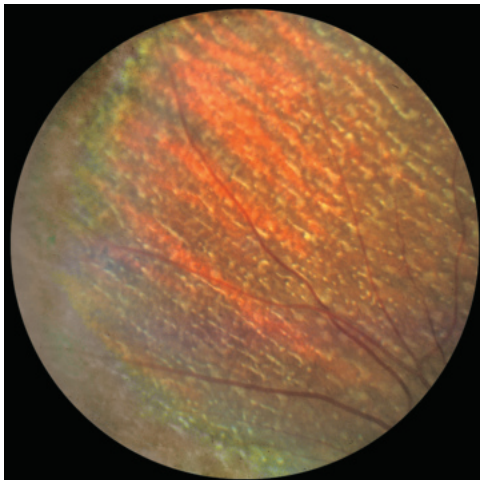


Figure 12-4 Fundus photograph of a patient with retinitis punctata albes-cens shows numerous deep retinal white dots. (Courtesy of John R. Heckenlively, MD.)

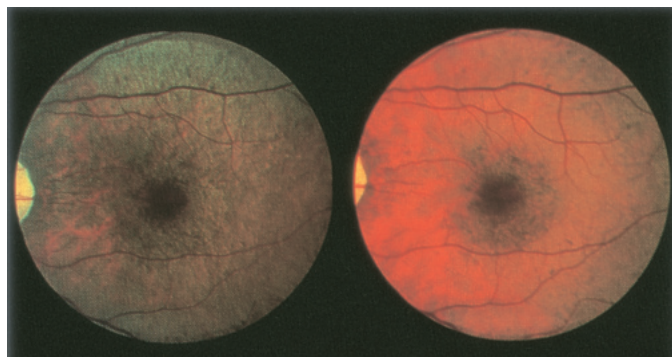


Figure 12-5 Fundus photographs showing the Mizuo-Nakamura phenomenon. The fundus of this patient with X-linked cone dystrophy is unremarkable in a dark-adapted state (*right*) but has a yellow iridescent sheen after exposure to light (*left*).

De Silva SR, Arno G, Robson AG, et al. The X-linked retinopathies: physiological insights, pathogenic mechanisms, phenotypic features and novel therapies. *Prog Retin Eye Res.* 2021;82:100898.

Zeitz C, Robson AG, Audo I. Congenital stationary night blindness: an analysis and update of genotype-phenotype correlations and pathogenic mechanisms. *Prog Retin Eye Res.* 2015;45:58–110.

Retinal and Choroidal Dystrophies

Classification and Terminology

Most retinal and choroidal dystrophies were originally named and described purely on the basis of ophthalmoscopic appearance and clinical course, many years before the discovery of DNA. Over time, identification of additional affected patients and families, coupled with advances in gene mapping and molecular biology, has led to a compendium of specific gene defects associated with previously known phenotypes.

The Online Mendelian Inheritance in Man website (www.omim.org) lists nearly 1000 genetic disorders with significant involvement of the retina, choroid, or both. The Retinal Information Network, RetNet (<https://sph.uth.edu/retnet/>), lists more than 300 different retinal degenerations for which the gene locus and often the specific gene defect have been identified. These websites are regularly updated with the most current information regarding genetic aspects of retinal and choroidal disorders.

Growing knowledge of the genetic basis for these diseases further demonstrates the complexity of the association of genotype and phenotype. For example, in families in which a single mutation has been identified, the onset, severity, and course of disease can vary widely among family members (termed *variable expressivity*). Some diseases and syndromes display distinctive clinical features and are associated with only 1 gene. However, most conditions are associated with multiple genes that give rise to a similar clinical picture (termed *genetic heterogeneity*).

Historically, retinal and choroidal dystrophies have been classified in various ways, each with its logic and limitations:

- On the basis of which retinal layer is involved, such as retina, RPE, choroid, and vitreoretinal interface. These distinctions are helpful clinically but do not always correspond to the site(s) of expression of the causative gene.
- On the basis of inheritance pattern of the disease (eg, autosomal dominant, X-linked recessive, etc). However, due to genetic heterogeneity, the same phenotype may be caused in some cases by a gene on an autosomal chromosome and in other cases by a gene on the X chromosome, and each may be transmitted in either a dominant or recessive pattern.
- On the basis of disease phenotype through clinical examination and electrophysiological and psychophysical testing. However, different genes can give rise to similar phenotypes.

For convenience, this chapter organizes the retinal and choroidal dystrophies on the basis of clinical phenotypes and anatomical involvement rather than on molecular genetics. Thus, the reader will note that some genes are causative across multiple phenotypes (genetic heterogeneity), and only in rare instances is a specific phenotype defined by a unique causative gene. In this schema, disorders that typically affect the photoreceptors of the entire retina are classified separately from those that typically affect the macula predominantly, as the symptoms and prognoses of these disorders often differ. The category of disorders that affect photoreceptors diffusely or “retina-wide” is further subdivided into diseases that affect predominantly rods (*rod-cone dystrophies*), diseases that affect predominantly cones (*cone-rod dystrophies*), and diseases that affect predominantly the choroid.

Daiger SP, Sullivan LS, Bowne SJ. Genetic mechanisms of retinal disease. In: Schachat AP, Wilkinson CP, Hinton DR, Sadda SR, Wiedemann P, eds. *Ryan's Retina*. Vol 2. 6th ed. Elsevier/Saunders; 2018:711–721.

General Diagnostic Considerations

With rare exceptions, hereditary diseases of the eye have bilateral, symmetric involvement. If ocular involvement is unilateral, other causes—such as birth defects, intrauterine or antenatal infections, inflammatory diseases, or trauma—should be considered. Because retinal degenerations can also occur as part of a systemic disorder, obtaining a thorough medical history is crucial, as is ruling out any reversible or treatable cause of retinal dysfunction, such as vitamin A deficiency, autoimmune disorders, and paraneoplastic or infectious retinopathy.

Clinical diagnostic evaluation, assessment of disease severity, and monitoring of progression of chorioretinal dystrophies usually involve some combination of fundus autofluorescence (FAF), optical coherence tomography (OCT), perimetric testing, ERG, and genetic testing. Several photoreceptor dystrophies have typical phenotypes, such as the deep retinal white dots or flecks in retinitis punctata albescens (see Fig 12-4), choriocapillaris atrophy in choroideremia (*CHM*), or the crystalline deposits associated with Bietti crystalline dystrophy (*CYP4V2*). Distinctive phenotypes are the exception, however.

Generally, panretinal dystrophies or degenerations of the RPE and retina are divided into 2 groups: nonsyndromic retinopathies and syndromic retinopathies. The term *nonsyndromic*

panretinal dystrophies refers to hereditary disorders that diffusely involve photoreceptor and pigment epithelial function; these conditions are characterized by progressive visual field loss, central vision loss, and subnormal ERG responses. The disease process is confined to the eyes and is not associated with systemic manifestations. In *syndromic (secondary) panretinal dystrophies*, the retinal degeneration is associated with 1 or more organ systems, such as hearing loss (in Usher syndrome) or neurodegeneration and nephronophthisis (in Joubert syndrome; for discussion of retinal degenerations associated with systemic disease, see Chapter 13). Occasionally, when the etiology is unknown and no associated disease is present, the term *pigmentary retinopathy* is used to describe the disorder. The focus of this chapter is on the nonsyndromic retinopathies.

General Genetic Considerations

All inheritance patterns are represented among the currently known inherited retinal dystrophies. Thus, obtaining an accurate and complete family history is essential in determining the dystrophy's inheritance pattern (ie, autosomal dominant, autosomal recessive, X-linked recessive, X-linked dominant, or mitochondrial). However, patients with retinal dystrophies may have a negative family history for a variety of reasons, including lack of information, variable expressivity or incomplete penetrance within the family, or *de novo* mutations. It is helpful to examine relatives for any signs of asymptomatic retinal degeneration.

Molecular genetic testing helps to confirm a suspected diagnosis of retinal degeneration, to identify the causative gene(s) of a generalized phenotype, to uncover a *de novo* mutation, and to identify asymptomatic relatives and carriers. This type of testing is also useful for identifying syndromic versus nonsyndromic causes of retinal dystrophies, but it does not predict the penetrance, expressivity, or rate of progression of these conditions. Testing asymptomatic individuals to determine a potential future risk of vision loss is generally not warranted (unless a treatment is available), given the wide variability of expressivity.

Stone EM, Aldave AJ, Drack AV, et al. Recommendations of the American Academy of Ophthalmology Task Force on Genetic Testing. February 2014. Accessed January 5, 2022. www.aao.org/clinical-statement/recommendations-genetic-testing-of-inherited-eye-d

General Management Considerations

Management of patients with retinal degeneration should include ophthalmic evaluations every 1–2 years. Follow-up visits are appropriate to address refractive management and to monitor for the development of treatable ocular conditions: cystoid macular edema (CME), cataract, glaucoma, and retinal exudation. CME develops in 10%–20% of patients with retinal degenerations.

Patients with retinal dystrophies may understandably fear that they will become blind in the near future. The clinician should help these patients understand that total blindness is an infrequent endpoint but that the disease's impact on visual function (eg, reduced visual acuity, reduced visual field) may affect their activities and quality of life. Patients and their family members may benefit from psychological and genetic counseling. Patients with subnormal visual acuity may benefit from low vision aids, while those with advanced disease may need vocational rehabilitation and mobility training. The American Academy

of Ophthalmology's Initiative in Vision Rehabilitation, available on the ONE Network, provides information and a variety of resources, including a patient handout (www.aao.org/low-vision-and-vision-rehab).

Diffuse Dystrophies: Photoreceptor Dystrophies

Rod–cone dystrophies

Patients with rod–cone dystrophies, usually referred to as *retinitis pigmentosa* (RP), often present with history of nyctalopia and peripheral visual field loss. These findings correlate with the location and primary function of rod photoreceptors. The history may not be clear; patients may assume that their visual function is normal, because it is “normal” for them not to be able to see in the dark. Validated methods and instruments (such as dark-adapted ERG and visual field testing or low-luminance questionnaires) are also available for quantification of visual dysfunction.

Typical fundus findings in rod–cone dystrophy include arteriolar narrowing, with or without optic nerve head pallor, and variable amounts of bone spicule–like pigmentary changes (Fig 12-6). These pigmentary changes result from intraretinal pigment deposition by macrophages that migrate into the retina to process degenerating retinal cells. This form of pigment deposition within the retina occurs in regions of outer retinal atrophy (eg, following retinal detachment or inflammatory retinopathies) and is not specific to hereditary retinopathies. The peripheral retina and RPE may be atrophic even if intraretinal pigment is absent (*RP sine pigmento*), and the macula typically shows a loss of the foveal reflex and irregularity of the vitreoretinal interface. Autofluorescence imaging can often identify additional areas of retinal involvement that are not evident on clinical examination.

Vitreous cells, CME, epiretinal membranes, optic disc drusen, and posterior subcapsular cataracts are commonly observed in eyes with panretinal dystrophies. CME, which is detected by OCT in about one-quarter of cases, may be treatable with oral carbonic anhydrase inhibitors (Fig 12-7). In approximately 2%–5% of patients with panretinal dystrophies, areas of vascular hyperpermeability and areas of exudative retinopathy (the so-called *Coats reaction*; Fig 12-8) will develop. Eyes with rod–cone degenerations typically develop partial- to full-ring scotomata in midequatorial regions; these often expand into the periphery, leaving only a small central island of visual field (Fig 12-9). The coexistence of cataract, vitreous cells, and macular edema can sometimes lead to the mistaken diagnosis of uveitis.

The ERG response in eyes with rod–cone dystrophies typically shows a marked reduction in rod-derived responses, more than in cone-derived responses. Both a- and b-waves are reduced because the photoreceptors are primarily involved. The b-waves are characteristically prolonged in duration and diminished in amplitude. Individuals with the carrier state of X-linked recessive RP often show a mild reduction or delay in b-wave responses. Eyes with postinflammatory retinopathies (eg, retinopathies resulting from rubella) often have better preservation of the ERG than eyes with similar-appearing pigmentary changes from a hereditary retinopathy. Although the rod and cone amplitudes are reduced in postinflammatory retinopathies, the implicit times are usually within normal ranges because the remaining photoreceptors are essentially normal. In contrast, in patients with a hereditary retinopathy, the remaining photoreceptors are impaired by the

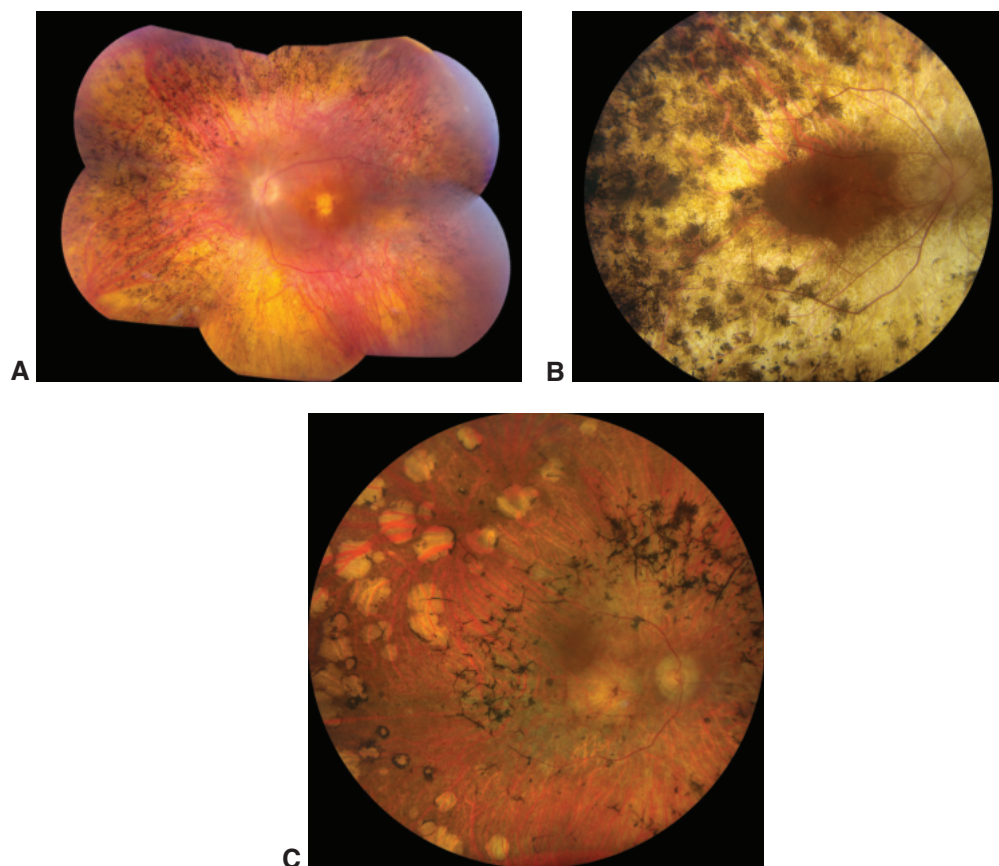


Figure 12-6 Examples of fundus findings characteristic of rod-cone dystrophy. **A**, Fundus of a 54-year-old woman with *USH2A* mutation shows optic nerve head pallor, arteriolar attenuation, macular atrophy, and widespread peripheral pigmentary alteration. Corrected distance visual acuity (CDVA) was hand motions. **B**, Fundus of a 66-year-old man with *USH2A* mutation shows extensive peripheral retinal pigment epithelium (RPE) atrophy but relative preservation of the optic nerve, macula, and arterioles. CDVA was 20/30. Note the wide differences in phenotypes between panels A and B, despite involvement of the same gene. **C**, Fundus of a 45-year-old woman with mutations in the *PCARE* and *CRB1* genes shows arteriolar attenuation, prominent RPE hyperplasia (so-called *bone spicules*) posterior to the equator, and lacunar RPE atrophy in the periphery. A tiny island of healthy retina remains in the fovea. CDVA was 20/100. (Courtesy of Franco M. Recchia, MD.)

genetic condition, and the ERG response shows prolonged implicit times. In conventional testing of many rod-cone dystrophies, the ERG responses may initially present as undetectable or become undetectable over time. Unless the patient has a treatable condition, such as vitamin A deficiency or an autoimmune retinopathy, repetitive ERG testing has minimal benefit for monitoring disease progression.

Sector RP refers to disease that involves only 1 or 2 sectors of the fundus (Fig 12-10). This condition is generally symmetric between eyes, which helps rule out acquired damage (eg, from trauma, vascular insult, or inflammation). Unilateral RP is extremely rare. Typical causes of unexplained unilateral pigmentary retinopathy are infection (rubella,

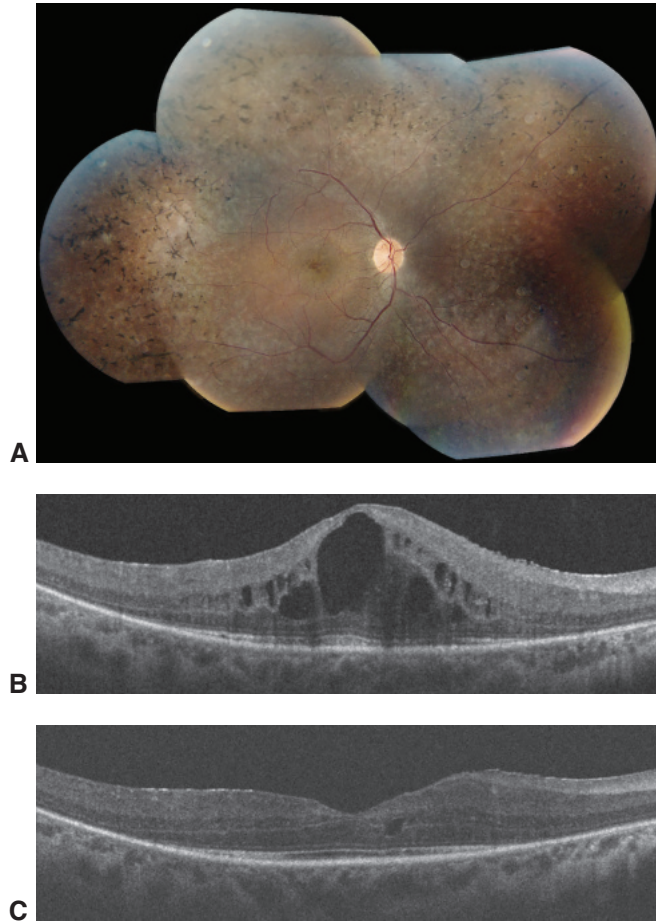


Figure 12-7 Rod-cone dystrophy (associated with a pathogenic *RDH12* variant) complicated by cystoid macular edema (CME). Montage fundus photograph (**A**) and spectral-domain optical coherence tomography (SD-OCT) (**B**) at presentation show cysts in the foveal area. CDVA was 20/50. **C**, SD-OCT 3 months after treatment was initiated with oral acetazolamide, 500 mg daily, shows a substantial reduction in macular edema. CDVA was 20/40. (Courtesy of Franco M. Recchia, MD.)

syphilis), inflammation, remote trauma, and retained intraocular metallic foreign body. Most cases of pigmented paravenous retinopathy are postinflammatory, have interocular asymmetry, and are usually nonprogressive.

When a suspected panretinal dystrophy is being evaluated in a patient with a negative family history (*sporadic retinal dystrophy*), it is important to consider acquired causes of retinal degeneration that can mimic hereditary conditions, including previous bilateral ophthalmic artery occlusions, diffuse uveitis, infections (eg, syphilis), paraneoplastic syndromes, and retinal drug toxicity. Syndromic forms of pigmentary retinopathy associated with metabolic or other organ system disease must also be considered (see Chapter 13).

Gregory-Evans K, Pennesi ME, Weleber RG. Retinitis pigmentosa and allied disorders. In: Schachat AP, Wilkinson CP, Hinton DR, Sadda SR, Wiedemann P, eds. *Ryan's Retina*. Vol 2. 6th ed. Elsevier/Saunders; 2018:861–935.

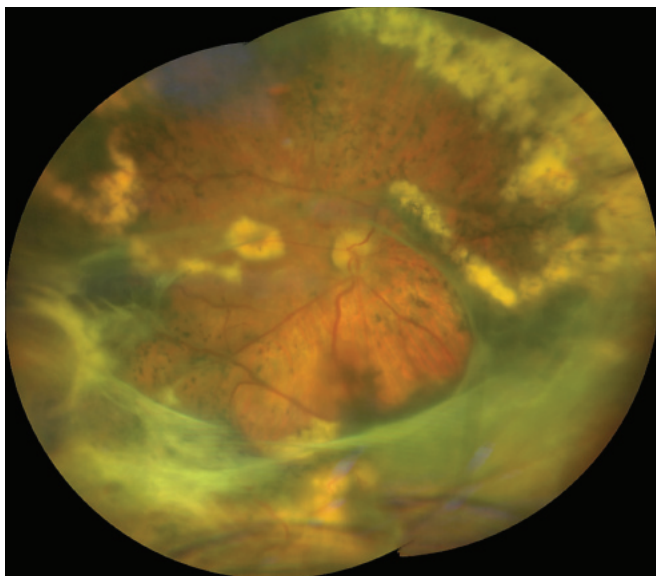


Figure 12-8 Exudative retinopathy and subsequent traction-exudative retinal detachment complicating a case of *USH2A*-associated rod-cone dystrophy. Background arteriolar attenuation and peripheral pigmentary changes are also present. (Courtesy of Franco M. Recchia, MD.)

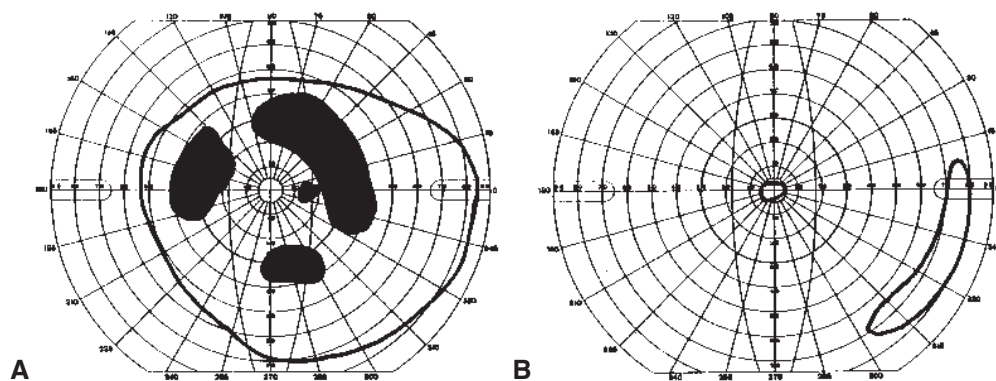


Figure 12-9 Examples of visual fields in retinitis pigmentosa (RP), which were obtained with a Goldmann III-4 test object. **A**, Early disease: midperipheral scotomata. **B**, Late disease: severe loss, sparing only a central tunnel and a far-peripheral island, which may eventually disappear. (Courtesy of Michael F. Marmor, MD.)

Management One large study reported that high daily doses of vitamin A palmitate (15,000 IU/day) slowed the decline in ERG response in eyes with RP. A slight benefit from supplementation with omega-3 and omega-6 fatty acids has also been reported. The modest benefit of high-dose vitamin A supplementation must be weighed against the risks of long-term liver toxicity, vitamin A-related intracranial hypertension, and teratogenicity.

Excessive light exposure may play a role in retinal degenerations caused by rhodopsin mutations and/or genes that contribute to lipofuscin accumulation, such as *ABCA4*. Recommendations for patients to wear UV-absorbing sunglasses and brimmed hats for

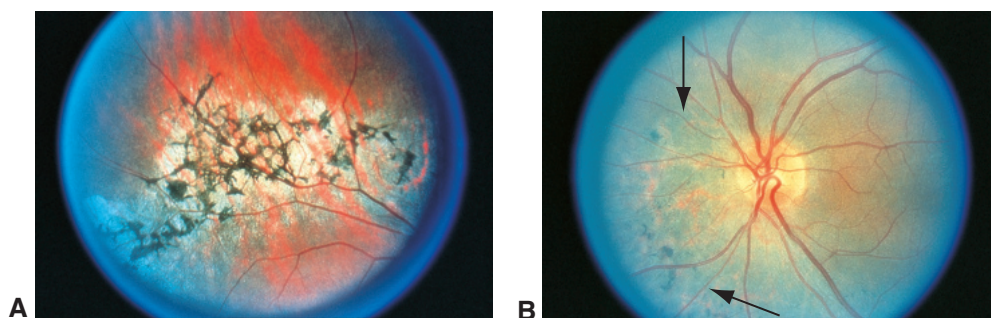


Figure 12-10 Fundus photographs of delimited forms of inherited retinal dystrophies. Note the sharp demarcation between the areas of degeneration and other regions of the fundus that appear healthy. It is important to assess interocular symmetry and the pattern of cell damage to consider acquired forms of retinopathy (such as pigmented paravenous retinopathy). **A**, Fundus with degenerative changes near the arcades. **B**, Fundus with sector RP (*between arrows*), showing vascular narrowing and spicules only in the inferonasal quadrant. (Courtesy of Michael F. Marmor, MD.)

protection from high levels of light exposure seem prudent, despite the absence of direct evidence of benefit.

Efforts to restore at least some vision in patients rendered completely blind from RP have included the use of electronic chips that interface with the remaining retinal tissue or directly with the visual cortex. At least 5 variations of a “retinal prosthesis” have been, or continue to be, investigated. Other therapeutic investigative efforts involve gene therapy and stem cell transplantation.

Makiyama Y, Oishi A, Otani A, et al. Prevalence and spatial distribution of cystoid spaces in retinitis pigmentosa: investigation with spectral domain optical coherence tomography. *Retina*. 2014;34(5):981–988.

Salvatore S, Fishman GA, Genead MA. Treatment of cystic macular lesions in hereditary retinal dystrophies. *Surv Ophthalmol*. 2013;58(6):560–584.

Cone and cone-rod dystrophies

The cone dystrophies comprise a heterogeneous group of hereditary diseases with more than 25 identified causative genes. Patients with *cone dystrophy* typically present with progressive loss of central vision and color discrimination (reflecting the primary location and function of cone photoreceptors). They may also experience hemeralopia (day blindness) and photophobia (discomfort and/or pain in the presence of normal levels of light). Onset of symptoms typically occurs in the teenage years or later adulthood. Ophthalmoscopy may be normal early in the course of the disease. In other patients, ophthalmoscopy may reveal the typical symmetric bull’s-eye pattern of macular atrophy (Fig 12-11) or more severe atrophy, such as demarcated circular macular lesions. Mild to severe temporal optic atrophy and tapetal retinal reflexes (with a glistening greenish or golden sheen) may also be present. Unlike macular dystrophies, the cone dystrophies are more associated with color discrimination symptoms and photophobia; and as such, they must be differentiated from color vision defects.

Cone dystrophies are diagnosed when ERG results indicate a subnormal or undetectable photopic ERG response and a normal or near-normal rod-isolated ERG response. When present, the LA 3.0 30-Hz ERG response is almost invariably delayed, in keeping with generalized

Figure 12-11 Fundus photograph of cone dystrophy shows the bull's-eye pattern of central atrophy.



cone system dysfunction. Peripheral visual fields may remain normal. The cone dystrophies are progressive. In some patients, secondary rod photoreceptor involvement develops in later life, suggesting overlap between progressive cone dystrophies and cone-rod dystrophies.

Similar to patients with cone dystrophies, patients with *cone-rod dystrophies* typically present with reduced central vision and symptoms of dyschromatopsia and photophobia. On visual field testing, some patients show a tight ring or central scotoma within the central 20° or 30° of the visual field. Ophthalmoscopy may initially be normal; later, it may demonstrate intraretinal pigment in areas of retinal atrophy in the fundus periphery, and patients may report progressive nyctalopia. The diagnostic ERG hallmark of a cone-rod dystrophy is that the cone-derived full-field ERG responses are more subnormal than the rod ERG responses (see Chapter 3, Fig 3-2).

Leber congenital amaurosis

The dystrophies that are typified by early onset and rapid progression of severe bilateral vision loss are collectively termed *Leber congenital amaurosis* (LCA; see also BCSC Section 6, *Pediatric Ophthalmology and Strabismus*, Chapter 24). LCA is characterized by severely reduced vision from birth, usually associated with wandering nystagmus. Infants exhibit limited to no visual response, and visual acuities tend to range between 20/200 and no light perception. Some infants with LCA rub or poke their eyes (the *oculodigital reflex*) in order to create visual stimulation, as do other infants with poor vision.

In the early stages, obvious fundus changes are rare, and molecular genetic testing offers the best method of distinguishing stationary and progressive hereditary retinopathies. In addition, because there are both syndromic and nonsyndromic forms of LCA, a molecular genetic diagnosis can help identify potential systemic features that warrant medical management. Some forms of LCA involve developmental defects, while others appear to represent degenerations of normally formed retina. Postinfectious etiologies should be considered based on history and clinical findings. Central macular atrophic lesions (sometimes incorrectly referred to as *macular colobomas*) are often seen in eyes with LCA, in addition to early-onset cataracts and keratoconus in older children. Most children

with nonsyndromic LCA have normal intelligence, and some of the observed psychomotor impairment may be secondary to sensory deprivation.

The ERG response is typically minimal or undetectable, but ERG testing cannot differentiate stationary (CSNB or achromatopsia) from progressive (rod–cone dystrophy or cone–rod dystrophy) conditions. LCA typically progresses the most rapidly of these conditions.

Autosomal dominant and autosomal recessive inheritance of LCA have been linked to at least 3 genes and 23 genes, respectively. There is some overlap in the genes responsible for LCA and those that cause later-onset retinal dystrophies (both rod–cone and cone–rod). In 2017, the US Food and Drug Administration issued the first approval for a gene therapy, voretigene neparvovec-rzyl (Luxturna, Spark Therapeutics), for *RPE65*-linked LCA in individuals aged 1 year or older. See Chapter 20 for further discussion of gene therapy.

Russell S, Bennett J, Wellman JA, et al. Efficacy and safety of voretigene neparvovec (AAV2-hRPE65v2) in patients with RPE65-mediated inherited retinal dystrophy: a randomised, controlled, open-label, phase 3 trial. *Lancet*. 2017;390(10097):849–860. Published correction appears in *Lancet*. 2017;390(10097):848.

Enhanced S-cone syndrome

The most prominent features of the severe form of enhanced S-cone syndrome (ESCS), also known as *Goldmann-Favre syndrome*, include nyctalopia, increased sensitivity to blue light, pigmentary retinal degeneration, an optically empty vitreous, hyperopia, pathognomonic ERG abnormalities, and varying degrees of peripheral to midperipheral visual field loss (Fig 12-12). The posterior pole may show round, yellow, sheenlike lesions along the arcades, accompanied by areas of diffuse degeneration. Deep nummular pigmentary deposition is usually observed at the level of the RPE around the vascular arcades. Macular (and sometimes peripheral) schisis may be present, overlapping the phenotype of X-linked retinoschisis. The ERG response includes no detectable DA 0.01 signal; delayed and simplified responses to a brighter flash that have the same waveform under both DA and LA conditions; and a LA 3.0 30-Hz response of lower amplitude than that of the LA 3.0 (photopic single-flash) a-wave.

Eyes with ESCS have an overabundance of blue cones, a reduced number of red and green cones, and few, if any, functional rods. This condition is unique in that it is both a developmental and degenerative photoreceptor retinopathy. ESCS is autosomal recessive and results from homozygous or compound heterozygous mutations in *NR2E3*. The visual prognosis is highly variable.

Diffuse Dystrophies: Choroidal Dystrophies

Widespread primary retinal or RPE disease that causes advanced atrophy of the choriocapillaris occurs in choroideremia, gyrate atrophy, Bietti crystalline dystrophy, and phenothiazine-related retinal toxicity (see also Chapter 14). In FAF imaging, hypoautofluorescence in the areas of atrophy is typically observed in all of these conditions and is therefore helpful for monitoring the disease progression.

Choroideremia

Patients with choroideremia have nyctalopia and show progressive peripheral visual field loss over 3–5 decades. Most patients maintain good visual acuity until a central island of

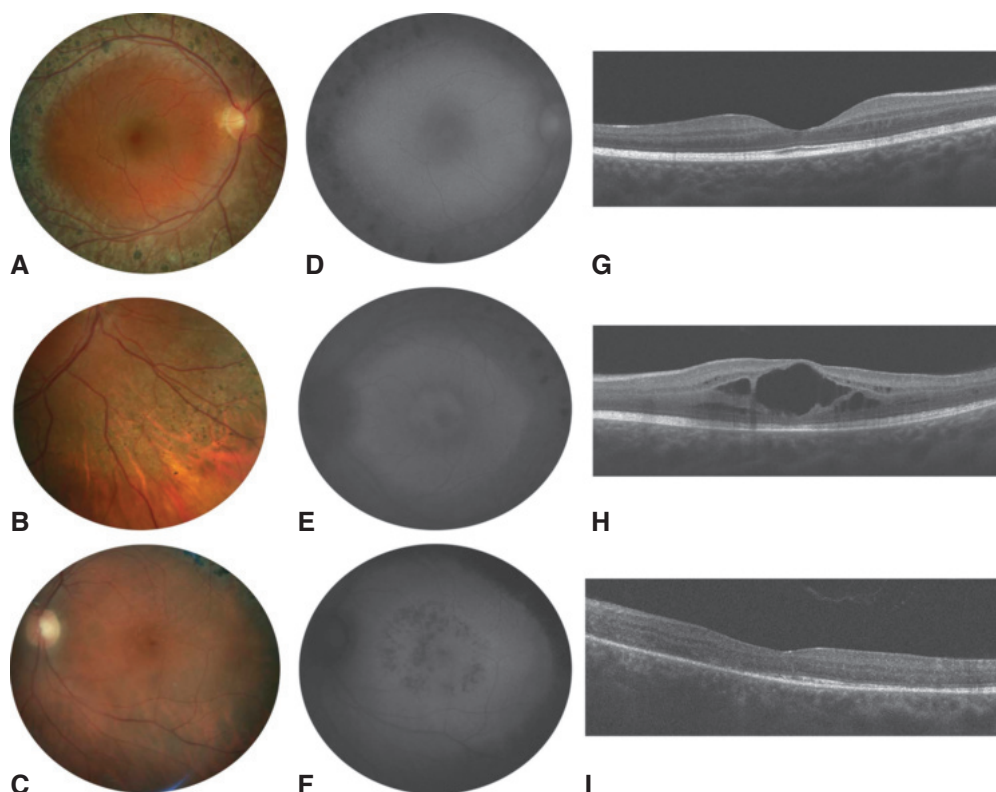


Figure 12-12 Clinical characteristics of enhanced S-cone syndrome. In the early stages, the fundus may be normal. In older subjects, the fundus usually shows 360° nummular pigmentary changes outside the vascular arcades at the level of the RPE (**A–C**). The macula may show changes resulting from schisis or nonspecific pigment epithelial changes (**C**). The autofluorescence is variable (**D–F**). There may be hyperautofluorescence within the arcades that either spares or involves the foveal region. SD-OCT imaging of the macula may be normal (**G**) or show schitic and/or cystoid changes (**H**) or outer retinal abnormalities (**I**). (Reproduced with permission from Vincent A, Robson AG, Holder GE. Pathognomonic (diagnostic) ERGs. A review and update. *Retina*. 2013;33(1):5–12. doi:10.1097/IAE.0b013e31827e2306)

foveal vision is lost. The degeneration initially manifests as mottled areas of pigmentation in the anterior equatorial region and macula. The anterior areas gradually degenerate toward the posterior pole to form confluent scalloped areas of RPE and choriocapillaris loss; larger choroidal vessels are preserved (Fig 12-13). The retinal vessels appear normal, and there is no optic atrophy.

On fluorescein angiography, the changes are pronounced: the scalloped areas of missing choriocapillaris appear hypofluorescent next to brightly hyperfluorescent areas of perfused choriocapillaris with intact overlying RPE. FAF imaging shows a characteristic speckled pattern of autofluorescence in the nonatrophic areas. The ERG response is sub-normal early in the course of the disease and is generally extinguished by midlife. Because phenotypes can overlap with other conditions, especially other choroidal dystrophies, the clinical and imaging features should not be considered pathognomonic.



Figure 12-13 Montage fundus photograph of a 22-year-old patient with choroideremia. (Courtesy of Cagri G. Besirli, MD.)

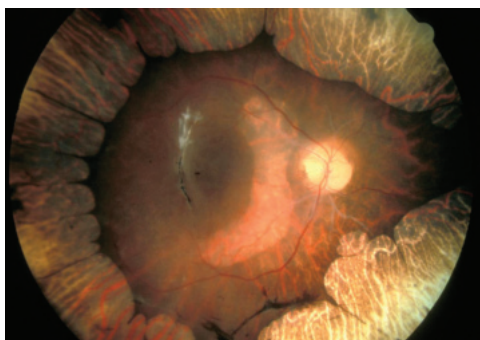
Choroideremia is X-linked and caused by mutations in *CHM*, which is constitutively expressed and encodes geranylgeranyl transferase Rab escort protein (REP1). REP1 plays an essential role in the intracellular trafficking of proteins, substrates, and organelles by mediating proper lipid modification (prenylation) of specific G proteins called *Rab proteins*. Carriers of choroideremia are usually asymptomatic and have normal ERGs. However, they often show patches of subretinal black mottled pigment, and occasionally, older female carriers show a lobular pattern of choriocapillaris and RPE loss. Gene therapy trials for choroideremia are ongoing.

Edwards TL, Jolly JK, Groppe M, et al. Visual acuity after retinal gene therapy for choroideremia. *N Engl J Med*. 2016;374(20):1996–1998.

Gyrate atrophy

Patients affected by gyrate atrophy usually develop nyctalopia during the first decade of life and experience progressive loss of visual field and visual acuity later in the course of the disease. Macular edema is commonly present. In the early stages of the disease, patients have large, geographic, peripheral paving-stone–like areas of atrophy of the RPE and choriocapillaris, which gradually coalesce to form a characteristic scalloped border at the junction of normal and abnormal RPE (Fig 12-14). Gyrate atrophy is an autosomal recessive dystrophy caused by mutations in *OAT*, the gene for ornithine aminotransferase. The diagnosis is supported by elevated plasma levels of ornithine, as well as by genetic testing for mutations of *OAT*. If started at a young age, aggressive dietary restriction of

Figure 12-14 Gyrate atrophy. Wide-angle fundus photograph shows scalloped edges of the remaining posterior retina, as is typically seen in gyrate atrophy. A crescent of nasal macular atrophy is also present. (Courtesy of Colin A. McCannel, MD.)



arginine intake and, in some cases, vitamin B₆ supplementation can slow or halt progression of the retinal degeneration.

Bietti crystalline dystrophy

Individuals with Bietti crystalline dystrophy develop symptoms of nyctalopia, decreased vision, and paracentral scotomata in the second to fourth decades of life. On examination, intraretinal yellow-white crystals are visible in the posterior retina and in the peripheral cornea near the limbus. As the disease progresses, widespread retinochoroidal atrophy develops and peripheral vision worsens. The condition is a very rare autosomal recessive disorder caused by mutations in the gene *CYP4V2*. There is no known treatment.

Macular Dystrophies

Stargardt disease

With an incidence of roughly 1 in 10,000, Stargardt disease is the most common juvenile macular dystrophy and a common cause of central vision loss in adults younger than 50 years. The visual acuity in Stargardt disease typically ranges from 20/50 to 20/200.

The classic Stargardt phenotype is characterized by a juvenile-onset foveal atrophy surrounded by discrete, yellowish, round or pisciform (fish-shaped) flecks at the level of the RPE (Fig 12-15). These flecks represent excessive accumulation of lipofuscin, a waste product of RPE metabolism, within the RPE cells. On fluorescein angiography, 80% or more of patients with Stargardt disease have a “dark choroid,” in which blocking of choroidal fluorescence by swollen, lipofuscin-laden RPE cells accentuates the retinal circulation (see Fig 12-15B). FAF imaging is a more reliable means of demonstrating elevated background autofluorescence and characteristic findings, including peripapillary sparing of RPE changes, central macular hypoautofluorescence, and over time, an outward expanding pattern of hyperautofluorescent flecks that leave hypoautofluorescent areas in their wake. Full-field ERGs are not diagnostic for this condition.

The age at onset and presentation of the clinical features in Stargardt disease vary, sometimes even among individuals in the same family. The condition is usually slowly progressive with the accumulation of lipofuscin in the RPE (Fig 12-16). In later stages, atrophic maculopathy, with or without lipofuscin flecks and panretinal degeneration, can be observed.

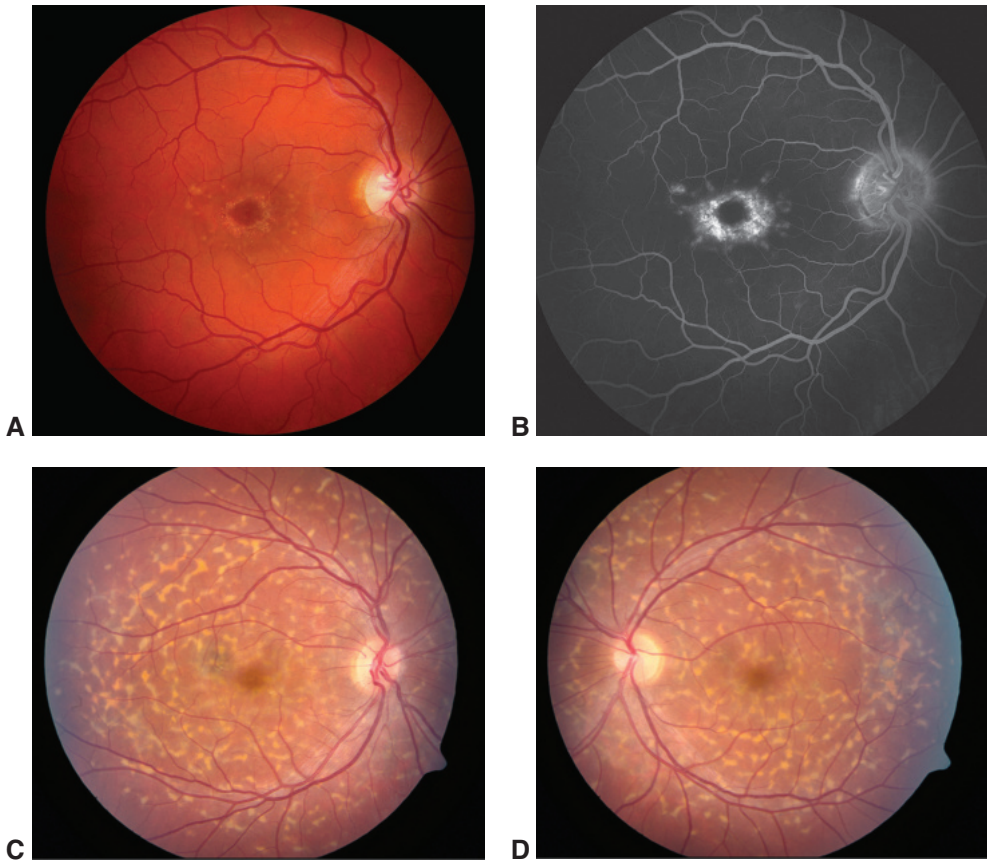


Figure 12-15 Examples of Stargardt disease. **A**, Fundus photograph shows paramacular yellowish flecks and “beaten-bronze” central macular atrophy. **B**, Fluorescein angiography image of the same eye shows a dark choroid, hyperfluorescence associated with the flecks, and bull’s-eye pattern of macular transmission defect. **C**, **D**, Fundus photographs of the right and left eye, respectively, show classic multiple, discrete, yellowish, pisciform (fish-shaped) flecks scattered throughout the posterior pole. (Parts A and B courtesy of Mark W. Johnson, MD; parts C and D courtesy of Paul Sternberg Jr, MD.)

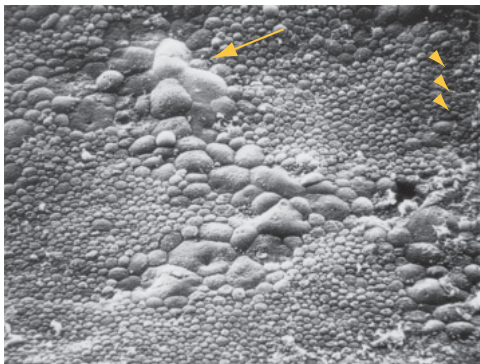


Figure 12-16 Scanning electron micrograph of the RPE in Stargardt disease. The regions of RPE cells engorged with abnormal lipofuscin-like material (arrow) are seen clinically as yellowish flecks. Note that the cells comprising the normal RPE monolayer are substantially smaller (arrowheads). (Reproduced from Eagle RC Jr, Lucier AC, Bernardino VB Jr, Yanoff M. Retinal pigment epithelial abnormalities in fundus flavimaculatus: a light and electron microscopic study. *Ophthalmology*. 1980;87(12):1189–1200. Copyright 1980, modified with permission from Elsevier.)

Most cases of Stargardt disease are autosomal recessive and are caused by mutations in *ABCA4*. However, autosomal dominant transmission patterns can result from mutations in other genes, most notably *ELOVL4*, *PROM1*, and *PRPH2* (*RDS/peripherin*). The *ABCA4* gene encodes an adenosine triphosphate (ATP)-binding cassette transporter protein expressed by rod outer segments and RPE. Dysfunction of this transporter protein impairs the proper disposal of lipofuscin, which is toxic to RPE cells. In animal models of *ABCA4*-related disease, vitamin A supplementation accelerates the accumulation of lipofuscin pigments in the RPE and, in conjunction with blue light, also accelerates retinal cell death. Drug therapies to reduce lipofuscin accumulation, gene therapies, and stem cell treatments are currently undergoing clinical trials.

A clinical variant termed *fundus flavimaculatus* results from mutations in the same genes that cause Stargardt disease and can be present in families with the classic Stargardt phenotype. In patients with the variant, the flecks are widely scattered throughout the fundus but spare the macula.

Best disease, or Best vitelliform dystrophy

Individuals affected by Best disease frequently develop a yellow, egg yolk-like (*vitelliform*) macular lesion in childhood. The solid-appearing vitelliform lesion eventually breaks down, leaving a mottled geographic atrophy appearance (Fig 12-17). The breakdown of the solid lesion can proceed over years or even decades. Late in the course of the disease, the geographic atrophy may be difficult to distinguish from other types of macular degeneration or dystrophy. Some patients (up to 30% in some series) have extrafoveal vitelliform lesions in the fundus. The macular appearance in all stages is deceptive, as most patients maintain relatively good visual acuity throughout the course of the disease. Even patients with “scrambled-egg” macular lesions typically have visual acuities from 20/30 to 20/60. In approximately 20% of patients, a choroidal neovascular membrane develops in at least 1 eye.

The ERG response is characteristically normal, but the electro-oculogram (EOG) result is almost always abnormal, even in apparently unaffected, asymptomatic individuals who have the causative genetic variant but have normal-appearing fundi (ie, carriers). The light peak to dark trough ratio (Arden ratio) of the EOG (see Chapter 3) is typically 1.5 or less. Before ordering an EOG to rule out Best disease, the clinician should ensure that the full-field ERG is normal.

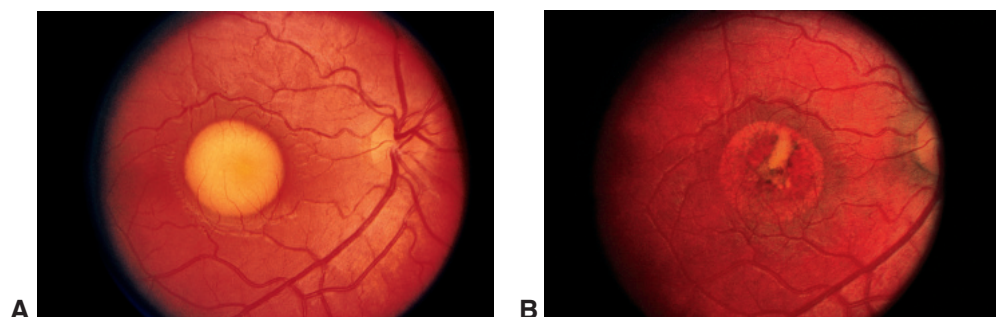


Figure 12-17 Fundus photographs of Best vitelliform dystrophy. **A**, Characteristic “yolk” stage, during which visual acuity is typically good. **B**, Atrophy and scarring after the yolk breaks down. (Courtesy of Mark W. Johnson, MD.)

Best disease is an autosomal dominant maculopathy caused by mutations in the *BEST1* gene (also known as *VMD2*). The encoded protein bestrophin localizes to the basolateral plasma membrane of the RPE and functions as a transmembrane ion channel. Although some *BEST1* variants cause autosomal dominant disease, other mutations, when present as homozygous or compound heterozygous variants, can give rise to *autosomal recessive bestrophinopathy* (ARB). Unlike Best disease, ARB is associated with progressive retinal dysfunction on the full-field ERG, loss of visual acuity, diffuse irregularity of the RPE, and dispersed punctate flecks that are distinct from extramacular vitelliform lesions.

Agarwal A. *Gass' Atlas of Macular Diseases*. 5th ed. Saunders; 2011:278–280.

Boon CJ, Klevering BJ, Leroy BP, Hoyng CB, Keunen JE, den Hollander AI. The spectrum of ocular phenotypes caused by mutations in the *BEST1* gene. *Prog Retin Eye Res*. 2009; 28(3):187–205.

Conditions and disorders with adult-onset vitelliform lesions

Several conditions and disorders feature adult-onset macular vitelliform lesions. The most common of these disorders, *adult-onset foveomacular vitelliform dystrophy*, is one of the pattern dystrophies (discussed later in this chapter). It is characterized by yellow subfoveal lesions that are bilateral, round or oval, and typically one-third disc diameter in size; they often contain a central pigmented spot (Fig 12-18). Occasionally, when the lesions are larger, the patient may be misdiagnosed as having Best disease or even age-related macular degeneration. This dystrophy generally appears in the fourth to sixth decades of life in patients who either are visually asymptomatic or have mild blurring and metamorphopsia. Eventually, the lesions may fade, leaving an area of RPE atrophy, but most patients retain reading vision in at least 1 eye throughout their lives. Autosomal dominant inheritance has been recognized in some affected families. The most common causative gene is *PRPH2*, and there is evidence of genetic heterogeneity for this phenotype.

Patients with numerous basal laminar (cuticular) drusen may develop an unusual *vitelliform exudative macular detachment* (Fig 12-19), which can be mistaken for choroidal neovascularization (CNV) because of the subretinal hyporefectivity on OCT. The diagnosis of CNV can be confirmed by the presence of leakage (enlarging and increasing hyperfluorescence over time) on fluorescein angiography or OCT angiography. In the absence of CNV, the angiographic findings are early blockage by the subretinal material and late staining without lesion enlargement.

Some patients with large soft drusen have a large, central coalescence of drusen, or *drusenoid RPE detachment*, which may occasionally mimic a macular vitelliform lesion (Fig 12-20). Such lesions often have pigment mottling on their surface and are surrounded by numerous other individual or confluent soft drusen. They may remain stable (and allow good vision) for many years, but eventually they tend to flatten and evolve into geographic atrophy.

Early-onset “drusenoid” macular dystrophies

Drusen are commonly seen in the aging fundus but are also a component of age-related macular degeneration (AMD), which is exceedingly rare before the age of 50. The term *early-onset drusen*, therefore, refers to the spectrum of deep and subretinal yellow-white lesions that occur in younger patients. Macular dystrophies associated with early-onset drusen are entities that are typically distinct from AMD in their presentation and clinical course. However,

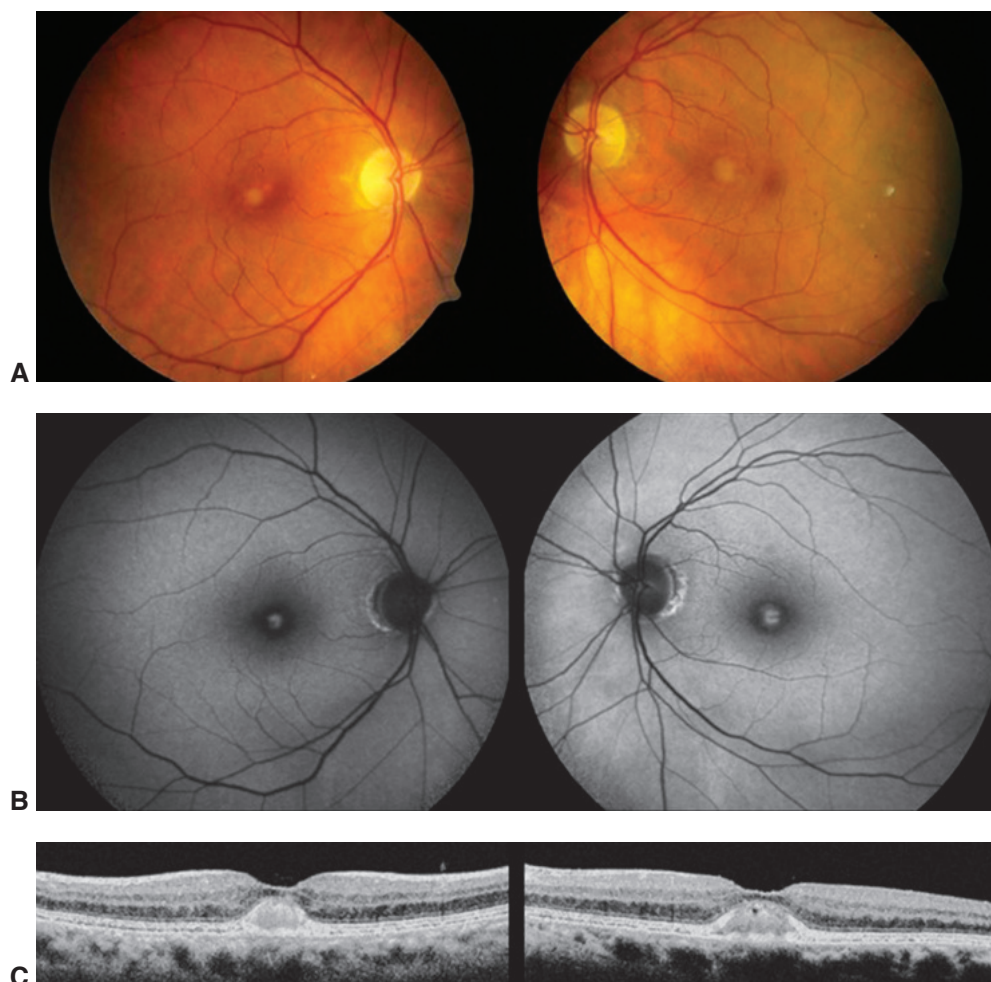


Figure 12-18 Adult-onset foveomacular vitelliform dystrophy. (*Left panels* in each part show the right eye, and *right panels* show the left eye of the same patient.) **A**, Fundus photographs demonstrate small, round, yellow subfoveal lesions. **B**, The lesions are hyperautofluorescent on autofluorescence imaging. **C**, SD-OCT images show the reflective, dome-shaped subfoveal material elevating the overlying neurosensory retina. (Courtesy of Stephen J. Kim, MD.)

the causative genes in several juvenile and early-onset macular dystrophies are the same as the genes that have been implicated in the complex genetic disorder of AMD. Although they are frequently referred to as *familial* or *autosomal dominant drusen*, the clinician needs to establish whether other family members are affected before assuming an inheritance pattern.

Drusen are numerous and of various sizes, typically extending beyond the vascular arcades and nasal to the optic nerve head (Fig 12-21). Early-onset drusen have been classified into 3 entities: large colloid drusen, Malattia Leventinese drusen, and cuticular drusen (Fig 12-22). On fundus examination, large colloid drusen appear as bilateral large, yellowish lesions located in the macula and/or the periphery of the retina. The vitelliform lesions are hyperautofluorescent on FAF and are thought to be made up of lipofuscin, while the associated

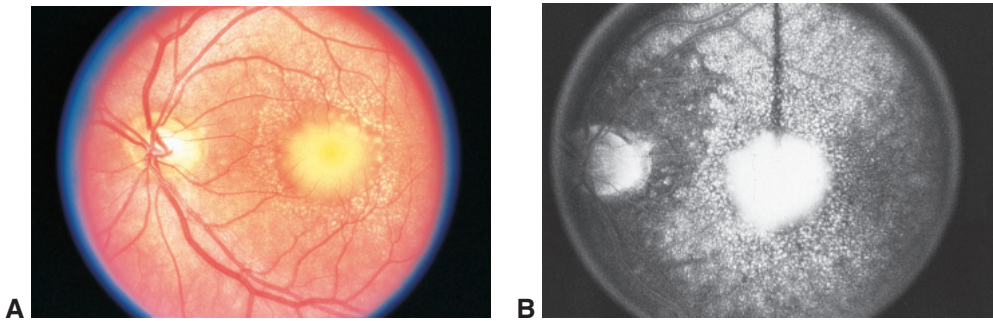


Figure 12-19 Vitelliform exudative macular detachment. **A**, Fundus photograph of a vitelliform lesion associated with numerous cuticular (basal laminar) drusen. **B**, Corresponding late-phase fluorescein angiography image shows staining of the drusen and vitelliform lesion. (Courtesy of Michael F. Marmor, MD.)



Figure 12-20 Fundus photograph shows central coalescence of large drusen simulating a macular vitelliform lesion. (Courtesy of Mark W. Johnson, MD.)

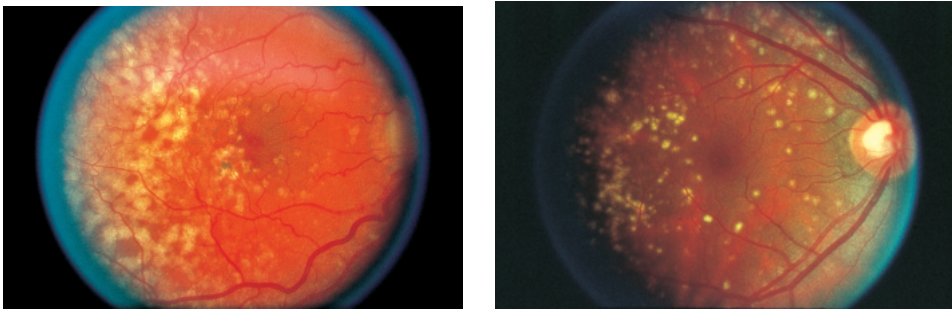


Figure 12-21 Fundus photographs of different manifestations of early-onset drusen. Variable size and distribution of the drusen are evident. (Courtesy of Michael F. Marmor, MD.)

surrounding cuticular drusen and/or subretinal drusenoid deposits are generally not autofluorescent. The drusen of *Malattia Leventinese* (also called *Doyne honeycomb dystrophy*) often show a distinctive pattern of radial extensions of small and intermediate-sized deposits emanating from the fovea. The condition is caused by a shared single autosomal dominant mutation in the gene *EFEMP1*, which to date has not been associated with AMD risk. Patients generally retain good central visual acuity through their sixth decade, after which visual acuity generally deteriorates to 20/200 or worse because of progressive RPE atrophy.



Figure 12-22 Basal laminar (cuticular) drusen. Fundus photographs of the right (**A**) and left (**B**) eyes of a 38-year-old man with numerous round, yellow drusen scattered in the macula. Basal laminar (cuticular) drusen are present between the plasma membrane of the RPE and its basement membrane and are more easily seen on angiography and in young patients with brunette fundi. (Courtesy of Stephen J. Kim, MD.)

Sorsby macular dystrophy (SMD) is a rare cause of bilateral central vision loss by the fifth decade of life. Early signs of SMD are yellowish-gray drusenlike deposits or a confluent plaque of yellow material at the level of Bruch membrane within the macula and along the temporal arcades. The deposits progress over time to include the central macula and take on the appearance of geographic atrophy, with pronounced clumps of black pigmentation around the central ischemic and atrophic zone (a pseudoinflammatory appearance). Vision loss results from expansion of macular atrophy or from development of subfoveal CNV (Fig 12-23). SMD is inherited in an autosomal dominant pattern and results from mutations in *TIMP3*, which plays an important role in the regulation of extracellular matrix turnover. Both common and rare variants of *TIMP3* have been implicated in the pathogenesis of AMD.

Other drusenlike deposits that manifest before 50 years of age include those associated with several hereditary basement membrane abnormalities that lead to significant renal disease. They include Alport syndrome, membranoproliferative glomerulonephritis type II, and atypical hemolytic uremia syndromes.

Pattern dystrophies

The pattern dystrophies are a group of disorders characterized by the development, typically in midlife, of various patterns of yellow, orange, or gray pigment deposition at the level of the RPE within the macula. These dystrophies have been divided into 5 major subtypes according to the distribution of pigment deposits:

- adult-onset foveomacular vitelliform dystrophy (discussed earlier in this chapter)
- butterfly-type pattern dystrophy (Fig 12-24)
- reticular-type pattern dystrophy (Fig 12-25)
- multifocal pattern dystrophy simulating fundus flavimaculatus (Fig 12-26A)
- fundus pulverulentus (“dustlike,” coarse pigment mottling (Fig 12-26B)

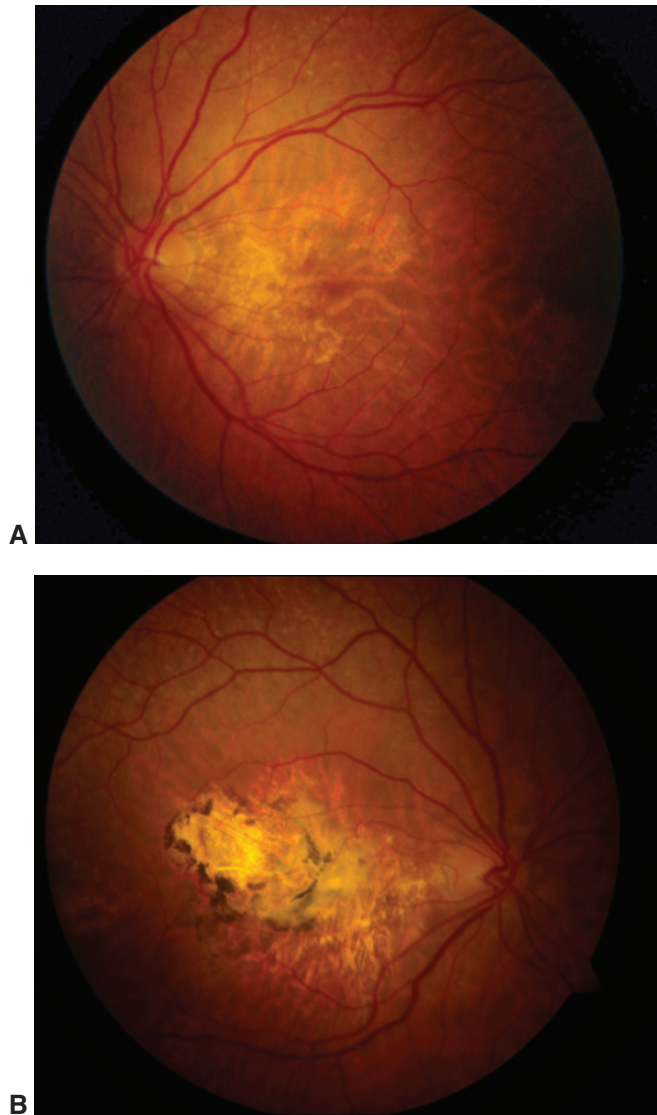


Figure 12-23 Fundus photographs from a 54-year-old woman with Sorsby macular dystrophy. Characteristic pale drusen are seen just outside the macula in both eyes. **A**, There is fovea-sparing geographic atrophy in the left eye. **B**, The more severely affected right eye has subretinal fibrosis as well as geographic atrophy. (Courtesy of Cagri G. Besirli, MD.)

Pattern dystrophy may best be considered as a single disease with variable expressivity. Different patterns are known to occur in members of the same family carrying an identical mutation. Furthermore, one pattern can evolve into another within a single patient.

Patients are often asymptomatic and diagnosed incidentally. The most common presenting symptom is diminished visual acuity or mild metamorphopsia. Overall, the visual prognosis is good, as the risk of developing CNV is low. Geographic macular atrophy may eventually develop in some cases.

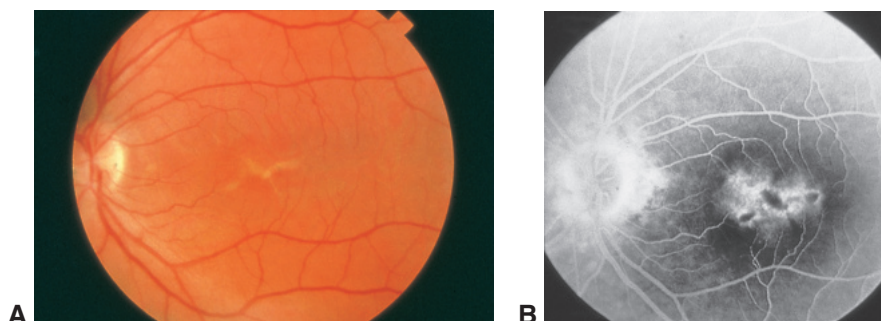


Figure 12-24 Butterfly-type pattern dystrophy. **A**, Color fundus photograph from a 56-year-old woman shows a typical yellow macular pigment pattern. **B**, Fluorescein angiography image shows blocked fluorescence of the pigment lesion itself and a rim of hyperfluorescence from surrounding RPE atrophy. (Reproduced from Song M-K, Small KW. Macular dystrophies. In: Regillo CD, Brown GC, Flynn HW Jr, eds. Vitreoretinal Disease: The Essentials. Thieme; 1999:297. With permission from Thieme. www.thieme.com)

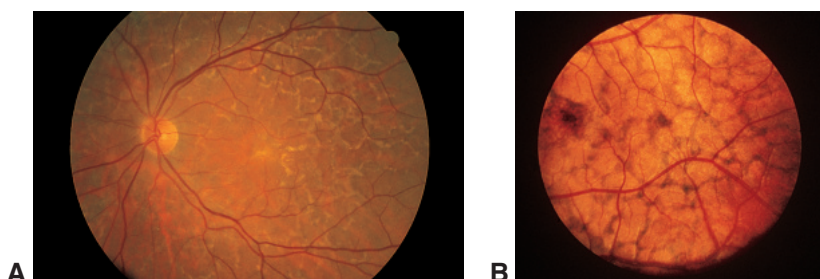


Figure 12-25 Fundus photographs show 2 examples of reticular-type pattern dystrophy, characterized by a “fishnet” pattern of yellowish-orange (**A**) or brown (**B**) pigment deposition in the posterior fundus. (Courtesy of Mark W. Johnson, MD.)

The pattern of inheritance is often autosomal dominant, but other modes of inheritance have been observed, including autosomal recessive and mitochondrial. Most cases of autosomal dominant pattern dystrophy have been associated with mutations in *PRPH2*. Mutations in *BEST1* and *CTNNA1* have also been identified. Associations of pattern dystrophy with pseudoxanthoma elasticum and various forms of muscular dystrophy have been reported.

Atypical and occult macular dystrophies

Several atypical macular dystrophies have been described. Among them are central areolar choroidal dystrophy, North Carolina macular dystrophy, and occult macular dystrophy.

Central areolar choroidal dystrophy is a hereditary (usually autosomal dominant) retinal disorder typically resulting in a well-defined area of atrophy of the RPE and choriocapillaris in the center of the macula (Fig 12-27). Dysfunction of macular photoreceptors usually leads to a decrease in visual acuity by the age of 30–60 years. The genes *PRPH2*, *GUCY2D*, and *GUCA1A* have been identified as causative.

North Carolina macular dystrophy is an autosomal dominant, completely penetrant, congenital, and stationary maldevelopment of the macula. There is substantial phenotypic

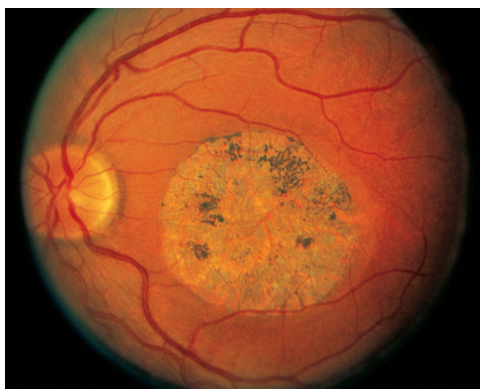


Figure 12-26 Two additional patterns of early-onset macular dystrophy. **A**, Multifocal pattern dystrophy simulating fundus flavimaculatus. **B**, Fundus pulverulentus. (Courtesy of Franco M. Recchia, MD.)

variability, with 3 grades of severity: grade 1, drusen; grade 2, confluent drusen; and grade 3, coloboma-like excavated defects in the macula that sometimes resemble the lesions of toxoplasmosis (Fig 12-28). The visual acuity in eyes with North Carolina macular dystrophy can be surprisingly good, given the appearance of the macula. However, CNV and fibrosis can develop and lead to deterioration in visual acuity. Three chromosomal loci, from which 1 gene (*PROM1*) has been identified, have been implicated.

Occult macular dystrophy was first described by Miyake as a hereditary (autosomal dominant) macular dystrophy without visible fundus abnormalities. In all patients, the

Figure 12-27 Fundus photograph of central areolar choroidal dystrophy in a patient with an autosomal dominant inheritance pattern. (Courtesy of Mark W. Johnson, MD.)



results of focal macular ERG were significantly subnormal, making this test the gold standard for diagnosis. Several years later, after patients with similar findings were described in other parts of the world, the condition was named occult macular dystrophy, and mutations in *RP1L1* and *MFSD8* have been reported to give rise to this phenotype. The most striking clinical finding is disruption (either focal or diffuse) of the central ellipsoid layer on OCT.

Rahman N, Georgiou M, Khan KN, Michaelides M. Macular dystrophies: clinical and imaging features, molecular genetics and therapeutic options. *Br J Ophthalmol*. 2020; 104(4):451–460.

Inner Retinal Dystrophies

X-linked retinoschisis

X-linked retinoschisis (XLRS) is the most common form of juvenile-onset retinal degeneration in male adolescents. Female carriers are almost always unaffected. XLRS typically presents in the first to second decade of life in a variety of ways, depending on the severity of disease (Fig 12-29). The most severe cases are diagnosed in infants presenting with nystagmus, strabismus, or decreased visual behavior and found to have dense vitreous hemorrhage or bullous retinal detachment (see Fig 12-29F, G). Less severe cases are usually diagnosed in later childhood by routine vision screening or as a result of decreased central vision.

Retinoschisis refers to a splitting of the neurosensory retina. These hallmark splits are typically seen in the macula and appear ophthalmoscopically as spokelike folds or fine striae radiating from the fovea (see Fig 12-29A, B). Approximately 50% of affected male adolescents also have peripheral schisis, involving the outer plexiform and nerve fiber layers (see Fig 12-29D). Extensive elevation of the peripheral inner retinal layers may be virtually indistinguishable from retinal detachment. Other clinical findings include a metallic sheen of the fundus, pigmentary changes, white spiculations, “vitreous veils” of condensed posterior vitreous or inner retinal tissue, and vitreous hemorrhage arising from shearing of retinal vessels traversing the schisis cavity (see Fig 12-29C, D). Pigmentary deposits may develop in peripheral areas destroyed by the disease process such that advanced cases of XLRS may be mistaken for RP (see Fig 12-29E).

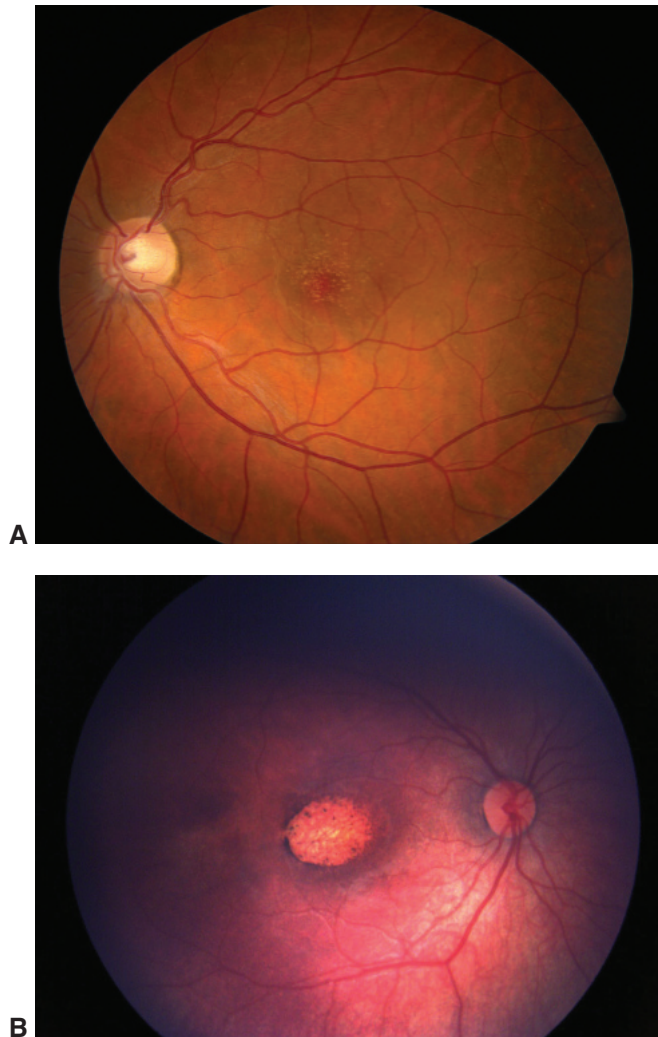


Figure 12-28 Fundus photographs showing clinical variations of North Carolina macular dystrophy in 2 members of the same family. **A**, The father has nonconfluent drusen typical of grade 1 of the disease. **B**, His 1-year-old son has an atrophic, coloboma-like defect characteristic of grade 3. (Courtesy of Cagri G. Besirli, MD.)

CLINICAL PEARL

X-linked retinoschisis is high in the differential diagnosis of vitreous hemorrhage in a boy, along with trauma and pars planitis.

OCT can readily show splitting of the retinal layers (see Fig 12-29B). Angiography reveals a petaloid pattern of hyperfluorescence without leakage. The panretinal involvement and inner retinal location of the disease are reflected in the ERG response, which

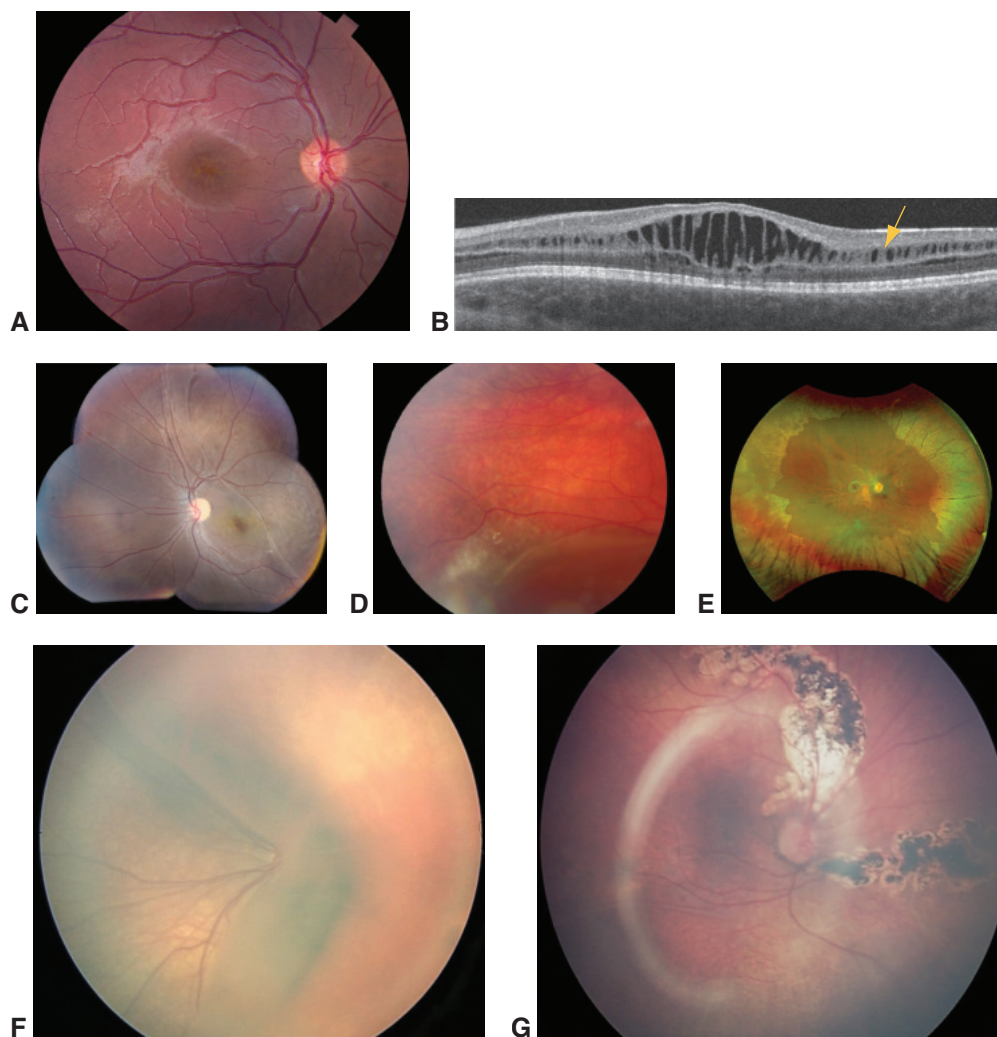


Figure 12-29 Spectrum of clinical findings in congenital retinoschisis. All examples are from boys with mutations in the *RS1* gene. **A**, Fundus photograph shows the central radial yellow spokes consistent with foveal schisis. (The whitish patches in the outer macula represent light reflex from healthy internal limiting membrane and is a typical, normal finding in children.) **B**, Corresponding SD-OCT shows macular schisis. Compared with OCT findings in CME, those in macular schisis include more pronounced elongation of the inner retinal cavitations centrally and involvement beyond the parafoveal region (*arrow*). **C**, Montage photograph shows radial striae in the macula, “vitreous veils” traversing obliquely, and whitish spiculations in the superior and temporal periphery. **D**, Inferior periphery of the right eye shows a smooth, domed, convex elevation consistent with peripheral retinoschisis. **E**, Ultra-wide-field fundus photograph shows extensive central and peripheral RPE atrophy consistent with advanced X-linked retinoschisis that is easily confused with rod-cone dystrophy. **F**, This 7-month-old boy, referred for nystagmus and strabismus, was found to have bilateral bullous schisis involving the superior macula (right eye is shown). **G**, Postoperative fundus photograph 2 months after vitrectomy, inner wall retinectomy, endolaser photocoagulation, and placement of silicone oil. (Courtesy of Franco M. Recchia, MD.)

has a negative waveform in which the a-wave is normal or near normal, but the b-wave is reduced (see Chapter 3, Fig 3-2).

The vast majority of cases of XLRS are caused by variants in the *RS1* gene. *RS1* encodes an adhesion protein called *retinoschisin*, which is crucial for the structural integrity of the retina provided by the Müller cells; it also acts in neurosynaptic transmission.

Retinal Degenerations Associated With Systemic Disease

Highlights

- Many systemic diseases can have retinal manifestations.
- A multidisciplinary approach to management is often warranted for retinal degenerations associated with systemic disease.
- Gene therapies are under investigation for many systemic diseases with retinal degenerations.

Introduction

For many of the conditions discussed in this chapter, a correct diagnosis could lead to meaningful, and in some cases life-saving, interventions. Important diagnostic and prognostic questions that arise in evaluating a patient who presents with retinal degeneration include the following:

- Is the degeneration hereditary or acquired?
- Is the condition stable or progressive?
- Can a precise diagnosis be made?

Systemic diseases with retinal degenerations are a highly heterogeneous group that often require multidisciplinary subspecialty care because of potentially severe associated morbidities and mortality. Gene therapies are under investigation for many of these diseases.

Retinal Degeneration With Systemic Involvement

Pigmentary retinopathy and retinal degenerations may be associated with a wide spectrum of genetic or acquired diseases. The term *pigmentary retinopathy* refers broadly to a panretinal disturbance of the retina and retinal pigment epithelium (RPE). Pigment deposits define most pigmentary retinopathies and typically present in the form of pigment clumps or spicules. In some diseases, there is generalized depigmentation characterized by atrophy and little or no pigment deposition. This section summarizes some important examples of these disorders (Table 13-1).

Table 13-1 Selected Systemic Diseases With Pigmentary Retinopathies

Disorder	Features
Autosomal dominant disorders	
Arteriohepatic dysplasia (Alagille syndrome)	Intrahepatic cholestatic syndrome, posterior embryotoxon, Axenfeld anomaly, congenital heart disease, flattened facies and bridge of nose, bony abnormalities, myopia, pigmentary retinopathy
Charcot-Marie-Tooth disease	Pigmentary retinopathy, degeneration of lateral horn of spinal cord, optic atrophy
Myotonic dystrophy (Steinert disease)	Muscle wasting, "Christmas tree" cataract, retinal degeneration, pattern dystrophy or reticular degeneration; ERG response subnormal
Oculodentodigital dysplasia (oculodentodigital syndrome)	Thin nose with hypoplastic alae, narrow nostrils, abnormality of fourth and fifth fingers, hypoplastic dental enamel, congenital cataract, colobomas
Olivopontocerebellar atrophy	Retinal degeneration (peripheral and/or macular), cerebellar ataxia, possible external ophthalmoplegia
Stickler syndrome	Progressive myopia with myopic retinal degeneration, arthropathy including joint hypermobility and arthritis, midfacial hypoplasia, high arched or cleft palate, bifid uvula; retinal detachment common; ERG response subnormal
arthro-ophthalmopathy)	
Waardenburg syndrome	Hypertelorism, wide bridge of nose, cochlear deafness, white forelock, heterochromia iridis, poliosis, pigment disturbance of RPE, choroidal vitiligo; ERG response normal to subnormal
Wagner hereditary vitreoretinal degeneration	Narrowed and sheathed retinal vessels, pigmented spots in the retinal periphery and along retinal vessels, choroidal atrophy and optic atrophy, extensive liquefaction and membranous condensation of vitreous body; subnormal ERG response; overlapping features with Stickler syndrome
Autosomal recessive disorders	
Bardet-Biedl syndrome	Pigmentary retinopathy, bull's-eye maculopathy, mild cognitive disabilities, polydactyly, obesity, hypogenitalism, renal abnormalities, progressive visual field loss; ERG response severely diminished to undetectable
Bietti crystalline dystrophy	Yellow-white crystals scattered in posterior pole, round subretinal pigment deposits, confluent loss of RPE and choriocapillaris on fluorescein angiogram, possible crystals in limbal cornea
Homocystinuria	Fine pigmentary or cystic degeneration of retina, marfanoid appearance, myopia, lens subluxation or dislocation, cardiovascular abnormalities (thromboses), glaucoma, cognitive disabilities
α-Mannosidosis	Macroglossia (enlarged tongue), flat nose, large head and ears, skeletal abnormalities, possible hepatosplenomegaly, storage material in retina; resembles severe mucopolysaccharidosis I
Mucopolysaccharidosis I (severe; Hurler syndrome)	Early corneal clouding, retinal pigmentary degeneration, coarse facies, deafness, cognitive disabilities, dwarfism, skeletal abnormalities, hepatosplenomegaly, optic atrophy; subnormal ERG response
Mucopolysaccharidosis I (attenuated; Scheie syndrome)	Coarse facies, aortic regurgitation, stiff joints, early clouding of the cornea, normal life span, normal intellect, pigmentary retinopathy
Mucopolysaccharidosis III (Sanfilippo syndrome)	Milder somatic stigmata than in severe mucopolysaccharidosis I, but severe pigmentary retinopathy

Disorder	Features
Neonatal adrenoleukodystrophy (Zellweger spectrum disorder)	Pigmentary retinopathy, optic atrophy, seizures, hypotonia, adrenal cortical atrophy, psychomotor impairment; extinguished ERG response
Neuronal ceroid lipofuscinoses (CLN; Batten disease)	Infantile (CLN1, Hattia-Santavuori): onset age 6–18 months with rapid deterioration, fine granular inclusions, bull's-eye maculopathy Late infantile (CLN2, Jansky-Bielschowsky): onset age 2–4 years, rapid CNS deterioration, curvilinear body inclusions Lake-Cavanagh: onset 4–6 years, ataxia, dementia, curvilinear and fingerprint-like inclusions Juvenile (CLN3, Batten-Spielmeyer-Vogt): onset age 6–8 years, slowly progressive, fingerprint-like inclusions, pigmentary retinopathy, bull's-eye maculopathy
Refsum disease	Elevations of phytanic acid, pigmentary retinopathy, optic atrophy, partial deafness, cerebellar ataxia, ichthyosis
Spinocerebellar degeneration	Ataxia, limb incoordination, nerve deafness, maculopathy, retinal degeneration, optic atrophy
Usher syndrome	Congenital deafness (partial or profound), pigmentary retinopathy, vestibular areflexia (type 1)
Zellweger (cerebrohepatorenal) syndrome (Zellweger spectrum disorder)	Hypotonia, high forehead and hypertelorism, hepatomegaly, deficient cerebral myelination, nystagmus, cataract, microphthalmia, retinal degeneration; undetectable ERG response
X-linked disorders	
Incontinentia pigmenti (Bloch-Sulzberger syndrome)	Skin pigmentation in lines and whorls, alopecia, dental and CNS anomalies, optic atrophy, falciform folds, cataract, nystagmus, strabismus, patchy mottling of fundi, conjunctival pigmentation
Mucopolysaccharidosis II (Hunter syndrome)	Minimal or no corneal clouding, mild clinical course; onset of signs at age 2–4 years: full lips, large and rounded cheeks, broad nose, enlarged tongue, possible cognitive disabilities, pigmentary retinopathy; subnormal ERG response; over time, voice changes from vocal cord enlargement; possible airway obstruction from airway narrowing
Pelizaeus-Merzbacher disease	Infantile progressive leukodystrophy, cerebellar ataxia, limb spasticity, cognitive impairment, possible pigmentary retinopathy with absent foveal reflex
Mitochondrial disorders	
Kearns-Sayre syndrome; maternally inherited diabetes and deafness (MIDD); mitochondrial encephalopathy, lactic acidosis, stroke like episodes (MELAS)	Chronic progressive external ophthalmoplegia, ptosis, pigmentary retinopathy and/or macular atrophy, heart block (Kearns-Sayre syndrome); normal to subnormal ERG response

CNS = central nervous system; ERG = electroretinogram; RPE = retinal pigment epithelium.

Information from Rimoin DL, Connor JM, Pyeritz RE, Korf BR, eds. *Emery and Rimoin's Principles and Practice of Medical Genetics*. 3 vols. 4th ed. Churchill Livingstone; 2002:chap 137.

Infantile-Onset to Early Childhood–Onset Syndromes

The dystrophies characterized by early onset and rapid progression of severe bilateral vision loss are collectively called *Leber congenital amaurosis (LCA)*. In any infant suspected of having poor or declining vision, LCA should be considered when a severely diminished or extinguished electroretinogram (ERG) signal is present at birth (see Chapter 12 for further discussion). When the ERG signal is diminished and the changes in vision are progressive, evaluation should include careful screening for congenital syndromes and metabolic disorders that affect the retina.

Huang CH, Yang CM, Yang CH, Hou YC, Chen TC. Leber's congenital amaurosis: current concepts of genotype-phenotype correlations. *Genes (Basel)*. 2021;12(8):1261. doi:10.3390/genes12081261.

Bardet-Biedl Syndrome

Bardet-Biedl syndrome is a genetically and clinically heterogeneous disorder of ciliary function. Many different types have been identified and have a similar constellation of findings, including pigmentary retinopathy (with or without pigment deposits), obesity, polydactyly, hypogonadism, cognitive disability, and renal abnormalities (see the section “Renal diseases”). Patients with Bardet-Biedl syndrome typically demonstrate a form of rod–cone dystrophy with variable severity, usually sine pigmento, with a bull’s-eye atrophic maculopathy (Fig 13-1). These disorders are sometimes classified as autosomal recessive, but molecular studies strongly suggest that many are multigenic, with 2 or even 3 different mutations contributing to the phenotype. Increasing evidence suggests that the primary function of the proteins affected in Bardet-Biedl syndrome are to mediate and regulate microtubule-based intracellular transport processes.

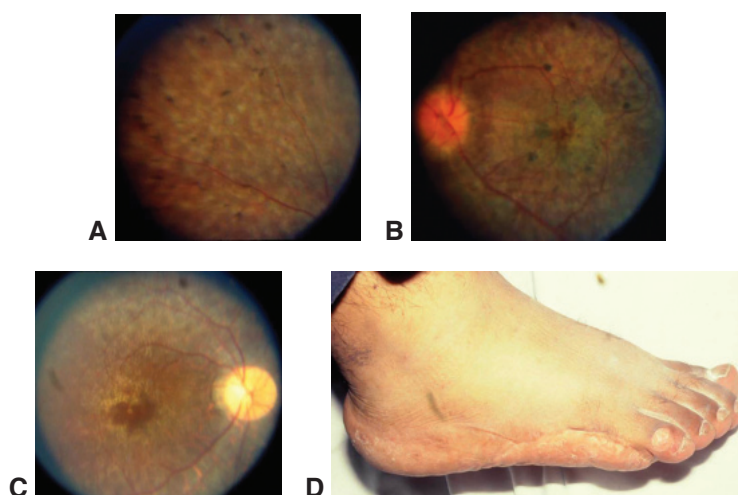


Figure 13-1 Bardet-Biedl syndrome. **A, B**, Fundus photographs show pigmentary alterations in the periphery and macula. **C**, Fundus photograph from the sibling of the patient in **A** and **B** demonstrates similar macular changes. **D**, Clinical photograph of a patient's foot with 6 toes (polydactyly). (Courtesy of David Sarraf, MD.)

M'hamdi O, Ouertani I, Chaabouni-Bouhamed H. Update on the genetics of Bardet-Biedl syndrome. *Mol Syndromol*. 2014;5(2):51–56.

Hearing Loss and Pigmentary Retinopathy: Usher Syndrome

Usher syndrome is the most common name used to describe the association of retinitis pigmentosa (RP) with congenital sensorineural hearing loss, whether partial or profound. The prevalence of Usher syndrome is thought to be 3 cases per 100,000 persons. There are 3 types of Usher syndrome, with types 1 and 2 being more common than type 3. Patients with type 1 have early and profound deafness, RP, and vestibular areflexia. Patients with type 2 are born with moderate to severe hearing loss and develop RP within the second decade of life but have normal vestibular function. Patients with type 3 have progressive hearing loss, RP of variable severity, and sporadic vestibular function.

All forms show autosomal recessive inheritance. Currently, 16 genetic loci have been identified as associated with Usher syndrome. The proteins encoded by these genes are part of a dynamic protein complex present in the cilia of the inner ear and in the cone outer segments of the photoreceptor cells of the retina. See Table 13-2 for other genetic conditions that may lead to pigmentary retinopathy and hearing loss.

Mathur P, Yang J. Usher syndrome: hearing loss, retinal degeneration and associated abnormalities. *Biochim Biophys Acta*. 2015;1852(3):406–420.

Neuromuscular Disorders

Pigmentary retinopathy associated with neuromuscular pathology is present in a variety of disorders (see Table 13-1). ERG abnormalities found in these neurologic disorders confirm the presence of retinopathy but are not diagnostic for any one disorder.

Although *Duchenne muscular dystrophy* does not cause a pigmentary retinopathy, it deserves mention because the ERG signal shows a negative waveform similar to that found in patients with congenital stationary night blindness—specifically, a normal a-wave but a reduced b-wave (see Chapters 3 and 12). This ERG response suggests a defective “on-response” pathway, but patients with this disorder do not have nyctalopia (night blindness). Interestingly, Duchenne muscular dystrophy is caused by mutations in the gene for dystrophin, a protein that is abundant in muscle but also found in neural synaptic regions and in the retina.

Barboni MT, Nagy BV, de Araújo Moura AL, et al. ON and OFF electroretinography and contrast sensitivity in Duchenne muscular dystrophy. *Invest Ophthalmol Vis Sci*. 2013; 54(5):3195–3204.

Table 13-2 Disorders Causing Pigmentary Retinopathy and Hearing Loss

Alport syndrome
Alström syndrome
Cockayne syndrome
Congenital rubella syndrome
Mucopolysaccharidosis I (severe; also known as <i>Hurler syndrome</i>)
Refsum disease
Spondyloepiphyseal dysplasia congenita

Diseases Affecting Other Organ Systems

Most retinopathies associated with diseases affecting other organ systems are rare and genetic. Clinicians may find the OMIM, Online Mendelian Inheritance in Man, website (www.omim.org) useful in recognizing these disorders.

Renal diseases

Several forms of congenital renal disease are ciliopathies associated with retinal degeneration. *Familial juvenile nephronophthisis* (also called *Senior-Løken syndrome*, *renal-retinal dysplasia*) is one of a group of diseases characterized by autosomal recessive inheritance, retinal degeneration, and childhood onset of end-stage renal disease. Individuals with *Joubert syndrome* have cerebellar malformation (a characteristic “molar tooth” deformity that can be observed on magnetic resonance imaging of the brain) and may also have associated chorioretinal coloboma. Patients with *Bardet-Biedl syndrome* (discussed earlier) commonly have urethral reflux with pyelonephritis and kidney damage, whereas patients with *Alström syndrome* may demonstrate obesity and have short stature and cardiomyopathy in addition to renal disease. *Jeune syndrome* is a retinal ciliopathy that is complicated by cystic kidney disease and asphyxiating thoracic dystrophy.

Liver disease

Patients with *arteriohepatic dysplasia* (also called *Alagille syndrome*) present with hepatorenal abnormalities, including cholestatic jaundice. Characteristic ocular findings, which include posterior embryotoxon and pigmentary retinopathy, can have a peripapillary and macular predilection.

Gastrointestinal tract disease

Familial adenomatous polyposis (FAP; also known as *Gardner syndrome*) is associated with pigmented lesions that are similar to those found in congenital hypertrophy of the RPE. However, the lesions in FAP are ovoid, more variegated than the classic isolated lesions of congenital hypertrophy of the RPE, and typically multiple and bilateral. The presence of more than 4 widely spaced, small (<0.5–disc diameter) lesions per eye and bilateral involvement suggest FAP. Note that congenital grouped pigmentation (bear tracks) is not associated with FAP (Fig 13-2). Caused by mutations in the adenomatous polyposis gene (*APC*), FAP has an autosomal dominant inheritance pattern with incomplete expression. The pigmented retinal lesions are an important marker for identifying family members at risk for colonic polyps, which have a high malignant potential (see BCSC Section 4, *Ophthalmic Pathology and Intraocular Tumors*).

Nusliha A, Dalpatadu U, Amarasinghe B, Chandrasinghe PC, Deen KI. Congenital hypertrophy of retinal pigment epithelium (CHRPE) in patients with familial adenomatous polyposis (FAP): a polyposis registry experience. *BMC Res Notes* 7, 734 (2014). <https://doi.org/10.1186/1756-0500-7-734>

Dermatologic diseases

Ichthyosis, comprising abnormal scaling, dryness, and tightness of the skin, may be found in conjunction with the pigmentary retinopathy of Refsum disease and the crystalline maculopathy of Sjögren-Larsson syndrome (Fig 13-3). *Incontinentia pigmenti* (*Bloch-Sulzberger syndrome*) is a rare X-linked disorder that presents only in females; the syndrome is lethal

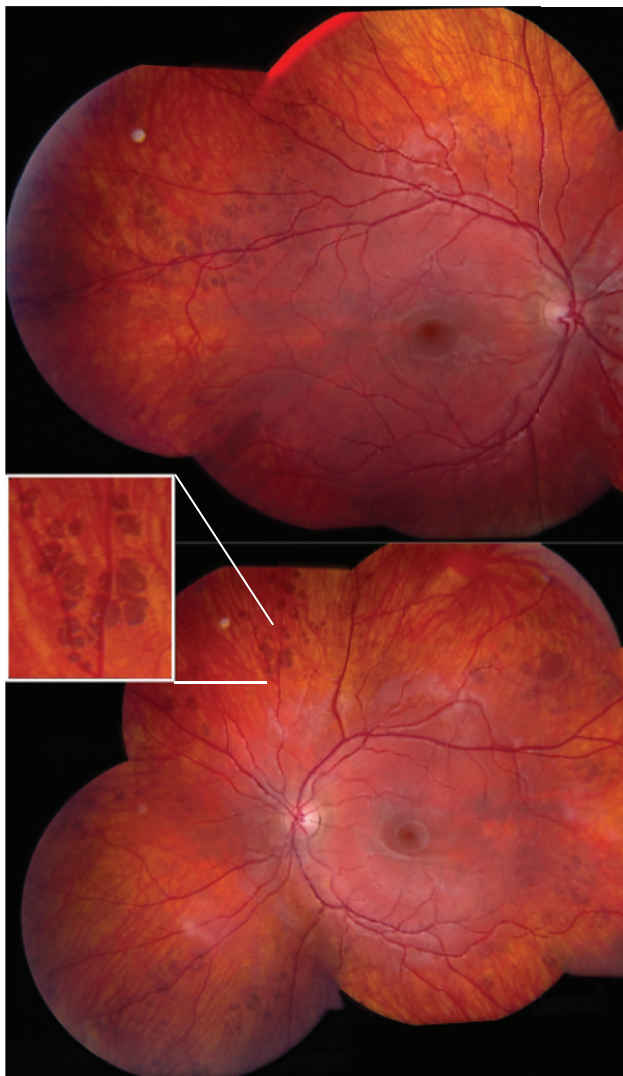


Figure 13-2 Bilateral, extensive bear tracks in congenital hypertrophy of the retinal pigment epithelium (CHRPE). *Inset* shows a magnified cluster, highlighting the sharp borders and location deep to the retina (under the retinal vessels), consistent with localization at the level of the RPE. In contrast, pigmented lesions in familial adenomatous polyposis are more widely spaced, larger, and typically ovoid compared to the bear track lesions in this fundus photograph. (Courtesy of Anthony B. Daniels, MD, MSc.)

in utero to males. It is characterized by streaky skin lesions and abnormalities of the teeth and central nervous system (CNS). Ocular involvement occurs in approximately 35%–77% of affected females and includes pigmentary abnormalities as well as peripheral retinal non-perfusion and neovascularization that may cause traction and cicatricial retinal detachment (see also BCSC Section 6, *Pediatric Ophthalmology and Strabismus*). *Pseudoxanthoma elasticum* is associated with a “plucked chicken” skin appearance, peripapillary angioid streaks, and a peau d’orange fundus appearance (see Chapter 4).

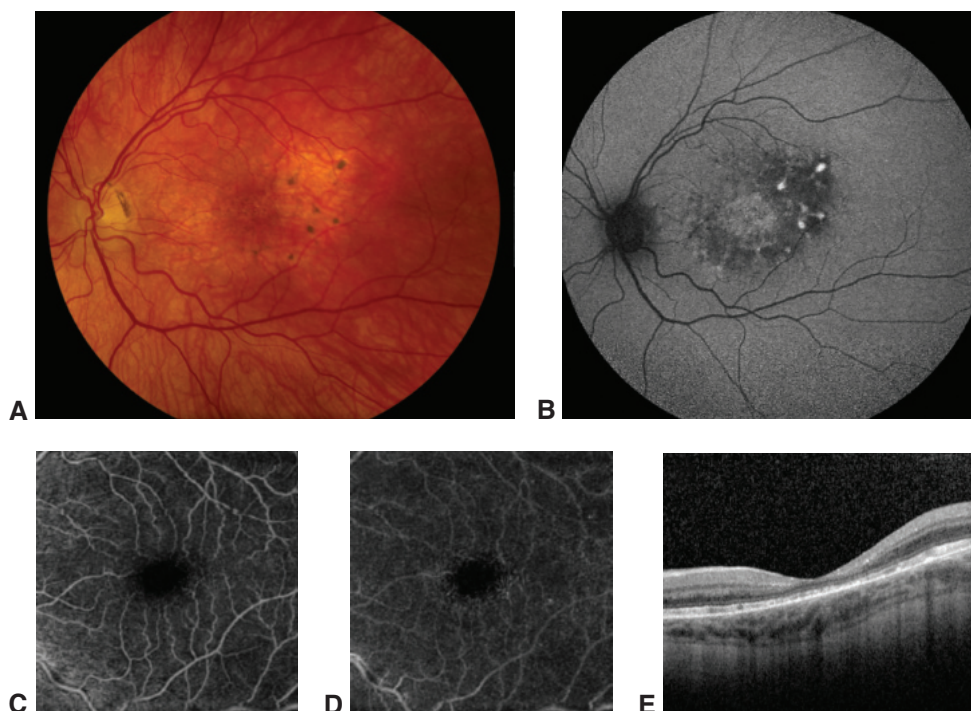


Figure 13-3 Images from a patient with late-stage Sjögren-Larsson syndrome. **A**, Fundus images demonstrate RPE changes and atrophy with lipofuscin deposits in the macula. **B**, Fundus autofluorescence reveals hyperautofluorescence of lipofuscin deposits. **C, D**, Increased flow voids, vessel dilation, and decreased capillary density in the superficial and deep retinal capillary plexuses are displayed with optical coherence tomography (OCT) angiography. **E**, Spectral-domain OCT (SD-OCT) shows hyperreflective dots in the inner retina and RPE and disruption of the ellipsoid zone. (Courtesy of Jaclyn L. Kovach, MD.)

Swinney CC, Han DP, Karth PA. Incontinentia pigmenti: a comprehensive review and update. *Ophthalmic Surg Lasers Imaging Retina*. 2015;46(6):650–657.

Dental disease

Amelogenesis imperfecta is a genetic disease that causes abnormalities in dentition development resulting from defective enamel production. When associated with a cone-rod dystrophy, this condition is referred to as *Jalili syndrome* and has a wide range of clinical retinal manifestations, including macular coloboma and pigmentary retinopathy.

Paraneoplastic and Autoimmune Retinopathies

Occasionally, retinal degeneration is a complication of cancer resulting from a paraneoplastic immunologic mechanism. BCSC Section 9, *Uveitis and Ocular Inflammation*, explains the role of the immune system in this process. The 2 main paraneoplastic retinopathy syndromes are *cancer-associated retinopathy* (CAR; Fig 13-4) and *melanoma-associated retinopathy* (MAR). Patients with these syndromes can have normal-appearing

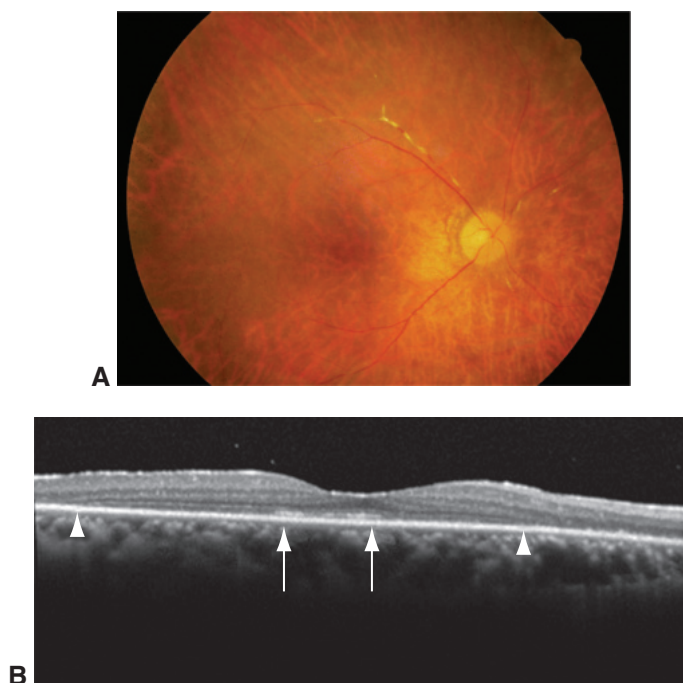


Figure 13-4 Cancer-associated retinopathy (CAR). **A**, Fundus photograph of CAR in a patient with ovarian carcinoma. Note the severe vascular attenuation without obvious pigmentary alterations. **B**, Fourier-domain cross-sectional OCT of an eye with CAR that shows disruption (*arrowheads*) of the outer nuclear layer and external limiting membrane as well as decreases in reflectivity of the inner segment ellipsoid zone (*arrows*). (Part A courtesy of John R. Heckenlively, MD; part B modified from Mesiwala NK, Shemonski N, Sandrian MG, et al. Retinal imaging with en face and cross-sectional optical coherence tomography delineates outer retinal changes in cancer-associated retinopathy secondary to Merkel cell carcinoma. *J Ophthalmic Inflamm Infect.* 2015;5(1):53. <https://doi.org/10.1186/s12348-015-0053-0>)

fundi. The characteristic ERG findings in MAR are a preserved dark-adapted a-wave followed by a strikingly reduced b-wave, resulting in an electronegative ERG, which is similar to the ERG findings in congenital stationary night blindness. Patients with MAR usually present with acquired nyctalopia and shimmering photopsias. In CAR, the ERG shows decreased or extinguished a- and b-waves.

A third entity, *autoimmune retinopathy*, refers to an acquired, presumed immunologically mediated, retinal degeneration that resembles paraneoplastic retinopathy but there is no identifiable systemic malignancy.

Bilateral diffuse uveal melanocytic proliferation (BDUMP) is a paraneoplastic syndrome characterized by multiple melanocytic lesions of the choroid that may be associated with rapidly progressive posterior subcapsular cataract, iris and ciliary body cysts, and exudative retinal detachment. BDUMP has been associated with various systemic malignancies (see Chapter 9). *Acute exudative polymorphous vitelliform maculopathy*, which is characterized by multiple waxing and waning subretinal vitelliform lesions, has been reported in association with metastatic cutaneous melanoma and other systemic malignancies.

Fox AR, Gordon LK, Heckenlively JR, et al. Consensus on the diagnosis and management of nonparaneoplastic autoimmune retinopathy using a modified Delphi approach. *Am J Ophthalmol*. 2016;168:183–190.

Grange L, Dalal M, Nussenblatt RB, Sen HN. Autoimmune retinopathy. *Am J Ophthalmol*. 2014;157(2):266–272.

Rahimy E, Sarraf D. Paraneoplastic and non-paraneoplastic retinopathy and optic neuropathy: evaluation and management. *Surv Ophthalmol*. 2013;58(5):430–458.

Metabolic Diseases

When patients with retinal degeneration are being evaluated, it is important to consider metabolic diseases, as some of these disorders are potentially lethal and others have severe morbidities. Disorders such as abetalipoproteinemia and Refsum disease are among the differential diagnostic concerns for RP even though the retinopathy associated with these diseases can be granular and atypical. See BCSC Section 6, *Pediatric Ophthalmology and Strabismus*, which covers many of the entities discussed in the following subsections, including albinism.

Albinism

In albinism, the synthesis of melanin is reduced or absent. When the reduction in melanin biosynthesis affects the eyes, skin, and hair follicles, the disease is called *oculocutaneous albinism* (OCA). There are several different types, which are usually inherited in an autosomal recessive pattern. If the skin and hair appear normally pigmented and only ocular pigmentation is affected, the condition is called *ocular albinism*. Ocular albinism typically has an X-linked inheritance pattern. Female carriers of X-linked ocular albinism may show partial iris transillumination and fundus pigment mosaicism.

Regardless of the type of albinism, ocular involvement generally conforms to 1 of 2 clinical patterns: (1) congenitally subnormal visual acuity (typically 20/100–20/400) and nystagmus; or (2) normal or minimally reduced visual acuity without nystagmus. The first pattern is true albinism; the second has been termed *albinoidism* because of its milder visual consequences. Both patterns share the clinical features of photophobia, iris transillumination, and hypopigmented fundi (Fig 13-5A). They differ according to whether or not the fovea develops normally; in true albinism, the fovea is hypoplastic, with no foveal pit or reflex and no evident luteal pigment (Fig 13-5B, C). The gold standard for diagnosis of true albinism is the finding of characteristic abnormalities of the flash and pattern visual evoked potentials (VEP): in albinism, stimulation of 1 eye results in an asymmetric occipital response, which is due to the greater number of decussating fibers in individuals with this disorder and contrasts with the symmetric VEP in persons without albinism.

OCA has 2 forms that are potentially lethal. The first, Chédiak-Higashi syndrome, is characterized by albinism, neutropenia, and an extreme susceptibility to infections, as well as other complications such as bleeding (caused by deficient platelets). The second, Hermansky-Pudlak syndrome, is characterized by a platelet defect that causes easy bruising and bleeding. In the United States, most patients with Hermansky-Pudlak syndrome are of Puerto Rican descent.

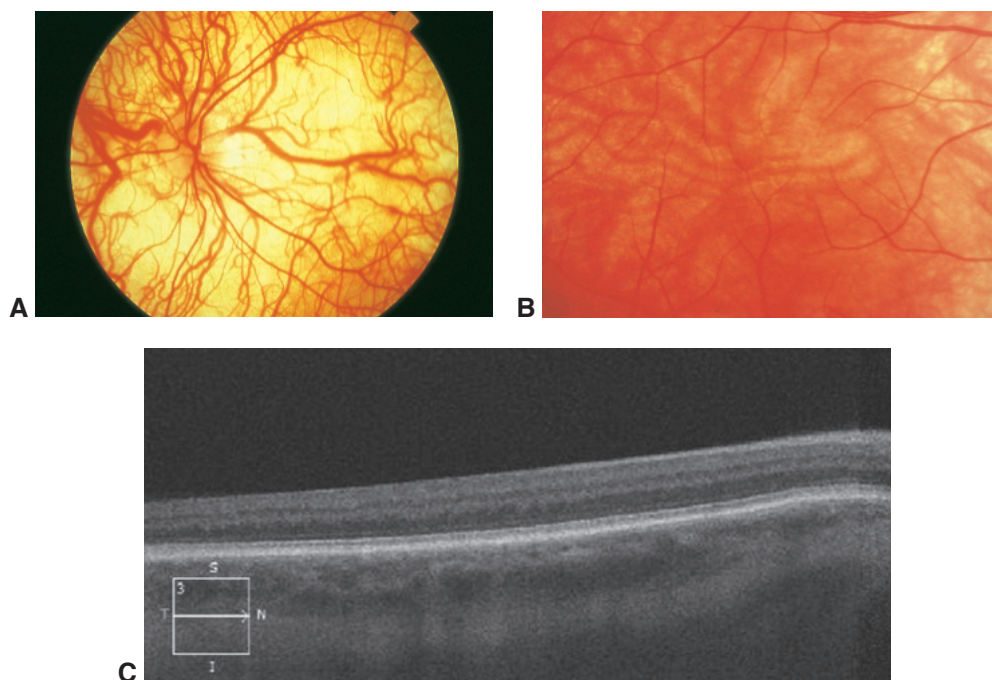


Figure 13-5 Albinism. **A**, Fundus photograph shows generalized fundus hypopigmentation. **B**, High-magnification fundus photograph shows foveal hypoplasia. No foveal reflex or luteal pigment is evident. **C**, SD-OCT image shows the lack of a foveal pit. Eccentric fixation was also present, resulting in superior decentration of the scans. (Parts A and B courtesy of Carl D. Regillo, MD; part C courtesy of David Browning, MD.)

King RA, Jackson IJ, Oetting WS. Human albinism and mouse models. In: Wright AE, Jay B, eds. *Molecular Genetics of Inherited Eye Disorders*. Harwood Academic; 1994:89–122.

Metabolic Diseases With Central Nervous System Abnormalities

The following subsections discuss some of the major inherited metabolic diseases known to affect the CNS and retina (see Table 13-1). See BCSC Section 6, *Pediatric Ophthalmology and Strabismus*, for a list of the ocular findings in inborn errors of metabolism.

Neuronal ceroid lipofuscinoses

The neuronal ceroid lipofuscinoses (NCLs) are a group of autosomal recessive diseases caused by the accumulation of waxy lipopigments (eg, ceroid and lipofuscin) within the lysosomes of neurons and other cells. These disorders usually become evident in early childhood and are characterized by progressive dementia, seizures, vision loss associated with a pigmentary retinopathy in early-onset cases, and variable life expectancy. A diagnosis can be made with genetic testing, in addition to a peripheral blood smear or biopsy and electron microscopy of conjunctival or other tissues, which can reveal the characteristic curvilinear, fingerprint-like or granular inclusions. The infantile and juvenile types

of NCLs are associated with pigmentary retinopathies (see Table 13-1). Ocular findings in infantile NCL include optic atrophy; macular pigmentary changes including bull's-eye atrophic maculopathy, mottling of the fundus periphery, and retinal vascular attenuation; and reduced or absent ERG signals (Fig 13-6). The 2 adult forms of NCL do not have ocular manifestations.

Haltia M. The neuronal ceroid-lipofuscinoses: from past to present. *Biochim Biophys Acta*. 2006;1762(10):850–856.

Abetalipoproteinemia and vitamin A deficiency

Abetalipoproteinemia is an autosomal recessive disorder in which apolipoprotein B is not synthesized, which causes fat malabsorption, resulting in deficiency of fat-soluble vitamins and retinal and spinocerebellar degeneration. Supplementation with vitamins A and E is needed to prevent or ameliorate the retinal degeneration. The most common form of vitamin A deficiency retinopathy occurs in patients who have undergone gastric bypass surgery for obesity or small-bowel resection for Crohn disease. These patients have malabsorption of fat-soluble vitamins and may develop a blind loop syndrome, in which an overgrowth of bacteria consumes vitamin A. Patients experience nyctalopia, and if the condition remains untreated, they eventually demonstrate vision loss and diffuse, drusen-like spots similar to those observed in retinitis punctata albescens.

Zellweger spectrum disorders

Zellweger spectrum refers to a group of related peroxisomal disorders that are mostly autosomal recessive diseases and are caused by the dysfunction or absence of peroxisomes or peroxisomal enzymes, which leads to defective oxidation and accumulation of very-long-chain fatty acids. *Zellweger syndrome* is the most severe of the disorders in the spectrum. Severe infantile-onset retinal degeneration is associated with hypotonia, psychomotor

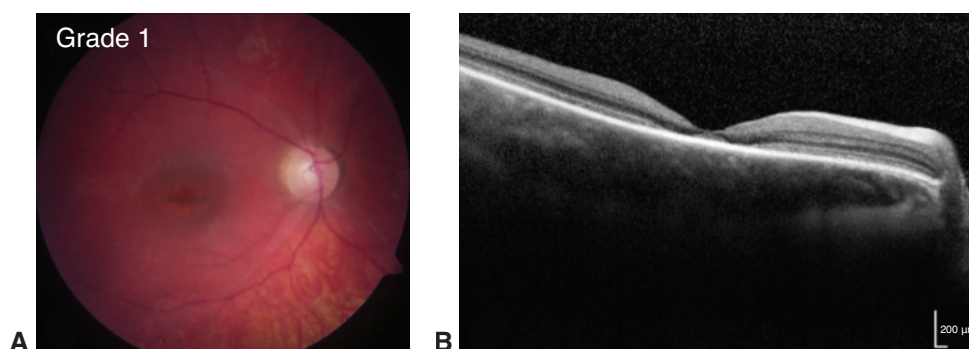


Figure 13-6 **A**, Fundus photograph from a patient with neuronal ceroid lipofuscinosis (Batten disease; *CLN3*, juvenile onset) shows bull's eye maculopathy, an early manifestation of the disease. **B**, SD-OCT shows foveal atrophy in a "flying saucer" pattern. (Reproduced from Dulz S, Atiskova Y, Wibbeler E, et al. An ophthalmic rating scale to assess ocular involvement in juvenile *CLN3* disease. *Am J Ophthalmol*. 2020;220:64–71. Copyright 2020, with permission from Elsevier.)

impairment, seizures, characteristic facies, renal cysts, and hepatic interstitial fibrosis. Death usually occurs in infancy. Patients with *neonatal adrenoleukodystrophy*, the intermediate form in the spectrum, also present in infancy but generally survive until the age of 7–10 years (Fig 13-7). Similar but less severe findings are present in *infantile Refsum disease*, which is characterized by pigmentary retinopathy with reduced or extinguished ERG signals, cerebellar ataxia, polyneuropathy, anosmia, hearing loss, and cardiomyopathy. Diagnosis is made by demonstrating elevated plasma levels of phytanic acid or reduced phytanic acid oxidase activity in cultured fibroblasts. Dietary restriction of phytanic acid precursors may slow or stabilize the neuropathy but typically not the retinal degeneration.

Mucopolysaccharidoses

The systemic *mucopolysaccharidoses* (MPSs) are caused by inherited defects in catabolic lysosomal enzymes that degrade the glycosaminoglycans dermatan sulfate, keratan sulfate, and heparan sulfate. The MPSs are transmitted as autosomal recessive traits except for type II, which is an X-linked recessive disorder (see Table 13-1).

Only those MPSs in which heparan sulfate is stored are associated with retinal dystrophy. These include severe MPS I (also known as *Hurler syndrome*) and attenuated MPS I (*Hurler-Scheie* and *Scheie syndromes*), the clinical features of which include coarse facies, cognitive disabilities (severe MPS I only), corneal clouding, and retinal degeneration. The retinal pigmentary changes may be subtle, but the ERG response is subnormal. MPS II (Hunter syndrome) also features pigmentary retinopathy but corneal clouding, if present, is only mild; patients have coarse facies and short stature and may show cognitive disabilities. In MPS type III (Sanfilippo syndrome), somatic stigmata are mild, but pigmentary retinopathy is severe.



Figure 13-7 Neonatal adrenoleukodystrophy (Zellweger spectrum disorder). Fundus photograph shows retinal arteriolar attenuation, diffuse pigmentary alterations, and mild optic atrophy. (Courtesy of Mark W. Johnson, MD.)

Other lysosomal metabolic disorders

Tay-Sachs disease (GM₂ gangliosidosis type I), caused by a mutation in the hexosaminidase subunit alpha gene (*HEXA*), is the most common ganglioside storage disease, with an incidence of 1 in 320,000 births in the United States. Glycolipid accumulation in the brain and retina causes cognitive disability and blindness, respectively, and death generally occurs between the ages of 2 and 5 years. Ganglion cells surrounding the fovea become filled with ganglioside, and areas with such cells appear grayish or white, in contrast with the fovea, which lacks these cells, causing a cherry-red spot (Fig 13-8).

The chronic nonneuronopathic adult form of *Gaucher disease* does not have cerebral involvement. This disease is characterized by large accumulations of glucosylceramide in the liver, spleen, lymph nodes, skin, and bone marrow. Some patients have a cherry-red spot; others show whitish superficial lesions in the midperiphery of the fundus. Spectral-domain optical coherence tomography analysis demonstrates multiple characteristic hyperreflective lesions located along the retinal surface.

The various types of *Niemann-Pick disease* (NPD) are caused by the absence of different sphingomyelinase isoenzymes and resultant accumulation of sphingomyelin in the liver, spleen, lung, brain, and other organs. In NPD type A (acute neuronopathic), a cherry-red spot is present in approximately 50% of cases. NPD type B (chronic), also known as *sea-blue histiocyte syndrome*, is the mildest, and there is no functional involvement of the CNS; these patients have a macular halo that is considered diagnostic (Fig 13-9).

Fabry disease (*angiokeratoma corporis diffusum*) is an X-linked condition caused by mutations in the gene encoding α -galactosidase A. Ceramide trihexoside accumulates in the smooth muscle of blood vessels in the kidneys, skin, gastrointestinal tract, CNS, heart,

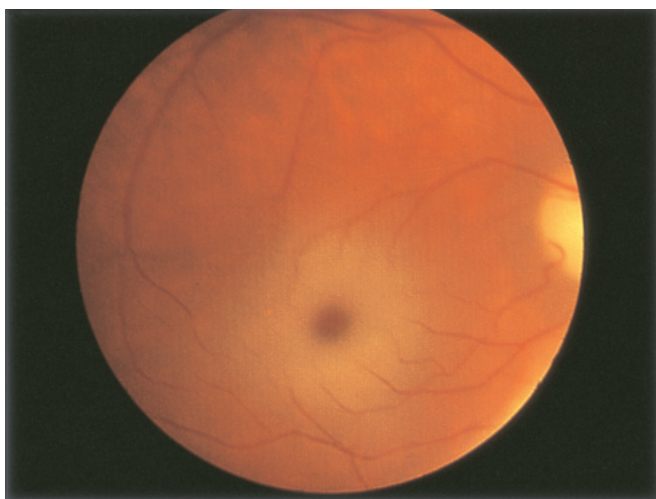


Figure 13-8 Tay-Sachs disease. Fundus photograph shows a cherry-red spot.



Figure 13-9 Chronic Niemann-Pick disease. Fundus photograph shows a macular halo. (Courtesy of Mark W. Johnson, MD.)

and reticuloendothelial system. Ocular signs include cornea verticillata (whorls), tortuous conjunctival vessels, tortuous and dilated retinal vessels, and lens changes. Tortuosity of conjunctival and retinal vessels is also characteristic of *fucosidosis*, a rare lysosomal storage disorder caused by buildup of complex sugars due to reduced or absent activity of the α -L-fucosidase enzyme. CNS abnormalities may include hemiparesis, vertigo, diplopia, dysarthria, nystagmus, and ataxia.

Gregory-Evans K, Pennesi ME, Weleber RG. Retinitis pigmentosa and allied disorders.

In: Schachat AP, Wilkinson CP, Hinton DR, Sadda SR, Wiedemann P, eds. *Ryan's Retina*.

6th ed. Elsevier/Saunders; 2018:861–935.

Amino Acid Disorders

In *cystinosis*, intralysosomal cystine accumulates because of a deficiency in the carrier protein cystinosisin, which typically transports cystine out of lysosomes. Three types are recognized, all autosomal recessive: nephropathic, late-onset (or intermediate), and benign. Cystine crystals accumulate in the cornea and conjunctiva in all 3 types, but retinopathy develops only in patients with the nephropathic type; these patients present early (8 to 15 months of age) with progressive renal failure, growth delays, renal rickets, and hypothyroidism. The retinopathy is characterized by areas of patchy depigmentation of the RPE alternating with irregularly distributed pigment clumps and associated fine retinal crystals, but no significant visual disturbance. Treatment with cysteamine may be beneficial. *Bietti crystalline dystrophy* may also cause crystalline keratopathy and retinopathy associated with patchy loss of the choriocapillaris and RPE and with associated photoreceptor loss.

Oishi A, Oishi M, Miyata M, et al. Multimodal imaging for differential diagnosis of Bietti crystalline dystrophy. *Ophthalmol Retina*. 2018;2(10):1071–1077.

Mitochondrial Disorders

Chronic progressive external ophthalmoplegia (CPEO) belongs to a group of diseases collectively termed *mitochondrial myopathies* (Fig 13-10), in which mitochondria are abnormally shaped and increased in number. Muscle biopsy specimens may reveal ragged red fibers. In addition to CPEO, the syndrome is associated with atypical RP and various systemic abnormalities. When associated with cardiomyopathy and cardiac conduction defects (heart block), the disorder is known as *Kearns-Sayre syndrome*; onset is usually before the age of 10 years. The severity of the pigmentary retinopathy is highly variable. Many patients retain good visual function and a normal ERG signal. Other mitochondrial myopathies with pigmentary retinopathy include *MIDD* (*maternally inherited diabetes and deafness*; Fig 13-11), *MELAS* (*mitochondrial encephalomyopathy, lactic acidosis, and stroke*), and *NARP* (*neurogenic muscle weakness, ataxia, and retinitis pigmentosa*) syndromes.

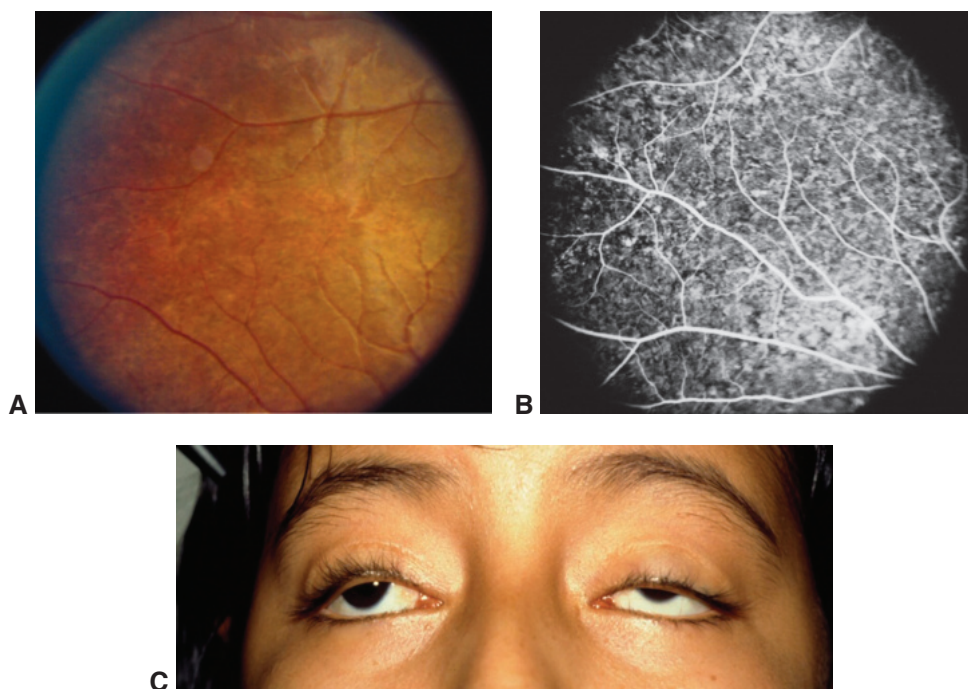


Figure 13-10 Chronic progressive external ophthalmoplegia (CPEO) and retinopathy associated with mitochondrial myopathy. **A**, Fundus photograph shows diffuse RPE mottling. **B**, Corresponding mottled hyper- and hypofluorescence in the arteriovenous phase of fluorescein angiography. **C**, Photograph shows bilateral ptotic eyelids and eyes in a misaligned exotropic position from poor extraocular muscle function, features consistent with CPEO caused by a mitochondrial mutation. (Courtesy of David Sarraf, MD.)

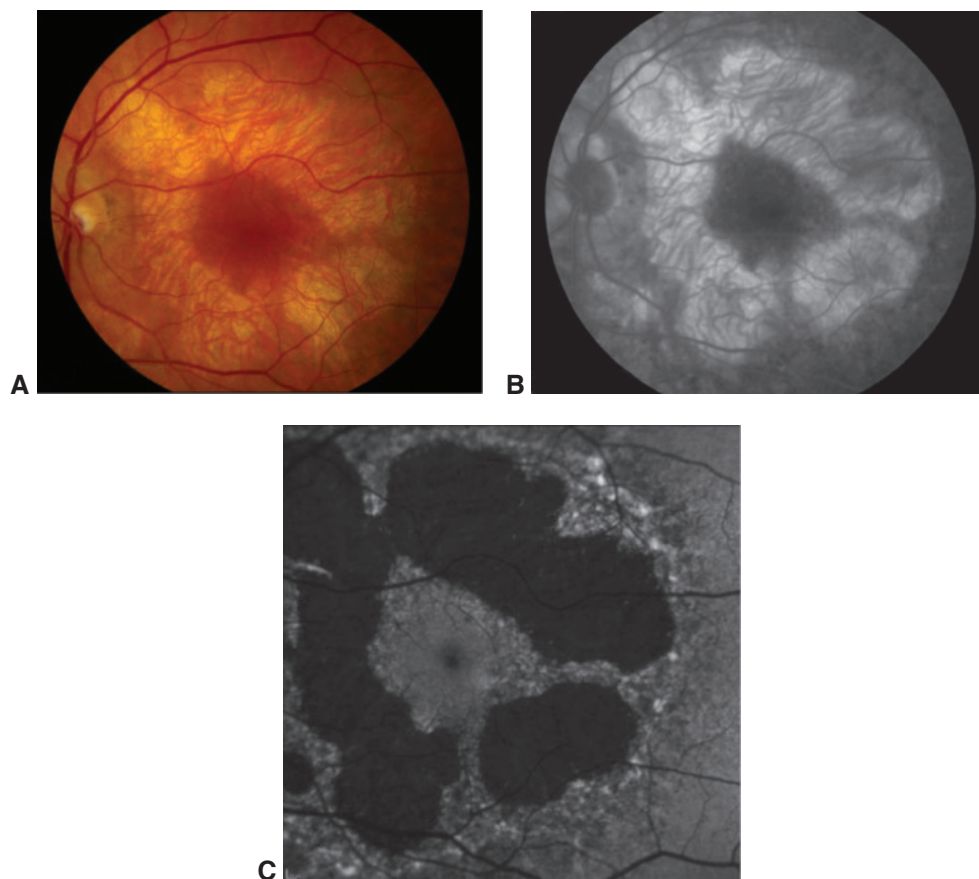


Figure 13-11 Maternally inherited diabetes and deafness (MIDD) caused by a mitochondrial mutation. Color fundus photograph **(A)**, late fluorescein angiography frame **(B)**, and fundus autofluorescence image **(C)** show RPE atrophy in a perifoveal distribution. These findings were all symmetrically present in the fellow eye. (Courtesy of Herb Cantrill, MD.)

Systemic Drug–Induced Retinal Toxicity

Highlights

- Early detection of hydroxychloroquine toxicity is critical and requires the presence of abnormalities on 2 modalities (spectral-domain optical coherence tomography [OCT] and automated threshold visual field testing).
- In Asian patients with hydroxychloroquine toxicity, more peripheral changes may develop, which are best captured with long OCT scans and Humphrey 24-2 or 30-2 visual fields.
- Tamoxifen-related maculopathy can have many of the same features as macular telangiectasia type 2 (MacTel 2) and should be considered in the differential diagnosis of MacTel 2.

Overview

Retinal toxicities caused by systemic therapeutic agents may be categorized according to the retinal level affected and the pattern of toxicity. Broadly, these toxicities manifest as (1) abnormalities at the level of the retinal pigment epithelium (RPE)/photoreceptor complex; (2) occlusive retinopathy or microvasculopathy; (3) ganglion cell and optic nerve damage; and (4) other abnormalities, which include macular edema, crystalline retinopathy, and alterations in color vision and electroretinogram (ERG) responses.

Drugs Causing Abnormalities of the Retinal Pigment Epithelium/Photoreceptor Complex

Chloroquine Derivatives

Although retinal toxicity from *chloroquine* use remains a problem in many parts of the world, it is rare in the United States, where this medication has largely been replaced by the much safer, related drug *hydroxychloroquine*. These medications are used for the treatment of malaria and rheumatologic and dermatologic diseases. Both medications bind to melanin in the RPE, which may concentrate or prolong their effects. Although the

incidence of toxicity is low, it is a serious concern because associated vision loss rarely recovers. Patients and their primary care physicians must be made aware of the ophthalmic risks and the need for regular screening examinations to detect retinal toxicity at an early stage, before vision loss occurs. Typical symptoms include paracentral scotomata, central vision decline, and/or reading difficulty.

The earliest signs of toxicity include bilateral paracentral visual field defects and/or inner segment ellipsoid loss in a paracentral location, which appears as the “flying saucer” sign on spectral-domain optical coherence tomography (SD-OCT) images (Fig 14-1). However, most patients of Asian descent will show initial damage in a more peripheral distribution outside the macular area (Fig 14-2). When there is continued drug exposure, progressive pigmentary changes may develop, and a bilateral atrophic bull’s-eye maculopathy may ensue (Fig 14-3). End-stage cases of advanced toxicity may show panretinal degeneration that simulates retinitis pigmentosa. In some patients, corneal intraepithelial deposits, usually referred to as *cornea verticillata*, may also be noted.

Ophthalmic screening of patients receiving chloroquine or hydroxychloroquine is aimed primarily at early detection and minimization of toxicity. As summarized in a 2016 Clinical Statement from the American Academy of Ophthalmology (<https://www.aao.org/clinical-statement/revised-recommendations-on-screening-chloroquine-h>), the risk of toxicity is low for individuals who have no complicating conditions and take less than 6.5 mg/kg/d of hydroxychloroquine or 3 mg/kg/d of chloroquine. The most recent data suggest that a hydroxychloroquine dosage of 5 mg/kg/d or less and a chloroquine dosage of 2.3 mg/kg/d or less based on the patient’s real body weight may be safer across all body mass indexes than the dosage recommendation of 6.5 mg/kg/d and 3 mg/kg/d, respectively using the patient’s ideal body weight.

Cumulative total doses greater than 1000 g of hydroxychloroquine and 460 g of chloroquine place patients at high risk of toxicity. Additional risk factors include duration of use (>5 years), kidney disease, concomitant use of tamoxifen (fivefold increase), and concomitant

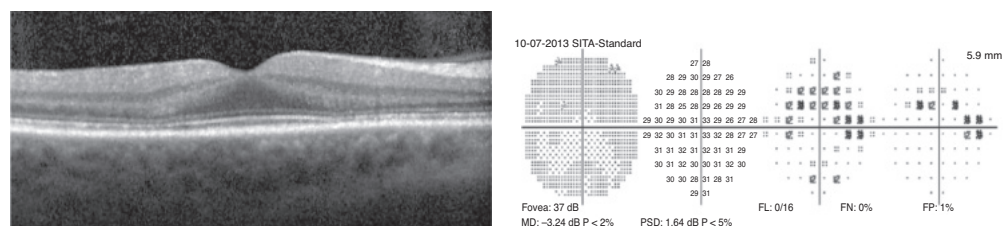


Figure 14-1 Spectral-domain optical coherence tomography (SD-OCT) image and Humphrey visual field (HVF) from a 50-year-old woman who had been using Plaquenil 400 mg daily for 10 years to treat systemic lupus erythematosus. Notably, she also had lupus-related nephrotic syndrome. Her Plaquenil dosage, which was based on actual body weight, was 4.4 mg/kg/d. She was completely asymptomatic. However, SD-OCT (*left*) showed attenuation of the ellipsoid zone and interdigitation zone in a perifoveal pattern, with early “flying saucer” sign with relative preservation of the central photoreceptors. Given the characteristic superior arcuate defect on the 10-2 HVF (*right*), Plaquenil was stopped. It is likely that renal disease accelerated the presentation in this patient despite the dose being within the American Academy of Ophthalmology recommendation of 5 mg/kg/d or less. Therefore, clinicians should maintain heightened vigilance in patients with renal disease, especially when no alternatives to Plaquenil can be safely used.

(Courtesy of Amani Fawzi, MD.)

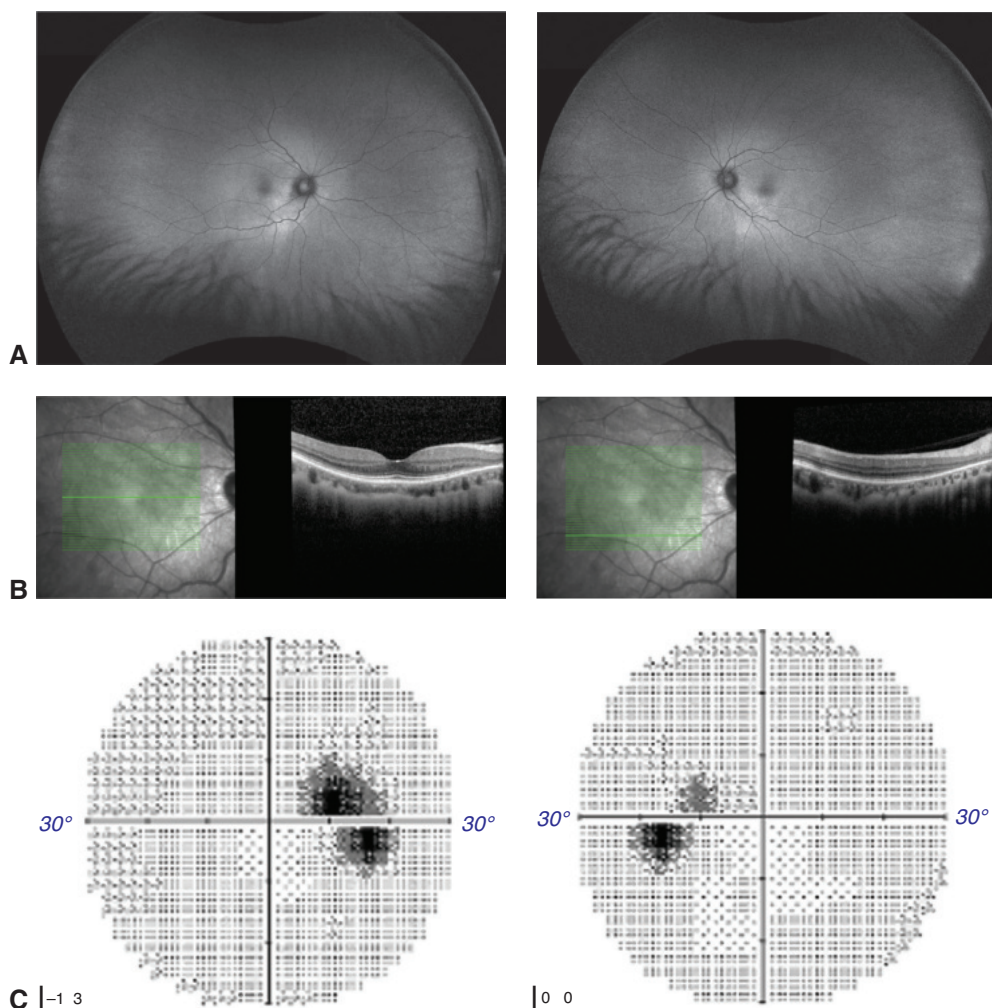


Figure 14-2 Peripheral retinal manifestations of hydroxychloroquine toxicity in Asian patients. **A**, Fundus autofluorescence (FAF) shows hyperautofluorescence along the inferior arcade in both eyes. **B**, OCT scan through the right fovea (*left*) shows disruption of the outer retina and loss of the ellipsoid zone temporal to the optic nerve. More inferior scans (*right*) highlight the extension of this loss along the inferior arcade. This photoreceptor loss explains the unmasking of the retinal pigment epithelium (RPE) autofluorescence and relative hyperautofluorescence in this region. **C**, 30-2 HVF illustrates the peripheral localization of the visual field defects, which would be missed on 10-2 HVF. (Courtesy of Amani Fawzi, MD.)

retinal disease such as age-related macular degeneration. The latter can also make early detection of toxicity difficult. Furthermore, well-documented but rare cases of hydroxychloroquine maculopathy have occurred with “safe” daily doses and in the absence of other risk factors.

Baseline evaluation for patients beginning treatment with a chloroquine derivative should include a complete ophthalmic examination. For follow-up comparison, the ophthalmologist can employ SD-OCT as well as automated threshold visual field testing with a white pattern (Humphrey white 10-2 protocol), although some clinicians prefer red for

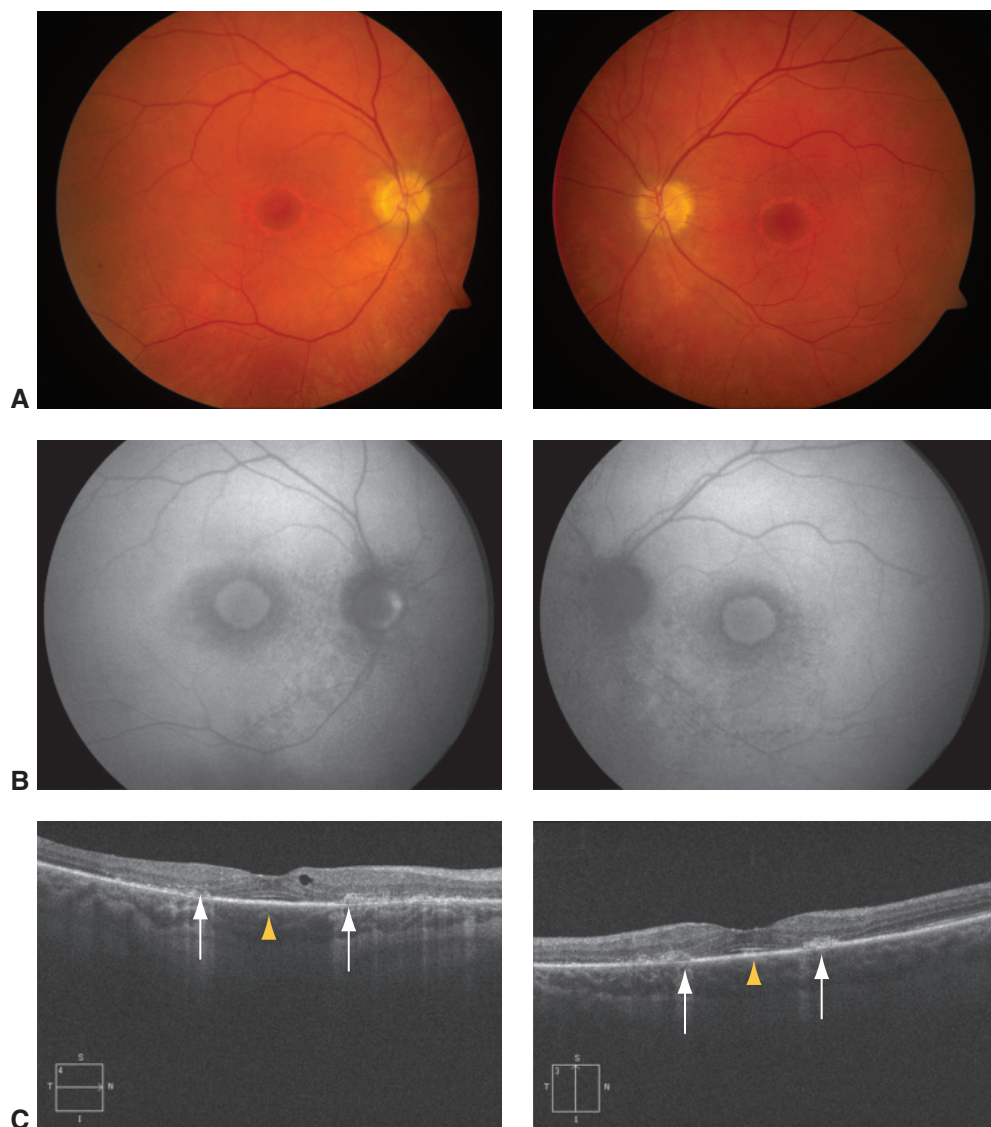


Figure 14-3 Bilateral, symmetric bull's-eye maculopathy in a patient with hydroxychloroquine toxicity. **A**, Fundus photographs of right and left eyes. **B**, Corresponding FAF images. **C**, SD-OCT images demonstrate the characteristic "flying saucer" sign (*arrowhead*): the ovoid appearance of the central fovea due to preservation of the outer retinal structures in the central fovea surrounded by perifoveal loss of the outer retinal structures. With progression of the toxic effect, pigment migration into the outer retina can be seen (*arrows*). (Courtesy of Stephen J. Kim, MD.)

its increased sensitivity. In Asian patients with hydroxychloroquine toxicity, more peripheral changes may develop, which are best captured with long OCT scans and Humphrey 24-2 or 30-2 visual fields.

Current guidelines recommend a baseline fundus examination within the first year of use and then annual screening after 5 years of use in patients at low risk for toxicity.

However, many practitioners screen patients every 6 to 12 months with a combination of Humphrey 10-2 testing and SD-OCT for 5 years and then every 6 months thereafter. Patients who are at risk of toxicity or who have unclear symptoms can be further assessed with fundus autofluorescence and multifocal electroretinography (mfERG). Signs of toxicity include a paracentral ring of hyperautofluorescence or hypoautofluorescence and paracentral mfERG depressions.

- Marmor MF, Kellner U, Lai TY, Melles RB, Mieler WF; American Academy of Ophthalmology. Recommendations on screening for chloroquine and hydroxychloroquine retinopathy (2016 revision). *Ophthalmology*. 2016;123(6):1386–1394.
- Melles RB, Marmor MF. Pericentral retinopathy and racial differences in hydroxychloroquine toxicity. *Ophthalmology*. 2015;122(1):110–116.
- Melles RB, Marmor MF. The risk of toxic retinopathy in patients on long-term hydroxy-chloroquine therapy. *JAMA Ophthalmol*. 2014;132(12):1453–1460.
- Mititelu M, Wong BJ, Brenner M, Bryar PJ, Jampol LM, Fawzi AA. Progression of hydroxy-chloroquine toxic effects after drug therapy cessation: new evidence from multimodal imaging. *JAMA Ophthalmol*. 2013;131(9):1187–1197. doi:10.1001/jamaophthalmol.2013.4244

Phenothiazines

Phenothiazines, including *chlorpromazine* and *thioridazine*, are antipsychotic tranquilizing medications that are concentrated in uveal tissue and RPE by binding to melanin granules. High-dose chlorpromazine therapy commonly causes abnormal pigmentation of the eyelids, interpalpebral conjunctiva, cornea, and anterior lens capsule. Anterior and posterior subcapsular cataracts may also develop. However, pigmentary retinopathy from chlorpromazine therapy is unusual.

In contrast, high-dose thioridazine treatment can cause development of a severe pigmentary retinopathy within a few weeks or months of dosing initiation (Fig 14-4). Toxicity is rare at doses of 800 mg/d or lower. Initially, patients experience blurred vision, and the fundus shows coarse RPE stippling in the posterior pole. Eventually, patchy nummular atrophy of the RPE and choriocapillaris may develop. The late stages may be mistaken for choroideremia or Bietti crystalline dystrophy; late-stage signs and symptoms include visual field loss and nyctalopia (night blindness).

Generally, patients receiving thioridazine are not monitored ophthalmoscopically because toxicity is rare at standard doses. However, symptomatic patients or patients suspected of having a toxic reaction, especially those who have taken high doses of the drug, should undergo a full retinal examination.

Miscellaneous Medications

Other systemic medications that can induce toxicity of the RPE include clofazimine, deferoxamine (Fig 14-5), and nucleoside reverse transcriptase inhibitors (NRTIs; Table 14-1). *Clofazimine* is a phenazine dye used to treat dapsone-resistant leprosy and various autoimmune disorders, such as psoriasis and systemic lupus erythematosus. Its toxicity manifests as a bull's-eye maculopathy. *Deferoxamine*, an iron-chelating agent, can cause reticular or vitelliform pigment epithelial changes in the macula (see Fig 14-5B) and can

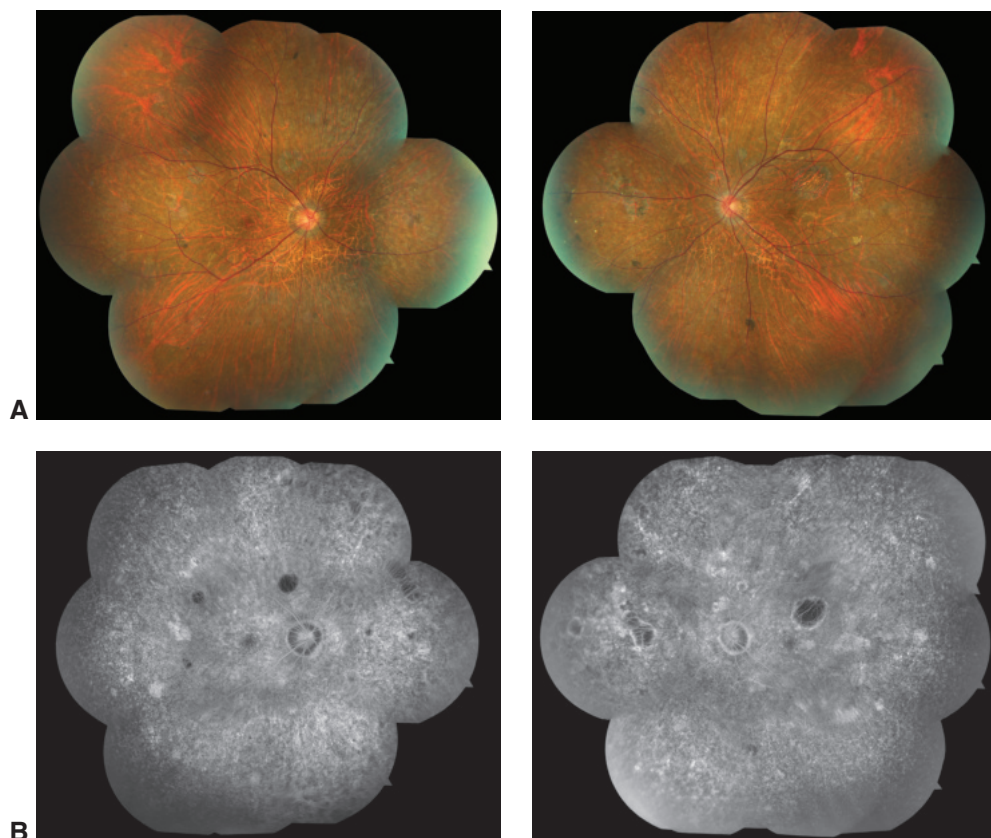


Figure 14-4 Thioridazine toxicity in a patient with schizophrenia. **A**, Fundus photograph montages of right and left eyes. **B**, Corresponding fluorescein angiography montages. Note the diffuse nummular loss of RPE in the posterior pole and periphery of each eye. (Courtesy of David Sarraf, MD.)

be associated with macular edema caused by RPE pump failure. NRTIs such as didanosine (formerly, *dideoxydinostine*) have been used in the systemic treatment of patients infected with HIV to inhibit replication of the virus. This class of medications can cause mitochondrial toxicity and damage to tissues with high oxygen requirements, such as the optic nerve and RPE. Patients may develop peripheral vision loss associated with a bilateral, symmetric, and midperipheral pattern of concentric mottling and atrophy of the RPE and choriocapillaris.

Mitogen-activated protein kinase kinase (MEK) inhibitors, a class of drugs used as chemotherapeutic agents in the treatment of metastatic cancers, can cause a condition similar to central serous chorioretinopathy. This condition is characterized by multifocal serous retinal detachments (Fig 14-6). *Immune checkpoint inhibitors*, a class of immunomodulatory drugs for treatment of metastatic cancers, have been associated with a variety of ocular manifestations, including serous retinal detachments, all thought to be related to autoimmune dysregulation. In rare instances, the use of *sildenafil* has been associated with serous macular detachment and central serous chorioretinopathy, presumably

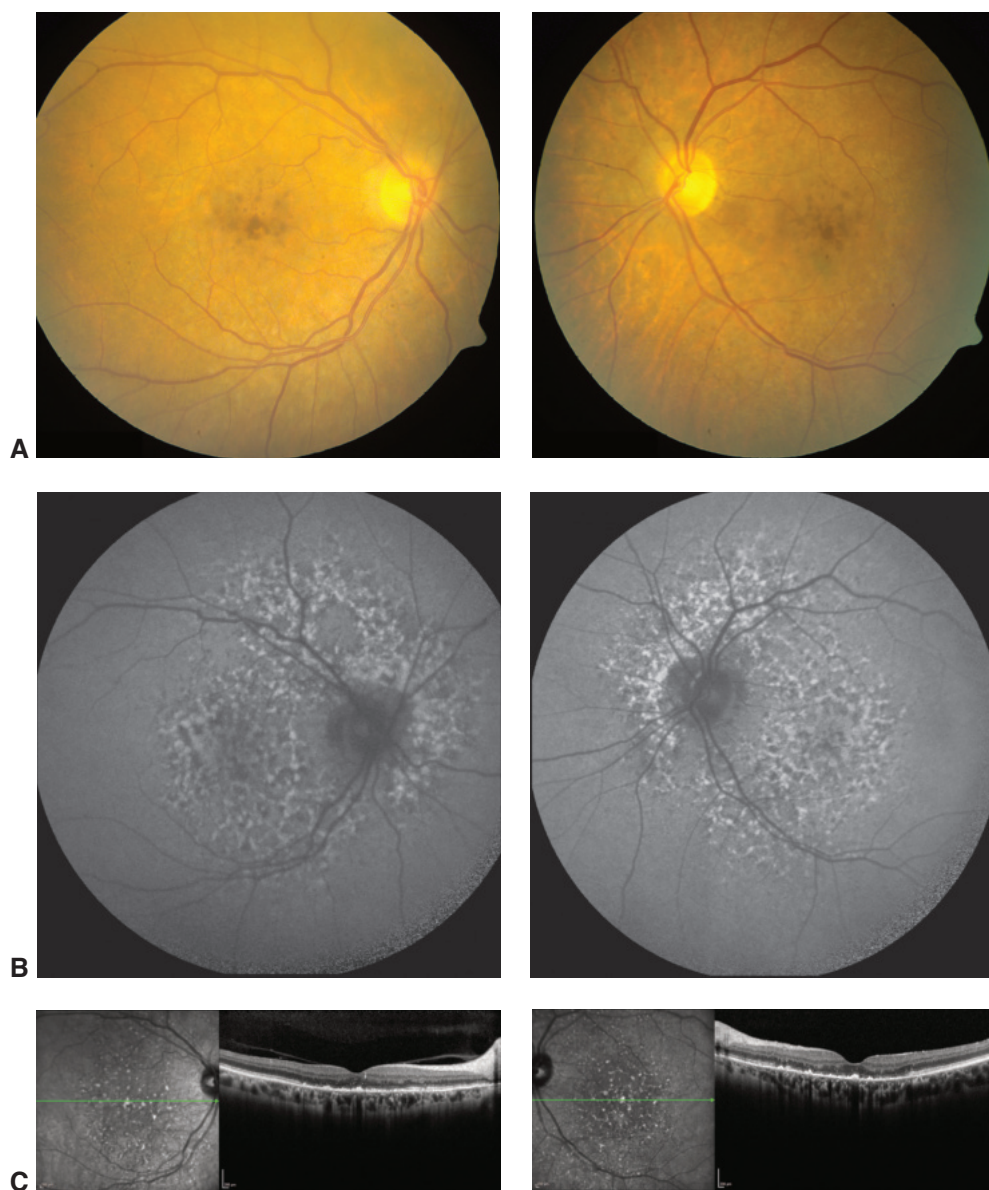


Figure 14-5 Deferoxamine (also called *desferrioxamine*) toxicity. **A**, Fundus photographs show pigmentary macular changes in a patient with sickle cell disease who was receiving deferoxamine for transfusional hemosiderosis. **B**, Corresponding FAF images highlight the classic reticular pigment epithelial changes. **C**, SD-OCT demonstrates ellipsoid loss and hyperreflective deposits at the level of the RPE. (Courtesy of Kenneth Taubenslag, MD, Edward Cherney, MD, and Anita Agarwal, MD.)

caused by choroidal vascular dilation and choroidal congestion manifesting as increased choroidal thickness on enhanced depth imaging (EDI) SD-OCT. *Corticosteroids* are the most common medications to be associated with the development of central serous chorioretinopathy.

Table 14-1 Miscellaneous Medications Causing RPE/Photoreceptor Complex Toxicity

Medication	Use	Complication
Alkyl nitrites (poppers)	Recreational use; euphoric and smooth muscle relaxant usually used in preparation for male-male sexual contact	Foveal outer retinal defect at the photoreceptor level
Clofazimine	Treatment of dapsone-resistant leprosy, autoimmune disorders	Bull's-eye maculopathy
Corticosteroids	Many indications	Central serous chorioretinopathy
Deferoxamine	Iron-chelating agent	Reticular or vitelliform maculopathy
Didanosine (dideoxyinosine)	Nucleoside reverse transcriptase inhibitor; inhibit replication of HIV	Macular edema Mitochondrial toxicity Peripheral pigmentary retinopathy
Immune checkpoint inhibitors	Immunomodulatory therapy for metastatic cancer	Various ocular manifestations, serous retinal detachment, inflammatory
Mitogen-activated protein kinase kinase (MEK) inhibitors	Chemotherapeutic, for metastatic cancer	Multifocal serous retinal detachments, self-limited
Pentosan polysulfate sodium	Treatment of interstitial cystitis	Maculopathy with pigmentary changes and dark-adaptation defects

RPE = retinal pigment epithelium.

Alkyl nitrites (“poppers”) are a class of drugs used for recreation and can cause a toxic maculopathy. Patients present with a central scotoma or photopsia. Fundus examination may reveal a yellow spot on the fovea. SD-OCT imaging may reveal focal disruption of the central inner segment ellipsoid band, indicating an abnormality of the foveal cones (Fig 14-7).

Pentosan polysulfate sodium, which is approved by the US Food and Drug Administration for the treatment of interstitial cystitis, has recently been associated with a pigmentary maculopathy with characteristic bilateral findings of parafoveal pigmentary changes, dense hypo- and hyperautofluorescence, and nodular RPE thickening on OCT (Fig 14-8).

Dalvin LA, Shields CL, Orloff M, Sato T, Shields JA. Checkpoint inhibitor immune therapy: systemic indications and ophthalmic side effects. *Retina*. 2018;38(6):1063–1078.

Davies AJ, Kelly SP, Naylor SG, et al. Adverse ophthalmic reaction in poppers users: case series of ‘poppers maculopathy’. *Eye (Lond)*. 2012;26(11):1479–1486.

Gabrielian A, MacCumber MM, Kukuyev A, Mitsuyasu R, Holland GN, Sarraf D. Didanosine-associated retinal toxicity in adults infected with human immunodeficiency virus. *JAMA Ophthalmol*. 2013;131(2):255–259.

McCannel TA, Chmielowski B, Finn RS, et al. Bilateral subfoveal neurosensory retinal detachment associated with MEK inhibitor use for metastatic cancer. *JAMA Ophthalmol*. 2014;132(8):1005–1009.

Pearce WA, Chen R, Jain N. Pigmentary maculopathy associated with chronic exposure to pentosan polysulfate sodium. *Ophthalmology*. 2018;125(11):1793–1802.

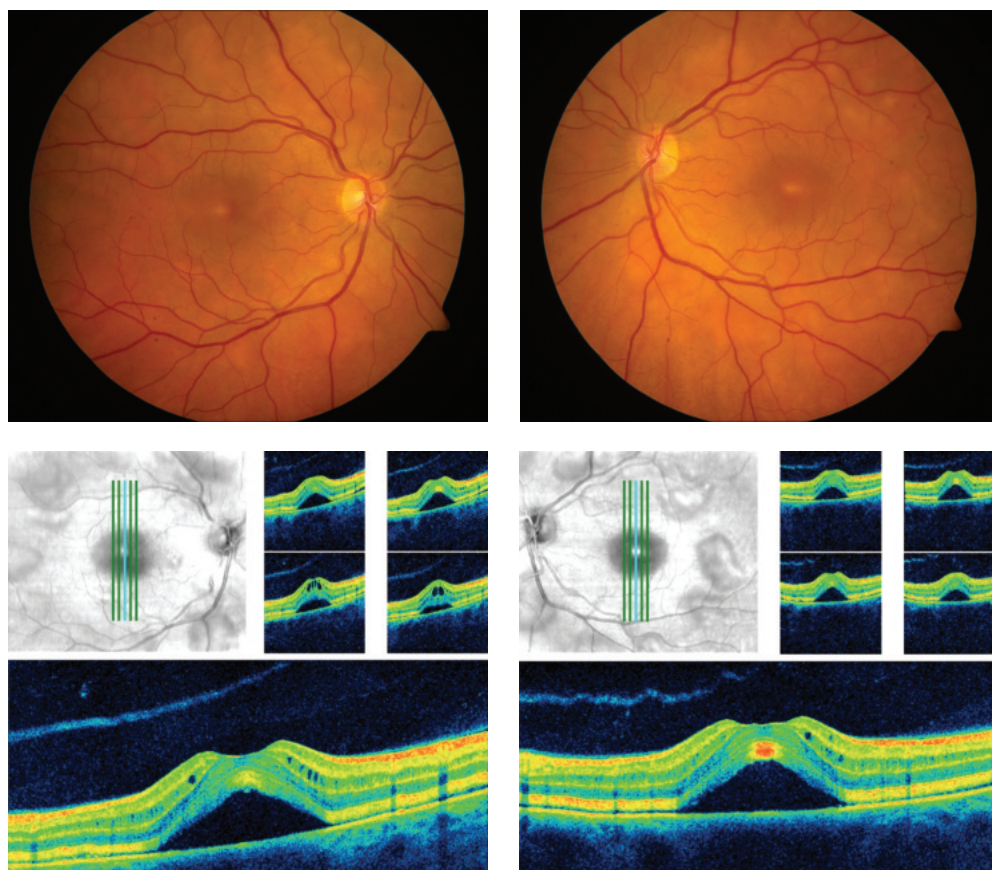


Figure 14-6 MEK toxicity. Fundus photographs and OCT images of both eyes demonstrate multifocal serous detachments involving the fovea and the area around the arcades. The patient reported decreased vision 3 weeks after starting the MEK inhibitor trametinib for metastatic cutaneous melanoma. Subsequent stoppage of trametinib resulted in complete resolution. (Courtesy of Stephen J. Kim, MD.)

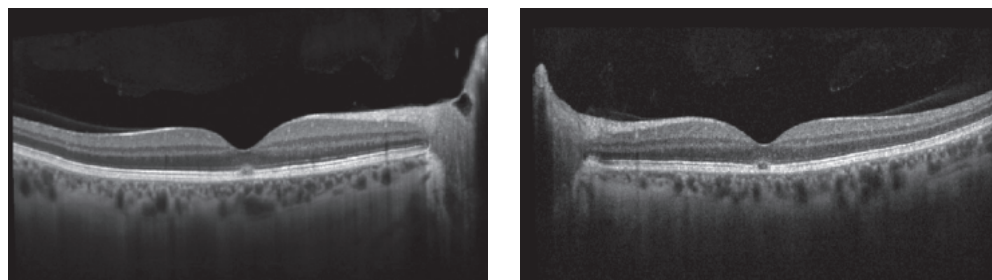


Figure 14-7 SD-OCT images from a 40-year-old man with a 6-month history of blurred vision, who admitted to long-term use of alkyl nitrites (“poppers”). Corrected distance visual acuity (also called *best-corrected visual acuity*) was 20/40 OD, 20/50 OS. SD-OCT of both eyes showed bilateral focal disruption of the central inner segment ellipsoid band in the fovea. (Courtesy of Manjot K. Gill, MD.)

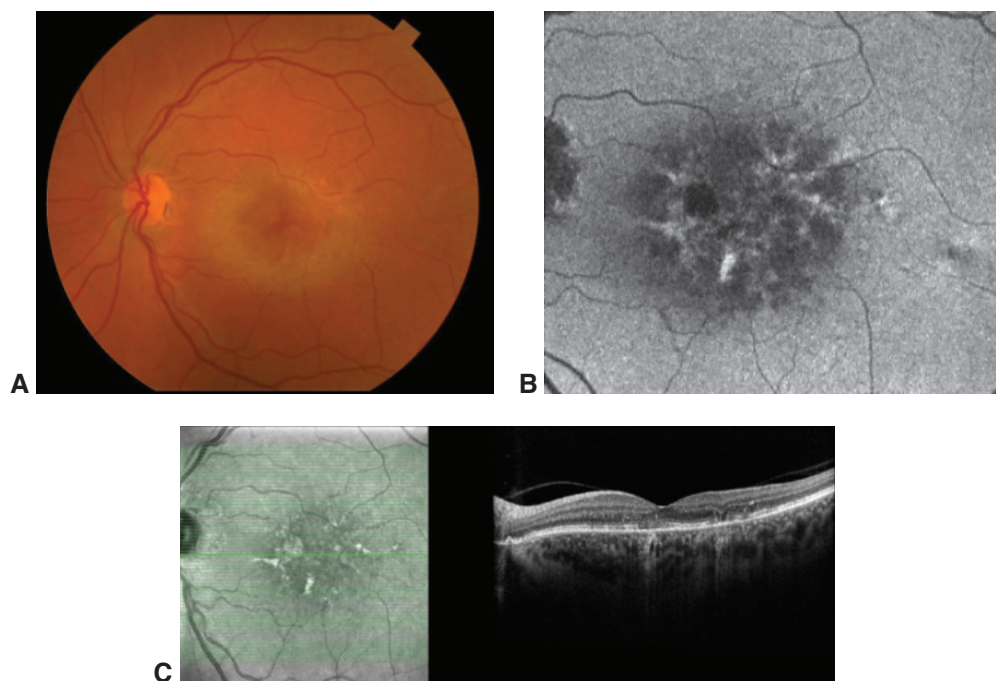


Figure 14-8 Presumed pentosan polysulfate toxicity. A 64-year-old woman reported a yellow discoloration to her vision and difficulties adjusting to light. She had been using pentosan polysulfate sodium for 30 years to treat interstitial cystitis. **A**, Color fundus photograph shows subtle pigmentary changes, while FAF (**B**) and infrared (**C**, left) images reveal alternating hyper- and hypoautofluorescent/reflective lesions that are characteristic. **C** (right), OCT shows subtle photoreceptor and RPE changes. (Courtesy of Amani Fawzi, MD.)

Drugs Causing Occlusive Retinopathy or Microvasculopathy

Interferon alfa-2a is an antiviral and immunomodulatory drug used for the treatment of viral hepatitis. This treatment may be complicated by the development of cotton-wool spots and retinal hemorrhages. *Ergot alkaloids* (vasoconstrictors used to treat migraine) and oral contraceptives have been associated with thrombotic complications, including retinal vein and retinal artery occlusions. *Procainamide* is an antiarrhythmic agent that can induce systemic lupus erythematosus and cause extensive “pruning” of second-order retinal vessels and infarction of the retina, leading to severe vision loss.

A few drugs administered intraocularly but not systemically deserve special mention. The aminoglycosides *amikacin* and especially *gentamicin* antibiotics can cause macular infarction and severe macular ischemia, leading to irreversible central vision loss. Recently, intracameral *vancomycin*, used for prophylaxis of endophthalmitis, has been associated with hemorrhagic occlusive retinal vasculitis (HORV). Postmarketing research studies of *brovacizumab*, a newer anti-vascular endothelial growth factor agent approved for the treatment of neovascular age-related macular degeneration, have reported an association with intraocular inflammation and occlusive retinal vasculitis.

- Baumal CR, Spaide RF, Vajzovic L, et al. Retinal vasculitis and intraocular inflammation after intravitreal injection of brodalumab. *Ophthalmology*. 2020;127(10):1345–1359.
- Narkewicz MR, Rosenthal P, Schwarz KB, et al; PEDS-C Study Group. Ophthalmologic complications in children with chronic hepatitis C treated with pegylated interferon. *J Pediatr Gastroenterol Nutr*. 2010;51(2):183–186.
- Raza A, Mittal S, Sood GK. Interferon-associated retinopathy during the treatment of chronic hepatitis C: a systematic review. *J Viral Hepat*. 2013;20(9):593–599.
- Witkin AJ, Shah AR, Engstrom RE, et al. Postoperative hemorrhagic occlusive retinal vasculitis: expanding the clinical spectrum and possible association with vancomycin. *Ophthalmology*. 2015;122(7):1438–1451.

Drugs Causing Ganglion Cell Damage and Optic Neuropathy

Quinine is used as a muscle relaxant for leg cramps and as an antimalarial. It has a narrow therapeutic index that is safe at doses under 2 g, but it causes morbidity at doses greater than 4 g and mortality at doses greater than 8 g. At toxic levels, acute severe vision loss may occur as a result of retinal ganglion cell toxicity, mimicking a central retinal artery occlusion. A cherry-red spot may be observed, and SD-OCT imaging may demonstrate ganglion cell layer thickening and hyperreflectivity. Diffuse inner retinal atrophy will ensue, accompanied by retinal vascular attenuation and optic atrophy. Full-field ERG testing will show a negative waveform, similar to that observed with a central retinal artery occlusion (Fig 14-9). Blindness caused by quinine toxicity is permanent.

Methanol toxicity, usually occurring as a result of ingesting contaminated or “cheap” alcohol, causes acute blindness. Posterior segment manifestations include acute transient optic nerve head and macular edema. In histologic studies of acute methanol toxicity, the retina, RPE, and optic nerve demonstrate vacuolization, a sign of cell death. Eventually, optic atrophy and occasionally retinal vascular attenuation caused by diffuse ganglion cell loss may develop. Full-field ERG testing shows a negative waveform. The most commonly reported sequela of methanol toxicity is optic atrophy.

Drugs Causing Macular Edema

The *taxanes* are a class of microtubule inhibitors that include *paclitaxel*, albumin-bound *paclitaxel*, and *docetaxel*. These drugs are employed as chemotherapeutics for the treatment of various cancers, including breast carcinoma. In rare cases, they are associated with cystoid macular edema (CME) that is visible on examination or SD-OCT but not on fluorescein angiography. Similarly, the cholesterol-lowering agent niacin, also called *nicotinic acid*, can produce angiographically silent CME. Initially, central vision may be impaired, but full recovery follows discontinuation of the drug and resolution of the cystoid edema.

The glitazones *rosiglitazone* and *pioglitazone* are oral hypoglycemics used for the treatment of diabetes mellitus. They can cause severe fluid retention, leading to pulmonary edema, and are occasionally associated with the development or exacerbation of macular edema. *Fingolimod*, an oral agent used in the management of relapsing forms of multiple sclerosis, can infrequently cause macular edema, usually within 3 months of initiation of treatment; the

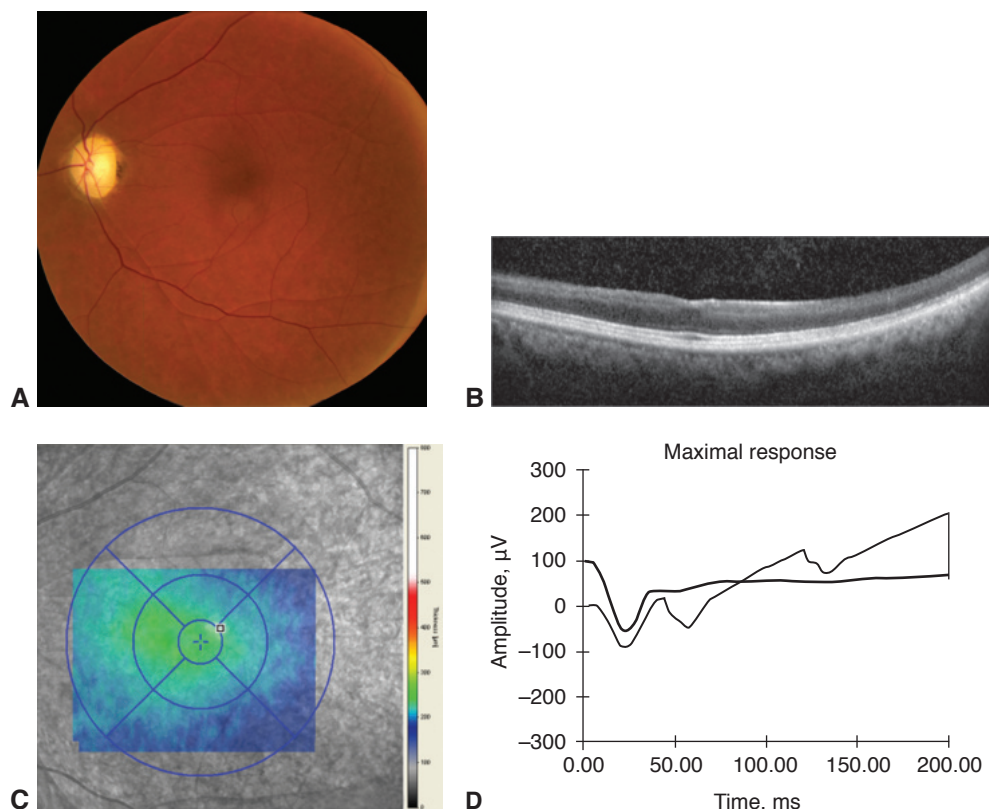


Figure 14-9 Quinine toxicity. **A**, Fundus photograph shows optic nerve head pallor and retinal vascular attenuation. **B**, SD-OCT image demonstrates diffuse inner retinal atrophy. **C**, OCT map analysis shows diffuse retinal thinning. **D**, Full-field electroretinogram shows an electronegative response (the positive b-wave amplitude is less than the negative a-wave amplitude). (Courtesy of David Sarraf, MD.)

edema resolves with cessation but warrants monitoring and differentiation of visual symptoms related to optic neuritis. Topical *prostaglandin F_{2α}* analogs, used in treating glaucoma, have been reported in small case series to cause macular edema. *Deferoxamine* may also cause secondary macular edema due to RPE toxicity, as mentioned earlier in the chapter.

Drugs Causing Crystalline Retinopathy

Crystalline retinopathies can be caused by systemic medications and other agents and can be associated with several ocular and systemic diseases; these diseases are discussed elsewhere in this book or the BCSC series (Fig 14-10, Table 14-2). *Tamoxifen* is an antiestrogen drug used as adjuvant therapy following primary treatment of breast cancer. Retinopathy is rare at typical doses (20 mg daily), but crystalline retinopathy has been reported in patients receiving high-dose tamoxifen therapy (daily doses >200 mg or cumulative doses

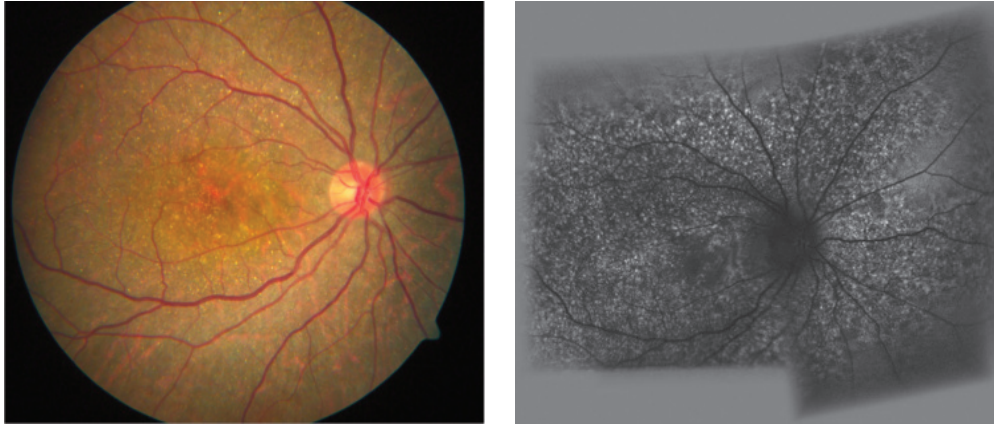


Figure 14-10 Fundus photograph (*left*) shows scattered hyperreflective, crystalline lesions throughout the fundus in a patient with Bietti crystalline dystrophy. FAF image (*right*; same patient) illustrates the hyperautofluorescent crystalline deposits as well as hypoautofluorescence seen in areas of RPE atrophy. (Reproduced from Berry JL, Fawzi A. *Heritable disorders of the retinal pigment epithelium, Bruch's membrane, and the choriocapillaris*. In: Wright KW, Strube YNJ. *Pediatric Ophthalmology and Strabismus*. 3rd ed. Oxford University Press; 2012, Figures 2 and 28. Copyright 2012, used with permission.)

Table 14-2 Causes of Crystalline Retinopathy

Systemic diseases

- Cystinosis
- Primary hereditary hyperoxaluria (primary oxalosis)
- Sjögren-Larsson syndrome

Drug-induced causes

- Canthaxanthine toxicity
- Ethylene glycol ingestion (secondary oxalosis)
- Methoxyflurane anesthesia (secondary oxalosis)
- Nitrofurantoin toxicity
- Talc emboli (caused by long-term intravenous drug use with methylphenidate)
- Tamoxifen toxicity (see Fig 14-11)
- Triamcinolone acetonide injection–associated crystalline maculopathy (caused by intravitreal triamcinolone injection)

Ocular diseases

- Bietti crystalline dystrophy (see Fig 14-10)
- Calcific drusen
- Gyrate atrophy
- Retinal telangiectasia

>100 g). The maculopathy is characterized by brilliant inner retinal crystalline deposits clustered around the fovea and may be associated with CME and substantial vision loss in severe cases; it may be irreversible. In rare instances, SD-OCT imaging has revealed central loss of the inner segment ellipsoid band in patients receiving low-dose tamoxifen therapy, without crystals visible on ophthalmoscopic examination (Fig 14-11). On fluorescein angiography and OCT angiography, eyes with tamoxifen maculopathy may also

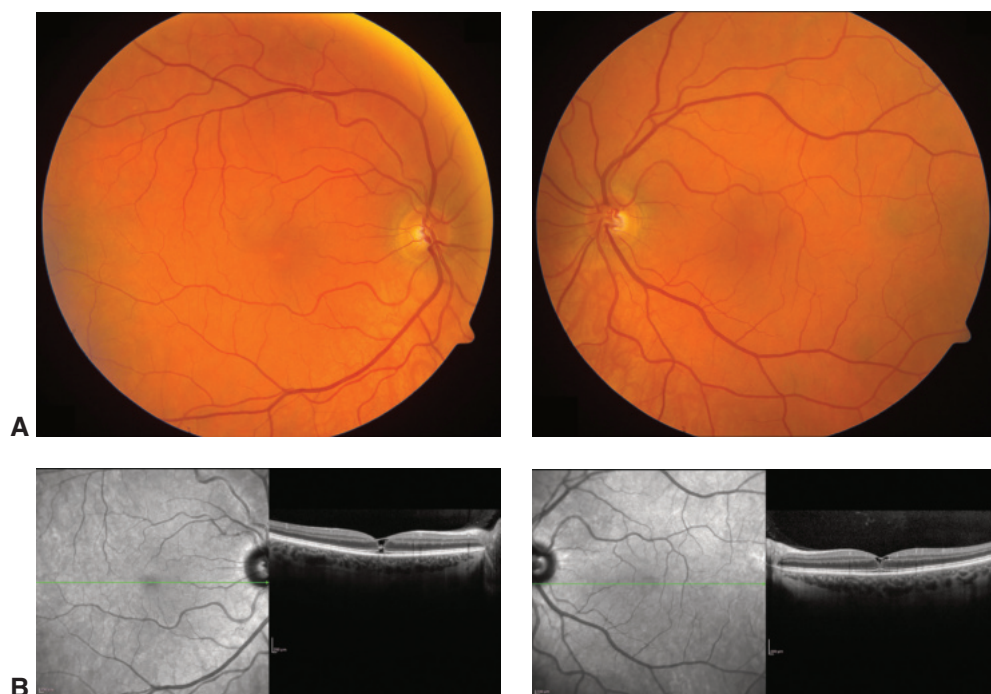


Figure 14-11 Crystalline retinopathy in a woman receiving tamoxifen for treatment of breast cancer. **A**, Fundus photographs show punctate pigmentary changes. Rare inner retinal crystals were noted on slit-lamp biomicroscopy. **B**, SD-OCT of the right eye shows subtle but characteristic inner layer foveal cystic changes with central disruption and loss of the ellipsoid band; the left eye demonstrates inner layer foveal cystic changes only. (Courtesy of Kenneth Taubenslag, MD, and Stephen J. Kim, MD.)

show telangiectasia, masquerading as macular telangiectasia type 2 (MacTel 2); thus, this maculopathy should be considered in the differential diagnosis of MacTel 2.

A crystalline maculopathy may also occur after ingestion of high doses of *canthaxanthine*, a widely available carotenoid used to simulate tanning. In the inner retina, canthaxanthine deposits distribute in a doughnut pattern around the macula, with a predilection for the juxtapapillary region. They do not typically cause vision loss and may resolve after the medication is discontinued.

Intravascular crystalline deposits of oxalate have been observed after the ingestion of *ethylene glycol* and after prolonged administration of *methoxyflurane* anesthesia (an agent that is no longer used in the United States) in patients with renal dysfunction. Other retinal crystals that may be deposited intravascularly include talc emboli, which are injected along with drugs such as methylphenidate in persons who inject drugs. The refractile talc deposits usually embolize in the smaller-caliber perifoveal retinal arterioles and may cause peripheral retinal neovascularization in rare cases; they do not typically cause vision loss.

Drenser K, Sarraf D, Jain A, Small KW. Crystalline retinopathies. *Surv Ophthalmol.* 2006;51(6): 535–549.

Drugs Causing Color Vision or ERG Abnormalities

Phosphodiesterase 5 (PDE-5) inhibitors such as *sildenafil* and *tadalafil* can also partially inhibit PDE-6, an integral enzyme in the phototransduction cascade. Transient blue tinting of vision and temporarily subnormal ERG responses (including a delayed cone b-wave implicit time) have been observed in patients taking high doses of sildenafil. These changes may occur in up to 50% of patients ingesting doses greater than 100 mg, but no permanent retinal toxic effects have been reported. Reversible yellow tinting of vision, or *xanthopsia*, may be caused by the cardiac glycoside *digitalis*.

Some patients taking isotretinoin for the treatment of acne have reported poor night vision and have been found to have abnormal dark-adaptation curves and ERG responses. Toxicity seems to be infrequent but is more likely in patients undergoing repetitive courses of therapy. The changes are largely reversible.

The antiepileptic drug vigabatrin can cause visual field constriction and ERG abnormalities, including depression of the 30-Hz cone amplitude.

Drugs Causing Other Ocular Toxicities

The use of *rifabutin* has been associated with vision loss arising from anterior and posterior uveitis with hypopyon and hypotony. Certain sulfur-derived medications such as *acetazolamide* and *topiramate* can cause medication-induced myopia and associated retinal and choroidal folds and macular edema. Vision loss may be mild (caused by isolated macular folds) or severe (caused by ciliochoroidal effusion, leading to angle-closure glaucoma) and may be reversed with early recognition and prompt discontinuation of the drug. There are rare reports of *bupropion* causing choroidal effusion.

Ocular argyrosis may develop after colloidal silver ingestion over a period longer than 1 year; this condition manifests as ocular pigmentation, black tears, and a dark choroid caused by brown-black granules diffusely deposited in Bruch membrane, which can lead to “leopard spotting” and drusenlike deposition.

Diseases of the Vitreous and Vitreoretinal Interface



This chapter includes related activities. Go to www.aao.org/bcscactivity_section12 or scan the QR codes in the text to access this content.

Highlights

- Posterior vitreous detachment occurs commonly with age and can be associated with vitreous hemorrhage or retinal tears.
- There are 3 recognized categories of vitreomacular traction disease: vitreomacular adhesion, vitreomacular traction syndrome, and macular hole.
- Phenotypically similar to retinopathy of prematurity, familial exudative vitreoretinopathy is characterized by failure of the temporal retina to vascularize in an individual born at full term with normal respiratory status.

Posterior Vitreous Detachment

The vitreous is a transparent gel composed mainly of water, collagen, and hyaluronan (hyaluronic acid) that is attached to the basal lamina of the lens, optic nerve, and retina, and fills the vitreous cavity of the eye. A posterior vitreous detachment (PVD) is the separation of the posterior cortical gel from the retinal surface, including its adhesions at the optic nerve head (the area of Martegiani), macula, and blood vessels. At its base, the vitreous remains firmly attached to the retina. Because of this firm attachment, the basal cortical vitreous collagen cannot be peeled off the retina; instead, the vitreous must be “shaved” during vitrectomy, instead of being removed.

With increasing age, the vitreous gel undergoes both liquefaction (synchysis) and collapse (syneresis). The viscous hyaluronan accumulates in lacunae, which are surrounded by displaced collagen fibers. The gel can then contract. With this contraction, the posterior cortical gel detaches toward the firmly attached vitreous base. Clinical studies typically reveal a low occurrence of PVD in patients younger than 50 years. Autopsy studies demonstrate PVD in less than 10% of patients younger than 50 years but in 63% of those older than 70 years. The prevalence of PVD is increased in conditions such as aphakia, pseudophakia with open posterior capsule, inflammatory disease, trauma, vitreous

hemorrhage, and axial myopia. Localized regions of the posterior cortical gel can separate slowly, over the course of many years, with few if any symptoms, compared with the more acute, symptomatic event. Common symptoms of an acute PVD include the appreciation of floaters that can take many forms or of a cloud that can follow eye movement.

The diagnosis of PVD is often made with indirect ophthalmoscopy or slit-lamp biomicroscopy, with which the posterior vitreous face may be observed a few millimeters in front of the retinal surface. In eyes with a PVD, a translucent ring of fibroglial tissue (the “Weiss” or “Vogt” ring) (Fig 15-1) is frequently torn loose from the surface of the optic nerve head, and its observation helps the clinician make the diagnosis. Although a shallow detachment of the posterior cortical gel may be difficult or impossible to observe with biomicroscopy, this type of detachment may be revealed on contact B-scan ultrasonography as a thin, hyperreflective line bounding the posterior vitreous. Optical coherence tomography (OCT) has shown that PVDs often start as a localized detachment of the vitreous over the perifovea, called a *posterior perifoveal vitreous detachment*, later spreading anteriorly to involve larger areas.

Persistent focal attachment of the vitreous to the retina can cause a number of pathologic conditions. Vitreous contraction as well as traction caused by ocular saccades may lead to breaks, particularly at the posterior edge of the vitreous base. Persistent attachment to the macula may lead to vitreomacular traction syndrome (Fig 15-2). Focal attachment to the foveola can induce foveal cavitation and macular hole formation. Remnants of the vitreous often remain on the internal limiting membrane (ILM) after a posterior vitreous “detachment.” For this reason, some authorities state that a presumed PVD often is actually posterior vitreoschisis that is internal or external to the layer of hyalocytes. These vitreous remnants may have a role in epiretinal membrane or macular hole formation and can contribute to traction detachments in patients with pathologic myopia and to macular edema in patients with diabetes. Plaques of these adherent remnants of cortical vitreous can often be highlighted during vitreous surgery by applying triamcinolone (Fig 15-3).

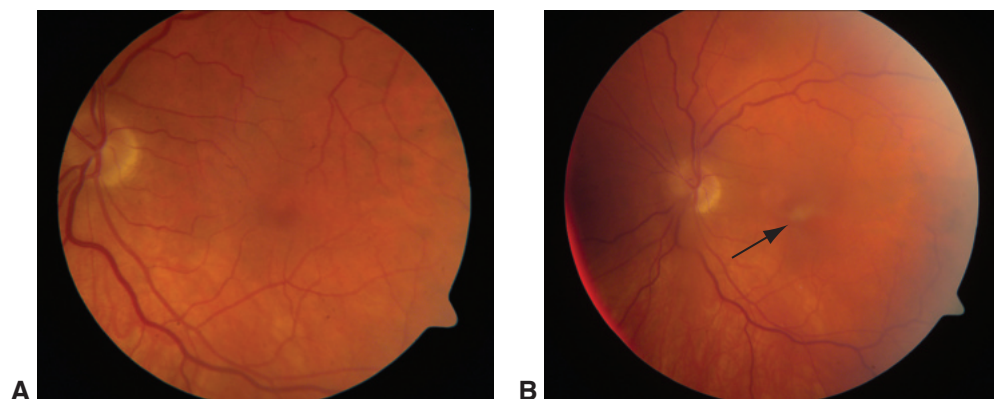


Figure 15-1 Posterior vitreous detachment. Color fundus photographs show attached vitreous (**A**) and an acute Weiss ring over the fovea with obscuration (*arrow*) occurring several days later (**B**). (Courtesy of Stephen J. Kim, MD.)

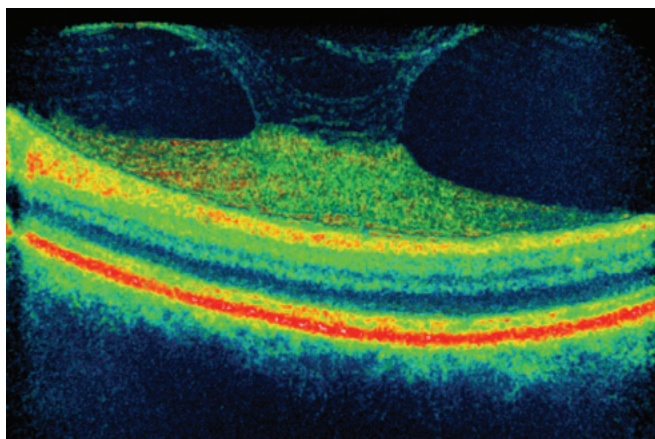


Figure 15-2 A 3-dimensional rendering of spectral-domain optical coherence tomography (SD-OCT) imaging of vitreomacular traction syndrome. The cone of vitreous is attached to and elevates the central fovea. (Courtesy of Richard F. Spaide, MD.)

Gishti O, van den Nieuwenhof R, Verhoeckx J, van Overdam K. Symptoms related to posterior vitreous detachment and the risk of developing retinal tears: a systematic review. *Acta Ophthalmol.* 2019;97(4):347–352.

Epiretinal Membranes

An epiretinal membrane (ERM) is a transparent, avascular, fibrocellular membrane on the inner retinal surface that adheres to and covers the ILM of the retina. Proliferation of glia, retinal pigment epithelium (RPE), or hyalocytes at the vitreoretinal interface, especially at the posterior pole, results in ERM formation.

ERMs are relatively common; at autopsy, they are discovered in 2% of persons older than 50 years and in 20% older than 75 years. Both sexes are equally affected. Bilaterality occurs in approximately 10%–20% of cases, and severity is usually asymmetric. Detachment or separation of the posterior vitreous is present in almost all eyes with idiopathic ERMs and may be a requisite for ERM development. Schisis of the posterior vitreous may leave variable portions of the posterior cortical vitreous attached to the macula, allowing glial cells from the retina to proliferate along the retinal surface and hyalocytes to proliferate on posterior cortical vitreous remnants on the retinal surface. Secondary ERMs occur regardless of age or sex in association with abnormal vitreoretinal adhesions, occult retinal tears, and areas of inflammation, as well as following retinal detachment or retinal bleeding.

Signs and symptoms

Epiretinal proliferation is generally located in the central macula—over, surrounding, or eccentric to the fovea (Fig 15-4). The membranes usually appear as a mild sheen or glint on the retinal surface. Over time, ERMs may become more extensive, increasing retinal distortion and thickening (Activities 15-1, 15-2), which can lead to a decline in visual acuity and to image distortion. However, their rate of progression and severity vary greatly. In some cases, the ERM may become opaque, obscuring underlying retinal details. A “pseudohole” appearance

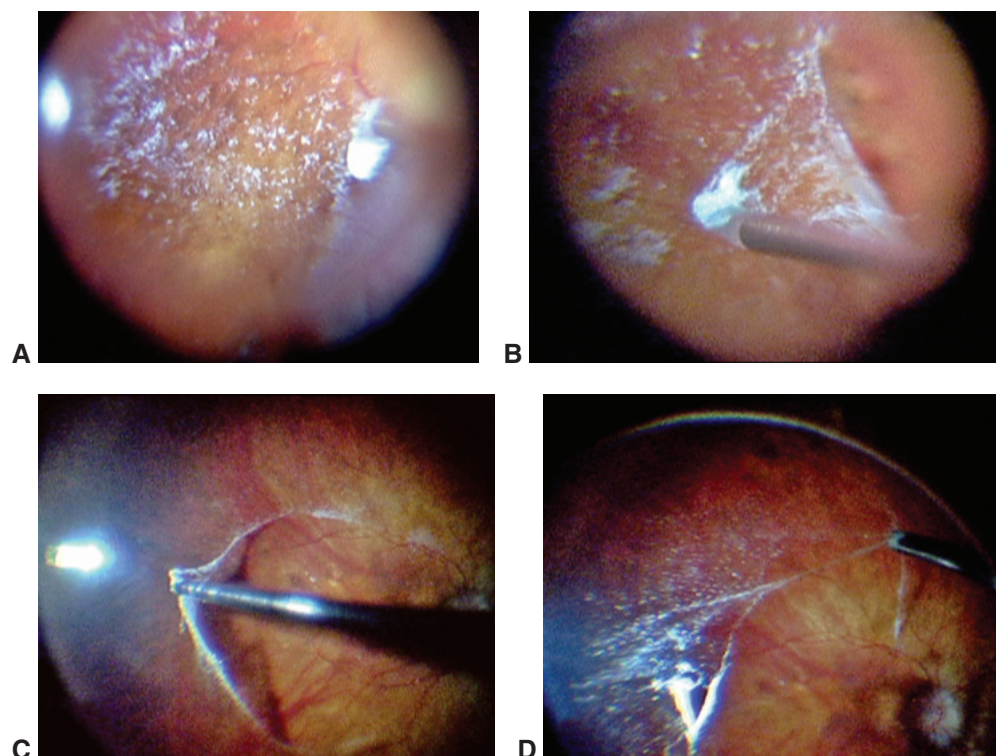


Figure 15-3 Visualization of a thin layer of adherent vitreous during vitrectomy with the use of triamcinolone. This patient appeared to have a posterior vitreous detachment (PVD) and underwent a vitrectomy. **A**, A small amount of triamcinolone was injected into the vitreous cavity; the excess was aspirated from the surface of the retina, leaving a fine distribution of triamcinolone sticking to the adherent vitreous. **B**, The vitreous membrane was elevated using a diamond-dusted silicone scraper. Note that the vitreous is difficult to see; the sheet of triamcinolone is the clue to its presence. **C**, A wide-angle viewing system then was used to visualize the elevation of the adherent vitreous, and the vitrector was set to suction only. **D**, Note the extent of the adherent vitreous sheet, which was removed with the vitrector set to cut. (Courtesy of Richard F. Spaide, MD.)

is produced when this preretinal membrane contracts to the edge of the clivus, steepening the gentle slope around the fovea into a cylindrical depression. Occasionally, intraretinal hemorrhages or whitened patches of superficial retina representing delayed axoplasmic flow in the nerve fiber layer and edema may be present, which can imitate a retinal vein occlusion. *Lamellar hole-associated epiretinal proliferation (LHEP)* features an avascular tissue layer of medium reflectivity that covers the premacular surface and surrounds a foveal defect without a tractional component. The cellular origin of ERMs is still under debate. Histologic examination reveals mainly RPE cells and retinal glial cells (astrocytes and Müller cells); however, myofibroblasts, fibroblasts, hyalocytes, and macrophages have also been identified.



ACTIVITY 15-1 OCT Activity: Epiretinal membrane.

Courtesy of Colin A. McCannel, MD.





Figure 15-4 Epiretinal membrane (ERM). **A**, Multicolor fundus image obtained with the scanning laser ophthalmoscope (30° field of view) reveals an ERM in the central macula with radiating striae of the internal limiting membrane (ILM) in the superior, temporal, and inferior macula. The colors in reflectance multicolor images are not exactly true to life. **B**, OCT scan through the fovea shows increased retinal thickening and cystoid edema with a large central cyst. The ERM is distorting the retinal surface temporally, which appears as several small optical voids between the ERM and the retina. (Courtesy of Colin A. McCannel, MD.)



ACTIVITY 15-2 OCT Activity: Epiretinal membrane progression.

Courtesy of Colin A. McCannel, MD.



Contracture of ERMs produces distortion and wrinkling of the inner surface of the retina, called *cellophane maculopathy* or *preretinal macular fibrosis*. It can range from mild to severe, with *wrinkling* or *striae* to severe *macular puckering*. Increased traction may cause shallow macular detachment, diffuse thickening, or cystic changes. Furthermore, traction on retinal vessels results in increased vascular tortuosity and straightening of the perimacular vessels. Fluorescein angiography (FA) may show staining of the optic nerve and capillary leakage in the central macula. The most common OCT findings are a highly reflective epiretinal reflective layer, loss of the normal retinal contour, and retinal thickening. Additional findings include irregularities of the inner retinal surface and cystic edema.

Treatment

When ERMs are asymptomatic and visual acuity is good, intervention is not indicated. Asymptomatic ERMs should be monitored periodically because they will often worsen, sometimes over a relatively short period, after being stable. In rare cases, an ERM may spontaneously detach from the inner retinal surface, with concomitant improvement or resolution of the retinal distortion and improvement in symptoms and vision. OCT can be used to monitor the integrity of the ellipsoid zone for progressive disruption. This metric can also provide information about prognosis, which can be useful in surgical decision-making, and about postoperative visual potential. If the patient is bothered by reduced vision or metamorphopsia, vitrectomy should be considered (see also Chapter 19). The goal of surgery is to optimize vision, reduce metamorphopsia, and restore binocularity if it was affected preoperatively.

Johnson TM, Johnson MW. Epiretinal membrane. In: Yanoff M, Duker JS. *Ophthalmology*. 4th ed. Elsevier; 2014:614–619.

Vitreomacular Traction Diseases

Vitreomacular traction (VMT) diseases include abnormalities that arise from focal or broad vitreomacular adhesions in the presence of detaching or otherwise detached posterior vitreous. The 3 recognized categories of VMT disease are vitreomacular adhesion, VMT syndrome, and macular hole. Table 15-1 summarizes a useful classification system for VMT diseases that relies on OCT findings.

Vitreomacular adhesions

Vitreomacular adhesions typically do not cause visual symptoms. They can be focal or broad and may lead to secondary traction disease, that is, VMT and macular holes.

Vitreomacular traction syndrome

In VMT syndrome, the posterior hyaloid is abnormally adherent to the macula (eg, a vitreomacular adhesion). As the vitreous detaches, the posterior hyaloid remains tethered

Table 15-1 The International Vitreomacular Traction Study Classification System for Vitreomacular Adhesion, Traction, and Macular Hole

Classification	Subclassification
Vitreomacular adhesion	Size: focal ($\leq 1500\ \mu\text{m}$) or broad ($>1500\ \mu\text{m}$) Isolated or concurrent
Vitreomacular traction	Size: focal ($\leq 1500\ \mu\text{m}$) or broad ($>1500\ \mu\text{m}$) Isolated or concurrent
Full-thickness macular hole	Size (diameter): small ($\leq 250\ \mu\text{m}$), medium ($>250\text{--}\leq 400\ \mu\text{m}$), or large ($>400\ \mu\text{m}$) Status of vitreous: with or without vitreomacular traction Cause: primary or secondary

Modified from Duker JS, Kaiser PK, Binder S, et al. The International Vitreomacular Traction Study Group classification of vitreomacular adhesion, traction, and macular hole. *Ophthalmology*. 2013;120(12): 2611–2619. Copyright 2013, with permission from Elsevier.

at the macula, usually the fovea, causing tractional foveal distortion, cystic edema, and in severe cases, traction foveal detachment. These changes lead to metamorphopsia, decreased vision, and often vague reports about poor vision in the affected eye that are out of proportion to the measured visual acuity. VMT syndrome is differentiated clinically from typical ERM. The fundus examination is often normal. VMT syndrome is best diagnosed and differentiated from ERM with the aid of OCT, which is useful for demonstrating the vitreoretinal interface abnormalities and the tractional effects of the syndrome on foveal architecture, particularly the outer retinal layers. VMT syndrome is often progressive and is associated with a greater loss of vision compared with ERM alone. Chronic traction is generally understood to be harmful over the long term, particularly when cystic edema is present or when the patient's vision is affected. Close observation may be appropriate, as traction can spontaneously release. Spontaneous separation of the focal vitreoretinal adhesion, with resolution of all clinical features, occurs in approximately 50% of cases and less commonly when there is an associated ERM or when the adhesion is broad (Fig 15-5).

Voo I, Mavrofrides EC, Puliafito CA. Clinical applications of optical coherence tomography for the diagnosis and management of macular diseases. *Ophthalmol Clin North Am.* 2004; 17(1):21–31.

Idiopathic Macular Holes

The incidence rate of idiopathic macular holes is approximately 8 per 100,000 persons per year, and the female to male ratio is 2 to 1. Macular holes occur mostly in the sixth through eighth decades of life but can appear at a younger age in myopic eyes. Idiopathic macular holes are bilateral in approximately 10% of patients. Investigations using OCT suggest that idiopathic macular holes are caused by the same tractional forces as the forces associated with perifoveal vitreous detachment and thus are likely an early stage of age-related PVD.

The following description of the stages of macular hole formation is useful for making management decisions (Fig 15-6):

- A *stage 0*, or pre-macular, hole occurs when a PVD with persistent foveal attachment develops. Subtle loss of the foveal depression can be observed, and visual acuity is usually unaffected. Most stage 0 holes do not progress to advanced stages. This stage represents a vitreomacular adhesion.

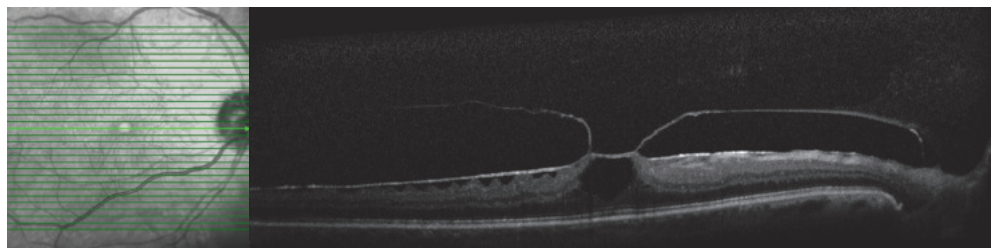


Figure 15-5 Vitreomacular traction syndrome. OCT scan of the macula through the fovea shows vitreomacular traction causing a large foveal cyst and distortion of the inner retina. An ERM is also present. (Courtesy of Tara A. McCannel, MD, PhD.)

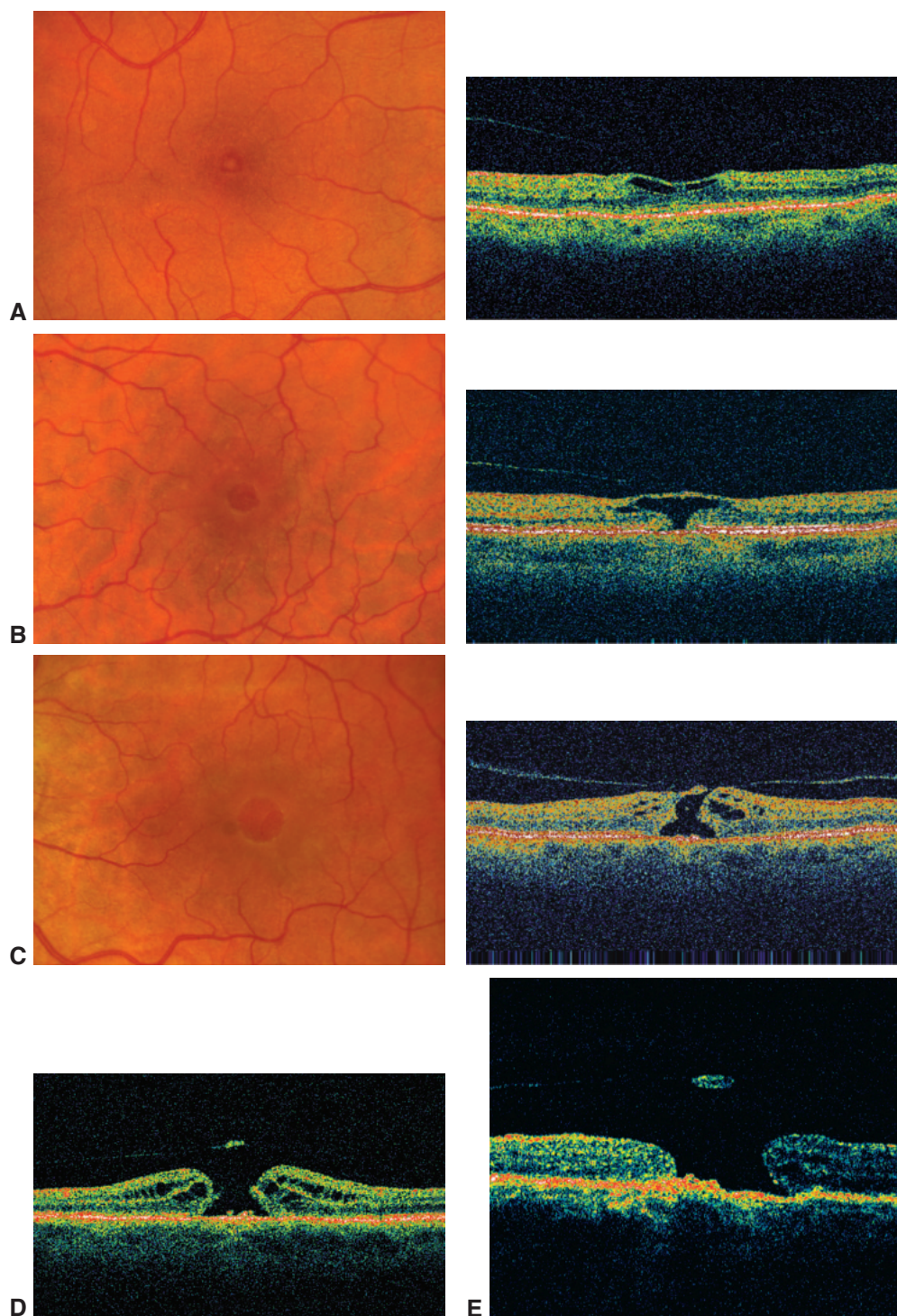


Figure 15-6 Stages of macular hole formation. **A**, Stage 1A. Color fundus photograph and corresponding OCT scan, the latter demonstrating horizontal splitting of retinal layers. **B**, Stage 1B. Fundus photograph and corresponding OCT scan. **C**, Stage 2. Fundus photograph shows a hole with a small opening in the inner layer eccentrically. Corresponding OCT scan of stage 2. **D**, Stage 3. OCT scan shows a full-thickness hole with elevation of adjacent retinal edges. **E**, Stage 4. OCT scan shows a full-thickness hole with operculum. (Courtesy of Mark W. Johnson, MD, and Peter K. Kaiser, MD.)

- A *stage 1* macular hole (impending macular hole) typically causes visual symptoms of metamorphopsia and central vision decline, usually to a visual acuity range of 20/25 to 20/60. The characteristic findings are either a small yellow spot (stage 1A) or a yellow ring (stage 1B) in the fovea. OCT examination reveals that a stage 1A hole is a foveal “pseudocyst,” or horizontal splitting (schisis), associated with vitreous traction on the foveal center. A stage 1B hole indicates a break in the outer fovea, the margins of which constitute the yellow ring noted clinically. Spontaneous resolution of a stage 1 hole occurs in approximately 50% of cases without ERM. This stage represents VMT syndrome.
- *Stage 2* represents an early full-thickness macular hole that is less than 400 μm in diameter. As a tractional break develops in the “roof” (inner layer) of a foveal pseudocyst, foveal schisis progresses to a full-thickness dehiscence. Progression to stage 2 is accompanied by a further decline in visual acuity. OCT demonstrates the full-thickness defect and the continuing attachment of the posterior hyaloid to the foveal center. This stage represents VMT syndrome with a small- to medium-sized macular hole.
- A *stage 3* macular hole is a fully developed hole ($\geq 400 \mu\text{m}$ in diameter), typically surrounded by a rim of thickened and detached retina. Visual acuity varies widely. The posterior hyaloid remains attached to the optic nerve head but is detached from the fovea. An operculum suspended by the posterior hyaloid may be seen overlying the hole. On OCT, this stage represents a large macular hole with no VMT (Fig 15-7, Activity 15-3).
- A *stage 4* macular hole is a fully developed hole with a complete PVD, as evidenced by the presence of a Weiss ring. On OCT, this stage represents a large macular hole with no VMT.

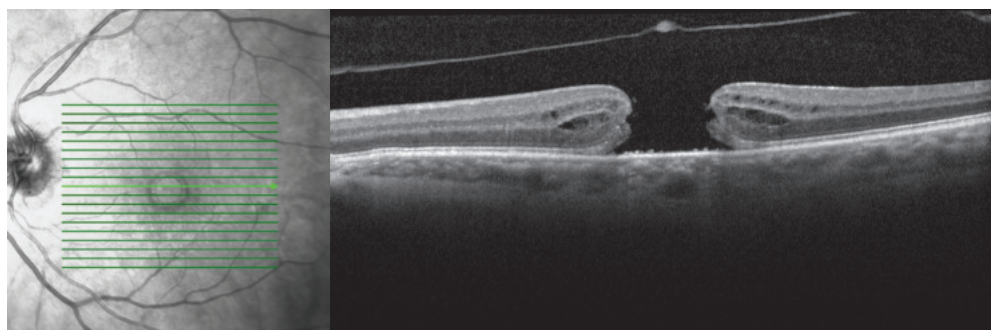


Figure 15-7 SD-OCT line cube scan of the left macula of a 62-year-old woman who had vision loss 18 months before presentation. At the time of the scan, the visual acuity of this eye was 20/40 (eccentric fixation). The infrared reflectance image (*left*) shows a hole in the central macular retina. See also Activity 15-3; scrolling through the images, a discontinuity of the retina in the central macular scans can be seen, corresponding to the macular hole. The scan through the macular hole (scan 10) shows an operculum. This operculum represents a small glial plug that helps keep the fovea together; when it is pulled away by the posterior vitreous, a macular hole is facilitated. Histologic studies indicate that the number of photoreceptors attached to the plug can vary, from none to many. The prominent posterior vitreous face can also be seen; its contour suggests that it is likely attached at the optic nerve head and peripheral macula (dome-shaped configuration), which is typical in idiopathic macular holes. (Courtesy of Colin A. McCannel, MD.)

**ACTIVITY 15-3** OCT Activity: Stage 3 macular hole.

Courtesy of Colin A. McCannel, MD.



The fellow-eye risk of macular hole development depends on the vitreous attachment status. If a complete vitreous detachment is present in the fellow eye, there is little, if any, risk of macular hole development. However, if the fellow eye has stage 1A abnormalities, there is a substantial risk of progression to a full-thickness macular hole. When the fellow eye is normal and its vitreous is attached, the risk of developing a macular hole in that eye is approximately 10%, the rate of bilaterality.

Management options

Stage 1 macular holes without ERM have an approximate 50% rate of spontaneous resolution and thus are usually monitored. For stage 2 or higher macular holes, surgical intervention is indicated—specifically, pars plana vitrectomy usually performed with ILM peeling and gas tamponade. In most recent case series, the success rate of this procedure for closure and vision improvement was greater than 90% (see Chapter 19). Modifications of routine macular hole surgery are usually reserved for very large, chronic, or nonclosing holes; these include inverted ILM flaps and autologous retinal grafts composed of peripheral retina. Although these techniques may achieve anatomical hole closure, visual acuity may not improve.

Duker JS, Kaiser PK, Binder S, et al. The International Vitreomacular Traction Study Group classification of vitreomacular adhesion, traction, and macular hole. *Ophthalmology*. 2013; 120(12):2611–2619.

Developmental Abnormalities

Tunica Vasculosa Lentis

Remnants of the tunica vasculosa lentis and hyaloid artery are commonly noted and are usually not visually significant. *Mittendorf dot*, an anterior remnant, is a small, dense, and white round plaque attached to the posterior lens capsule nasally and inferiorly to its posterior pole (Fig 15-8). *Bergmeister papilla*, a prepapillary remnant, is a fibroglial tuft of tissue extending from the margin of the optic nerve head into the vitreous for a short distance. The entire hyaloid artery may persist from optic nerve head to lens as multilayered fenestrated sheaths forming the Cloquet canal.

Prepapillary Vascular Loops

Initially thought to be remnants of the hyaloid artery, prepapillary vascular loops are normal retinal vessels that have grown into Bergmeister papilla before returning to the retina (Fig 15-9). The loops typically extend less than 5 mm into the vitreous. These vessels may supply 1 or more quadrants of the retina. FA has shown that 95% of these vessels are arterial and 5% are venous. Complications associated with prepapillary vascular loops include branch retinal artery occlusion, amaurosis fugax, and vitreous hemorrhage.

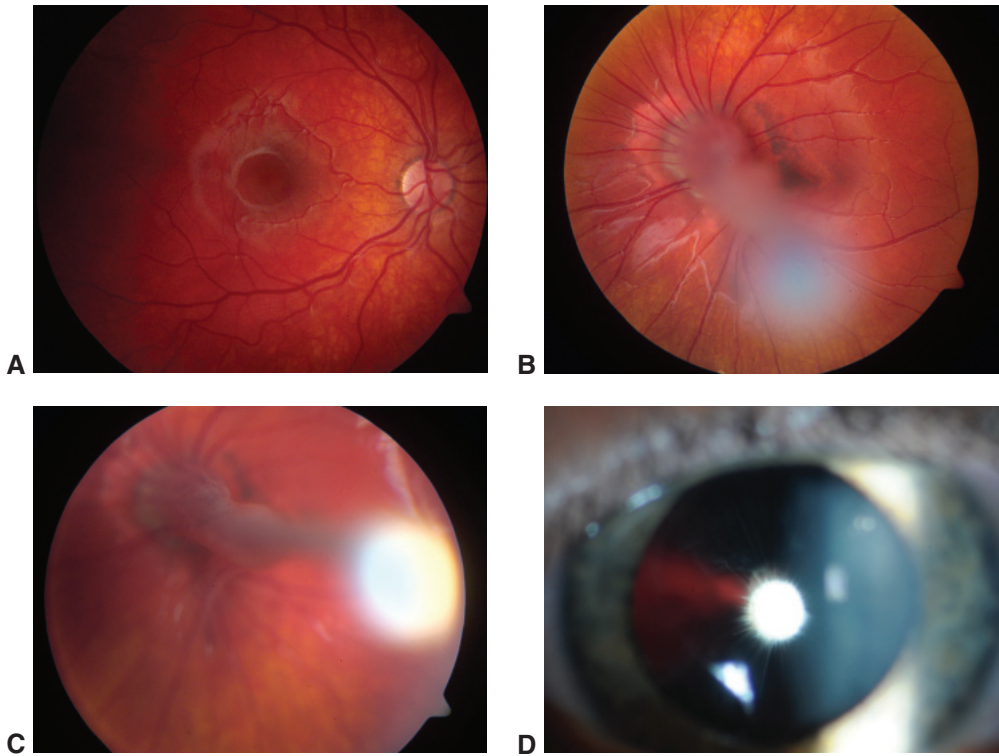


Figure 15-8 Persisting hyaloid artery. **A**, Healthy right eye. **B, C**, In the left eye, the hyaloid artery can be seen from the optic nerve head, traveling through the vitreous cavity to the lens as multilayered sheaths forming the Cloquet canal. **D**, Mittendorf dot. (Courtesy of Stephen J. Kim, MD.)



Figure 15-9 Color fundus photograph shows a prepapillary vascular loop. (Courtesy of M. Gilbert Grand, MD.)

Persistent Fetal Vasculature

Persistent fetal vasculature (PFV) is a congenital anomaly thought to result from failure of the primary vascular vitreous to regress. The disorder is unilateral in 90% of cases and usually has no associated systemic findings. Anterior, posterior, and combined forms of this developmental abnormality have been described. Most cases are sporadic, but PFV can occur as either an autosomal recessive (mutations in *ATOH7*) or autosomal dominant trait. In some patients with *ATOH7* mutations, the disease is bilateral and asymmetric, with the fellow eye showing a variety of changes, including avascularity. See also BCSC Section 6, *Pediatric Ophthalmology and Strabismus*.

Anterior persistent fetal vasculature

In anterior PFV, the hyaloid artery remains, and a white fibrovascular membrane or mass is present behind the lens. Associated findings include microphthalmos, a shallow anterior chamber, and elongated ciliary processes that are visible around the small lens. Leukocoria is often present at birth. A dehiscence of the posterior lens capsule may, in many cases, cause swelling of the lens and cataract as well as secondary angle-closure glaucoma. In addition, glaucoma may result from incomplete development of the anterior chamber angle.

Anterior PFV may result in blindness in the most advanced cases. Lensectomy and removal of the fibrovascular retrolental membrane prevent angle-closure glaucoma in some cases; however, development of a secondary cataract is common. Deprivation amblyopia and refractive amblyopia are serious postoperative challenges in patients with PFV. Anterior PFV should be considered in the differential diagnosis of leukocoria.

Posterior persistent fetal vasculature

Posterior PFV may occur in association with anterior PFV or as an isolated finding. The eye may be microphthalmic, but the anterior chamber is usually normal and the lens is typically clear and without a retrolental membrane. A stalk of tissue emanates from the optic nerve head and courses toward the retrolental region, often running along the apex of a retinal fold that may extend anteriorly from the optic nerve head, usually in an inferior quadrant. The stalk fans out circumferentially toward the anterior retina. Posterior PFV should be distinguished from retinopathy of prematurity (ROP), familial exudative vitreoretinopathy, and ocular toxocariasis. Surgical repair of posterior PFV consists of lensectomy and vitrectomy, which result in formed vision in approximately 70% of cases.

Goldberg MF. Persistent fetal vasculature (PFV): an integrated interpretation of signs and symptoms associated with persistent hyperplastic primary vitreous (PHPV). LIV Edward Jackson Memorial Lecture. *Am J Ophthalmol*. 1997;124(5):587–626.

Sisk RA, Berrocal AM, Feuer WJ, Murray TG. Visual and anatomic outcomes with or without surgery in persistent fetal vasculature. *Ophthalmology*. 2010;117(11):2178–2183.

Hereditary Hyaloideoretinopathies With Optically Empty Vitreous: Wagner and Stickler Syndromes

The hallmark of the group of conditions known as *hereditary hyaloideoretinopathies* is vitreous liquefaction that results in an optically empty cavity except for a thin layer of cortical

vitreous behind the lens and threadlike, avascular membranes that run circumferentially and adhere to the retina. Fundus abnormalities include equatorial and perivascular (radial) lattice degeneration. The electroretinogram response may be subnormal.

In *Wagner syndrome*, the optically empty vitreous is accompanied by myopia, strabismus, and cataract. It is not associated with retinal detachment. The syndrome is inherited in an autosomal dominant manner, and there are no associated systemic findings.

Stickler syndrome is the most common form of hereditary hyaloideoretinopathy with associated systemic findings and is transmitted as an autosomal dominant trait (Fig 15-10). Most patients have a mutation in *COL2A1*, which encodes type II procollagen. Various mutations may produce Stickler syndrome phenotypes of differing severity. Additional ocular abnormalities include myopia, open-angle glaucoma, and cataract. Orofacial findings include midfacial flattening and the Pierre Robin malformation complex of cleft palate, micrognathia, and glossoptosis. These abnormalities may be dramatic at birth, requiring tracheostomy, or they may not be obvious at all. Generalized skeletal abnormalities include joint hyperextensibility and enlargement; arthritis, particularly of the knees; and mild spondyloepiphyseal dysplasia.

Early recognition of Stickler syndrome is important because of the high occurrence of retinal detachment. In one case series, retinal tears were associated with mutations in *COL2A1* in 91% of cases and retinal detachments in 53%. The detachments may be difficult to repair because of multiple, posterior, or large breaks and the tendency for proliferative vitreoretinopathy to develop in these cases. Patients with this condition typically have cortical vitreous condensations that are firmly adherent to the retina. For this reason, prophylactic treatment of retinal breaks should be performed (see the section Prophylactic Treatment of Retinal Breaks in Chapter 16).

Other forms of hereditary hyaloideoretinopathy associated with systemic abnormalities include Weill-Marchesani syndrome and some varieties of dwarfism.

Rose PS, Levy HP, Liberfarb RM, et al. Stickler syndrome: clinical characteristics and diagnostic criteria. *Am J Med Genet A*. 2005;138A(3):199–207.

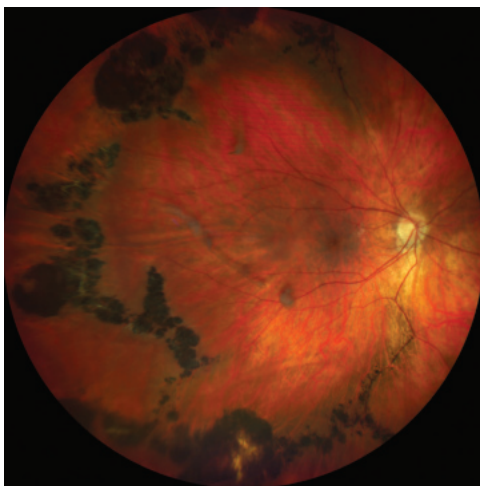


Figure 15-10 Color fundus photograph shows extensive lattice degeneration and pigmentary change in a patient with Stickler syndrome. (Courtesy of Franco M. Recchia, MD.)

Familial Exudative Vitreoretinopathy

Familial exudative vitreoretinopathy (FEVR) is characterized by failure of the temporal retina to vascularize and is phenotypically similar to ROP (Table 15-2). Retinal folds and peripheral fibrovascular proliferation, as well as traction and exudative retinal detachments, are often associated with FEVR (Fig 15-11). Temporal dragging of the macula may cause the patient to appear to have exotropia. Late-onset rhegmatogenous retinal detachments may occur. Generally, the earlier the disease presents, the more severe the manifestations.

The condition is frequently bilateral, although the severity of ocular involvement may be asymmetric. Unlike patients with ROP, individuals with FEVR are born full term and have normal respiratory status. In FEVR, the peripheral retinal vessels are dragged and straightened, and they end abruptly a variable distance from the ora serrata (brush border). Distinguishing FEVR from ROP is also aided by the family history and a careful examination of all family members. The only finding in some family members with FEVR may be a straightening of vessels and peripheral retinal nonperfusion. Parents and siblings of affected children may be mildly affected and asymptomatic. FA with peripheral sweeps or wide-field angiography is indispensable when examining family members. Treatment of affected family members may consist of laser therapy applied to the avascular retina, guided by FA.

FEVR is usually inherited as an autosomal dominant trait, but X-linked transmission also occurs. Several gene loci have been associated with the FEVR phenotype. A number of genetic disorders can present with the retinal characteristics of FEVR, including dyskeratosis congenita, Coats plus syndrome, facioscapulohumeral muscular dystrophy, and progressive hemifacial atrophy (Parry-Romberg syndrome). It is important to differentiate these diseases genetically.

Ranchod TM, Ho LY, Drenser KA, Capone A Jr, Trese MT. Clinical presentation of familial exudative vitreoretinopathy. *Ophthalmology*. 2011;118(10):2070–2075.

Table 15-2 Features of Familial Exudative Vitreoretinopathy and Retinopathy of Prematurity

	Familial Exudative Vitreoretinopathy	Retinopathy of Prematurity
Prematurity	Absent	Present
Normal respiratory status	Present	Absent
Birth weight	Often normal	Often low
Family history	Present	Absent
Exudates	Present	Absent
Course of disease	Unpredictable	Predictable
Late stage	Reactivation common	Cicatrization common

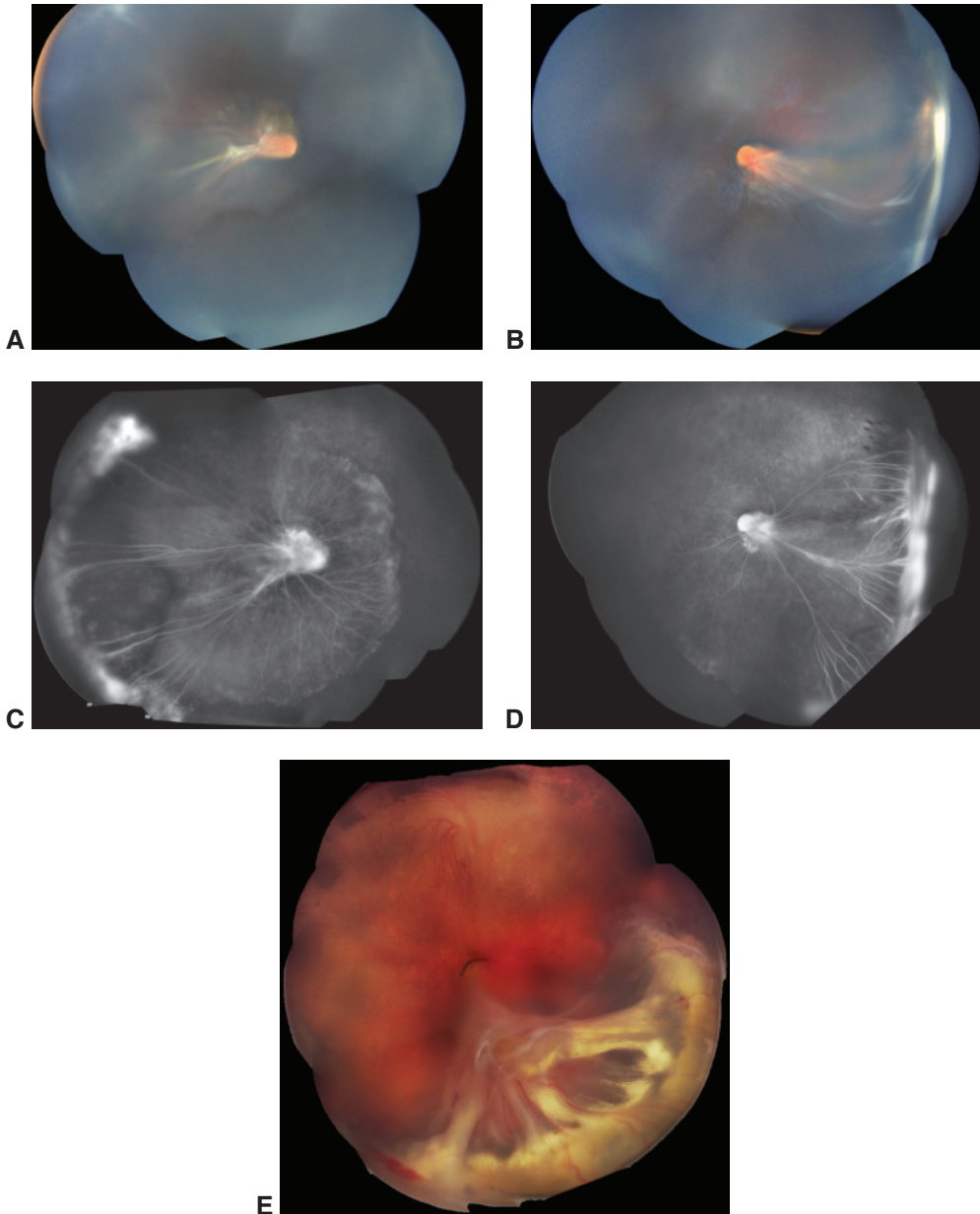


Figure 15-11 Familial exudative vitreoretinopathy (FEVR) due to the *LRP5* mutation. **A, B,** The temporal retina shows a zone of nonperfusion that is horizontally V-shaped, causing a tractional macular fold. **C, D,** Fluorescein angiography images from the same patient demonstrate dragging of the vasculature. There is evidence of leakage and avascularity. **E,** Color fundus image montage from a different patient with FEVR shows folding of the retina with massive exudation. (Courtesy of Audina M. Berrocal, MD.)

Vitreous Opacities

Opacities Associated With Vitreous Degeneration and Detachment

Synchysis and syneresis result in loss of the highly organized vitreous anatomy. The collagen fibers that make up the vitreous can coalesce, or tangle, producing small areas that are no longer transparent and can cast shadows. These shadows are perceived by patients as floaters, which patients may find bothersome.

Following vitreous detachment, the coalescence and tangling of vitreous collagen fibers can worsen. In addition, areas where the vitreous was attached more firmly, such as at the optic nerve, are less transparent. When these opacities move away from the retinal surface, they too can cast shadows and may be perceived as floaters.

Over time, as the vitreous continues to liquefy, the opacities may sink inferiorly and become less noticeable. Also, the brain has the capacity to learn to selectively ignore the floaters. As a result, most patients become asymptomatic or minimally symptomatic and do not require any intervention.

Asteroid Hyalosis

In asteroid hyalosis, minute white opacities composed of calcium-containing phospholipids are evenly dispersed in the otherwise normal vitreous (Fig 15-12). Clinical studies have confirmed a relationship between asteroid hyalosis and both diabetes and hypertension. The overall prevalence of asteroid hyalosis is 1 in 200 persons, most often in people older than 50 years. The condition is unilateral in 75% of cases, and significant decreases in visual acuity are rare. However, when PVD occurs, compression of the material occurs, and visual acuity may decrease. When asteroid hyalosis blocks the view of the posterior fundus

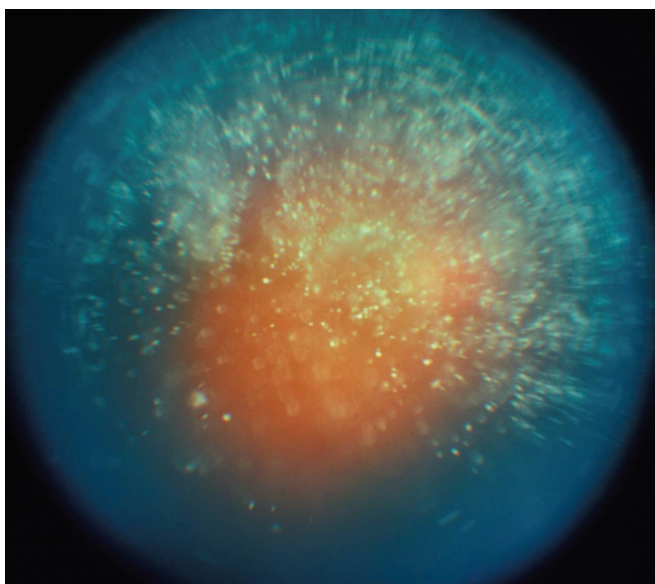


Figure 15-12 Color fundus photograph of asteroid hyalosis. (Courtesy of Hermann D. Schubert, MD.)

and retinal pathology is suspected, FA is usually successful in imaging the abnormalities. Occasionally, vitrectomy may be necessary to remove visually significant opacities or to facilitate treatment of underlying retinal abnormalities such as proliferative retinopathy.

Mochizuki Y, Hata Y, Kita T, et al. Anatomical findings of vitreoretinal interface in eyes with asteroid hyalosis. *Graefes Arch Clin Exp Ophthalmol*. 2009;247(9):1173–1177.

Vitreous Hemorrhage

A common cause of emergency visits to ophthalmology offices is sudden vision loss due to vitreous hemorrhage not associated with ocular trauma. In adults, the most common causes include proliferative diabetic retinopathy (see Chapter 5), PVD, central retinal vein occlusion, and retinal neovascularization from a variety of other causes (see Chapter 7, Table 7-2). Bleeding can be exacerbated by the use of systemic anticoagulants. Vitreous hemorrhage may arise from avulsion of the superficial retinal or prepapillary vessels or from rupture of retinal vessels that cross retinal tears. In cases of vitreous hemorrhage associated with an acute PVD, retinal tears are found in approximately 50%–70% of eyes; clinical retinal detachment, in 8%–12%. In children, X-linked hereditary retinoschisis and pars planitis are common causes of vitreous hemorrhage; however, trauma must always be considered in the differential diagnosis (see Chapter 17).

In most cases of vitreous hemorrhage, the underlying cause can be determined by obtaining a history or on retinal examination. If the hemorrhage is too dense to permit indirect ophthalmoscopy or biomicroscopy, suggestive clues can be obtained from examination of the fellow eye. Diagnostic ultrasonography can be performed to detect any tractional tear (often superotemporally) and to rule out retinal detachment or tumor. Bilateral eye patching with bed rest for a few hours to several days, with the head of the bed elevated, may permit the intrahyaloid and retrohyaloid blood to settle, allowing a better view of the posterior segment. If the etiology still cannot be established, the ophthalmologist should consider frequent reexamination with repeated ultrasonography until the cause is found. Alternatively, prompt diagnostic vitrectomy in nondiabetic patients may be considered and may help prevent progression of a retinal tear to retinal detachment. Ghost cell glaucoma can result from long-standing vitreous hemorrhage.

El-Sanhouri AA, Foster RE, Petersen MR, et al. Retinal tears after posterior vitreous detachment and vitreous hemorrhage in patients on systemic anticoagulants. *Eye (Lond)*. 2011;25(8):1016–1019.

Sarrafizadeh R, Hassan TS, Ruby AJ, et al. Incidence of retinal detachment and visual outcome in eyes presenting with posterior vitreous separation and dense fundus-obscuring vitreous hemorrhage. *Ophthalmology*. 2001;108(12):2273–2278.

Witmer MT, Cohen SM. Oral anticoagulation and the risk of vitreous hemorrhage and retinal tears in eyes with acute posterior vitreous detachment. *Retina*. 2013;33(3):621–626.

Pigment Granules

In a patient without uveitis, retinitis pigmentosa, or a history of surgical or accidental eye trauma, the presence of pigmented cells in the anterior vitreous (“tobacco dust”), known as a *Shafer sign*, is highly suggestive of a retinal break. See Chapter 16.

Cholesterolosis

Numerous yellow-white, gold, or multicolored cholesterol crystals are present in the vitreous and anterior chamber in cholesterolosis, also known as *synchysis scintillans*. This condition appears almost exclusively in eyes that have undergone repeated or severe accidental or surgical trauma causing large intravitreal hemorrhages. The descriptive term *synchysis scintillans* refers to the highly refractile appearance of the cholesterol-containing crystals. In contrast to eyes with asteroid hyalosis, in which the opacities are evenly distributed throughout the vitreous, eyes with cholesterolosis frequently have a PVD, which allows the crystals to settle inferiorly.

Amyloidosis

Bilateral vitreous opacification may occur as an early manifestation of the dominantly inherited form of hereditary familial amyloidosis, which is most commonly associated with a transthyretin mutation (Fig 15-13). Amyloid infiltration of the vitreous is rare in

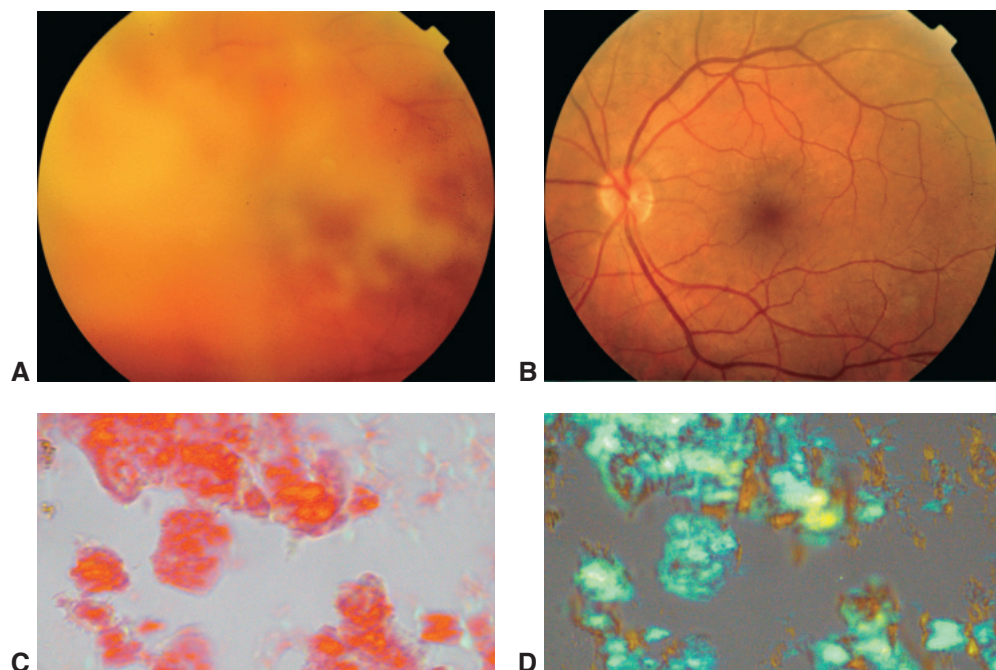


Figure 15-13 Amyloidosis. Images from a 57-year-old woman with a history of vitrectomy for floaters in the right eye. A cataract subsequently developed in the right eye and was extracted. Her vision then decreased in the left eye, which she ascribed to a cataract. **A**, Color fundus photograph of the left eye showed a dense vitreous infiltration; there was no cataract, and intraocular pressure was markedly elevated. Review of systems revealed carpal tunnel syndrome in both wrists. **B**, After vitrectomy on the left eye, there was a clear view to the posterior pole. **C**, The removed vitreous material, stained with Congo red. **D**, The material demonstrated birefringence. The patient was found to have a mutation affecting transthyretin. Glaucoma commonly develops in patients with transthyretin-related familial amyloidotic polyneuropathy. (Courtesy of Richard F. Spaide, MD.)

nonfamilial cases. In addition to the vitreous, amyloid may be deposited in the retinal vasculature, the choroid, and the trabecular meshwork.

Retinal findings include hemorrhages, exudates, cotton-wool spots, and peripheral neovascularization. In addition, infiltrations may be present in the orbit, extraocular muscles, eyelids, conjunctiva, cornea, and iris. Nonocular manifestations of amyloidosis include upper- and lower-extremity polyneuropathy and central nervous system abnormalities. Amyloid may be deposited in several organs, including the heart and skin, and in the gastrointestinal tract.

Initially, the extracellular vitreous opacities appear to lie adjacent to retinal vessels posteriorly; they later develop anteriorly. At first, the opacities appear granular and have wispy fringes, but as they enlarge and aggregate, the vitreous takes on a “glass wool” appearance.

The differential diagnosis of amyloidosis includes chronic (dehemoglobinized) vitreous hemorrhage, lymphoma, sarcoidosis, and Whipple disease. Vitrectomy may be indicated for vitreous opacities when symptoms warrant intervention, but recurrent opacities may develop in residual vitreous. Histologic examination of removed vitreous shows material with a fibrillar appearance and a staining reaction to Congo red, characteristic of amyloid. Birefringence and electron microscopic studies are confirmatory.

Sandgren O. Ocular amyloidosis, with special reference to the hereditary forms with vitreous involvement. *Surv Ophthalmol.* 1995;40(3):173–196.

CHAPTER 16

Retinal Detachment and Predisposing Lesions



This chapter includes a related activity. Go to www.aao.org/bcscactivity_section12 or scan the QR code in the text to access this content.

Highlights

- Lattice degeneration is present in 6%–10% of people and may predispose eyes to retinal detachment (RD).
- Although symptomatic retinal breaks typically are treated in most eyes, the complete clinical scenario is important to consider when clinicians are determining whether asymptomatic lesions, including lattice and retinal breaks, should be observed or treated.
- Retinal detachments are categorized as rhegmatogenous, traction (or tractional), or exudative.
- Retinoschisis can be differentiated from rhegmatogenous RD by examination and imaging.
- Retinoschisis without RD typically does not require treatment.

Examination and Management of Posterior Vitreous Detachment

The vitreous gel is attached most firmly at the *vitreous base*, a circumferential zone straddling the ora serrata that extends approximately 2 mm anterior and 3–4 mm posterior to the ora. Vitreous collagen fibers at this base are so firmly attached to the anterior retina and pars plana epithelium that the vitreous typically cannot be separated from these tissues without tearing them. The vitreous is also firmly attached at the margin of the optic nerve head, at the macula, along major vessels, at the margins of lattice degeneration, and at chorioretinal scars.

Most *retinal tears* result from traction caused by posterior vitreous detachment (PVD). The predisposing event is syneresis (collapse) of the central vitreous. Vitreous traction on the retina can produce a *retinal break*, a full-thickness defect in the neurosensory retina; in this setting, the break usually occurs at the posterior edge of the vitreous base (Fig 16-1).

Many patients do not report acute symptoms when a PVD occurs. Symptoms of PVD at the initial examination include the entoptic phenomena of photopsias (flashing lights), multiple floaters, and the appearance of a curtain or cloud across the visual field. Patients with

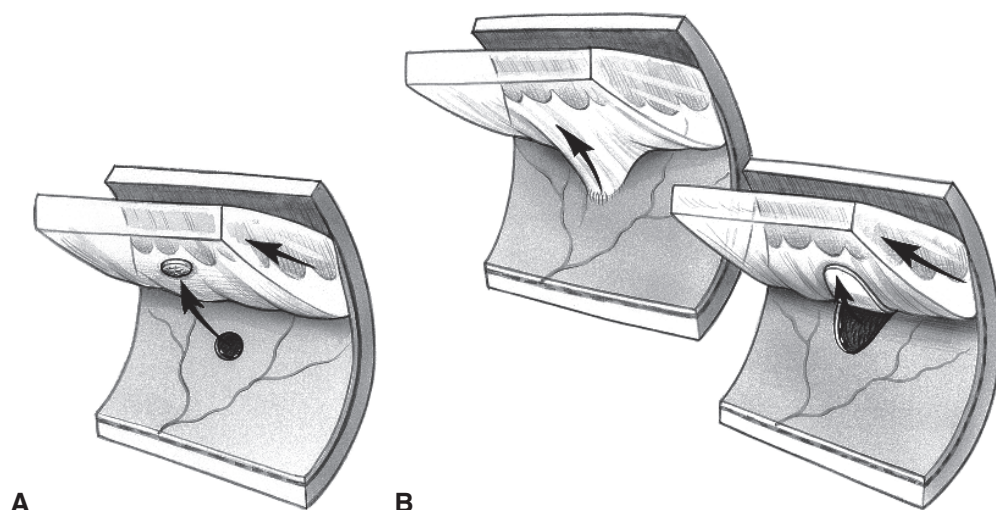


Figure 16-1 Schematic representations of mechanisms of retinal tear formation associated with posterior vitreous separation. **A**, Round or oval hole. **B**, Flap tear: posterior extension of vitreous base with firm vitreoretinal attachment. (Illustration by Christine Gralapp, based on illustrations by Tim Hengst.)

these symptoms should be examined promptly, and office staff should be made aware of the urgency of these symptoms. Photopsias are caused by the physical stimulus of vitreoretinal traction on the retina. Floaters are caused by vitreous opacities such as blood, glial cells torn from the optic nerve head, or aggregated collagen fibers, all of which can cast shadows on the retina.

Vitreous hemorrhage may arise from avulsion of superficial retinal or prepapillary vessels or from rupture of retinal vessels that cross retinal tears. Overall, 7%–18% of patients with acute symptomatic PVD have retinal tears. If vitreous hemorrhage is present, 50%–70% of patients have retinal tears, versus 7%–12% without vitreous hemorrhage. Patients with an acute PVD complicated by a retinal tear are 7 times more likely to present with vitreous pigment or granules than are those without a tear.

Indirect ophthalmoscopy with scleral depression or slit-lamp biomicroscopy are used to clinically diagnose PVD and rule out retinal breaks or detachment. Optical coherence tomography (OCT) can also be employed to visualize the state of the vitreous gel on the optic nerve head and throughout the posterior pole. Reexamination of the patient 2–4 weeks after presentation may be appropriate, because as the PVD evolves over time, new retinal breaks may occur. Additional risk factors to consider in follow-up determination include trauma, aphakia, myopia, fellow-eye history, family history of retinal detachment (RD), and signs of Stickler syndrome. All patients should be instructed to return to the ophthalmologist immediately if they notice a change in symptoms, such as increasing numbers of floaters or the development of visual field loss. They should also be told that a PVD may occur in the fellow eye. Four to 8 weeks after initial presentation and examination, if clinical symptoms of flashes and floaters are stable or improving, the risk of new retinal breaks is low.

If a large vitreous hemorrhage precludes complete examination, ultrasonography may be performed to evaluate for flap tears and rule out RD and other fundus lesions.

In addition, bilateral ocular patching and bed rest, with the patient's head elevated 45° or more for a few days, may allow the hemorrhage to settle sufficiently to permit detection of superior breaks. If the cause of the hemorrhage cannot be identified, the patient should be reexamined at frequent intervals, and early vitrectomy may be considered.

- Byer NE. Natural history of posterior vitreous detachment with early management as the premier line of defense against retinal detachment. *Ophthalmology*. 1994;101(9):1503–1514.
- van Overdam KA, Bettink-Remeijer MW, Klaver CC, Mulder PG, Moll AC, van Meurs JC. Symptoms and findings predictive for the development of new retinal breaks. *Arch Ophthalmol*. 2005;123(4):479–484.

Lesions That Predispose Eyes to Retinal Detachment

Lattice Degeneration

Lattice degeneration, a vitreoretinal interface abnormality, is present in 6%–10% of the general population and is bilateral in one-third to one-half of affected patients. It occurs more commonly in—but is not limited to—myopic eyes; there is a familial predilection. Examination findings characteristic of lattice include well-defined oval or linear regions of retinal thinning classically with white crossing lines. There may be 1 or more lesions, and they may contain areas of hyperpigmentation, hypopigmentation, or atrophic retinal holes.

Lattice may predispose eyes to retinal breaks and detachment. The most important histologic features include varying degrees of atrophy and irregularity of the inner retinal layers, an overlying pocket of liquefied vitreous, condensation, and adherence of vitreous at the margin of the lesion (Figs 16-2, 16-3).

Lattice is found in approximately 20%–30% of all patients who present with rhegmatogenous retinal detachments (RRDs). However, because lattice is not necessarily causative, prophylactic laser treatment is not universally recommended. When lattice is the cause of RD, a tractional tear at the lateral or posterior margin of the lattice or, less commonly, an atrophic hole within the zone of lattice may be found (see Fig 16-3). RDs secondary to atrophic holes typically occur in younger patients with myopia and absence of PVD; they are often asymptomatic until fixation is involved.

- Byer NE. Lattice degeneration of the retina. *Surv Ophthalmol*. 1979;23(4):213–248.
- Byer NE. Long-term natural history of lattice degeneration of the retina. *Ophthalmology*. 1989;96(9):1396–1402.

Vitreoretinal Tufts

Peripheral retinal tufts are small, focal areas of elevated glial hyperplasia associated with vitreous or zonular attachment and traction, which may be overlooked if careful peripheral examination with scleral depression is not performed. Tractional tufts are classified according to anatomical, pathogenetic, and clinical distinctions into the following groups:

- noncystic retinal tufts (Fig 16-4)
- cystic retinal tufts
- zonular traction retinal tufts (Fig 16-5)

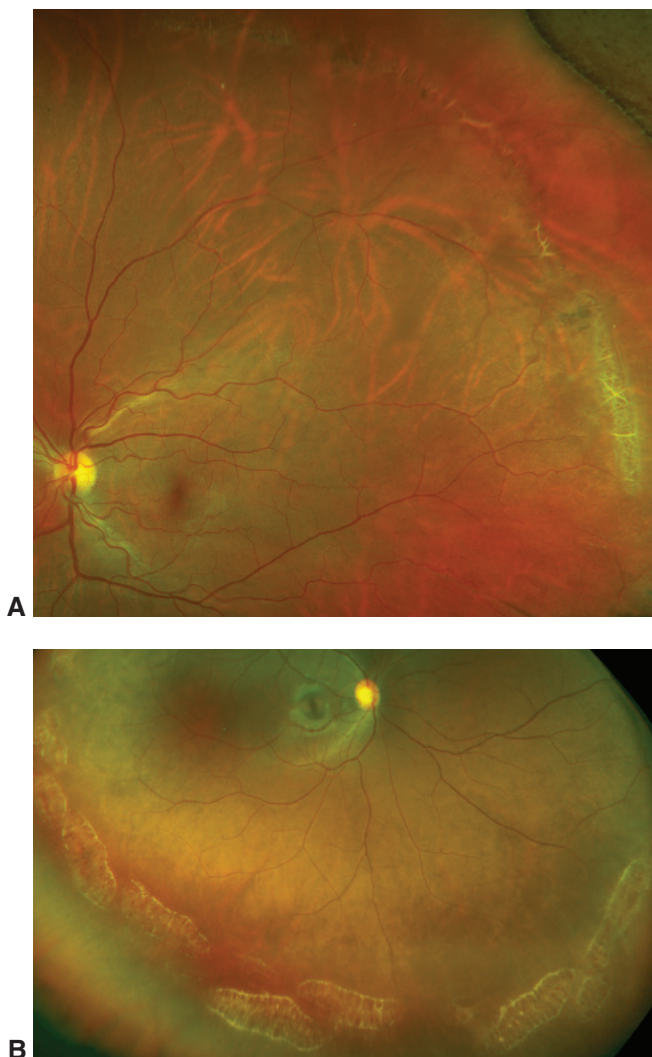


Figure 16-2 Lattice degeneration. **A**, Wide-field color fundus photograph of lattice degeneration. Vascular sheathing is apparent where vessels cross the area of lattice. Characteristic white lattice lines are visible. **B**, Color fundus photograph from another patient shows lattice degeneration inferiorly that appears similar to "snail track" degeneration, with multiple small atrophic retinal holes. (Courtesy of Hannah J. Yu, BS, and Charles C. Wyckoff, MD, PhD.)

Retinal pigment epithelial hyperplasia may surround the tuft. Cystic and zonular traction retinal tufts, both with firm vitreoretinal adhesions, may predispose eyes to retinal tears and detachment.

Byer NE. Cystic retinal tufts and their relationship to retinal detachment. *Arch Ophthalmol.* 1981;99(10):1788–1790.

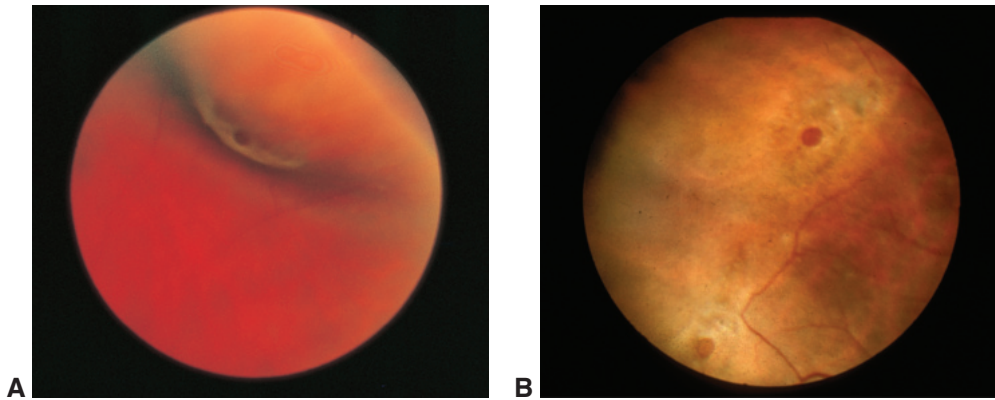


Figure 16-3 Lattice degeneration with atrophic hole. **A**, Fundus photograph of lattice degeneration with a small atrophic hole as viewed with scleral depression. **B**, Fundus photograph of atrophic holes as viewed without scleral depression. (Part A courtesy of Norman E. Byer, MD.)

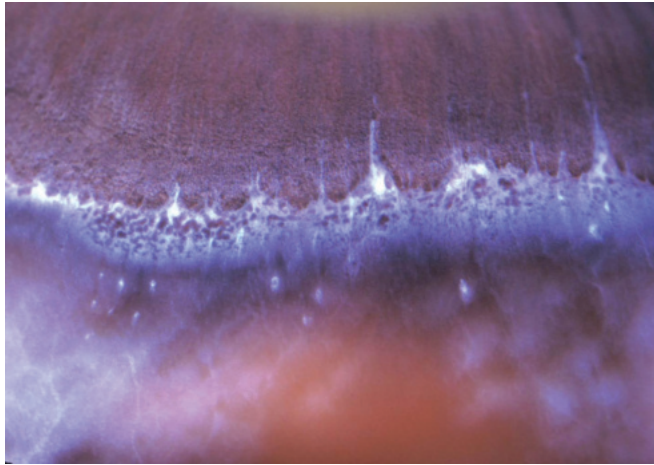


Figure 16-4 Color photograph of a gross eye specimen shows a cluster of white surface nodules with characteristic gross appearance and location of noncystic retinal tufts. (Reproduced with permission from Foos RY, Silverstein RN, eds. System of Ocular Pathology. Vol. 3. iPATH Press; 2004.)

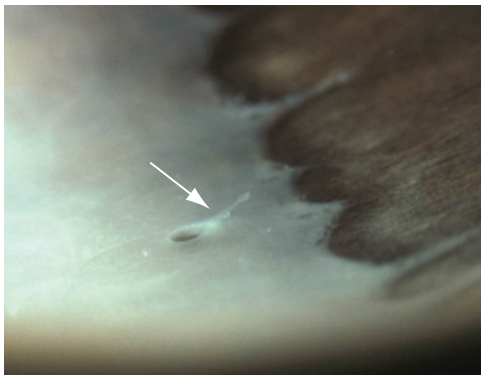


Figure 16-5 Color photograph of a gross eye specimen shows a small zonal traction retinal tuft (arrow) with cystic base. Note that the tuft points anteriorly toward the peripheral lens. (Reproduced with permission from Foos RY, Silverstein RN, eds. System of Ocular Pathology. Vol. 3. iPATH Press; 2004.)

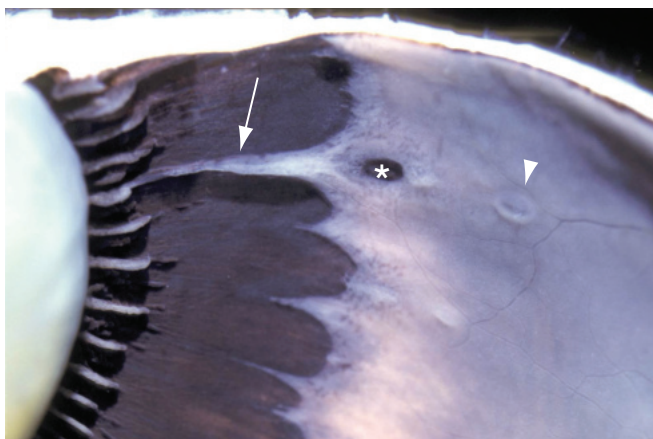


Figure 16-6 Color photograph of a gross eye specimen shows a meridional complex, consisting of an atypical and large dentate process (*white arrow*) that is continuous with a ciliary process of the pars plicata and an area of enclosed pars plana and ora bay (*asterisk*). Slightly posterior to the complex is a small area in the same meridian that appears to be excavated but is in fact a cyst (*arrowhead*). (Modified with permission from Foos RY, Silverstein RN, eds. *System of Ocular Pathology*. Vol. 3. iPATH Press; 2004.)

Meridional Folds, Enclosed Ora Bays, and Peripheral Retinal Excavations

Meridional folds are folds of redundant retina, usually located superonasally. They are usually associated with dentate processes but may also extend posteriorly from ora bays. Occasionally, tears associated with PVD occur at the most posterior limit of the folds (see Chapter 1, Fig 1-3). Retinal tears can also occur at or near the posterior margins of enclosed ora bays, which are oval islands of pars plana epithelium located immediately posterior to the ora serrata and completely or almost completely surrounded by peripheral retina (Fig 16-6). Occasionally, tears may occur at the site of peripheral retinal excavations, which represent a mild form of lattice degeneration. The excavations may have firm vitreoretinal adhesions and are found adjacent to, or up to 4 disc diameters (DDs) posterior to, the ora serrata. They are often aligned with meridional folds.

Engstrom RE Jr, Glasgow BJ, Foos RY, Straatsma BR. Degenerative diseases of the peripheral retina. In: Tasman W, Jaeger EA, eds. *Duane's Clinical Ophthalmology on DVD-ROM*. Vol 3. Lippincott Williams & Wilkins; 2013:chap 26.

Lesions That Do Not Predispose Eyes to Retinal Detachment

Paving-Stone Degeneration

Cobblestone (or paving-stone) degeneration is characterized by peripheral, discrete areas of retinal atrophy (Fig 16-7); it appears in 22% of individuals older than 20 years. The atrophic areas may occur singly or in groups and are sometimes confluent. On histologic examination, these “paving stones” are characterized by atrophy of the retinal pigment epithelium (RPE) and outer retinal layers, attenuation or absence of the choriocapillaris, and adhesions

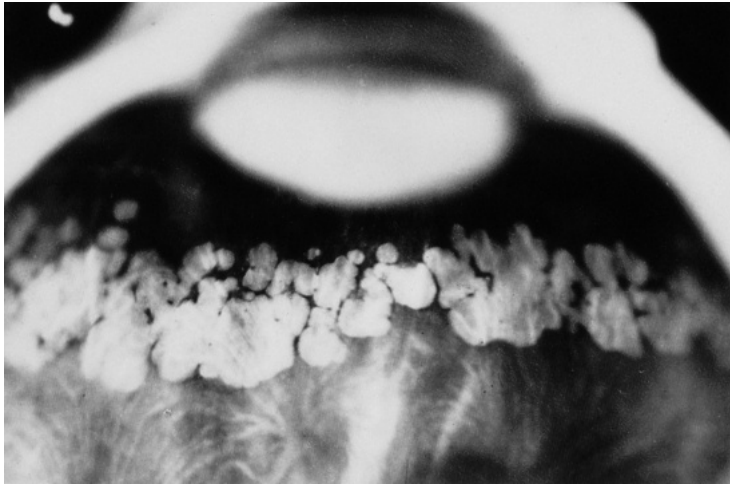


Figure 16-7 Gross appearance of paving-stone degeneration. (Reproduced with permission from Green WR. *Pathology of the retina*. In: Frayer WC, ed. *Lancaster Course in Ophthalmic Histopathology*, unit 9. FA Davis; 1988:181.)

between the remaining neuroepithelial layers and Bruch membrane. These lesions are most common in the inferior quadrants, anterior to the equator. Ophthalmoscopically, they appear yellowish white and are sometimes surrounded by a rim of hypertrophic RPE. Because the RPE is absent or hypoplastic, large choroidal vessels can be visible beneath the lesions.

Retinal Pigment Epithelial Hyperplasia

When stimulated by chronic low-grade traction, RPE cells proliferate. Diffuse retinal pigment epithelial hyperplasia may be observed straddling the ora serrata, in latitudes that correspond roughly to the insertion of the vitreous base. Focal hyperplasia may also occur on the pars plana and in the peripheral retina, especially in areas of focal traction such as vitreoretinal tufts and lattice degeneration. Areas of previous inflammation and trauma may also be sites of retinal pigment epithelial hyperplasia.

Retinal Pigment Epithelial Hypertrophy

Acquired retinal pigment epithelial hypertrophy is a degenerative change associated with aging that commonly occurs in the periphery, often in a reticular pattern. Histologically, it is characterized by large cells and by large, spherical melanin granules. Similar histologic features are present in congenital hypertrophy of the RPE (eg, grouped pigmentation, or “bear tracks”), for which possible associations with systemic findings such as familial adenomatous polyposis (Gardner syndrome) should be considered.

Peripheral Cystoid Degeneration

Typical peripheral cystoid degeneration, characterized by zones of microcysts in the far-peripheral retina, is present in the eyes of almost all adults older than 20 years. Although retinal holes may form in these areas, they rarely cause RD. *Reticular peripheral cystoid*

degeneration, found in approximately 20% of adult eyes, is almost always located posterior to typical peripheral cystoid degeneration. It usually occurs in the inner retina and presents with a linear or reticular pattern that follows the retinal vessels. This form may develop into reticular degenerative retinoschisis. See also the section Retinoschisis.

Retinal Breaks

Retinal breaks are clinically significant in that they may allow liquid from the vitreous cavity to enter the potential space between the neurosensory retina and the RPE, thereby causing an RRD. Some breaks are caused by vitreoretinal traction (tears); others result from atrophy of the retinal layers (holes). Traumatic breaks are discussed in the next section. Retinal breaks may be classified as

- flap, or horseshoe, tears
- giant retinal tears
- operculated holes
- retinal dialyses
- atrophic retinal holes

A *flap tear* occurs when a strip of retina is pulled anteriorly by vitreoretinal traction, often during a PVD or secondary to trauma (Fig 16-8). A tear is considered symptomatic when the patient reports photopsias, floaters, or both. A *giant retinal tear* extends 90° (3 clock-hours) or more circumferentially and usually occurs along the posterior edge of the vitreous base. An *operculated hole* occurs when traction is sufficient to tear a piece of retina completely free from the adjacent retinal surface. A *retinal dialysis* is a circumferential, linear break that occurs at the ora serrata, with vitreous base attached to the retina posterior to the tear's edge; it is commonly a consequence of blunt trauma. An *atrophic retinal hole* is generally not associated with vitreoretinal traction and has not been linked to an increased risk of RD.

American Academy of Ophthalmology Retina/Vitreous Panel. Preferred Practice Pattern Guidelines. *Posterior Vitreous Detachment, Retinal Breaks, and Lattice Degeneration*. American Academy of Ophthalmology; 2019. www.aao.org/ppp

Traumatic Breaks

Blunt or penetrating eye trauma can cause retinal breaks by direct retinal perforation, contusion, or vitreous traction. Fibrocellular proliferation occurring later at the site of an injury may cause vitreoretinal traction and subsequent detachment. Also see Chapter 17.

Blunt trauma can cause retinal breaks by direct contusive injury to the globe through 2 mechanisms: (1) coup, adjacent to the point of trauma, and (2) contrecoup, opposite the point of trauma. Blunt trauma compresses the eye along its anteroposterior axis and expands it in the equatorial plane. Because the vitreous body is viscoelastic, slow compression of the eye has no deleterious effect on the retina. However, rapid compression of the eye results in severe traction on the vitreous base that may tear the retina.

Contusion injury may cause large, ragged equatorial breaks; dialysis; or a macular hole. Traumatic breaks are often multiple, and they are commonly found in the inferotemporal

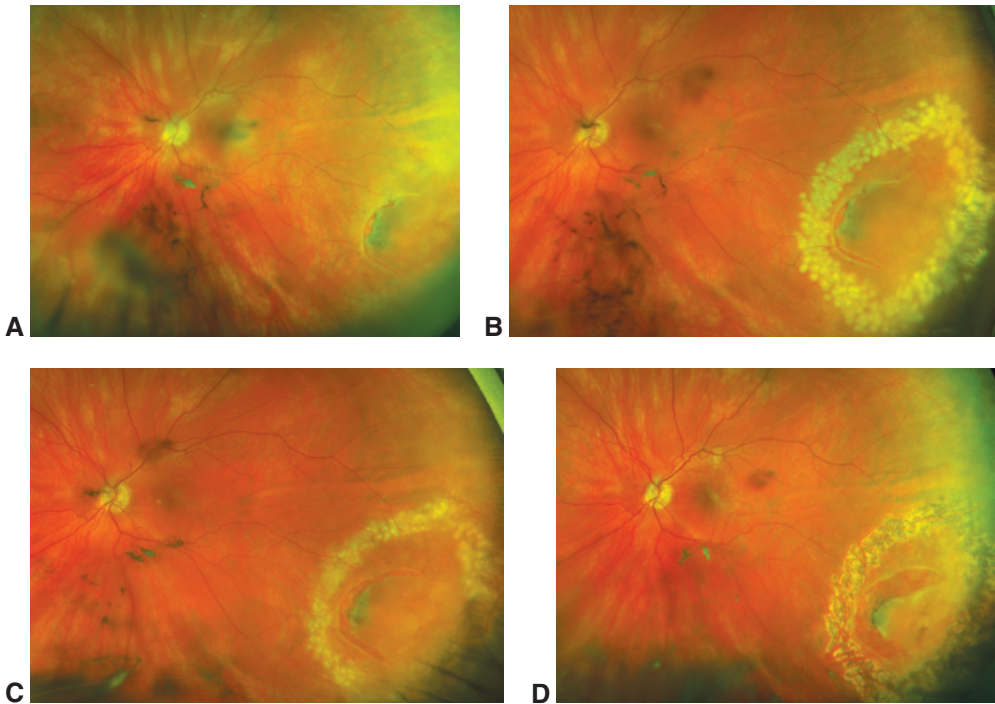


Figure 16-8 Flap retinal tear. Sequence of color fundus photographs of a large, temporally located flap tear with associated small cuff of subretinal fluid and multiple small ruptured bridging retinal vessels with mild vitreous hemorrhage. **A**, At presentation. **B**, Immediately following laser demarcation. **C**, One week after laser demarcation. **D**, One month after laser demarcation. (Courtesy of Hannah J. Yu, BS, and Charles C. Wykoff, MD, PhD.)

and superonasal quadrants. The most common contusion injuries are dialyses, which may be as small as 1 ora bay (the distance between 2 retinal dentate processes at the latitude of the ora serrata) or may extend 90° or more. Dialyses are usually located at the posterior border of the vitreous base but can also occur at the anterior border (Fig 16-9, Activity 16-1). Avulsion of the vitreous base may be associated with dialysis and is considered pathognomonic of ocular contusion. The vitreous base can be avulsed from the underlying retina and nonpigmented epithelium of the pars plana without tearing either one; generally, however, one or both may also be torn in the process. Less common types of breaks caused by blunt trauma are horseshoe tears (which may occur at the posterior margin of the vitreous base, at the posterior end of a meridional fold, or at the equator) and operculated holes.



ACTIVITY 16-1 Anatomy Marker Activity: Retinal tears and holes.

Courtesy of Mark M. Miller and Colin McCannel, MD.



Trauma in Young Eyes

Although young patients have a higher incidence of eye injury than do other age groups, only in rare instances does the retina detach immediately after blunt trauma because

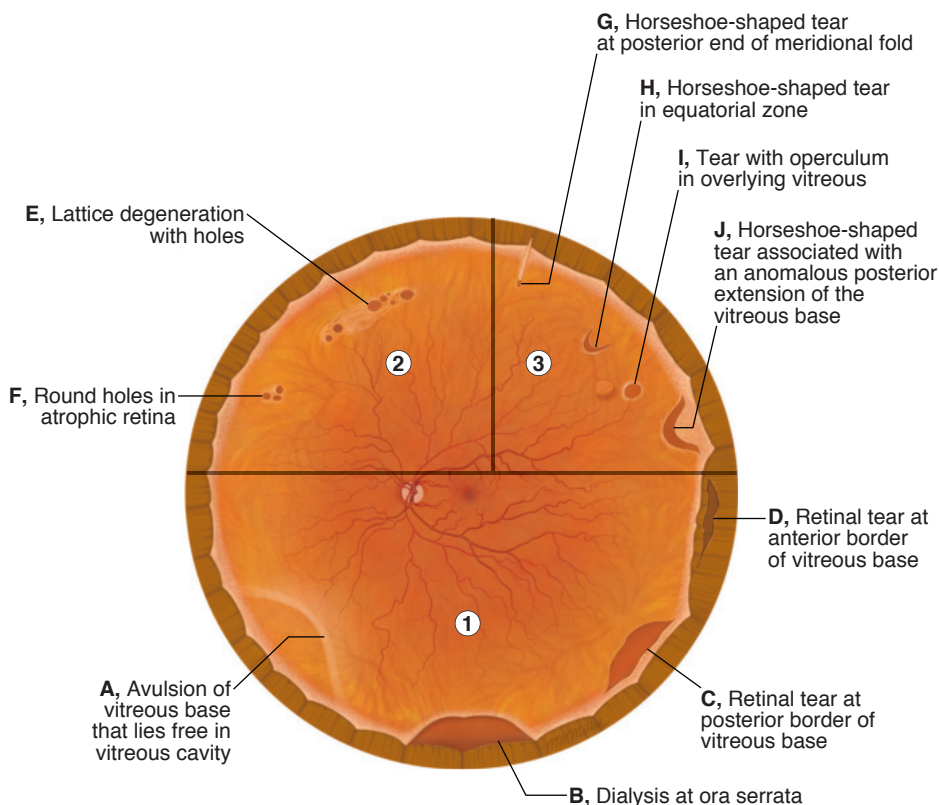


Figure 16-9 Schematic illustration of retinal tears and holes. **Part 1:** Retinal breaks at borders of the vitreous base. **A**, Avulsion of the vitreous base that lies free in the vitreous cavity. **B**, Dialysis of the ora serrata. **C**, Retinal tear at the posterior border of the vitreous base. **D**, Retinal tear at the anterior border of the vitreous base. **Part 2:** Retinal breaks with areas of abnormal vitreoretinal interface (lattice degeneration). **E**, Lattice degeneration with holes. **F**, Round holes in atrophic retina. **Part 3:** Retinal breaks associated with abnormal vitreoretinal attachments. **G**, Flap, or horseshoe, tear at the posterior end of a meridional fold. **H**, Horseshoe tear in the equatorial zone. **I**, Tear with operculum in the overlying vitreous. **J**, Horseshoe tear associated with an anomalous posterior extension of the vitreous base. (Illustration by Mark M. Miller.)

young vitreous has not yet undergone synchysis (liquefaction). The vitreous, therefore, does not allow fluid movement through the retinal tears or dialyses. With time, however, the vitreous may liquefy over a tear, allowing fluid to pass through the break to detach the retina. The clinical presentation of the RD is thus usually delayed:

- 12% of detachments identified immediately
- 30% identified within 1 month
- 50% identified within 8 months
- 80% identified within 24 months

Traumatic RDs in young patients may be shallow and often show signs of chronicity, including multiple demarcation lines, subretinal deposits, and areas of intraretinal schisis.

When posterior vitreous separation is present or occurs later after trauma, retinal breaks are often associated with abnormal vitreoretinal attachments and may resemble nontraumatic breaks. RDs may occur acutely in these patients.

Prophylactic Treatment of Retinal Breaks

Any retinal break can cause an RD by allowing liquid from the vitreous cavity to pass through the break and separate the sensory retina from the RPE. However, the vast majority of retinal holes and breaks do not cause a detachment.

The ophthalmologist may consider prophylactic treatment of breaks in an attempt to reduce the risk of RD (Table 16-1). Treatment does not eliminate the risk of new tears or detachment, an important point for patient counseling.

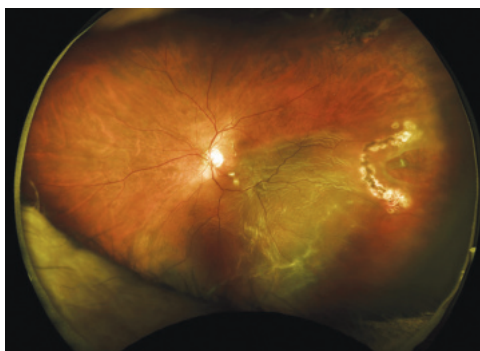
The goal of prophylactic laser treatment or cryotherapy for retinal breaks is the creation of a chorioretinal adhesion around each break to prevent fluid from entering the subretinal space. When subretinal fluid is present, treatment is applied so that it fully surrounds the area of subretinal fluid (see Fig 16-8). When insufficient treatment is applied, vitreous traction can lead to anterior extension of horseshoe tears and RD (Fig 16-10). Similarly, when lattice degeneration is treated, typically the entire lesion is surrounded with treatment applications.

When considering prophylaxis, the ophthalmologist weighs numerous factors, including symptoms, family history, residual traction, size and location of the break, phakic status, refractive error, status of the fellow eye, presence of subretinal fluid, and availability of the patient for follow-up evaluation. The following discussion serves only as a broad guideline, because individual patient characteristics and clinical factors must be considered for each patient (see also the discussion of hereditary hyaloideoretinopathies with optically empty vitreous in Chapter 15).

Table 16-1 Prophylactic Treatment of Retinal Breaks

Type of Retinal Lesion	Treatment
Acute symptomatic dialysis	Treat promptly
Acute symptomatic flap, or horseshoe, tear	Treat promptly
Acute symptomatic operculated hole	Consider treatment
Asymptomatic atrophic hole	Often observed without treatment, but consider treatment in specific clinical circumstances
Asymptomatic dialysis	No consensus guidelines, but consider treatment
Asymptomatic horseshoe tear (no subretinal fluid)	Consider treatment
Asymptomatic lattice degeneration, with or without atrophic holes (no subretinal fluid)	Often observed without treatment, but consider treatment in specific clinical circumstances
Asymptomatic operculated hole	Often observed without treatment, but consider treatment in specific clinical circumstances
Eyes with lattice degeneration, atrophic holes, or asymptomatic retinal tear where the fellow eye has had a retinal detachment	No consensus guidelines, but consider treatment

Figure 16-10 Wide-field image shows a horse-shoe tear inadequately surrounded by laser applications and subsequent retinal detachment (RD). (Courtesy of Stephen J. Kim, MD.)



Symptomatic Retinal Breaks

Overall, 7%–18% of eyes with a symptomatic PVD are found to have 1 or more tractional tears at initial examination. Numerous clinical studies have demonstrated that acute symptomatic breaks are at substantial risk of progressing to RD, especially when there is associated vitreous hemorrhage. Therefore, acute symptomatic flap tears are commonly treated prophylactically.

Acute symptomatic operculated holes may be less likely to cause detachment because there may be no residual traction on the adjacent retina. Typically, prophylactic treatment is performed when evaluation reveals persistent vitreous traction at the margin of an operculated hole, when the hole is large or located superiorly, or when there is vitreous hemorrhage.

Atrophic holes may be incidental findings in a patient who presents with an acute PVD, and treatment may not be necessary for these holes.

Asymptomatic Retinal Breaks

Asymptomatic flap tears progress to RD in approximately 5% of cases. Because of this risk, treatment may be considered but may not be universally recommended in emmetropic, phakic eyes. Asymptomatic flap tears accompanied by additional clinically relevant findings such as lattice degeneration, myopia, or subclinical detachment, or by aphakia, pseudophakia, or history of RD in the fellow eye may confer an increased risk of progression to RD, and treatment may be recommended. Asymptomatic operculated holes and atrophic holes rarely cause RD, so treatment is generally not recommended unless the patient is at high risk for RD.

Lattice Degeneration

Although limited data are available, an 11-year follow-up study of patients with untreated lattice degeneration and no symptomatic tears showed that RD occurred in approximately 1% of cases. Thus, the presence of lattice, with or without atrophic holes, generally does not require prophylaxis in the absence of other risk factors or symptoms. If lattice degeneration is present in a patient with additional risk factors, such as RD in the fellow eye, flap tears, pseudophakia, or aphakia, prophylactic treatment may be considered.

Wilkinson CP. Interventions for asymptomatic retinal breaks and lattice degeneration for preventing retinal detachment. *Cochrane Database Syst Rev.* 2014;(9):CD003170.

Aphakia and Pseudophakia

Removal of the native crystalline lens can lead to anterior shifting of the vitreous and subsequent retinal traction. Because aphakic and pseudophakic eyes have higher risks of RD (1%–3%) than phakic eyes, such patients should be warned of potential symptoms of RD and carefully examined if they occur. These symptoms overlap with symptoms associated with PVD and include new flashes, floaters, or the appearance of curtains in the visual field. In a population-based 25-year follow-up study comparing eyes that underwent cataract surgery with eyes that did not, the probability of RD following cataract surgery was greatest in the first year (an approximately 11-fold difference, compared with approximately fourfold in years 5 through 20). The cumulative risk of RD steadily increased to 1.79% at 20 years. Risk factors for the development of RD following cataract surgery include male sex, younger age, myopia, increased axial length, posterior capsule tear, and absence of a PVD.

Erie JC, Raecker MA, Baratz KH, Schleck CD, Burke JP, Robertson DM. Risk of retinal detachment after cataract extraction, 1980–2004: a population-based study. *Ophthalmology*. 2006;113(11):2026–2032.

Fellow Eye in Patients With Retinal Detachment

In patients with RD, the fellow-eye risk of detachment is approximately 10% for phakic patients and substantially higher for aphakic and pseudophakic patients. Vitreous status may play a role in determining this clinical risk. Complete retinal evaluation, including peripheral evaluation with 360° scleral depression, may be considered for patients developing concerning symptoms. Prophylactic treatment of retinal breaks and lattice degeneration, even if asymptomatic, may be considered. Additional clinical scenarios, including Stickler syndrome, may indicate the need for fellow-eye prophylactic treatment to decrease the risk of RD development.

Folk JC, Arrindell EL, Klugman MR. The fellow eye of patients with phakic lattice retinal detachment. *Ophthalmology*. 1989;96(1):72–79.

Subclinical Retinal Detachment

The term *subclinical RD* is used in various ways in the literature. It can refer to an asymptomatic RD, or a detachment in which subretinal fluid extends more than 1 DD from the break but not more than 2 DDs posterior to the equator. Because approximately 30% of such detachments progress, treatment may be considered. Treatment may be advised particularly for symptomatic patients and cases involving traction on the break. Presence of a demarcation line suggests a lower risk; however, progression may occur through the demarcation line.

Brod RD, Flynn HW Jr, Lightman DA. Asymptomatic rhegmatogenous retinal detachments. *Arch Ophthalmol*. 1995;113(8):1030–1032.

Retinal Detachment

Retinal detachments are classified as rhegmatogenous, traction, or exudative. The most common are *rhegmatogenous retinal detachments (RRDs)*. The term is derived from the

Greek *rhegma*, meaning “break.” RRDs are caused by fluid passing from the vitreous cavity through a retinal break into the potential space between the neurosensory retina and the RPE. Less common than RRDs, *traction* (also called *tractional*) *detachments* are caused by proliferative membranes that contract and elevate the retina. Combinations of traction and rhegmatogenous pathophysiologic components may also lead to RD. *Exudative*, or *serous*, *detachments* are caused by retinal or choroidal diseases in which fluid accumulates beneath the neurosensory retina.

The differential diagnosis of RD includes retinoschisis, choroidal tumors, and retinal elevation secondary to detachment of the choroid. Table 16-2 lists diagnostic features of the 3 types of RD.

Rhegmatogenous Retinal Detachment

The Rochester epidemiology project determined that RRD has an annual incidence of 12.6 per 100,000 persons in a primarily White population. A given individual's risk is affected by the presence or absence of certain factors, including high myopia, family history of RD, fellow-eye retinal tear or detachment, recent vitreous detachment, pseudophakia, trauma, peripheral high-risk lesions, and vitreoretinal degenerations.

In 90%–95% of RRDs, a definite retinal break can be found, often with the help of Lincoff rules (Fig 16-11). In the remainder, an occult break is presumed to be present. If no break can be found, the ophthalmologist must rule out all other causes of retinal elevation. Half of patients with RRD have photopsias or floaters. The intraocular pressure is usually lower in the affected eye than in the fellow eye but may occasionally be higher, for example, when associated with Schwartz-Matsuo syndrome. A Shafer sign, descriptively termed “tobacco dust” because of the small clumps of pigmented cells in the anterior vitreous, is frequently present. The retina typically detaches progressively from the periphery to the optic nerve head; usually it has convex borders and contours and a corrugated appearance, especially in recent RDs, and undulates with eye movements. In contrast, in a long-standing RRD, the retina may appear smoother and thinner. Further, retinal macrocysts, arising from the outer plexiform layer, can be seen in long-standing RRD, particularly of the traumatic type with retinal dialysis (Fig 16-12). Fixed folds resulting from proliferative vitreoretinopathy (PVR) almost always indicate an RRD. Shifting fluid may occur, but it is uncommon and more typical of exudative RDs.

PVR is the most common cause of failure after surgical repair of an RRD. In PVR, retinal pigment epithelial, glial, and other cells grow and migrate on both the inner and outer retinal surfaces and on the vitreous face, forming membranes. Contraction of these membranes causes fixed retinal folds, often appearing as star-shaped folds; equatorial traction; detachment of the nonpigmented epithelium from the pars plana; and generalized retinal shrinkage (Fig 16-13). As a result, the causative retinal breaks may reopen, new breaks may occur, or a traction detachment may develop.

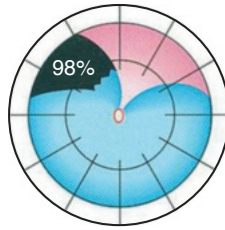
To better compare preoperative anatomy with postoperative outcomes, a classification scheme of PVR was created (Table 16-3). The classification lists 3 grades of PVR (A, B, and C), which correspond to increasing severity of disease. Anterior and posterior involvement (CA, CP) are distinguished and subclassified into focal, diffuse, circumferential, subretinal, and anterior displacement, and the extent of the pathology is described in clock-hours.

Table 16-2 Diagnostic Features of the 3 Types of Retinal Detachments

	Rhegmatogenous (Primary)	Nonrhegmatogenous (Secondary) Traction	Exudative
History	Aphakia, myopia, blunt trauma, photopsia, floaters, visual field defect; progressive, generally healthy	Diabetes, ischemic venous occlusive disease, sickle cell disease, penetrating trauma, prematurity	Systemic factors such as malignant hypertension, eclampsia, renal failure, severe central serous chorioretinopathy
Retinal break	Tears or holes identified in 90%–95% of cases	None or may develop secondarily	None, or coincidental
Extent and characteristics of detachment	Extends ora serrata to optic nerve head early, has convex borders and surfaces and corrugated appearance; gravity dependent	Frequently does not extend to ora serrata, may be central or peripheral, has concave borders and surfaces	Volume and gravity dependent; extension to ora serrata is variable, may be central or peripheral, smooth surface
Retinal mobility	Undulating bullae or folds	Taut retina, peaks to traction points	Smoothly elevated bullae, usually without folds
Evidence of chronicity	Demarcation lines, intraretinal macrocysts, atrophic retina	Demarcation lines	Usually none
Pigment in vitreous	Present in 70% of cases	Present in trauma cases	Not present
Vitreous changes	Frequently synergetic; posterior vitreous detachment, traction on flap of tear	Vitreoretinal traction with preretinal proliferative membranes	Usually clear, except in uveitis
Subretinal fluid	Clear	Clear, no shift	May be turbid and shift rapidly to dependent location with changes in head position
Choroidal mass	None	None	May be present
Intraocular pressure	Frequently low	Usually normal	Varies
Transillumination	Normal	Normal	Normal; however, blocked transillumination if pigmented choroidal lesion present
Examples of conditions causing detachment	Retinal break	Proliferative diabetic retinopathy, retinopathy of prematurity, toxocariasis, sickle cell retinopathy, posttraumatic vitreous traction	Uveitis, metastatic tumor, malignant melanoma, Coats disease, Vogt-Koyanagi-Harada syndrome, retinoblastoma, choroidal hemangioma, senile exudative maculopathy, exudative detachment after cryotherapy or diathermy

Modified from Hilton GF, McLean EB, Brinton DA, eds. *Retinal Detachment: Principles and Practice*. 2nd ed. Ophthalmology Monograph 1. American Academy of Ophthalmology; 1995.

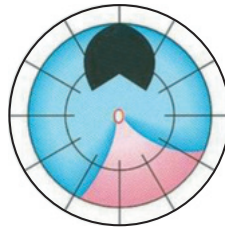
Rules to Find the Primary Break



Rule 1:

Superior temporal or nasal detachments:

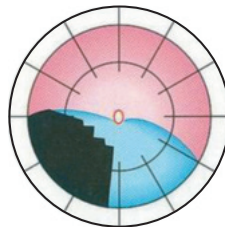
In 98%, the primary break lies within $1\frac{1}{2}$ clock-hours of the highest border.



Rule 2:

Total or superior detachments that cross the 12 o'clock meridian:

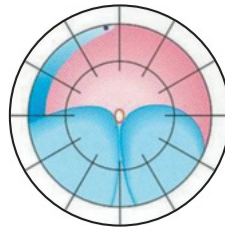
In 93%, the primary break is at 12 o'clock or in a triangle, the apex of which is at the ora serrata, and the sides of which extend $1\frac{1}{2}$ clock-hours to either side of 12 o'clock.



Rule 3:

Inferior detachments:

In 95%, the higher side of the detachment indicates on which side of the disc an inferior break lies.



Rule 4:

"Inferior" bullous detachment:

Inferior bullae in a rhegmatogenous detachment originate from a superior break.

Figure 16-11 Lincoff rules for finding the primary retinal break. Guttering, as illustrated in Rule 4, may be difficult to identify and may require indirect ophthalmoscopy with scleral depression for visualization. (Reproduced with permission from Kreissig I. A Practical Guide to Minimal Surgery for Retinal Detachment. Vol 1. Thieme Medical Publishers, Inc; 2000:13–18. www.thieme.com.)

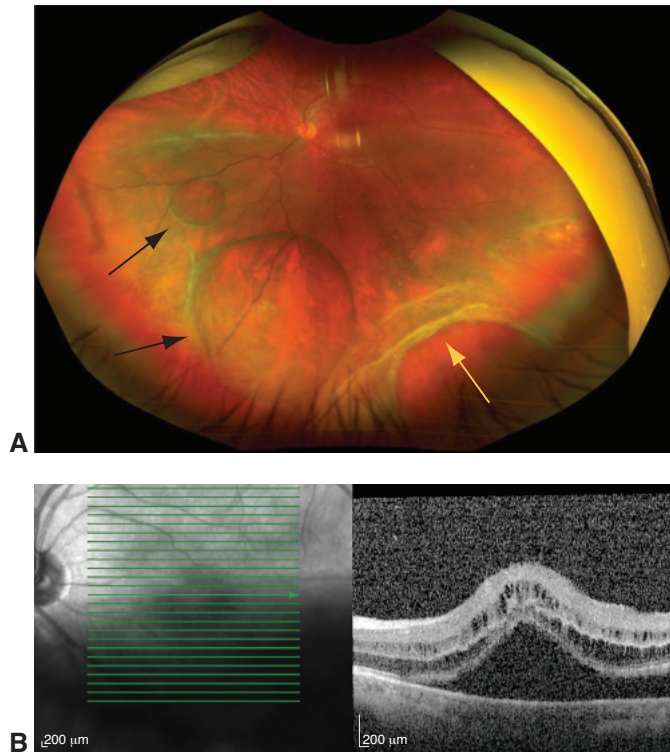


Figure 16-12 Retinal dialysis and macrocysts. **A**, Wide-field color fundus photograph shows a long-standing macula-off RD with an inferotemporal dialysis (yellow arrow) and large nasal and inferior macrocysts (black arrows) that arise from the outer plexiform layer. **B**, OCT shows that the detachment extends through the macula. (Courtesy of Avni P. Finn, MD, MBA.)

Han DP, Lean JS. Proliferative vitreoretinopathy. In: Albert DM, Miller JW, Azar DT, Blodi BA, eds. *Albert & Jakobiec's Principles and Practice of Ophthalmology*. Saunders; 2008:chap 183.

Rowe JA, Erie JC, Baratz KH, et al. Retinal detachment in Olmsted County, Minnesota, 1976 through 1995. *Ophthalmology*. 1999;106(1):154–159.

Management of rhegmatogenous retinal detachment

The principles of surgery for RD are as follows:

- Find all retinal breaks.
- Create a chorioretinal irritation around each break.
- Close the retinal breaks.

The most important element in management of RD is a careful retinal examination. Retinal breaks can be closed by several methods, all of which involve bringing the RPE and choroid into contact with the retina long enough to produce a chorioretinal adhesion that will permanently wall off the subretinal space. This process usually involves 1 of 3 approaches: (1) *scleral buckling*, (2) *vitrectomy*, or (3) *pneumatic retinopexy*. For acute,

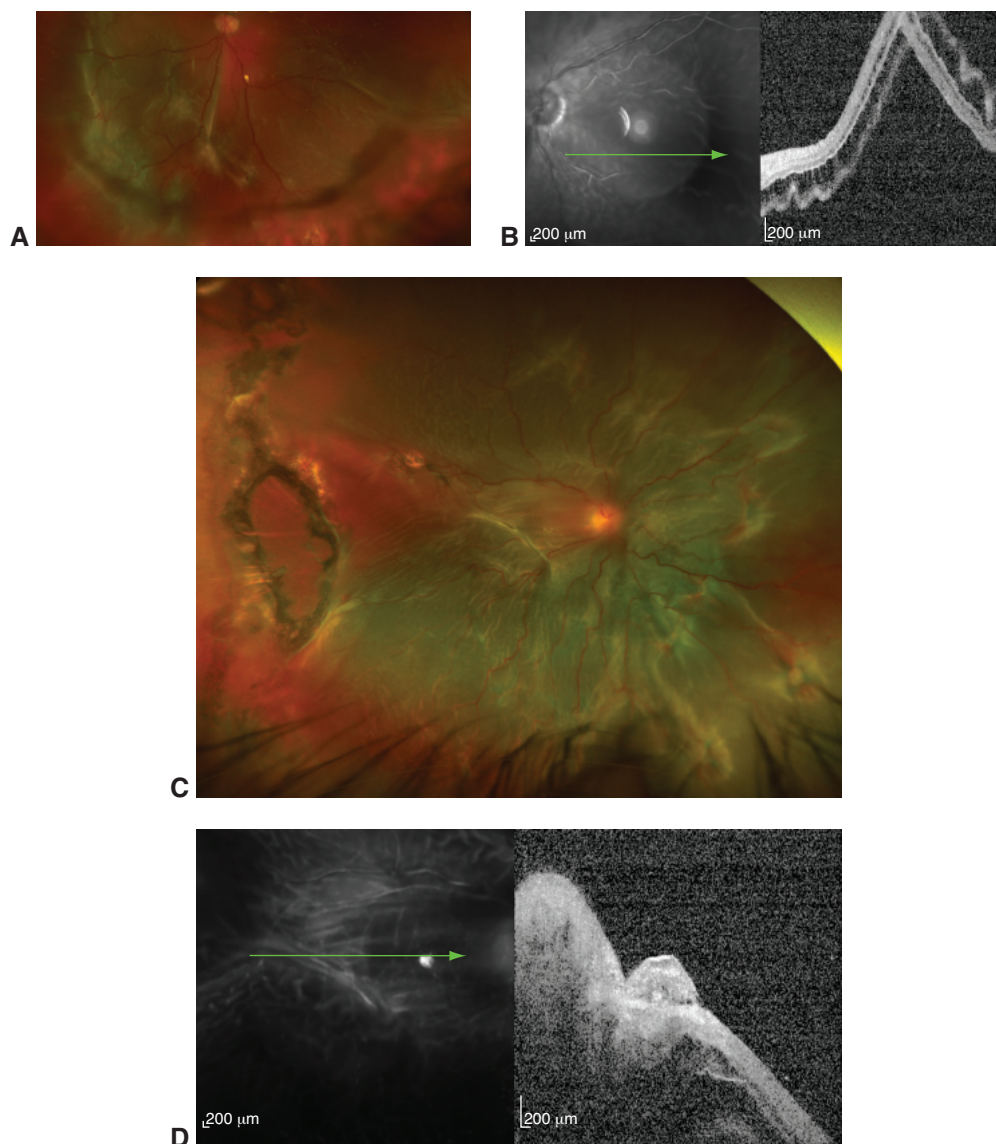


Figure 16-13 Proliferative vitreoretinopathy. **A**, Wide-field color fundus photograph of rhegmatogenous retinal detachment (RRD) with multiple early fixed retinal folds in the inferonasal quadrant. Underlying indentation of the peripheral retinal pigment epithelium is visualized because of a previously placed encircling scleral buckle. **B**, Corresponding near-infrared reflectance image from the same patient (*left*). *Green arrow* marks the location of the spectral-domain optical coherence tomography (SD-OCT) image (*right*), which shows RD with no appreciable preretinal proliferative tissues posteriorly. **C**, Wide-field color fundus photograph (different patient) of total RRD with extensive and severe preretinal proliferative tissues with retinal contraction, multiple fixed retinal folds, and a large retinal break temporally. **D**, Corresponding near-infrared reflectance image from the same patient (*left*). *Green arrow* marks the location of the SD-OCT image (*right*), which shows RD with thick preretinal proliferative tissues posteriorly. (Courtesy of Tien P. Wong, MD, and Charles C. Wyckoff, MD, PhD.)

Table 16-3 Classification of Proliferative Vitreoretinopathy, 1991

Grade	Features
A	Vitreous haze, vitreous pigment clumps, pigment clusters on inferior retina
B	Wrinkling of inner retinal surface, retinal stiffness, vessel tortuosity, rolled and irregular edge of retinal break, decreased mobility of vitreous
CP 1–12	Posterior to equator: focal, diffuse, or circumferential full-thickness folds, ^a subretinal strands ^a
CA 1–12	Anterior to equator: focal, diffuse, or circumferential full-thickness folds, ^a subretinal strands, ^a anterior displacement, ^a condensed vitreous with strands

^aExpressed in number of clock-hours involved.

Used with permission from Machemer R, Aaberg TM, Freeman HM, Irvine AR, Lean JS, Michels RM. An updated classification of retinal detachment with proliferative vitreoretinopathy. *Am J Ophthalmol.* 1991;112(2):159–165.

macula-on RDs with symptoms, surgery is typically performed urgently. Preoperatively, minimizing patient eye movement, particularly saccadic movements while reading, and head positioning to orient the RD in a dependent position can minimize the risk of subretinal fluid extension into the fovea. In contrast, in eyes with chronic RDs with pigmented demarcation lines, treatment may be delayed or may not be needed (Fig 16-14). See Chapter 19 for a more detailed discussion of these management approaches.

Traction Retinal Detachment

Vitreous membranes caused by penetrating injuries or by proliferative retinopathies such as diabetic retinopathy can pull the neurosensory retina away from the RPE, causing a traction RD (Fig 16-15). The retina characteristically has a smooth concave surface and contours and is immobile. The detachment may be central or peripheral and, in rare cases, may extend from the optic nerve head to the ora serrata. In most cases, the causative

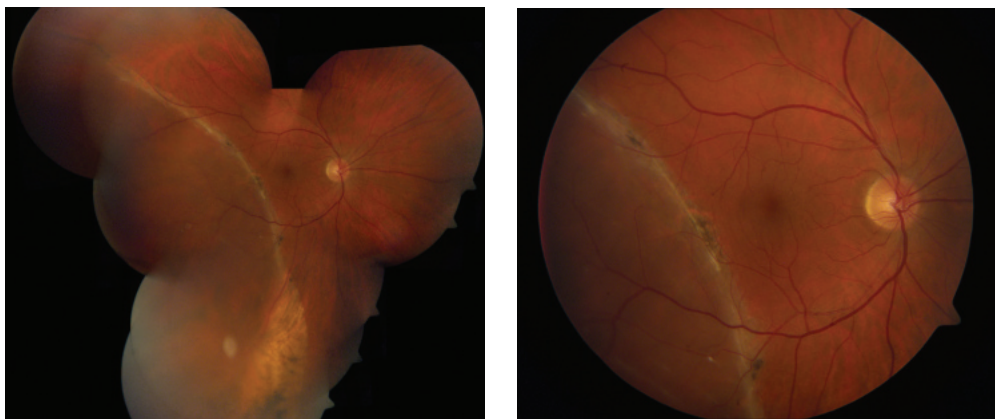


Figure 16-14 Chronic RD. At initial examination (*left*), the patient presented with an asymptomatic large RD with a pigmented and atrophic demarcation line. No progression was observed over several weeks, and surgery was performed electively (*right*). (Courtesy of Stephen J. Kim, MD.)

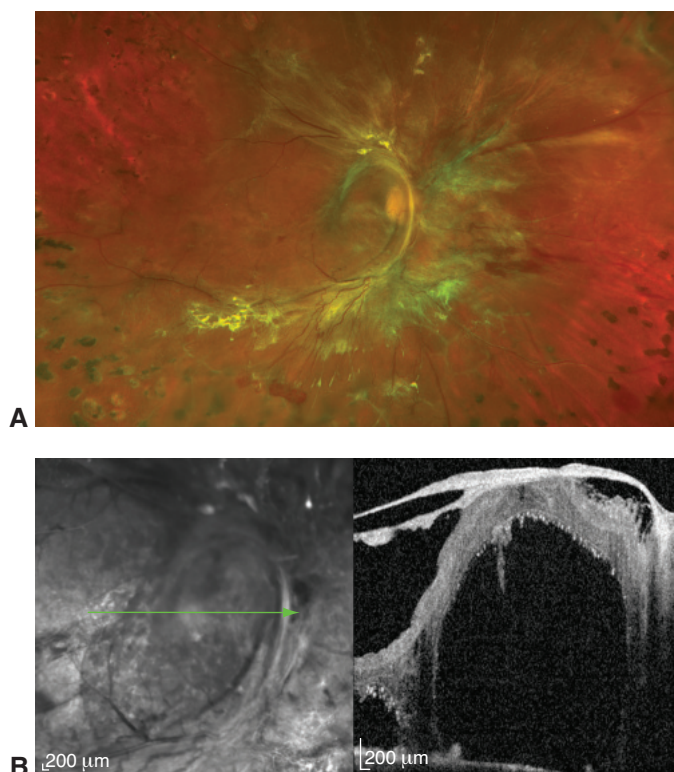


Figure 16-15 Traction RD secondary to proliferative diabetic retinopathy. **A**, Wide-field color fundus photograph of macula-involving traction RD. Extensive fibrotic neovascularization of the optic nerve head extending along the arcade vasculature is visible with associated severe retinal traction. Peripheral panretinal photocoagulation marks are visible. **B**, Corresponding near-infrared reflectance image from the same patient (*left*). *Green arrow* marks the location of the SD-OCT image (*right*), which shows separation of the neurosensory retina from the underlying retinal pigment epithelium due to thick preretinal proliferative tissues. (Courtesy of Tien P. Wong, MD, and Charles C. Wykoff, MD, PhD.)

vitreous membrane can be visualized. If the traction can be released by vitrectomy, the detachment may resolve without evacuation of the subretinal fluid.

In some cases, traction may tear the retina and cause a combined traction and rhegmatogenous detachment. Clinically, the retina loses its concave surface and assumes a convex shape similar to that in an RRD. Retinal mobility is often limited because of the tethering by proliferative tissue. In addition, corrugations characteristic of an RRD are present, and subretinal fluid, which is more extensive than in traction RD, may extend from the optic nerve head to the ora.

Exudative Retinal Detachment

Recognizing that an RD is exudative is crucial because, unlike with other types of RDs, the management of exudative RD is usually nonsurgical. Exudative detachment occurs when either retinal blood vessels leak or the RPE is damaged, allowing fluid to accumulate in the

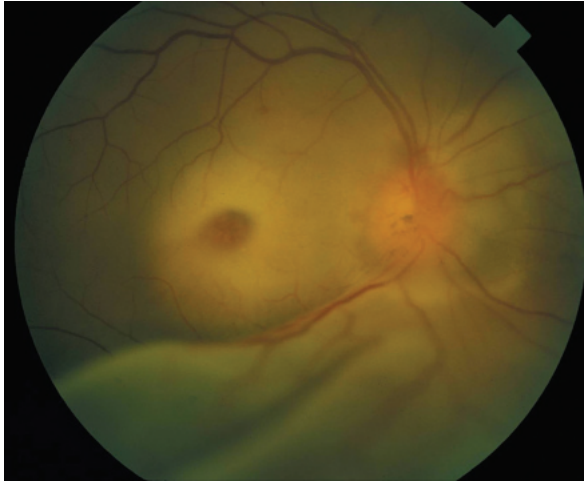


Figure 16-16 Color fundus photograph of an exudative RD that resulted from metastatic breast carcinoma. (Courtesy of Hermann D. Schubert, MD.)

subretinal space (Fig 16-16). Neoplasia and inflammatory diseases are the leading causes of large exudative detachments.

The presence of shifting fluid strongly suggests an exudative RD. Because the subretinal fluid responds to gravity, it causes detachment of the area of retina in which it accumulates. For example, when the patient is sitting, the inferior retina is detached. When the patient becomes supine, the fluid moves posteriorly in a matter of seconds or minutes, detaching the macula. Another characteristic of exudative detachments is the smoothness of the detached retinal surface, in contrast to the corrugated appearance in eyes with RRDs. Included in the differential diagnosis is rhegmatogenous inferior bullous detachment associated with a superior retinal tear, in which the subretinal fluid may shift (see Fig 16-11, Rule 4). Fixed retinal folds, which usually indicate PVR, are rarely, if ever, present in exudative detachments. Occasionally, the retina is sufficiently elevated in exudative detachments to be visible directly behind the lens (eg, in Coats disease), a rare occurrence in RRDs.

Differential Diagnosis of Retinal Detachment

Retinoschisis

Typical peripheral cystoid degeneration is present in virtually all adult eyes bilaterally. Contiguous with and extending up to 2–3 mm posterior to the ora serrata, the area of degeneration, which is best visualized with scleral depression, has a “bubbly” appearance. The cystoid cavities in the outer plexiform layer contain a hyaluronidase-sensitive mucopolysaccharide. The only known complications of typical cystoid degeneration are coalescence and extension of the cavities and progression to typical degenerative retinoschisis.

Reticular peripheral cystoid degeneration is almost always located posterior to and continuous with typical peripheral cystoid degeneration, but it is considerably less common. It

has a linear or reticular pattern that corresponds to the retinal vessels and a finely stippled internal surface. The cystoid spaces are in the nerve fiber layer. This condition may progress to reticular degenerative retinoschisis, also known as *bullous retinoschisis* (Fig 16-17).

Although degenerative retinoschisis is sometimes divided into typical and reticular forms, clinical differentiation is difficult. The complications of posterior extension and progression to RD are associated with the reticular form. Retinoschisis is bilateral in 50%–80% of affected patients, often occurs in the inferotemporal quadrant, and is commonly associated with hyperopia.

In *typical degenerative retinoschisis*, the retina splits in the outer plexiform layer. The outer layer is irregular and appears pockmarked on scleral depression. The inner layer is thin and appears clinically as a smooth, oval elevation, usually in the inferotemporal quadrant but sometimes located superotemporally. Occasionally, small, irregular white dots (“snowflakes”) are present; these are footplates of Müller cells and neurons that bridge or formerly bridged the cavity. The retinal vessels may appear sclerotic. In all cases, peripheral cystoid degeneration with a typical bubbly appearance can be found anterior to the

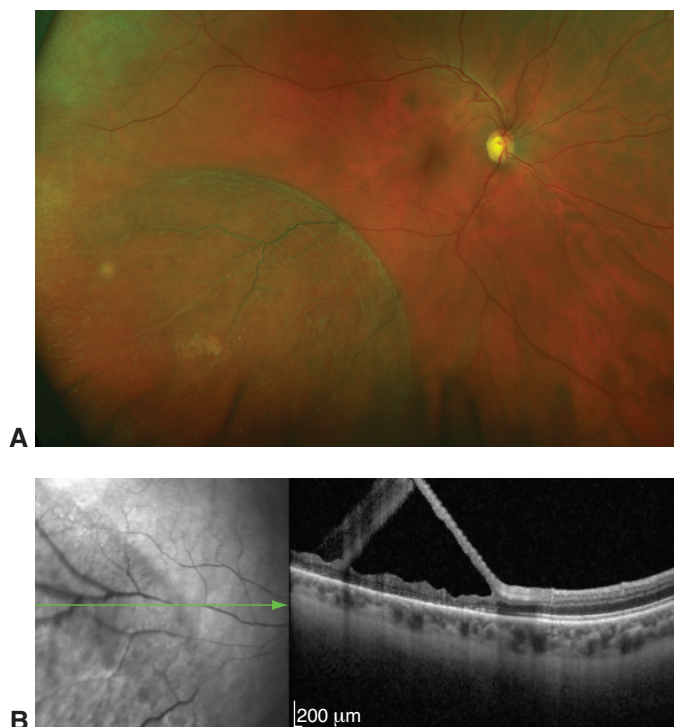


Figure 16-17 Bullous degenerative retinoschisis, also referred to as *reticular degenerative retinoschisis*. **A**, Wide-field color fundus photograph of inferotemporal bullous retinoschisis with visible “snowflakes.” **B**, Corresponding near-infrared reflectance image from the same patient (*left*). The area of retinoschisis is visible as the slightly darker area to the left with flat posterior retina to the right. *Green arrow* marks the location of the SD-OCT image (*right*), which shows the transition into the area of retinoschisis with splitting of the retina in the outer plexiform layer and thinning of the inner layer compared with the uninvolved more posterior retina. (Courtesy of Hannah J. Yu, BS, and Charles C. Wykoff, MD, PhD.)

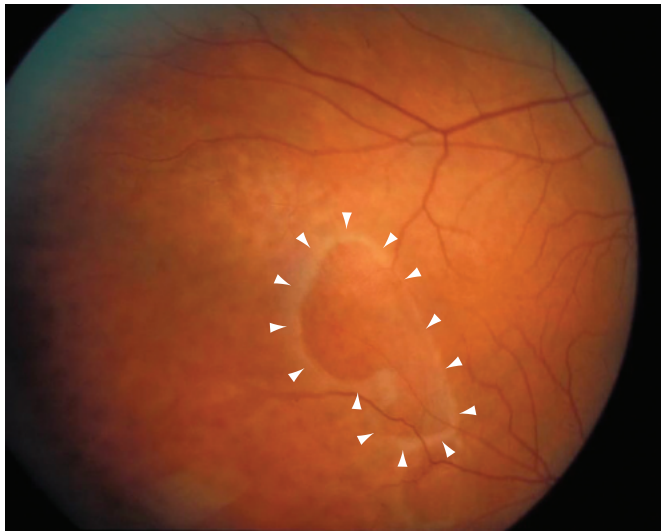


Figure 16-18 Retinoschisis with large, irregular outer-schisis-layer holes (outlined by arrowheads) and yellow dots on the inner surface. (Courtesy of Colin A. McCannel, MD.)

schisis cavity. The schisis may extend posteriorly to the equator, but complications such as hole formation, RD, or marked posterior extension are rare. The split in the retina almost never extends as far posteriorly as the macula. Laser barricade is generally not effective.

In *reticular degenerative retinoschisis*, the splitting occurs in the nerve fiber layer. The very thin inner layer may be markedly elevated. As in typical retinoschisis, the outer layer appears pockmarked, and the retinal vessels may appear sclerotic. Posterior extension is more common in reticular than in typical retinoschisis. Approximately 23% of cases have holes in the outer wall that may be large and have rolled edges (Fig 16-18).

Reed D, Garg AJ. Degenerative retinoschisis. In: Schachat AP, Wilkinson CP, Hinton DR, Sadda SR, Wiedemann P, eds. *Ryan's Retina*. 6th ed. Elsevier/Saunders; 2018:chap 100.

Differentiation of Retinoschisis From Rhegmatogenous Retinal Detachment

Retinoschisis must be differentiated from RRD (Table 16-4); this can be accomplished by examination and imaging. Retinoschisis causes an absolute scotoma, whereas RRD causes a relative scotoma. Tobacco dust, hemorrhage, or both are present in the vitreous

Table 16-4 Differentiation of Retinoschisis From Rhegmatogenous Retinal Detachment		
Clinical Feature	Retinoschisis	Rhegmatogenous Retinal Detachment
Retinal surface	Smooth-domed	Corrugated
Hemorrhage or pigment	Usually absent	Present
Scotoma	Absolute	Relative
Response to photocoagulation	Generally present	Absent
Shifting fluid	Absent	Usually absent
Optical coherence tomography	Subretinal fluid generally absent	Subretinal fluid present

with retinoschisis only in rare instances, whereas they are commonly observed with RRD. In retinoschisis, the retina has a smooth surface and usually appears dome shaped; in contrast, in eyes with RRD, the retina often has a corrugated, irregular surface. In long-standing RRD, however, the retina also may appear smooth and thin, similar to its appearance in retinoschisis. In addition, atrophy of the underlying RPE, demarcation line(s), and degenerative retinal macrocysts may be present in eyes with long-standing RRD, whereas the underlying RPE is normal in eyes with retinoschisis.

Retinoschisis is associated with approximately 3% of RDs. Two types of schisis-related detachments occur. In the first type, holes are present in the outer but not the inner wall of the schisis cavity, so cavity contents can migrate through a hole in the outer wall and slowly detach the retina (see Fig 16-18). Demarcation lines and degeneration of the underlying RPE are common. A demarcation line in an eye with retinoschisis suggests that a full-thickness detachment is present or was formerly present and has spontaneously regressed. This type of retinoschisis detachment usually does not progress, or it may progress slowly and seldom requires treatment.

In the second type of schisis-related detachment, holes are present in both the inner and outer layers of the schisis cavity, which may collapse, resulting in a progressive RRD. Such detachments often progress rapidly and usually require treatment. The causative breaks may be located very posteriorly and thus may be difficult to repair with scleral buckling, often requiring vitrectomy.

Byer NE. Long-term natural history study of senile retinoschisis with implications for management. *Ophthalmology*. 1986;93(9):1127–1137.

Gotzaris EV, Georgalas I, Petrou P, Assi AC, Sullivan P. Surgical treatment of retinal detachment associated with degenerative retinoschisis. *Semin Ophthalmol*. 2014;29(3):136–141.

Ip M, Garza-Karren C, Duker JS, et al. Differentiation of degenerative retinoschisis from retinal detachment using optical coherence tomography. *Ophthalmology*. 1999;106(3):600–605.

Xue K, Muqit MMK, Ezra E, et al. Incidence, mechanism and outcomes of schisis retinal detachments revealed through a prospective population-based study. *Br J Ophthalmol*. 2017;101(8):1022–1026.

Macular Lesions Associated With Retinal Detachment

Optic Pit Maculopathy

Optic nerve pits are small, hypopigmented, excavated colobomatous defects of the optic nerve. These oval or round, yellow or whitish defects are usually found within the inferior temporal portion of the optic nerve head margin (Fig 16-19). Most are unilateral, asymptomatic, and congenital, but they can be acquired in the setting of glaucomatous excavation. Optic nerve pits may lead to serous macular detachments with a potentially poor prognosis if left untreated. The macular retinal thickening and detachment typically extend from the optic nerve pit in an oval shape toward the fovea. OCT imaging reveals macular schisis as well as subretinal fluid. Whether the subretinal fluid is liquid vitreous or cerebrospinal fluid is controversial; a proteomic analysis of fluid in 1 adult case

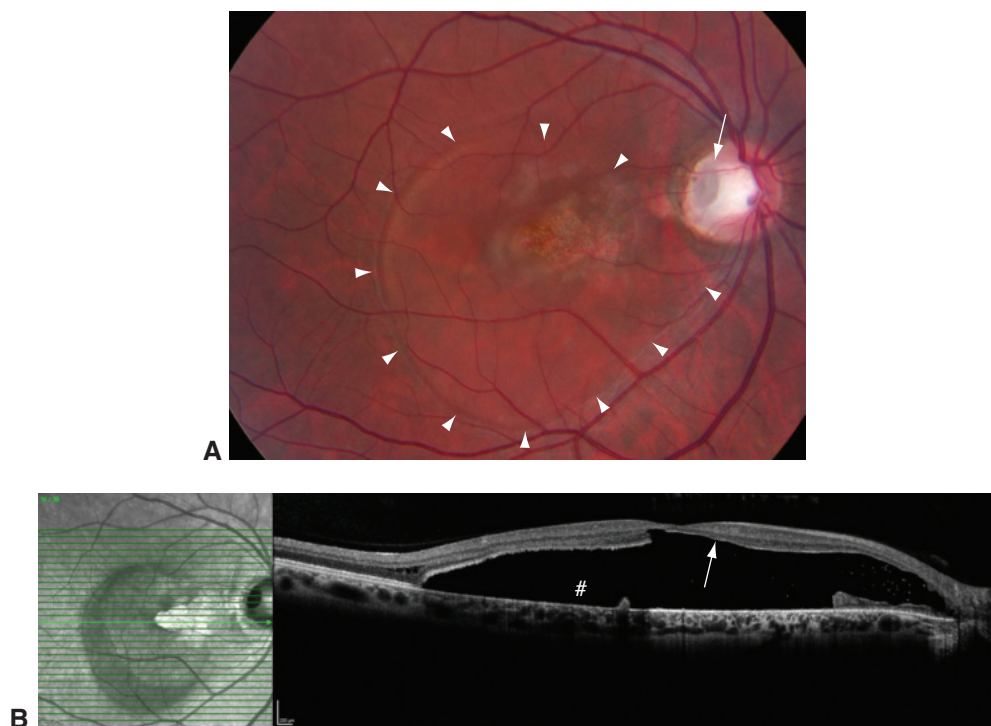


Figure 16-19 Optic nerve pit with macular detachment, retinal thinning, and retinal pigment epithelial atrophy. **A**, Fundus photograph shows an abnormal temporal optic nerve head appearance with an excavation, or pit (arrow). The adjacent retina is thickened and elevated, extending into the macula (outlined by arrowheads). **B**, OCT scan illustrates subretinal fluid (pound sign) associated with the optic nerve pit. Note the degenerated outer segments (arrow) of the photoreceptors. (Courtesy of Colin A. McCannel, MD.)

confirmed that vitreous was the definite source. Many cases can be observed. When treatment is indicated, many approaches have been reported. The associated schisis as well as subretinal fluid can recur following surgical resolution.

The differential diagnosis of optic nerve pits includes glaucomatous nerve damage, such as optic pit–like changes that may occur at the inferior or superior pole of the optic nerve. Optic nerve pits are included in the differential diagnosis of macular thickening or detachment. Careful examination of the optic nerve head margin is important for recognizing this condition.

Bottoni F, Cereda M, Secondi R, Bochicchio S, Staurenghi G. Vitrectomy for optic disc pit maculopathy: a long-term follow-up study *Graefes Arch Clin Exp Ophthalmol*. 2018; 256(4):675–682.

Jain N, Johnson MW. Pathogenesis and treatment of maculopathy associated with cavitory optic disc anomalies. *Am J Ophthalmol*. 2014;158(3):423–435.

Patel S, Ling J, Kim SJ, Schey KL, Rose K, Kuchtey RW. Proteomic analysis of macular fluid associated with advanced glaucomatous excavation. *JAMA Ophthalmol*. 2016; 134(1):108–110.

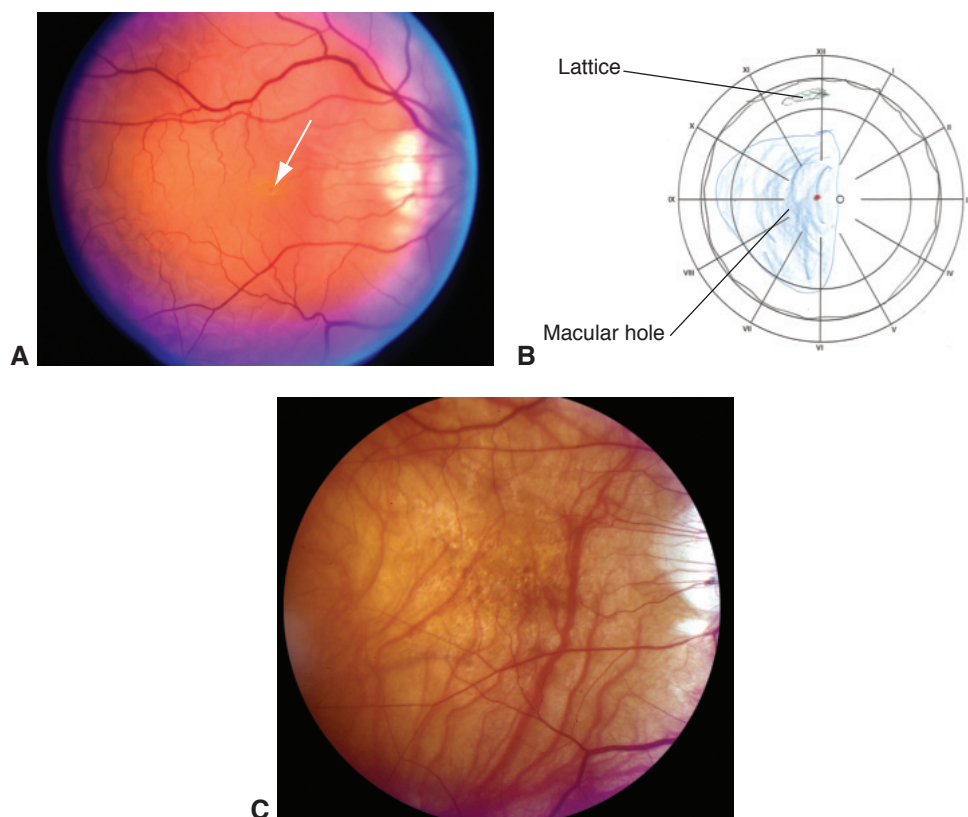


Figure 16-20 A case of RRD caused by a macular hole. **A**, Fundus photograph (50-degree camera) of the detached retina with a hole visible in the center of the macula (arrow). **B**, A retinal drawing of the extent of the detachment. The area within the blue outline is detached; the red dot symbolizes the macular hole. At presentation, the detachment did not extend to the ora serrata; lack of such an extension is uncharacteristic even for a limited RRD arising from a peripheral break. A lattice lesion with pigmentation is drawn superiorly. **C**, Fundus photograph (30-degree camera) of the macula after successful retinal reattachment using vitrectomy with gas tamponade. Typical myopic fundus features include retinal pigment epithelial changes from myopic degeneration, fair pigmentation, peripapillary scleral crescent, and prominent large choroidal vessels. (Courtesy of Colin A. McCannel, MD.)

Macular Holes in High Myopia

A distinct variant of RRD is caused by macular holes, almost always in the setting of a posterior staphyloma in highly myopic eyes (Fig 16-20). Vitreous cavity fluid enters the subretinal space through the macular hole and initiates the detachment. The success rate for surgical repair is lower for this variant than for either macular holes without RRD or typical RRDs.

Ando Y, Hirakata A, Ohara A, et al. Vitrectomy and scleral imbrication in patients with myopic traction maculopathy and macular hole retinal detachment. *Graefes Arch Clin Exp Ophthalmol*. 2017;255(4):673–680.

Ho TC, Ho A, Chen MS. Vitrectomy with a modified temporal inverted limiting membrane flap to reconstruct the foveolar architecture for macular hole retinal detachment in highly myopic eyes. *Acta Ophthalmol*. 2018;96(1):e46–e53.

Posterior Segment Manifestations of Trauma



This chapter includes related videos. Go to www.aao.org/bcscvideo_section12 or scan the QR codes in the text to access this content.

Highlights

- In the initial evaluation of an ocular injury, the clinician should try to determine whether the globe is open or closed and whether an intraocular foreign body (IOFB) is present.
- In cases of ocular or orbital trauma, an IOFB should always be suspected and ruled out. If the foreign body material is unknown, a computed tomography scan is the preferred imaging modality over magnetic resonance imaging.
- Endophthalmitis occurs following 2%–7% of penetrating injuries; the incidence is higher in association with IOFBs and in rural settings.

Classification of Ocular Globe Trauma

Ocular trauma is an important cause of visual impairment worldwide. Ocular globe trauma can be classified as follows (terminology based on the Birmingham Eye Trauma Terminology System; Video 17-1):

- Closed-globe injuries
 - contusion (blunt trauma *without* break in eye wall)
 - lamellar laceration (partial-thickness wound of the eye wall)
 - superficial foreign bodies
- Open-globe injuries
 - rupture (blunt trauma *with* break in eye wall)
 - laceration (full-thickness wound of the eye wall, caused by a sharp object)
 - penetrating injury (entrance break; no exit break in eye wall)
 - perforating injury (both entrance and exit breaks in eye wall)
 - intraocular foreign bodies, penetrating or perforating

This chapter focuses on closed- and open-globe injuries primarily affecting the posterior segment of the eye.



VIDEO 17-1 Birmingham Eye Trauma Terminology System.
Animation developed by Shriji Patel, MD, MBA.



Microsurgical techniques have improved the ability to repair corneal and scleral lacerations, and vitrectomy techniques allow management of severe intraocular injuries (see Chapter 19). Ocular trauma is also discussed in BCSC Section 6, *Pediatric Ophthalmology and Strabismus*; Section 7, *Oculofacial Plastic and Orbital Surgery*; and Section 8, *External Disease and Cornea*.

Evaluation of the Patient After Ocular Trauma

In the initial evaluation of an ocular injury, the clinician should try to determine whether the globe is open or closed and whether an intraocular foreign body (IOFB) is present. The evaluation includes obtaining a complete history (Table 17-1) and performing a thorough examination. If possible, the visual acuity of each eye should be measured separately and the pupils evaluated for an afferent pupillary defect. To the extent possible, the clinician should perform external, slit-lamp, and fundus examinations and measure intraocular pressure (IOP) with care to avoid exacerbating the injury. Severe chemosis, ecchymosis, eyelid edema, low IOP, presence of an entrance wound, iris damage or incarceration, cataract, or other anterior segment pathology may suggest an ocular rupture or laceration. Normal IOP and/or absence of findings on examination does not exclude an occult penetration of the globe.

Table 17-1 Important Questions to Ask in Cases of Ocular Trauma

When exactly did the injury occur?
What was the exact mechanism of injury?
How forceful was the injury?
Was there any object (eg, wood stick, nail, knife) that may have penetrated the eye? If so, what was the object's material?
Is the presence of an intraocular foreign body a possibility? Could it be wood or organic material?
Was the patient hammering metal on metal or working near machinery that could have caused a projectile to enter the eye?
Was the patient wearing spectacles or was he or she close to shattered glass?
Was the patient wearing eye protection?
What was the health status of the eye before the injury?
Has the patient had previous ocular surgery, including laser in situ keratomileusis (LASIK), penetrating keratoplasty, and/or cataract surgery?
Are there concomitant systemic injuries?
What emergency measures were taken, if any (eg, tetanus shot given, antibiotics administered)?
When was the last tetanus toxoid administered?
When was the patient's last oral intake (in case surgery is required)?
Was the injury work related?

If an open-globe injury is suspected but cannot be confirmed on the basis of findings or because of lack of patient cooperation, a thorough examination with possible surgical exploration should be performed under general anesthesia in the operating room.

Multimodal imaging can help assess the status of the injured eye and facilitate detection of an IOFB, particularly in the presence of media opacities. For acute injury, the 2 most helpful imaging systems are computed tomography (CT) of the eye and orbits and ocular ultrasonography (B-scan). A CT scan without contrast should be considered for any trauma patient when an IOFB is suspected on the basis of the mechanism of injury. CT can also aid in identifying periocular trauma, including orbital fractures. When B-scan examination is performed, care must be taken to avoid expulsion of intraocular matter. It is advisable to perform ultrasonography through the patient's closed eyelids, aided by copious amounts of ultrasound gel. B-scan ultrasonography can be particularly helpful in detecting nonradiopaque IOFBs, such as wood and plastic. Signs of a scleral rupture that are visible on ultrasonography include the entrapment of vitreous strands into the rupture site. Intraocular air may cause image artifacts that can complicate image interpretation.

CT is very helpful in detecting radiopaque IOFBs; however, dense IOFBs may introduce image artifacts that cause them to appear larger than they really are, making exact localization difficult. Although magnetic resonance imaging (MRI) is not usually used with acute injuries, it can be helpful in visualizing detailed ocular anatomy and in identifying the presence and location of IOFBs, including those that are not radiopaque. However, MRI should be used only after the presence of ferromagnetic foreign bodies has been definitively ruled out, because of the possibility that the magnetic field will move such foreign bodies, causing additional damage. When the foreign body material is unknown, CT is preferred over MRI as the imaging modality.

Blunt Trauma Without a Break in the Eye Wall

In blunt trauma, the object does not penetrate the eye but may cause rupture of the eye wall. Serious sequelae from blunt trauma affecting the anterior segment include

- angle recession (see BCSC Section 10, *Glaucoma*)
- iridodialysis (see BCSC Section 8, *External Disease and Cornea*)
- iritis (see BCSC Section 9, *Uveitis and Ocular Inflammation*)
- hemorrhage into the anterior chamber (hyphema) (see BCSC Section 8, *External Disease and Cornea*)
- subluxated or dislocated lens (see BCSC Section 11, *Lens and Cataract*)

Serious sequelae from blunt trauma affecting the posterior segment include

- commotio retinae
- choroidal rupture
- macular hole
- suprachoroidal hemorrhage
- retinal tears or detachment
- vitreous hemorrhage

- traumatic chorioretinal disruption (chorioretinitis sclopetaria)
- vitreous base avulsion
- optic nerve avulsion

See Chapter 16 for discussion of traumatic retinal breaks and retinal detachment and Chapter 19 for discussion of suprachoroidal hemorrhage. Sequelae of blunt trauma affecting the posterior segment are discussed in the following sections.

Commotio Retinae

The term *commotio retinae* refers to damage to the outer retinal layers caused by shock waves that traverse the eye from the site of impact following blunt trauma. Ophthalmoscopic examination reveals a sheenlike retinal whitening that appears some hours after the injury (Fig 17-1). This retinal whitening occurs most commonly in the posterior pole but may also be found peripherally. Spectral-domain optical coherence tomography (SD-OCT) findings suggest that the major site of disruption is in the photoreceptor and retinal pigment epithelial (RPE) layers, resulting in the observed retinal opacification (Fig 17-2). With foveal involvement, a cherry-red spot may appear because the cells involved in the whitening are not present in the foveola. Commotio retinae in the posterior pole may reduce visual acuity to as low as 20/200. Gradual visual recovery may occur if there is no associated macular pigment epitheliopathy, choroidal rupture, or macular hole formation. Disruption of the cone outer segment tips, ellipsoid zone, and external limiting membrane is associated with poorer visual and anatomical outcomes.

Choroidal Rupture

When the eye is compressed along its anteroposterior axis, tears may occur in Bruch membrane, which has little elasticity, as well as in the overlying RPE and fibrous tissue around the choriocapillaris. Adjacent subretinal hemorrhage is common. Choroidal ruptures may be single or multiple and occur typically in the periphery and concentric to the optic nerve

Figure 17-1 Extensive commotio retinae with sheenlike retinal whitening (*arrow*) and preretinal hemorrhage (*asterisk*) following blunt ocular trauma due to a rubber bullet. (Reproduced from Barnes AC, Hudson LE, Jain N. Rubber bullet ocular trauma. *Ophthalmology*. 2020;127(9):1190. Copyright 2020, with permission from Elsevier.)

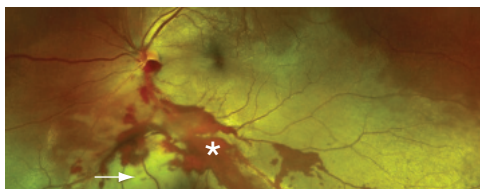
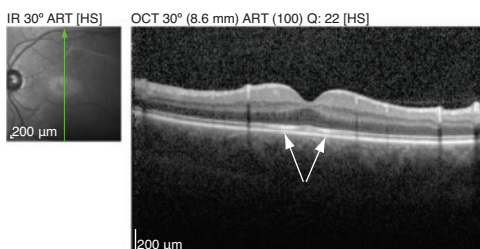


Figure 17-2 Spectral-domain optical coherence tomography (SD-OCT) image of the left eye of a patient who experienced a rock injury at work. Examination revealed macular retinal whitening with visual acuity (VA) decreased to 20/100. OCT image demonstrates increased reflectivity of the parafoveal ellipsoid zone (*arrows*). (Courtesy of Shrijji Patel, MD, MBA.)



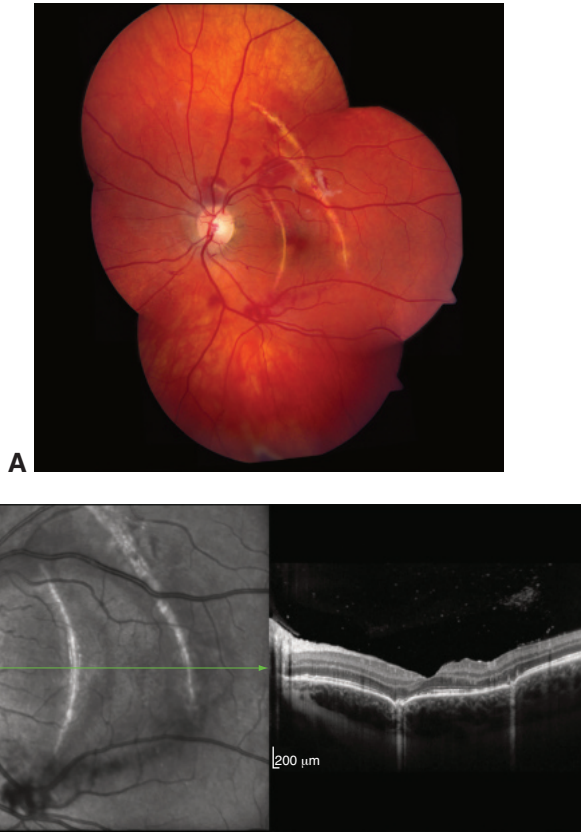


Figure 17-3 Images from a 24-year-old after a motor vehicle accident. **A**, Color fundus photograph montage reveals choroidal ruptures with subretinal hemorrhage along the superior arcade. **B**, SD-OCT shows breaks in the retinal pigment epithelium (RPE)–Bruch membrane complex with a highly reflective choroidal signal beneath the choroidal ruptures due to greater coherence of light penetration. (Courtesy of Kenneth Taubenslag, MD, and Edward Chaum, MD, PhD.)

head (Fig 17-3). Ruptures that extend through the fovea may cause permanent vision loss. There is no effective treatment.

Occasionally, choroidal neovascularization (CNV) develops as a late complication after damage to Bruch membrane (Fig 17-4). A patient with a choroidal rupture near the macula requires ongoing monitoring and should be alerted to the risk of CNV. Subfoveal CNV, if present, is generally treated with a vascular endothelial growth factor (VEGF) inhibitor. See Chapter 4 for information on the management of CNV.

Posttraumatic Macular Hole

Blunt trauma may cause a full-thickness macular hole by various mechanisms, including contusion necrosis and vitreous traction. Holes may be observed immediately after blunt trauma that causes severe commotio retinae, following a submacular hemorrhage caused by a choroidal rupture, or after a whiplash separation of the vitreous from the retina. In

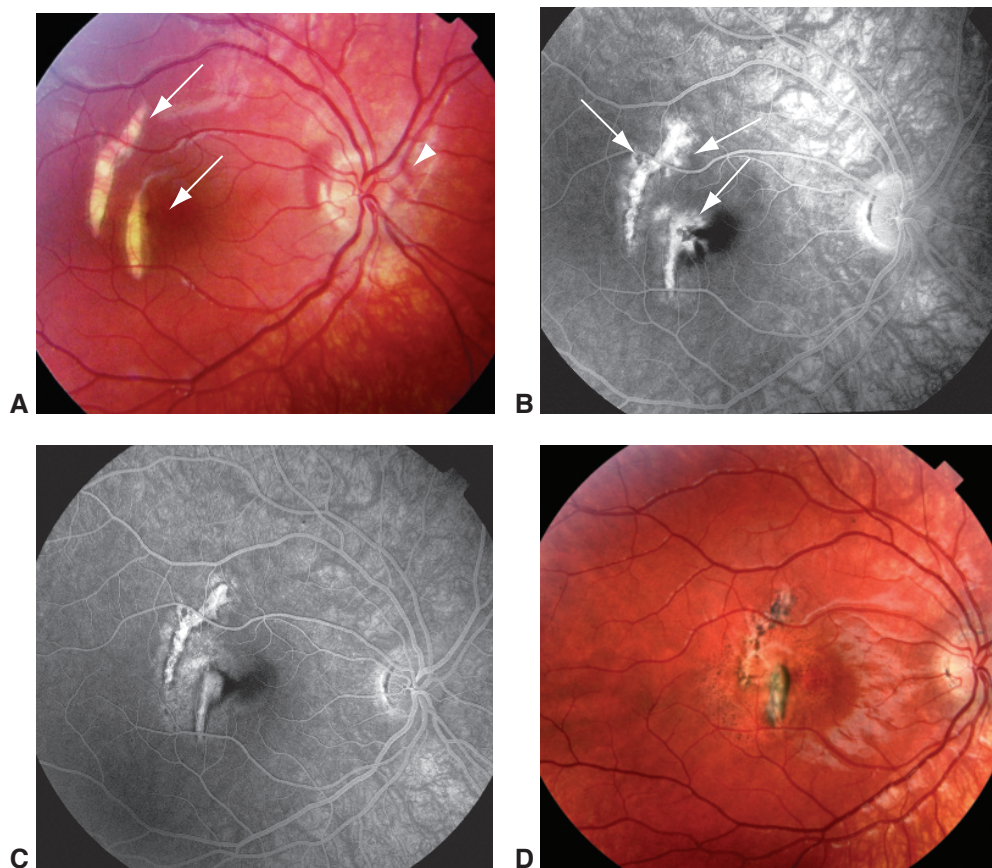


Figure 17-4 Images from a 10-year-old who was hit in the eye with a tennis ball. **A**, Color fundus photograph reveals choroidal ruptures (*arrows*). A subretinal hemorrhage is present around the optic nerve head (*arrowhead*). VA was 20/30. **B**, Six weeks later, VA decreased to 20/400. Late-phase fluorescein angiography image shows multiple fronds of choroidal neovascularization (CNV) arising from the choroidal ruptures (*arrows*). **C**, Late-phase fluorescein angiography image taken 2 weeks after treatment with corticosteroids and photodynamic therapy shows that the CNV has regressed dramatically. **D**, Color fundus photograph taken 6 months after treatment. The scarring around the choroidal ruptures obscures their characteristic appearance. Some pigmentary changes have occurred in the macula as well, but VA is 20/25. (Courtesy of Richard F. Spaide, MD.)

addition, central depressions, or macular pits (similar to those observed in patients after sun gazing), have been described following blunt trauma to the eye and whiplash injuries. Lightning and electrical injury can also cause macular holes; patients with these injuries usually have signs of cataract and can have acute peripapillary retinal whitening. Posttraumatic macular holes may close spontaneously or may be successfully closed surgically.

Vitreous Hemorrhage

Vitreous hemorrhage is a common sequela of ocular trauma. Because a hemorrhage that is loculated at presentation can later become diffuse, a determination of the cause of the

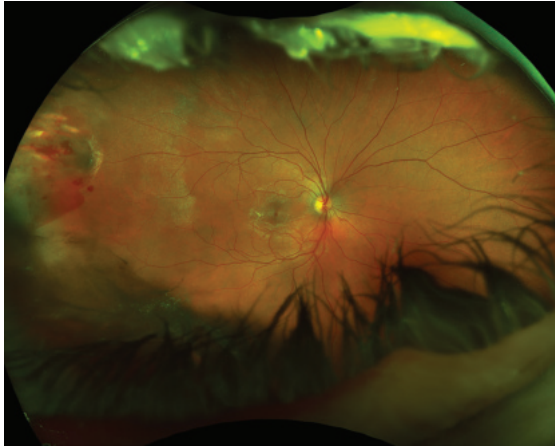


Figure 17-5 Wide-field color fundus photograph from a 32-year-old woman who presented after blunt trauma to her right eye. There is evidence of chorioretinitis sclopetaria, including temporal preretinal and subretinal hemorrhage and areas of whitening that are associated with bare sclera. (Courtesy of Franco M. Recchia, MD.)

hemorrhage should always be undertaken as soon as possible. Bed rest with elevation of the head may enable the hemorrhage to settle sufficiently to allow a more detailed ophthalmoscopic examination. If vitreous hemorrhage obscures the view of the posterior segment, B-scan or radiologic ocular imaging should be considered given the increased incidence of retinal tear and detachment in this setting. See also Chapter 19.

Traumatic Chorioretinal Disruption

Chorioretinitis sclopetaria is an unusual retinal pathology produced by high-speed projectile injuries to the orbit, leading to large areas of choroidal and retinal disruption combined with extensive subretinal, retinal, or vitreous hemorrhage (Fig 17-5). As the blood resorbs, the injured area is repaired by extensive scar formation and widespread pigmentary alteration. If the macula is involved, there is significant vision loss. Secondary retinal detachment rarely develops. The pattern of damage is ascribed to shock waves generated by the deceleration of the projectile passing close to the sclera. Blunt trauma due to injuries from paintballs or other projectiles may produce a similar fundus appearance.

Open-Globe Injuries

Open-globe injuries generally have a guarded prognosis regarding visual acuity outcomes (see the section Prognostication of Globe Injuries later in this chapter). The development of a retinal detachment is common; the detachment is usually caused by the primary injury or by traction resulting from proliferative vitreoretinopathy (PVR). In all cases of open-globe injuries, the presence of an IOFB should be ruled out.

Scleral Rupture

Severe blunt injuries can rupture the globe. Rupture injuries may be very severe; there is often expulsion of intraocular content (to varying degrees). The most common locations

for rupture are (1) the corneal limbus, especially through previous surgical wounds; and (2) through areas of physiologic scleral thinning parallel to and under the insertions of the rectus muscles. Important diagnostic signs of rupture include the following:

- marked decrease in ocular ductions
- very boggy conjunctival chemosis with hemorrhage
- deepened anterior chamber
- severe vitreous hemorrhage

The IOP is usually very low but may be normal or even elevated.

CLINICAL PEARL

The presence of 360° of hemorrhagic chemosis is highly suggestive of occult scleral rupture; there should be a low threshold for surgical exploration.

Lacerating and Penetrating Injuries

Lacerating injuries result from cutting or tearing of the eye wall by objects of varying sharpness. In a penetrating injury of the globe, there is an entrance break but no exit break in the eye wall. The prognosis is related to the location and extent of the wound, as well as the associated damage and degree of hemorrhage. An uncommon iatrogenic injury is scleral penetration with a needle during retrobulbar or peribulbar anesthesia for intraocular surgery.

Perforating Injuries

A globe-perforating injury has both entrance and exit wounds. Globe-perforating injuries may be caused by objects of varying sharpness such as needles, knives, high-velocity pellets, or small fragments of metal. Studies have shown that, after perforating injuries, fibrous proliferation occurs along the scaffold of damaged vitreous between the entrance and exit wounds. The wounds are often closed by fibrosis within 5–7 days after the injury, depending on wound size. Small-gauge injuries with only a small amount of hemorrhage and no significant collateral damage may heal without serious sequelae. Posterior exit wounds may be identified with gentle B-scan ultrasonography or CT scan.

Surgical Management

In most instances, primary repair of open-globe injuries consists of suturing of the corneal and scleral wounds. Although there are some theoretical reasons for performing an early vitrectomy, the priority at the time of the acute injury is to close the globe. Primary wound closure should not be delayed, particularly because closure will facilitate a later vitrectomy if it is needed. For more on vitrectomy, see Chapter 19. Open-globe trauma surgery is best performed with the patient under general anesthesia; use of peribulbar anesthesia is avoided because injection of local anesthetics into the orbit can cause compression of the globe and expulsion of intraocular contents.

Primary repair

The principles of primary repair of open-globe injuries include careful, gentle microsurgical corneoscleral wound repair, during which incarcerated uvea is repositioned or excised. If a laceration crosses the limbus, or if there is any suspicion of a scleral laceration or rupture, a gentle and generous peritomy, usually 360°, should be considered for best possible exposure. Corneal lacerations may be closed with 10-0 nylon interrupted sutures, and scleral wounds may be closed with stronger 7-0, 8-0, or 9-0 nonabsorbable sutures. Vitreous should be excised from the wound and the anterior chamber re-formed. Any uvea or retina that protrudes should be amputated if devitalized or gently repositioned into the eye. Chapter 4 of BCSC Section 4, *Ophthalmic Pathology and Intraocular Tumors*, discusses wound healing in detail.

Attempts should be made to safely explore any scleral laceration until its posterior extent has been located. If no laceration or rupture can be seen, and a posterior rupture is suspected, a meticulous scleral exploration, including underneath the rectus muscles, should be performed. This may necessitate disinserting 1 or more extraocular muscles to achieve adequate exposure. If the wound is very posterior, the site should be left to heal without suturing; attempts to suture very posterior wounds may result in expulsion of intraocular content. Some ophthalmologists advocate placing a prophylactic encircling scleral buckle at the time of primary repair to reduce the likelihood of a later retinal detachment.

Immediate vitrectomy

Immediate vitrectomy may be necessary or advisable in some circumstances—for example, when evaluation suggests the possibility of an IOFB, retinal detachment, or endophthalmitis.

Some surgeons favor immediate vitrectomy at the time of the primary repair, before cellular proliferation (PVR) begins. Inducing a posterior vitreous detachment and thorough dissection of the vitreous remove some of the scaffold on which contractile membranes grow. This may reduce the risk of late complications such as traction (also called *tractional*) retinal detachments, cyclitic membrane formation, and phthisis bulbi. Separating the posterior cortical vitreous from the retina may be difficult, especially in children and young adults and in eyes with retinal breaks or retinal detachment. If the injury is perforating, the posterior wound may present challenges because infusate may leak from it, making the maintenance of IOP during surgery difficult.

Delayed vitrectomy

Most practitioners in the United States prefer initially performing a primary repair of the wound(s) to restore the globe and IOP, followed by delayed vitrectomy, if necessary. The following are some advantages of delayed vitrectomy:

- reduces the risk of intraoperative hemorrhage in eyes that are acutely inflamed and congested
- allows the cornea to clear and improve intraoperative visualization
- permits spontaneous separation of the vitreous from the retina, which facilitates a safer and more complete vitrectomy
- allows posterior wounds in perforating injuries to heal, so there is ocular integrity during vitrectomy

The optimal timing of vitrectomy after primary repair remains controversial. Many advocate waiting at least 5 days if there are unsutured (posterior) wounds. Vitrectomy that is delayed more than 2 weeks following the injury may contribute to substantial worsening of PVR and associated worse anatomical and visual outcomes.

Typical indications for vitrectomy include the following:

- the presence of moderate to severe vitreous hemorrhage
- uncontrolled IOP despite medical management
- other tissue damage that requires repair
- phacoanaphylactic uveitis, which may occur if the lens is damaged
- signs of developing transvitreal traction
- retinal detachment
- posttraumatic endophthalmitis

Kuhn F. The timing of reconstruction in severe mechanical trauma. *Ophthalmic Res.* 2014;51(2):67–72.

Mieler WF, Mittra RA. The role and timing of pars plana vitrectomy in penetrating ocular trauma. *Arch Ophthalmol.* 1997;115(9):1191–1192.

Intraocular Foreign Bodies

In some cases, an IOFB is observed (Fig 17-6), or it is suggested by the presence of an entry site or the reported mechanism of injury. A detailed history helps the clinician assess the likelihood of the presence of an IOFB. As previously discussed, ocular imaging can be very



Figure 17-6 Color montage photograph of an aluminum intraocular foreign body (IOFB) with retinal penetration and visible sclera. Note the minimal reactive inflammation to aluminum, which the eye tolerates better than copper or iron. (Courtesy of Edward Chaum, MD, PhD.)

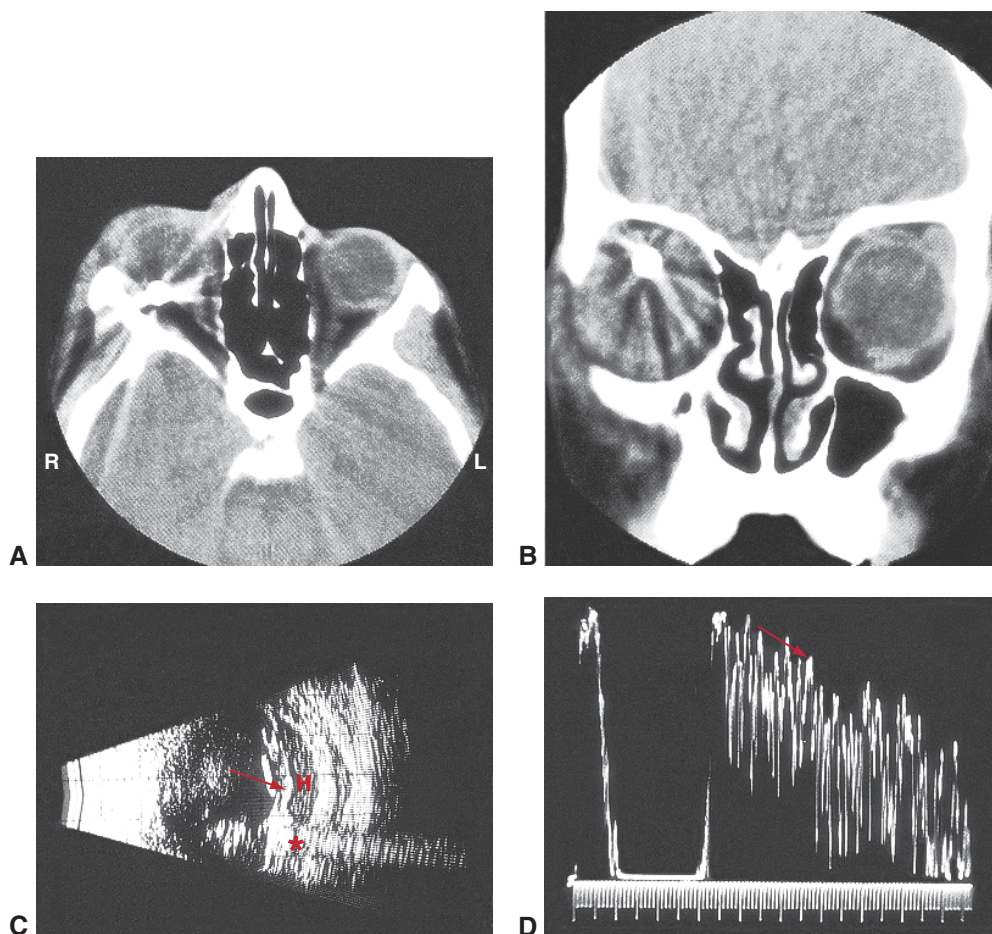


Figure 17-7 Images from a patient with an intraocular BB pellet. Axial (A) and coronal (B) computed tomography (CT) views show the pellet's position to be in the superior and posterior globe. B-scan (C) shows retinal detachment (arrow) and subretinal hemorrhage (H). A characteristic reverberation of echoes between the front and back surfaces of the round pellet gives a "trail of echoes" artifact that extends posterior to the foreign body on B-scan (asterisk) and on A-scan (D) (arrow).

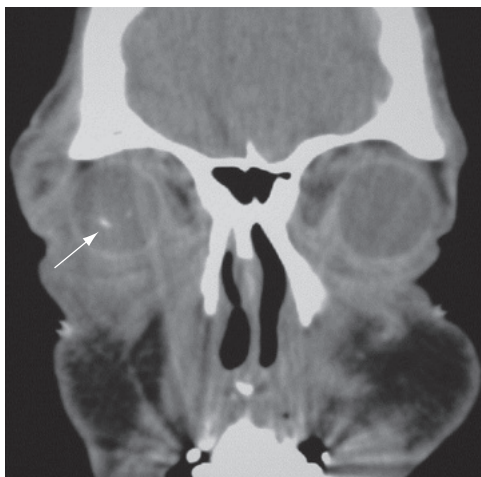
helpful in the detection of IOFBs (Figs 17-7, 17-8). If surgical removal of an IOFB cannot be accomplished promptly, intravitreal injection and systemic administration of antimicrobial agents should be considered in order to minimize the risk of endophthalmitis developing.

Surgical techniques for removal of intraocular foreign bodies

Surgical planning should address the following issues:

- location of the foreign body in the eye
- surgeon's ability to visualize and localize the foreign body
- size and shape of the foreign body
- composition of the foreign body (ferromagnetic vs nonferromagnetic)
- encapsulation of the foreign body

Figure 17-8 CT scan demonstrating a non-metallic IOFB. (Reproduced from Arey ML, Mootha VV, Whittemore AR, Chason DP, Blomquist PH. Computed tomography in the diagnosis of occult open-globe injuries. *Ophthalmology*. 2007;114(8):1448–1452. Copyright 2007, with permission from Elsevier.)



Pars plana vitrectomy allows removal of traumatized vitreous and facilitates controlled microsurgical extraction of IOFBs and media opacities such as cataract and hemorrhage (Video 17-2). Before forceps extraction is attempted, the IOFB should be freed of all attachments. A small rare-earth magnet or kidney stone basket may be used to engage and separate the foreign body from the retinal surface (Video 17-3). Although small foreign bodies can be removed through enlargement of the pars plana sclerotomy site, it may be safer to extract some large foreign bodies through the corneoscleral limbus or the initial wound to minimize collateral damage.



VIDEO 17-2 Intraocular foreign body with subhyaloid hypopyon.

Courtesy of Tomas A. Moreno, MD, and Shrijji Patel, MD, MBA.



VIDEO 17-3 Removal of an intraocular foreign body using a tipless kidney stone basket.

Courtesy of Shrijji Patel, MD, MBA.



Retained intraocular foreign bodies

The reaction of the eye to a retained foreign body varies widely and depends on the object's chemical composition, sterility, and location. Inert, sterile foreign bodies such as stone, sand, glass, porcelain, plastic, and cilia are generally well tolerated. If such material is found several days after the injury and does not appear to create an inflammatory reaction, it may be left in place, provided it is not obstructing vision.

Zinc, aluminum, copper, and iron are metals that are commonly reactive in the eye. Of these, zinc and aluminum tend to cause minimal inflammation (see Fig 17-6) and may become encapsulated. However, any very large foreign body may incite inflammation and thereby cause PVR. Epiretinal proliferations, traction retinal detachment, and phthisis bulbi may result.

Table 17-2 Symptoms and Signs of Siderosis Bulbi**Symptoms**

Nyctalopia
 Centrally constricted visual field
 Decreased vision

Signs

Rust-colored corneal stromal staining
 Heterochromia iridis
 Pupillary mydriasis and poor reactivity
 Brown deposits on the anterior lens capsule
 Cataract
 Vitreous opacities
 Peripheral retinal pigmentation (early)
 Diffuse retinal pigmentation (late)
 Narrowed retinal vessels
 Optic nerve head discoloration and atrophy
 Secondary open-angle glaucoma from iron accumulation in the trabecular meshwork

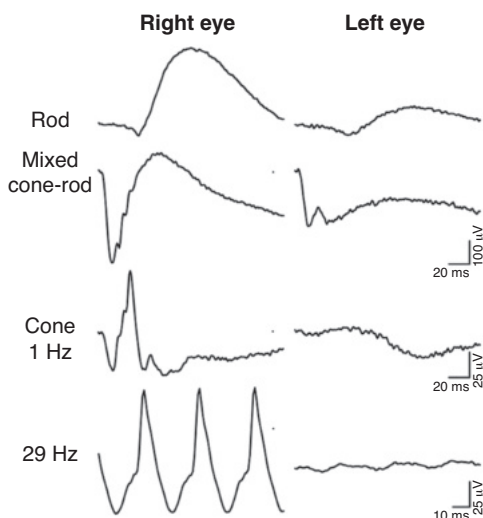
Chalcosis Pure copper (eg, copper wire) is especially toxic and causes *acute* chalcosis. Prompt removal is required to prevent severe inflammation that may lead to loss of the eye. Foreign bodies with a copper content of less than 85% (eg, brass, bronze) may cause *chronic chalcosis*. Typical findings in chronic chalcosis are deposits in Descemet membrane (a sign similar to the Kayser-Fleischer ring in Wilson disease and the result of copper's affinity for basement membranes), greenish aqueous particles, green discoloration of the iris, petal-shaped deposition of yellow or brown pigment in the lens capsule ("sunflower" cataract), brownish-red vitreous opacities and strand formation, and metallic flecks on retinal vessels and the internal limiting membrane in the macular region.

Siderosis bulbi In siderosis bulbi, iron from IOFBs is deposited primarily in neuroepithelial tissues such as the iris sphincter and dilator muscles, the nonpigmented ciliary epithelium, the lens epithelium (see BCSC Section 11, *Lens and Cataract*, Fig 5-17), the retina, and the RPE. Retinal photoreceptors and RPE cells are especially susceptible to damage from iron (Table 17-2). Electroretinography (ERG) changes in eyes with early siderosis include an increased a-wave and normal b-wave, a progressively diminishing b-wave amplitude over time, and eventually an undetectable signal during the final stage of iron toxicity of the retina (Fig 17-9).

Posttraumatic Endophthalmitis

Endophthalmitis occurs after 2%–7% of penetrating injuries; the incidence is higher in association with IOFBs and in rural settings. Posttraumatic endophthalmitis can progress rapidly. Its clinical signs include marked inflammation featuring hypopyon, fibrin, vitreous infiltration, and corneal opacification. The risk of endophthalmitis occurring after penetrating ocular injury may be reduced by prompt wound closure and early removal of IOFBs. Use of prophylactic subconjunctival, intravenous, or intravitreal antibiotics should be considered.

Figure 17-9 Standard full-field electroretinography (ERG) in the left eye of a patient with an iron IOFB removed several years after initial trauma. The ERG demonstrates moderate outer retinal dysfunction (a-wave reduction) and severe inner retinal dysfunction (b-wave loss) in the mixed cone- and rod-mediated responses, causing an electronegative configuration, as well as barely detectable cone responses. (Reproduced from Sulewski ME Jr, Serrano LW, Han G, Aleman TS, Nichols CW. Structural and electrophysiologic outcomes in a patient with retinal metallosis. *Ophthalmol Retina*. 2018;2(2):173–175. Copyright 2018 American Academy of Ophthalmology.)



Intravitreal or periocular aminoglycoside antibiotics should be avoided because of their high risk of retinal toxicity. Anterior chamber and vitreous cultures should be obtained, and if endophthalmitis is suspected, antibiotics should be injected.

CLINICAL PEARL

- In penetrating or perforating ocular injuries, involvement of the crystalline lens raises the risk of endophthalmitis (even in the absence of an IOFB). A common mechanism is a dirty wire or stick that perforates the cornea, inoculates the anterior chamber or vitreous cavity, and then retracts from the eye. In such cases, there should be a low threshold for intravitreal injection of antibiotics.
- Fluoroquinolones have acceptable vitreous penetration after systemic (intravenous or oral) administration. Levofloxacin 500 mg daily or moxifloxacin 400 mg daily is a good option for treatment of posttraumatic endophthalmitis in addition to intravitreal antibiotics.

Bacillus cereus, which rarely causes endophthalmitis in other settings, accounts for almost 25% of cases of posttraumatic endophthalmitis. Endophthalmitis caused by infection with *B cereus* has a rapid and severe course and, once established, leads to profound vision loss and often loss of the eye. Most commonly, *B cereus* endophthalmitis is associated with injuries caused by soil-contaminated objects, especially in the setting of IOFB. Gram-negative organisms are also frequent pathogens in posttraumatic endophthalmitis. When there is contamination with vegetable matter, posttraumatic fungal infection, most commonly *Candida*, should be considered.

Bhagat N, Nagori S, Zarbin M. Post-traumatic infectious endophthalmitis. *Surv Ophthalmol*. 2011;56(3):214–251.

Jindal A, Pathengay A, Mithal K, et al. Endophthalmitis after open globe injuries: changes in microbiological spectrum and isolate susceptibility patterns over 14 years. *J Ophthalmic Inflamm Infect.* 2014;4(1):5.

Prognostication of Globe Injuries

The severity of the damage to the eye and its function at presentation have prognostic significance. Functional assessments include measuring visual acuity, determining whether an afferent pupillary defect is present, and noting the injury descriptors, specifically the type of trauma and the zone of injury. A higher zone of injury increases the risk for retinal detachment and portends a worse visual prognosis. The Ocular Trauma Score assigns a point value based on these assessments (Table 17-3). In this system, visual acuity is the most important predictor of injury severity; other characteristics are assigned a negative point value that is subtracted from the visual acuity score to produce the total raw score. The higher the raw score, the better the final visual acuity prognosis. This system is a useful general guide to roughly estimate visual acuity outcomes following globe trauma, but the clinician should use it cautiously when counseling patients.

Table 17-3 Calculating the Ocular Trauma Score

Step 1: Record any variables present and their associated raw points.

Variables Used	Raw Points
A. Visual acuity at presentation	
NLP	60
LP/HM	70
1/200–19/200	80
20/200–20/50	90
≥20/40	100
B. Rupture	–23
C. Endophthalmitis	–17
D. Perforating injury	–14
E. Retinal detachment	–11
F. Afferent pupillary defect	–10

Step 2: Total the raw points of the applicable variables (A–F) to determine the raw score.

Step 3: Use the raw score to look up the estimate of the likelihood of various final visual acuity outcomes.

Raw Score	NLP	LP/HM	1/200–19/200	20/200–20/50	≥20/40
0–44	74%	15%	7%	3%	1%
45–65	27%	26%	18%	15%	15%
66–80	2%	11%	15%	31%	41%
81–91	1%	2%	3%	22%	73%
92–100	0%	1%	1%	5%	94%

HM = hand motions; LP = light perception; NLP = no light perception.

Adapted from Kuhn F, Maisiak R, Mann L, Mester V, Morris R, Witherspoon CD. The Ocular Trauma Score (OTS). *Ophthalmol Clin North Am.* 2002;15(2):163–165, vi. Copyright 2002, with permission from Elsevier.

Kuhn F, Maisiak R, Mann L, Mester V, Morris R, Witherspoon CD. The Ocular Trauma Score (OTS). *Ophthalmol Clin North Am*. 2002;15(2):163–165, vi.

Pieramici DJ, Au Eong KG, Sternberg P Jr, Marsh MJ. The prognostic significance of a system for classifying mechanical injuries of the eye (globe) in open-globe injuries. *J Trauma*. 2003; 54(4):750–754.

Sympathetic Ophthalmia

Sympathetic ophthalmia is a rare complication of penetrating ocular trauma in which the fellow, uninjured eye develops a severe autoimmune inflammatory reaction. Primary removal of the injured eye is not routinely necessary because the disorder is rare and treatable, and superior cosmetic and psychological outcomes are achieved with globe retention.

Avulsion of the Optic Nerve Head

A forceful backward dislocation of the optic nerve from the scleral canal can occur under several circumstances, including

- extreme rotation and forward displacement of the globe
- penetrating orbital injury, causing a backward pull on the optic nerve
- sudden increase in IOP, causing rupture of the lamina cribrosa

Total loss of vision characteristically occurs. Findings may vary from a pitlike depression of the optic nerve head to posterior hemorrhage and contusion necrosis (Fig 17-10). B-scan ultrasonography may reveal a hypoechoic defect in the area of the posterior sclera in the region of the optic nerve.

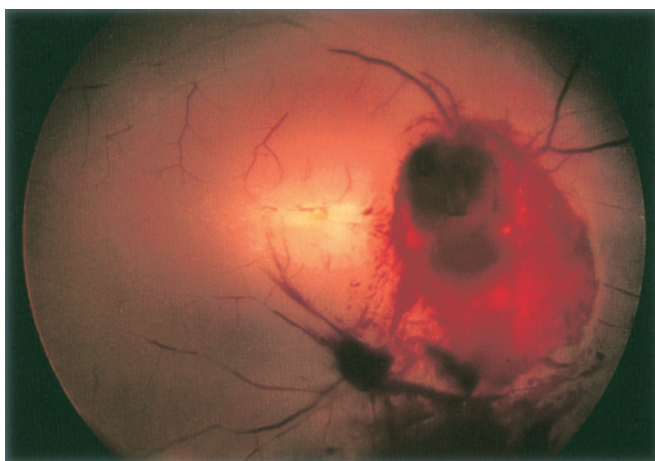


Figure 17-10 Avulsion of the optic nerve head. In this color fundus photograph, the nerve is obscured by hemorrhage, and a mixed vascular occlusion is present.

Abusive Head Trauma

Severe shaking of infants, a form of nonaccidental trauma, is the cause of abusive head trauma (formerly known as *shaken baby syndrome*). Patients with abusive head trauma are usually younger than 5 years and frequently younger than 12 months. The presenting sign of child abuse involves the eye in approximately 5% of cases. Any physician who suspects that child abuse may have occurred is required by law in every US state and Canadian province to report the incident to a designated government agency.

See BCSC Section 6, *Pediatric Ophthalmology and Strabismus*, for discussion of the multiple systemic symptoms associated with abusive head trauma. Ocular signs include

- retinal hemorrhages and cotton-wool spots (Fig 17-11)
- retinal folds
- hemorrhagic schisis cavities
- pigmentary maculopathy

The retinal hemorrhages associated with abusive head trauma often have a hemispheric contour. The retinopathy may resemble that observed in Terson syndrome or central retinal vein occlusion, neither of which is common in infants. Retinal hemorrhages may be present in cases of accidental trauma, blood dyscrasias, vaginal delivery, and sepsis.

Vitrectomy for vitreous hemorrhage should be considered when amblyopia is likely to occur but may be deferred when a bright-flash ERG response shows loss of the b-wave, which is indicative of extensive retinal damage.

Matthews GP, Das A. Dense vitreous hemorrhages predict poor visual and neurological prognosis in infants with shaken baby syndrome. *J Pediatr Ophthalmol Strabismus*. 1996;33(4):260–265.

Pierre-Kahn V, Roche O, Dureau P, et al. Ophthalmologic findings in suspected child abuse victims with subdural hematomas. *Ophthalmology*. 2003;110(9):1718–1723.

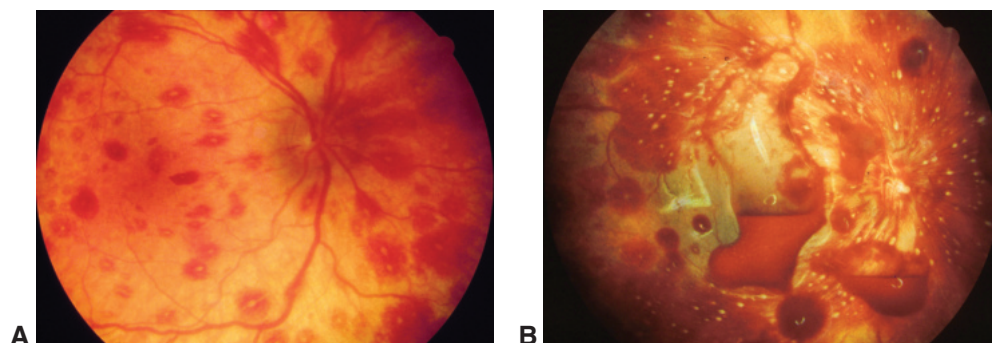


Figure 17-11 Color fundus photographs from a patient with abusive head trauma causing preretinal and retinal hemorrhages. **A**, Image taken several days after hospital admission, by which time many of the smaller hemorrhages had started to resorb. **B**, Numerous hemorrhages are located on and within the retina, and regions of hemorrhagic retinoschisis are observed centrally. Because the baby was upright, the red blood cells sank down into a dependent position within the larger regions of hemorrhagic retinoschisis. Some of the hemorrhages were white centered, whereas others had reflections of the flash from the fundus camera. (Reproduced with permission from Spaide RF, Swengel RM, Scharre DW, Mein CE. Shaken baby syndrome. *Am Fam Physician*. 1990;41(4):1145–1152.)

Photic Damage

The eye has several mechanisms to protect itself against light damage, including pupil constriction, light absorption by melanin in the RPE, and the presence of antioxidants, such as lutein and zeaxanthin, in the macula. Light injures the retina by 3 basic mechanisms: mechanical, thermal, and photochemical.

Mechanical injury occurs when the power of the absorbed light is high enough to form gas or water vapor or to produce acoustic shock waves that mechanically disrupt retinal tissues. The absorbed energy may be enough to strip electrons from molecules in the target tissue, producing a collection of ions and electrons referred to as *plasma*. For example, a Q-switched Nd:YAG laser produces its therapeutic effect through mechanical light damage and uses this effect to disrupt a cloudy posterior capsule behind an intraocular lens.

Thermal injury occurs when excessive light absorption by the RPE and surrounding structures causes local elevation of tissue temperature, leading to coagulation, inflammation, and scarring of the RPE and the surrounding neurosensory retina and choroid. A therapeutic application of thermal light injury is the retinal burn caused by laser photocoagulation. See Chapter 18 for discussion of photocoagulation.

Photochemical injury results from biochemical reactions that cause retinal tissue destruction without temperature elevation. It is the result of the transfer of light energy to a molecule; the excess energy initiates reactions that cause tissue damage. Damaging reactions can include oxidation, photoisomerization, photochemical cleavage, and electrocyclic reactions. Such changes occur primarily at the level of the outer segments of the photoreceptors, which are more sensitive than the inner segments. Examples of photochemical injury are solar retinopathy and photic retinopathy that occurs after excessive exposure to illumination from an operating microscope.

Mainster MA, Turner PL. Photic retinal injuries: mechanisms, hazards, and prevention.

In: Schachat AP, Wilkinson CP, Hinton DR, Sadda SR, Wiedemann P, eds. *Ryan's Retina*.

Vol 2. 6th ed. Elsevier/Saunders; 2018:chap 93.

Solar Retinopathy

Solar retinopathy, also known as *foveomacular retinitis*, *eclipse retinopathy*, or *solar retinitis*, is a thermally enhanced photochemical retinal injury caused by direct or indirect gazing at the sun; it may also occur after viewing a solar eclipse without proper eye protection. The extent of the damage depends on the duration and intensity of the exposure. Younger, emmetropic patients with clearer lenses are at increased risk of solar retinopathy. Symptoms include decreased vision, central scotomata, dyschromatopsia, metamorphopsia, micropsia, and frontal or temporal headache within hours of exposure. Visual acuity is typically reduced to 20/25–20/100 but may be worse depending on the degree of exposure. Most patients recover within 3–6 months, with visual acuity returning to the level of 20/20–20/40, but there may be residual metamorphopsia and paracentral scotomata. Typical findings include a central opacified area of the fovea acutely and hypopigmentation after the acute changes resolve (Fig 17-12). No known beneficial treatment exists, and therefore prevention through education is critically important.

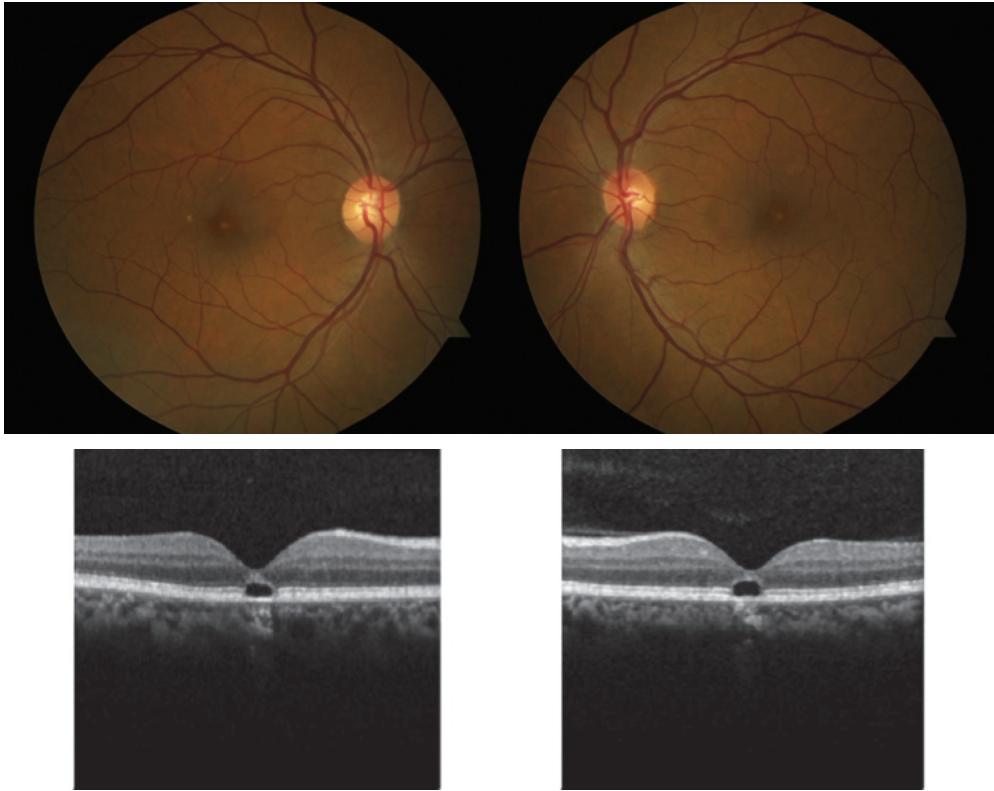


Figure 17-12 Solar retinopathy. The fundus photographs (*top*) show central foveal hypopigmentation. On OCT imaging (*bottom*), outer retinal cavitation in the fovea is typically seen. (Courtesy of David Sarraf, MD.)

Comander J, Gardiner M, Loewenstein J. High-resolution optical coherence tomography findings in solar maculopathy and the differential diagnosis of outer retinal holes. *Am J Ophthalmol*. 2011;152(3):413–419.e6.

Phototoxicity From Ophthalmic Instrumentation

There have been reports of injuries from operating microscopes and from fiber-optic endoilluminating probes used in vitrectomies. The incidence of photic retinopathy after contemporary cataract surgery is not known. However, cases continue to be reported after intraocular surgery. The incidence increases with prolonged operating times, but photic retinopathy can occur even with surgery times as short as 30 minutes. In retinal surgery, photic injury is more likely to occur with prolonged, focal exposure, especially when the light probe is held close to the retina, as it may be during macular hole and epiretinal membrane procedures.

Most affected patients are asymptomatic, but some will notice a paracentral scotoma on the first postoperative day. With acute injury, patients may have a deep, irregular yellow-white retinal lesion that is adjacent to the fovea and oval in shape, resembling the shape of

the light source. The lesion typically evolves to become a zone of mottled RPE that transmits background hyperfluorescence on fluorescein angiography.

Reports of photic macular lesions occurring after intraocular surgery underscore the need for prevention. During ocular surgery, the risk of photic retinopathy may be reduced by minimizing exposure time; avoiding the use of intense illumination; using oblique illumination when possible during parts of the surgery; filtering light wavelengths below 515 nm; and, when possible, using pupillary shields. See also BCSC Section 3, *Clinical Optics and Vision Rehabilitation*.

van den Biesen PR, Berenschot T, Verdaasdonk RM, van Weelden H, van Norren D.

Endoillumination during vitrectomy and phototoxicity thresholds. *Br J Ophthalmol*. 2000;84(12):1372–1375.

Youssef PN, Sheibani N, Albert DM. Retinal light toxicity. *Eye (Lond)*. 2011;25(1):1–14.

Occupational Light Toxicity

Occupational exposure to bright lights can lead to retinal damage. A common cause of this type of occupational injury is arc welding without the use of protective goggles. The damage from the visible blue light of the arc welder leads to photochemical damage similar to that observed in solar retinopathy. Occupational injury from stray laser exposure is also a serious concern.

Laser-Pointer Injury

The availability of high-power green and blue handheld laser devices has created a source of immediate accidental or purposeful sight-threatening macular injury (Fig 17-13). These

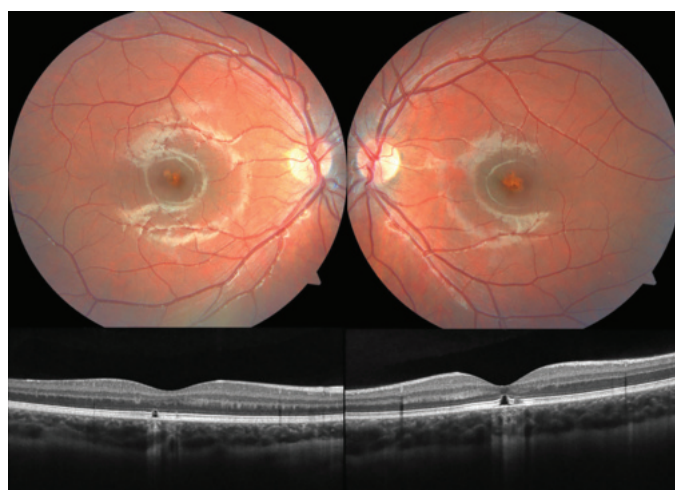


Figure 17-13 Fundus photographs and SD-OCT images from an 11-year-old boy with foveal atrophy and a focal, well-circumscribed area of photoreceptor loss bilaterally, which was due to prolonged laser-pointer exposure. (Reproduced from Snyder L, Patel S. *Laser pointer maculopathy*. *Ophthalmol Retina*. 2018;2(10):996. Copyright 2018, American Academy of Ophthalmology.)

devices are easily obtainable via the internet and resemble the much safer, ubiquitous low-power red laser pointers. The devices also have the potential to cause secondary harm by visually incapacitating individuals while they are performing visually demanding functions, such as firefighting and piloting planes.

Alsulaiman SM, Alrushood AA, Almasaud J, et al; King Khaled Eye Specialist Hospital Collaborative Retina Study Group. High-power handheld blue laser–induced maculopathy: the results of the King Khaled Eye Specialist Hospital Collaborative Retina Study Group. *Ophthalmology*. 2014;121(2):566–572.e1.

A large, solid yellow curved shape that starts from the left edge and curves upwards and to the right, filling the top half of the page.

PART III

Selected Therapeutic Topics

CHAPTER 18

Laser Therapy and Cryotherapy for Posterior Segment Diseases



This chapter includes a related video. Go to www.aaio.org/bcscvideo_section12 or scan the QR code in the text to access this content.

Highlights

- Laser setting parameters, including wavelength, power, duration, and spot size, are chosen with the goal of the laser treatment and the targeted tissue in mind.
- Although anti-vascular endothelial growth factor injections have replaced laser photocoagulation as the treatment of choice for several diseases, laser photocoagulation remains a useful treatment for proliferative retinopathies and ablation of retinal vascular lesions.
- Photodynamic therapy is effective for selective diseases, including idiopathic polypoidal choroidal vasculopathy and central serous chorioretinopathy.

Basic Principles of Photocoagulation

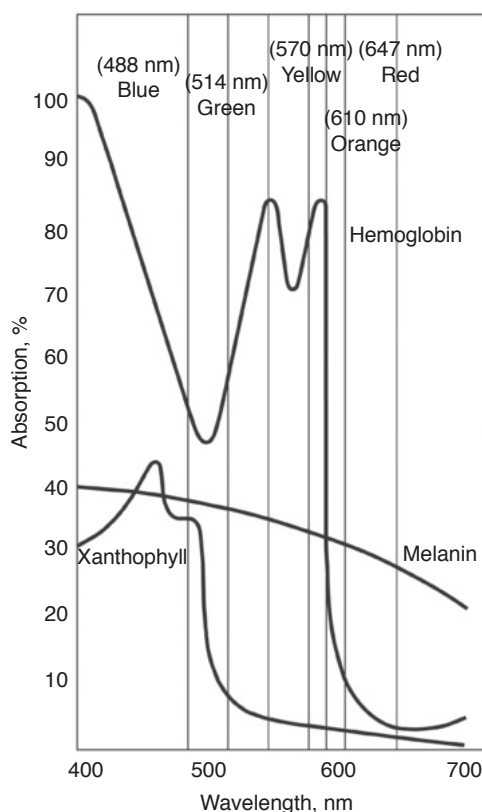
Photocoagulation uses light energy to coagulate tissue. After light energy is applied to the target tissue, it converts into thermal energy and the tissue temperature rises above 65°C, causing denaturation of tissue proteins and coagulative necrosis.

Current posterior segment laser delivery systems span the visible light spectrum of 400–700 nm (green, yellow, red) and venture into the infrared wavelengths (>700 nm). Delivery systems may use a transpupillary approach with slit-lamp or indirect ophthalmoscopic delivery, endophotocoagulation during vitrectomy, or transscleral application with a contact probe.

The effectiveness of photocoagulation depends on the transmission of light through ocular media and the absorption of that light by pigment in the target tissue. Light is absorbed principally by ocular tissues that contain melanin, xanthophyll, or hemoglobin. Figure 18-1 illustrates the absorption spectra of the key pigments found in ocular tissues:

- Melanin is an effective absorber of green, yellow, red, and infrared wavelengths.
- Macular xanthophyll readily absorbs blue wavelengths but minimally absorbs yellow and red wavelengths.
- Hemoglobin easily absorbs blue, green, and yellow wavelengths but has minimal absorption of red wavelength.

Figure 18-1 Absorption spectra of xanthophyll, hemoglobin, and melanin. (From Folk JC, Pulido JS. Laser Photocoagulation of the Retina and Choroid. *Ophthalmology Monograph 11*. American Academy of Ophthalmology; 1997:9.)



Choice of Laser Wavelength

Laser wavelength selection depends on the specific goals of treatment and the degree to which the photocoagulation must be targeted to the particular tissue while sparing adjacent healthy tissue. The *area* (depth and diameter) of effective coagulation is directly related to the *intensity* and *duration* of irradiation. For a specific set of laser parameters (spot size, duration, and power), the intensity of the burn obtained depends on the clarity of the ocular media and the degree of pigmentation.

The green laser produces light that is absorbed well by melanin and hemoglobin and less completely by xanthophyll. Because of these characteristics and the absence of undesirable short (blue) wavelengths, the green laser has replaced the blue-green laser for treatment of retinal vascular abnormalities and choroidal neovascularization (CNV).

The red laser penetrates through nuclear sclerotic cataracts and moderate vitreous hemorrhages better than lasers with other wavelengths do. In addition, it is minimally absorbed by xanthophyll and thus may be useful in treatments near the fovea. However, the red laser causes deeper burns with a higher rate of patient discomfort than other wavelengths and inhomogeneous absorption at the level of the choroid. The infrared laser has characteristics similar to those of the red laser with even deeper tissue penetration.

The advantages of the yellow laser include minimal scatter through nuclear sclerotic lenses, low xanthophyll absorption, and little potential for photochemical damage.

It appears to be useful for destroying vascular structures while minimizing damage to adjacent pigmented tissue; thus, it may be valuable for treating retinal vascular and CNV lesions.

Laser effects on posterior segment tissues include photochemical and thermal effects and vaporization. Photochemical reactions can be induced by ultraviolet or visible light that is absorbed by tissue molecules or by molecules of a photosensitizing medication (eg, verteporfin), producing cytotoxic reactive oxygen species (eg, free radicals). Absorption of laser energy by pigment results in a temperature rise by tens of degrees and subsequent protein denaturation; the exact temperature rise depends on laser wavelength, laser power, duration of laser application, and spot size. Vaporization is generated by the rise in water temperature above the boiling point, which causes microexplosions, as can occur in overly intense burns. For further discussion of laser light characteristics and light–tissue interactions, see BCSC Section 3, *Clinical Optics and Vision Rehabilitation*, Chapter 2.

Atebara NH, Thall EH. Principles of lasers. In: Yanoff M, Duker JS. *Ophthalmology*. 4th ed. Elsevier/Saunders; 2014:32–37.

Palanker D, Blumenkranz MS. Retinal laser therapy: biophysical basis and applications. In: Schachar AP, Wilkinson CP, Hinton DR, Sadda SR, Wiedemann P, eds. *Ryan's Retina*; vol 1. 6th ed. Elsevier/Saunders; 2018:chap 41.

Practical Aspects of Laser Photocoagulation

Anesthesia

Topical, peribulbar, or retrobulbar anesthesia may be necessary to facilitate delivery of laser photocoagulation.

Lenses

Two types of contact lenses are available to assist in slit-lamp delivery of photocoagulation: negative-power planoconcave lenses and high-plus-power lenses. Planoconcave lenses provide an upright image with superior resolution of a small retinal area, and most clinicians favor their use for macular treatments. Mirrored planoconcave lenses facilitate viewing and photocoagulation of more peripheral retina. In general, planoconcave lenses provide the same retinal spot size as that selected on the slit-lamp setting.

High-plus-power lenses provide an inverted image with some loss of fine resolution, but they offer a wide field of view, which facilitates efficient treatment over a broad area. High-plus-power lenses provide a spot size that is magnified over the laser setting size; the magnification factor depends on the lens used (Table 18-1).

Parameters and indications

Selection of laser setting parameters depends on the treatment goals, the clarity of the ocular media, and the fundus pigmentation. As a rule, smaller spot sizes require less energy than larger spot sizes, and longer-duration exposures require less energy than shorter-duration exposures to achieve the same intensity effects.

Macular laser Although intravitreal anti-vascular endothelial growth factor injections have replaced laser as the treatment of choice for many etiologies of macular edema and

Table 18-1 Magnification Factors for Common Laser Lenses

Lens	Magnification	Laser Spot Magnification
Panretinal photocoagulation lenses		
Ocular Mainster PRP 165	0.51×	1.96×
Ocular Mainster Wide Field PDT	0.68×	1.5×
Ocular Pro Retina	0.5×	2.0×
Rodenstock Panfunduscope	0.7×	1.43×
Volk Equator Plus	0.44×	2.27×
Volk HR Wide Field	0.5×	2.0×
Volk QuadrAspheric	0.51×	1.97×
Volk SuperQuad 160	0.5×	2.0×
Focal laser lenses		
Goldmann 3-mirror (central)	0.93×	1.08×
Ocular Fundus Laser	0.93×	1.08×
Ocular Mainster High Magnification	1.25×	0.8×
Ocular PDT 1.6×	0.63×	1.6×
Ocular Reichel-Mainster 1× Retina	0.95×	1.05×
Ocular Reichel-Mainster 2× Retina	0.5×	2.0×
Ocular Yannuzzi Fundus	0.93×	1.08×
Volk Area Centralis	1.06×	0.94×
Volk Centralis Direct	0.9×	1.11×
Volk Fundus 20	1.44×	0.7×
Volk Fundus Laser	1.25×	0.8×
Volk HR Centralis	1.08×	0.93×
Volk HR Wide Field	0.5×	2.0×
Volk PDT Lens	0.66×	1.5×
Volk Super Macula 2.2	1.49×	0.67×

CNV, laser photocoagulation still has a role in the management of some forms of macular edema, extrafoveal CNV, and focal retinal pigment epithelium (RPE) abnormalities with leakage, such as those seen in central serous chorioretinopathy and around retinal arterial macroaneurysms. To avoid central scotomata, treatment should not be administered within 500 μm of the foveal center. Macular laser treatment for edema generally uses a small spot size (50–200 μm) and short duration (≤ 0.1 second) to achieve smaller, less-intense burns. For diabetic macular edema, green or yellow direct laser therapy is typically applied to all leaking microaneurysms located between 500 μm and 3000 μm from the center of the macula. For zones of capillary nonperfusion and diffuse leakage more than 500 μm from the center of the macula and 500 μm from the temporal margin of the optic nerve head, a light-intensity grid pattern is applied using a green or yellow laser. A similar strategy is used to treat macular edema caused by branch retinal vein occlusion. In the treatment of CNV or RPE leakage spots, the aim is to achieve a more intense burn of the entire lesion or area of leakage.

Peripheral retinal photocoagulation Peripheral retinal photocoagulation may be performed with either a slit-lamp or indirect ophthalmoscopic delivery system. In panretinal photocoagulation (PRP) or laser retinopexy, spot size typically is 200–500 μm and laser power is adjusted to achieve gray or light-cream burns. For PRP, burns are usually one-half to one burn width apart (see Chapter 5, Fig 5-10) and should spare the macula. For milder retinopathy,

one can leave approximately 1–2 disc diameters of retina outside the macula and optic nerve head untreated, whereas more severe retinopathy may require treatment up to the arcade vessels and closer to the optic nerve (Fig 18-2). Initial treatment should be concentrated in the inferior retina in case of subsequent vitreous hemorrhage and to preserve the temporal, nasal, and inferior visual field. The posterior ciliary nerves in the 3 and 9 o'clock meridians should be avoided, and any coexisting macular edema should be treated beforehand to avoid exacerbation. Typically, 1200–1400 laser applications of 500- μm spot size, or the equivalent of smaller burns, are placed.

Laser retinopexy is used to create a chorioretinal adhesion around retinal tears or for demarcation of a (small) retinal detachment. Usually, 2 or 3 rows of photocoagulation around the break are sufficient.

Laser ablation of retinal vascular lesions Vascular lesions, such as retinal arterial macroaneurysms, are often treated using a large spot size ($\geq 500\ \mu\text{m}$), low power, and long duration so each lesion slowly heats up and coagulates “from the inside out.” High-intensity burns whiten the surface of retinal vascular lesions, after which visible-light laser does not penetrate well, making it difficult to achieve the treatment goal.

Alternative laser delivery systems and strategies

Recent innovations in slit-lamp delivery systems include pattern scanners that deliver an entire array of laser applications with each foot-pedal depression; the high-intensity laser pulses are ultrashort (20–50 milliseconds) and are delivered in rapid succession. This approach may increase the efficiency of treatment, but it may not achieve an effect equivalent to that of traditional laser treatment on a spot number-to-spot number comparison.

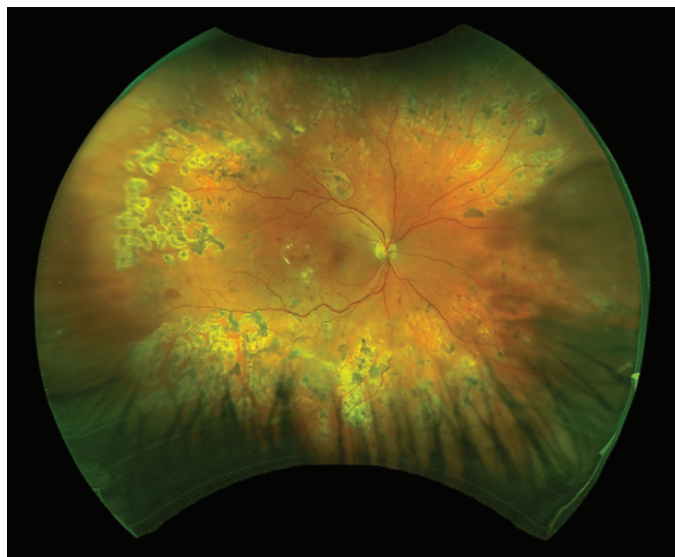


Figure 18-2 Illustration of the posterior extent of full panretinal photocoagulation showing sparing of the 3 and 9 o'clock meridians to avoid damage to the posterior ciliary nerves. (Courtesy of Gaurav K. Shah, MD.)

Some laser delivery systems incorporate real-time retinal image overlay and registration. This configuration allows for computer-assisted planning and precise targeting of the retinal lesions during treatments.

Delivery systems that apply subthreshold (ie, barely visible to invisible) laser spots administer micropulses (≤ 0.1 millisecond) that confine heat conduction to the RPE while limiting thermal damage to the photoreceptors and choriocapillaris. These systems have been effective in treating diabetic macular edema and may reduce the number and size of scotomata. Titration of burn intensity and monitoring of the area of placement of invisible laser spots during laser delivery is facilitated by commercial laser systems using endpoint software technology.

Bauman CR, Ip M, Puliafito CA. Light and laser injury. In: Yanoff M, Duker JS.

Ophthalmology. 4th ed. Saunders/Elsevier; 2013:461–466.

Chappelaw AV, Tan K, Waheed NK, Kaiser PK. Panretinal photocoagulation for proliferative diabetic retinopathy: pattern scan laser versus argon laser. *Am J*

Ophthalmol. 2012;153(1):137–142.e2.

Complications of Photocoagulation

The most serious complications of photocoagulation are caused by the use of excessive energy or misdirected light. These complications include inadvertent corneal and iris burns, which can lead to corneal opacities, and iritis and zones of iris atrophy, respectively. Thermal damage to the posterior ciliary nerves in the suprachoroidal space and/or the iris sphincter muscle can lead to persistent mydriasis, loss of accommodation, and corneal anesthesia with subsequent dry eye, whereas absorption by lens pigments may create lenticular burns and resultant opacities. Optic neuropathy may occur from treatment directly to or adjacent to the optic nerve head, and nerve fiber damage may follow intense absorption in zones of intraretinal hemorrhage, increased pigmentation, or retinal thinning. Chorioretinal complications include foveal burns, Bruch membrane ruptures, creation of retinal or choroidal lesions, and exudative choroidal or retinal detachment. When the retinal nerve fiber layer is damaged during laser treatment, visual field loss may extend beyond the local area.

Accidental foveal burns

Great care should be taken to identify the fovea by means of biomicroscopy. To maintain orientation, frequent reference to the foveal center throughout the procedure is helpful. In some instances, the risk of foveal burns may be reduced by immobilizing the globe with peribulbar or retrobulbar anesthesia.

Bruch membrane ruptures

Small spot size, high power, and short duration of laser applications all increase the risk of a rupture in Bruch membrane, which may subsequently give rise to hemorrhage from the choriocapillaris and development of CNV.

Retinal lesions

Intense photocoagulation may cause full-thickness retinal holes. Similarly, intense treatment may lead to fibrous proliferation, striae, and foveal distortion, with resultant meta-

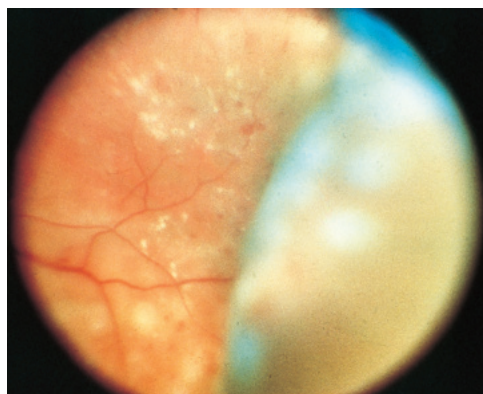


Figure 18-3 Color fundus photograph shows choroidal detachment that occurred after panretinal scatter photocoagulation for diabetic retinopathy. (Courtesy of M. Gilbert Grand, MD.)

morphopsia or diplopia. Focal treatment with small-diameter, high-intensity burns may cause vascular occlusion or perforate blood vessels, leading to preretinal or vitreous hemorrhage. In addition, extensive panretinal treatment may induce or exacerbate macular edema, particularly in patients with diabetes.

Choroidal lesions

Treatment of CNV may be complicated by subretinal hemorrhage, choroidal ischemia, and additional CNV or chorioretinal anastomosis. Progressive atrophy of the RPE may occur at the margin of photocoagulation scars, resulting in enlarged scotomata. Also, photocoagulation may precipitate tears of the pigment epithelium.

Exudative retinal and choroidal detachment

Extensive, intense photocoagulation may lead to massive chorioretinal edema and resultant serous retinal and choroidal detachment (Fig 18-3). In turn, the latter may lead to narrowing of the anterior chamber angle from forward rotation of the ciliary body, elevated intraocular pressure, and in rare cases, aqueous misdirection. Limiting the extent of the laser burns delivered in one session of PRP may prevent this complication.

Palanker D, Lavinsky D, Blumenkranz MS, Marcellino G. The impact of pulse duration and burn grade on size of retinal photocoagulation lesion: implications for pattern density. *Retina*. 2011;31(8):1664–1669.

Transpupillary Thermotherapy

Transpupillary thermotherapy (TTT) acts in a subthreshold manner by slightly raising the choroidal temperature, thus causing minimal thermal damage to the RPE and overlying retina. TTT is administered with an infrared laser (810 nm) using beam sizes from 0.8 mm to 3.0 mm, power settings between 250 mW and 750 mW, and a 1-minute exposure time. For choroidal melanoma, TTT may be considered as a stand-alone treatment for tumors less than 4 mm thick; however, for thicker tumors, a combination of TTT and plaque radiotherapy provides better local tumor control than TTT alone.

Photodynamic Therapy

Photodynamic therapy (PDT) using the photosensitizing drug verteporfin is approved by the US Food and Drug Administration for treating certain types of subfoveal CNV in age-related macular degeneration and secondary to ocular histoplasmosis syndrome and myopia. Because more effective treatments have become available, PDT has generally fallen out of favor; however, it is still a valuable option for the treatment of leaking polyps in idiopathic polypoidal choroidal vasculopathy. It is also useful in central serous chorioretinopathy and some ocular tumors.

PDT is a 2-step procedure:

1. intravenous administration of the photosensitizing drug, which localizes to endothelial cells of vessels present in CNV and tumors
2. local activation of the drug by a laser wavelength preferentially absorbed by the sensitizing drug

The low-intensity laser energy induces a photochemical reaction, leading to the formation of reactive oxygen species, including free radicals. These radicals cause endothelial cell damage, platelet adherence, vascular thrombosis, and capillary closure.

Complications of Photodynamic Therapy

The most serious adverse effects of PDT are photosensitivity reactions that range from mild to second-degree burns of sun-exposed skin. These can be avoided by having the patient minimize exposure to sunlight for 5 days after treatment. Severe vision loss may occur in approximately 4% of patients after standard-fluence PDT of subfoveal lesions. To minimize choriocapillaris nonperfusion, treatment using half-fluence PDT (25 J/cm² energy; 300 mW/cm² light intensity) has become more common. Another method to approximate (but not duplicate) half-fluence is to use full fluence for 41–42 seconds, or half the typical time of 83 seconds.

Cryotherapy

Cryotherapy involves the freezing and thawing of tissue, resulting in cell injury and death. In practice, cryotherapy is most often used to treat retinal breaks (cryopexy), either as a stand-alone procedure or as part of retinal detachment repair. When media opacity, light pigmentation, far peripheral breaks, and subretinal fluid around the tear could impede laser uptake, cryopexy may be preferable over laser retinopexy. Cryotherapy is also used to treat retinal vascular tumors and pars planitis.

Cryotherapy freezes the tissue that is in direct contact with a handheld probe. The freezing interface progresses in an outward direction, resulting in a temperature distribution that is coldest at the point of contact with the probe. After reaching a temperature below -40°C , cells at the center of the cryoablated tissue die from the disruptive process of extracellular and intracellular ice formation. Peripheral cells that do not reach -40°C die primarily from apoptosis and necrosis. Cryotherapy also induces ischemia by causing

vascular stasis and disruption of small-caliber vessels and may lead to breakdown of the blood–ocular barrier. Subsequent chorioretinal scarring produces a firm adhesion between the retina and choroid.

Cryopexy Technique

Before cryotherapy is applied to the eye, the surgeon should confirm that the cryoprobe tip is cooling properly. When the cryoprobe is initially applied to the conjunctiva or sclera, however, the tip should be at room temperature. Using indirect ophthalmoscopy or a surgical microscope for visualization, the surgeon begins by positioning the cryopexy probe tip near the retinal tear and pressing down gently, creating an indentation. Typically, a footswitch is depressed to allow coolant to flow to the tip, causing an ice ball to form and turning the tissue a whitish color. Because strong adhesion is created with freezing, the probe should not be moved at this time to avoid tearing the tissue. Once the probe has been allowed to thaw, it can be repositioned for another application. This sequence continues until the entire tear has been completely surrounded by cryopexy. See Video 18-1 for an example of cryopexy used to treat a retinal break.



VIDEO 18-1 Intraoperative cryopexy for a peripheral retinal break.

Courtesy of Franco M. Recchia, MD.



Inadvertent freezing of the macula may occur if indentation of the shaft of the cryotherapy probe is mistaken for the tip. Other treatment complications include eyelid damage from inadvertent freezing from the probe shaft, transitory uveitis, temporary chemosis, and subconjunctival hemorrhage.

Vitreoretinal Surgery and Intravitreal Injections



This chapter includes related videos. Go to www.aao.org/bcscvideo_section12 or scan the QR codes in the text to access this content.

Highlights

- Pars plana vitrectomy is typically used for removing vitreous opacities (vitreous hemorrhage), relieving vitreoretinal traction, restoring the normal anatomical relationship of the retina and retinal pigment epithelium, and accessing the subretinal space.
- There are 3 surgical techniques for eyes with primary uncomplicated rhegmatogenous retinal detachment: *pneumatic retinopexy*, *scleral buckling*, and *primary vitrectomy with or without scleral buckling*. The common goals of these procedures are to identify and treat all causative retinal breaks while providing support through external and internal tamponade as needed.
- Intravitreal injection is the most common procedure in ophthalmology and in medicine in general.

Pars Plana Vitrectomy

Pars plana vitrectomy is usually used for removing vitreous opacities (vitreous hemorrhage), relieving vitreoretinal traction, restoring the normal anatomical relationship of the retina and retinal pigment epithelium (RPE), and accessing the subretinal space. This vitreoretinal surgical technique involves a closed-system approach in which 3 ports are placed 3–4 mm posterior to the surgical limbus, depending on the status of the patient's lens. One port is dedicated to infusion of balanced salt solution into the vitreous cavity to maintain the desired intraocular pressure. Epinephrine can be added to the infusion solution to induce mydriasis and to cause vasoconstriction for reduction of intraoperative bleeding; however, it may promote ischemia and inflammation. Dextrose is often added to infusions to reduce cataractogenesis in phakic diabetic patients. The remaining ports are used to access and visualize the vitreous cavity with tools such as a fiberoptic endo-illuminator and instruments to manipulate, dissect, or remove intraocular tissues, fluids, and objects.

Vitrectomy is performed with the use of an operating microscope in conjunction with a contact lens or noncontact viewing system. Direct and indirect visualization are possible; the latter requires the use of an inverting system to orient the image. The advantages of indirect visualization include a wider viewing angle, which enables visualization through media opacities and miotic pupils, as well as when the eye is filled with gas. Although direct viewing systems offer greater magnification and enhanced stereopsis for macular work, their field of view is smaller.

Instrumentation includes a high-speed vitreous cutter, intraocular forceps, endolaser probe, micro-pic forceps, intraocular scissors, extrusion cannula, and fragmatome. Visualization aids include indocyanine green (ICG) or brilliant blue G (BBG) dyes and triamcinolone suspension (Video 19-1). These substances aid in visualization of the internal limiting membrane (ILM) and, in the case of triamcinolone, identification of the vitreous. Perfluorocarbon liquids, which are heavier than water, can be used to temporarily stabilize the retina during dissection and facilitate anterior drainage of subretinal fluid during retinal detachment repair. Tamponade of the retina can be accomplished with use of air, gas, or silicone oil as a vitreous substitute. Commonly used gases include sulfur hexafluoride (SF_6) and perfluoropropane (C_3F_8), which last approximately 2 and 8 weeks, respectively, at nonexpansile, isovolumic concentrations (Table 19-1).



VIDEO 19-1 Triamcinolone-aided pars plana vitrectomy.
Courtesy of Shrijji Patel, MD, MBA.



The development of smaller-gauge vitrectomy instrumentation has facilitated trans-conjunctival, sutureless vitrectomy techniques. With these systems, surgeons place 23-gauge, 25-gauge, or 27-gauge trocar cannulas to align conjunctival and scleral openings and to allow instrument insertions. These cannulas obviate the need for conjunctival peritomy and do not usually require suture closure. The diameter of 20-gauge sclerotomies is 1 mm, compared with 0.7 mm, 0.5 mm, and 0.4 mm for 23-gauge, 25-gauge, and 27-gauge instrumentation, respectively. Potential advantages of small-gauge vitrectomy include fewer

Table 19-1 Properties of Commonly Used Intraocular Tamponades

	Chemical Formula	Expected Expansion	Time to Expansion (hr)	Nonexpansile Concentration	Approximate Duration Inside Eye	Surface Tension (milli-Newton/ meter)
Air		—	—	—	5–7 d	70
Sulfur hexafluoride	SF_6	2×	24–48	20%	2 wk	70
Perfluoropropane	C_3F_8	4×	72–96	14%	6–8 wk	70
Silicone oil (1000 cSt)		NA	NA	NA	Until removal in OR	21
Silicone oil (5000 cSt)		NA	NA	NA	Until removal in OR	21

cSt = centistokes (a measure of viscosity); NA = not applicable; OR = operating room.

Information from Schachat AP, Wilkinson CP, Hinton DR, Sadda SR, Wiedemann P, eds. *Ryan's Retina*. Vol 3. 6th ed. Elsevier/Saunders; 2018:2040–2043.

intraoperative iatrogenic retinal tears, shorter operative time, increased postoperative patient comfort, faster visual recovery, and reduced conjunctival scarring.

Chen GH, Tzekov R, Jiang FZ, Mao SH, Tong YH, Li WS. Iatrogenic retinal breaks and postoperative retinal detachments in microincision vitrectomy surgery compared with conventional 20-gauge vitrectomy: a meta-analysis. *Eye (Lond)*. 2019;33(5):785–795.

Vitrectomy for Selected Macular Diseases

Macular Epiretinal Membranes

Epiretinal membranes (ERMs; Fig 19-1) have a variable clinical course. See Chapter 15 for discussion of ERM signs, symptoms, and treatment. There are generally 2 indications for surgery: (1) reduced visual acuity or (2) distortion causing dysfunction of binocularity. In general, ERM peel may be advised if visual acuity is reduced (Video 19-2). However, even if the visual acuity is good, vitrectomy may be indicated if difficulty in fusing a normal and a distorted image results in disruption of binocularity.



VIDEO 19-2 Vitrectomy for epiretinal membrane peel.

Courtesy of Colin A. McCannel, MD.

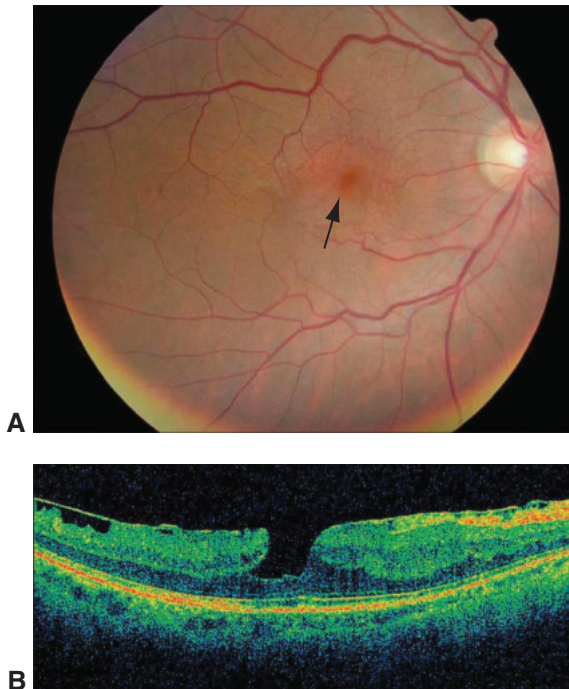


Figure 19-1 Epiretinal membrane. **A**, Fundus photograph shows an epiretinal membrane (ERM) with a pseudohole (*arrow*). **B**, Optical coherence tomography (OCT) confirms the ERM with pseudohole formation and steepened foveal slope due to contraction of the ERM. (© 2021 American Academy of Ophthalmology.)

After surgery, approximately two-thirds of patients achieve an improvement in visual acuity of 2 or more lines. Maximal improvement may take up to 6–12 months (Fig 19-2). Preoperative patient counseling is critical. Although improvement in metamorphopsia is common, complete resolution usually does not occur.

Vitreomacular Traction Diseases

Vitreomacular traction syndrome

Vitreomacular traction (VMT) syndrome is a distinct vitreoretinal interface disorder that is differentiated clinically from typical ERM. VMT syndrome stems from anomalous, incomplete posterior vitreous separation at the macula. The disorder may create focal elevation of the fovea (Fig 19-3) and, occasionally, a shallow retinal detachment. Classically, in eyes with this syndrome, the hyaloid tightly inserts into the macula, usually at or near the fovea, creating traction. Symptoms include metamorphopsia and decreased vision. Surgical treatment consists of a pars plana vitrectomy and peeling of the cortical vitreous from the surface of the retina. Intraoperative use of triamcinolone may aid visualization of the cortical vitreous. See Chapter 15 for further discussion of VMT syndrome.

Idiopathic macular holes

The stages of macular hole formation are discussed in Chapter 15. Vitrectomy is not generally recommended for stage 1 macular holes because approximately 50% of cases without ERMs resolve spontaneously. It is typically indicated for recent full-thickness macular holes (stages 2, 3, and 4). Early intervention for full-thickness macular holes is important; shorter time between the development and the closure of a macular hole has been associated with improved anatomical and functional outcomes.

Figure 19-2 OCT images of an ERM forming a pseudohole in a patient with visual distortion and reduced visual acuity (20/50). **A**, A preretinal membrane distorts the retinal contour, and intraretinal edema is present. **B**, Image taken 2 months after surgery shows continued restoration of normal macular contour and absence of the preretinal membrane and traction; visual acuity had improved to 20/25. (Courtesy of Edward F. Cherney, MD.)

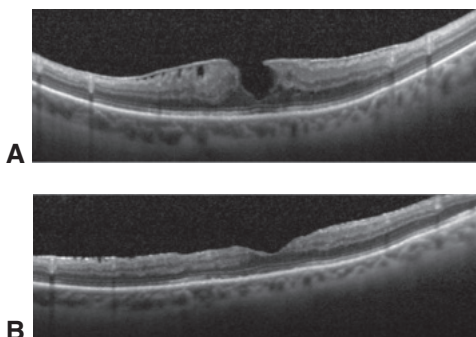
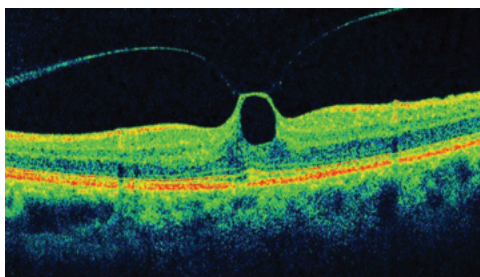


Figure 19-3 Vitreomacular traction syndrome in a patient with visual acuity of 20/60 and mild ophthalmoscopic findings. OCT scan shows a partial posterior detachment with persistent hyaloidal insertion at the center of the macula. Note the elevated fovea with complete loss of contour and inner schisis cavity. Pars plana vitrectomy with membrane peeling led to an improved visual acuity of 20/25 and resolution of symptomatic distortion. (Courtesy of Stephen J. Kim, MD.)



Surgery for full-thickness macular holes typically consists of (1) pars plana vitrectomy, (2) separation and removal of the posterior cortical vitreous, (3) removal of the ILM, and (4) use of intraocular air or gas tamponade (Video 19-3). Various studies have demonstrated that ILM peeling improves the rate of hole closure, particularly for larger stage 3 or 4 holes, and reduces reopening rates. *ILM inverted flap* is a newer surgical technique that can be used to close any macular hole (Video 19-4). Intraoperative dyes (eg, ICG, trypan blue, BBG) or other visualization techniques (eg, triamcinolone) are widely used to aid in peeling the ILM. Duration of face-down positioning after surgery ranges from a few hours to 2 or more weeks. Since the early 2000s, most studies have reported macular hole closure at rates higher than 90%, especially for smaller holes (Fig 19-4). After successful closure, it is uncommon for the hole to reopen; however, this may occur if severe cystoid macular edema or ERM develops.



VIDEO 19-3 Vitrectomy with ILM peeling for macular hole repair.

Courtesy of Colin A. McCannel, MD.



VIDEO 19-4 Inverted ILM flap for macular hole closure.

Courtesy of María H. Berrocal, MD.

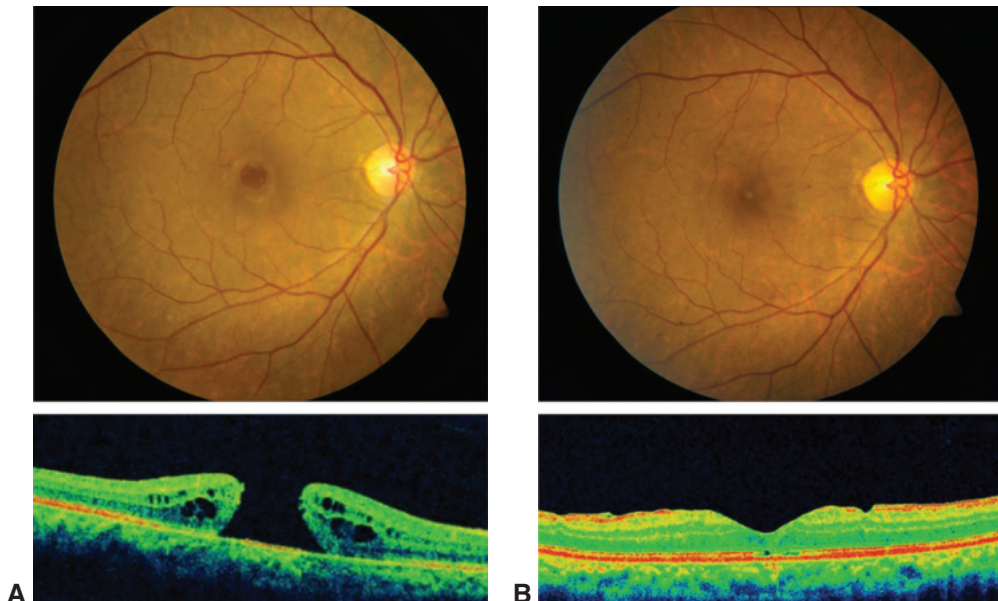


Figure 19-4 Idiopathic macular hole. **A**, Color fundus photograph and corresponding OCT image of a full-thickness macular hole in a patient who had experienced reduced visual acuity (20/100) for 3 months. **B**, Postoperative fundus photograph and OCT image from the same patient. After vitrectomy, membrane peeling, and fluid–gas exchange, the macular hole closed, normal foveal anatomy was restored, and visual acuity improved to 20/25. (*Courtesy of Stephen J. Kim, MD.*)

Kelly NE, Wendel RT. Vitreous surgery for idiopathic macular holes. Results of a pilot study.

Arch Ophthalmol. 1991;109(5):654–659.

Kumagai K, Furukawa M, Ogino N, Uemura A, Demizu S, Larson E. Vitreous surgery

with and without internal limiting membrane peeling for macular hole repair. *Retina.*

2004;24(5):721–727.

Submacular Hemorrhage

Patients with neovascular age-related macular degeneration (AMD) and larger submacular hemorrhages generally have poor visual outcomes. Pars plana vitrectomy techniques may be considered for thick submacular hemorrhage. The surgery involves pneumatic displacement of subretinal blood away from the macular center without attempting to drain the hemorrhage. This technique can be performed with vitrectomy, subretinal injection of tissue plasminogen activator (tPA) via a 39-gauge to 41-gauge cannula, and partial air–fluid exchange (Video 19-5). Postoperative face-down positioning can result in substantial inferior extramacular displacement of the blood (Fig 19-5). Intravitreal injection of expansile gas (eg, SF₆ or C₃F₈) and face-down positioning, with or without adjunctive intravitreal tPA administration, has also been performed in an office setting. Resolution of submacular hemorrhage with improvement of visual acuity can be achieved with administration of

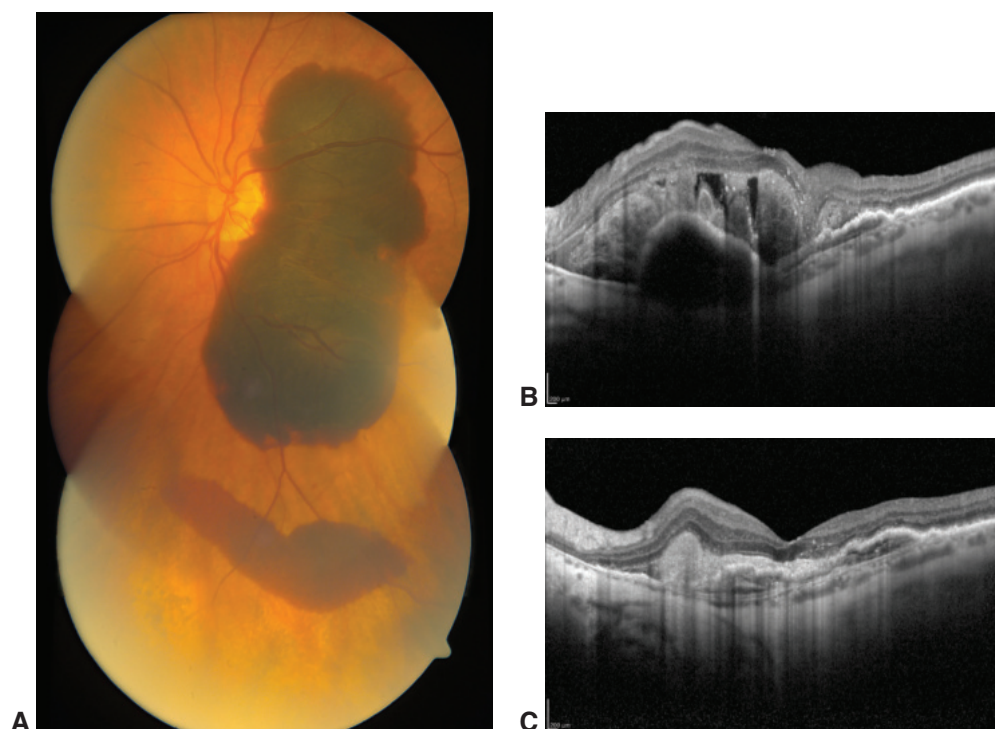


Figure 19-5 Submacular hemorrhage. **A**, Fundus photograph montage shows a large submacular hemorrhage in the setting of neovascular age-related macular degeneration (AMD). **B**, OCT shows large pigment epithelial detachment with overlying subretinal hemorrhage. **C**, OCT taken after pars plana vitrectomy with subretinal tissue plasminogen activator shows resolution of the subretinal hemorrhage with fibrosis. Vision improved from counting fingers to 20/150. (Courtesy of Shriji Patel, MD, MBA.)

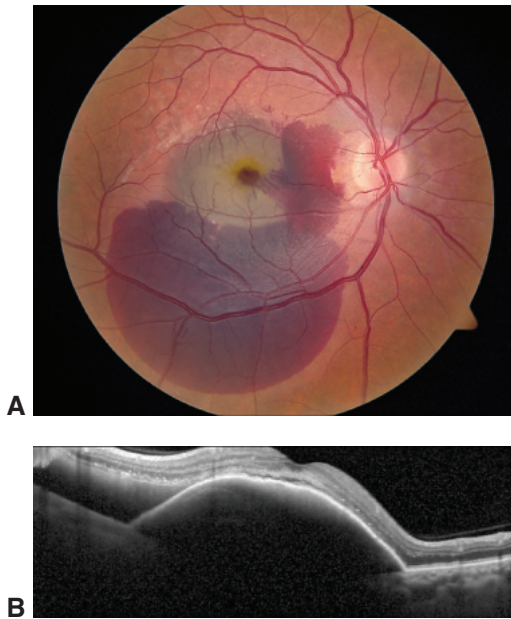


Figure 19-6 Submacular hemorrhage. **A**, Color fundus photograph from a 74-year-old man with 2 days of vision loss and 20/400 visual acuity. Note the lighter-appearing blood in the sub-retinal pigment epithelium (sub-RPE) space in the center and temporal macula versus the darker-appearing blood in the subretinal space in the nasal macula and inferior retina. **B**, Spectral-domain OCT vertical line scan through the macula shows inferior (*left*) subretinal hemorrhage and central sub-RPE hemorrhage. Sub-RPE hemorrhage is not amenable to pneumatic displacement; thus, the patient was treated with intravitreal anti-vascular endothelial growth factor (anti-VEGF) alone, and visual acuity improved to 20/60. (Courtesy of Kenneth Taubenslag, MD.)

anti-vascular endothelial growth factor (anti-VEGF) agents alone, which is the only viable option for blood predominantly located in the sub-RPE space (Fig 19-6). Following treatment of the hemorrhage, most patients require anti-VEGF treatment for the exudative AMD.



VIDEO 19-5 Subretinal tPA for macular hemorrhage.

Courtesy of Shriji Patel, MD, MBA.



Vitrectomy for Vitreous Opacities

The majority of patients with vitreous opacities experience improvement without intervention. Nevertheless, surgery to remove vitreous opacities or symptomatic floaters has become more common. Appropriate case selection is necessary, given the 2.6% return to the operating room rate for retinal detachment. YAG vitreolysis can be used as an alternative to surgical removal of floaters, but there is limited high-quality scientific literature assessing the efficacy of this technique, and vision-threatening complications have been reported.

Hahn P, Schneider EW, Tabandeh H, Wong RW, Emerson GG; American Society of Retina Specialists Research and Safety in Therapeutics (ASRS ReST) Committee. Reported complications following laser vitreolysis. *JAMA Ophthalmol.* 2017;135(9):973–976.

Rubino SM, Parke DW III, Lum F. Return to the operating room after vitrectomy for vitreous opacities: Intelligent Research in Sight Registry analysis. *Ophthalmol Retina.* 2021;5(1):4–8.

Vitrectomy for Complications of Diabetic Retinopathy

Advances in vitreoretinal surgical techniques have facilitated earlier surgical intervention in patients with diabetic retinopathy and have resulted in reduced surgical morbidity and

shorter surgical times. In addition, preoperative use of anti-VEGF agents can help reduce intraoperative bleeding; however, it can lead to traction retinal detachment if surgery is significantly delayed after the injection.

Vitreous Hemorrhage

Vitreous hemorrhage is a common complication in patients with diabetic retinopathy. Vitrectomy is indicated when a vitreous hemorrhage fails to clear spontaneously. The timing of the surgery is determined by the surgeon's preference and the patient's visual requirements. Possible indications for more prompt intervention include monocular vision, bilateral vitreous hemorrhages, or ultrasonographic evidence of a retinal tear or underlying retinal detachment that threatens the macula. In the absence of ophthalmoscopic visualization, serial ultrasonography helps the clinician assess the anatomical condition of the retina.

If surgery is indicated, treatment involves pars plana vitrectomy with removal of vitreous hemorrhage (Video 19-6) and release of the hyaloid from fronds of retinal neovascularization. If present, vitreoretinal traction at the optic nerve head and along the arcade vessels is addressed at the time of surgery, along with any macular ERMs. Complete panretinal photocoagulation and hemostasis should generally be achieved during the procedure. To prevent bleeding or rebleeding, the eye may be filled with air or a short-acting gas to tamponade possible bleeding sites.



VIDEO 19-6 Vitrectomy for vitreous hemorrhage.

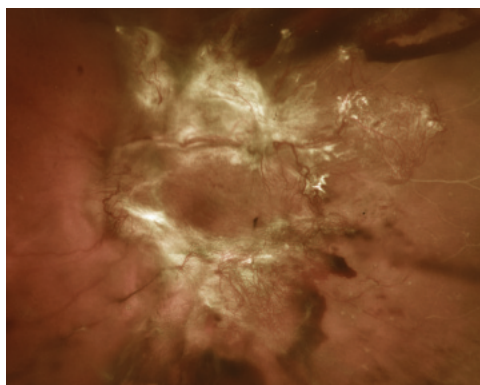
Courtesy of Colin A. McCannel, MD.



Diabetic Traction Retinal Detachment

Traction (also called *tractional*) retinal detachment (TRD) occurs when the hyaloid contracts but fronds of neovascular ingrowth prevent it from separating from the retinal interface. The tractional forces are transmitted to full-thickness retina and, in the absence of a retinal break, cause schisis and/or detachment of the underlying retina from the corresponding RPE (Fig 19-7). Vitrectomy is indicated when progression of a TRD threatens or involves the macula. In certain complex cases, spontaneous breaks can also occur in an atrophic retina under traction, resulting in combined traction and rhegmatogenous detachments. Although

Figure 19-7 Traction retinal detachment in a patient with proliferative diabetic retinopathy. Fibrosis with extensive neovascularization can be seen along the superior and inferior arcades. There is vitreous and preretinal hemorrhage along with sclerotic vessels temporally. (Courtesy of Shrijji Patel, MD, MBA.)



panretinal photocoagulation should precede vitrectomy whenever possible, it can be more difficult to accomplish in the presence of vitreous hemorrhage. A preoperative adjunctive intravitreal injection of an anti-VEGF agent (3–5 days before surgery) may induce regression of neovascularization, facilitating dissection and minimizing intraoperative bleeding.

During vitrectomy for TRD, the cortical vitreous and posterior hyaloid are removed from the retinal surface (Video 19-7). Point adhesions of cortical vitreous to surface retinal neovascularization can be relieved with use of various instruments, including scissors or the vitreous cutter. Surgical approaches to fibrovascular tissue include segmentation and delamination. In *segmentation*, bands of fibrovascular tissue causing traction are cut, but the epiretinal proliferations are not completely removed. In *delamination*, the epiretinal proliferations are completely, or almost completely, dissected off the retinal surface to relieve the traction. After tractional membranes are removed, diathermy may be used to treat fibrovascular tufts and achieve hemostasis, and supplementary laser treatment may be applied in the periphery to reduce ischemia.

Brunner S, Binder S. Surgery for proliferative diabetic retinopathy. In: Schachat AP, Wilkinson CP, Hinton DR, Sadda SR, Wiedemann P, eds. *Ryan's Retina*. Vol 3. 6th ed. Elsevier/Saunders; 2018.



VIDEO 19-7 Tractional retinal detachment repair with subretinal hemorrhage removal.
Courtesy of Enchun M. Liu, MD.



Diabetic Macular Edema

The current mainstays of treatment for diabetic macular edema are intravitreal anti-VEGF, corticosteroid pharmacotherapy, and photocoagulation (for more information about pharmacologic agents, see Chapter 5). However, vitrectomy with membrane peeling may be considered for recalcitrant cases in which the posterior hyaloid or epiretinal membrane is exerting traction on the macula.

Vitrectomy for Posterior Segment Complications of Anterior Segment Surgery

Postoperative Endophthalmitis

Postoperative endophthalmitis is classified on the basis of time of onset: *acute onset* occurs within 6 weeks after surgery, and *delayed onset* occurs more than 6 weeks after surgery. A specific subtype of endophthalmitis that occurs following filtering bleb surgery has a markedly different spectrum of causative organisms.

Acute-onset postoperative endophthalmitis

Clinical features of acute-onset postoperative endophthalmitis include intraocular inflammation, often with hypopyon, conjunctival vascular hyperemia, and corneal and eyelid edema. Symptoms include pain and vision loss. Common causative organisms are coagulase-negative *Staphylococcus* species, *Staphylococcus aureus*, *Streptococcus* species,

and gram-negative organisms. Monitoring includes obtaining intraocular cultures. A vitreous specimen can be obtained either by needle tap or with a vitrectomy instrument. A *vitreous needle tap* is typically performed with a 25-gauge, 5/8-inch needle on a 3-mL syringe (to provide greater vacuum) introduced through the pars plana and directed toward the midvitreous cavity. Independent of vitreous sample collection, an anterior chamber specimen may be obtained by using a 30-gauge needle on a tuberculin syringe. Vitreous specimens are more likely to yield a positive culture. Management includes administering intravitreal antibiotics; see Table 19-2 for typical dosing regimens.

Intravitreal antibiotic injections should always be administered after culture samples are collected. Commonly used agents include ceftazidime and vancomycin. Ceftazidime has largely replaced amikacin or gentamicin in clinical practice because of concerns of potential aminoglycoside toxicity. Intravitreal dexamethasone may reduce posttreatment inflammation, but its role in endophthalmitis management remains controversial.

The use of vitrectomy for acute-onset post-cataract surgery endophthalmitis may be guided by the results of the Endophthalmitis Vitrectomy Study (EVS; Clinical Trial 19-1). In the EVS, patients were randomly assigned to undergo either vitrectomy or vitreous tap/biopsy. Both groups received intravitreal and subconjunctival antibiotics (vancomycin and amikacin). The EVS concluded that vitrectomy was indicated in patients with acute-onset postoperative endophthalmitis (within 6 weeks of cataract extraction) with light perception vision (Fig 19-8). Patients with hand motions visual acuity or better had equivalent outcomes in both treatment groups.

Endophthalmitis Vitrectomy Study Group. Results of the Endophthalmitis Vitrectomy Study. A randomized trial of immediate vitrectomy and of intravenous antibiotics for the treatment of postoperative bacterial endophthalmitis. *Arch Ophthalmol.* 1995;113(12):1479–1496.

Chronic endophthalmitis

Chronic (delayed-onset) endophthalmitis has a progressive or indolent course over months or years. Common causative organisms are *Propionibacterium acnes*, coagulase-negative *Staphylococcus* spp, and fungi. Endophthalmitis caused by *P acnes* characteristically induces a peripheral white plaque within the capsular bag and an associated chronic granulomatous inflammation (Fig 19-9A). An injection of antibiotics into the capsular bag or vitreous cavity usually does not eliminate the infection; instead, the preferred treatment is pars plana vitrectomy, partial capsulectomy with selective removal of intracapsular white plaque, and injection of 1 mg intravitreal vancomycin adjacent to or inside the capsular bag (Fig 19-9B). If the condition recurs after vitrectomy, removal of the entire capsular bag, with removal or exchange of the intraocular lens, should be considered.

Table 19-2 Dosing of Commonly Used Intravitreal Antimicrobials

Vancomycin	1.0 mg/0.1 mL
Ceftazidime	2.25 mg/0.1 mL
Clindamycin	1 mg/0.1 mL
Amikacin	400 µg/0.1 mL
Voriconazole	100 µg/0.1 mL

CLINICAL TRIAL 19-1**Endophthalmitis Vitrectomy Study**

Objective: To evaluate the role of pars plana vitrectomy and intravenous antibiotics in the management of postoperative bacterial endophthalmitis.

Participants: Patients with clinical signs and symptoms of bacterial endophthalmitis in an eye after cataract surgery or intraocular lens implantation; onset of infection occurred within 6 weeks of surgery.

Randomization: Patients were randomly assigned to immediate pars plana vitrectomy or to immediate tap and inject. Patients were randomly assigned to receive systemic antibiotics or no systemic antibiotics and evaluated at regular intervals after treatment.

Outcome measures: Standardized visual acuity testing and media clarity.

Outcomes:

1. No difference in final visual acuity or media clarity whether or not systemic antibiotics (amikacin/ceftazidime) were used.
2. No difference in outcomes between the 3-port pars plana vitrectomy group and the immediate tap/biopsy group for patients with better than light perception visual acuity at the study entry examination.
3. For patients with light perception visual acuity, much better results in the immediate pars plana vitrectomy group:
 - a. Three times more likely to achieve $\geq 20/40$ (33% vs 11%)
 - b. Almost 2 times more likely to achieve $\geq 20/100$ (56% vs 30%)
 - c. Less likely to incur $< 5/200$ (20% vs 47%)

Clinical impact: This study, completed in 1995, revolutionized treatment of post-cataract surgery endophthalmitis by making tap and inject an office procedure for most eyes.

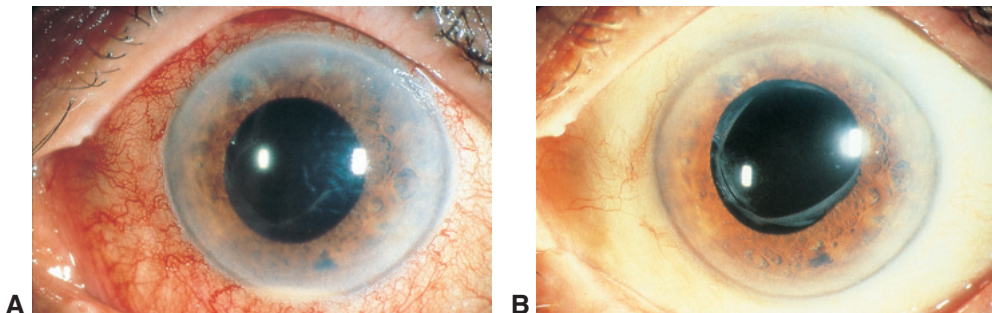


Figure 19-8 Acute-onset endophthalmitis. **A**, Patient with marked epibulbar hyperemia, iritis, and hypopyon indicative of endophthalmitis 5 days after cataract surgery. **B**, After a needle tap of vitreous and injection of intravitreal antibiotics, the inflammation resolved and visual acuity improved to 20/30. (Courtesy of Harry W. Flynn Jr, MD.)

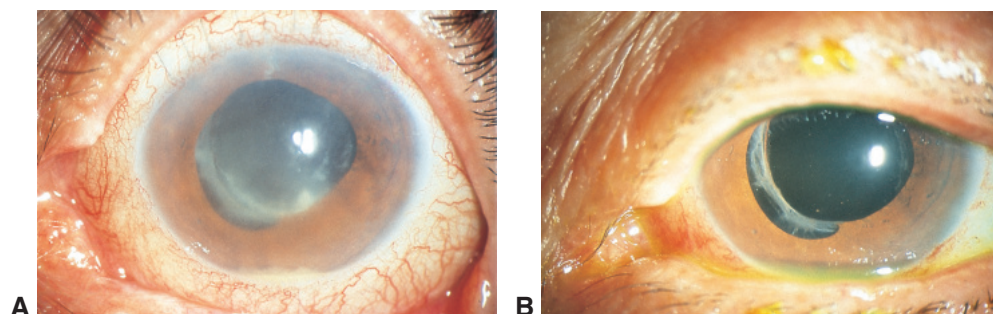


Figure 19-9 Chronic (delayed-onset) postoperative endophthalmitis. **A**, Endophthalmitis in a patient with progressive intraocular inflammation 3 months after cataract surgery. **B**, Same patient after pars plana vitrectomy, capsulectomy, and injection of intravitreal antibiotics. Culture results confirmed a diagnosis of *Propionibacterium acnes* endophthalmitis. (Courtesy of Harry W. Flynn Jr, MD.)

Clark WL, Kaiser PK, Flynn HW Jr, Belfort A, Miller D, Meisler DM. Treatment strategies and visual acuity outcomes in chronic postoperative *Propionibacterium acnes* endophthalmitis. *Ophthalmology*. 1999;106(9):1665–1670.

Endophthalmitis associated with glaucoma surgery

Except for the additional sign of a purulent bleb, the clinical features of conjunctival filtering bleb–associated endophthalmitis are similar to those of acute-onset postoperative endophthalmitis. These features include conjunctival vascular hyperemia and noticeable intraocular inflammation, often with hypopyon (occurring months or years after glaucoma filtering surgery; Fig 19-10A). The initial infection may involve the bleb only (*blebitis*), without anterior chamber or vitreous involvement. Blebitis without endophthalmitis can be treated with frequent applications of topical and subconjunctival antibiotics and close follow-up. However, if blebitis progresses to bleb-associated endophthalmitis, patients are treated with intravitreal antibiotics with or without vitrectomy (Fig 19-10B). Likewise, exposed glaucoma drainage implants or microinvasive glaucoma surgery can result in endophthalmitis, typically months to years after surgery.

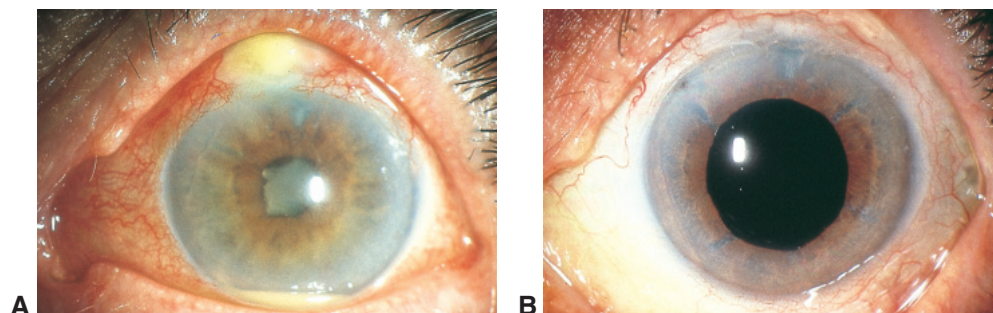


Figure 19-10 Bleb-associated endophthalmitis. **A**, Patient with endophthalmitis who had sudden onset of decreased vision, redness, and pain 2 years after glaucoma filtering surgery. **B**, Same patient after treatment with pars plana vitrectomy and injection of intravitreal antibiotics. (Courtesy of Harry W. Flynn Jr, MD.)

Causative organisms frequently include *Streptococcus* spp, *Haemophilus* species, and other gram-positive organisms. The recommended intravitreal antibiotics are similar to those used in acute-onset postoperative endophthalmitis. However, the most common causative organisms in bleb-associated endophthalmitis are more virulent than the most frequently encountered organisms in endophthalmitis that occurs after other intraocular surgeries (such as cataract surgery). Even with prompt treatment, bleb-associated endophthalmitis has visual outcomes that are generally worse than those for acute-onset endophthalmitis after cataract surgery.

Retained Lens Fragments After Phacoemulsification

The incidence of posteriorly displaced, or retained, lens fragments during cataract surgery ranges from 0.3% to 1.1% in reported series. Retained lens fragments may cause severe intraocular inflammation and secondary glaucoma. Nuclear fragments usually continue to cause chronic intraocular inflammation, whereas cortical remnants typically resorb spontaneously (Table 19-3).

Indications for vitrectomy include secondary glaucoma, lens-induced uveitis, and the presence of large nuclear fragments. In the 4 largest reported case series, 52% of patients with retained lens fragments had an intraocular pressure (IOP) of at least 30 mm Hg before vitrectomy. Removal of the lens fragments reduced this incidence by 50% or more in these series. Pars plana vitrectomy, with or without use of a fragmatome, is the preferred approach to remove harder pieces of the lens nucleus (Video 19-8). After the lens fragments are removed, the retinal periphery should be examined for retinal tears or retinal detachment.

Table 19-3 General Recommendations for Management of Retained Lens Fragments

For the anterior segment surgeon

- Attempt retrieval of displaced lens fragments only if they are readily accessible.
- Perform anterior vitrectomy as necessary to avoid vitreous prolapse into the wound.
- Insert an intraocular lens if possible.
- Close the cataract wound with interrupted sutures.
- Prescribe topical medications as needed.
- Refer the patient to a vitreoretinal consultant.

For the vitreoretinal surgeon

- Observe eyes with minimal inflammation and/or a small lens fragment.
 - Continue topical medications as needed.
 - Schedule vitrectomy
 - if inflammation or intraocular pressure is not controlled.
 - if a nuclear fragment or nonresolving cortical fragment is present.
 - Delay vitrectomy if necessary to allow clearing of corneal edema.
 - Perform maximal core vitrectomy before phacofragmentation.
 - Start with low fragmentation power (5%–10%) for more efficient removal of the nucleus.
 - Prepare for secondary intraocular lens insertion if necessary.
 - Examine the retinal periphery for retinal tears or retinal detachment.
-

Modified with permission from Flynn HW Jr, Smiddy WE, Vilar NF. Management of retained lens fragments after cataract surgery. In: Saer JB, ed. *Vitreo-Retinal and Uveitis Update: Proceedings of the New Orleans Academy of Ophthalmology Symposium*. Kugler Publications; 1998:149, 150.

**VIDEO 19-8** Vitrectomy for removal of retained lens fragment.

Courtesy of Colin A. McCannel, MD.



Studies with long-term follow-up have reported that retinal detachment occurs in approximately 15% of eyes with retained lens fragments. Aggressive attempts to retrieve posterior lens fragments through a limbal approach are sometimes complicated by retinal detachments caused by giant retinal tears. Giant retinal tears are more commonly found 180° away from the incision used for cataract surgery.

Aaberg TM Jr, Rubsamens PE, Flynn HW Jr, Chang S, Mieler WF, Smiddy WE. Giant retinal tear as a complication of attempted removal of intravitreal lens fragments during cataract surgery. *Am J Ophthalmol.* 1997;124(2):222–226.

Modi YS, Epstein A, Smiddy WE, Murray TG, Feuer W, Flynn HW Jr. Retained lens fragments after cataract surgery: outcomes of same-day versus later pars plana vitrectomy. *Am J Ophthalmol.* 2013;156(3):454–459.e1.

Vanner EA, Stewart MW. Vitrectomy timing for retained lens fragments after surgery for age-related cataracts: a systematic review and meta-analysis. *Am J Ophthalmol.* 2011;152(3):345–357.e3.

Posteriorly Dislocated Intraocular Lenses

Posterior chamber intraocular lenses (PCIOLs) may become dislocated despite seemingly satisfactory capsular support at the time of the initial surgery. Factors to consider when placing a sulcus-fixated IOL include the presence of zonular dehiscence, total amount of anterior capsule support (eg, >180°), size of the eye, and haptic-to-haptic diameter of the IOL. Foldable IOLs have a haptic-to-haptic length of 12.5–13.0 mm. This length, which is frequently smaller than the sulcus-to-sulcus diameter into which the haptics are placed, may contribute to postoperative subluxation or dislocation of the IOL. A flexible IOL may also become dislocated following Nd:YAG laser capsulotomy performed soon after cataract surgery. Late dislocation of the IOL (from several months to decades after surgery) is less common but may occur as a result of trauma or spontaneous loss of zonular support in eyes with pseudoexfoliation syndrome. Treatment options in such cases include observation only, surgical repositioning, IOL exchange, or IOL removal.

In vitrectomy for posteriorly dislocated IOLs, all vitreous adhesions to the IOL are removed in order to minimize vitreous traction on the retina when the lens is manipulated back into the anterior chamber. The IOL may be placed into the ciliary sulcus provided that there is adequate support. If capsular support is inadequate, the IOL may be fixated by suturing the haptics to the iris (*iris fixation*) or sclera (*scleral fixation*) or by placing the haptics into intrascleral tunnels (*intrascleral fixation*). Alternatively, the PCIOL can be removed through a limbal incision and exchanged for an anterior chamber IOL (Video 19-9) or scleral-sutured IOL (Video 19-10).

**VIDEO 19-9** Vitrectomy for retrieval of posteriorly dislocated IOL.

Courtesy of Colin A. McCannel, MD.



**VIDEO 19-10** Scleral-sutured IOL.

Courtesy of Shriji Patel, MD, MBA.



Smiddy WE, Flynn HW Jr. Managing retained lens fragments and dislocated posterior chamber IOLs after cataract surgery. *Focal Points: Clinical Modules for Ophthalmologists*. American Academy of Ophthalmology; 1996, module 7.

Cystoid Macular Edema

Cystoid macular edema (CME) that develops after anterior segment surgery usually resolves spontaneously. Treatment with corticosteroid and nonsteroidal anti-inflammatory eyedrops is the first-line approach for patients with persistent CME. Periocular or intravitreal corticosteroids may be used in recalcitrant cases. Oral acetazolamide may also be useful in some cases. Lysis of isolated vitreous wicks in the anterior chamber can be performed with the Nd:YAG laser. Pars plana vitrectomy may be required for more extensive adhesions or anterior chamber vitreous migration. Removal of vitreous adhesions to anterior segment structures may promote resolution of CME and improve visual acuity in select cases (Fig 19-11). An IOL may require repositioning, exchange, or removal if it is thought to be irritating the iris by chafing or capture.

Suprachoroidal Hemorrhage

Suprachoroidal hemorrhage can occur during or after any type of intraocular surgery, particularly glaucoma surgery, in which large variations in IOP are commonplace. By definition, such hemorrhages accumulate in the supraciliary and suprachoroidal space, a potential space between the sclera and uvea that is modified by uveal adhesions and entries of vessels. When retinal surfaces touch one another, the choroidal hemorrhage is termed *appositional*, or “kissing.” These hemorrhages may be further classified as *expulsive*

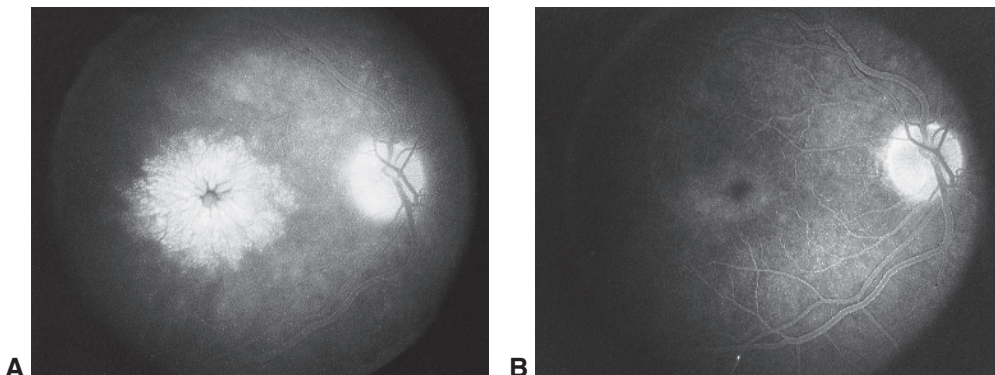


Figure 19-11 Fundus photographs of pseudophakic cystoid macular edema (CME). **A**, Patient has nonresolving CME, vitreous strands adhering to the cataract wound, and a dislocated intraocular lens (IOL). **B**, Same patient after pars plana vitrectomy, removal of vitreous strands, repositioning of IOL, and periocular administration of corticosteroids. CME has improved markedly. (Courtesy of Harry W. Flynn Jr, MD.)

or *nonexpulsive*; the expulsive type involves extrusion of intraocular contents. Reported risk factors for suprachoroidal hemorrhage include

- advanced age
- aphakia
- arteriosclerotic cardiovascular disease
- glaucoma
- hypertension
- intraoperative tachycardia
- myopia
- Sturge-Weber–associated choroidal hemangiomas
- use of anticoagulant drugs

Transient hypotony is a common feature of all incisional ocular surgery; in a small percentage of patients, it may be associated with suprachoroidal hemorrhage from rupture of the long or short posterior ciliary arteries.

Surgical management strategies are controversial. Most studies recommend immediate closure of ocular surgical incisions and removal of vitreous incarcerated in the wound, if possible; the primary goal is to prevent or limit expulsion. Successful intraoperative drainage of a suprachoroidal hemorrhage is rare, however, because the blood coagulates rapidly. Most surgeons recommend observation of suprachoroidal hemorrhages for 7–14 days to allow some degree of liquefaction of the hemorrhage. Determining the timing of secondary surgical intervention is aided by B-scan ultrasonography, which enables evaluation of ultrasonographic features of clot liquefaction. Indications for surgical drainage include recalcitrant pain, increased IOP, retinal detachment, and appositional choroidal detachments associated with ciliary body rotation and angle closure. In addition, prolonged IOP elevation in the presence of an anterior chamber hemorrhage (*hyphema*) increases the risk of corneal blood staining and is an indication for surgical intervention.

In surgical management of suprachoroidal hemorrhage, an anterior chamber infusion line is placed to maintain IOP (Fig 19-12, Video 19-11). A full-thickness sclerotomy is

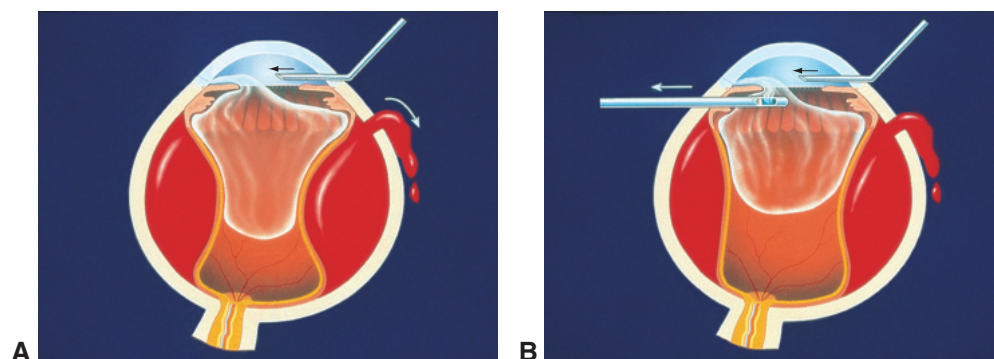


Figure 19-12 Schematic of suprachoroidal hemorrhage drainage. **A**, Anterior infusion and simultaneous drainage of suprachoroidal hemorrhage through pars plana sclerotomy. **B**, Pars plana vitrectomy removes vitreous prolapse while drainage of suprachoroidal hemorrhage continues. (Courtesy of Harry W. Flynn Jr, MD.)

then placed subjacent to the site of maximum accumulation of blood. After the suprachoroidal blood drains, pars plana vitrectomy may be performed. Appositional and closed-funnel suprachoroidal hemorrhage, prolonged elevation of IOP, and retinal detachment all portend a poor visual prognosis.



VIDEO 19-11 How to drain a suprachoroidal hemorrhage.

Courtesy of Christina Y. Weng, MD, MBA.



Scott IU, Flynn HW Jr, Schiffman J, Smiddy WE, Murray TG, Ehli F. Visual acuity outcomes among patients with appositional suprachoroidal hemorrhage. *Ophthalmology*. 1997;104(12):2039–2046. Published correction appears in *Ophthalmology*. 1998;105(3):394.

Needle Injury of the Globe

Factors predisposing patients to needle penetration of the globe during retrobulbar block include

- axial high myopia
- inexperience of the surgeon
- poor patient cooperation at the time of the injection
- posterior staphyloma
- previous scleral buckling surgery
- scleromalacia

Care should be taken to avoid iatrogenic globe penetration at the time of retrobulbar and peribulbar injection of anesthetic or medication (Video 19-12). Resulting injury can occur based on the depth and location of needle penetration, intraocular injection of drug, and globe perforation (Fig 19-13A). Management options vary with the severity of the intraocular damage. Often, blood obscures and surrounds the retinal penetration site, making laser treatment difficult. Observation or transscleral cryotherapy may be considered in such cases. When retinal detachment is present, early vitrectomy with or without scleral buckling is often recommended (Fig 19-13B). Posterior pole damage from needle extension into the macula or optic nerve is associated with a very poor visual prognosis.



VIDEO 19-12 Retrobulbar injection: technique and tips.

Courtesy of Julian D. Perry, MD, Alexander D. Blandford, MD, Joseph D. Boss, MD, and Rishi P. Singh, MD.



Rhegmatogenous Retinal Detachment Surgery

Rhegmatogenous retinal detachment (RRD) occurs when a retinal break (or multiple breaks) allows ingress of fluid from the vitreous cavity into the subretinal space (Fig 19-14). Breaks can be atrophic, often associated with lattice degeneration, or they may be tractional tears related to vitreous traction on the retina and posterior vitreous detachment (PVD). The risk of RRD in otherwise normal eyes is approximately 5 new cases in 100,000 persons per year; lifetime risk is approximately 1 in 300 persons. The most significant risk factors are high myopia,

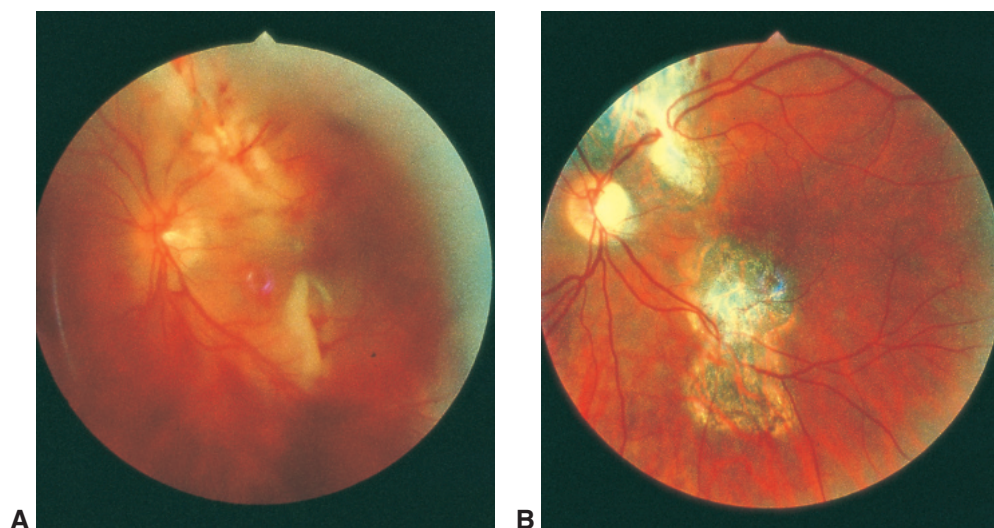
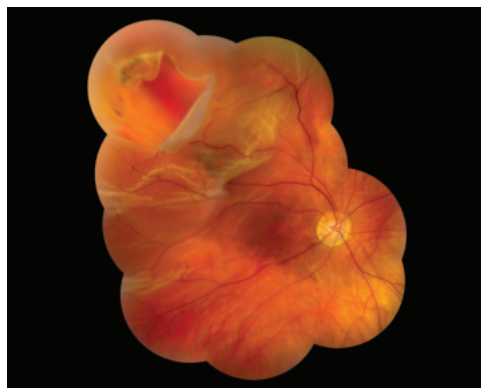


Figure 19-13 Damage caused by needle penetration of the globe. **A**, Multiple retinal breaks and damage to the macula caused by needle penetration of the globe. **B**, After retinal detachment, treatment consisted of vitrectomy, fluid–gas exchange, and endolaser photocoagulation of retinal breaks. Although retinal reattachment was achieved, the patient's visual acuity remained very poor. (Courtesy of Harry W. Flynn Jr, MD.)

Figure 19-14 Color fundus photograph montage of a patient with symptomatic retinal detachment from a large superotemporal break following cataract surgery. (Courtesy of Nancy M. Holekamp, MD.)



family history of retinal detachment, and fellow-eye retinal detachment. Pseudophakia is also an important risk factor; the reported incidence after cataract surgery is less than 1% but increases over time. Patient characteristics that increase the risk of pseudophakic retinal detachment include younger age at the time of cataract extraction, male sex, and longer axial length. A surgical complication such as posterior capsule rupture with vitreous loss has been estimated to increase the risk of retinal detachment as much as 20-fold.

Management options for RRD include laser demarcation of the detachment, pneumatic retinopexy, scleral buckling procedure, and vitrectomy with or without scleral buckling. In rare cases, observation may be considered for select patients with localized retinal detachment surrounded by demarcation line and no associated symptoms (subclinical retinal detachment).

Clark A, Morlet N, Ng JQ, Preen DB, Semmens JB. Risk for retinal detachment after phacoemulsification: a whole-population study of cataract surgery outcomes. *Arch Ophthalmol*. 2012;130(7):882–888.

Powell SK, Olson RJ. Incidence of retinal detachment after cataract surgery and neodymium:YAG laser capsulotomy. *J Cataract Refract Surg*. 1995;21(2):132–135.

Techniques for Surgical Repair of Retinal Detachments

There are 3 surgical techniques for eyes with primary uncomplicated RRD: *pneumatic retinopexy*, *scleral buckling*, and *primary vitrectomy with or without scleral buckling*. The common goals of these procedures are to identify and treat all causative retinal breaks while supporting such breaks through external and internal tamponade as needed.

Campo RV, Sipperley JO, Sneed SR, et al. Pars plana vitrectomy without scleral buckle for pseudophakic retinal detachments. *Ophthalmology*. 1999;106(9):1811–1816.

Kreissig I, ed. *Primary Retinal Detachment: Options for Repair*. Springer-Verlag; 2005.

Pneumatic retinopexy

Pneumatic retinopexy closes retinal breaks by using an intraocular gas bubble for a sufficient time to allow the subretinal fluid to resorb and a chorioretinal adhesion to form around the causative break(s) (Fig 19-15). The classic indications for pneumatic retinopexy include

- confidence that all retinal breaks have been identified
- retinal breaks that are confined to the superior 8 clock-hours
- a single retinal break or multiple breaks within 1–2 clock-hours
- the absence of proliferative vitreoretinopathy (PVR) grade CP or CA according to the updated Retina Society Classification
- a cooperative patient who can maintain proper positioning
- clear media

With direct pneumatic occlusion of the causative retinal breaks in acute detachments, subretinal fluid is often completely resorbed within 6–8 hours.

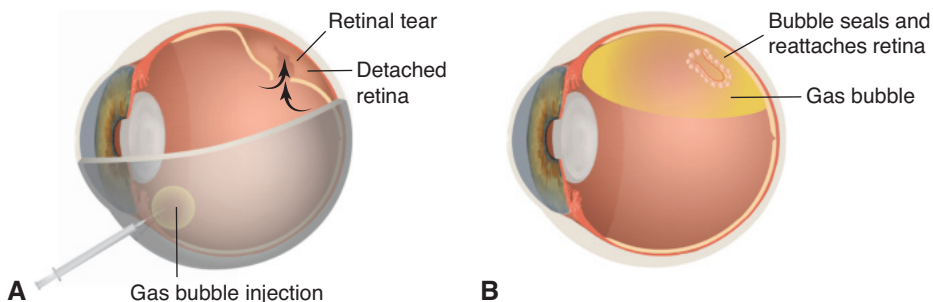


Figure 19-15 Schematic of pneumatic retinopexy. **A**, A small expansile gas bubble is injected into the vitreous cavity. **B**, The bubble enlarges. The patient is positioned so that the gas bubble occludes the retinal break, allowing for retinal reattachment. The break is sealed with either cryotherapy or laser. (Illustration by Cyndie C. H. Wooley. Part A adapted with permission from Elsevier. From Bairo F. Towards an ideal biomaterial for vitreous replacement: historical overview and future trends. *Acta Biomater*. 2011;7(3):921–935. doi:10.1016/j.actbio.2010.10.030)

Transconjunctival cryopexy can be performed on the causative retinal breaks; alternatively, *laser retinopexy* may be performed after retinal apposition. A variety of intraocular gases (eg, air, SF₆, C₃F₈) can be used for tamponade, and a concomitant anterior chamber paracentesis is generally required to normalize the elevated IOP that results from the gas injection. The patient must maintain a predetermined head posture to place the breaks in the least dependent position.

A prospective multicenter randomized clinical trial comparing pneumatic retinopexy with scleral buckling demonstrated successful retinal reattachment in 73% of patients who underwent pneumatic retinopexy and in 82% of those who received scleral buckling procedures; this difference was not statistically significant. Complications from pneumatic retinopexy include subretinal gas migration, anterior chamber gas migration, endophthalmitis, cataract, and recurrent retinal detachment from the formation of new retinal breaks.

Gilca M, Duval R, Goodyear E, Olivier S, Cordahi G. Factors associated with outcomes of pneumatic retinopexy for rhegmatogenous retinal detachments: a retrospective review of 422 cases. *Retina*. 2014;34(4):693–699.

Tornambe PE, Hilton GF. Pneumatic retinopexy. A multicenter randomized controlled clinical trial comparing pneumatic retinopexy with scleral buckling. The Retinal Detachment Study Group. *Ophthalmology*. 1989;96(6):772–784.

Scleral buckling

Scleral buckling closes retinal breaks through external scleral indentation. Transscleral cryopexy is used to create a permanent adhesion between the retina and RPE at the sites of retinal breaks. The buckling material is then carefully positioned to support the causative breaks by scleral imbrication.

The surgeon chooses the scleral buckling technique (eg, encircling, segmental, or radial placement of the sponge, sutured versus scleral tunnels) according to the number and position of retinal breaks, eye size, age of patient, presence of PVD and associated vitreoretinal findings (eg, lattice degeneration, vitreoretinal traction, aphakia), and individual preference and training (Fig 19-16, Video 19-13). Scleral buckling is specifically

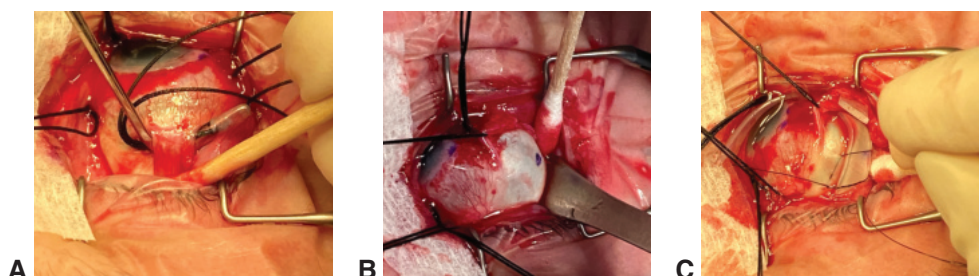


Figure 19-16 Scleral buckling procedure (see also Video 19-13). **A**, The conjunctiva is opened; the rectus muscles are isolated and tagged with a silk suture. **B**, The eye is rotated so the sclera is exposed. Using calipers, the surgeon measures and marks the location for the anterior and posterior scleral pass for the radial mattress suture. **C**, A forceps is used to pass the encircling element under the rectus muscle. Partial-thickness scleral suture passes are made anterior and posterior to the target buckle position. The tied-up radial mattress suture is shown, which will hold the buckle in place. The element can then be tightened to create the desired imbrication. (Courtesy of Gaurav K. Shah, MD.)

useful in younger, phakic patients with attached posterior hyaloid, complex detachments involving multiple retinal breaks, and detachments due to retinal dialysis.



VIDEO 19-13 Scleral buckle for rhegmatogenous retinal detachment.

Courtesy of Ravi Pandit, MD, David Xu, MD, and Ajay Kuriyan, MD.



An increase in IOP related to compression from the buckling effect may indicate the need for external drainage of the subretinal fluid, anterior chamber paracentesis, or both. Chronic viscous subretinal fluid, “fish-mouthing” of large retinal breaks, and bullous retinal detachments may necessitate treatment with intraocular gas tamponade, drainage, or both. Complications of scleral buckling include induced myopia, anterior ocular ischemia, diplopia, extraocular muscle disinsertion, ptosis, orbital cellulitis, subretinal hemorrhage from drainage, and retinal incarceration at the drainage site.

Primary vitrectomy

Traction on focal areas of adhesion of the vitreous to the peripheral retina (frequently at the posterior vitreous base insertion) may cause retinal breaks, allowing intraocular fluid to migrate into the subretinal space, which leads to retinal detachment. Consequently, the goals of primary vitrectomy are to remove cortical vitreous adherent to retinal breaks, directly drain the subretinal fluid, tamponade the breaks (using air, gas, or silicone oil), and create chorioretinal adhesions around each retinal break with endolaser photocoagulation or cryopexy.

In general, the 3-port vitrectomy technique is used, employing 20-, 23-, 25-, or 27-gauge instruments. At the surgeon’s discretion, vitrectomy can be combined with a scleral buckling procedure. During vitrectomy, a complete posterior vitreous separation is ensured, and the peripheral cortical vitreous is carefully shaved toward the vitreous base to relieve traction on the retinal breaks (Fig 19-17, Video 19-14). The use of intraoperative triamcinolone can confirm complete vitreous separation. To drain the subretinal fluid and achieve intraoperative retinal reattachment, the surgeon can either drain through the causative break, create a drainage retinotomy, or use perfluorocarbon liquid. If PVR is present, it may be necessary to peel the epiretinal (and, less commonly, subretinal) membranes to facilitate the retinal reattachment. For extensive PVR, a relaxing retinotomy or retinectomy may be required.

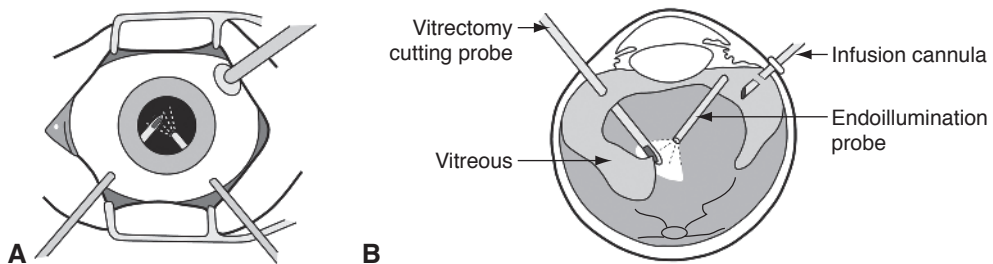


Figure 19-17 Schematic of vitrectomy. **A**, Surgeon’s view of a 3-port pars plana vitrectomy. **B**, Cross-sectional view shows an infusion cannula, endoillumination probe, and vitrectomy cutting probe. (Illustration by Dave Yates.)

Once the retina is flattened, chorioretinal laser photocoagulation or cryopexy can be applied. Postoperative tamponade is generally provided by intraocular air or nonexpansile concentrations of SF₆ or C₃F₈ gas, although silicone oil may be required in complex cases. Complications of vitrectomy for retinal detachment include postvitrectomy nuclear sclerosis (in phakic eyes), glaucoma, PVR, and recurrent retinal detachment.



VIDEO 19-14 Vitrectomy for rhegmatogenous retinal detachment.
Courtesy of Colin A. McCannel, MD.



Features of *complex retinal detachment* include giant retinal tears, recurrent retinal detachment, vitreous hemorrhage, and PVR. The surgeon may employ pars plana vitrectomy techniques to address the common features of PVR, including proliferative membranes, retinal folds, and media opacities. In the past, controversy surrounded the use of long-acting gas versus silicone oil for retinal tamponade in eyes with complex retinal detachment caused by advanced grades of PVR. This issue was explored in the Silicone Study, a prospective multicenter randomized trial, which concluded that tamponade with SF₆ was inferior to long-term tamponade with either C₃F₈ or silicone oil. Although differences in outcomes between the use of C₃F₈ and silicone oil were statistically insignificant, patients treated with silicone oil experienced a lower rate of hypotony than those treated with C₃F₈.

Vitrectomy with silicone oil or sulfur hexafluoride gas in eyes with severe proliferative vitreoretinopathy: results of a randomized clinical trial. Silicone Study Report 1. *Arch Ophthalmol.* 1992;110(6):770–779.

Vitrectomy with silicone oil or perfluoropropane gas in eyes with severe proliferative vitreoretinopathy: results of a randomized clinical trial. Silicone Study Report 2. *Arch Ophthalmol.* 1992;110(6):780–792.

Outcomes Following Retinal Reattachment Surgery

Anatomical reattachment

In the absence of PVR, the overall rate of anatomical reattachment with current techniques is 80%–90% for the primary surgery. In patients with PVR (an indicator of chronicity) or who have had previous reattachment surgeries, success rates are in the 70% range. However, rates for final reattachment, even if multiple procedures are required, are in the 90%–100% range. Retinal detachments caused by dialyses or small holes or that are associated with demarcation lines have a better prognosis. Aphakic and pseudophakic eyes have a slightly less favorable prognosis. Detachments caused by giant tears or that are associated with PVR, uveitis, choroidal detachments, or posterior breaks secondary to trauma have the worst prognosis for anatomical reattachment.

Sullivan P. Techniques of scleral buckling. In: Schachat AP, Wilkinson CP, Hinton DR, Sadda SR, Wiedemann P, eds. *Ryan's Retina*. Vol 3. 6th ed. Elsevier/Saunders; 2018.

Postoperative visual acuity

The status of the macula—whether it is detached and for how long—is the primary presurgical determinant of postoperative visual acuity. If the macula is not detached

(“*macula-on*” *retinal detachment*) and the retinal detachment is successfully repaired, restoration of preoperative visual acuity is usually expected.

If the macula is detached preoperatively (“*macula-off*” *retinal detachment*), damage to—or degeneration of—photoreceptors may prevent good postoperative visual acuity. Only approximately one-third to one-half of eyes with a detached macula recover visual acuity to the level of 20/50 or better. Among patients with a macular detachment of less than 1 week’s duration, 75% will obtain a final visual acuity of 20/70 or better, as opposed to 50% with a macular detachment of a duration exceeding 7–10 days but less than 8 weeks.

In addition to photoreceptor damage from the detachment, factors associated with visual acuity deterioration or incomplete recovery following successful retinal reattachment surgery include irregular astigmatism, cataract progression, persistent subfoveal fluid, macular edema, or macular pucker.

Complications of Pars Plana Vitrectomy

Nuclear sclerotic cataract is the most common complication of vitrectomy. Within 3–6 months after vitrectomy, as many as 90% of phakic eyes in patients older than 50 years may develop visually significant nuclear sclerotic cataract. Vitrectomy may also increase the long-term risk of open-angle glaucoma. Both cataract progression and glaucoma are speculated to be the result of increased oxygen tension in the eye after vitrectomy, which in turn leads to oxidative damage to the lens and trabecular meshwork, respectively.

Other complications of pars plana vitrectomy include intraoperative retinal tears (approximately 1%–5%), postoperative detachment (approximately 1%–2%), retention of subretinal perfluorocarbon liquid (when used), retinal and vitreous incarceration, endophthalmitis (approximately 0.05%), suprachoroidal hemorrhage, and vitreous hemorrhage (approximately less than 1%; up to 5% and higher in patients with diabetes). Table 19-4 lists some of the complications of pars plana vitrectomy.

Table 19-4 Complications of Pars Plana Vitrectomy

Complications associated with pars plana vitrectomy
Postoperative nuclear sclerotic cataract
Long-term risk of open-angle glaucoma
Intraoperative or postoperative retinal break
Intraoperative or postoperative retinal detachment
Intraoperative cataract
Postoperative vitreous hemorrhage
Postoperative massive fibrin exudation
Postoperative anterior segment neovascularization
Endophthalmitis
Retinal phototoxicity
Complications associated with silicone oil
Glaucoma
Band keratopathy
Corneal decompensation

Banker AS, Freeman WR, Kim JW, Munguia D, Azen SP; Vitrectomy for Macular Hole Study Group. Vision-threatening complications of surgery for full-thickness macular holes. *Ophthalmology*. 1997;104(9):1442–1453.

Chang S. LXII Edward Jackson lecture: open angle glaucoma after vitrectomy. *Am J Ophthalmol*. 2006;141(6):1033–1043.

Thompson JT. The role of patient age and intraocular gases in cataract progression following vitrectomy for macular holes and epiretinal membranes. *Trans Am Ophthalmol Soc*. 2003;101:485–498.

Intravitreal Injections

Intravitreal injection is the most common procedure in ophthalmology and in medicine in general (Fig 19-18, Video 19-15). The number of injections performed in the United States, estimated from Medicare procedure codes, increased from fewer than 3000 per year in 1999 to an estimated 6.5 million in 2016. The most common indications for these injections include AMD, diabetic retinopathy, and macular edema associated with venous occlusive disease. Intravitreal injections are used most frequently to administer antiangiogenic agents such as aflibercept, bevacizumab, and ranibizumab. Intravitreal injections are also used to deliver steroid preparations and sustained-delivery devices, antimicrobial medications, and various medications currently in clinical trials. The number of intravitreal injections continues to increase as a result of the aging population, the availability of new medications, and an expanding list of indications.



VIDEO 19-15 Intravitreal injection of a pharmacologic agent.

Courtesy of Stephen J. Kim, MD.



Injections can be accomplished safely 3–4 mm posterior to the limbus, depending on the lens status (Table 19-5). Commonly employed methods for administering anesthesia before intravitreal injections include use of pledgets or cotton-tipped applicators soaked with anesthetic and held on the site of injection, application of topical (including viscous) formulations of anesthetic, and subconjunctival injection of lidocaine. There is no

Figure 19-18 Intravitreal injection. The ocular surface was anesthetized with subconjunctival injection of lidocaine, 2%, in the inferotemporal quadrant. An eyelid speculum was inserted, and povidone-iodine, 5%, applied to the ocular surface. After 2 minutes, povidone-iodine was reapplied over the injection site and—after proper hand placement and no talking by the patient or the clinician—the injection was made approximately 4 mm from the limbus.

(Courtesy of Stephen J. Kim, MD.)



Table 19-5 Steps for Performing Intravitreal Injections

1. Obtain informed consent before performing the injection.
2. Administer appropriate anesthesia (topical or subconjunctival).
3. Insert lid speculum according to provider preference.
4. Apply topical povidone-iodine, 5%, to the ocular surface for a minimum of 90 seconds.
5. Inject the medicine 3–4 mm posterior to the limbus (depending on lens status) with needle tip directed toward the midvitreal.
6. Rinse the ocular surface with sterile saline; topical antibiotics should be avoided as they can promote bacterial resistance.
7. Confirm optic nerve perfusion before patient is discharged from the office. Perform anterior chamber paracentesis if the intraocular pressure remains dangerously elevated.

consensus regarding the optimal method of anesthesia for patient comfort and reduced risk of infection. However, some evidence has suggested that topical lidocaine gel formulations could form a physical barrier that blocks contact between the povidone-iodine used for antisepsis and the ocular surface flora.

Strict aseptic technique, including avoiding contact with the eyelid to prevent contamination of the needle tip from the margin and lashes, is recommended. The application of povidone-iodine, 5%, to the ocular surface for at least 90 seconds prior to injection is widely considered beneficial. Antibiotic eyedrop use before or after injections is not recommended for routine procedures; repeated application of topical antibiotics can lead to development of resistant ocular flora.

Endophthalmitis remains the most-feared complication of intravitreal injection, and the reported incidence ranges from 0.02% to 0.2%. Although respiratory organisms can cause endophthalmitis, the most common source of infection is presumed to be the patient's own conjunctiva or eyelids. Thus, potential mechanisms of infection include direct inoculation of ocular surface bacteria into the vitreous or subsequent entry through a wound track. In addition, multiple studies have reported that *Streptococcus viridans*, a common component of oral flora, is a cause of endophthalmitis after intravitreal injections, presumably from contamination by respiratory droplets. Therefore, restricting talking by both the patient and provider during the procedure and the use of face masks (with the nasal bridge taped to reduce upward airflow) are reasonable practices. In addition, excessive manipulation of the eyelid margin should be avoided to limit expression of bacteria-laden secretions from the meibomian glands, and aggressive treatment of blepharitis should be considered for patients with severe disease.

Outbreaks of endophthalmitis from contaminated bevacizumab have prompted periodic review of compounding pharmacy practices and accreditation status to reduce the risk of future outbreaks. To minimize patient risk when bilateral injections are performed, many practitioners have adopted a workflow in which different lot numbers of compounded medications are used for each eye.

Other complications include the development of elevated IOP following intravitreal injections of anti-VEGF agents or as a common adverse effect of steroid injections. A complication unique to the dexamethasone sustained-release implant is severe corneal endothelial toxicity if the implant migrates into the anterior chamber.

Common patient-reported symptoms after intravitreal injection include ocular surface irritation, subconjunctival hemorrhage, and visualization of injected medication or an air bubble from the syringe. Certain silicone-lubricated syringes can leave microdroplets of intravitreal silicone oil.

Khurana RN, Appa SN, McCannel CA, et al. Dexamethasone implant anterior chamber migration: risk factors, complications, and management strategies. *Ophthalmology*. 2014;121(1):67–71.

Kim SJ, Chomsky AS, Sternberg P Jr. Reducing the risk of endophthalmitis after intravitreal injection. *JAMA Ophthalmol*. 2013;131(5):674–675.

Kim SJ, Toma HS. Antimicrobial resistance and ophthalmic antibiotics: 1-year results of a longitudinal controlled study of patients undergoing intravitreal injections. *Arch Ophthalmol*. 2011;129(9):1180–1188.

McCannel CA. Meta-analysis of endophthalmitis after intravitreal injection of anti-vascular endothelial growth factor agents: causative organisms and possible prevention strategies. *Retina*. 2011;31(4):654–661.

Patel SN, Gangaputra S, Sternberg P Jr, Kim SJ. Prophylaxis measures for postinjection endophthalmitis. *Surv Ophthalmol*. 2020;65(4):408–420.

Gene Therapy



This chapter includes a related video. Go to www.aao.org/bcscvideo_section12 or scan the QR code in the text to access this content.

Highlights

- Gene therapy is a quickly evolving field that offers great potential for the treatment of progressive, visually debilitating inherited retinal diseases.
- Although currently approved (and soon to be approved) gene therapies have targeted inherited retinal diseases, studies investigating treatment of age-related macular degeneration are also under way.
- Gene augmentation therapy involves replacement of mutated genes in affected cells or tissues with a normal, functional copy of the gene.

Introduction

The last decade has fostered major advancements in the field of gene therapy, including promising new treatments for cancer, heart disease, and diabetes. The eye is also a potential target for gene therapies, given that the retina is an immune-privileged tissue with low risk of systemic dissemination and only small amounts of vector are needed to achieve a therapeutic response. Inherited retinal diseases (IRDs), a rare and diverse group of disorders causing progressive photoreceptor cell death and vision loss, are considered particularly amenable to gene therapies, as mutations in more than 300 disease-related genes, all critical to retinal function, have been identified. Currently, approximately 200,000 people in the United States and 4.5 million people worldwide are affected by these progressively debilitating visual disorders.

In general, approaches to and applications of gene therapy vary depending on the different nucleic acids used and how they are delivered. For IRDs, investigational therapies involve modifying the genome of retinal cells primarily through the introduction of normal genes or the inactivation of disease genes (Table 20-1). In contrast, gene therapies under investigation for neovascular age-related macular degeneration use vector systems to express antiangiogenic proteins that block the vascular endothelial growth factor pathway (Table 20-2).

Although RNA and compound therapies are available, most gene therapies, such as voretigene neparvovec-rzyl, are DNA based. Common types of DNA therapy include gene augmentation, optogenetics, and genome editing.

Table 20-1 Gene Therapy Trials for Inherited Retinal Diseases^a

Target Disease	Sponsor	Viral Vector	Gene Delivered	NCT #
Achromatopsia	AGTC	AAV2 — subretinal	<i>CNGA3</i>	NCT02935517
	AGTC	AAV2 — subretinal	<i>CNGB3</i>	NCT02599922
	MeiraGTx UK II Ltd	AAV2/8 — subretinal	<i>CNGA3</i>	NCT03758404
	MeiraGTx UK II Ltd	AAV2/8 — subretinal	<i>CNGB3</i>	NCT03001310
Choroideremia	Spark Therapeutics	AAV2 — subretinal	<i>CHM</i>	NCT02341807
	Biogen	AAV2 — subretinal	<i>CHM</i>	NCT03496012
Retinoschisis	AGTC	AAV2 — intravitreal	<i>RS1</i>	NCT02416622
	NIH/NEI	AAV8 — intravitreal	<i>RS1</i>	NCT02317887
Stargardt disease	Sanofi	Lentivirus — subretinal	<i>ABCA4</i>	NCT01367444
Usher syndrome 1B	Sanofi	Lentivirus — subretinal	<i>MYO7A</i>	NCT01505062
X-linked RP	AGTC	AAV2 — subretinal	<i>RPGR</i>	NCT03316560
	MeiraGTx UK II Ltd	AAV2/5 — subretinal	<i>RPGR</i>	NCT03252847
	Biogen	AAV8 — subretinal	<i>RPGR</i>	NCT03116113

AAV = adeno-associated virus; AGTC = Applied Genetic Technologies Corp; NCT = National Clinical Trial; NEI = National Eye Institute; NIH = National Institutes of Health; RP = retinitis pigmentosa.

^aData from National Institutes of Health. Clinicaltrials.gov website. Accessed July 2020.

Table 20-2 Gene Therapy Trials for Age-Related Macular Degeneration

Target Disease	Name/Sponsor	Vector	Mechanism of Action
Neovascular AMD	RGX-314 RegenxBio	AAV8 — subretinal/ suprachoroidal	Encodes anti-VEGF Fab protein similar to ranibizumab
Neovascular AMD	ADVM-022 Adverum Biotechnologies	AAV2 — intravitreal	Promotes production of aflibercept protein
Neovascular and nonneovascular AMD	AAVCAGsCD59 Hemera Biosciences	AAV2 — intravitreal	Soluble form of CD59 inhibits MAC formation

AAV = adeno-associated virus; AMD = age-related macular degeneration; MAC = membrane attack complex; VEGF = vascular endothelial growth factor.

Adapted with permission from Sabbagh O, Mehra A, Maldonado RS. Gene therapy in AMD: promises and challenges. *Retina Specialist*. Published March 21, 2020. Accessed February 13, 2022. <https://www.retina-specialist.com/article/gene-therapy-in-amd-promises-and-challenges>

See also Part III, Genetics, and the appendix in BCSC Section 2, *Fundamentals and Principles of Ophthalmology*, for additional discussion and a genetics glossary.

Gene Augmentation Therapy

Augmentation is the most straightforward gene therapy. Often referred to as *gene replacement therapy*, gene augmentation involves the introduction of a normal, functional copy of a protein-coding gene into a host cell to replace a mutated gene (Fig 20-1). The normal copy then typically remains in an episomal state while promoters and enhancers facilitate its expression. This type of therapy is useful mainly for recessively inherited retinal

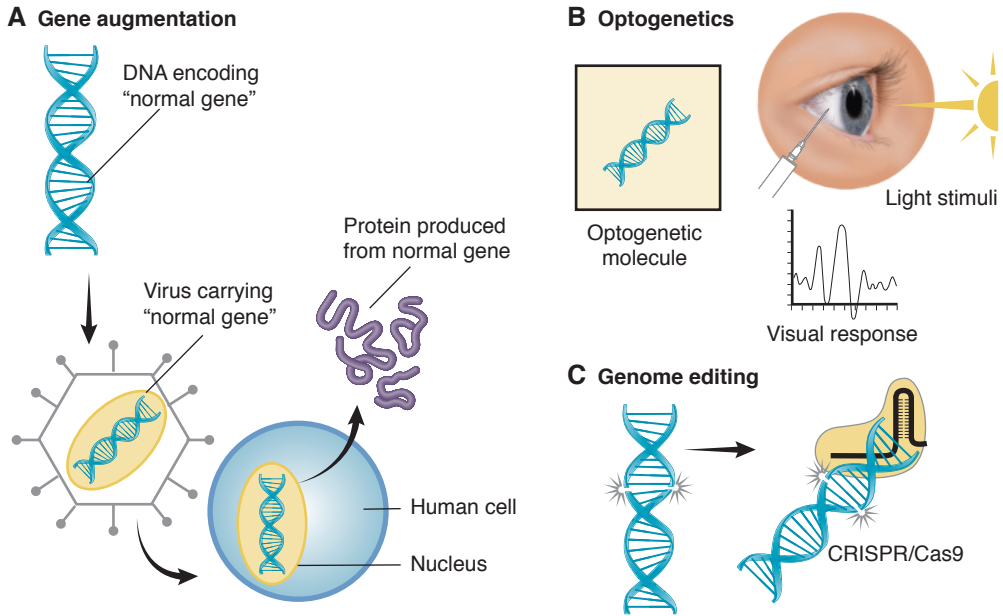


Figure 20-1 Three types of gene therapy: gene augmentation (**A**), optogenetics (**B**), and genome editing (**C**). (Illustration by Cyndie C. H. Wooley. Part A modified from Kay C. *Gene therapy: the new frontier for inherited retinal disease*. Retina Specialist. Published February 20, 2017. Accessed February 13, 2022. <https://www.retina-specialist.com/article/gene-therapy-the-new-frontier-for-inherited-retinal-disease/>)

diseases, in which neither of the 2 mutated alleles can produce functional gene products. Delivery of a correct copy of the gene is expected to restore production of normal proteins, overriding the defective or missing proteins and modulating the disease phenotype.

Autosomal dominant IRDs are not amenable to gene replacement therapy because the mutant gene product continues to interact or interfere with normal protein function, even when the protein has come from an exogenous source. In patients with a dominant disease, gene editing is used instead to inactivate the mutant protein or ablate the mutant gene at the DNA level, providing longer-term treatment (see the section Genome Editing).

In gene augmentation therapy, DNA may be delivered into the host cell by several therapeutic vectors; however, adeno-associated viral (AAV) vectors are most often used because of their high tropism for retinal cells and their low immunogenicity. Other vectors under study include lentiviruses and nanoparticles, which have larger cargo capacities to accommodate larger genes.

For vector delivery into the eye, intravitreal, subretinal, or suprachoroidal options are available. Intravitreal injections, administered during an in-office visit, facilitate targeting of the inner retina and have a relatively low complication rate. Subretinal delivery enables vector transduction in retinal pigment epithelium cells and/or photoreceptors but requires a vitrectomy and retinotomy, limiting treatment to only a localized area of the retina. Suprachoroidal delivery, another in-office procedure, potentially allows widespread delivery throughout the eye and is an attractive route for treating neovascular age-related macular degeneration and other conditions affecting the choroid.

In 2017, the US Food and Drug Administration approved the first in vivo gene replacement therapy (ie, voretigene neparvovec-rzyl) for treatment of *RPE65*-related retinopathies

in patients with confirmed pathogenic variants in both alleles. These patients typically have autosomal recessive Leber congenital amaurosis or retinitis pigmentosa and experience progressive vision loss, which may be severe in early childhood. Voretigene neparvovec-rzyl delivers a normal copy of the gene encoding the human RPE65 protein to the retinal cells of individuals with a reduced or absent level of the biologically active protein. In a phase 3 trial, voretigene gene replacement therapy improved not only participants' ability to navigate in dim light but also their full-field light sensitivity threshold and visual field (Video 20-1).



VIDEO 20-1 Voretigene gene replacement surgery.

Courtesy of Audina M. Berrocal, MD.



Optogenetics

Although gene augmentation therapy is an attractive approach in patients with a known genotype or early-stage IRD, it is not suitable for those with more advanced disease (ie, in patients who have lost most of their photoreceptors). For these patients, optogenetics is an alternative treatment involving the genetic introduction of light-sensitive proteins into retinal cells to monitor or control neural activity (see Fig 20-1). This strategy is often used to convert secondary or tertiary neurons into “photoreceptors” or to restore the sensitivity of degenerating photoreceptors.

Genome Editing

Another emerging DNA therapy is gene editing using CRISPR/Cas9-based technology (see Fig 20-1). With this technique, clustered, regularly interspaced, short palindromic repeats (CRISPR) are complexed with a CRISPR-associated (Cas) nuclease to create controlled or targeted breaks in DNA sequences. This technique is especially useful in treating dominant IRDs.

Current Limitations

Although gene therapy holds tremendous promise for treating retinal diseases, many challenges must be overcome before it can be broadly implemented. They include the rare and heterogeneous nature of IRDs; the large size of affected genes, which can exceed the cargo capacity of AAV vectors; the inaccessibility of the target tissue (eg, the retina and/or retinal pigment epithelium); the lack of long-term safety data; and cost. Despite these obstacles, the number of retinal gene therapy trials is expected to increase dramatically over the coming years.

Prado DA, Acosta-Acero M, Maldonado RS. Gene therapy beyond Luxturna: a new horizon of the treatment for inherited retinal disease. *Curr Opin Ophthalmol*. 2020;31(3):147–154.

Vázquez-Domínguez I, Garanto A, Collin RWJ. Molecular therapies for inherited retinal diseases-current standing, opportunities and challenges. *Genes (Basel)*. 2019;10(9):654.

Ziccardi L, Cordeddu V, Gaddini L, et al. Gene therapy in retinal dystrophies. *Int J Mol Sci*. 2019;20(22):5722.

Additional Materials and Resources

Related Academy Materials

The American Academy of Ophthalmology is dedicated to providing a wealth of high-quality clinical education resources for ophthalmologists.

Print Publications and Electronic Products

For a complete listing of Academy products related to topics covered in this BCSC Section, visit our online store at: <https://store.aao.org/clinical-education/topic/retina-vitreous.html>

Or call Customer Service at 866.561.8558 (toll free, US only) or +1 415.561.8540, Monday through Friday, between 8:00 AM and 5:00 PM (PST).

Online Resources

Visit the Ophthalmic News and Education (ONE®) Network at <https://www.aao.org/retina-vitreous> to find relevant videos, online courses, journal articles, practice guidelines, self-assessment quizzes, images, and more. The ONE Network is a free Academy-member benefit.

Access free, trusted articles and content with the Academy's collaborative online encyclopedia, EyeWiki, at aao.org/eyewiki.

Get mobile access to the *Wills Eye Manual*, watch the latest 1-minute videos, and set up alerts for clinical updates relevant to you with the AAO Ophthalmic Education App. Download today: Search for "AAO Ophthalmic Education" in the Apple app store or in Google Play.

Basic Texts and Additional Resources

Agarwal A. *Gass' Atlas of Macular Diseases*. 5th ed. Elsevier/Saunders; 2012.

Chow D, Chaves de Olivera PR. *OCT Angiography*. Thieme; 2017.

Duker JS, Waheed NK, Goldman DR, eds. *Handbook of Retinal OCT: Optical Coherence Tomography*. 2nd ed. Elsevier; 2022.

Freund KB, Sarraf D, Mieler WF, Yannuzzi LA. *The Retinal Atlas*. 2nd ed. Elsevier; 2017.

Gupta AK, Aggarwal VK, Goel N. *Handbook of Clinical Trials in Ophthalmology*. Jaypee Brothers Medical Publishers; 2014.

Hartnett ME. *Pediatric Retina*. 3rd ed. Wolters Kluwer; 2020.

Ho AC, Regillo CD, eds. *Age-related Macular Degeneration Diagnosis and Treatment*. Springer; 2011.

Landry DA, Kashani AH. *Optical Coherence Tomography and OCT Angiography: Clinical Reference and Case Studies*. Bryson Taylor Publishing; 2016.

- Rizzo S, Patelli F, Chow DR, eds. *Vitreo-retinal Surgery: Progress III*. Springer-Verlag; 2009. *Essentials in Ophthalmology*.
- Saxena S, Meyer CH, Ohji M, Akduman L, eds. *Vitreoretinal Surgery*. Jaypee Brothers Medical Publishers; 2012.
- Schachat AP, Wilkinson CP, Hinton DR, Sadda SR, Wiedemann P, eds. *Ryan's Retina*. 6th ed. Elsevier; 2018.
- Sebag J, ed. *Vitreous: In Health and Disease*. Springer-Verlag; 2014.
- Tabandeh H, Goldberg MF. *The Retina in Systemic Disease: A Color Manual of Ophthalmoscopy*. Thieme; 2009.
- Tasman WS, Jaeger EA, eds. *Duane's Ophthalmology on DVD-ROM*. Lippincott Williams & Wilkins; 2013.
- Wilkinson CP, Rice TA. *Michels Retinal Detachment*. 2nd ed. Mosby; 1997.

Requesting Continuing Medical Education Credit

The American Academy of Ophthalmology is accredited by the Accreditation Council for Continuing Medical Education (ACCME) to provide continuing medical education for physicians.

The American Academy of Ophthalmology designates this enduring material for a maximum of 15 *AMA PRA Category 1 Credits™*. Physicians should claim only the credit commensurate with the extent of their participation in the activity.

To claim *AMA PRA Category 1 Credits™* upon completion of this activity, learners must demonstrate appropriate knowledge and participation in the activity by taking the posttest for Section 12 and achieving a score of 80% or higher.

This activity meets the Self-Assessment CME requirements defined by the American Board of Ophthalmology (ABO). Please be advised that the ABO is not an accrediting body for purposes of any CME program. ABO does not sponsor this or any outside activity, and ABO does not endorse any particular CME activity. Complete information regarding the ABO Self-Assessment CME Maintenance of Certification requirements is available at <https://abop.org/maintain-certification/cme-self-assessment/>.

To take the posttest and request CME credit online:

1. Go to www.aao.org/cme-central and log in.
2. Click on “Claim CME Credit and View My CME Transcript” and then “Report AAO Credits.”
3. Select the appropriate media type and then the Academy activity. You will be directed to the posttest.
4. Once you have passed the test with a score of 80% or higher, you will be directed to your transcript. *If you are not an Academy member, you will be able to print out a certificate of participation once you have passed the test.*

CME expiration date: June 1, 2025. *AMA PRA Category 1 Credits™* may be claimed only once between June 1, 2022, and the expiration date.

For assistance, contact the Academy’s Customer Service department at 866-561-8558 (US only) or +1 415-561-8540 between 8:00 AM and 5:00 PM (PST), Monday through Friday, or send an email to customer_service@aao.org.

Study Questions

Please note that these questions are not part of your CME reporting process. They are provided here for your own educational use and for identification of any professional practice gaps. The required CME posttest is available online (see “Requesting Continuing Medical Education Credit”). Following the questions are answers with discussions. Although a concerted effort has been made to avoid ambiguity and redundancy in these questions, the authors recognize that differences of opinion may occur regarding the “best” answer. The discussions are provided to demonstrate the rationale used to derive the answer. They may also be helpful in confirming that your approach to the problem was correct or, if necessary, in fixing the principle in your memory. The Section 12 faculty thanks the Resident Self-Assessment Committee for developing these self-assessment questions and the discussions that follow.

1. What is the main glycosaminoglycan component of vitreous?
 - a. chondroitin
 - b. dermatan
 - c. hyaluronic acid (hyaluronan)
 - d. keratan
2. Within the retina, the density of rods is greatest at what degree of fixation?
 - a. 90
 - b. 45
 - c. 12
 - d. 0
3. What is the most common systemic condition associated with angioid streaks?
 - a. oculocutaneous albinism
 - b. Crohn disease
 - c. pseudoxanthoma elasticum
 - d. ulcerative colitis
4. What symptom following intravitreal injection would be unexpected and warrant immediate evaluation?
 - a. progressive floaters with progressive blurring of vision
 - b. sharp pain following the injection
 - c. foreign body sensation
 - d. small floaters that are noticed immediately after injection

5. A patient with long-standing poorly controlled diabetes presents with vision loss (20/200) in 1 eye. Clinical examination shows mild inferior vitreous hemorrhage, minimal macular edema outside the central macula, and a well-perfused optic nerve. Fluorescein angiography demonstrates an area of neovascularization elsewhere and a foveal avascular zone diameter of 1500 μm . What is the most likely cause of the poor vision?
 - a. ischemic maculopathy
 - b. capillary leakage
 - c. traction (tractional) detachment
 - d. bleeding from neovascularization
6. What traumatic extraocular condition is associated with a branch retinal artery occlusion?
 - a. pelvic fracture
 - b. femur fracture
 - c. subarachnoid hemorrhage
 - d. pancreatitis
7. What is the most significant risk factor for central retinal vein occlusion (CRVO)?
 - a. hypertension
 - b. older age
 - c. hypercoagulable state
 - d. glaucoma
8. What treatment has been proven to be effective for branch retinal vein occlusion–associated macular edema?
 - a. panretinal photocoagulation
 - b. verteporfin
 - c. fluocinolone acetonide intravitreal implant
 - d. ranibizumab
9. What is the most common cause of decreased visual acuity in patients who present with acute CRVO?
 - a. macular ischemia
 - b. macular edema
 - c. vitreous hemorrhage
 - d. neovascular glaucoma
10. A 5-year-old boy is found to have unilateral telangiectatic retinal vessels with an exudative retinal detachment. What histologic findings are characteristic of the likely diagnosis?
 - a. “foamy” histiocytes and cholesterol crystals
 - b. loss of capillary pericytes and thickening of the retinal capillary basement membrane
 - c. dilated, thin-walled vascular channels between the retinal pigment epithelium (RPE) and outer aspect of Bruch membrane
 - d. focal sclerosis of retinal vessels with an overlying pocket of liquefied vitreous

11. What is the mode of inheritance for von Hippel–Lindau syndrome?
 - a. autosomal recessive
 - b. autosomal dominant
 - c. X-linked
 - d. sporadic
12. What cause of leukocoria is associated with microphthalmos?
 - a. persistent fetal vasculature
 - b. infection with *Toxocara* species
 - c. Coats disease
 - d. retinoblastoma
13. How is threshold retinopathy of prematurity (ROP) defined?
 - a. 3 contiguous or 10 cumulative clock-hours of extraretinal fibrovascular proliferation in zone II with any vascular engorgement
 - b. at least 5 contiguous clock-hours of extraretinal neovascularization or 8 cumulative clock-hours of extraretinal neovascularization with plus disease as well as retinal vessels ending in zone I or II
 - c. 6 clock-hours of any extraretinal fibrovascular proliferation in zone III with any vascular engorgement
 - d. 3 contiguous or 8 cumulative clock-hours of extraretinal fibrovascular proliferation in zone III with any vascular engorgement
14. A 35-year-old otherwise healthy man presents with recent onset of unilateral slightly blurred vision. On evaluation, the right eye has a visual acuity of 20/25, there is serous subretinal fluid in the macula, and the choroid is thickened. The patient is minimally symptomatic. What is the most appropriate initial management?
 - a. observation
 - b. topical steroids
 - c. photodynamic therapy
 - d. laser photocoagulation therapy
15. A 24-year-old woman presents with acute-onset, paracentral “flashing lights” in 1 eye; nasal visual field loss by confrontation testing in both eyes; and normal visual acuity in both eyes. Vitreous cells are present posteriorly in both eyes. The fundus is otherwise unremarkable. Visual field, multifocal electroretinogram (mfERG), and optical coherence tomography (OCT) testing reveal scotomata corresponding to focally decreased mfERG responses and outer retinal layer disruption in both eyes. What is the most likely diagnosis?
 - a. multiple evanescent white dot syndrome (MEWDS)
 - b. acute zonal occult outer retinopathy (AZOOR)
 - c. acute macular neuroretinopathy (AMN)
 - d. intermediate uveitis

16. A 42-year-old man reports decreased vision in his right eye over the past 3 days. He does not report significant pain or discomfort, but on review of systems, the ophthalmologist discovers that he also has ulcers on the inside of his mouth. For which HLA haplotype would the patient most likely be positive?
 - a. HLA-A29
 - b. HLA-B27
 - c. HLA-B51
 - d. HLA-DR4
17. Once the diagnosis of sympathetic ophthalmia is established, what is the preferred initial management?
 - a. intraocular injection of foscarnet to the sympathizing eye
 - b. panretinal photocoagulation to the sympathizing eye
 - c. enucleation of the exciting eye
 - d. administration of oral corticosteroids
18. What bilateral white dot syndrome is characterized by acute vision loss that is typically followed by full or near-full vision recovery?
 - a. acute posterior multifocal placoid pigment epitheliopathy (APMPPE)
 - b. birdshot chorioretinopathy (vitiliginous chorioretinitis)
 - c. MEWDS
 - d. serpiginous choroiditis
19. What is the best oral induction treatment option for a patient with varicella-zoster virus–associated acute retinal necrosis?
 - a. acyclovir 800 mg 5 times daily
 - b. valacyclovir 1 g 3 times daily
 - c. valacyclovir 2 g 3 times daily
 - d. valganciclovir 900 mg 2 times daily
20. A 30-year-old woman presents with blurred vision and photopsias that started in her right eye and then affected her left eye as well. She had a fever, malaise, and headache 1 week ago. Her fundus examination reveals multiple yellow-white placoid lesions 1–2 disc areas in size. What is the most likely diagnosis?
 - a. AZOOR
 - b. APMPPE
 - c. MEWDS
 - d. serpiginous choroiditis

21. What is the most common pattern of color confusion associated with acquired color vision defects?
 - a. blue-yellow
 - b. red-yellow
 - c. blue-green
 - d. red-green
22. What is the inheritance pattern of choroideremia?
 - a. autosomal recessive
 - b. autosomal dominant
 - c. mitochondrial DNA
 - d. X-linked recessive
23. What ophthalmologic diagnostic test is characteristically expected to give a normal result in patients with Best disease?
 - a. fluorescein angiography (FA)
 - b. electroretinogram (ERG)
 - c. electro-oculogram (EOG)
 - d. OCT
24. What is the mode of inheritance of Best disease?
 - a. autosomal recessive
 - b. autosomal dominant
 - c. X-linked recessive
 - d. mitochondrial
25. What is the characteristic fundus appearance of dominant (familial) drusen?
 - a. large soft drusen with irregular borders
 - b. RPE hyperplasia
 - c. drusen distribution beyond the vascular arcades and nasal to the optic nerve head
 - d. clustering of lesions predominantly in the macula
26. Dermal erythema and bullae are a presenting feature of what retinal condition?
 - a. X-linked retinitis pigmentosa
 - b. severe form of enhanced S-cone syndrome (Goldmann-Favre syndrome)
 - c. gyrate atrophy
 - d. incontinentia pigmenti

27. Sorsby macular dystrophy results from mutations in which gene?
 - a. *EFEMP1*
 - b. *NYX*
 - c. *CFH*
 - d. *TIMP3*
28. Mutations in *CYP4V2* may lead to characteristic crystalline deposits in the retina with initially normal visual function but with enlarging regions of geographic-like paracentral atrophy. What disorder does this mutation cause?
 - a. cystinosis
 - b. oxalosis
 - c. Bietti crystalline dystrophy
 - d. macular telangiectasia type 2
29. A bull's-eye maculopathy may be present in what disease?
 - a. Tay-Sachs disease
 - b. cystinosis
 - c. Fabry disease
 - d. Batten disease
30. A male patient presents with photophobia, iris transillumination, hypopigmented fundi, and nystagmus. His skin and hair have normal pigmentation. What is the most likely inheritance pattern of this patient's condition?
 - a. X-linked recessive
 - b. autosomal dominant
 - c. autosomal recessive
 - d. X-linked dominant
31. A 60-year-old woman with unexplained peripheral neuropathy but no additional ophthalmic or medical history reports bilateral visually significant floaters. What is the most likely diagnosis?
 - a. asteroid hyalosis
 - b. cholesterosis
 - c. amyloidosis
 - d. chronic vitreous hemorrhage
32. A 1-year-old boy presents with peripheral traction retinal detachment with temporal displacement of the maculae bilaterally. The child's father is similarly affected. There is no history of premature birth. What is the most likely diagnosis?
 - a. familial exudative vitreoretinopathy
 - b. congenital retinal telangiectasia
 - c. juvenile retinoschisis
 - d. incontinentia pigmenti

33. Where is the vitreous most firmly attached to intraocular tissue?
 - a. optic nerve head
 - b. macula
 - c. retinal blood vessels
 - d. vitreous base
34. Atrophic retinal holes are commonly associated with what condition?
 - a. vitreous hemorrhage
 - b. retinal detachment
 - c. posterior vitreous detachment
 - d. lattice degeneration
35. In an eye with retinoschisis, what examination findings are associated with an increased risk of progression to retinal detachment?
 - a. demarcation line
 - b. hyperopia
 - c. inner and outer layer holes
 - d. typical peripheral cystoid degeneration
36. What is a known risk factor for degenerative retinoschisis?
 - a. prior retinal detachment
 - b. hyperopia
 - c. lattice degeneration
 - d. collagen vascular disease
37. A stage 3 macular hole has at least what diameter?
 - a. 200 μm
 - b. 300 μm
 - c. 400 μm
 - d. 500 μm
38. What finding is most consistent with siderosis bulbi?
 - a. dense vitritis
 - b. sunflower cataract
 - c. deposits in Descemet membrane
 - d. peripheral retinal pigmentation

39. An ophthalmologist is surgically exploring a blunt globe injury secondary to racquetball trauma. The patient presented with 360° of hemorrhagic chemosis and an intraocular pressure of 3 mm Hg. Intraoperatively, a complete 360° peritomy is performed, and no globe rupture is identified. What is the most appropriate next step?
- closure of peritomy
 - exploration under the rectus muscles
 - pars plana vitrectomy
 - placement of a scleral buckle
40. What is the most common ophthalmic manifestation of abusive head trauma?
- cranial nerve paresis
 - bilateral intraocular hemorrhages
 - papilledema
 - exudative retinal detachment
41. A 68-year-old man reports a “missing spot” in his vision 1 week after cataract extraction by a first-year resident. Corrected distance visual acuity (also called *best-corrected visual acuity*) is 20/100. In addition to normal postoperative findings, the examination is significant only for subtle foveal hypopigmentation. Macular OCT demonstrates an outer retinal lucency. What is the most likely diagnosis?
- nonexudative age-related macular degeneration
 - photoc retinopathy
 - macular hole
 - cystoid macular edema
42. A 19-year-old man is struck in the left eye with a paintball. Visual acuity is 20/200 OS. Examination shows no afferent pupillary defect. Intraocular pressure is 18 mm Hg. There is no subconjunctival hemorrhage. The anterior chamber is formed. Fundus examination shows thickened, sheenlike retinal whitening in the macula. What is the most appropriate management for this patient?
- laser photocoagulation
 - anterior chamber paracentesis
 - high-dose intravenous corticosteroids
 - observation
43. What imaging modality best helps determine the optimal time to surgically drain a suprachoroidal hemorrhage?
- B-scan ultrasonography
 - FA
 - OCT
 - computed tomography

44. What surgical procedure is most indicated for a total retinal detachment with proliferative vitreoretinopathy and multiple posterior retinal breaks?
- a. vitrectomy
 - b. indirect laser retinopexy
 - c. pneumatic retinopexy with cryotherapy
 - d. scleral buckle
45. Nine weeks after routine cataract surgery, a patient develops a steroid-responsive granulomatous uveitis/endophthalmitis, with a white plaque on her intraocular lens. What would be the most appropriate management of this condition?
- a. injection of intravitreal antibiotics
 - b. observation
 - c. pars plana vitrectomy and partial capsulectomy with injection of intravitreal antibiotic
 - d. topical antibiotics and steroids
46. What agent used for retinal tamponade persists in the eye for approximately 2 months after pars plana vitrectomy?
- a. perfluoropropane gas
 - b. silicone oil
 - c. perfluorocarbon liquid
 - d. sulfur hexafluoride gas

Answers

1. **c.** Hyaluronic acid (hyaluronan) is the main glycosaminoglycan found in vitreous. Other major components include water and collagen. Although dermatan, chondroitin, and keratan are glycosaminoglycans, they are not the principal ones found in the vitreous.
2. **c.** The rod photoreceptors have their greatest density (approximately 160,000 rods/mm²) within the retina at around 12° of fixation. Rod density decreases toward the peripheral retina. Cone density is greatest (exceeding 140,000 cones/mm²) in the fovea. Within the central fovea, only cones are observed. The fovea is defined as a concave central retinal depression seen on slit-lamp examination; it is approximately 1.5 mm in diameter.
3. **c.** Angioid streaks have been associated with a number of systemic disorders and with aging. The most common systemic association is with pseudoxanthoma elasticum (PXE), a predominantly autosomal recessive disorder caused by a mutation in *ABCC6*. PXE results in calcification and other mineralization of elastin, most visibly as yellow papules in the flexor regions of the skin (“plucked chicken” appearance). Angioid streaks are typically more prominent adjacent to or can extend from the optic nerve head, in contrast to Bruch membrane ruptures from trauma or high myopia (“lacquer cracks”). Other systemic diseases associated with angioid streaks include Paget disease of bone, β -thalassemia, sickle cell disease, and Ehlers-Danlos syndrome. Angioid streaks are not a feature of oculocutaneous albinism (OCA); patients with OCA may have depigmented skin spots but not papules. Crohn disease and ulcerative colitis are associated with uveitis but not angioid streaks.
4. **a.** Vitritis, or inflammation of the vitreous, is the first presenting feature of injection-related endophthalmitis. It is perceived by patients as progressive floaters and blurring of vision, often culminating in essentially no formed vision (eg, light perception only). Immediate evaluation is necessary to determine whether endophthalmitis is present. Sharp pain following the injection or foreign body sensation is likely caused by surface irritation or damage from the povidone-iodine solution, the manipulation of the conjunctiva, or the needle stick. Occasionally, patients may have severe pain that begins within 24 hours of the injection, which may be caused by corneal abrasions. Small floaters that are noticed immediately after injection are usually caused by small air bubbles in the injected liquid, a common occurrence. Less commonly, these floaters are due to silicone oil bubbles from the syringe lubricant. Air bubbles usually disappear after a few hours, whereas silicone oil bubbles persist but usually float out of view.
5. **a.** In patients with diabetic retinopathy, vision loss can be associated with capillary leakage, ischemic maculopathy (capillary occlusion), and sequelae from ischemia-induced neovascularization. Vitreous hemorrhage, macular edema, traction detachment, and macular ischemia can all cause vision loss. In this patient, macular ischemia (normal foveal avascular zone is approximately 500 μ m in diameter) is the most likely cause because the vitreous hemorrhage is outside the visual axis (inferior) and the macular edema is noncentral.
6. **b.** A branch retinal artery occlusion (BRAO) is the result of embolization or thrombosis of the affected vessel. Common types of emboli include cholesterol emboli arising in the carotid arteries, platelet-fibrin emboli associated with large-vessel arteriosclerosis, and calcific emboli arising from diseased cardiac valves. Rare causes of a BRAO include emboli

resulting from cardiac myxoma, long-bone fractures (fat emboli), infective endocarditis (septic emboli), and intravenous drug use (talc emboli). Subarachnoid hemorrhage may be associated with intraocular hemorrhage or Terson syndrome. Traumatic pancreatitis is associated with Purtscher retinopathy, which is characterized by focal areas of retinal whitening that may superficially resemble a BRAO but are not a BRAO.

7. **b.** The most important risk factor for central retinal vein occlusion (CRVO) is age; 90% of affected patients are older than 50 years at the time of diagnosis. Other significant risk factors for development of CRVO include systemic hypertension, open-angle glaucoma, hypercoagulable states, diabetes mellitus, and hyperlipidemia.
8. **d.** The 2008 study Ranibizumab for Macular Edema Following Branch Retinal Vein Occlusion (BRAVO) found ranibizumab to be an effective treatment for macular edema associated with branch retinal vein occlusion (BRVO); monthly injection of either 0.5 mg or 0.3 mg of ranibizumab was superior to sham injection for improving visual acuity. Verteporfin is used in photodynamic therapy and is not an approved treatment for macular edema associated with BRVO. Fluocinolone acetonide intravitreal implant and panretinal photocoagulation are not used for treating macular edema associated with BRVO.
9. **b.** Patients with acute CRVO commonly present with reduced visual acuity secondary to macular edema. Neovascularization of the iris usually occurs 3 to 5 months after symptom onset. Peripheral ischemia with capillary dropout is seen in some severe cases of CRVO and can promote neovascularization, resulting in vitreous hemorrhage. Macular ischemia can occur as well but is a less likely cause of decreased acuity on presentation.
10. **a.** Coats disease is clinically evident within the first decade of life and is more common in boys. It is characterized by a unilateral retinal telangiectasia with mild to severe leakage and possible exudative retinal detachment. “Foamy” histiocytes and cholesterol crystals in the subretinal space are common histologic findings. Loss of capillary pericytes and thickening of the retinal capillary basement membrane may be seen in diabetic retinopathy. Dilated, thin-walled vascular channels between the retinal pigment epithelium (RPE) and the outer aspect of Bruch membrane are found in polypoidal choroidal vasculopathy. Focal sclerosis of retinal vessels with an overlying pocket of liquefied vitreous is found in lattice degeneration.
11. **b.** Von Hippel–Lindau syndrome is caused by a tumor suppressor gene mutation on the short arm of chromosome 3 (3p26–p25), the inheritance of which is autosomal dominant with incomplete penetrance and variable expression.
12. **a.** All of the conditions listed as answer choices (persistent fetal vasculature, Coats disease, retinoblastoma, and infection with *Toxocara* species) can cause unilateral leukocoria. However, only persistent fetal vasculature is associated with microphthalmos. It is also associated with elongated ciliary processes, cataract, retinal detachment, and angle-closure glaucoma.
13. **b.** The term *threshold retinopathy of prematurity* (ROP) was coined in the mid-1980s by investigators in the Cryotherapy for ROP (CRYO-ROP) study to define disease with equal chances of spontaneous regression or progression to an unfavorable outcome. Threshold disease is characterized by at least 5 contiguous clock-hours of extraretinal neovascularization or 8 cumulative clock-hours of extraretinal neovascularization with plus disease as well as retinal vessels ending in zone I or II.
14. **a.** The patient almost certainly has central serous chorioretinopathy (CSC). In most cases, initial observation, with the expectation of spontaneous resolution of the subretinal fluid, is the most appropriate management. Photodynamic therapy may be considered for CSC

when the patient is symptomatic or when the subretinal fluid does not resolve after a period of observation. Verteporfin photodynamic therapy (PDT) has been shown to decrease or eliminate subretinal fluid; it also decreases choroidal thickness and reduces choroidal vascular hyperpermeability. Laser photocoagulation therapy is no longer preferred for CSC. Moreover, unlike PDT, photocoagulation has no effect on choroidal thickness. Steroids are contraindicated in patients with CSC.

15. **b.** The findings are most consistent with those in acute zonal occult outer retinopathy (AZOOR), an idiopathic condition that typically affects young women with myopia. Acute onset of posterior photopsias may occur in many posterior inflammatory conditions, including multiple evanescent white dot syndrome (MEWDS) and multifocal choroiditis; however, the disruption of the outer retina observed on optical coherence tomography (OCT) differentiates AZOOR from both MEWDS and multifocal choroiditis. MEWDS is characterized by multiple small gray, white, or yellow-white dots at the level of the outer retina in and around the posterior pole and typically presents unilaterally. Acute macular neuroretinopathy is characterized clinically by reddish-brown teardrop or wedge-shaped lesions around the fovea, the tips of which point centrally; the lesions correspond in size and location to subjective paracentral scotomata. Intermediate uveitis is characterized by vitreous cells.
16. **c.** The clinical presentation is consistent with that of Behçet disease. Panuveitis with occlusive retinal vasculitis is the most common presentation. HLA-B51 is commonly associated with Behçet disease with ocular manifestations. However, the diagnosis of Behçet is clinical, and laboratory tests are of little value in confirming the diagnosis. HLA-A29 is more common in patients with birdshot chorioretinopathy, HLA-B27 is associated with acute anterior uveitis, and HLA-DR4 is weakly associated with Vogt-Koyanagi-Harada disease (or syndrome).
17. **d.** In the rare instances when sympathetic ophthalmia does follow either ocular injury or surgery, standard treatments such as corticosteroids almost always control the inflammation. Therefore, enucleation or evisceration of an injured eye to minimize risk of sympathetic ophthalmia is rarely practiced. Panretinal photocoagulation has no place in managing this form of uveitis. Foscarnet is an antiviral antibiotic that is used to treat cytomegalovirus retinitis or other herpes viral retinitis, such as that occurring in acute retinal necrosis or as a complication of iatrogenic or infectious immunosuppression.
18. **a.** Acute posterior multifocal placoid pigment epitheliopathy (APMPPE) is an uncommon, bilateral inflammatory disease characterized by acute-onset vision loss, usually followed by substantial or near-complete improvement weeks to months later. In the acute stage, fluorescein angiography (FA) of active lesions shows early blockage followed by progressive late leakage and staining. There is no definitive evidence that treatment with corticosteroids is beneficial in altering the outcome for APMPPE. Birdshot chorioretinopathy is chronic, progressive, and prone to recurrent episodes of inflammation. MEWDS is typically unilateral. Symptoms include decreased vision, scotomata, and sometimes photopsias. In most patients, the symptoms and fundus findings begin to improve in 2–6 weeks without treatment. Serpiginous choroiditis is an often vision-threatening, recurring inflammatory disease involving the outer retina, RPE, and inner choroid (the choriocapillaris). Persistent scotomata and decreased central vision are common symptoms.
19. **c.** While intravenous acyclovir 10 mg/kg every 8 hours for 10–14 days may be used for induction treatment in acute retinal necrosis, oral valacyclovir 2 g 3 times daily is considered to be an equally effective alternative. Oral acyclovir 800 mg 5 times daily or valacyclovir 1 g 3 times

daily is the appropriate maintenance dosage after induction has been completed. Oral valganciclovir is reserved for cytomegalovirus-associated intraocular infections.

20. **b.** Acute APMPE is a bilateral inflammatory disease that typically occurs in otherwise healthy young adults, with men and women affected equally. Patients may have a viral prodrome. In rare cases, cerebrovasculitis occurs. The characteristic examination finding is multiple yellow-white placoid lesions that vary in size and involve the outer retina (RPE) and inner choroid (choriocapillaris). MEWDS can also have a viral prodrome but is usually unilateral. In some patients, a transient foveal granularity also develops and is highly suggestive of the condition. On initial presentation, eyes with AZOOR may have a normal-appearing fundus or show evidence of mild vitritis. Permanent visual field loss is often associated with late development of fundus changes. Depigmentation of large zones of RPE usually corresponds to scotomata; narrowed retinal vessels may be visible within these areas. In serpiginous choroiditis, lesions first appear at or near the optic nerve head and extend centrifugally in a serpentine pattern. With numerous recurrences, a serpiginous (pseudopodial) or geographic (maplike) pattern of chorioretinal scarring develops.
21. **a.** Acquired color vision defects are most frequently blue-yellow, or *tritan*, abnormalities; they affect males and females equally. Blue-yellow color defects often accompany an optic neuropathy but also can occur in a maculopathy. Hereditary color vision defects are most frequently red-green abnormalities. They are most often X-linked recessive and affect 5%–8% of males and 0.5% of females.
22. **d.** Choroideremia is an X-linked recessive degeneration of the choriocapillaris of the choroid, and of the overlying RPE and retina. Patients with choroideremia have nyctalopia and show progressive peripheral visual field loss over 3–5 decades. Most patients maintain good visual acuity until a central island of foveal vision is lost.
23. **b.** In Best disease, the electroretinogram (ERG) response is characteristically normal, and the electro-oculogram result is almost always abnormal, showing a severe loss of light response. OCT and FA results are abnormal in Best disease and reflect the changes in the macular lesion from vitelliform stage to atrophic appearance.
24. **b.** Best disease is an autosomal dominant maculopathy caused by mutations in the *BEST1* (*VMD2*) gene. The encoded protein bestrophin localizes to the basolateral plasma membrane of the RPE and functions as a transmembrane ion channel.
25. **c.** Dominant (familial) drusen typically extend beyond the vascular arcades and nasal to the optic nerve head. A single missense mutation (Arg345Trp) on exon 10 in the *EFEMP1* gene of some patients with dominant drusen results in a fibrillin-like extracellular matrix protein expressed in the RPE and retina. Typically, the clinical findings first manifest bilaterally in the third to fourth decade of life. Although usually asymptomatic, choroidal neovascularization may develop in this patient population and lead to loss of vision. In contrast to drusen of age-related macular degeneration (AMD), the lesions of dominant drusen are typically small and round. Clumping and hyperplasia of the RPE and drusen clustering in the macula are features of AMD, not familial drusen.
26. **d.** Incontinentia pigmenti (Bloch-Sulzberger syndrome) is an X-linked dominant condition characterized by streaky skin lesions and abnormalities of the teeth and central nervous system. Ocular involvement includes pigmentary abnormalities as well as peripheral retinal nonperfusion and neovascularization that may cause traction (also called *tractional*) and cicatricial retinal detachment. In incontinentia pigmenti, erythema and bullae develop in the first few days of life.

X-linked retinitis pigmentosa is a retinal degeneration associated with vision loss and pigmentary retinopathy, but no dermatologic manifestations. The severe form of enhanced S-cone syndrome (also called *Goldmann-Favre syndrome*) is also a pigmentary retinopathy and is associated with pathognomonic ERG abnormalities and nyctalopia but no skin findings. Gyrate atrophy is an autosomal recessive congenital deficiency in ornithine aminotransferase that leads to large, geographic, peripheral paving-stone-like areas of atrophy of the RPE and choriocapillaris. It has no association with dermatologic changes.

27. **d.** Sorsby macular dystrophy (SMD) results from mutations in *TIMP3*, which plays an important role in the regulation of extracellular matrix turnover. Early signs of SMD are yellowish-gray drusenlike deposits or a confluent plaque of yellow material at the level of Bruch membrane within the macula and along the temporal arcades. The deposits progress over time to include the central macula and take on the appearance of geographic atrophy. Vision loss results from expansion of macular atrophy or from development of subfoveal choroidal neovascularization.

Malattia Leventinese (also called *Doyle honeycomb dystrophy*) is caused by a mutation in *EFEMP1*. The drusen in this condition often show a distinctive pattern of radial extensions of small and intermediate-sized deposits emanating from the fovea. The clinical syndrome of cuticular (also called *basal laminar*) drusen features small clustered drusen and occurs in young adults. Although this syndrome is associated with mutation in complement factor H, it is not a monogenic disorder. Mutations in *NYX* are associated with congenital stationary night blindness.

28. **c.** The clinical description is most consistent with that of Bietti crystalline dystrophy, which is associated with mutations in *CYP4Y2*. Oxalosis is a rare inherited disorder of primary hyperoxaluria, which has been associated with mutations in 3 genes (*AGXT*, *GRHPR*, *DHDPSL*). Cystinosis is an abnormality of cystine accumulation that may result from genetic causes (mutation in *CTNS*) or exposure to some anesthetics. Typically, patients with oxalosis and cystinosis have renal insufficiency or failure resulting from amino acid crystallization in the kidneys. Characteristic findings in macular telangiectasia type 2 include a reduced foveolar reflex, loss of retinal transparency (retinal graying), superficial retinal crystalline deposits, and foveal atrophy, but the disease is not associated with *CYP4V2*; it is associated with serine metabolism abnormalities.
29. **d.** Batten disease, an example of a neuronal ceroid lipofuscinosis, may have retinal findings, including an atrophic bull's-eye maculopathy, optic nerve pallor, and attenuation of retinal vessels. The ophthalmic symptoms and signs may be the first, earliest manifestations of this disorder. The cherry-red spots seen in Tay-Sachs disease result from ganglioside accumulation within ganglion cells. Pigmentary abnormalities and fine retinal crystals are present in cystinosis (nephropathic type). Tortuous and dilated retinal vessels, as well as cornea verticillata and tortuous conjunctival vessels, are present in Fabry disease.
30. **a.** The clinical presentation described is consistent with ocular albinism, which is typically transmitted as an X-linked (recessive) trait. Albinism includes a group of different genetic abnormalities in which the synthesis of melanin is reduced or absent. A number of genes are associated with both oculocutaneous and ocular albinism. Oculocutaneous albinism is typically transmitted as an autosomal recessive trait.
31. **c.** Vitreous opacities may be one of the initial signs of the dominantly inherited form of hereditary familial amyloidosis. In addition to the vitreous, amyloid may be deposited in the retinal vasculature, the choroid, and the trabecular meshwork. Nonocular manifestations of

amyloidosis include upper- and lower-extremity polyneuropathy and central nervous system abnormalities. Congo red staining of vitreous samples can confirm the diagnosis. Asteroid hyalosis is typically unilateral and is rarely visually significant. Cholesterosis, or *synchysis scintillans*, occurs in eyes with a history of intravitreal hemorrhage usually related to prior accidental or surgical ocular trauma. Although prior ophthalmic pathology leading to dehemoglobinized vitreous hemorrhage should always be considered, it is less likely in this scenario.

32. **a.** Unlike patients with ROP, individuals with familial exudative vitreoretinopathy (FEVR) are born full term. FEVR is characterized by failure of the temporal retina to vascularize. Retinal folds and peripheral fibrovascular proliferation, as well as traction and exudative retinal detachments, are often associated with FEVR. FEVR is usually inherited as an autosomal dominant trait, but X-linked transmission also occurs. Congenital retinal telangiectasia and juvenile retinoschisis are not typically associated with a traction retinal detachment. Incontinentia pigmenti is typically lethal in utero to males.
33. **d.** The vitreous is most tightly adherent at its base, where the vitreous remains firmly adherent to the anterior retina and pars plana epithelium. This attachment is so strong that it can lead to vitreous base avulsion after severe trauma. The vitreous is also firmly attached to the posterior lens capsule, retinal vessels, optic nerve, and fovea. With age, the vitreous contracts, which can result in a posterior vitreous detachment. With this contraction, the posterior cortical gel detaches toward the firmly attached vitreous base.
34. **d.** Atrophic retinal holes are commonly associated with lattice degeneration. They are infrequently the cause of rhegmatogenous retinal detachment. They represent atrophic rather than tractional retinal breaks, so they are not caused by posterior vitreous detachment, and they are not associated with vitreous hemorrhage.
35. **c.** The presence of inner and outer layer holes in retinoschisis is associated with an increased risk of retinal detachment. However, the presence of outer layer holes can lead to a localized retinal detachment that usually does not progress and seldom requires treatment. The presence of hyperopia and typical peripheral cystoid degeneration does not predispose to retinal detachment. Finally, the presence of a demarcation line in an eye with retinoschisis suggests that a full-thickness detachment is present or was formerly present and has spontaneously regressed; this is not likely to lead to a progressive retinal detachment.
36. **b.** Degenerative retinoschisis is commonly associated with hyperopia. Lattice degeneration is more common in myopic eyes. Collagen vascular disease and prior retinal detachment do not increase the risk of degenerative retinoschisis.
37. **c.** Stage 3 holes are full-thickness holes at least 400 μm in diameter. Stage 0 holes (pre-macular hole) represent vitreomacular adhesion (VMA). OCT examination shows that a stage 1A hole is a foveal “pseudocyst,” or horizontal splitting (schisis), associated with vitreous traction on the foveal center. A stage 1B hole indicates a break in the outer fovea. Stage 2 holes are early full-thickness holes less than 400 μm in diameter. Stage 4 holes are full-thickness holes at least 400 μm in diameter in association with a complete posterior vitreous detachment.
38. **d.** The chalcosis and siderosis bulbi that result from retaining intraocular copper and iron, respectively, have distinct manifestations. Pure copper can cause an intense inflammatory response, whereas a copper content less than 85% can result in chronic chalcosis, with findings that include sunflower cataract and a Kayser-Fleischer–like ring of deposits in Descemet membrane. Intraocular iron deposits in neuroepithelial tissues produce findings that include retinal pigmentation. ERG can be used to assess retinal toxicity in siderosis bulbi.

39. **b.** Severe blunt trauma can cause scleral rupture. The most common sites of scleral rupture are at the corneal limbus and through areas of physiologic scleral thinning parallel to and under the rectus muscle insertions. Scleral rupture is associated with markedly decreased ocular ducts; boggy conjunctival chemosis with hemorrhage; deepened anterior chamber; severe vitreous hemorrhage; and usually hypotony, although intraocular pressure may also be normal or elevated. In this case, suspicion of occult scleral rupture is high, warranting further exploration, with disinsertion of 1 of more rectus muscles in order to identify the rupture site. Scleral lacerations or ruptures are typically closed with 7-0, 8-0, or 9-0 non-absorbable suture. Some specialists recommend prophylactic vitrectomy and/or placement of a scleral buckle at the time of primary repair of some perforating ocular injuries, but the primary goal of most open-globe repairs is to achieve corneoscleral wound closure.
40. **b.** Retinal hemorrhages are the cardinal manifestation of abusive head trauma (AHT, formerly called *shaken baby syndrome*). The presenting sign of child abuse involves the eye in approximately 5% of cases. Ocular signs include retinal hemorrhages and cotton-wool spots, retinal folds, hemorrhagic schisis cavities, and pigmentary maculopathy. The retinal hemorrhages associated with AHT often have a hemispheric contour. Papilledema occurs in less than 10% of cases of AHT. Cranial nerve paresis and exudative retinal detachment are not commonly associated with AHT.
41. **b.** Nonexudative AMD, macular holes, and cystoid macular edema can decrease central visual acuity; however, in the setting of recent (and likely prolonged) ophthalmic surgery and outer retinal lucency, photic retinopathy secondary to exposure to the operating microscope light source is the most likely diagnosis. Although this retinopathy is more common following retinal surgery, it can occur with surgery times as short as 30 minutes; prolonged focal exposure can cause photochemical injury to the fovea, much like solar retinopathy. Patients typically present with central or paracentral scotomata, hypopigmented foveal lesions, and outer retinal cavitation. Most patients recover vision somewhat over a period of 3–6 months.
42. **d.** The clinical presentation described is consistent with commotio retinae, and the appropriate management is observation. High-dose intravenous steroids have no role in the management of commotio retinae. Anterior chamber paracentesis may be used in cases of acute retinal artery occlusion but has no role in commotio retinae. Laser photocoagulation may be used for a retinal break but is not used for commotio retinae.
43. **a.** When suprachoroidal hemorrhage occurs intraoperatively, immediate drainage is rarely effective, because of rapid coagulation of the blood. Waiting 7 to 14 days often allows the hemorrhage to liquefy. B-scan ultrasonography is useful to help identify clot liquefaction. It is also useful to determine whether appositional (“kissing”) suprachoroidal hemorrhage is present and whether there is concurrent retinal detachment. In the presence of a large suprachoroidal hemorrhage, often no view is possible for OCT or FA. Computed tomography is not indicated for monitoring suprachoroidal hemorrhage.
44. **a.** For a total retinal detachment with proliferative vitreoretinopathy (PVR) and multiple posterior retinal breaks, pars plana vitrectomy with or without scleral buckle is indicated, along with membrane peeling to relieve traction, retinectomy (in case of incarceration or retinal shortening), flattening retina by using air or perfluorocarbon liquid, endolaser photocoagulation or cryopexy, and gas or silicone oil tamponade. Pneumatic retinopexy is contraindicated in the presence of PVR. Laser demarcation is not effective for a total retinal detachment. Scleral buckle alone is typically not effective in the presence of multiple posterior retinal breaks.

45. **c.** The clinical history is characteristic of *Propionibacterium acnes* endophthalmitis. Although injection of intravitreal antibiotics may clear the infection in up to 50% of cases, the most appropriate management is pars plana vitrectomy with partial capsulectomy and injection of 1 mg intravitreal vancomycin adjacent to or inside the capsular bag. Occasionally, removal of the intraocular lens and the entire capsular bag is required to definitively treat the condition. Observation is not appropriate for chronic endophthalmitis. Although topical antibiotics and steroids will treat the symptoms, they will not eradicate the infection.
46. **a.** Perfluoropropane gas (C_3F_8) lasts for approximately 2 months in the eye after a vitrectomy and thus provides a longer-lasting tamponade than sulfur hexafluoride gas (SF_6), which lasts for 2 to 3 weeks. Perfluorocarbon liquids such as perfluoro-*n*-octane, which are heavier than water, can be used for temporary intraoperative stabilization of the retina, but they are not left in the eye. Silicone oil must be surgically removed.

Index

(*f*= figure; *t*= table)

- AAV. *See* Adeno-associated viral vectors
- ABCA4 gene, 294, 302
- ABCA4 retinopathy, 47–48, 50*f*
- ABCC6 gene, 95
- Abetalipoproteinemia, 324, 326
- Ablation (laser), 423. *See also* Photocoagulation
- Absolute scotoma, 391, 391*t*
- Abusive head trauma, 411, 411*f*
- ACCORD (study), 100, 105, 111
- ACCORDION (study), 100, 105
- Acetazolamide, 178, 293*f*, 347, 443
- Achromatopsia, 284, 284*t*, 456*t*
- Acute exudative polymorphous vitelliform maculopathy, 323
- Acute idiopathic maculopathy (AIM), 250, 259–260, 260*f*
- Acute macular neuroretinopathy (AMN), 250, 257–259, 259*f*
- Acute-onset postoperative endophthalmitis, 437–438, 438*t*, 439*f*
- Acute posterior multifocal placoid pigment epitheliopathy (APMPPE), 225–226, 226*f*, 250–252, 251*t*, 252*f*, 253
- Acute retinal ischemia, 160–161, 161*f*
- Acute retinal necrosis (ARN), 268, 268*f*
- Acute syphilitic posterior placoid chorioretinitis (ASPPC), 274, 275*f*
- Acute zonal occult outer retinopathy (AZOOR), 54, 250, 257, 258*f*
- Acyclovir, 269
- Adaptive optics imaging, 11*f*, 32
- Adeno-associated viral (AAV) vectors, 457, 458
- Adult-onset foveomacular vitelliform dystrophy (AOFVD), 74, 74*f*, 303, 304*f*, 306
- Adult-onset vitelliform lesions, 303, 304–305*f*
- Adult-onset vitelliform maculopathy, 74, 74*f*, 177*f*
- Advanced AMD, 66–67. *See also* Neovascular age-related macular degeneration; Nonneovascular age-related macular degeneration
- Aedes aegypti* mosquito, 279
- Afferent pupillary defect, 396, 409, 409*t*
- Aflibercept
 - adverse effects, 111
 - diabetic macular edema treatment, 112*t*, 124–125, 126
 - neovascular AMD treatment, 89*t*, 90
 - polypoidal choroidal vasculopathy treatment, 85
 - retinal vein occlusion treatment, 136*f*, 138*f*, 142–143*t*, 144
 - route of administration, 452
- African American patients, 167, 174–175, 262
- Age
 - choroidal changes, 18, 227–229, 229*f*, 242
 - electroretinography testing controls for, 47
 - macular changes. *See* Age-related macular degeneration
 - retinal changes, 237
 - retinal vein occlusion and, 135
 - vitreous changes, 349
- Age-related choroidal atrophy, 227–229, 229*f*
- Age-related macular degeneration (AMD), 65–97
 - about, 65–68, 67*f*
 - differential diagnosis, 303–304
 - epidemiology and etiology, 66, 68–69, 75
 - genetics, 68–69, 304, 306
 - management, 74–77, 76*t*, 86–93, 88*f*, 89*t*, 92*t*, 455, 456*t*, 457
 - neovascular, 77–93. *See also* Neovascular age-related macular degeneration
 - nonneovascular, 69–77. *See also* Nonneovascular age-related macular degeneration
 - precautions, 335
 - risk factor education, 74, 75, 75*t*
 - risk factors, 68
 - stages, 66–67
 - studies, 65–66
- Aggressive (posterior) retinopathy of prematurity (A-ROP), 195*t*, 196–197, 199*f*
- AIDS. *See* HIV/AIDS
- AIM. *See* Acute idiopathic maculopathy
- Alagille syndrome, 316*t*, 320
- Albinism, 324–325, 325*f*
- Albinoidism, 324
- Alkyl nitrites (“poppers”), 340, 340*t*, 341*f*
- Alphavirus*, 281
- α -Mannosidosis, 316*t*
- Alport syndrome, 306, 319*t*
- Alström syndrome, 319*t*, 320
- Aluminum, 404*f*, 406
- Amacrine cells, 13, 14*f*
- Amalric triangles, 225
- Amblyopia, 209–210, 360
- AMD. *See* Age-related macular degeneration
- Amelogenesis imperfecta, 322
- American Academy of Ophthalmology, 162
- American Diabetes Association, 100
- American Heart Association, 160, 162
- Amikacin, 342, 438, 438*t*
- Amino acid disorders, 329
- Aminoglycosides, 342, 408
- AMN. *See* Acute macular neuroretinopathy
- Amniotic fluid embolism, 192
- Amphotericin B, 272, 273*f*
- Amsler grid testing, 76, 77
- Amyloidosis, 366–367, 366*f*
- Anaphylaxis, 39
- ANCHOR (study), 65, 88–89, 88*f*, 89*t*
- Ancylostoma caninum*, 279
- Anemia, 108
- Anesthesia, 421, 452–453
- Aneurysmal telangiectasia, 180–181, 181–183*f*
- Aneurysms
 - macroaneurysms, 132–133, 165–166, 166*f*, 176, 190
 - microaneurysms, 108–109, 109*f*, 178, 179*f*, 188, 239
- Angiogenesis, 87, 193. *See also* Antiangiogenic therapies

- Angiography
 fluorescein, 32–38. *See also* Fluorescein angiography
 indocyanine green, 23, 38–39, 38–39*f*
 optical coherence tomographic angiography, 28–29, 30*f*
 scanning laser ophthalmoscopy and, 25–26, 25*f*
 Angioid streaks, 17, 95–96, 95*f*, 171, 174, 321
 Angiokeratoma corporis diffusum, 328–329
 Annular gap, 5–7
 Anomaloscope, 57
 Anomalous foveal anatomy, 210, 212*f*
 Anomalous trichromatism, 283–284
 Anterior capsular phimosis, 129
 Anterior chamber, 41, 119, 161
 Anterior ciliary arteries, 222
 Anterior cortical gel, 5
 Anterior hyaloid, 6*f*
 Anterior ischemic optic neuropathy, 134
 Anterior persistent fetal vasculature, 360
 Anterior segment
 blunt trauma sequelae, 397
 neovascularization
 in central retinal artery occlusion, 162
 in central retinal vein occlusion, 137, 148, 149, 151–152
 in ocular ischemic syndrome, 152, 152*f*, 154
 surgery complication management, 437–445, 438*t*, 439–440*f*, 441*t*
 Antiangiogenic therapies, 87–93
 about, 87
 adverse effects, 81, 91, 111
 alternatives, 127
 choroidal neovascularization treatment, 240, 241*f*
 clinical approaches, 87
 Coats disease treatment, 179
 combination therapies, 93
 diabetic macular edema treatment, 116*f*, 122, 124–126, 125*f*
 diabetic retinopathy treatment, 111, 115–117, 116*f*, 119, 120
 imaging findings following, 80*f*
 macular telangiectasia treatment, 180
 pathologic myopia treatment, 96–97
 radiation retinopathy treatment, 189
 retinal venous occlusion treatment, 136*f*, 138–139, 138*f*, 141–143*t*, 144, 149
 retinopathy of prematurity treatment, 207–209
 specific agents, 88–91, 88*f*, 89*t*, 92
 Antibiotics. *See also specific antibiotics*
 for globe injuries, 407–408
 microvasculopathy complications, 342
 postoperative endophthalmitis treatment, 438–441, 438*t*, 439–440*f*
 Anticoagulants, 365
 Antioxidants, 75, 76*t*
 Anti-VEGF therapy. *See* Antiangiogenic therapies
 AOFVD. *See* Adult-onset foveomacular vitelliform dystrophy
 APC gene, 320
 Aphakia, 381
 APMPE. *See* Acute posterior multifocal placoid pigment epitheliopathy
 Apolipoprotein B, 326
 Appositional choroidal detachment (“kissing choroidals”), 40*f*, 443
 Appositional suprachoroidal hemorrhage, 443, 445
 ARB. *See* Autosomal recessive bestrophinopathy
 Arden index (ratio), 54
 Area centralis, 7, 7*f*, 8*t*
 Area of Martegiani, 6*f*, 7, 349
 AREDS (study), 66, 70, 75, 75*t*
 AREDS2 (study), 66, 75–76, 76*t*
 Arginine, 300
 Argyrosis, ocular, 347
 ARMS2 gene, 68
 ARN. *See* Acute retinal necrosis
 A-ROP. *See* Aggressive retinopathy of prematurity
 Arrestin, 287
 Arterial occlusive disease, 154–164
 acute retinal ischemia and, 160–161, 161*f*
 branch, 155–156, 156–157*f*, 157*t*, 172*f*, 176
 central, 158–162. *See also* Central retinal artery occlusion
 cilioretinal artery occlusion, 162, 163*f*
 cotton-wool spots, 154, 155*f*, 155*t*, 157*f*
 drug-induced, 342, 343
 etiology, 155, 157*t*, 159–160
 ophthalmic artery occlusion, 162–163, 164*f*
 paracentral acute middle maculopathy, 164, 165*f*, 259, 259*f*
 radiation retinopathy complication, 188
 Arteriohepatic dysplasia, 316*t*, 320
 Arteriosclerotic retinopathy, 132
 Arteritic ischemic optic neuropathy, 222, 222*f*
 Arthro-ophthalmopathy, 316*t*
 Artifacts, 29
 Artificial intelligence, 104
 A-scans, 26
 Ascorbate, 7
 Asian patients, 334, 335*f*, 336
Aspergillus endophthalmitis, 272, 272*f*
 Aspirin, 107
 ASPPC. *See* Acute syphilitic posterior placoid chorioretinitis
 Asteroid hyalosis, 364–365, 364*f*, 366
 Atherosclerosis, 153
 ATOH7 gene, 360
 Atrophic creep, 96
 Atrophic retinal holes, 210*f*, 371, 372–373*f*, 376, 378*f*, 379*t*, 380
 Atrophy. *See also* Geographic atrophy
 of choriocapillaris, 289
 choroidal, 226, 227–229, 229*f*, 242–243, 243*f*
 of gyrate, 299–300, 300*f*
 macular, 292*f*, 295, 296*f*, 302, 302*f*, 306, 307, 307*f*
 optic atrophy, 51, 188
 of retinal pigment epithelium, 66, 70, 71–73, 72*f*, 119*f*, 226, 303, 331*f*, 425
 Atropine, 236
 Attenuated mucopolysaccharidosis, 316*t*
 Atypical hemolytic uremia syndromes, 306
 Atypical macular dystrophies, 308–309
 Aurora borealis effect, 265
 Autoimmune retinopathy, 323
 Autoimmunity
 central serous retinopathy association, 217

- inflammatory vasculitis, 261–262, 261*t*, 262*f*
 intraocular lymphoma, 264–267, 265–266*f*
 lupus vasculitis, 262, 262*f*
 retinopathy, 323
 sympathetic ophthalmia, 263
 Vogt-Koyanagi-Harada disease, 263, 264*f*
 Autoinfarction, 171, 173*f*
 Autosomal dominant drusen, 304
 Autosomal dominant inherited retinal diseases, 457
 Autosomal recessive bestrophinopathy (ARB), 54, 303
 a-waves
 electroretinography, 45–47, 46*f*, 52, 285
 in macular dystrophies, 313
 in rod–cone dystrophies, 291
 Azathioprine, 261
 AZOOR. *See* Acute zonal occult outer retinopathy
- Bacillus cereus* endophthalmitis, 408
 Background diabetic retinopathy, 101
 Bacterial endophthalmitis, 270–271, 271*f*, 408
 Bardet-Biedl syndrome, 316*t*, 318–319, 318*f*, 320
Bartonella henselae, 274, 276*f*
 Bartonellosis, 274, 276*f*
 Basal laminar (cuticular) drusen, 304–305, 306*f*
 Basilar laminar deposits, 67, 67*f*, 69–70
 Basilar linear deposits, 67, 67*f*, 70
 Batten disease (neuronal ceroid lipofuscinoses), 316*t*,
 317*t*, 325–326, 326*f*
Baylisascaris procyonis, 279
 BCM. *See* Blue-cone monochromatism
 BDUMP. *See* Bilateral diffuse uveal melanocytic
 proliferation
 Bear tracks, 320, 321*f*
 “Beaten-bronze,” 301*f*
 BEAT-ROP (study), 206*t*, 207–208, 209
 Behçet disease, 261, 261*t*
 Berger space, 5, 6*f*
 Bergmeister papilla, 358
 Best disease, 54, 55*f*, 302–303, 302*f*
BEST1 gene, 54, 303, 308
 Bestrophin, 54, 303
 Best vitelliform dystrophy, 54, 55*f*, 302–303, 302*f*
 Bevacizumab
 adverse effects, 91
 choroidal neovascularization treatment, 241*f*
 diabetic macular edema treatment, 112*t*, 124–125
 neovascular AMD treatment, 90–91, 92*t*
 retinal vein occlusion treatment, 142–143*t*, 144, 144*f*
 retinopathy of prematurity treatment, 206*t*, 207–208
 route of administration, 452
 Bietti crystalline dystrophy, 300, 316*t*, 329, 345*f*
 Bilateral diffuse uveal melanocytic proliferation
 (BDUMP), 233–234, 234*f*, 323
 Binocular indirect ophthalmoscopes/ophthalmoscopy,
 22
 Bipolar cells (BPCs), 13, 14*f*, 45
 Birdshot chorioretinopathy, 39, 53, 251*t*, 255–256, 255*f*
 Birdshot uveitis, 265, 266
 Birdshot uveitis-like fundus appearance, 265–266, 266*f*
 Bisretinoids, 29–30
 Black “sunburst” lesions, 168
 Bleb-associated endophthalmitis, 440–441, 440*f*
 Blebitis, 440
- Blind loop syndrome, 326
 Blindness
 age-related macular degeneration progression to, 93
 drug-induced, 343
 persistent fetal vasculature as cause of, 360
 Bloch-Sulzberger syndrome, 317*t*, 320
 Blocked fluorescence, 35
 Blood–brain barrier, 14
 Blood hyperviscosity, 150
 Blood–ocular barrier, 33
 Blood–retina barrier, 33, 35–36, 36*f*, 121–122, 121*f*, 123
 Blue-cone monochromatism (BCM), 49*f*, 284, 285
 Blue cones, 57
 Blue–yellow color deficiency, 57
 Blunt trauma, 376, 397–401. *See also* Closed-globe
 injuries
 Bone spicules, 292*f*
Borrelia burgdorferi, 278
 “Boxcarring” of blood flow, 157*f*
 BPCs. *See* Bipolar cells
 Bradyopsia, 53
 BRAMD (study), 92*t*
 Branch retinal artery occlusion (BRAO), 155–156,
 156–157*f*, 157*t*, 172*f*, 176
 Branch retinal vein occlusion (BRVO), 134–148
 about, 134, 145
 clinical findings, 134, 135–136*f*
 complications, 132–133, 137–138, 139*f*
 cystoid macular edema etiology, 176
 differential diagnosis, 179
 electroretinography findings, 47
 management
 pharmacologic, 138–139, 140–143*t*, 144–145, 144*f*,
 146
 surgical, 146–148, 147*f*
 pathogenesis, 134–135
 prognosis, 145–146, 146*f*
 risk factors, 135–137
 BRAO. *See* Branch retinal artery occlusion
 BRAVO (study), 141*t*, 144, 145
 “Bridge arch-shaped” serous pigment epithelial
 detachment (PED), 81
 Brilocizumab, 342
 Bruch membrane
 age-related changes, 67, 67*f*, 69–70, 77, 78*f*
 anatomy, 16*f*, 17
 angioid streaks and, 95
 degeneration of, 17
 myopia and, 239, 240*f*, 243, 246, 246*f*
 rupture of, 424
 tears, 398
 Brunette fundi, 306*f*
 BRVO. *See* Branch retinal vein occlusion
 B-scan optical coherence tomography, 83*f*
 B-scans (ultrasonography), 26, 27*f*, 39–41, 40–41*f*, 397
 “Bubbly” appearance, 389, 390–391
 Bullous retinoschisis, 310, 312*f*, 390, 390*f*
 Bull’s-eye maculopathy, 318, 326, 326*f*, 334, 336*f*
 Bull’s-eye pattern
 in acute idiopathic maculopathy, 260
 in Bardet-Biedl syndrome, 318
 in cone dystrophies, 295, 296*f*
 in Stargardt disease, 301*f*

- Bull's-eye rash, 278
 Bupropion, 347
 Burns, 412, 424
 Butterfly-type pattern dystrophy, 306, 308f
 BVOS (study), 140t
 b-waves, 45–47, 46f, 53, 285, 291, 313
- CACNA1F* gene, 286
 Calcific drusen, 73
 Calcific emboli, 156
 Cancer, 322–323, 323f, 389f
 Cancer-associated retinopathy (CAR), 322–323, 323f
Candida endophthalmitis, 265f, 272, 273f, 408
 Canthaxanthine, 346
 Capillary plexus, 13–14
 CAR. *See* Cancer-associated retinopathy
 Carbogen therapy, 161
 Carbonic anhydrase inhibitors, 174, 291
 Cardiac myxoma, 156
 Cardiovascular disease. *See* Arterial occlusive disease;
 Hypertension; Ocular ischemic syndrome; Retinal
 venous occlusion
 Carotid-cavernous fistulas, 226, 228f
 Carotid occlusive disease, 108, 152–153f, 152–154
 Cataractous lens, 41f
 Cataracts, 47, 212f, 291, 296
 Cataract surgery
 age-related macular degeneration progression
 affected by, 76
 complications, 441–442, 441t
 cystoid macular edema etiology, 176, 178
 diabetic macular edema treatment and, 124
 diabetic patient precautions, 128–129
 photoc retinopathy after, 413
 retinal detachment after, 381
 Cat-scratch disease, 274, 275f
 CATT (study), 66, 91, 92t
 Cavernous hemangioma, 186–187, 187f
 Ceftazidime, 438, 438t
 Cellophane maculopathy, 353
 Center-involved diabetic macular edema, 101, 112t, 122,
 123f, 126
 Central areolar choroidal dystrophy, 308, 310f
 Central blindness, 93
 Central nervous system
 Behçet disease involvement of, 261
 incontinentia pigmenti and retinal degeneration, 321
 metabolic diseases and
 abetalipoproteinemia, 324, 326
 Fabry disease, 328–329
 mucopolysaccharidoses, 316t, 319t, 327
 neuronal ceroid lipofuscinoses, 317t, 325–326,
 326f
 Tay-Sachs disease, 328, 328–329f
 Zellweger spectrum disorders, 317t, 326–327, 327f
 primary vitreoretinal lymphoma involvement of, 264,
 266
 Central retinal artery, 13, 15f
 Central retinal artery occlusion (CRAO)
 about, 157–159f, 158–160, 162
 causes, 15f, 188, 343
 imaging techniques, 53
 management, 160–162, 161f
- Central retinal vein occlusion (CRVO)
 about, 134–137, 148
 clinical findings, 134, 137f, 149
 complications, 132–133, 137–138, 139f
 cystoid macular edema etiology, 176
 differential diagnosis, 134, 150–151, 153
 drug-induced, 343
 evaluation, 53, 151
 management
 follow-up evaluations, 151
 pharmacologic, 138–139, 140–143t, 144–145, 144f,
 151
 surgical, 151–152
 pathogenesis, 134–135
 risk factors, 135–137
 sickle cell retinopathy and, 168
 types, 148–149, 149–150f
- Central serous chorioretinopathy (CSC)
 clinical variations, 216–217, 216f
 differential diagnosis, 73–74, 86, 218–221
 drug-induced, 338–339
 epidemiology, 215–216
 imaging techniques, 32, 39, 217–218, 217–221f
 management, 221
 systemic associations, 217
- Central serous retinopathy (CRS), 215
 Ceramide trihexoside, 328
 Cerebral vasculitis, 250
 Cerebrohepatorenal syndrome (Zellweger spectrum
 disorders), 317t, 326–327, 327f
- Ceroid, 325
CFH gene, 68
 Chalcosis, 407
 Charcot-Marie-Tooth disease, 316t
 Chédiak-Higashi syndrome, 324
 Chemical-induced diabetes, 100
 Chemotherapy, 265, 269f
 Cherry-red spot
 central retinal artery occlusion finding, 158, 158f, 161f
 drug-induced, 343
 lysosomal metabolic disorder finding, 328, 328f
 ophthalmic artery occlusion finding, 163
 trauma-related, 398
- Chikungunya virus retinitis, 281
 Children. *See also specific congenital disorders*
 Coats disease, 178–179, 179f
 developmental abnormalities, 358–361
 electrophysiologic testing modalities for, 53, 56
 trauma-related injuries, 377–379, 411, 411f
- Chloroquine, 333–335
 Chloroquine derivatives, 333–337, 334–336f
 Chlorpromazine, 337
CHM gene, 299
 Cholesterol emboli, 156, 157f, 159
 Cholesterosis, 366
 Choriocapillaris
 about, 225–226, 226–227f
 age-related changes, 67, 67f, 77, 78f
 anatomy, 14, 17, 18, 18f
 atrophy of, 289
 hypertensive choroidopathy and, 133–134
 imaging techniques, 30f
- Chorioretinal disruption, 398, 401, 401f

- Chorioretinal edema, 425
- Chorioretinal folds, 230, 230f, 231t
- Chorioretinal scars, 275
- Chorioretinitis sclopeteria, 398, 401, 401f
- Chorioretinopathy
- birdshot, 39, 53, 251t, 255–256, 255f
 - central serous chorioretinopathy, 215–221. *See also* Central serous chorioretinopathy
 - diagnostic imaging, 32, 36, 39
 - management, 426
- Choroid
- anatomy, 14, 17–19, 18f, 222
 - effusions, 40f, 41, 347
 - imaging techniques, 25, 33, 33f, 34–35, 39, 39f
 - myopia and, 239–243, 240–244f
 - thinning of, 240–242, 242f
- Choroidal detachments
- differential diagnosis, 382
 - imaging techniques, 40
 - photocoagulation-related, 118, 424, 425, 425f
- Choroidal dystrophies
- Bietti crystalline dystrophy, 289, 300, 316t
 - central areolar, 308, 310f
 - choroideremia, 289, 297–299, 299f
 - classification, 289
 - diagnostic considerations, 289–290
 - genetics, 290
 - gyrate atrophy, 299–300, 300f
 - management, 290–291
 - terminology, 288
- Choroidal folds, 230, 230f, 231t
- Choroidal granulomas, 273f
- Choroidal hemangiomas, 231, 232f
- Choroidal inflammatory disease, 249–281
- about, 249
 - autoimmune conditions, 261–263, 261t, 262f, 263f
 - infectious, 272–281
 - white dot syndromes, 250–257, 251t, 253f, 255–257f
- Choroidal melanomas, 425
- Choroidal neovascularization (CNV)
- about, 65–67, 93, 97t
 - acute posterior multifocal placoid pigment epitheliopathy association, 252
 - Best disease association, 302
 - causes
 - age-related macular degeneration, 77–93. *See also* Neovascular age-related macular degeneration
 - angioid streaks, 95–96, 95f
 - idiopathic and miscellaneous, 97, 97t
 - laser treatments, 127
 - miscellaneous, 97
 - ocular histoplasmosis syndrome, 93–95, 94f
 - pathologic myopia, 96–97, 96f
 - choroidal folds association, 230, 231t
 - choroidal rupture complication, 399, 400f
 - classification, 77–78, 78f
 - differential diagnosis, 218, 303
 - imaging techniques, 30, 31f, 36, 37f, 39, 39f
 - macular dystrophy association, 306, 307f
 - management, 86–93, 88f, 89t, 92t, 422, 426
 - multifocal choroiditis in, 257, 257f
 - myopic, 239–240, 240–244f
 - ocular histoplasmosis syndrome and, 93–95, 94f
 - pathologic myopia and, 96–97, 96f, 239–240, 241–244f
- Choroidal nevi, 25
- Choroidal noninflammatory disease, 215–234
- age-related choroidal atrophy, 227–229, 229f
 - bilateral diffuse uveal melanocytic proliferation, 233–234, 234f, 323
 - central serous chorioretinopathy, 215–221. *See also* Central serous chorioretinopathy
 - choroidal folds, 230, 230f, 231t
 - choroidal hemangiomas, 231, 232f
 - choroidal perfusion abnormalities, 222–227
 - uveal effusion syndrome, 231–232, 233f
- Choroidal perfusion abnormalities, 222–227
- arteritic disease, 222, 222–223f
 - choriocapillaris blood flow abnormalities, 225–226, 226–227f
 - increased venous pressure, 226–227, 228f
 - nonarteritic disease, 222–225, 224–225f
- Choroidal polyps, 34f
- Choroidal rupture, 95–96, 397, 398–399, 399–400f
- Choroidal tumors, 382
- Choroideremia, 53, 289, 297–299, 299f, 456t
- Choroidopathy, 133–134
- Choroid photocoagulation-related lesions, 425
- Chronic progressive external ophthalmoplegia (CPEO), 330, 330f
- CHRPE. *See* Congenital hypertrophy of the retinal pigment epithelium
- Cicatricial retinal detachment, 321
- Cigarette smoking, 68, 135
- Ciliary arteries, 222
- Ciliary body, 7, 9f, 15, 41
- Cilioretinal artery, 13, 15f, 158, 158f
- Cilioretinal artery occlusion, 162, 163f
- Cilium, 11, 12f
- Circle of Zinn-Haller, 246
- 11-*cis*-retinaldehyde, 17
- 11-*cis*-retinol dehydrogenase, 286
- Cisterns, in vitreous, 7
- CLARITY (study), 100
- Classic choroidal neovascularization (CNV), 77, 79
- Clindamycin, 276, 438t
- Clinically significant diabetic macular edema (CSME), 101, 122, 127
- Clinically significant retinopathy of prematurity (CSROP), 203
- Clofazimine, 337, 340t
- Cloquet canal, 6f, 7, 358, 359f
- Closed-globe injuries, 397–401
- choroidal rupture, 95–96, 397, 398–399, 399–400f
 - classification, 395
 - commotio retinae, 397, 398, 398f
 - evaluations, 396–397, 396t
 - posttraumatic macular hole, 399–400
 - prognostication, 409–410, 409t
 - sequelae, 397–398
 - traumatic chorioretinal disruption, 401, 401f
 - vitreous hemorrhage and, 397, 400–401
- CME. *See* Cystoid macular edema
- CMV. *See* Cytomegalovirus retinitis
- CNV. *See* Choroidal neovascularization

- Coats disease, 178–179, 179*f*, 180
 Coats reaction, 179, 185, 291
 Cobblestone degeneration, 374–375, 375*f*
 Cockayne syndrome, 319*t*
 COL2A1 gene, 361
 Collagen fibers, in vitreous, 7
 Collagen vascular disease, 192
 Collateral vessels, 137–138, 139*f*
 Colloidal silver, 347
 Coloboma-like excavated macular defect, 309, 311*f*
 Color vision
 about, 57
 dysfunctions, 118, 283–285, 284*t*, 286*f*, 347
 testing of, 57–59, 58–59*f*
 “Comet” sign, 95, 95*f*
 Comma sign, 171
 Commotio retinae, 397, 398, 398*f*
 Complete achromatopsia, 284–285
 Complete congenital stationary night blindness (CSNB), 49*f*, 286, 286*f*
 Complex retinal detachment, 450
 Computed tomography (CT), 397
 COMRADE C (study), 141*t*, 145
 Cone dystrophies, 47–48, 48*f*, 52–53
 Cone-rod dystrophies, 47–48, 295–296, 296*f*, 322
 Cone(s)
 age-related changes, 67
 anatomy, 11–13, 12*f*
 color vision and, 57
 density and distribution of, 9–11
 electroretinography testing, 45–51, 46*f*, 48–49*f*
 psychophysical evaluations, 61
 shedding by, 17
 Confluent drusen, 69*f*, 70
 Congenital color deficiency, 283–285, 284*t*, 286*f*
 Congenital hypertrophy of the retinal pigment epithelium (CHRPE), 321*f*
 Congenital nystagmus, 284
 Congenital rubella syndrome, 319*t*
 Congenital stationary night blindness (CSNB), 49*f*, 52, 285–286, 286*f*, 319
 Congenital toxoplasmosis, 275
 Conjunctival filtering blebs, 440, 440*f*
 Contact B-scan ultrasonography, 39–40, 40*f*
 Contact lenses, 23, 421, 422*t*, 441–442, 441*t*
 Contrast sensitivity (CS), 57, 59–60, 60*f*, 118
 Contusion trauma, 376–377, 395
 COPERNICUS, 142*t*, 144
 Copper, 406, 407
 Corkscrew vessels, 228*f*
 Corneal burns, 424
 Corneal lacerations, 403
 Cornea verticillata, 329, 334
 Corticosteroids
 acute posterior multifocal placoid pigment epitheliopathy treatment, 250–252
 adverse effects, 145, 217, 222, 268, 339, 340*t*
 cystoid macular edema treatment, 178, 443
 diabetic macular edema treatment, 111, 126–127
 diabetic retinopathy treatment, 117
 giant cell arteritis treatment, 160
 implants, 126, 145
 precautions, 265
 progressive outer retinal necrosis syndrome treatment, 268
 pseudophakic cystoid macular edema treatment, 177*f*, 178
 radiation retinopathy treatment, 189
 retinal venous occlusion treatment, 139, 140–141*t*, 145
 route of administration, 452
 Susac syndrome treatment, 176
 toxoplasmic retinochoroiditis treatment, 276
 Cotton-wool spots
 amyloidosis finding, 367
 arterial occlusive disease findings, 154, 155*f*, 155*t*, 157*f*
 causes of, 155*t*
 diabetic retinopathy finding, 108, 114*f*, 154
 differential diagnosis, 267
 drug-induced, 342
 hypertensive retinopathy findings, 132, 132–133*f*
 Purtscher and Purtscher-like retinopathy finding, 190, 191*f*
 radiation retinopathy finding, 188, 188*f*
 retinal venous occlusion finding, 134, 135*f*
 systemic lupus erythematosus finding, 262
 trauma-related, 411
 Coxsackievirus infection, 260
 CPEO. *See* Chronic progressive external ophthalmoplegia
 CRAO. *See* Central retinal artery occlusion
 CRAVE (study), 142*t*
 CRB1-associated RP1, 179
 CRB1 gene, 292*f*
 CRISPR/Cas9-based technology, 458
 Crohn disease, 175*f*
 CRS. *See* Central serous retinopathy
 CRUISE (study), 142*t*, 144
 CRVO. *See* Central retinal vein occlusion
 Cryopexy, 427, 448
 CRYO-ROP (study), 194, 204, 205*t*
 Cryotherapy
 about, 426–427
 cryopexy technique, 427, 448
 hemangioma treatment, 231
 retinal break treatment, 379
 retinal cavernous hemangioma treatment, 187
 retinopathy of prematurity treatment, 205*t*, 207
 von Hippel–Lindau syndrome treatment, 184–185
 Cryotherapy for Retinopathy of Prematurity Cooperative Group, 194
 Crystalline retinopathy, 329, 344–346, 345–346*f*, 346*t*
 CS. *See* Contrast sensitivity
 CSC. *See* Central serous chorioretinopathy
 C-scans, 26
 CSME. *See* Clinically significant diabetic macular edema
 CSNB. *See* Congenital stationary night blindness
 CSROP. *See* Clinically significant retinopathy of prematurity
 CT. *See* Computed tomography
 CTNNA1 gene, 308
 Culex mosquitoes, 279
 Cushing syndrome, 217
 Cuticular (basal laminar) drusen, 304–305, 306*f*
 CVOS (study), 140*t*, 149*f*

- Cyclodialysis clefts, 41
 Cyclosporine, 261
 CYP4V2 gene, 289, 300
 Cysteamine, 329
 Cystic retinal tufts, 371–372, 373f
 Cystinosis, 329
 Cystoid macular edema (CME)
 about, 176, 177f
 age-related macular degeneration finding, 77, 79
 birdshot chorioretinopathy association, 255–256
 cytomegalovirus retinitis association, 268
 differential diagnosis, 178
 drug-induced, 343
 etiology, 146, 146f, 176–178
 imaging techniques, 36f, 176
 macular telangiectasia association, 180
 management, 144, 144f, 178, 443, 443f
 pseudophakic, 176–178, 177f
 in retinal dystrophies, 290, 291, 293f
 toxocariasis association, 277
 Cysts, 41, 375–376, 382, 385f, 392
 Cytomegalovirus (CMV) retinitis, 267–268, 267f, 269, 270t
- Dalen-Fuchs nodules, 263
 Dark adaptation responses
 in electro-oculography, 53–54, 54–55f
 in electroretinography, 44f, 45, 46f, 47, 48–50f, 52–53, 52f
 psychophysical evaluations, 61
 Dark adaptometry, 61
 “Dark-choroid,” 300
 Day blindness, 295
 DCCT (study), 100, 104–105, 106f
 Deafness, 226
 Deep capillary plexus, 13–14, 30f
 Deferoxamine (desferrioxamine), 337–338, 339f, 340t, 344
 Delamination, 437
 Demarcation lines, 378, 381, 387, 387f, 392
 Demyelinating optic neuritis, visual evoked potentials
 in, 55
 Dental diseases, 322
 Dentate processes, 9, 9f
 Dermatologic diseases, 320–322, 322f
 Descemet membrane, 407
 Desferrioxamine (deferoxamine), 337–338, 339f, 340t, 344
 Deutan red-green color deficiency, 57, 59
 Developmental abnormalities, 358–361
 persistent fetal vasculature, 360
 prepapillary vascular loops, 358, 359f
 tunica vasculosa lentis, 358, 359f
 Dexamethasone, 141t, 145, 276, 438, 453
 Dexamethasone implants, 126, 145
 DHA. *See* Docosahexaenoic acid
 Diabetes mellitus
 asteroid hyalosis association, 364
 cataract surgery precautions, 128–129
 choroidal perfusion abnormalities association, 226
 classification, 100
 examination recommendations, 103–104, 104–105t
 hypertension and, 132, 133, 161
 ocular ischemic syndrome association, 153f
 photocoagulation precautions, 425
 retinal venous occlusion risk factor, 135, 136
 terminology, 100
 Diabetic macular edema (DME), 121–128
 about, 121–122, 121f
 classification, 101, 122–123, 122–123f
 defined, 101
 etiology, 111
 evaluations, 59
 management
 about, 123–124, 437
 nonpharmacologic, 127–128
 pharmacologic, 111, 116f, 124–126, 125f
 photocoagulation for, 422
 subthreshold laser delivery systems for, 424
 systemic management, 108
 studies, 100, 112f
 vision loss and, 108, 109–110
 Diabetic nephropathy, 108
 Diabetic papillopathy, 120, 134
 Diabetic retinopathy, 99–129
 about, 99
 classification, 100–101
 cotton-wool spot finding, 108, 114f, 154
 cystoid macular edema etiology, 176
 diabetic macular edema, 121–128. *See also* Diabetic macular edema
 differential diagnosis, 179, 188
 epidemiology, 101–102
 examination recommendations, 103–104, 104–105t
 hypertension and, 132–133
 management, 104–108, 106–107t, 435–437, 436f
 nonproliferative, 101, 108–111. *See also* Nonproliferative diabetic retinopathy
 pathogenesis, 102, 103f
 proliferative, 101, 111–120. *See also* Proliferative diabetic retinopathy
 studies, 100
 terminology, 100–101
 vision loss clinical signs, 108
 Diabetic Retinopathy Clinical Research Network, 116.
 See also DRCR Retina Network
 Dialyses, 376, 377, 379t, 382, 385f
 Dichromacy, 284, 284t
 Dichromatism, 284, 284t
 Didanosine, 338, 340t
 Dideoxyinosine, 338, 340t
 Diet, retinopathy of prematurity and, 204
 Diffuse macular edema, 123
 Diffuse unilateral subacute neuroretinitis (DUSN), 279, 280f
 Digital Diagnostics (IDx-DR), 104
 Digitalis, 347
 Diplopia, 425
 Direct ophthalmoscope/ophthalmoscopy, 22–23.
 See also Ophthalmoscopy
 Disseminated intravascular coagulation, 223
 DME. *See* Diabetic macular edema
 Docetaxel, 343
 Docosahexaenoic acid (DHA), 75
 Dominant (familial) exudative vitreoretinopathy (FEVR), 179

- Dot form, 216, 216f
- Doughnut pattern, 347
- Doxycycline, 279
- Doyme honeycomb dystrophy, 305
- DRCR Retina Network (studies), 109, 111, 112–113t, 115–116, 116f, 117, 120, 124, 125f, 126, 128
- DRS (study), 100, 107t, 117–118, 118f
- Drug-induced diabetes, 100
- Drusen
- age-related choroidal degeneration finding, 229f
 - age-related macular degeneration finding, 67, 67f, 69–71, 69f, 71f, 75
 - categorization of, 70
 - choroidal neovascularization, 39
 - confluent, 69f, 70
 - hard, 70
 - imaging techniques, 24f, 27f, 34f, 39, 40, 69f, 70–72
 - macular dystrophy finding, 303–306, 305–307f, 309, 311f
 - pseudoxanthoma elasticum finding, 95
 - soft, 229f, 303
- Drusenoid pigment epithelial detachment (PED), 70, 303, 305f
- DRVS (study), 100, 120
- “Dry” age-related macular degeneration. *See* Nonneovascular age-related macular degeneration
- Duchenne muscular dystrophy, 319
- Dural arteriovenous malformations, 226
- DUSN. *See* Diffuse unilateral subacute neuroretinitis
- “Dustlike” pigment mottling, 306, 308f
- Dwarfism, 361
- Dyschromatopsias, 283–285
- Dystrophic lipidization, 73
- Dystrophies. *See also* Cone dystrophies; Macular dystrophies; Rod–cone dystrophies
- choroidal, 297–300, 299–300f, 316t. *See also* Choroidal dystrophies
 - cone–rod, 322
 - macular, 300–310. *See also* Macular dystrophies
 - retinal, 288–297, 310–313. *See also* Retinal dystrophies
 - rod–cone, 318. *See also* Retinitis pigmentosa
- Dystrophin, 319
- Eales disease, 176, 272
- Early-onset “drusenoid” macular dystrophies, 303–306, 305–306f
- Early Treatment of Retinopathy of Prematurity (ETROP), 194, 204, 205t, 210
- Ebola virus (EBOV) panuveitis, 281
- Eclampsia, 223, 224f
- Eclipse retinopathy, 412–413, 413f
- EDI-OCT. *See* Enhanced depth imaging optical coherence tomography
- EFEMP1 gene, 305
- Egg yolk–like (vitelliform) macular lesion, 302–303, 302f
- Ehlers-Danlos syndrome, 95
- Eicosapentaenoic acid (EPA), 75
- Electrical injuries, 400
- Electro-oculography/electro-oculogram (EOG), 44t, 53–55, 54–55f
- Electrophysiologic testing, 43–56
- about, 43–44, 44t, 56–57
 - electro-oculography, 53–55, 54–55f
 - electroretinography, 44–53. *See also* Electoretinography
 - microperimetry, 56
 - visual evoked potentials, 51, 55–56, 56f
- Electoretinography (ERG), 44–53
- about, 44, 44t
 - clinical considerations, 48–49f, 52–53
 - dark adaptometry comparison, 61
 - drug-induced abnormalities, 347
 - electrodes for, 44
 - full-field electoretinography, 45–48, 46f, 48–50f, 51, 52f
 - melanoma-associated retinopathy findings, 323
 - multifocal electoretinography, 49–51, 50f, 52f
 - ocular ischemic syndrome findings, 153
 - pattern electoretinography, 50f, 51, 52f
- Ellipsoid, 11–13
- Ellipsoidal mirror, 25–26, 25f
- ELM. *See* External limiting membrane
- ELOVL4 gene, 302
- Elschnig spots, 134, 225, 225f
- Embolism
- arterial macroaneurysms and, 165–166
 - arterial occlusive disease etiology, 156, 157–158f, 159
 - choroidal perfusion abnormalities and, 222
 - differential diagnosis, 176, 192
 - talc, 347
- Encephalofacial hemangiomatosis, 231
- Enclosed ora bays, 374, 374f
- Endogenous bacterial endophthalmitis, 270–271, 271f
- Endogenous fungal endophthalmitis, 271, 273f
- Endophthalmitis
- antiangiogenic therapy complication, 91, 125
 - bacterial, 270–271, 271f
 - fungal, 271–272, 272–273f
 - intravitreal injection complication, 453
 - postoperative, 437–441, 438t, 439–440f
 - trauma-related, 407–409
 - yeast, 272, 273f
- Endophthalmitis Vitrectomy Study (EVS), 438–439, 440f
- En face scans, 26, 29
- Enhanced depth imaging optical coherence tomography (EDI-OCT), 26, 39, 71, 74, 85, 86
- Enhanced S-cone syndrome (ESCS), 53, 297, 298f
- Enucleation, for penetrating ocular injury, 263
- EOG. *See* Electro-oculography/electro-oculogram
- EPA. *See* Eicosapentaenoic acid
- Epiretinal membranes (ERMs), 351–354
- about, 351
 - clinical findings, 351–353, 353f, 355f
 - differential diagnosis, 355
 - etiology and epidemiology, 351
 - management, 354, 431–432, 431–432f
- Eplerenone, 221
- Equatorial retina, 8
- ERG. *See* Electoretinography
- Ergot alkaloids, 342
- ERMs. *See* Epiretinal membranes
- Erythema chronicum migrans, 278

- Erythroclastic (red blood cell-induced) glaucoma, 119
 ESCD. *See* Enhanced S-cone syndrome
Escherichia coli, 270
 ESCS. *See* Enhanced S-cone syndrome
 ETDRS (study), 88, 100, 107*t*, 108–109, 115, 118, 122, 124, 127, 147
 Ethambutol hydrochloride, 273
 Ethylene glycol, 346
 ETROP. *See* Early Treatment of Retinopathy of Prematurity
 EVEREST studies, 85
 Evisceration, for penetrating ocular injury, 263
 EVS. *See* Endophthalmitis Vitrectomy Study
 EXCITE (study), 66, 88
 Exogenous fungal endophthalmitis, 271
 Expulsive suprachoroidal hemorrhage, 443–444
 External limiting membrane (ELM), 10*f*, 12*f*, 13, 14*f*
 Extra-areal periphery, 8
 Extraretinal fibrovascular proliferation, 114
 Exudates
 hard, 132, 145–146, 179, 185
 macular, 133*f*, 134, 184, 184*f*
 soft, 132
 Exudative age-related macular degeneration (AMD), 67
 Exudative retinal detachment
 diagnostic features, 383*t*, 388–389, 389*f*
 differential diagnosis, 389
 drug-induced, 338, 341*f*
 etiology, 389, 389*f*
 familial exudative vitreoretinopathy association, 362
 lupus vasculitis association, 262
 photocoagulation-related, 424, 425
 retinopathy of prematurity association, 210, 211*f*
 Exudative retinopathy, 291, 294*f*
 EyeArt (Eyenuk), 104
 Eye Disease Case-Control Study, 135–136
 Eye movement tracking, 28, 29, 56
- FA. *See* Fluorescein angiography
 Fabry disease, 328–329
 Facioscapulohumeral muscular dystrophy, 179
 FAF. *See* Fundus autofluorescence
 Familial adenomatous polyposis (FAP), 320, 321*f*, 362–363, 362*t*, 363*f*
 Familial cerebelloretinal angiomas, 181–182
 Familial drusen, 304
 Familial exudative vitreoretinopathy (FEVR), 179, 360, 362–363, 362*t*
 Familial juvenile nephronophthisis, 320
 FAP. *See* Familial adenomatous polyposis
 Farnsworth-Munsell 100-hue test, 58
 Farnsworth Panel D-15 test, 58–59, 59*f*
 Fat emboli/embolism, 156, 192
 FAZ. *See* Foveal avascular zone
 Fenofibrate, 111
 FEVR. *See* Familial exudative vitreoretinopathy
 ffERG. *See* Full-field electroretinography
 Fibrovascular pigment epithelial detachment (PED), 77, 79, 81, 85, 91
 FIELD (study), 100, 111
 Fingolimod, 343–344
 FIPTs. *See* Focal intraretinal periartertiolar transudates
 “Fishnet” pigment deposition, 308*f*
 Fish-shaped (pisciform) flecks, 300, 301*f*, 302
 Flap tears, of retina, 376, 377*f*, 379*t*, 380
 Flash visual evoked potentials (flash VEPs), 55, 56
Flaviviridae, 279
 Flecken, 190, 191*f*
 Floaters
 in birdshot chorioretinopathy, 255
 in cytomegalovirus retinitis, 267
 management, 435
 in posterior vitreous detachment, 350, 369–370
 in retinal detachments, 382
 in toxocariasis, 277
 in toxoplasmic retinochoroiditis, 275
 “Flower petal” pattern, 176, 177*f*
 Fluconazole, for yeast endophthalmitis, 271
 Flulike prodrome, 250, 254, 259
 Fluocinolone acetonide implants, 126
 Fluorescein angiography (FA), 32–38
 about, 32–35, 33–34*f*
 adverse effects of, 36–37
 with fundus camera, 23
 hyperfluorescence patterns, 34*f*, 35–36, 35*t*, 36–37*f*
 hypofluorescence patterns, 34*f*, 35
 landmarks, 8
 laser therapy guidance with, 127
 OCT angiography comparison, 29
 scanning laser ophthalmoscopy and, 25
 Fluorophores, 29–32
 Fluoroquinolones, 408
 “Flying saucer” sign, 326*f*, 334, 334*f*, 336*f*
 Focal chorioretinitis, 271, 271*f*
 Focal intraretinal periartertiolar transudates (FIPTs), 132, 132–133*f*
 Focal laser photocoagulation, 122, 124, 127
 Focal macular edema, 123
 Footplates of Müller cells, 13
 Form-deprivation errors, 245
 Foscarnet, 267–268, 269, 270*t*
 4:2:1 rule, for diabetic retinopathy, 108–109
 Fovea
 anatomy, 7–8, 7*f*, 8*t*, 10*f*, 210, 212*f*
 atrophy of, 72–73
 diabetic macular edema and, 121–122
 imaging techniques, 35
 photoreceptors of, 9
 Fovea centralis, 7–8, 7*f*, 8*t*
 Fovea plana, 212*f*
 Foveal avascular zone (FAZ), 8, 83*f*, 171*f*, 181*f*
 Foveal burns, 424
 Foveal detachment, 355
 Foveal schisis, 312
 Foveola, 7–8, 7*f*, 8*t*, 9
 Foveomacular retinitis, 412–413, 413*f*
 “Frosted branch” angitis, 267
 Fuchs spot, 240
 Fucosidosis, 329
 Full-field (Ganzfeld) electroretinography (ffERG), 45–48, 46*f*, 48–50*f*, 51, 52*f*
 Fundus
 imaging techniques, 22–25, 24*f*, 27*f*, 29–32, 31*f*, 72, 72*f*, 74, 74*f*
 rod-cone dystrophy findings, 291, 292*f*
 “sunset glow” appearance of, 263

- Fundus albipunctatus, 286–287, 286–287f
 Fundus autofluorescence (FAF), 23, 24f, 29–32, 31f, 72, 72f, 74, 74f
 Fundus flavimaculatus, 47–48, 50f, 302, 306
 Fundus pulverulentus, 306
 Fungal endophthalmitis, 271–272, 272–273f, 408
 Fungemia, 271
Fusarium endophthalmitis, 272
- GALILEO (study), 142t, 144
 Ganciclovir, 267–268, 269, 270t
 Ganglion cell layer (GCL), 13, 14f, 343, 344f
 Ganglion cell(s), 13
 Ganglioside storage disease, 328
 Ganzfeld ERG. *See* Full-field electroretinography
 Gardner syndrome, 320. *See also* Familial adenomatous polyposis
 Gastrointestinal tract disease, retinal degeneration associated with, 320, 321f
 Gaucher disease, 328
 GCA. *See* Giant cell arteritis
 GCL. *See* Ganglion cell layer
 GEFAL (study), 92t
 Gene augmentation therapy, 456–457, 457f
 General anesthesia, 53
 Gene replacement therapy, 456–457, 457f
 Gene therapy
 about, 455–456
 for age-related macular degeneration, 456t
 for choroideremia, 299
 current limitations, 458
 for Leber congenital amaurosis, 297
 for retinal dystrophies, 288, 290, 295, 456t
 for Stargardt disease, 302
 types, 456–458, 457f
 Genetic heterogeneity, 288, 289
 Genetics. *See also* X-linked disorders; *specific genes*
 of age-related macular degeneration, 68–69, 304, 306
 of cavernous hemangiomas, 186
 of Coats disease, 178
 of cone and cone-rod dystrophies, 297
 of dystrophies, 288–289
 of night vision abnormalities, 285–286
 of von Hippel–Lindau syndrome, 181–182
 Genetic testing, 68, 290
 GENEVA (study), 141t, 145
 Genome editing, 457, 457f, 458
 Gentamicin, 342, 438
 Geographic atrophy
 choroidal, 226, 229
 macular, 302, 302f, 306, 307, 307f
 of retinal pigment epithelium, 66, 70, 71–73, 72f
 Geographic choroiditis, 253
 Ghost cell glaucoma, 119, 365
 Ghost vessels, 226
 Giant cell arteritis (GCA), 159–160, 222, 222–223f
 Giant tears, of retina, 376
 “Giraffe skin,” 232, 233f
 Glaucoma
 ghost cell, 365
 management, 119, 440–441, 440f
 myopia and, 246f, 247
 neovascular, 188
 nerve damage caused by, 392–393
 open-angle, 136, 151
 retinopathy of prematurity association, 210
 Glia, 176, 177f
 Glitazones, 343
 Globe injuries, 395–415
 abusive head trauma and, 411, 411f
 classification, 395–396
 closed, 397–401
 choroidal rupture, 397, 398–399, 399–400f
 classification, 395
 commotio retinae, 397, 398, 398f
 posttraumatic macular hole, 399–400
 sequelae, 397–398
 traumatic chorioretinal disruption, 401, 401f
 vitreous hemorrhage, 400–401
 evaluation, 396–397, 396t
 foreign bodies, 404–407. *See also* Intraocular foreign bodies
 management, 402–404
 needle injuries, 445, 446f
 open, 401–407
 classification, 395–396
 lacerating and penetrating, 395, 402, 408
 perforating, 395, 402, 408
 scleral rupture, 401–402
 sequelae, 401
 optic nerve head avulsion, 398, 410, 410f
 photoc damage, 412–415, 413f
 posttraumatic endophthalmitis, 407–409
 prognostication of, 409–410, 409t
 sympathetic ophthalmia, 410
 Glucosylceramide, 328
 Glycemic control, 104–105, 106t, 123–124
 GM₂ gangliosidosis type I, 328
 Goldmann-Favre disease, 178
 Goldmann-Favre syndrome, 297
 Goldmann-Weekers (G-W) adaptometer, 61
 Granulomas
 choroidal, 273f
 posterior pole, 277
 in toxocariasis, 277
 Granulomatosis with polyangiitis, 222, 223f
 Green cones, 57
 GRK1 gene, 287
 Grönblad-Strandberg syndrome, 95
 GUCY2D, and GUCA1A genes, 308
 Guttering, 384f
 G-W adaptometer. *See* Goldmann-Weekers adaptometer
 Gyrate atrophy, 299–300, 300f
- Haemophilus* spp, 441
 Haller layer, 18
 Handheld laser-pointer injury, 414–415, 414f
 HARBOR (study), 66, 89t
 Hard exudates, 132, 145–146, 179, 185
 Hardy-Rand-Rittler plates, 58
 HARRIER (study), 91
 HAWK (study), 91
 HbAs. *See* Sickle cell trait
 HbSC. *See* Sickle cell-hemoglobin C disease
 HbSS disease. *See* Homozygous sickle cell disease
 “Headlight in the fog,” 277f

- Hearing loss, 319, 319*t*
 Helicoid peripapillary choroidopathy, 253. *See also*
 Serpiginous choroidopathy
 HELLP (hemolysis, elevated liver enzymes, and low
 platelet count) syndrome, 224*f*
 Hemangioblastomas, 179, 182–185, 184–185*f*, 186
 Hemangiomas, 186–187, 186–187*f*, 231, 232*f*
 Hemeralopia, 295
 Hemicentral retinal vein occlusion (HRVO), 134, 138*f*
 Hemoglobin, 419–420, 420*f*
 Hemoglobin A_{1c} (HgA_{1c}), 105
 Hemorrhage
 diabetic retinopathy finding, 108, 114, 114*f*, 120
 hypemas, 444
 internal limiting membrane, 189, 189*f*
 intraretinal. *See* Intraretinal hemorrhage
 optic nerve, 190
 preretinal, 114, 114*f*, 425
 retinal, 342, 411, 411*f*
 salmon-patch, 168, 170*f*
 submacular, 93, 399, 434–435, 434–435*f*
 subretinal, 85, 86, 190, 239, 398, 399*f*, 425
 suprachoroidal, 397, 443–445, 444*f*
 vitreous. *See* Vitreous hemorrhage
 Hemorrhagic occlusive retinal vasculitis (HORV), 342
 Henle fiber layer, 8*t*, 9, 176, 177*f*, 237
 Heparan sulfate, 327
 Hereditary dystrophies, 316*t*
 Hereditary hyaloideoretinopathies with optically empty
 vitreous, 360–361, 361*f*
 Hermansky-Pudlak syndrome, 324
 Herpes simplex virus (HSV), 268, 269, 270*t*
 HEXA gene, 328
 HgA_{1c} (hemoglobin A_{1c}), 105
 High myopia. *See* Pathologic myopia
 Histiocytic lymphoma. *See* Primary vitreoretinal
 lymphoma
Histoplasma capsulatum, 94
 Histoplasmosis, 93–95, 94*f*
 “Histo spots,” 94
 HIV/AIDS
 cytomegalovirus retinitis association, 267, 268
 intraocular lymphoma risks, 264–265
 non-CMV necrotizing herpetic retinitis association,
 269
 syphilitic retinochoroiditis association, 274
 toxoplasmic retinochoroiditis association, 276
 Hives, 37
 HLA-A29, 255
 HLA-B5, 261
 HLA-B51, 261
 Hollenhorst plaques, 157, 157*f*, 159
 HOME (study), 77
 Homocystinuria, 316*t*
 Homozygous sickle cell (HbSS) disease, 168, 171, 174
 HORIZON (study), 66, 89*t*
 Horseshoe retinal tears, 376, 377, 377–378*f*, 379, 379*t*,
 380*f*
 HORV. *See* Hemorrhagic occlusive retinal vasculitis
 HSV. *See* Herpes simplex virus
 Human leukocyte antigens, 255, 261
 Hunter syndrome, 317*t*, 327
 Hurler-Scheie syndrome, 327
 Hurler syndrome, 316*t*, 327
 Hyalocytes, 7
 Hyaloid artery, 358, 359*f*, 360
 Hyaluronan (hyaluronic acid), 349
 Hydroxychloroquine, 51, 52*f*, 333–335
 Hyperacuity testing, 76–77
 Hypercoagulability, 136
 Hypercortisolism, 217
 Hyperfluorescence, 30–32, 34*f*, 35–36, 35*t*, 36–37*f*, 110*f*
 Hyperlipidemia, 105, 108, 124, 136
 Hyperopia, 230, 231*t*, 232
 Hypertension
 asteroid hyalosis association, 364
 central serous retinopathy association, 217
 choroidal perfusion abnormalities and, 223–224, 225*f*
 diabetic macular edema association, 124
 diabetic retinopathy association, 105, 108
 hypertensive choroidopathy, 133–134
 hypertensive optic neuropathy, 133*f*, 134
 hypertensive retinopathy, 132–133, 132–133*f*
 malignant, 223
 retinal vascular diseases association, 131–135
 Hypertensive choroidopathy, 133–134
 Hypertensive optic neuropathy, 133*f*, 134
 Hypertensive retinopathy, 132–133, 132–133*f*
 Hyperviscosity retinopathy, 150
 Hyphemas, 41, 174–175, 444
 Hypofluorescence, 30, 31*f*, 34*f*, 35
 Hypoglycemic drugs, 347
 Hypogonadism, 318
 Hypopyon, 440
 Hypotension, fluorescein adverse effect, 37
 Hypothyroidism, 136
 Hypotony, 444
 Hypotony maculopathy, 230, 231*t*
 ICG. *See* Indocyanine green
 ICGA. *See* Indocyanine green angiography
 Ichthyosis, 320
 ICROP. *See* International Classification of ROP
 iCSNB. *See* Incomplete congenital stationary night
 blindness
 Idiopathic macular holes, 355–358, 356*f*, 432–433, 433*f*
 Idiopathic multifocal choroiditis, 256
 Idiopathic polypoidal choroidopathy, 34*f*, 426
 Idiopathic retinal vasculitis, aneurysms, and
 neuroretinitis (IRVAN), 176
 IDx-DR (Digital Diagnostics), 104
 IGA. *See* Indocyanine green angiography
 ILM. *See* Internal limiting membrane
 ILM inverted flap, 433
 Imaging technologies, 23–41
 about, 21
 adaptive optics imaging, 32
 fluorescein angiography, 32–38. *See also* Fluorescein
 angiography
 fundus autofluorescence, 23, 24*f*, 29–32, 31*f*, 72, 72*f*,
 74, 74*f*
 fundus camera imaging, 23, 24, 24*f*, 27*f*, 30–32
 indocyanine green angiography, 23, 38–39, 38–39*f*
 ophthalmoscopy, 22–23. *See also* Ophthalmoscopy
 optical coherence tomography, 26–28, 27–28*f*, 32.
 See also Optical coherence tomography

- optical coherence tomography angiography, 28–29, 30*f*
- scanning laser ophthalmoscopy, 24–26, 25*f*, 30–32, 31*f*
- ultrasonography, 26, 27*f*, 39–41, 40–41*f*, 397
- Immune checkpoint inhibitors, 338, 340*t*
- Implantable miniature telescopes, 93
- Implantable telescopes, 93
- Incomplete congenital stationary night blindness (iCSNB), 49*f*, 286, 286*f*
- Incontinentia pigmenti, 317*t*, 320
- Indirect ophthalmoscope/ophthalmoscopy, 22–23
- Indocyanine green (ICG), 38
- Indocyanine green angiography (ICGA), 23, 38–39, 38–39*f*
- Infantile neuronal ceroid lipofuscinoses (NCLs), 325–326
- Infantile nystagmus syndrome, 284
- Infantile Refsum disease, 327
- Infants. *See also specific congenital disorders*
 - abusive head trauma in, 411, 411*f*
 - congenital toxoplasmosis in, 275
 - developmental abnormalities, 358–361
 - electrophysiologic testing modalities for, 47, 53, 56
 - electroretinography testing controls for, 47, 53
 - Leber congenital amaurosis in, 296
 - neuronal ceroid lipofuscinoses in, 325–326
 - Refsum disease in, 327
 - retinopathy of prematurity and, 193–194. *See also* Retinopathy of prematurity
 - trauma-related injuries, 377–379, 411, 411*f*
- Infectious diseases. *See also* Endophthalmitis
 - Chikungunya virus retinitis, 281
 - cytomegalovirus retinitis, 267–268, 267*f*, 269, 270*t*
 - diffuse unilateral subacute neuroretinitis, 279, 280*f*
 - Ebola virus panuveitis, 281
 - non-CMV necrotizing herpetic retinitis, 268–269*f*, 268–270, 270*t*
 - ocular bartonellosis, 274, 276*f*
 - ocular Lyme borreliosis, 278–279
 - ocular tuberculosis, 272–273, 273*f*
 - syphilitic retinochoroiditis, 274, 275*f*
 - toxocariasis, 277–278, 278*f*, 360
 - toxoplasmic chorioretinitis, 274–277, 277*f*
 - trauma-related, 408
 - West Nile virus chorioretinitis, 279, 280*f*
 - Zika virus chorioretinitis, 279–281
- Inferior staphyloma syndrome, 245, 245*f*
- Inflammation, electroretinography findings, 47
- Inflammatory vasculitis, 261–262, 261*t*, 262*f*
- Inherited retinal diseases (IRDs), 455–458
- Inner nuclear layer (INL), 10*f*, 13, 14*f*, 45, 164
- Inner-outer segment junction, 13
- Inner plexiform layer (IPL), 10*f*, 13
- Inner retinal dystrophies, 310–313, 312*f*
- Inner segments, 11, 12*f*, 13
- Insulin-dependent diabetes mellitus, 100
- Interferogram, 26
- Interferon, 261, 342
- Intermediate capillary plexus, 14
- Intermediate uveitis, 277
- Internal limiting membrane (ILM)
 - anatomy, 13, 14*f*
 - diabetic retinopathy findings, 108
 - myopia and, 237–239
 - sickle cell retinopathy findings, 168
 - Valsalva retinopathy hemorrhagic detachment, 189, 189*f*
- International Classification of ROP (ICROP), 194–198
- International Society for Clinical Electrophysiology of Vision (ISCEV), 44, 45–47, 46*f*
- International Vitreomacular Traction Study Classification System, 354*t*
- Intracranial hemangiomas, 185, 186
- Intraocular foreign bodies (IOFBs)
 - about, 404–406, 404–406*f*, 407*t*
 - classification, 395
 - imaging techniques, 40, 41, 397
 - retained, 404*f*, 406–407, 407*t*, 408*f*, 441–442, 441*t*
- Intraocular lenses (IOLs), 41, 442–443
- Intraocular lymphoma, 264–267, 265–266*f*
- Intraocular pressure (IOP)
 - decreased, 230, 382
 - elevated, 153, 174
 - intravitreal injection complication, 453
 - risk factors, 145
 - in trauma patients, 396, 402, 404
- Intraretinal fluid, 77, 79*f*, 81*f*, 82, 96*f*
- Intraretinal hemorrhage
 - Behçet disease finding, 261
 - branch retinal vein occlusion complication, 134, 135–136*f*
 - diabetic retinopathy finding, 108–109, 109*f*
 - radiation retinopathy complication, 188
- Intraretinal microvascular abnormalities (IRMAs), 108–109, 110*f*
- Intrascleral fixation, 442
- Intravitreal injections, 111, 117, 452–454, 452*f*, 453*t*, 457
- Inverted ILM technique, 238, 358
- IOFBs. *See* Intraocular foreign bodies
- IOLs. *See* Intraocular lenses
- Ionizing radiation, retinopathy caused by exposure to, 187–189
- IOP. *See* Intraocular pressure
- IPL. *See* Inner plexiform layer
- Ipsilateral facial nevus flammeus (port-wine birthmark), 231
- IRDs. *See* Inherited retinal diseases
- Iris burns, 424
- Iris fixation, 442
- Iris imaging techniques, 41
- Iris neovascularization
 - diabetic retinopathy complication, 119
 - in ocular ischemic syndrome, 152–153
 - in radiation retinopathy, 188
 - in retinal artery occlusion, 162
 - in retinal vein occlusion, 148, 149, 152, 152*f*
- IRMAs. *See* Intraretinal microvascular abnormalities
- Iron, as foreign body, 406, 407, 407*t*, 408*f*
- IRVAN. *See* Idiopathic retinal vasculitis, aneurysms, and neuroretinitis
- Irvine-Gass syndrome, 176
- ISCEV. *See* International Society for Clinical Electrophysiology of Vision
- Ischemic (nonperfused) central retinal venous occlusion (CRVO), 148–149, 150*f*

- Ishihara plates, 58
 Isotretinoin, 347
 IVAN (study), 92*t*

 Jalili syndrome, 322
 Jeune syndrome, 320
 Joubert syndrome, 320
 Juxtafoveal retinal telangiectasia, 179, 180–181, 181–183*f*

 Kayser-Fleischer ring, 407
KCNV2 gene, 53
 Kearns-Sayre syndrome, 317*t*, 330
 Keratitis, 272, 278
 Keratoconus, 296
 “Kissing choroidals” (appositional choroidal detachment), 40*f*, 443
Klebsiella pneumoniae endophthalmitis, 270
 Kyrieleis plaques, 277*f*

 Lacerating injuries, 395, 402
 Lacquer cracks, 239, 240*f*
 Lamellar hole–associated epiretinal proliferation (LHEP), 27*f*, 352
 Lamina cribrosa dehiscence, 247, 247*f*
 L’Anthony Panel D-15 test, 58, 59
 Large colloid drusen, 304
 Laryngeal spasm, 37
 Laser ablation, 423. *See also* Photocoagulation
 Laser-pointer injury, 414–415, 414*f*
 Laser retinopexy, 422–423, 423*f*
 Late leakage from an undetermined source, 79
 Lattice degeneration
 clinical findings, 371, 372*f*, 378*f*
 etiology and epidemiology, 371
 hereditary hyaloideoretinopathy finding, 361, 361*f*
 management, 379, 379*t*, 380, 381
 myopia finding, 236*t*, 237
 retinal detachment association, 369, 371, 372–373*f*, 374, 378*f*
 retinal pigment epithelium hyperplasia finding, 375
 LCA. *See* Leber congenital amaurosis
 L cones, 57
 LCPUFAs. *See* Long-chain polyunsaturated fatty acids
 Leakage hyperfluorescence, 34*f*, 35–36, 35*t*, 37*f*
 LEAVO (study), 143*t*, 144
 Leber congenital amaurosis (LCA), 296–297, 318, 458
 Leber hereditary optic neuropathy, 51
 Leber stellate neuroretinitis, 274
 Lensectomy, 360
 Lenses, 23, 421, 422*t*, 441–442, 441*t*
 Lentiviruses, 457
 “Leopard spotting,” 347
 Leptochoroid, 18
 Leukocoria, 178, 179*f*, 360
 Levofloxacin, 408
 LHEP. *See* Lamellar hole–associated epiretinal proliferation
 Lifestyle changes, for age-related macular degeneration, 76
 Ligament of Wieger, 5, 6*f*
 Light adaptation
 in electro-oculography, 53–54, 54–55*f*
 in electroretinography, 44*f*, 45, 46*f*, 47, 48–50*f*, 51, 52*f*

 Light injuries, 412–415, 413*f*
 Lightning injuries, 400
 Limiting membrane
 external, 10*f*, 12*f*, 13, 14*f*
 internal, 13, 14*f*, 168, 189–190, 237–239
 middle, 13, 14*f*
 Lincoff rules, 382, 384*f*
 Lipofuscin, 29–30, 32, 300, 302, 304–305, 322*f*, 325
 Lipogranuloma, 179
 Liver disease, retinal degeneration associated with, 320
 Long-chain polyunsaturated fatty acids (LCPUFAs), 75
 Long-wavelength sensitive cones, 57
 Low-coherence light, 26
LRP5 gene, 363*f*
 LUCAS (study), 92*t*
 Lupus choroidopathy, 262
 Lupus vasculitis, 262, 262*f*
 Lutein, 75–76, 76*t*, 412
 Lyme borreliosis, 278–279
 Lymphomas, 264–267, 265–266*f*, 367
 Lysosomal metabolic diseases, 327–329, 328–329*f*

 Macroaneurysms, 132–133, 165–166, 166*f*, 176, 190
 Macrocysts, 382, 385*f*, 392
 MacTel Project, 180
 Macula
 adaptive optics scanning laser ophthalmoscopy of, 11*f*
 anatomy, 7–8, 7*f*, 8*t*
 atrophy of, 292*f*, 295, 296*f*, 302, 302*f*, 306, 307, 307*f*
 infarction of, 342
 photoreceptors of, 10–11*f*, 11
 Macular branch retinal venous occlusion, 134, 136*f*
 Macular colobomas, 296
 Macular degeneration, 59, 66. *See also* Age-related macular degeneration
 Macular detachment, 303, 305*f*, 338–339, 392, 393*f*
 Macular dragging, 210, 210–212*f*
 Macular dystrophies, 300–310
 adult-onset vitelliform lesions, 303, 304–305*f*
 atypical and occult macular, 308–310, 310*f*
 Best disease, 302–303, 302*f*
 early-onset “drusenoid,” 303–306, 305–306*f*
 electroretinography findings, 47–48, 48*f*, 56
 pattern dystrophies, 306–308, 308–309*f*
 Stargardt disease, 300–302, 301*f*. *See also* Stargardt disease
 Macular edema
 cystoid, 176–178. *See also* Cystoid macular edema
 diabetic, 121–128. *See also* Diabetic macular edema
 drug-induced, 343–344, 347
 in gyrate atrophy, 299
 management, 123–128, 144, 144*f*, 178, 422, 443, 443*f*
 photocoagulation complication, 118, 425
 radiation retinopathy finding, 188
 retinal venous occlusion association, 134, 136*f*, 139, 148
 studies, 100
 Macular epiretinal membrane, 431–432, 431–432*f*
 Macular exudates, 133*f*, 134, 184, 184*f*
 Macular halo, 328, 329*f*
 Macular holes
 full-thickness, 354*t*
 idiopathic, 355–358, 356*f*, 432–433, 433*f*
 imaging techniques, 27–28*f*

- management, 358
- myopia and, 238–239, 238*f*
- posterior vitreous detachment sequelae, 350
- retinal detachment association, 394, 394*f*
- stages, 355–357, 356*f*
- trauma-related, 397, 399–400
- Macular ischemia, 134
- Macular laser, 421–422. *See also* Photocoagulation
- Macular neovascularization (MNV), 66–67, 77–87, 78*f*, 82–84*f*
- Macular pits, 400
- Macular puckering, 353
- Macular schisis, 96*f*, 237–238, 238*f*, 391–392, 391*f*
- Macular telangiectasia, 86, 180–181, 181–183*f*, 346
- Macular translocation surgery, 93
- Maculopathy
 - acute exudative polymorphous vitelliform, 323
 - acute idiopathic, 250, 259–260, 260*f*
 - adult-onset vitelliform, 74, 74*f*, 177*f*
 - bull's-eye, 318, 326, 326*f*, 334, 336*f*
 - cellophane, 353
 - drug-induced, 334, 335, 340, 345–346
 - hypotony, 230, 231*t*
 - optic pit, 392–393, 392*f*
 - paracentral acute middle, 164, 165*f*, 259, 259*f*
 - retinal detachment association, 392–393, 393*f*
 - trauma-related, 411
- Magnetic resonance imaging (MRI), 397
- Malattia Leventinese drusen, 304–305
- Malignant hypertension, 223
- α -Mannosidosis, 316*t*
- MANTA (study), 92*t*
- MAR. *See* Melanoma-associated retinopathy
- MARINA (study), 66, 88–89, 88*f*, 89*t*
- MARVEL (study), 143*t*
- Maternally inherited diabetes and deafness (MIDD), 317*t*, 330, 331*f*
- Maximal intensity projection, 29
- M cones, 57
- Mechanical photic damage, 412
- Medium-wavelength sensitive cones, 57
- MEK inhibitors. *See* Mitogen-activated protein kinase inhibitors
- Melanin, 29–30, 32, 412, 419–420, 420*f*
- Melanolipofuscin, 32
- Melanolysosomes, 32
- Melanoma-associated retinopathy (MAR), 322–323
- Melanomas, 425
- Melanosomes, 15, 16*f*
- MELAS. *See* Mitochondrial encephalopathy, lactic acidosis, stroke-like episodes
- Membranoproliferative glomerulonephritis type II, 306
- Meridional complex, 9, 9*f*
- Meridional folds, 9, 374, 374*f*, 377
- MESA (study), 66, 68
- Metabolic diseases, with retinal degeneration
 - albinism, 324–325, 325*f*
 - amino acid disorders, 329
 - central nervous system abnormalities, 316–317*t*, 325–329, 326–329*f*
 - mitochondrial disorders, 330, 330–331*f*
- Metamorphopsia, 74, 77, 95, 355
- Methanol toxicity, 343
- Methotrexate, 265
- Methoxyflurane, 346
- Methylphenidate, 346
- MEWDS. *See* Multiple evanescent white dot syndrome
- MFC. *See* Multifocal choroiditis
- MFCPU. *See* Multifocal choroiditis and panuveitis
- mfERG. *See* Multifocal electroretinography
- MFSD8 gene, 310
- Microaneurysms, 108–109, 109*f*, 178, 179*f*, 188, 239
- Microcysts, 375–376
- Micronutrients, for age-related macular degeneration, 74, 75–76, 75–76*t*
- Microperimetry, 56
- Microphthalmos, 360
- Microvasculopathy, 342–343
- MIDD. *See* Maternally inherited diabetes and deafness
- Middle limiting membrane (MLM), 13, 14*f*
- Midget bipolar cell, 13
- “Milky Way” sign, 263, 264*f*
- Mineralocorticoid receptor antagonists, 221
- Miniature telescopes (implantable), 93
- Minimally classic choroidal neovascularization (CNV), 77, 79
- Mitochondrial disorders, 317*t*, 330, 330–331*f*
- Mitochondrial encephalopathy, lactic acidosis, stroke-like episodes (MELAS), 317*t*, 330
- Mitogen-activated protein kinase (MEK) inhibitors, 338, 340*t*, 341*f*
- Mittendorf dot, 358
- Mizuo-Nakamura phenomenon, 287, 288*f*
- MLM. *See* Middle limiting membrane
- MNV. *See* Macular neovascularization
- Modified Scheie Classification of Hypertensive Retinopathy, 132
- Monochromatism, 284, 284*t*
- Morphopsia, 425
- Mosquito-borne diseases, 279–281
- “Mother spot,” 181. *See also* Phakomatoses
- Motion artifacts, 29
- Motion contrast, 28–29
- Moxifloxacin, 408
- MPSS. *See* Mucopolysaccharidoses
- MRI. *See* Magnetic resonance imaging
- Mucopolysaccharidoses (MPSs), 316*t*, 319*t*, 327
- Müller cells, 13, 14*f*, 180, 313, 390
- Multifocal choroiditis (MFC), 39, 95, 239, 250, 251*t*, 256–257, 256–257*f*, 272
- Multifocal choroiditis and panuveitis (MFCPU), 256
- Multifocal electroretinography (mfERG), 49–51, 50*f*, 52*f*
- Multifocal pattern dystrophy, 306
- Multiple evanescent white dot syndrome (MEWDS), 251*t*, 254–255, 254*f*
- Multiple sclerosis, 55
- Mycobacterium tuberculosis*, 272
- Myoid, 11, 13
- Myopia
 - age-related choroidal degeneration association, 227
 - drug-induced, 347
 - electroretinography testing and, 47
 - pathologic, 235–247. *See also* Pathologic myopia
 - retinopathy of prematurity association, 209–210
- Myopic macular schisis, 96*f*, 237–238, 238*f*
- Myotonic dystrophy, 316*t*

- Nanoparticles, 457
- NARP. *See* Neurogenic muscle weakness, ataxia, and retinitis pigmentosa
- National Stroke Association, 160
- Nausea and vomiting, fluorescein angiography as cause of, 36–37
- NCLs. *See* Neuronal ceroid lipofuscinoses
- Nd:YAG laser, 178, 412, 442, 443
- Near-infrared fundus autofluorescence, 32, 50f, 52f
- Near periphery, 8
- Necrotizing herpetic retinitis, 268–269f, 268–270, 270t
- Necrotizing retinochoroiditis, 275–276
- Needle injuries, 402, 445, 446f
- Neonatal adrenoleukodystrophy, 317t, 326, 327f
- Neoplasms, 230
- Neovascular age-related macular degeneration (AMD), 77–93
 about, 77
 anatomical classification, 77–78, 78f
 clinical findings, 77
 differential diagnosis, 82, 86
 gene therapy for, 456t, 457
 hemorrhage in, 434–435, 434f
 imaging techniques, 78–85, 79–84f
 management, 86–93, 88f, 89t, 92t
 nonexudative, 78
 polypoidal choroidal vasculopathy and, 85–86, 85–86f
 risk factors, 70
- Neovascular glaucoma, 188
- Neovascularization
 in branch retinal vein occlusion, 137, 145–146, 146–147f
 in central retinal artery occlusion, 162
 in central retinal vein occlusion, 137, 148, 149, 151–152
 in central serous chorioretinopathy, 218
 choroidal. *See* Choroidal neovascularization
 iris. *See* Iris neovascularization
 in ocular ischemic syndrome, 152–153, 152–153f, 154
 optic nerve, 188
 optic nerve head, 114, 137, 139f, 145–146, 146–147f, 188, 388f
 pathogenesis, 135, 137
 in peripheral retinal, 168, 169–171, 169f, 173f, 174t, 367
 in retinopathy of prematurity, 196–197
 sea fan lesions, 168, 171, 173f, 175
 subretinal, 180
- Neovascularization elsewhere (NVE), 114, 114f
- Neovascularization of the disc (NVD), 114, 114f
- Nerve fiber layer (NFL)
 anatomy, 10f, 13
 cotton-wool spots of, 132, 132–133f, 154, 155f
- Nerve head sign of sickling, 171
- Neurogenic muscle weakness, ataxia, and retinitis pigmentosa (NARP), 330
- Neuromuscular disorders, 316t, 319
- Neuronal ceroid lipofuscinoses (NCLs), 317t, 325–326, 326f
- Neuroretinitis, 134, 274
- NFL. *See* Nerve fiber layer
- Niacin, 343
- Nicotinic acid, 178, 343
- Niemann-Pick disease (NPD), 328, 329f
- Night blindness. *See* Nyctalopia
- N95, 51
- Nodular posterior scleritis, 230f
- Nonarteritic anterior ischemic optic neuropathy, visual evoked potentials in, 55
- Non-center-involved diabetic macular edema, 101, 122, 123f
- Non-CMV necrotizing herpetic retinitis, 268–269f, 268–270, 270t
- Noncontact indirect biomicroscopy, 22
- Noncystic retinal tufts, 371, 373f
- Nonexpulsive suprachoroidal hemorrhage, 444
- Nonexudative macular degeneration, 59, 66
- Nonexudative neovascular age-related macular degeneration (AMD), 78
- Non-Hodgkin diffuse large B-cell lymphoma, 264
- Non-insulin dependent diabetes mellitus, 100
- Nonischemic (perfused) central retinal venous occlusion (CRVO), 148, 149f
- Nonneovascular age-related macular degeneration (AMD), 69–77
 about, 69
 differential diagnosis, 73–74, 74f
 drusen, 67, 67f, 69–71, 69f, 71f, 75
 management, 74–77, 76t
 prognosis, 75t
 retinal pigment epithelium abnormalities, 71–73, 72–73f
- Nonperfused (ischemic) central retinal venous occlusion (CRVO), 148–149, 150f
- Nonproliferative diabetic retinopathy (NPDR), 108–111
 defined, 100–101
 examination schedules, 105t
 progression of, 108–111, 109–110f
 studies, 105
 treatment, 111, 112–113t
- Nonproliferative sickle cell retinopathy (NPSR), 168, 169–172f
- Nonsteroidal anti-inflammatory drugs (NSAIDs), 177f, 178
- Nonsyndromic panretinal dystrophies, 289–290
- North Carolina macular dystrophy, 308–309, 311f
- NPD. *See* Niemann-Pick disease
- NPDR. *See* Nonproliferative diabetic retinopathy
- NPSR. *See* Nonproliferative sickle cell retinopathy
- NR2E3 gene, 53, 297
- NRTIs. *See* Nucleoside reverse transcriptase inhibitors
- NSAIDs. *See* Nonsteroidal anti-inflammatory drugs
- Nuclear sclerotic cataract, 420–421, 451
- Nucleoside reverse transcriptase inhibitors (NRTIs), 337–338
- NVD. *See* Neovascularization of the disc
- NVE. *See* Neovascularization elsewhere
- Nyctalopia
 about, 285–288, 286–288f
 Bietti crystalline dystrophy association, 300
 birdshot chorioretinopathy finding, 255
 cone-rod dystrophy association, 296
 drug-induced, 337, 347
 electroretinography findings, 49f, 52
 Goldmann-Favre disease and, 297
 gyrate atrophy association, 299

- melanoma-associated, 323
- psychophysical evaluations, 61
- rod-cone dystrophy association, 291
- vitamin A deficiency and, 326
- Nystagmus, 56, 284–285, 296
- NYX gene, 286
- OAT gene, 299
- Occlusive ischemic syndrome, 108
- Occlusive retinopathy, 342–343
- Occlusive vascular diseases. *See* Arterial occlusive disease; Retinal venous occlusion
- Occult choroidal neovascularization (CNV), 37f, 77, 78f, 79
- Occult macular dystrophies, 309–310
- Occupational light toxicity, 414
- OCT. *See* Optical coherence tomography
- OCTA. *See* Optical coherence tomographic angiography
- Ocular albinism, 56, 284, 324
- Ocular argyrosis, 347
- Ocular bartonellosis, 274, 276f
- Ocular globe trauma. *See* Globe injuries
- Ocular histoplasmosis syndrome (OHS), 93–95, 94f
- Ocular ischemic syndrome (OIS)
 - clinical findings, 152–153, 152–153f
 - course and prognosis, 154
 - differential diagnosis, 150, 153
 - etiology, 153
 - management, 154
- Ocular Lyme borreliosis, 278–279
- Ocular trauma. *See* Trauma
- Ocular Trauma Score, 409, 409t
- Ocular tuberculosis, 272–273, 273f
- Oculocutaneous albinism, 56, 324
- Oculodentodigital dysplasia (syndrome), 316t
- Oculodigital reflex, 296
- Oguchi disease, 287
- “Ohno” sign, 263
- OHS. *See* Ocular histoplasmosis syndrome
- OIS. *See* Ocular ischemic syndrome
- Olivopontocerebellar atrophy, 316t
- Omega-3 and omega-6 fatty acids, 75, 294
- OMIC. *See* Ophthalmic Mutual Insurance Company
- OMIM. *See* Online Mendelian Inheritance in Man website
- Onion sign, 81
- ONL. *See* Outer nuclear layer
- Online Mendelian Inheritance in Man (OMIM) website, 288
- Onset-offset (pattern-reversal pattern) visual evoked potentials (VEPs), 55, 56, 56f
- Opacities, vitreous, 364–367, 364f, 366f, 429, 435
- Open-angle glaucoma, 136, 151
- Open-globe injuries, 401–407
 - classification, 395–396
 - evaluations, 396–397, 396t
 - lacerating and penetrating, 263, 395, 402, 408
 - management, 402–404
 - perforating, 395, 402, 408
 - prognostication, 409–410, 409t
 - scleral rupture, 401–402
 - sequelae, 401
- Operculated retinal holes, 376, 377, 379t, 380
- Operculum, 356–357f, 357, 378f
- Ophthalmic artery occlusion, 162–163, 164f
- Ophthalmic Mutual Insurance Company (OMIC), 213
- Ophthalmoscopy
 - direct, 22
 - indirect, 22–23
 - scanning laser, 24–26, 25f, 30–32, 31f
- OPL. *See* Outer plexiform layer
- Opportunistic infections, 267
- Optical coherence tomography (OCT)
 - about, 26–28, 27–28f, 32
 - angiography, 28–29, 30f
 - laser therapy guidance with, 127
 - spectral-domain, 26–27, 50f, 52f
- Optical coherence tomography angiography (OCTA), 28–29, 30f
- Optic atrophy, 51, 188
- Optic disc drusen, 40, 95, 95f
- Optic nerve
 - anatomy, 13
 - electrophysiologic evaluations, 55
 - myopia and, 246–247, 246–247f
 - racemose hemangiomas of, 186, 186f
- Optic nerve head (optic disc)
 - avulsion of, 398, 410, 410f
 - drusen of, 291, 304
 - edema, 120, 133f, 134, 188, 190
 - hemangiomas of, 186
 - hemorrhage and, 190, 398, 399f
 - neovascularization of, 114, 137, 139f, 145–146, 146–147f, 188, 388f
- Optic nerve pit(s), 392–393, 393f
- Optic neuritis, 55, 56f
- Optic neuropathy, 133f, 134, 188, 343, 424
- Optic pit maculopathy, 392–393, 393f
- Optociliary shunt vessels, 137–138, 139f
- Optogenetics, 457f, 458
- Ora bays, 9, 9f, 374, 374f, 377
- Oral contraceptives, 342
- Orange reflex, 158
- Ora serrata, 8, 9f, 22
- Ornithine, 299
- Oscillatory potentials, 47, 49f, 51
- Outer nuclear layer (ONL), 10f
- Outer plexiform layer, 10f, 13, 14
- Outer retinal tubulation, 73, 73f
- Outer-schisis-layer holes, 391f
- Outer segments, 12f, 13, 15–17, 16f
- Oxalate, 346
- Oxygen, 7, 13, 18, 199
- Pachychoroid, 18, 85
- Pachychoroid phenotype, 219
- Pachychoroid pigment epitheliopathy, 219
- Pachychoroid spectrum, 219–220
- Pachyvessel, 219
- Paclitaxel, 343
- Paget disease of bone, 95
- PAMM. *See* Paracentral acute middle maculopathy
- Pancreatitis, 192
- Panel tests, 58–59, 59f
- Panophthalmitis, 271

- PANORAMA (study), 100, 111
- Panretinal dystrophies, 289–290, 291
- Panretinal photocoagulation (PRP)
- about, 422–423, 423*f*
 - diabetic macular edema treatment, 127
 - diabetic retinopathy treatment, 111, 112*t*, 115, 116–120, 119*f*
 - ocular ischemic syndrome treatment, 154
 - retinal venous occlusion treatment, 140*t*, 146, 151
- Panuveitis
- Behçet disease association, 261
 - differential diagnosis, 95
 - Ebola virus association, 281
 - imaging techniques, 39
 - syphilitic, 274
 - toxocariasis association, 277
 - Vogt-Koyanagi-Harada disease association, 263
- Papilledema, 231*t*
- Papillopathy, 120
- Paracentral acute middle maculopathy (PAMM), 164, 165*f*, 259, 259*f*
- Paracentral scotomata (scotomas), 77, 95, 127, 259, 412, 413–414
- Parafovea, 7*f*, 8, 8*t*, 168
- Paraneoplastic retinopathies, 322–323, 323*f*
- Parasitic infections, 279
- Parinaud oculoglandular syndrome, 274
- Pars plana, 9, 9*f*
- Pars plana vitrectomy
- complications, 451–452, 451*t*
 - diabetic macular edema treatment, 127
 - diabetic retinopathy treatment, 119
 - foreign-body removal, 406
 - macular hole treatment, 358
 - principles of, 429–431, 430*t*
 - retinal venous occlusion treatment, 148, 152
 - vitreous hemorrhage association, 365
- Patch atrophy, 243
- Patellar fossa, 5
- Patent foramen ovale, 15*f*
- Pathologic myopia, 235–247
- about, 235
 - clinical findings, 235, 236*t*
 - management, 238–240, 241*f*
 - pathogenesis
 - Bruch membrane, 239, 240*f*, 246, 246*f*
 - choroid, 239–243, 240–244*f*
 - optic nerve, 246–247, 246–247*f*
 - retina, 236–239, 237–238*f*
 - sclera, 237*f*, 243–246, 245*f*
- Pattern-appearance stimulation, of visual evoked potentials, 56
- Pattern dystrophies, 74, 303, 304*f*, 306–308, 308–309*f*
- Pattern electroretinography (PERG), 50*f*, 51, 52*f*
- Pattern-reversal pattern (onset-offset) visual evoked potentials (VEPs), 55, 56, 56*f*
- Pattern scanners, 423
- Patton lines, 230, 231*t*
- Paving-stone degeneration, 374–375, 375*f*
- PCARE mutation, 292*f*
- PCIOs. *See* Posterior chamber intraocular lenses
- PCV. *See* Polypoidal choroidal vasculopathy
- PDE-5. *See* Phosphodiesterase-5 inhibitors
- PDR. *See* Proliferative diabetic retinopathy
- PDT. *See* Photodynamic therapy
- Peau d'orange, 95, 95*f*
- PED. *See* Pigment epithelial detachment
- Pediatric eye trauma, 377–379
- Pegaptanib, 88
- Pelizaeus-Merzbacher disease, 317*t*
- Pelli-Robson test, 60, 60*f*
- Penetrating injuries, 263, 395, 402, 408
- Penicillin, 279
- Pentosan polysulfate, 340, 340*t*, 342*f*
- Perfluorocarbon, 430, 449, 451
- Perfluoropropane, 430
- Perforating injuries, 395, 402, 408
- Perfused central retinal venous occlusion (CRVO), 148, 149*f*
- PERG. *See* Pattern electroretinography
- Pericytes, 102
- Perifovea, 7*f*, 8, 8*t*, 176
- Peripapillary intrachoroidal cavitations, 243, 244*f*
- Peripheral anterior synechiae, 119
- Peripheral cystoid degeneration, 375–376, 390–391
- Peripheral granuloma, in toxocariasis, 277
- Peripheral necrotizing herpetic retinitis, 268*f*
- Peripheral retina, 8
- Peripheral retinal excavations, 374
- Peripheral retinal neovascularization
- amyloidosis finding, 367
 - differential diagnosis, 174*t*
 - in sickle cell retinopathy, 168, 169–171, 169*f*, 173*f*
- Peripheral retinal photocoagulation, 422–423, 423*f*.
See also Photocoagulation
- Peripheral schisis, 310
- Peripheral vision field loss, 118, 291
- Periphlebitis, 267
- Peroxisomal disorders, 326–327
- Persistent fetal vasculature (PFV), 360
- Persistent placoid maculopathy, 252
- Petaloid pattern, 176, 177*f*
- P50, 51
- PFV. *See* Persistent fetal vasculature
- Phacoemulsification, 441
- Phagocytosis, 13, 16–17, 32, 217, 218*f*
- Phakomatoses, 181–187
- about, 181
 - retinal cavernous hemangioma, 186–187, 187*f*
 - von Hippel-Lindau syndrome, 181–185, 184–185*f*
 - Wyburn-Mason syndrome, 186, 186*f*
- Phenothiazines, 337, 338*f*
- Phlebectasias, 178
- Phosphodiesterase-5 inhibitors (PDE-5), 347
- Photoc damage, 412–415, 413*f*
- Photochemical injuries, 412
- Photocoagulation
- aneurysm treatment, 165–166
 - Coats disease treatment, 179
 - complications, 175, 424–425
 - cystoid macular edema treatment, 178
 - diabetic macular edema treatment, 112*t*, 122, 124, 125*f*, 126, 127–128
 - diabetic retinopathy treatment, 104, 107*t*, 111, 112*t*, 115, 116–120, 118–119*f*, 118*f*
 - hemangioma treatment, 231

- myopic choroidal neovascularization treatment, 239
- neovascular age-related macular degeneration
 - treatment, 87
- principles of, 419–425
 - alternative laser delivery systems, 423–424
 - anesthesia for, 421
 - laser wavelength, 420–421
 - lenses, 421, 422*f*
 - overview, 419, 420*f*
 - parameters and indications, 421–423
- radiation retinopathy treatment, 189
- retinal break treatment, 379
- retinal cavernous hemangioma treatment, 187
- retinal venous occlusion treatment, 139, 140*t*, 145, 146, 147, 147*f*, 151
- retinopathy of prematurity treatment, 200*f*, 205*t*, 207, 208
- sickle cell retinopathy treatment, 175
- types of, 421–423
- von Hippel–Lindau syndrome treatment, 184
- Photodynamic therapy (PDT)
 - about, 426
 - age-related macular degeneration treatment, 87, 93
 - central serous chorioretinopathy treatment, 221
 - choroidal neovascularization treatment, 239, 241*f*
 - combination treatments that include, 93
 - complications, 426
 - diabetic retinopathy treatment, 88
 - hemangioma treatment, 231
 - pathologic myopia treatment, 96
 - polypoidal choroidal vasculopathy treatment, 85, 426
 - von Hippel–Lindau syndrome treatment, 184–185, 185*f*
- Photophobia, 52–53, 295
- Photopsias. *See also* Floaters
 - electrophysiologic evaluations, 53
 - photocoagulation adverse effect, 118
 - in posterior vitreous detachment, 369–370
 - in retinal detachments, 382
- Photoreceptor dystrophies
 - cone dystrophies, 47–48, 48*f*, 52–53
 - cone–rod dystrophies, 47–48, 295–296, 296*f*, 322
 - rod–cone, 291–295, 292–295*f*. *See also* Retinitis pigmentosa
- Photoreceptor(s). *See also* Cone(s); Rod(s)
 - age-related changes, 67, 67*f*
 - anatomy, 11–13, 12*f*, 15–17, 16*f*
 - density and distribution of, 9–11, 10–11*f*
 - electroretinography testing of, 45–51, 46*f*, 48–49*f*
 - gene therapy for, 458
 - imaging, 32
 - phagocytosis of, 32
 - posttraumatic injuries, 398
 - shaggy, 218*f*
- Photo-ROP Cooperative Group, 203
- Phototoxicity from ophthalmic instrumentation, 413–414
- PHP. *See* Preferential hyperacuity perimetry
- Physiological testing. *See* Electrophysiologic testing
- PIC. *See* Punctate inner choroiditis
- PIER (study), 66, 88, 88*f*
- Pigmentary maculopathy, 340, 411
- Pigmentary retinopathy
 - about, 290, 315
 - didanosine complication, 340*t*
 - phenothiazine complication, 337
 - syndromic
 - Bardet–Biedl syndrome association, 318–319, 318*f*
 - dental disease association, 322
 - dermatologic disease association, 320–322, 322*f*
 - gastrointestinal tract disease association, 320, 321*f*
 - liver disease association, 320
 - metabolic diseases with CNS abnormalities, 325, 326, 327
 - mitochondrial disorder association, 330
 - neuromuscular disorder association, 316*t*, 319, 319*t*
 - overview, 315, 316–317*t*
 - Usher syndrome association, 319, 319*t*
 - unilateral, 292–293
- Pigmented paravenous retinopathy, 293
- Pigment epithelial detachment (PED)
 - drusen formation and, 70
 - fibrovascular, 77, 79, 81, 85, 91
 - imaging, 80–81*f*, 81
 - serous, 81
 - subfoveal, 81*f*
 - vascularized serous, 79, 80*f*
- Pigment granules, 365
- Pioglitazone, 343
- PIOL. *See* Primary intraocular lymphoma
- Pisciform (fish-shaped) flecks, 300, 301*f*, 302
- PLANET (study), 66, 85
- Platelet–fibrin emboli, 156, 158*f*
- “Plucked chicken” skin, 96, 321
- Plus disease, 195*t*, 197*f*, 198*f*
- Pneumatic displacement, 93
- Pneumatic retinopexy, 447–448, 447*f*
- POHS. *See* Presumed ocular histoplasmosis syndrome
- Poliosis, 263
- Polydactyly, 318, 318*f*
- Polypoidal choroidal vasculopathy (PCV)
 - description of, 85–86, 85–86*f*
 - differential diagnosis, 218, 219
 - imaging techniques, 39, 39*f*
 - management, 85, 93
- Polypoidal choroidopathy, 34*f*
- Pooling hyperfluorescence, 34*f*, 35, 35*t*, 36
- “Poppers” (alkyl nitrites), 340, 340*t*, 341*f*
- PORN. *See* Progressive outer retinal necrosis syndrome
- Port-wine birthmark (ipsilateral facial nevus flammeus), 231
- Posterior (aggressive) retinopathy of prematurity, 195*t*, 196–197, 199*f*
- Posterior chamber intraocular lenses (PCIOs), 442–443
- Posterior ciliary arteries, 17–18, 18*f*, 222, 223*f*
- Posterior perifoveal vitreous detachment, 350
- Posterior persistent fetal vasculature, 360
- Posterior pole, 7*f*, 8*t*
- Posterior pole granuloma, 277
- Posterior scleritis, 230*f*
- Posterior segment, blunt trauma sequelae, 397–398, 401. *See also* Closed-globe injuries; Open-globe injuries
- Posterior uveal bleeding syndrome, 85. *See also* Polypoidal choroidal vasculopathy

- Posterior uveitis, 34*f*, 47, 265
 Posterior vitreoschisis, 350, 351
 Posterior vitreous detachment (PVD)
 about, 349
 astteroid hyalosis association, 364
 cholesterolosis association, 366
 clinical findings, 369–370, 370*f*
 diagnosis, 350, 350–352*f*
 differential diagnosis, 190
 epiretinal membranes and, 351–354, 353*f*, 355, 355*f*
 etiology and epidemiology, 349–350
 idiopathic macular holes, 355–358, 356–357*f*
 management, 370–371
 myopia macular retinoschisis in, 237–238, 238*f*
 retinal tears caused by, 369
 vitreomacular traction diseases and, 350, 351*f*, 354–355, 354*t*, 355*f*
 vitreous hemorrhage association, 365
 Postoperative endophthalmitis, 437–441, 438*t*, 439–440*f*
 Posttraumatic endophthalmitis, 407–409
 Posttraumatic macular hole, 399–400
 Precortical vitreous pocket, 6*f*, 7
 Prednisone, 276
 Preeclampsia, 223–225, 224*f*
 Preferential hyperacuity perimetry (PHP), 77
 Pregnancy
 central serous retinopathy association, 217
 diabetic retinopathy association, 103–104, 104*t*
 diagnostic imaging precautions, 38
 premature births, 193–194, 199
 Toxoplasma gondii exposure, 275
 Zika virus exposure during, 279–281
 Premacular bursa, 6*f*, 7
 Premature births, 193–194, 199
 Prepapillary vascular loops, 358, 359*f*
 Preretinal hemorrhage, 114, 114*f*, 425
 Preretinal macular fibrosis, 353
 Preretinal tract, 5
 Preserved para-arteriolar retinal pigment epithelium phenotype, 179
 Presumed ocular histoplasmosis syndrome (POHS), 94
 Prethreshold disease, 194, 199*t*
 Primary intraocular lymphoma (PIOL), 264
 Primary repair, of open-globe injuries, 403
 Primary vitrectomy, 449–450, 449*f*
 Primary vitreoretinal lymphoma, 264–265
 Procainamide, 342
 Progressive outer retinal necrosis (PORN) syndrome, 268, 269*f*
 Projection artifacts, 29
 Proliferative diabetic retinopathy (PDR), 111–120
 complications, 119–120
 epidemiology, 101
 eye examination schedules, 105*t*
 high-risk characteristics, 114–115, 114*f*
 management
 complications, 175
 goals of, 115
 mandatory treatment, 114–115, 114*f*
 nonpharmacologic, 104, 117–119, 118–119*f*
 pharmacologic, 115–117, 116*f*
 neovascularization and, 169–171
 pregnancy-related, 104
 progression of, 111, 114–115
 studies, 105
 traction retinal detachment association, 388*f*
 vitreous hemorrhage association, 365
 Proliferative vitreoretinopathy (PVR), 382, 386*f*, 387*t*, 401
PROM1 gene, 302, 309
Propionibacterium acnes, 438, 440*f*
 Prostaglandin F_{2a} analogs, 344
 Prosthesis, retinal, 295
 Protan red-green color deficiency, 57, 59
 PRP. *See* Panretinal photocoagulation
PRPH2 gene, 302, 303, 308
 Pseudodrusen
 age-related choroidal degeneration association, 229, 229*f*
 imaging techniques, 25
 in pseudoxanthoma elasticum, 226
 reticular, 70, 71*f*
 “Pseudohole” appearance, 351–352, 431–432*f*
 Pseudoisochromatic plates, 58, 58*f*
 Pseudophakia, 381, 446
 Pseudophakic cystoid macular edema, 176–178, 177*f*
 Pseudo-POHS. *See* Pseudo-presumed ocular histoplasmosis syndrome
 Pseudo-presumed ocular histoplasmosis syndrome (pseudo-POHS), 256
 Pseudoxanthoma elasticum (PXE), 95–96, 95*f*, 226, 227*f*, 308, 321
 Psychophysical tests, 56–61
 about, 56–57
 color vision, 57–59, 58–59*f*
 contrast sensitivity, 59–60, 60*f*
 dark adaptometry, 61
 “Punched-out” chorioretinal scars, 94
 Punctate inner choroiditis (PIC), 250, 251*t*, 256
 Pupillary dilation, 118
 Purtscher flecken, 190, 191*f*
 Purtscher-like retinopathy, 190*t*, 191–192, 191*f*
 Purtscher retinopathy, 190, 190*t*
 PVD. *See* Posterior vitreous detachment
 PVR. *See* Proliferative vitreoretinopathy
 PXE. *See* Pseudoxanthoma elasticum
 Pyrimethamine, 276
 Quadruple therapy, for toxoplasmic retinochoroiditis, 276
 Quinine, 343, 344*f*
R9AP gene, 53
 Rab escort protein (REP1), 299
 Rab proteins, 299
 Race and ethnicity
 age-related macular degeneration prevalence, 68
 Behçet disease and, 261
 birdshot chorioretinopathy and, 255
 diabetic retinopathy and, 101–102
 drug-induced toxicity and, 334
 polypoidal choroidal vasculopathy and, 85
 sickle cell hemoglobinopathies and, 167, 174–175
 systemic lupus erythematosus and, 262
 Vogt-Koyanagi-Harada disease and, 263
 Racemose hemangiomas, 186, 186*f*

- Radial peripapillary capillary network, 13
- Radial striae, 310, 312
- Radiation, 187–189, 231, 265
- Radiation papillopathy, 134
- Radiation retinopathy, 179, 187–189, 188f
- RAINBOW (study), 206t, 208, 209
- Ranibizumab
- age-related macular degeneration treatment, 66, 85, 88–93, 88f, 89t, 92t
 - diabetic macular edema treatment, 112t, 124–125, 125f
 - diabetic retinopathy treatment, 88, 111, 115
 - retinal venous occlusion treatment, 141–143t, 144, 145
 - retinopathy of prematurity treatment, 206t, 208
 - route of administration, 452
- RAPs. *See* Retinal angiomatous proliferations
- RDH5* gene, 286
- Reactive retinal astrocytic tumor, 179
- Recurrent multifocal choroiditis (RMC), 256
- Red blood cell–induced (erythroclastic) glaucoma, 119
- Red cones, 57
- Red-green color deficiency, 57
- Refractile spots, 168
- Refsum disease, 316t, 319t, 324, 327
- Relentless placoid chorioretinitis, 252
- Renal diseases, 318, 320, 334
- Renal-retinal dysplasia, 320
- REP1. *See* Rab escort protein
- Retained foreign bodies, 404f, 406–407, 407t, 408f, 441–442, 441t
- Reticular degenerative retinoschisis, 390, 390f, 391
- Reticular peripheral cystoid degeneration, 375–376, 389–390
- Reticular pseudodrusen, 70, 71f
- Reticular-type pattern dystrophy, 306, 308f
- Reticulum cell sarcoma. *See* Primary vitreoretinal lymphoma
- Retina
- anatomy. *See also* Retinal pigment epithelium layers and neurosensory elements, 9–13, 10–12f, 14f, 15–17, 16f
 - topography, 7–8, 7f, 7t, 9f
 - vasculature and oxygen supply, 13–14, 15f, 18–19, 193, 194
 - electrophysiologic testing, 43–56. *See also* Electrophysiologic testing
 - myopia and, 236–249, 237–238f
 - psychophysical testing of. *See* Psychophysical tests
- Retinal angiomatous proliferations (RAPs), 39, 78, 79
- Retinal artery occlusion. *See* Arterial occlusive disease
- Retinal breaks
- classification, 376, 377f
 - clinical findings, 384f
 - defined, 369
 - etiology, 376–379, 377–378f
 - formation of, 369, 371, 378f
 - management
 - closure, 385–387
 - prophylactic treatment, 379–381, 379t, 380f
- Retinal burns, 412, 424
- Retinal capillaries, 109, 122, 176
- Retinal cavernous hemangioma, 186–187, 187f
- Retinal degeneration
- about, 315
 - metabolic diseases with
 - albinism, 324–325
 - amino acid disorders, 329
 - central nervous system abnormalities, 316–317t, 325–329, 326–329f
 - mitochondrial disorders, 330, 330–331f
 - with systemic involvement, 315–324. *See also* Systemic diseases, with retinal degeneration
- Retinal detachment, 369–394. *See also* Exudative retinal detachment
- about, 369
 - bullous, 310
 - causes, 115, 120
 - central serous chorioretinopathy as cause of, 215
 - classification, 381–382
 - complex, 450
 - differential diagnosis, 382, 389–391, 390–391f
 - electroretinography findings, 47
 - fellow-eye risk, 381
 - hypertension and, 223
 - hypertensive choroidopathy association, 134
 - imaging techniques, 34f, 40
 - lesions, not predisposing to, 374–376, 375f
 - lesions, predisposing to, 371–374, 372–374f
 - macular lesion association, 392–394, 393–394f
 - management
 - outcomes following surgery, 450–451
 - surgery, 436–437, 436f, 445–451, 446–449f
 - myopia and, 237
 - non-CMV necrotizing herpetic retinitis association, 269–270
 - posterior vitreous detachment and, 369–371, 370f
 - prevention, 379–381, 379t
 - psychophysical tests, 56–61. *See also* Psychophysical tests
 - retained lens fragment complication, 442
 - retinal breaks and
 - prophylactic treatment, 379–381, 379t, 380f
 - types of, 376–379, 377–378f
 - retinal tears and, 365
 - retinopathy of prematurity association, 210, 210–211f
 - sickle cell retinopathy association, 175
 - Stickler syndrome association, 361
 - trauma-related, 397, 401
 - types of. *See* Exudative retinal detachment; Rhegmatogenous retinal detachment; Traction retinal detachment
 - von Hippel–Lindau syndrome association, 184, 184f
- Retinal dialyses, 376, 377, 379t, 382, 385f
- Retinal dystrophies
- classification, 289
 - diagnostic considerations, 289–290
 - genetics, 290
 - management, 290–291
 - photoreceptor dystrophies
 - cone and cone–rod, 295–296, 296f
 - rod–cone, 287, 291–295, 292–295f
 - systemic disease association, 318
 - terminology, 288
 - X-linked retinoschisis, 310–313, 312f

- Retinal folds
 developmental abnormality, 360, 362
 proliferative vitreoretinopathy finding, 387*t*, 389
 trauma-related, 411
- Retinal grafts, 358
- Retinal hemangioblastomas (RH), 179, 181–185,
 184–185*f*, 186
- Retinal hemorrhage, 342, 411, 411*f*
- Retinal holes
 atrophic, 371, 372–373*f*, 376, 378*f*, 379*t*, 380
 photocoagulation-related, 424–425
- Retinal Information Network, 288
- Retinal ischemia, 108, 111, 145, 160–161, 161*f*
- Retinal pigment epithelium (RPE)
 age-related changes, 67, 67*f*, 69–70, 69*f*, 71–73,
 72–73*f*, 77
 anatomy and physiology of, 15–17, 16*f*, 18
 atrophy of, 66, 70, 71–73, 72*f*, 119*f*, 226, 303, 331*f*, 425
 Bardet-Biedl syndrome, 318–319, 318*f*
 central serous chorioretinopathy and, 215, 216–217,
 216*f*, 218*f*
 choroidal perfusion abnormalities association, 226
 choroidal thinning and, 242–243, 243*f*
 degeneration of, 289–290
 depigmentation of, 257, 258*f*
 detachment of. *See* Pigment epithelial detachment
 drug-induced abnormalities, 333–337, 334–336*f*, 338*f*
 electrophysiologic evaluations, 53–55, 54*f*
 functions, 13, 15–17, 32, 217, 218*f*
 hyperpigmentation of, 119*f*
 hyperplasia of, 372, 375
 hypertrophy of, 375
 overview, 315, 316–317*t*
 pigmentary retinopathy and, 315–322, 316–317*t*.
See also Pigmentary retinopathy
 Stargardt disease findings, 300, 301*f*, 302
 tears, 30, 31–32, 31*f*, 91
- Retinal precipitates, 274
- Retinal tears. *See also* Retinal breaks
 anatomy, 8
 defined, 369
 formation of, 378*f*
 imaging techniques, 40
 lesions, predisposing, 371, 372, 374
 management, 379–380, 379*t*, 423, 427
 myopia and, 237
 retained lens fragment complication, 442
 retinopathy of prematurity association, 212*f*
 Stickler syndrome association, 361
 trauma-related, 397
 vitreous hemorrhage association, 365
- Retinal telangiectasia, 178, 179*f*, 186
- Retinal tufts, 371–372, 373*f*
- Retinal vasculitis, 29, 34*f*, 175–176, 175*f*
- Retinal vasoproliferative tumor (VPT), 179, 185
- Retinal venous occlusion (RVO), 134–152
 about, 134
 branch, 145–148. *See also* Branch retinal vein
 occlusion
 central. *See* Central retinal vein occlusion
 clinical findings, 134, 135–138*f*
 complications, 137–138, 139*f*
 cystoid macular edema etiology, 176
 differential diagnosis, 179
 drug-induced, 342
 management, 138–139, 140–143*t*, 144–145, 144*f*
 pathogenesis, 134–135
 risk factors, 135–137
- Retinitis, 249–281
 about, 249
 Chikungunya virus, 281
 chorioretinitis sclopetaria, 398, 401, 401*f*
 cytomegalovirus, 267–268, 267*f*, 269, 270*t*
 infectious diseases, 267–280
 necrotizing herpetic, 268–269*f*, 268–270, 270*t*
 neuroretinitis, 274
 solar retinitis, 412–413, 413*f*
 white dot syndromes, 250–260. *See also* White dot
 syndromes
- Retinitis pigmentosa (RP; rod-cone dystrophies)
 clinical findings, 179, 291–293, 292–295*f*
 cystoid macular edema etiology, 176, 178
 differential diagnosis, 178, 285, 287, 297, 310, 324, 334
 electrophysiologic findings, 47, 48*f*, 53, 54
 electroretinography evaluations, 45–47, 46*f*, 52
 gene therapy for, 458
 management, 294–295
 sector retinitis pigmentosa, 47, 291–293, 295*f*
 systemic disease association, 219, 318, 319, 330
 X-linked, 53, 291, 456, 456*t*, 458
- Retinitis pigmentosa sine pigmento, 291, 318
- Retinitis punctata albescens, 287, 287*f*
- Retinitis sclopetaria, 401*f*
- Retinopathy. *See also* Chorioretinopathy; Diabetic
 retinopathy; Pigmentary retinopathy; Retinopathy
 of prematurity; Sickle cell retinopathy
 ABCA4 retinopathy, 47–48, 50*f*
 acute macular neuroretinopathy, 250, 257–259, 259*f*
 cancer-associated, 322–323, 323*f*
 drug-induced, 342–343, 344–346, 345–346*f*, 346*t*
 familial exudative vitreoretinopathy, 179, 360,
 362–363, 362*t*
 hypertensive retinopathy, 132–133, 132–133*f*
 hyperviscosity retinopathy, 150
 Purtscher and Purtscher-like retinopathy, 190*t*,
 191–192, 191*f*
 radiation retinopathy, 179, 187–189, 188*f*
 Valsalva retinopathy, 189–190, 189*f*
 venous stasis retinopathy, 153
- Retinopathy of prematurity (ROP), 193–213
 about, 193
 associated conditions, 209–210
 classification, 194, 195–200*f*, 195*t*
 clinical findings, 362*t*
 differential diagnosis, 179, 360, 362, 362*t*
 etiology and epidemiology, 193–194, 362*t*
 fundus photographic screening, 203
 management, 204, 205–206*t*, 207–209
 medicolegal aspects of, 211–213
 pathogenesis, 199–201
 prevention, 203–204
 screening recommendations, 201–203
 sequelae of, 210, 210–212*f*
 terminology, 194–199, 199*t*
- Retinopexy, 422–423, 423*f*, 447–448, 447*f*
- Retinoschisin, 313

- Retinoschisis
 differential diagnosis, 382, 389–392, 390–391*f*, 391*t*
 gene therapy for, 456*t*
 X-linked, 49*f*, 53, 178, 310–313, 312*f*, 328–329, 365
- RetNet, 288
- Retrobulbar tumor, 134
- Retrolental fibroplasia, 193. *See also* Retinopathy of prematurity
- RGS9 gene, 53
- RH. *See* Retinal hemangioblastomas
- Rhegmatogenous inferior bulbous detachment, 389
- Rhegmatogenous retinal detachment (RRD)
 chronic, 387, 387*f*
 diabetic retinopathy treatment complication, 115
 diagnostic features, 371, 382, 383*t*, 384–386*f*, 387*t*
 differential diagnosis, 391–392, 391*f*, 391*t*
 etiology and epidemiology, 382, 394, 394*f*
 familial exudative vitreoretinopathy association, 362
 management, 119, 175, 385–387, 445–451, 446–449*f*
 retinopathy of prematurity association, 210, 210*f*
 scatter photocoagulation complication, 175
 terminology, 381–382
 vision loss caused by, 146
- Rhodopsin kinase, 287, 294
- RIDE and RISE (studies), 100, 124
- Rifabutin, 347
- Rituximab, 265
- RLBP1 gene, 287
- RMC. *See* Recurrent multifocal choroiditis
- Rod–cone dystrophies. *See* Retinitis pigmentosa
- Rod monochromatism, 284–285
- Rod(s)
 age-related changes, 67
 anatomy, 11–13, 12*f*
 density and distribution of, 9–11
 electro-oculography evaluations, 54
 electroretinography testing, 45–47, 46*f*
 night vision abnormalities and, 285–288, 286–288*f*
 psychophysical evaluations, 61
 shedding by, 16–17
- ROP. *See* Retinopathy of prematurity
- “ROP safety net,” 213
- Rosiglitazone, 343
- RP. *See* Retinitis pigmentosa
- RPIL1 gene, 310
- RPE. *See* Retinal pigment epithelium
- RPE65 gene, 297, 457–458
- RRD. *See* Rhegmatogenous retinal detachment
- RS1 gene, 312*f*, 313
- Rubeosis iridis, 154
- Rush disease, 195*t*, 196
- RVO. *See* Retinal venous occlusion
- SAG gene, 287
- Salmon-patch hemorrhage, 168, 170*f*
- Sanfilippo syndrome, 316*t*, 327
- Sarcoidosis, 250, 253, 262, 367
- Sattler layer, 18
- Scanning laser ophthalmoscopy (SLO), 24–26, 25*f*, 30–32, 31*f*
- Scatter photocoagulation, 147–148, 175. *See also* Photocoagulation
- Scheie syndrome, 316*t*, 327
- Schisis. *See also* X-linked retinoschisis
 bullous retinoschisis, 310, 312*f*, 390, 390*f*
 foveal, 312*f*
 macular, 96*f*, 237–238, 238*f*, 297, 298*f*, 312*f*, 391–392, 391*f*
 of posterior vitreous, 350, 351
 retinal, 310–313, 312*f*, 382, 389–392, 390–391*f*, 391*t*, 456*t*
 trauma-related, 411
- Schlaegel lines, 256, 256*f*
- Sclera
 anatomy, 19
 choroidal folds and, 230, 230*f*, 231*t*
 laceration of, 403
 myopia and, 237*f*, 243–246, 245*f*
 rupture of, 401–402
 thickness of/permeability of, 19
- Scleral buckling, 209, 385, 392, 448–449, 448*f*
- Scleral fixation, 442
- Scleral window surgery, 232
- Scleritis, 278
- Sclerotomy, 444–445, 444*f*
- S-cone (blue-cone) monochromatism, 49*f*, 284, 285
- S cones, 57
- SCORE (study), 140–141*t*
- SCORE2 (study), 142*t*, 144
- Scotoma
 absolute, 391, 391*t*
 acute macular neuroretinopathy association, 257
 multifocal choroiditis association, 256
 multiple evanescent white dot syndrome association, 254
 paracentral, 77, 95, 127, 259, 412, 413–414
 retina dystrophies association, 294*f*, 296
 retinoschisis association, 391, 391*t*
 rod–cone dystrophies association, 291, 294*f*
 serpiginous choroidopathy association, 253
 “Scrambled-egg” macular lesions, 302
- SDH. *See* Shape-discrimination hyperacuity
- SD-OCT. *See* Spectral-domain optical coherence tomography
- Sea-blue histiocyte syndrome, 328
- “Sea fan” pattern, of neovascularization, 77, 82*f*, 168, 171, 173*f*, 175
- Secondary panretinal dystrophies, 290
- Sector retinitis pigmentosa, 47, 291–293, 295*f*
- Segmentation, 437
- Senior-Løken syndrome, 320
- Septic emboli, 156
- Serous pigment epithelial detachment, 79, 80*f*, 81
- Serous retinal detachment. *See* Exudative retinal detachment
- Serpiginous choroidopathy, 251*t*, 252, 253, 254*f*, 272
- Shafer sign (“tobacco dust”), 365, 382
- Shaggy photoreceptors, 218*f*
- Shaken baby syndrome, 411, 411*f*
- Shape-discrimination hyperacuity (SDH), 77
- Sheenlike retinal whitening, 398, 398*f*
- Shimmering, electroretinography findings in, 53
- Shock, fluorescein adverse effect, 37
- Short-wavelength sensitive cones, 57
- Sickle cell anemia, 95
- Sickle cell disease, 167–168, 167*t*, 171, 174, 339*f*. *See also* Sickle cell retinopathy

- Sickle cell–hemoglobin C (HbSC) disease, 168, 173f
- Sickle cell retinopathy
 differential diagnosis, 169–171, 174t
 management, 174–175
 nonproliferative, 168, 169–172f
 other ocular abnormalities, 171–174
 proliferative, 168–171, 173f, 175
 stages of, 168, 169f
- Sickle cell-thalassemia (SThal), 168
- Sickle cell trait (HbAs), 169, 174
- Sickling hemoglobinopathy, 167t, 174
- Siderosis bulbi, 407, 407t, 408f
- Siegrist streaks, 134, 225
- Signal voids, 29
- Sildenafil, 338–339, 347
- Silicone oil, 450, 454
- Silicone Study, 450
- Sjögren-Larsson syndrome, 320, 322f
- Skin, fluorescein adverse effects on, 38
- SLE. *See* Systemic lupus erythematosus
- Sleep apnea, 217
- Slit lamp, indirect ophthalmoscopy with, 22–23
- Slit-lamp biomicroscopy, 122
- SLO. *See* Scanning laser ophthalmoscopy
- SMD. *See* Sorsby macular dystrophy
- Smokestack form, 216, 216f
- “Snail track” degeneration, 372f
- Snellen visual acuity, 59
- Snowbanks, 277
- “Snowflakes,” 390, 390f
- Social determinants, 93, 101
- Soft drusen, 67, 67f, 69–70, 69f, 85, 229f, 303
- Soft exudates, 132
- Solar retinitis, 412–413, 413f
- Solar retinopathy, 412–413, 413f
- Sorsby macular dystrophy (SMD), 306, 307f
- Spatial frequency, 59–60
- Spectral-domain optical coherence tomography (SD-OCT), 26–27, 50f, 52f
- Spinocerebellar degeneration, 316t
- Spironolactone, 221
- Spokelike folds, 310, 312f
- Spondyloepiphyseal dysplasia congenita, 319t
- Sporadic retinal dystrophy, 293
- Stable dyschromatopsias, 283
- Staining hyperfluorescence, 35, 35t, 36
- Standing potential, 53, 54f
- Staphylococcus* spp, 270, 437–438
- Staphyloma, 96f, 237f, 238–239, 245, 245f, 394
- Stargardt disease, 47–48, 50f, 300–302, 301f, 456t
- “Starry night” sign, 263, 264f
- Static dyschromatopsia, 283
- Static nyctalopia, 285
- Stationary dyschromatopsias, 283
- Stationary nyctalopia, 285
- Steinert disease, 316t
- Stem cell treatments, 295, 302
- Stereopsis, 22
- Steroid implants, 126
- Steroids. *See* Corticosteroids
- SThal. *See* Sickle cell–thalassemia
- Stickler syndrome, 316t, 361, 361f, 370, 381
- Strabismus, 209–210
- Streptococcus* spp, 270, 271f, 437–438, 441, 453
- Stress, 217
- Striae, of retina, 353
- “String-of-pearls” pattern, 85, 265, 265f, 273f
- Strokes, 154, 160, 161f, 176
- Sturge-Weber syndrome, 181, 231
- Subclinical retinal detachment, 381
- Subfoveal pigment epithelial detachment, 81f
- Submacular hemorrhage, 93, 399, 434–435, 434–435f
- Subretinal drusenoid deposits, 25
- Subretinal fibrosis, 127, 179, 257, 257f
- Subretinal fibrosis and uveitis syndrome, 256
- Subretinal fluid
 age-related changes, 77, 78, 79f, 81f, 82, 86
 in central serous chorioretinopathy, 86
 in pathologic myopia, 96f
- Subretinal hemorrhage
 differential diagnosis, 239
 myopia and, 239
 photocoagulation complication, 425
 in polypoidal choroidal vasculopathy, 85, 86
 trauma-related, 398, 399f
 in Valsalva retinopathy, 190
- Subretinal hyperreflective material (SHRM), 81–82, 81f
- Subretinal neovascularization, 180
- Subretinal space, 17
- Sub-Tenon space, 19
- “Sugiura” sign, 263
- Sulfadiazine, 276
- Sulfa drugs, 347
- “Sunburst” lesions, 168
- “Sunflower” cataract, 407
- “Sunset glow” sign, 263
- Superficial vascular plexus, 13, 30f
- “Supertraction” or “supertraction crescent,” 239
- Suprachoroidal hemorrhage, 397, 443–445, 444f
- Susac syndrome, 176
- SUSTAIN (study), 66, 89
- Swept-source optical coherence tomography (SS-OCT), 26
- Sympathetic ophthalmia, 263, 410
- Synchysis, vitreous, 378
- Synchysis scintillans, 366
- Syndromic panretinal dystrophies, 289–290
- Synechiae, 119
- Syneresis, vitreous, 349, 364, 369
- Syphilis, 250, 253, 269, 274
- Syphilitic chorioretinitis, 274, 275f
- Syphilitic retinochoroiditis, 274, 275f
- Systemic anticoagulation, 145
- Systemic arterial hypertension ocular diseases, 131–134, 132–133f, 135
- Systemic diseases
 with retinal degeneration
 autoimmune retinopathies, 323
 Bardet-Biedl syndrome, 316t, 318–319, 318f
 Leber congenital amaurosis, 318
 neuromuscular disorders, 316t, 319
 organ-specific diseases, 318, 320–322
 paraneoplastic retinopathies, 322–323, 323f
 Usher syndrome, 316t, 319, 319f
 retinal degeneration differential diagnosis
 albinism, 324–325
 amino acid disorders, 329

- central nervous system abnormalities, 316–317*t*, 325–329, 326–329*f*
- mitochondrial disorders, 330, 330–331*f*
- Systemic drug-induced retinal toxicity
 - argyrosis, 347
 - choroidal effusions, 347
 - color vision abnormalities, 347
 - crystalline retinopathy, 344–346, 345–346*f*, 345*t*
 - electroretinography abnormalities, 347
 - ganglion cell damage, 343, 344*f*
 - macular edema, 343–344, 347
 - microvasculopathy, 342–343
 - myopia, 347
 - optic neuropathy, 343
 - retinal pigment epithelium abnormalities
 - chloroquine derivatives, 333–337, 334–336*f*
 - miscellaneous medications, 337–340, 339*f*, 340*t*, 341–342*f*
 - phenothiazines, 337, 338*f*
 - retinopathy, 342–343
 - uveitis, 347
- Systemic lupus erythematosus (SLE), 192, 262, 262*f*
- Tadalafil, 347
- Talc emboli, 156, 346
- Tamoxifen, 334–335, 344–346, 346*f*
- Taxanes, 178, 343
- Tay-Sachs disease, 328, 328–329*f*
- Telangiectasia, macular, 86, 180–181, 181–183*f*, 346
- Telangiectasia, retinal, 178, 179*f*, 186
- Telemedicine screenings, 201, 203
- Terson syndrome, 192, 192*f*
- Tessellation, 242
- Tetracycline, 279
- Thalassemia, 167, 167*t*
- Thermal injuries, 412, 424
- Thermal laser, for neovascular age-related macular degeneration, 87
- Thiazolidinediones, 123
- Thioridazine, 337, 338*f*
- 3-mirror lens, 23
- Threshold (retinopathy of prematurity), 194, 199*t*
- Thrombi
 - comma-shaped, 171
 - differential diagnosis, 176
- Thromboembolic events, 125
- Thrombotic thrombocytopenic purpura, 223
- Tick-borne diseases, 278–279
- Tilted disc syndrome, 245, 245*f*
- Time-domain (TD) optical coherence tomography (OCT), 26
- Time-resolved fluorescence imaging, 32
- TIMP3* gene, 306
- Tissue plasminogen activator (tPA), 161–162
- T lymphocytes, 263
- “Tobacco dust,” 365, 391–392
- “Tomato ketchup fundus,” 231
- Topiramate, 230, 231*t*, 347
- Toxocara canis*, 277
- Toxocara cati*, 277
- Toxocara* spp, 277, 279
- Toxocariasis, 277–278, 278*f*, 360
- Toxoplasma gondii*, 269, 274–275
- Toxoplasmic chorioretinitis, 274–277, 277*f*
- Toxoplasmosis, 309
- tPA. *See* Tissue plasminogen activator
- TP-PA. *See* *Treponema pallidum* particle agglutination assay
- Traction (tractional) retinal detachment (TRD)
 - central nervous system abnormalities and, 321
 - diabetic, 436–437, 436*f*
 - diabetic retinopathy treatment complication, 115, 120
 - diagnostic features, 383*t*, 384*f*, 387–388, 388*f*
 - management, 119, 120, 436–437, 436*f*
 - radiation retinopathy complication, 188
 - retinopathy of prematurity association, 193, 201, 210, 211*f*
 - rod–cone dystrophies association, 294*f*
 - sickle cell retinopathy association, 168
 - toxocariasis association, 277
- Tractional tufts, 371–372, 373–374*f*
- Traction foveal detachment, 355
- “Trail of echoes” artifact, 405*f*
- Trametinib, 341*f*
- Transconjunctival cryopexy, 448
- Transient hypotony, 444
- Transmission (window) defect hyperfluorescence, 35, 35*t*, 36, 255
- Transpupillary thermotherapy (TTT), 425
- 11-*trans*-retinaldehyde, 17
- Transscleral cryotherapy, 445, 448
- Transthyretin mutation, 366, 366*f*
- Trauma
 - pediatric, 377–379
 - pigment granule finding, 365
 - Purtscher and Purtscher-like retinopathy and, 190–192, 190*t*, 191–192*f*
 - retinal break cause, 376–377
 - sympathetic ophthalmia and, 263
 - Terson syndrome and, 192*f*
- Traumatic hyphema, 174–175
- TREND (study), 66, 90
- Treponema pallidum* particle agglutination assay (TP-PA), 274
- Triamcinolone, 350, 352*f*
- Triamcinolone acetonide, 112*t*, 124, 125*f*, 126, 145
- Trichromacy, 283
- Trichromatism, 283, 284*t*
- Trimethoprim-sulfamethoxazole, 276
- Tritan, 284
- Tritan axis errors, 59
- TTT. *See* Transpupillary thermotherapy
- Tubercular seriginous-like choroiditis, 253
- Tuberculosis, 250, 253, 272–273, 273*f*
- Tumor necrosis factor inhibitors, 261
- Tunica vasculosa lentis, 207, 358, 359*f*
- Type 1 diabetes, 100, 101, 103, 104*t*
- Type 2 diabetes, 100, 101, 103, 104*t*, 108
- Typical degenerative retinoschisis, 389, 390, 391
- Typical peripheral cystoid degeneration, 375–376, 389
- UBM. *See* Ultrasound biomicroscopy
- UKPDS (study), 100, 104–105, 106*t*, 108
- Ultrasonography (B-scan), 26, 27*f*, 39–41, 40–41*f*, 397
- Ultrasound biomicroscopy (UBM), 41
- Umbo, 7*f*, 8, 8*t*
- Urticarial reactions, 37
- USH2A* gene, 292*f*, 294*f*

- Usher syndrome, 290, 316*t*, 319, 319*t*, 456*t*
 Uveal effusion syndrome, 231–232, 233*f*
 Uveal lymphoma, 265–266, 266*f*
 Uveitis
 Behçet disease association, 261
 cystoid macular edema etiology, 176
 differential diagnosis, 264–267, 291
 drug-induced, 347
 electroretinography findings, 47
 imaging techniques, 34*f*, 39
 immune recovery, 268
 intermediate, 277
 Lyme disease association, 278
 Mycobacterium tuberculosis, 272
 panuveitis, 39, 95, 261, 263, 274, 277, 281
 syphilitic, 274
 in toxocariasis, 277
 Vogt-Koyanagi-Harada disease association, 263
- Valacyclovir, 270*t*
 Valganciclovir, 267–268, 270*t*
 Valsalva retinopathy, 189–190, 189*f*
 Vancomycin, 342, 438, 438*t*
 Variable expressivity, 288
 Varicella-zoster virus (VZV), 268, 269, 269*f*, 270*t*
 Vascular endothelial growth factor (VEGF), 87, 135, 137, 200–201. *See also* Antiangiogenic therapies
 Vascular filling defects, in fluorescein angiography, 34*f*, 35
 Vascularized serous pigmented epithelial detachment (PED), 79, 80*f*
 Vascular leakage, 29
 Vasculitis
 differential diagnosis, 176
 inflammatory, 259*f*, 260, 262, 262*f*
 lupus, 262, 262*f*
 retinal, 175–176, 175*f*
 Vasculogenesis, 193, 194
 Vasoproliferative tumor (VPT), 179, 185
 VECs. *See* Visual evoked cortical potentials
 Vector delivery systems, 455, 457, 458
 VEGF. *See* Vascular endothelial growth factor
 VEGFR1 gene, 90
 VEGFR2 gene, 90
 VEGF Trap. *See* Aflibercept
 VEGF Trap-Eye, 144
 Venous beading, 108–109, 109*f*
 Venous stasis retinopathy, 153
 VEPs. *See* Visual evoked potentials
 VER. *See* Visual evoked response
 Vernier acuity, 76–77
 Verteporfin, 85, 87, 184, 221, 426. *See also* Photodynamic therapy
 Vestibular areflexia, 319
 VHL. *See* Von Hippel–Lindau syndrome
 VIBRANT (study), 142*t*, 144
 VIEW 1 (study), 66, 89*t*, 90
 VIEW 2 (study), 66, 89*t*, 90
 Vigabatrin, 347
 VISION (study), 88*f*
 Vision loss
 in birdshot chorioretinopathy, 256
 diabetic-related, 99, 101, 102, 104, 109–110, 121–122
 in diffuse unilateral subacute neuroretinitis, 279
 drug-induced, 111, 334, 342, 343, 345, 347
 electrophysiologic evaluations, 55, 56
 in endophthalmitis, 272
 pregnancy-related, 104
 in retinal dystrophies, 290–291
 in toxocariasis, 277–278
 in toxoplasmic chorioretinitis, 274–275
 in vascular occlusive diseases, 145–146, 159
 in vitreomacular traction syndrome, 355
 VISTA (study), 100, 124
 Visual acuity
 antiangiogenic therapies for, 88–91, 88*f*, 89*t*, 92*t*, 96–97
 testing for, 57
 Visual evoked cortical potentials (VECPs), 55
 Visual evoked potentials (VEPs), 44*t*, 51, 55–56, 56*f*, 324
 Visual evoked response (VER), 55
 Visual field testing, 57
 Vitamin A deficiency, 292, 294, 326
 Vitamin A supplementation, 294, 326
 Vitamin B₆ supplementation, 300
 Vitamin C supplementation, 75, 76*t*
 Vitamin E supplementation, 75, 76*t*
 Vitelliform (egg yolk-like) macular lesion, 302–303, 302*f*
 Vitelliform exudative macular detachment, 303, 305*f*
 Vitelliform lesions, 302–305, 302*f*, 304–305*f*
 Vitelliform macular dystrophy, 32, 54
 Vitiliginous chorioretinitis, 265, 266
 Vitiligo, 263, 264*f*
 Vitrectomy. *See also* Pars plana vitrectomy
 amyloidosis treatment, 366*f*, 367
 anterior segment surgery complication management, 437–445, 438*t*, 439–440*f*, 441*t*
 asteroid hyalosis treatment, 365
 cystoid macular edema treatment, 178, 443, 443*f*
 diabetic macular edema treatment, 127, 128
 diabetic retinopathy complication management, 435–437, 436*f*
 diabetic retinopathy treatment, 116, 119, 120
 endophthalmitis treatment, 272, 273*f*
 macular epiretinal membrane treatment, 431–432, 431–432*f*
 needle injuries, 445
 open-globe injury repair, 403–404
 persistent fetal vasculature treatment, 360
 posterior dislocated intraocular lens management, 442–443
 posterior vitreous detachment treatment, 349, 350, 352*f*
 retinal detachment treatment, 392
 retinopathy of prematurity treatment, 209
 submacular hemorrhage treatment, 434–435, 434–435*f*
 suprachoroidal hemorrhage treatment, 443–445, 444*f*
 Terson syndrome treatment, 192
 vitreomacular traction disease treatment, 432–433*f*, 432–434
 vitreous opacity treatment, 435
 Vitreomacular adhesions, 354, 354*t*
 Vitreomacular traction, 354, 354*t*
 Vitreomacular traction diseases, 432–434, 432–433*f*
 Vitreomacular traction (VMT) syndrome, 350, 351*f*, 354–355, 354*t*, 355*f*, 432, 432*f*
 Vitreoretinal adhesions, 351, 355
 Vitreoretinal lymphoma, 255
 Vitreoretinal surgery, 115, 120, 175

- Vitreoretinal tufts, 371–372, 373f
- Vitreous
- age-related changes in, 349
 - anatomy, 5–7, 6f, 349, 369
 - avulsion of base, 370f, 377, 398
 - developmental abnormalities, 358–361, 359f
 - imaging techniques, 26, 28f, 40–41, 41f
 - inflammation, 94–95
 - liquefaction of, 378
 - opacities, 364–367, 364f, 366f, 429, 435
 - syneresis of, 349, 364, 369
 - traction, myopia and, 237
- Vitreous detachment
- opacities association, 364
 - posterior, 349–358, 369–371. *See also* Posterior vitreous detachment
- Vitreous hemorrhage
- in central retinal vein occlusion, 145, 148
 - in diabetic retinopathy, 114, 114f, 120
 - differential diagnosis, 367
 - electroretinography testing, 47
 - etiology and epidemiology, 365
 - in macular dystrophy, 310, 311
 - management, 115, 117, 119, 120, 371, 380, 436
 - photocoagulation complication, 425
 - in polypoidal choroidal vasculopathy, 85
 - in posterior vitreous detachment, 370–371
 - in retinal detachment, 391–392
 - in retinal venous occlusion, 145, 148
 - in sickle cell retinopathy, 168
 - in Terson syndrome, 192, 192f
 - trauma-related, 397, 400–401, 411
 - in Valsalva retinopathy, 189–190
- Vitreous needle tap, 438
- Vitreous opacities, 364–367, 364f, 366f, 429, 435
- “Vitreous veils,” 310, 312f
- VIVID (study), 100, 124
- VKH disease. *See* Vogt-Koyanagi-Harada disease
- VMD2 gene, 303
- VMT. *See* Vitreomacular traction syndrome
- Vogt-Koyanagi-Harada (VKH) disease (syndrome), 263, 264f
- Vogt ring, 350
- Volume scans and rendering, 26, 27–28, 27f
- Von Hippel lesions, 185
- Von Hippel–Lindau (VHL) syndrome, 179, 181–185, 184–185f
- Voretigene neparvec-rzyl, 455, 457–458
- Voriconazole, 271, 272, 438t
- Vortex veins, in choroid, 18
- VPT. *See* Vasoproliferative tumor
- VZV. *See* Varicella-zoster virus
- Waardenburg syndrome, 316t
- Wagner hereditary vitreoretinal degeneration, 316t
- Wagner syndrome, 361
- Wandering nystagmus, 296
- Wegener granulomatosis. *See* Granulomatosis with polyangiitis
- Weill-Marchesani syndrome, 361
- Weiss ring, 350, 350f, 357
- WESDR (study), 100, 101
- West Nile virus chorioretinitis, 279, 280f
- “Wet” age-related macular degeneration (AMD), 67.
- See also* Neovascular age-related macular degeneration
- Whiplash injuries, 399–400
- Whipple disease, 367
- White dot syndromes, 250–260
- about, 250, 251t
 - acute idiopathic maculopathy, 250, 259–260, 260f
 - acute macular neuroretinopathy, 250, 257–259, 259f
 - acute posterior multifocal placoid pigment epitheliopathy, 250–252, 251t, 252f, 253
 - acute zonal occult outer retinopathy, 250, 251t, 257, 258f
 - birdshot chorioretinopathy, 39, 53, 251t, 255–256, 255f
 - multifocal choroiditis, 250, 251t, 256–257, 256–257f
 - multiple evanescent white dot syndrome, 251t, 254–255, 254f
 - serpiginous choroidopathy, 251t, 253, 254f
- White infarct, 165
- Whorls, 329
- Wide-field contact lenses, 23
- Wieger ligament, 5, 6f
- Wilson disease, 407
- Window (transmission) defect hyperfluorescence, 35, 35t, 36, 255
- Wine birthmark (ipsilateral facial nevus flammeus), 231
- WINROP algorithm, 202
- Wrinkling, of retina, 353
- Wyburn-Mason syndrome, 186, 186f
- Xanthocoria, 178
- Xanthophyll, 419–421, 420f
- Xanthopsia, 347
- X-linked disorders. *See also* X-linked retinoschisis
- color vision dysfunction, 57, 284
 - cone dystrophy, 288f
 - congenital stationary night blindness, 285–286, 286f
 - familial exudative vitreoretinopathy, 179, 360, 362–363, 362t
 - incontinentia pigmenti, 317t, 320–321
 - mucopolysaccharidoses, 316t, 317t, 327
 - ocular albinism, 324
 - Pelizaeus-Merzbacher disease, 317t
 - retinitis pigmentosa, 53, 291, 456t, 458
- X-linked retinoschisis (XLRS)
- about, 310–313, 312f
 - differential diagnosis, 178, 365
 - electroretinography findings, 49f, 53
 - with retinal degeneration, 328–329
- YAG vitreolysis, 435
- Yeast endophthalmitis, 272, 273f
- Zeaxanthin, 75–76, 76t, 412
- Zellweger spectrum disorders (cerebrohepato renal syndrome), 317t, 326–327, 327f
- Zika virus chorioretinitis, 279–281
- Zinc
- age-related macular degeneration management, 75, 76, 76t
 - as foreign body, 406
- Zonulae occludentes, 15
- Zonular traction retinal tufts, 371–372, 373f

